Conference Proceeding

International Conference on

FRONTIERS IN SCIENCE AND TECHNOLOGY

ICFST - 2025

21st and 22nd November 2025

Organized by

R. E. Society's
R. P. Gogate Jogalekar College of Arts & Science And
R. V. Jogalekar College of Commerce (Autonomous), Ratnagiri

Under the aegis of

PM - USHA

Proceeding of

International Conference on Frontiers in Science and Technology (ICFST-2025)

Chief Editor

Prin. Dr. Makarand R. Sakhalkar

Co-Editors

Dr. Aparna Kulkarni
Professor and Head, Department of Chemistry

Dr. Madhura Mukadam
Professor and Head, Department of Zoology

Dr. Bhushan Dhale
Associate Professor and Head, Department of Physics

Dr. Sonali Kadam
Professor and Head, Department of Botany

Organized By
R. E. Society's
R. P. Gogate College of Arts & Science, and
R. V. Jogalekar College of Commerce (Autonomous),
Ratnagiri - 415612, Maharashtra, (India)

ISBN: 978-81-985929-5-8

Proceeding of
International Conference on Frontiers in Science and Technology
(ICFST-2025)

Published By:

R. E. Society's
R. P. Gogate College of Arts & Science and
R. V. Jogalekar College of Commerce (Autonomous)
Near District Court, Adv. N. V. Joshi Road
Ratnagiri – 415 612, Maharashtra, India
Mobile: 75882 64348
Email: gjcrtn@gmail.com

Published On:

21st November 2025

Published At:

Ratnagiri, Maharashtra (India)

ISBN: 978-81-985929-5-8

Disclaimer:

All papers published in these proceedings are based on the authors' original research work. The editors and publisher have taken reasonable steps to ensure the quality of the content; however, they do not accept any legal responsibility for any errors, interpretations, opinions, or consequences arising from the use of information presented herein. The responsibility for plagiarism, copyright permissions, data accuracy, and ethical compliance rests entirely with the authors.

Preface

It gives me immense pleasure to present the Conference Proceedings of the International Conference on Frontiers in Science and Technology (ICFST 2025), organized by the Science Faculty of Gogate Jogalekar College (Autonomous), Ratnagiri, which is run by the Ratnagiri Education Society, under the aegis of the PM-USHA Scheme (Pradhan Mantri Uchchatar Shiksha Abhiyan).

The ICFST 2025 has been conceived as a dynamic platform to bring together academicians, researchers, industry experts, and students from various scientific disciplines to exchange ideas and discuss recent innovations and emerging trends in the frontiers of science and technology. The conference represents our vision of fostering interdisciplinary collaboration, encouraging innovative research, and promoting scientific excellence at both national and international levels.

Through this conference, the Science Faculty endeavours to provide an opportunity for meaningful dialogue and networking among participants working in diverse areas such as Biological sciences, Environmental studies, Chemistry, Physics, Mathematics, Computer science, and Information technologies. The event also reflects our commitment to advancing the goals of the PM-USHA Scheme, which seeks to enhance the quality of higher education through innovation, capacity building, and academic integration.

We express our deepest gratitude to all authors, paper presenters, and delegates for their active participation and valuable research contributions that have enriched these proceedings. Our sincere thanks are due to the Ratnagiri Education Society for its continuous guidance and encouragement, as well as to the Advisory Committee, Organizing Committee, and Coordinators for their dedicated efforts in planning and executing this event successfully. We also acknowledge the support of our sponsors and collaborators, whose involvement has been vital to the success of the conference.

We firmly believe that this proceeding will serve as a valuable reference and inspiration for researchers, educators, and students engaged in scientific inquiry and technological innovation. The knowledge shared and the collaborations initiated through this conference will, continue to inspire future explorations in the ever-expanding frontiers of science and technology.

— Prof. Dr. Makarand R. Sakhalkar
Principal, Gogate Jogalekar College (Autonomous), Ratnagiri

Message from the Management

Ratnagiri Education Society, Ratnagiri

It gives me immense pleasure to note that the Science Faculty of Gogate Jogalekar College (Autonomous), Ratnagiri has successfully organized the International Conference on Frontiers in Science and Technology (ICFST 2025) under the aegis of the PM-USHA Scheme (Pradhan Mantri Uchchatar Shiksha Abhiyan).

The Ratnagiri Education Society has always been committed to fostering excellence in higher education and supporting initiatives that promote research, innovation, and interdisciplinary learning. This international conference is a reflection of that vision, providing a platform for academicians, researchers, and students to exchange ideas and explore new frontiers in scientific knowledge and technological advancement.

We are proud that our institution continues to uphold its legacy of academic leadership and social responsibility through such meaningful endeavours. The active participation of distinguished scholars and young researchers from diverse fields highlights the spirit of collaboration and intellectual curiosity that defines the essence of scientific progress.

On behalf of the Ratnagiri Education Society, I extend my heartfelt congratulations to the Principal, Convenor, Organizing Committee, Faculty Members, and Students for their dedicated efforts in making this event a resounding success. I also wish all participants fruitful discussions and productive outcomes that will contribute to future advancements in science and technology.

Smt. Shilpa Patwardhan
Chairperson,
Ratnagiri Education Society, Ratnagiri

Message from the PM – USHA Co-ordinator

It is my privilege to extend a warm welcome to all esteemed delegates, researchers, academicians, and industry professionals participating in the *International Conference on Frontiers in Science & Technology (ICFST-2025)*. As we gather to exchange knowledge and explore emerging trends, this conference serves as an important platform to celebrate scientific inquiry and to reaffirm our collective commitment to advancing human understanding. As Vice Principal of the Science Faculty and Chair of this conference, I am honored to oversee a platform dedicated to rigorous scientific exchange and interdisciplinary dialogue.

We are deeply honored to have Prof. R. D. Kulkarni, Vice Chancellor, University of Mumbai, delivering the keynote address, and Prof. Sanjay Bhave serving as the Chief Guest for the valedictory session. Their presence enriches this conference and inspires our scientific community.

Science today stands at a transformative juncture. Rapid innovation across material science, biotechnology, environmental studies, data analytics, and machine intelligence is reshaping the way we perceive the world and address global challenges. The contemporary scientific landscape is vibrant, dynamic, and filled with questions that demand creativity, collaboration, and courage.

Whether it is developing sustainable technologies, unlocking the potential of biotechnology, exploring the depths of environmental science, or harnessing the power of data and machine intelligence, every breakthrough begins with curiosity and the determination to push boundaries. The themes of this conference reflect these evolving frontiers—linking fundamental research with practical, sustainable, and socially relevant applications. ICFST-2025 aims to nurture this spirit by providing a platform where ideas can converge, evolve, and inspire future innovation.

I firmly believe that meaningful progress in science thrives on collaboration and interdisciplinary dialogue. As we engage in presentations, discussions, and knowledge exchange, let us remember that science advances not through isolated efforts, but through communities that think together, question together, and innovate together. I hope this conference ignites new connections, inspires meaningful research collaborations, and motivates young scientists to pursue inquiry with passion, curiosity, and integrity.

I extend my heartfelt gratitude to our esteemed advisory committees, keynote speakers, reviewers, organizing team, and participants from India and abroad for their dedication and enthusiasm. Your presence adds immense value to this scientific endeavor.

I wish all participants an engaging, insightful, and inspiring academic experience. May ICFST-2025 ignite curiosity, deepen scientific thought, and contribute meaningfully to the advancement of knowledge.

— Prof. Dr. Aparna Kulkarni
Conference Chair, ICFST 2025
Science Faculty, Gogate Jogalekar College (Autonomous), Ratnagiri

Message by the Convenor

It is a matter of great pride and satisfaction to present the **International Conference on Frontiers in Science and Technology (ICFST 2025),** organized by the **Science Faculty of Gogate Jogalekar College (Autonomous), Ratnagiri,** which is managed by the **Ratnagiri Education Society,** under the **aegis of the PM-USHA Scheme** (Pradhan Mantri Uchchatar Shiksha Abhiyan).

The conference has been envisioned as a platform to promote **academic dialogue, interdisciplinary research, and innovation** across various domains of science and technology. It brings together **scientists, academicians, industry professionals, and young researchers** to share their insights and recent findings, thereby fostering collaboration and intellectual exchange. The event reflects our ongoing commitment to advancing scientific learning, encouraging critical inquiry, and strengthening the bridge between education and research.

The organization of ICFST 2025 has been a rewarding journey made possible by the unwavering support and cooperation of many individuals and institutions. I take this opportunity to express my sincere gratitude to our **Principal, Dr. Makarand R. Sakhalkar**, for his constant encouragement and leadership. My heartfelt thanks also go to the **Advisory Committee, Organizing Committee, Coordinators, Faculty Members, and Technical Staff** for their dedication and teamwork in ensuring the smooth conduct of this event.

A special note of appreciation is extended to all **authors, presenters, and delegates** for their valuable contributions and active participation, which have greatly enriched the discussions and proceedings. Their enthusiasm and commitment to scientific exploration truly embody the spirit of this conference.

It is my firm belief that the deliberations and research shared during ICFST 2025 will inspire new perspectives, encourage future collaborations, and contribute meaningfully to the ever-expanding frontiers of science and technology.

— **Prof. Dr. Madhura Mukadam**
Convenor, ICFST 2025
Science Faculty, Gogate Jogalekar College (Autonomous), Ratnagiri

Acknowledgment

The Organising Committee of the International Conference on Frontiers in Science and Technology (ICFST 2025) expresses its profound gratitude to all individuals and institutions whose support and contributions have made this event a resounding success.

This conference, organised by the Science Faculty of Gogate Jogalekar College (Autonomous), Ratnagiri, under the aegis of the PM-USHA Scheme (Pradhan Mantri Uchchatar Shiksha Abhiyan) and managed by the Ratnagiri Education Society, has been a collaborative endeavour that reflects our collective commitment to academic excellence, innovation, and research.

We extend our sincere thanks to the Ministry of Education, Government of India, for the financial and institutional support through the PM-USHA Scheme, which has enabled us to enhance academic and research engagement at the college level.

Our heartfelt appreciation goes to Dr. Makarand R. Sakhalkar, Principal, for his constant guidance, encouragement, and leadership throughout the planning and organization of this conference. We are equally indebted to the Advisory Committee, whose scholarly insight and valuable suggestions enriched the academic quality of this event.

We acknowledge with gratitude the efforts of the Organizing Committee Members, Coordinators, Faculty Members, Technical Staff, and Student Volunteers, whose dedication and teamwork ensured the smooth execution of every phase of the conference.

Special thanks are due to all reviewers, keynote and invited speakers, session chairs, paper presenters, and participants for their active involvement and valuable research contributions. Their participation has significantly enhanced the scope and impact of this conference.

Finally, we express our appreciation to all sponsors, collaborators, and well-wishers for their continued support and cooperation in making ICFST 2025 a truly memorable and successful academic event.

— Organising Committee
ICFST 2025
Science Faculty, Gogate Jogalekar College (Autonomous), Ratnagiri

Funding Acknowledgment

This conference was supported under the PM-USHA Scheme (Pradhan Mantri Uchchatar Shiksha Abhiyan), an initiative of the Ministry of Education, Government of India. The organisers gratefully acknowledge this financial and institutional assistance, which enabled the successful conduct of the International Conference on Frontiers in Science and Technology (ICFST 2025) and the publication of these proceedings.

About the Conference

The International Conference on Frontiers in Science and Technology (ICFST 2025) was organized by the Science Faculty of Gogate Jogalekar College (Autonomous), Ratnagiri, under the aegis of the PM-USHA Scheme (Pandit Madan Mohan Malaviya National Mission on Teachers and Teaching) and managed by the Ratnagiri Education Society. The conference was conceived as a multidisciplinary platform aimed at promoting scientific dialogue, research collaboration, and innovation across various domains of science and technology.

The primary objective of ICFST 2025 was to bring together academicians, researchers, scientists, industry professionals, and students from diverse fields to share their findings, exchange ideas, and discuss emerging trends and challenges in contemporary scientific research. The conference provided an opportunity to explore the latest advancements in areas such as biological and environmental sciences, chemistry, physics, mathematics, computer science, biotechnology, and applied technologies.

This event sought to bridge the gap between fundamental research and practical applications, encouraging participants to adopt an interdisciplinary approach to problem-solving and sustainable development. The discussions and presentations highlighted how scientific innovation can be leveraged to address pressing global issues such as environmental conservation, renewable energy, health sciences, and digital transformation.

ICFST 2025 featured keynote and invited lectures, oral and poster presentations, and interactive sessions that fostered meaningful engagement among participants. The enthusiastic response from researchers and scholars from different institutions reflects the growing importance of cross-disciplinary collaboration in driving future discoveries.

The organizers hope that the knowledge exchanged and connections established during this conference will continue to inspire new ideas, research initiatives, and technological innovations that contribute to the advancement of science and society.

About the College

Gogate Jogalekar College (Autonomous), Ratnagiri, established in 1945, is one of the leading higher education institutions in the Konkan region of Maharashtra. The college is managed by the Ratnagiri Education Society, an organization committed to fostering academic excellence, research, and holistic development. Over the decades, the college has evolved into a multidisciplinary hub of learning, offering undergraduate and postgraduate programs in Arts, Science, and Commerce, along with several professional and skill-oriented courses.

The college was conferred Autonomous Status by the University Grants Commission (UGC), which has empowered it to design innovative curricula, adopt modern pedagogical practices, and promote research-oriented education. Affiliated to the University of Mumbai, the institution has consistently upheld high academic standards and contributed significantly to the intellectual growth of students in the region.

The Science Faculty of the college, comprising departments of Botany, Zoology, Chemistry, Physics, Mathematics, Biotechnology, and Computer Science, plays a pivotal role in promoting scientific inquiry and research. Faculty members are actively engaged in research projects, publications, and extension activities that address contemporary scientific and societal challenges.

Through initiatives like ICFST 2025, the Science Faculty continues to create platforms for knowledge exchange, innovation, and collaboration among scholars, researchers, and industry professionals. The college remains dedicated to its vision of nurturing competent, ethical, and socially responsible citizens equipped to meet the demands of the rapidly advancing world of science and technology.

Conference Committee

International Advisory Committee

Prof. D. P. Dubal - Queensland University of Technology, Australia
Prof. A. I. Inamdar - Dongguk University, South Korea
Dr. S. S. Mali - Chonnam National University, South Korea
Prof. K. G. Daniel - Broward College, Florida, USA
Mr. V. N. Jogalekar - Sr. Software Engineer, Google, USA

National Advisory Committee

Prof. Dr. R. V. Kulkarni - Vice Chancellor, University of Mumbai
Prof. Dr. V. J. Fulari - Vice Chancellor, Dr. B. A. Marathwada University
Prof. Dr. D. T. Shirke - Vice Chancellor, Shivaji University, Kolhapur
Dr. A. M. Deshmukh - President, Microbiology Society of India
and other distinguished academicians.

Organizing Committee

Chief Patron: Hon. Shri Shripad Naik, President, R. E. Society, Ratnagiri
Chairperson: Smt. Shilpa Patwardhan, R. E. Society, Ratnagiri
Principal: Prof. Dr. Makarand R. Sakhalkar
Chair: Dr. Aparna M. Kulkarni
Co-chair: Dr. V. V. Bhide
Convener: Prof. Dr. M. D. Mukadam
Co-convener: Dr. B. B. Dhale
Organizing Secretary: Dr. U. B. Sankpal
Treasurer: Mrs. A. A. Gharpure
Joint Secretary: Dr. S. L. Bhatar

INVITED TALKS

INDEX OF FULL-LENGTH PAPERS

INTERNATIONAL CONFERENCE ON FRONTIERS IN SCIENCE AND TECHNOLOGY
ICFST
2025
ORGANIZED BY
GOGATE JOGALEKAR COLLEGE
(AUTONOMOUS),
RATNAGIRI

Synthesis of Nanomaterials for Energy Storage and Green Hydrogen Generation

Akbar I. Inamdar
Division of Physics and Semiconductor Science, Dongguk University, Seoul 04620, South Korea

Maintaining an acceptable quality of life worldwide increasingly depends on the availability of clean and cost-effective energy supply. The worldwide power consumption expected to double by 2050. Therefore, the need for sustainable and affordable green energy and smart storage systems has become important to develop. It spurred innovative electrocatalysis research with the goal to develop materials and processes that are capable of producing environmentally friendly, carbon-neutral, clean, and green hydrogen fuel as an alternative to fossil fuel. Moreover, the materials which can serve as smart energy storage systems and act as electrochromic display simultaneously also gaining considerable attention due to worlds carbon zero mission. In this talk, I would like to discuss about the designing of the nanomaterials for the sustainable production of the green hydrogen via electrocatalysis process. Secondly, I will talk about the smart materials which works as supercapacitor and smart display devices, which are called as electrochromic storage devices (ECSD).

Authors to whom correspondence should be addressed:

akbarphysics2002@gmail.com (A. I. I.)

Oncolytic virotherapy platform for treatment of brain cancers

Dr. Yogesh Ostwal,
Max Planck Institute of Interdisciplinary Sciences, Germany

Oncolytic Virotherapy (OVT) is a promising platform for treating aggressive brain cancers, such as glioblastoma. It uses genetically modified viruses, like Herpes Simplex Virus (HSV) or Adenovirus, that are engineered to selectively infect and destroy cancer cells while sparing healthy tissue. The viruses replicate within the tumor cells, causing them to burst (oncolysis), which not only kills the cell directly but also releases tumor antigens. This process effectively turns an immunologically "cold" tumor into a "hot" one by activating a powerful anti-tumor immune response.

Generative AI (GenAI) models are becoming crucial for optimizing OVT platforms. GenAI can analyze complex datasets of virus-host interactions, tumor microenvironments, and patient-specific genomic data to design novel oncolytic viruses with enhanced tumor specificity and reduced off-target toxicity. Specifically, GenAI models can:

Predict the optimal viral modifications, such as identifying the best therapeutic transgenes to "arm" the virus for improved immune stimulation.

Model the dynamic interactions between the virus, the tumor, and the patient's immune system to determine optimal dosing and scheduling for clinical trials.

Personalize treatment by linking a patient’s unique molecular signature to the most effective oncolytic virus or combination therapy.

Authors to whom correspondence should be addressed:

Yogesh.ostwal@nucleovir.com

NANO catalysts for Energy and Environmental applications

Dr. Pradip Sarawade
Associate Professor, Department of Physics, University of Mumbai, Mumbai

Nanocatalysts have emerged as powerful platforms for addressing some of the most pressing challenges in modern energy conversion and environmental remediation. Their high surface-area-to-volume ratios, tunable electronic structures, and ability to host multifunctional active sites enable reaction pathways that are inaccessible to conventional bulk catalysts. This talk will highlight recent advances in the design, synthesis, and mechanistic understanding of nanocatalysts for key energy and environmental applications, including hydrogen production, CO_2 reduction, pollutant degradation, and advanced oxidation processes. Emphasis will be placed on structure–property relationships, stability under realistic operating conditions, and strategies for scaling nanocatalyst architectures for industrial deployment. By integrating insights from materials chemistry, surface science, and reaction engineering, this presentation will outline emerging opportunities for leveraging nanoscale catalytic systems to support a cleaner, more sustainable energy and environmental future.

Authors to whom correspondence should be addressed:

pradip.sarawade@physics.mu.ac.in

Emerging Contaminants and Ecosystem Health Along the Maharashtra Coast, India

Pradeep Kumkar
Department of Zoology and Fisheries, Faculty of Agrobiology, Food, and Natural Resources, Czech University of Life Sciences Prague, Czech Republic

The Maharashtra coast, extending over 720 km along the eastern Arabian Sea, represents one of India's most ecologically productive yet increasingly vulnerable coastal regions. Rapid urbanization, industrial discharge, and tourism-related pressures have accelerated the input of emerging contaminants into its estuarine and marine systems. To elucidate their distribution, interactions, and biological consequences, a series of integrated studies were undertaken linking pollution sources, contaminant profiles, and organismal responses. Comprehensive analyses of sediments and coastal waters revealed a high diversity of pollutants—microplastics (MPs), plasticisers, pharmaceuticals and personal care products (PPCPs), and heavy metal(loid)s— with the northern coast emerging as a contamination hotspot. Dominant polymers such as polyethylene, polypropylene, and polystyrene acted both as sources of leached plasticisers and as vectors for sorbed metals and pharmaceuticals, producing medium to high ecological risk indices for fish and crustaceans. Complementary assessments of the Ulhas River, a major industrial catchment, confirmed it as an important conduit of MPs and phthalates to the coastal sea. Laboratory and field experiments further demonstrated the biological effects of these pollutants: exposure to the plasticiser diethyl phthalate impaired predator–prey chemo recognition and survival in benthic loaches, while mudskippers inhabiting polluted estuaries selectively ingested filamentous MPs correlated with reduced body condition, hepatic stress, and altered feeding morphology. Concurrently, plastisphere investigations revealed dense colonization of aged polymer surfaces by diatoms and fungal hyphae, indicating shifts in microbial community structure and the potential for pathogen transport. Together, these findings illustrate a continuum of contamination from riverine to marine ecosystems, highlighting how interacting emerging pollutants disrupt ecological processes, degrade biodiversity, and threaten the sustainability of fisheries and coastal livelihoods. The study underscores the urgent need for integrated management strategies encompassing solid-waste reduction, effluent control, and long-term contaminant monitoring to protect the ecological integrity of India's western coastline.

Authors to whom correspondence should be addressed:

kumkarpradeep@gmail.com

Theme: Expanding Boundaries of Future with Applied Mathematics

Thermal Wave Propagation: Modelling, Analysis and Applications

Vinayak Kulkarni
Department of Mathematics, University of Mumbai, Mumbai-400098, Maharashtra, India

Thermal analysis techniques are in great demand in the basic sciences and engineering due to its ability to characterize materials and processes under various thermal conditions, ensuring product reliability and safety. Fourier law (1807) assumes that the heat conduction process in a homogeneous medium, the heat flux vector and temperature gradient appears at the same time instant and consequently thermal signals propagate with an infinite speed. In order to achieve the finite speed of thermal wave, Cattaneo and Vernotte (1958) have reconstructed the Fourier law in terms of the thermal relaxation parameter. Furthermore, to study the lagging behaviour of the heat conduction, Tzou (1995) proposed the dual-phase-lag theory by introducing delay time translations in heat flux vector and in temperature gradient. Moreover, Quintanilla (2008) has claimed that whenever a dual-phase-lag heat conduction law is coupled with the energy equation, then the problem may have a sequence of eigenvalues such that its real part is positive and goes to infinity. Consequently the resulting heat conduction model may be ill posed. However Quintanilla (2009) added that a dual-phase-lag heat conduction law if coupled with the constitutive equation of two temperature theory developed by Chen and Gurtin (1968), then the resulting heat conduction model is well posed. The proposed model is an attempt to design a well-posed heat conduction problem considering non-Fourier effects and study the influence of phase lag parameter in the wave like behaviour of heat conduction. The presence of relaxation time converts the corresponding heat conduction equation into a hyperbolic type that characterizes the combined diffusion and wave-like behaviour of heat conduction and predicts a finite speed of thermal wave propagation. The analytical solutions of governing equations could be achieved by converting the original boundary value problem into an eigenvalue problem by the application of the Integral transforms. The existing classical and non-classical theories of heat conduction have been recovered by considering the various special cases for two different translations under consideration. The micro structural interactions and corresponding thermal changes have been studied due to the involvement of relaxation time and delay time translations. Presenting models could establish the scientific role of phase-lags and the relaxation times to categorize the conducting materials in the mechanism of heat transfer. Mathematical analysis discussed helps understanding/ predicting thermal behaviour before it's built, enabling them to identify potential problems and optimize design. Also ensure materials meet specific thermal performance requirements, improving product quality and reliability. It has a wide scope of applications in diverse fields like designing of materials / structures and testing its thermal stability.

Authors to whom correspondence should be addressed:

vinayak.kulkarni@mathematics.mu.ac.in

Nature inspired organocatalytic enantioselective new bond formation

Swapandeep Singh Chimni
Department of Chemistry, Guru Nanak Dev University, Amritsar, India

Chemists have been inspired by Nature for a long time, not only trying to understand the chemistry that occurs in living systems, but also attempting to mimic Nature based on the learned facts. Learning from the mechanisms of action of enzymes, small organic molecules have been designed that can be used as catalysts. The greater activity in this field was initiated by the report of Barbas and List on the L-proline catalyzed aldol reaction involving enamine mechanism having similarity with catalytic mechanism of Aldolase I. Later on, our group and other reported the development of double hydrogen bonding catalysis, taking a clue from the activation of epoxide ring by two tyrosine residues in the catalytic site of epoxide hydrolase. This mode of activation was then extended for the activity of carbonyl and imine group. A variety of chiral organocatalysts have been developed incorporating double-hydrogen bonding such as ureas, thioureas, squaramides and bisphenols. These organocatalyst have been show to catalyze wide array of carbon-carbon, carbon-nitrogen and carbon-phosphorous bond formation reaction. In this context, our group have extensively used this strategy for enantioselective construction of carbon-carbon bond.

Authors to whom correspondence should be addressed:

sschimni@yahoo.com

Nanotechnology for Sustainable Lithium-Ion Battery Recycling

Vishwanath R. Patil
Department of Chemistry, University of Mumbai, Santacruz (E), Mumbai-400098, India,

Nanotechnology, with its ability to tailor materials at the nanoscale, has emerged as a key enabler for next-generation energy storage. By engineering structure, composition and interfaces at the nanometre level, nanomaterials can deliver high capacity, fast charge–discharge and long cycle life, while also reducing material consumption and improving device safety. This makes nanotechnology a natural ally in efforts to build cleaner, more efficient and more sustainable energy systems. At the same time, the rapid growth in lithium-ion battery (LIB) usage is generating large volumes of end-of-life cells, and conventional metal-centric recycling increasingly struggles to remain economically attractive, especially as cobalt content is reduced. Integrating nanotechnology with LIB recycling offers a route to directly convert recovered battery materials into high-value nanostructured electrodes, thereby linking waste minimisation, resource recovery and enhanced electrochemical performance within a circular-economy framework.

In this contribution, directly recovered battery materials are employed as precursors for nanostructured electrodes in both LIBs and supercapacitors. Chemically processed carbonaceous fractions are nanostructured, doped with phosphorus and combined with $BaTiO_3$ to form a P-doped graphene/$BaTiO_3$ (P-GN/BTO) nanocomposite anode, which delivers an initial discharge capacity of 824 mA h g^{-1} and a reversible capacity of 635 mA h g^{-1} at 0.1 A g^{-1}, while retaining 355 mA h g^{-1} at 2 A g^{-1} after 65 cycles. The same recovered fraction is also converted into mesoporous carbon (MC), which, when paired with P-GN/BTO in an asymmetric supercapacitor, provides a cell capacitance of 150 F g^{-1} at 1 A g^{-1} in the 0–2.0 V window, with an energy density of 83.3 Wh kg^{-1} at 3260 W kg^{-1} and excellent stability over 10,000 charge–discharge cycles. Alongside complementary nanostructured systems developed by our group—such as MnO_2–Co_3O_4@polypyrrole, V-doped Co–Bi oxides, ferrocene/PPy/graphene oxide and AQS/graphene oxide hybrids—these results demonstrate that nanotechnology applied directly to recovered battery materials can transform end-of-life LIBs into advanced electrode architectures, reduce reliance on virgin resources and strengthen sustainable, high-performance energy storage.

Authors to whom correspondence should be addressed:

vrpatil@chem.mu.ac.in

SYNTHESIS AND CHARACTERISATION OF MIXED HYBRID LANTHANIDE COMPLEX

S. S. Kadam, S. L. Bhattar*

Department of Chemistry, R.P. Gogate College of Arts and Science and R.V. Jogalekar College of Commerce (Autonomous), Ratnagiri, Maharashtra, India

Corresponding Author E-mail: slbhattar@gmail.com
Contact No. : +91 8999586859

Abstract: Lanthanide complexes have garnered considerable attention from researchers across diverse scientific domains, owing to their distinctive structural motifs and exceptional magnetic, catalytic, and optical properties. These features enable their critical deployment as magnetic probes, in nuclear medicine, optical amplifiers, and chemical sensors—where precise structural modulation of the complexes is pivotal to optimizing functional performance.

Lanthanide metal complexes were synthesized via a classical condensation method using lanthanide nitrate salts and a bidentate ligand in a 1:2:1 molar ratio (M:L:L). Their structures were confirmed by IR, TGA, XRD, elemental microanalysis, and SEM, while the free ligand was similarly characterized and subjected to microbial screening. The complexes exhibited strong in vitro antimicrobial activity against gram-positive (*S. pyogenes, S. aureus*) and gram-negative (*E. coli, P. aeruginosa*) strains, notable antifungal effects against *C. albicans, A. niger* and *A. clavatus* and significant antimalarial efficacy against *P. falciparum*. These results indicate their potential as promising candidates for antimicrobial and antimalarial drug development.

Keywords: Lanthanide complex, Optical and magnetic properties, chemical sensors, FTIR, Thermal analysis

INTRODUCTION

The coordination chemistry sector focusing on lanthanide (III) ions also known as rare earth metal ions, is quickly evolving as it finds applications in fundamental and applied research in diverse fields including chemistry, material science, and biology [1]. The electron configuration and lanthanide contraction play significant roles in determining the structures of complexes, which can pose difficulties in managing the coordination environment of metal ions [2]. The lanthanides are a group of 15 rare earth elements that span from cerium to lutetium in the Periodic Table, with atomic numbers 58 to 71. Some experts also include lanthanum 57 in this group, which comes before them in the Periodic Table, and the series is named after lanthanum. This series is characterized by a sequence of elements where the f orbital is either partially or completely filled with electrons, while the outer orbital remains vacant [3-6].

Within the lanthanide series, there exists a series of consecutive elements where the f orbital is either partially or completely filled with electrons, while the outer orbital remains unoccupied [5]. These elements exhibit oxidation states of +3 in their compounds, with some elements showing states of +2 and +4 as well. Notably, the +3 state is the most stable in lanthanum, gadolinium, and lutetium due to the vacancy of the 4f orbital, which undergoes half-filling before reaching complete filling [7]. Despite being classified as transition elements, these metals possess unique properties that distinguish them from other elements [6,8].

The main goal of this research project was to prepare and investigate the critical structural characteristics and biological activities of lanthanide complexes. The complexes were characterized using variety of techniques including elemental analysis, Fourier transform

infrared spectroscopy (FT-IR), thermogravimetric analysis (TGA), Scanning Electron Microscope (SEM), X-ray diffraction (XRD), and Fluorescence study.

EXPERIMENTAL

All chemicals and solvents used were of analytical grade. Lanthanum nitrate hexahydrate, 1,10-phenanthroline, and 8-hydroxyquinoline were obtained from Research Lab Fine Chem Industries, while nicotinic acid was purchased from Loba Chemie Pvt. Ltd. and used without further purification. Infrared spectra were recorded in KBr pellets on a Shimadzu spectrometer. Elemental analysis was performed using a Jeol JSM-IT200 analyzer, and XRD patterns were obtained with an Ultima IV diffractometer. Fluorescence measurements were carried out at room temperature using a Jasco spectrometer. Thermal gravimetric analysis (TGA) was conducted on a Mettler-Toledo instrument under an air atmosphere.

The synthesis process of La(1,10-phen)2(8-Hq) is illustrated in figure 1. The compound was obtained by reacting the ligands, 8-hydroxy quinoline (8-Hq), 1,10-Phenanthrolin (1,10-Phen), and Lanthanum Nitrate Hexahydrate (metal ligand) in a molar ratio of 1:2:1 in ethanol. To prepare the solution, 0.145 g (0.001 mol) of 8-hydroxy quinoline (8-Hq) and 0.396 g (0.002 mol) of 1,10-Phenanthrolin (1,10-Phen) were dissolved in 60 ml of absolute ethanol in a 100 ml three-neck flask. The mixture was stirred in an inert atmosphere at 90°C for 2 hours. Subsequently, it was cooled to 70°C, and a solution of Lanthanum Nitrate Hexahydrate (0.433 g, 0.001 mol) in 3 ml of deionized water was added dropwise. After stirring for an additional 2 hours, a yellowish precipitate of the complex formed. The precipitate was separated from the reaction mixture, filtered, and then dried at 90°C in an oven for 24 hours.

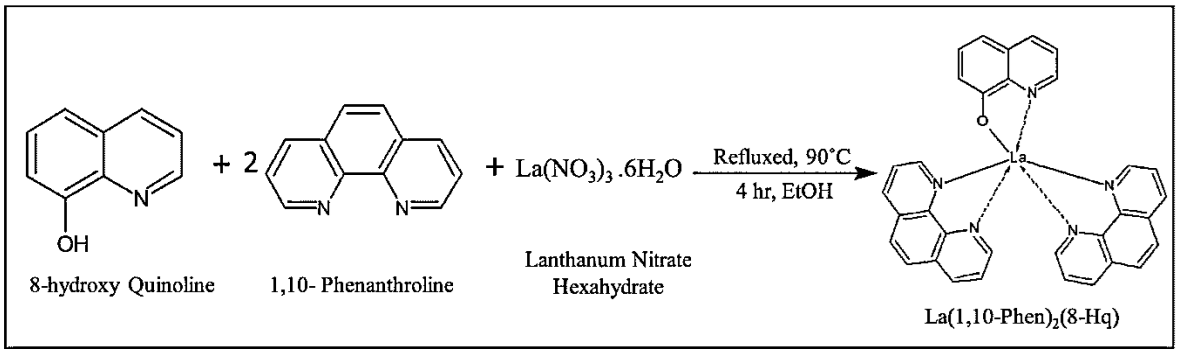

Figure 1 Preparation of complex (8-hydroxy quinoline) bis (1,10-Phenanthrolin) Lanthanum La(1,10-Phen)2(8- Hq)

RESULTS AND DISCUSSION

Infrared spectra: The material's characterization was conducted using spectroscopic techniques, specifically Fourier transformation infrared spectroscopy (FTIR). The absorption observed in the mid-wave number region (1600-500 cm^{-1}) corresponds to the in-plane and bending vibrations of the heavy atom (La). On the other hand, the absorption below 1000 cm^{-1} in the low wavenumber region is attributed to out-of-plane modes. The bands observed at 1600-1577 cm^{-1} are assigned to the stretching vibration of C=C from the quinoline ligand. The C=C/C=N stretching associated with the pyridyl group in La(1,10-Phen)$_2$(8-Hq) can be observed at 1500 cm^{-1}. The sharp peak at 1321 cm^{-1} is a result of C-N vibrational absorption. In the case of La(1,10-Phen)2(8-Hq) the vibrations at 1375 cm^{-1} are attributed to the C=C/C=N stretching in the quinoline fragments. Additionally, the presence of quinolinic rings is indicated by the characteristic peaks ranging from 600 to 800 cm^{-1}. [**9-11**]

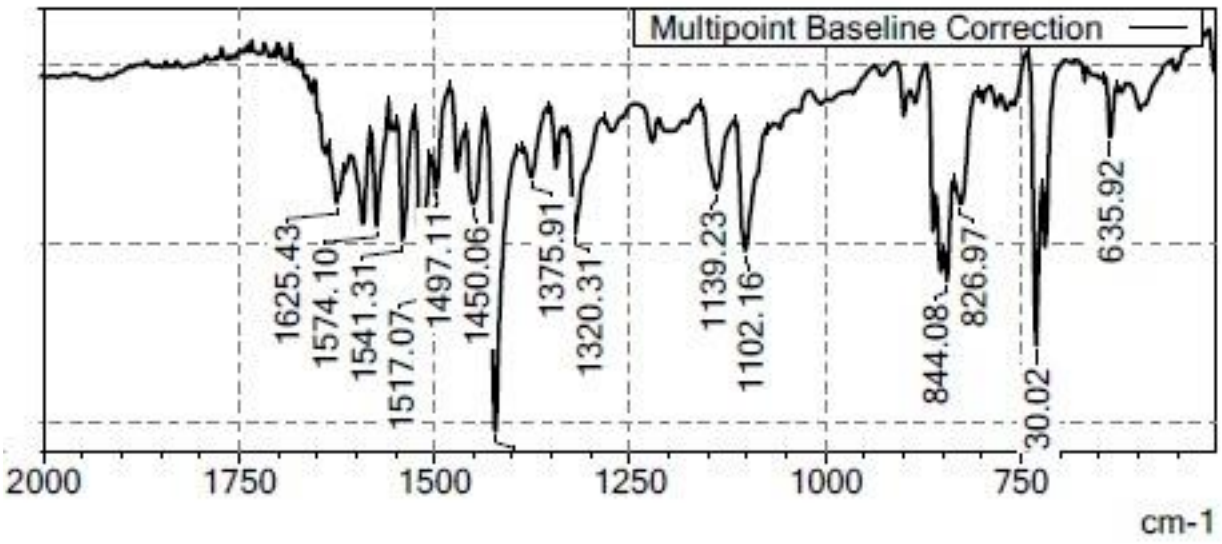

Figure 2 FT- IR spectra of complex (8-hydroxy quinoline) bis (1,10-Phenanthrolin) Lanthanum

Thermal analysis: The Thermogravimetric Differential Thermal Analysis (TG-DTA) was conducted under a nitrogen atmosphere, with a heating rate of 10°C/min, within the temperature range of 33-1000°C for both complexes. The thermal analysis of lanthanide complexes exhibited a multi-stage disintegration or loss process, which occurred in two distinct steps, indicating a remarkable level of thermal stability. Initially, the loss of water molecules located outside the coordination sphere took place, followed by subsequent stages that led to a gradual decrease in weight and the release of specific compounds from the prepared complexes. The temperature ranges at which these stages occurred varied depending on the nature of the ions involved in complex formation. The remaining material after the completion of the dissociation process may correspond to the Lanthanide oxide that constitutes the complex. The temperature ranges from 240 to 430ºC, resulting in a gradual decomposition of the complex and a decrease in mass of approximately 52% due to the elimination of a coordinated molecule. [**12-14**]

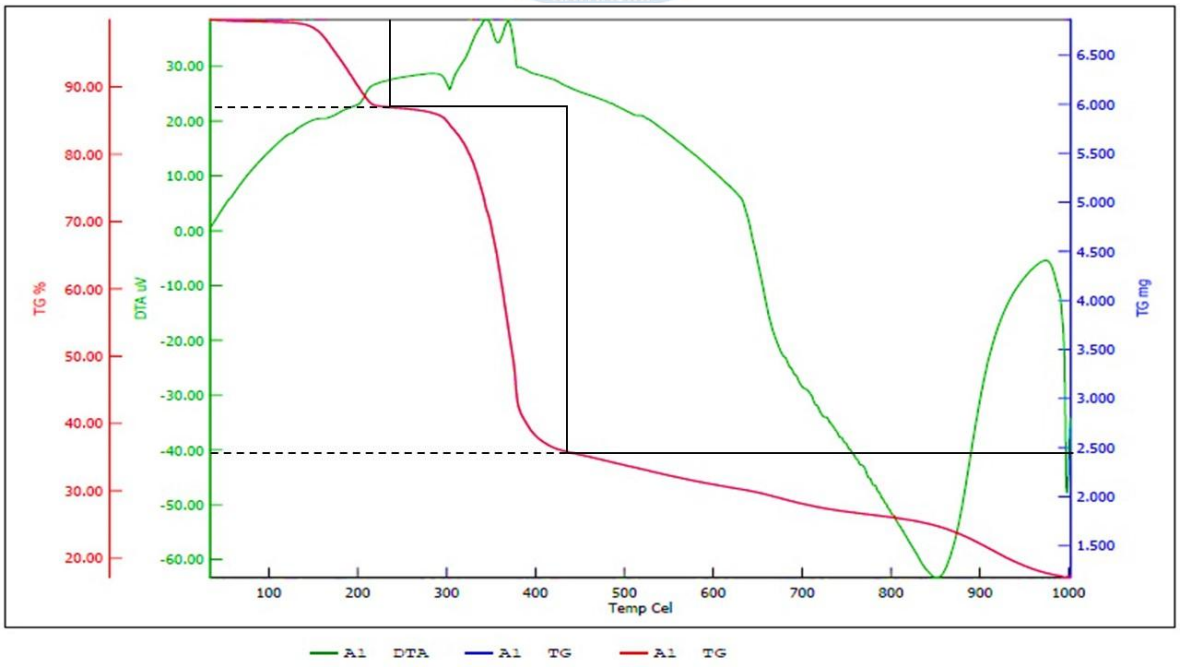

Figure 3 TGA thermograms of (8-hydroxy quinoline) bis (1,10-Phenanthrolin) Lanthanum

X-Ray Diffraction Studies: The flexible non-destructive analytical method known as X-ray diffraction (XRD) is used to examine the phase composition, crystal structure, and orientation of powder, solid, and liquid samples, among other physical parameters. Determining the purity of synthesized chemicals is mostly dependent on their XRD examination. In order to guarantee precise outcomes, every XRD pattern was acquired after the compounds underwent an array of processes, including washing, filtering, air-drying, and being exposed to air for a minimum of one week. Figures 4 show the X-ray diffraction patterns (PXRD) of the synthesized La(1,10-Phen)$_2$(8-Hq) compounds.[**15-17**]

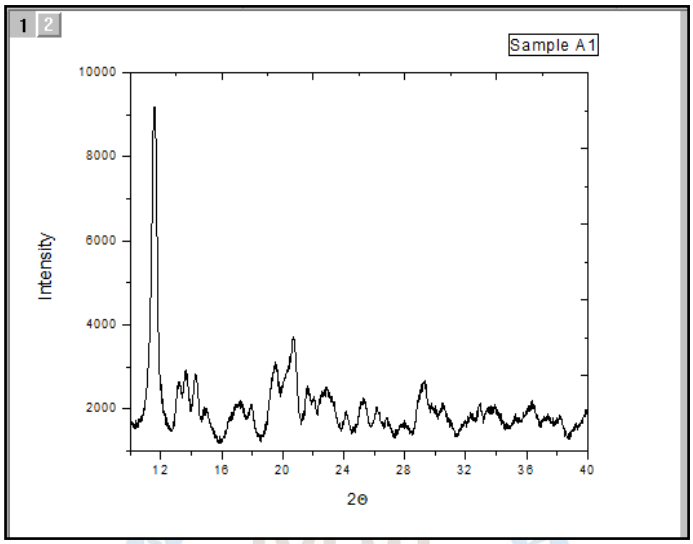

Figure 4 XRD pattern of complex (8-hydroxy quinoline) bis (1,10-Phenanthrolin) Lanthanum

Scanning Electron Microscopy (SEM) & Energy-dispersive X-ray (EDX) analysis: The surface morphology of lanthanide complexes is examined by employing a focused electron beam to scan the surface. From fig 3, the resulting SEM images exhibit a distinctive dumbbell and rod-like appearance with a smooth and polished aspect, showing the crystallinity of the complexes. To determine the chemical composition of the Ln (III) complexes, energy dispersive X-ray spectroscopy (EDX) is utilized. This analytical technique enables elemental analysis and chemical characterization of the samples. Additionally, the EDX analysis of the complexes provides valuable information regarding the presence of Lanthanides (La), carbon, oxygen, and nitrogen elements. Notably, the EDX profile of the La (III) complexes displays peaks corresponding to C, O, and Ln (III) elements, thereby corroborating the proposed structure.[**15-16**]

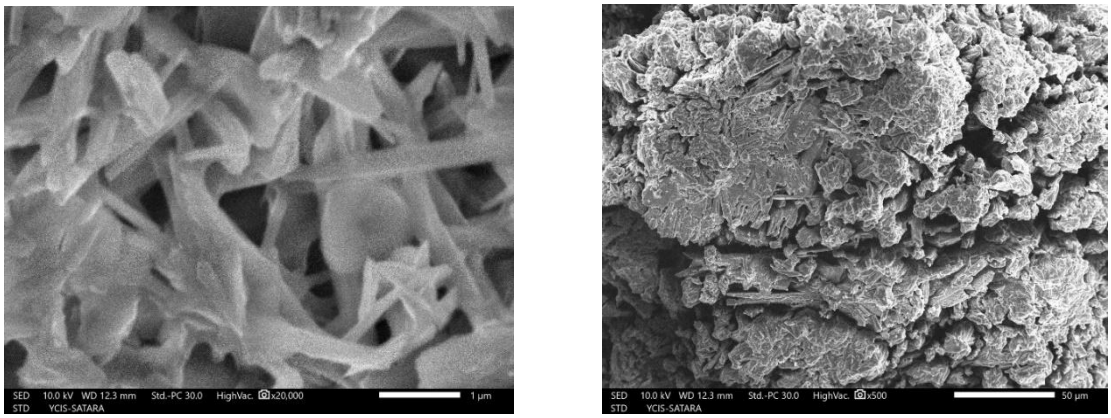

Figure 5 SEM and elemental images of complex (8-hydroxy quinoline) bis (1,10-Phenanthrolin) Lanthanum

Element	Line	Mass%	Atom%
C	K	45.22±3.01	54.82±3.65
N	K	16.71±4.73	17.37±4.92
O	K	29.59±5.80	26.93±5.28
La	L	8.48±14.82	0.89±1.55
Total		100.00	100.00
Spc_003			Fitting ratio 0.5109

CONCLUSION

Lanthanide complexes were synthesized from lanthanide nitrate hexahydrate, 1,10-phenanthroline, and 8-hydroxyquinoline, and characterized by elemental analysis, IR, SEM-EDX, and TG-DTA. Thermal studies revealed stepwise decomposition with intermediate formation, varying according to the lanthanide ion. X-ray diffraction confirmed the crystalline structure, while fluorescence spectroscopy demonstrated efficient intramolecular energy transfer from the ligand's triplet state to the lanthanide (III) ion, influencing their luminescence properties.

ACKNOWLEDGEMENTS

The authors gratefully acknowledge University Grant commission-CPE-II Phase for providing financial support for purchasing the instrument of Spectrofluorophotometer JASCO Model FP-8200.

We thankful to Dr. Namdev Harale, an assistant professor at SGM College in Karad (Satara), and Prof. Dr. Rohit Bhat of BKL Walawalkar Hospital in Ratnagiri performed the TG-DTA and Fourier transformation infrared spectroscopy (FTIR) measurements. We are also appreciative of Dr. Makarand Kulkarni of Punyashlok Ahilyadevi Holkar Solapur University in Solapur for providing the facilities for measurements of X-ray diffraction, energy-dispersive X-ray (EDX), and scanning electron microscopy (SEM).

CONFLICT OF INTEREST

The authors have declared that they have no conflict of interest.

REFERENCES

1. Paderni D., Giorgi L., Fusi V., Formica M., Ambrosi G. and Micheloni M., Chemical sensors for rare earth metal ions , Coord. Chem. Rev., Volume 429, 15 February 2021, 213639, https://doi.org/10.1016/j.ccr.2020.213639
2. Pospieszna-Markiewicz I., Fik-Jaskółka M. A., Hnatejko Z., Patroniak V. and Kubicki M., Synthesis and Characterization of Lanthanide Metal Ion Complexes of New Polydentate Hydrazone Schiff Base Ligand, Molecules 2022, 27(23), 8390 https://doi.org/10.3390/molecules27238390
3. Vernon R.E., The location and composition of Group 3 of the periodic table, Foundations of Chemistry (2021) 23:155–197 https://doi.org/10.1007/s10698-020-09384-2
4. Wedal J.C. and Evans W.J., A Rare-Earth Metal Retrospective to Stimulate All Fields, J. Am. Chem. Soc. 2021, 143, 44, 18354–18367 https://doi.org/10.1021/jacs.1c08288

5. Zasimov P., Amidani L., Retegan M., Walter O., Caciuffo R. and Kvashnina K.O., HERFD-XANES and RIXS Study on the Electronic Structure of Trivalent Lanthanides across a Series of Isostructural Compounds, Inorg. Chem. 2022, 61, 4, 1817–1830 https://doi.org/10.1021/acs.inorgchem.1c01525
6. Hussein K. A. and Shaalan N., Synthesis, Characterization, and Antibacterial Activity of Lanthanide Metal Complexes with Schiff Base Ligand Produced from Reaction of 4,4-Methylene Diantipyrine with Ethylenediamine, Indones. J. Chem., 2022, 22 (5), 1365 - 1375 https://doi.org/10.22146/ijc.74214
7. Nehra K., Dalal A. , Hooda A., Bhagwan S., Saini R.K., Mari B., Kumar S. and Singh D., Lanthanides β-diketonate complexes as energy-efficient emissive materials: A review, J. Mol. Struct., Volume 1249, 5 February 2022, 131531 https://doi.org/10.1016/j.molstruc.2021.131531
8. Prats H. and Stamatakis M., Atomistic and electronic structure of metal clusters supported on transition metal carbides: implications for catalysis, J. Mater. Chem. A, 2022,10, 1522-1534 https://doi.org/10.1039/D1TA08468B
9. Zhao J.-Y., Ren N., Zhang Y.-Y., Tang K. and Zhang J.-J., Five Dinuclear Lanthanide Complexes Based on 2,4-dimethylbenzoic Acid and 5,5′-dimethy-2,2′-bipyridine: Crystal Structures, Thermal Behaviour and Luminescent Property, Front. Chem. 9:726813. https://doi.org/10.3389/fchem.2021.726813
10. Niroomand S., Jahanara A., Jahani S., Sargazi G., Patrick B. O. , Noroozifar M. and Khorasani-Motlagh M., A novel binuclear Lanthanum complex containing 1,10-phenanthroline; from crystal structure to biological and antitumor activity, Journal of Photochemistry and Photobiology A: Chemistry, Volume 441, 1 July 2023, 114711 https://doi.org/10.1016/j.jphotocem.2023.114711
11. Vlasyuk D. & Łyszczek R., Effect of Different Synthesis Approaches on Structural and Thermal Properties of Lanthanide(III) Metal–Organic Frameworks Based on the 1H-Pyrazole-3,5-Dicarboxylate Linker, J Inorg Organomet Polym 31, 3534–3548 (2021) https://doi.org/10.1007/s10904-021-02018-w
12. Hussein K. A. & Shaalan N., Synthesis, Spectroscopy and Biological Activities Studies for New Complexes of Some Lanthanide Metals with Schiff's Bases Derived from Dimedone with 4-Aminoanitpyrine, Chem. Methodol. 2022, 6(2) 103-113 https://doi.org/10.22034/chemm.2022.2.3
13. Hao Y.-F., Xu S.-L., Zhao J.-J., Gao J., Ren N. and Zhang J.-J., New nitrogen-containing lanthanide complexes with novel structural, thermal, and fluorescence properties, Journal of Saudi Chemical Society, Volume 28, Issue 1, January 2024, 101792 https://doi.org/10.1016/j.jscs.2023.101792
14. Chiriac F. L., Iliş M., Madalan A., Manaila-Maximean D., Secu M. and Cîrcu V., Thermal and Emission Properties of a Series of Lanthanides Complexes with N-Biphenyl-Alkylated-4-Pyridone Ligands: Crystal Structure of a Terbium Complex with N-Benzyl-4-Pyridone, Molecules 2021, 26(7), 2017 https://doi.org/10.3390/molecules26072017
15. Paswan S., Anjum A., Singh A. P. & Dubey R. K., Synthesis and spectroscopic characterization of lanthanide complexes derived from 9,10-phenanthrenequinone and Schiff base ligands containing N, O donor atoms, Indian Journal of Chemistry Vol. 58A, April 2019, pp. 446-453 http://op.niscair.res.in/index.php/IJCA/article/view/22065

Impact of Green Catalysts on Product Yield in The Beckmann Rearrangement Reaction

R. S. Prasade, and Dr. M. E. Mhadaye*

Department of Chemistry, R. P. Gogate College of Arts and Science and R. V. Jogalekar College of Commerce (Autonomous), Ratnagiri, Maharashtra.

Email: rajprasade1234@gmail.com, meghanamhadaye03@gmail.com
Contact No. 9960220537

Abstract: The Beckmann rearrangement is an acid-catalyzed reaction that plays a crucial role in organic synthesis, particularly in the production of amides. Amides are fundamental functional groups in organic chemistry and biochemistry, widely utilized in pharmaceuticals, natural products, and industrial materials. The study involves the transformation of ketones into amides using traditional catalysts like concentrated sulfuric acid (H_2SO_4) and thionyl chloride ($SOCl_2$), as well as natural catalysts such as lemon juice, vinegar and egg shell catalyst. The product has been characterized by various spectral techniques such as IR, ^{1}H NMR, ^{13}CNMR.

Keywords: cyclohexanone, hydroxylamine hydrochloride, lemon juice, vinegar, egg shell catalyst.

Introduction

The Beckmann rearrangement is a classical reaction involving the acid-catalyzed transformation of oximes into N-substituted amides[1]. Since its discovery by Beckmann in 1886[2], this reaction has remained essential in both laboratory and industrial[3] organic synthesis. One of its most notable industrial applications is the large-scale synthesis of ε-caprolactam[3-5], a monomer used in the production of Nylon-6[1,6] a polymer of major commercial importance. The reaction also facilitates the synthesis of important aromatic amides such as acetanilide and benzanilide, both of which serve as intermediates in pharmaceuticals and fine chemicals[7-9].

Traditionally, the Beckmann rearrangement has been carried out using strong mineral acids like conc. H_2SO_4, sulphonyl chloride, $SOCl_2$ which, although effective, are corrosive, hazardous, and generate environmentally undesirable by-products[1,4,7-9]. In response to the growing emphasis on green chemistry, efforts have been directed toward developing safer and sustainable catalytic systems.

The present work focuses on evaluating both conventional and natural catalysts in the Beckmann rearrangement. The performance of thionyl chloride, sulfuric acid, lemon juice, vinegar, and an egg shell catalyst[10] were compared using cyclohexanone and cyclohexanone oxime as substrates. The aim was to determine a catalyst that provides high yield, purity, and environmental compatibility, thus supporting sustainable synthetic methodologies.

Methodology

All the chemicals used were of the analytical grade (AR) and of highest purity. The chemicals cyclohexanone, hydroxylamine hydrochloride, sodium hydroxide, conc. HCl, conc. H_2SO_4, pet ether, thionyl chloride was obtained from MOLYCHEM were used directly without further purification. Whenever A. R. grade chemicals were not available, the laboratory reagent

chemicals were used after purification. Solvents like chloroform, CCl_4, ethanol, methanol whenever used were distilled and purified according to standard procedures[11,12]. The progress of the reactions was monitored by thin-layer chromatography (TLC) on silica gel. Melting point was taken in an open glass capillary tube. IR spectra of sample were recorded in KBr on a Bruker Alpha II spectrometer in the region 4000-400 cm^{-1}, ^{1}H-NMR spectra were recorded in $CDCl_3$ on a Bruker Avance 400 MHz spectrometer and ^{13}C-NMR spectra were recorded in $CDCl_3$ on a Bruker Avance 400 MHz spectrometer.

Preparation of lemon juice catalyst: Fresh lemons were thoroughly washed with distilled water to remove surface impurities and cut into small pieces using a clean knife. The lemon pieces were manually pressed to extract the juice, which was then filtered through a cotton to remove any solid residues. The clear filtrate obtained was used directly as a natural acid catalyst in the reaction.

Preparation of vinegar catalyst: Commercial synthetic vinegar (Golden Dragon brand), manufactured by Sunblest Bijur Combine, was procured from the local market and used directly as a catalyst in the reaction.

Preparation of egg shell catalyst: Eggshells were collected in bulk and cleaned thoroughly with distilled water. The broken shells are then boiled in water to remove any adhesion. After cleaning, eggshells are dried in oven at 80°C and crushed into fine powder using mortar and pestle. This raw eggshell powder was then calcinated at a heating rate of 2°C/min in Muffle furnace to 900°C and this temperature was maintained for 3 hrs. The thermal treatment had two parts: in the first 30 minutes most of the organic materials were burnt out, whereas in the second part the eggshell gets transformed into white soft powder which was denominated as egg shell catalyst[14].

Experimental:

Synthesis of caprolactam involves two steps, first is the preparation of cyclohexanone oxime from cyclohexanone and second is the preparation of ε-caprolactum from cyclohexanone oxime by using traditional catalysts like conc. H_2SO_4, thionyl chloride, green catalyst like lemon juice, vinegar and egg shell catalyst.

Preparation of cyclohexanone oxime from cyclohexanone:

A mixture of hydroxylamine hydrochloride (0.0503 mol) and sodium acetate (0.0512 mol) was dissolved in 20 cm^3 of distilled water. To this solution, cyclohexanone (0.0483 mol) was added gradually in small portions with continuous stirring. The reaction mixture was shaken thoroughly and cooled in an ice-water bath, leading to the formation of crystalline cyclohexanone oxime. The precipitated crystals were collected by vacuum filtration using a Büchner funnel, washed with a small quantity of cold water, and air-dried. The percentage yield of cyclohexanone oxime was found to be 62.58 %. A small portion of the product was recrystallized from ethanol, and its melting point (89°C) was recorded to confirm purity[11,13].

Preparation of ε-caprolactum from cyclohexanone oxime by using traditional catalyst thionyl chloride

A 0.0101 mol of cyclohexanone oxime was dissolved in 20 cm^3 of anhydrous diethyl ether in a clean, dry conical flask. To this solution, 3 cm^3 of pure thionyl chloride was added dropwise with constant stirring. The reaction mixture was gently heated on a water bath, and the solvent along with volatile by-products was removed using a rotary evaporator. The residue was then

treated with 25 cm^3 of distilled water and boiled for several minutes and with occasional stirring to break up any solid lumps formed. After cooling, the supernatant liquid was decanted, and the crude product was recrystallized from hot ethanol in the same vessel. Upon cooling, pure ε-caprolactam was obtained as crystalline solid[11,13].

Preparation of ε-caprolactum from cyclohexanone oxime by using traditional catalysts like conc.H_2SO_4 and green catalyst like lemon juice, vinegar and egg shell catalyst.

A 0.0088 mol of cyclohexanone oxime was taken in a clean, dry flask. To this, the respective catalyst was added either concentrated sulfuric acid (1.6 cm^3 H_2SO_4 diluted with 2.0 cm^3 water), or lemon juice (3 cm^3), or vinegar (3 cm^3), or eggshell-derived CaO catalyst (0.5 g). The reaction mixture was gently warmed to initiate the reaction and then removed from the heat source, allowing the reaction to proceed at ambient temperature. Upon completion, the reaction mixture was cooled and 4 cm^3 of distilled water was added to it. A sodium hydroxide solution (0.08 mol NaOH in water) was prepared separately and added dropwise to the reaction mixture while maintaining the temperature at 0 °C, until the solution became alkaline. The resulting mixture was transferred to a separating funnel and extracted three times with 10 cm^3 portions of carbon tetrachloride. The organic layer was collected, and the solvent was removed to obtain a yellow oily product of pure ε-caprolactam, which solidified upon cooling.

Reaction Scheme: Synthesis of ε-caprolactam from cyclohexanone oxime

Step I:

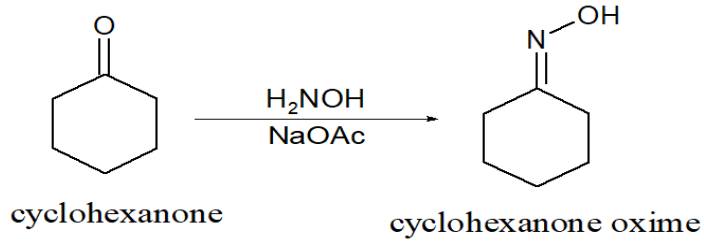

cyclohexanone cyclohexanone oxime

Step II:

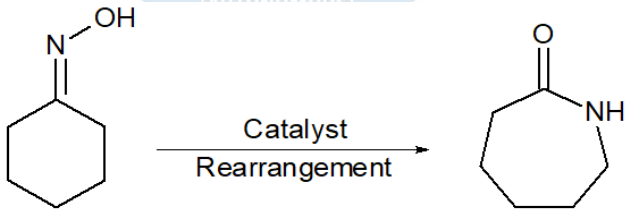

cyclohexanone oxime caprolactam

Result and Discussion:

Spectral characterization of ε-caprolactam (Lemon Juice Catalyst):

The structure of the synthesized ε-caprolactam, obtained using lemon juice as a natural catalyst, was confirmed by IR, ^1H NMR, and ^{13}C NMR spectroscopy.

The IR spectrum exhibited characteristic absorption bands at 3194 cm^{-1} (N–H stretching vibration of secondary amide), 2932 cm^{-1} (C-H stretching of methylene groups), 1664 cm^{-1} (C=O stretching of the amide group), 1480 cm^{-1} (N-H bending vibration), and 1351 cm^{-1} (C-H bending of methylene groups). The ^1H NMR spectrum (recorded in $CDCl_3$) showed multiplets in the range of δ 1.6-2.5 ppm corresponding to the methylene (-CH_2-) protons and a characteristic singlet at δ 8.9 ppm attributable to the amide (-NH) proton. The ^{13}C NMR

spectrum exhibited signals at δ 24–32 ppm corresponding to the methylene (-CH_2-) carbons and a prominent peak at δ 160 ppm, confirming the presence of the carbonyl carbon of the amide functional group[15, 16].

These spectral data collectively confirm the successful formation and purity of ε-caprolactam synthesized via the Beckmann rearrangement using lemon juice as a green catalyst.

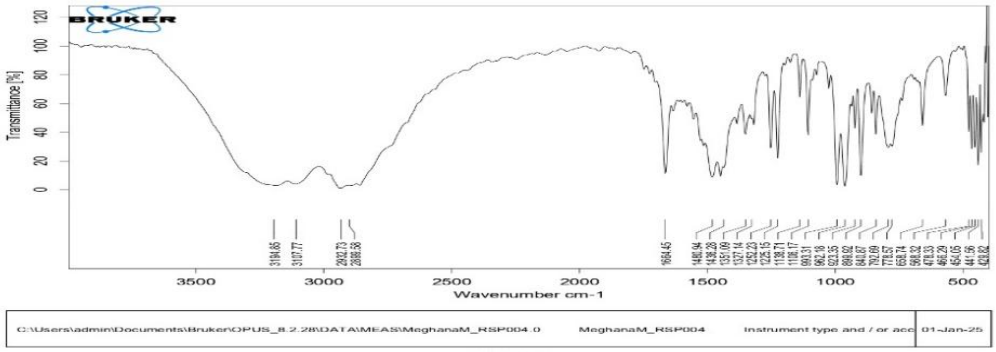

Fig. 1: IR spectra of ε-caprolactam obtained using lemon juice as a natural catalyst

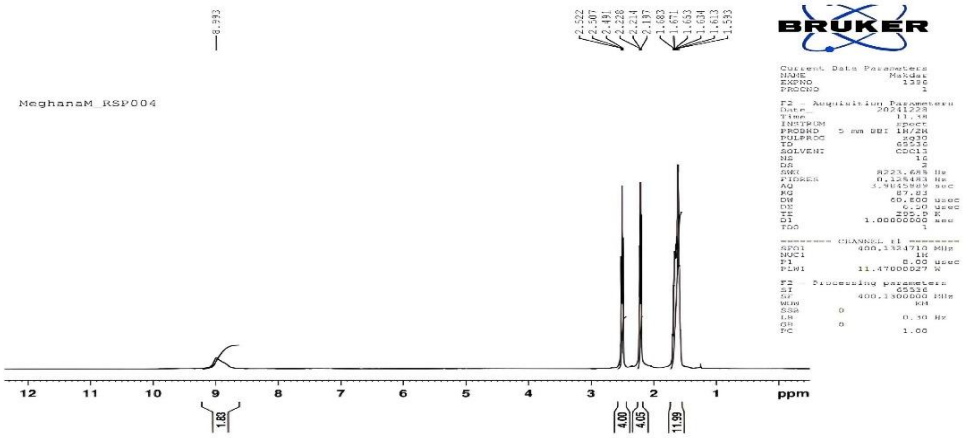

Fig. 2: ^{1}H NMR spectra of ε-caprolactam obtained using lemon juice as a natural catalyst

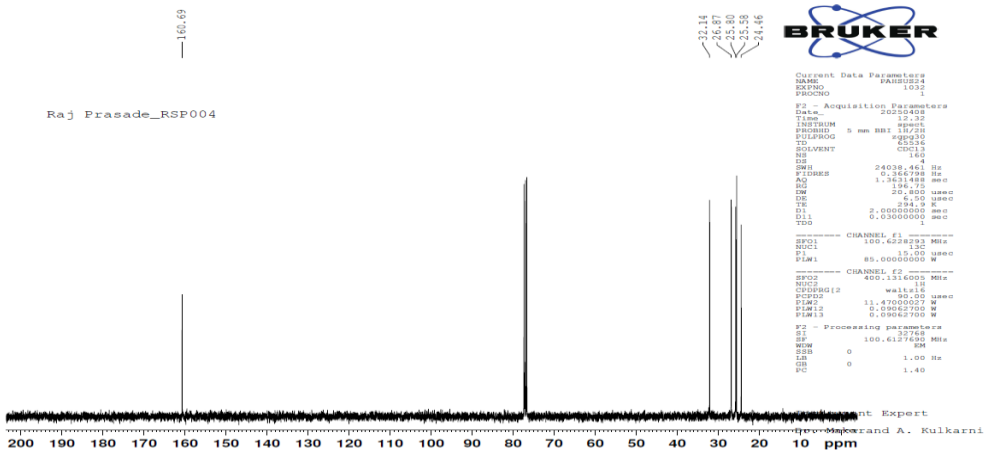

Fig. 3: ^{13}CNMR spectra of ε-caprolactam obtained using lemon juice as a natural catalyst

Table 1. Impact of catalysts on yield of ε-caprolactam

Catalysts	Thionyl chloride	Conc. H_2SO_4	Lemon juice	Vinegar	Egg shell catalyst
Observed yield of the product	0.594 g	0.384 g	0.367 g	0.290 g	0.411 g
Percentage yield of the product	59.40 %	38.40 %	36.70 %	29.00 %	41.10 %
Melting point	70 °C	70 °C	70 °C	70 °C	70 °C
Product					

Conclusion:

Catalysts play a crucial role in determining the efficiency, selectivity, and sustainability of chemical reactions. In the Beckmann rearrangement, ketoximes are transformed into their corresponding amides in the presence of acidic catalysts. Traditional catalysts such as thionyl chloride and concentrated sulfuric acid are highly effective and gives good yield. In the present study, various green and natural catalysts including lemon juice, vinegar, and egg shell catalyst were used which also give effective yield. In conclusion, our study demonstrated that green catalysts like lemon juice and egg shell catalyst can effectively catalysed the Beckmann rearrangement with comparable yields. This approach provides an eco-friendly alternative to conventional acidic catalysts.

References:

1. Rad et al., New Journal of Chemistry, 5, 2020.
2. Navjeet Kaur et al J. Chem. Pharm. Res., 4(4),1938-1946, 2012.
3. F. Manente, et al., Trifluoroacetic Acid Hydroxylamine System as Organocatalyst Reagent in a One-Pot Salt Free Process for the Synthesis of Caprolactam and Amides of Industrial Interest, 2021.
4. Jisong Zhang et al., Novel One-Step Synthesis Process from Cyclohexanone to Caprolactam in Trifluoroacetic Acid, American Chemical Society Publications, 2013.
5. Zhihui Li et al., Reactivity of hydroxylamine ionic liquid salts in the direct synthesis of caprolactam from cyclohexanone under mild conditions, The Royal Society of Chemistry, 2016.
6. Hong-Jun Pi, et al., Unexpected results from the re-investigation of the Beckmann rearrangement of ketoximes into amides by using TsCl, Elsevier Journal, Tetrahedron 65, 7790–7793, 2009.

7. Giuseppe Quartarone et al., Beckmann rearrangement of acetophenone oximes to the corresponding amides organo-catalyzed by trifluoroacetic acid for sustainable NSAIDs synthesis, Applied Catalysis A: General 472 ,167–177, 2014.
8. Xiaobin Mo et al., Scope and Mechanism of a True Organocatalytic Beckmann Rearrangement with a Boronic Acid / Perfluoropinacol System under Ambient Conditions, The Journal of American Chemical Society, 2018.
9. Yiping Zhang et al., Study on the Application of Beckmann Rearrangement in the Synthesis of Amides from Oximes, International Research Journal of Pure & Applied Chemistry, 15(4): 1-11, 2017; Article no. IRJPAC.39785, ISSN: 2231-3443, 2018.
10. Noraini Hamzah et al., Malaysian Journal of Chemistry, Vol. 23(2), 11 – 18, 2021.
11. B. S. Furnis, A.J. Hannaford, P.W.G. Smith and A. R. Tatchell, Vogel Textbook of Practical Organic Chemistry 5th Ed. ELBS Longman London, 1989.
12. D. D. Penine, W. L. F. Armarego and D. R. Penine, Purification of Laboratory Chemicals, 2nd Edition, A. Wheaton and Co. Ltd., Great Britain, 1980.
13. Advanced Practical Organic Chemistry, N. K. Vishnoi, 3rd edition, Vikas Publishing House PVT Ltd.
14. P. Kamaria, N. Kawathekar and P. Chaturvedi, Microwave Assisted Synthesis and Antimicrobial Evaluation of Schiff Bases of Indole-3-aldehyde, E-Journal of Chemistry, 2011, 8(1), 305-311.
15. P. S. Kalsi, Spectroscopy of Organic Compounds, 8th edition, New Age International Publishers.
16. Pavia, Lampman and Kriz, Introduction to spectroscopy, 3rd Edition, Harcourt College Publishers.

Microbial Fuel Cells: A Sustainable Method for Bioelectricity Production and Activated Sludge Utilization

Dr. Bharti.G. Wadekar & Mr. Mayur Patil

Assistant Professor & MSc. II Yr. Student,
Thakur Shyamnarayan Degree College, Mumbai.
Email Id: bhartiwadekar@tsdcmumbai.in

Abstract:

Microbial Fuel Cells (MFCs) are innovative bioelectrochemical devices that utilize activated sludge bacteria to produce electrical current through the metabolism of a diverse array of organic and inorganic substrates. These bioreactors efficiently convert chemical energy into electrical energy via microbial biocatalysis of various wastes, including agricultural residues, food waste, household waste, and sewage sludge from wastewater treatment plants. MFCs represent a sustainable technology that facilitates clean, green energy production, promotes waste recycling, and enables byproduct utilization from multiple sources. Recent advancements in MFC research, particularly in electrode material development and the use of activated sludge from rural and urban wastewater, have heightened interest in their practical applications. For large-scale implementation, MFCs offer an effective solution for managing diverse wastes while simultaneously generating electricity, addressing energy needs in rural or off-grid areas. By harnessing activated sludge, MFCs contribute to mitigating the global energy crisis and reducing reliance on non-renewable energy sources, supporting sustainable environmental management.

Keywords: Electricity generation, microbial fuel cells, sewage sludge, sludge reduction, *E.coli, Pseudomonas aerogenosa*

1. INTRODUCTION

Microbial fuel cells (MFCs) are bioelectrochemical systems that leverage the metabolic activities of microorganisms to convert the chemical energy in organic substrates into electrical energy, offering a sustainable approach to both energy production and wastewater treatment [Logan, 2008]. In MFCs, electroactive bacteria in the anode chamber oxidize organic matter, such as that found in activated sludge, releasing electrons that travel through an external circuit to the cathode, where a reduction reaction, typically involving oxygen, occurs [Rabaey and Verstraete, 2005]. This process generates electricity while simultaneously degrading organic pollutants, making MFCs a dual-purpose technology for energy recovery and environmental remediation [Du et al., 2007].

Activated sludge, a byproduct of conventional wastewater treatment, is rich in diverse microbial communities, making it an ideal inoculum for MFCs due to its ability to form electroactive biofilms and adapt to complex substrates [Zhang et al., 2011]. These biofilms facilitate electron transfer through direct mechanisms, such as microbial nanowires or outer-membrane cytochromes, or mediated pathways involving redox shuttles [Bond and Lovley, 2003]. Studies have shown that MFCs using activated sludge can achieve significant power outputs, with power densities reaching up to 52 mW/m² for glucose-fed systems, alongside

high organic matter removal rates (e.g., 94.4% for glucose) [Liu et al., 2005]. A key advantage of MFCs is their ability to reduce sludge volume, as the microbial degradation of organic matter during electricity generation minimizes excess sludge production, addressing a major challenge in wastewater treatment [Jiang et al., 2009].

The efficiency of MFCs depends on factors such as substrate concentration, electrode materials, pH, temperature (optimally 30-45°C), and internal resistance, all of which influence coulombic efficiency and power output [Logan, 2008]. Recent advancements, including mediator-less designs and electrode modifications, have improved performance and scalability, reducing operational costs [Rabaey and Verstraete, 2005]. By integrating energy generation with sludge reduction, MFCs provide a promising solution for sustainable wastewater management, reducing reliance on fossil fuels and mitigating environmental pollution [Du et al., 2007].

2. MFC Design and Development with Activated Sludge Bacteria

Microbial fuel cells (MFCs) are bioelectrochemical systems that utilize microorganisms to convert organic matter into electrical energy, offering a sustainable approach for simultaneous wastewater treatment and energy production [Logan, 2008]. The design and development of MFCs using activated sludge bacteria as the inoculum have gained significant attention due to the sludge's rich microbial diversity, cost-effectiveness, and ability to degrade complex organic substrates [Rabaey and Verstraete, 2005]. Below is a detailed description of the key components, design considerations, and development strategies for MFCs utilizing activated sludge bacteria, supported by relevant references.

2.a MFC Components and Configuration

MFCs typically consist of an anode and cathode chamber, often separated by a proton exchange membrane (PEM) to facilitate proton transfer while preventing oxygen diffusion into the anode [Du et al., 2007]. The anode, where activated sludge bacteria oxidize organic substrates, is typically made of carbon-based materials like carbon cloth or graphite felt due to their high conductivity and biocompatibility [Bond and Lovley, 2003]. The cathode, where reduction reactions (e.g., oxygen reduction to water) occur, may use materials like platinum-coated carbon or carbon-based catalysts to enhance reaction kinetics [Liu et al., 2005]. Activated sludge, sourced from wastewater treatment plants, serves as the microbial inoculum in the anode, forming electroactive biofilms that transfer electrons via direct electron transfer (DET) through microbial nanowires or outer-membrane cytochromes, or mediated electron transfer (MET) using redox shuttles [Zhang et al., 2011].

2.b Key Design Considerations

1. **Electrode Materials and Surface Area**: The anode's surface area and material significantly impact biofilm formation and electron transfer efficiency. High-surface-area materials like carbon nanotubes or graphene enhance microbial attachment and power output [Rabaey and Verstraete, 2005]. Cathode catalysts, such as manganese dioxide or biochar, are explored to replace costly platinum, improving cost-effectiveness [Jiang et al., 2009].

2. **Proton Exchange Membrane**: The PEM, often made of Nafion or sulfonated polymers, ensures proton transfer while maintaining separation between anaerobic anode and aerobic cathode conditions. Alternatives like ceramic membranes are being developed to reduce costs [Du et al., 2007].
3. **Reactor Configuration**: Single-chamber MFCs, which eliminate the PEM and expose the cathode to air, simplify design and reduce internal resistance, though they may face oxygen diffusion challenges [Liu et al., 2005]. Dual-chamber systems offer better control but increase complexity and cost.
4. **Substrate and Operating Conditions**: Activated sludge MFCs perform optimally with organic-rich substrates like glucose or acetate, with power densities reported up to 52 mW/m² for glucose [Liu et al., 2005]. Optimal conditions include a pH of 6.5–7.5 and temperature of 30–45°C to maximize microbial activity [Logan, 2008].

2.c Development Strategies with Activated Sludge

Activated sludge bacteria, due to their mixed microbial consortia, are highly adaptable and capable of degrading complex wastewater components, making them ideal for MFCs [Zhang et al., 2011]. Key development strategies include:

- **Pretreatment of Sludge**: Acid or heat pretreatment of activated sludge enhances the dominance of electroactive bacteria (e.g., *Geobacter* or *Shewanella* species), improving electron transfer efficiency [Bond and Lovley, 2003].
- **Biofilm Optimization**: Encouraging robust biofilm formation through electrode surface modifications (e.g., coating with conductive polymers) increases current density and stability [Jiang et al., 2009].
- **Mediator-Less Systems**: Modern MFCs aim to eliminate exogenous mediators, relying on direct electron transfer to reduce costs and environmental impact [Rabaey and Verstraete, 2005].
- **Scalability and Integration**: Stacked MFC designs and integration with existing wastewater treatment systems enhance practical applicability. For instance, continuous-flow MFCs using activated sludge have achieved up to 90% chemical oxygen demand (COD) removal alongside electricity generation [Du et al., 2007].

2.c.a. Single-Chamber MFC

Single-chamber MFCs consist of a single compartment housing both the anode and cathode, with the cathode typically exposed to air to facilitate oxygen reduction [Liu et al., 2005]. The absence of a proton exchange membrane (PEM) reduces internal resistance and construction costs, making this design simpler and more scalable [Rabaey and Verstraete, 2005]. Activated sludge, rich in electroactive bacteria like *Geobacter* and *Shewanella*, is inoculated in the anode region, where it oxidizes organic substrates (e.g., acetate or glucose) to produce electrons and protons [Bond and Lovley, 2003]. The air-cathode, often coated with catalysts like platinum or carbon-based materials, supports oxygen reduction. Single-chamber MFCs can achieve power densities up to 600 mW/m² with activated sludge and are effective for COD removal (up to

90%) [Liu et al., 2005]. However, challenges include oxygen diffusion to the anode, which can reduce coulombic efficiency, and cathode biofouling over time [Du et al., 2007].

2.c.b. Double-Chamber MFC

Double-chamber MFCs feature separate anode and cathode compartments, typically divided by a PEM (e.g., Nafion) to maintain anaerobic conditions at the anode and aerobic conditions at the cathode [Logan, 2008]. Activated sludge in the anode chamber degrades organic matter, releasing electrons that flow through an external circuit to the cathode, where electron acceptors like oxygen or ferricyanide are reduced [Rabaey and Verstraete, 2005]. These systems offer better control over reaction conditions and higher coulombic efficiency compared to single-chamber MFCs, with reported power densities of 52 mW/m² for glucose-fed sludge systems [Liu et al., 2005]. However, they are more complex and costly due to the PEM and separate chamber requirements. Activated sludge MFCs in double-chamber setups excel in wastewater treatment, achieving up to 94.4% organic matter degradation [Zhang et al., 2011].

2.c.d. Electrode Properties

The performance of MFCs relies heavily on electrode design, particularly for activated sludge-based systems, where microbial attachment and electron transfer are critical.

2.c.e. Surface Area and Porosity

High surface area and porosity of electrodes enhance microbial colonization and substrate diffusion, improving biofilm formation and electron transfer [Logan, 2008]. Carbon-based materials like carbon cloth, graphite felt, or graphene are commonly used for anodes due to their high surface area and porous structure, which support robust biofilm growth from activated sludge [Bond and Lovley, 2003]. For example, 3D porous carbon foam anodes have shown up to 2.5 times higher power density than flat electrodes due to increased microbial attachment [Jiang et al., 2009]. Cathodes benefit from porous structures like carbon mesh, which facilitate oxygen diffusion and reaction efficiency [Rabaey and Verstraete, 2005].

2.c.f. Electrical Conductivity

Electrodes must exhibit high electrical conductivity to minimize ohmic losses. Carbon-based materials, such as graphite or carbon nanotubes, are preferred for their excellent conductivity and biocompatibility with sludge bacteria [Du et al., 2007]. Modifications like coating anodes with conductive polymers (e.g., polyaniline) or nanomaterials (e.g., graphene oxide) further enhance conductivity and electron transfer efficiency, boosting power output by up to 30% in sludge-based MFCs [Zhang et al., 2011].

2.c.g Stability and Durability

Electr2.ode stability and durability are crucial for long-term MFC operation. Carbon-based anodes are chemically stable in the harsh, organic-rich environment of activated sludge, resisting degradation over months of operation [Logan, 2008]. Cathodes, however, may suffer from biofouling or catalyst degradation, particularly with costly platinum catalysts. Alternatives like activated carbon or manganese dioxide improve durability while reducing

costs [Jiang et al., 2009]. Surface treatments, such as acid washing or heat treatment of electrodes, enhance stability by preventing corrosion and maintaining performance [Rabaey and Verstraete, 2005].

2.c.f. Electron Transfer Mechanisms (ETC)

Electron transfer in activated sludge MFCs occurs via two primary mechanisms:

- **Direct Electron Transfer (DET)**: Electroactive bacteria in activated sludge, such as *Geobacter sulfurreducens*, transfer electrons directly to the anode through conductive pili (nanowires) or outer-membrane cytochromes [Bond and Lovley, 2003]. This mechanism is efficient and mediator-less, reducing operational costs.
- **Mediated Electron Transfer (MET)**: Some sludge bacteria use natural or artificial redox mediators (e.g., flavins or quinones) to shuttle electrons to the anode. While effective, MET may introduce toxicity or cost issues in large-scale systems [Rabaey and Verstraete, 2005]. Pretreatment of sludge (e.g., acid or heat) enhances DET by enriching electroactive species, improving overall efficiency [Zhang et al., 2011].

2.c.h. Role of Activated Sludge

Activated sludge, a microbial consortium from wastewater treatment plants, is an ideal inoculum for MFCs due to its diversity, adaptability, and ability to degrade complex organic compounds [Du et al., 2007]. It contains electroactive bacteria capable of forming biofilms on anodes, enabling efficient electron transfer and organic matter degradation (e.g., 90% COD removal) [Liu et al., 2005]. Pretreatment methods, such as heat or acid shock, select for robust electroactive species, increasing power output by up to 20% [Bond and Lovley, 2003]. Activated sludge also reduces excess sludge volume during MFC operation, addressing a key challenge in wastewater management [Jiang et al., 2009].

3. Other Substrates and their role

Substrate Name	Description	Maximum Electricity Produced	Presence of Bacteria	Advantages	Reference Name
Glucose	A simple sugar, readily metabolized by activated sludge bacteria, used in lab-scale MFCs due to high degradability.	600 mW/m² (single-chamber MFC, carbon cloth anode, Pt air-cathode); 52 mW/m² (double-chamber MFC, graphite anode, ferricyanide cathode).	Electroactive bacteria (e.g., *Geobacter*, *Shewanella*) in activated sludge form biofilms for efficient electron transfer.	High degradability (up to 94.4% COD removal), compatible with diverse sludge bacteria, high electron transfer rate.	Liu et al., 2005; Zhang et al., 2011

Acetate	A short-chain fatty acid, preferred by electroactive bacteria for direct electron transfer.	660 mW/m² (single-chamber MFC, carbon felt anode, carbon air-cathode); 431 mW/m² (double-chamber MFC, graphite anode, ferricyanide cathode).	*Geobacter* species dominate in sludge biofilms, enabling direct electron transfer via nanowires or cytochromes.	High coulombic efficiency (up to 80%), efficient metabolism by electroactive bacteria, widely studied for MFC optimization.	Bond and Lovley, 2003; Rabaey and Verstraete, 2005; Logan, 2008
Sewage Sludge/ Wastewater	Complex organic matter from wastewater treatment plants, practical for real-world applications.	200 mW/m² (double-chamber MFC, carbon cloth anode and cathode).	Diverse microbial consortia in activated sludge degrade complex organics, including *Geobacter* and *Shewanella*.	Enables simultaneous electricity generation and wastewater treatment, up to 90% COD removal, reduces sludge volume (up to 30% volatile solids).	Jiang et al., 2009; Du et al., 2007
Lactate	A simple organic acid, metabolized more slowly than acetate or glucose by sludge bacteria.	50–100 mW/m² (single- or double-chamber MFC, graphite or carbon cloth electrodes).	Mixed sludge bacteria, with lower abundance of electroactive species compared to acetate-fed systems.	Moderate degradability, suitable for specific bacterial strains, less efficient than acetate or glucose.	Zhang et al., 2011

Sucrose	A disaccharide, requires breakdown into simpler sugars, slower metabolism by sludge bacteria.	50–100 mW/m² (single- or double-chamber MFC, graphite or carbon cloth electrodes).	Mixed sludge bacteria, less selective for electroactive species, slower biofilm formation.	Readily available, but lower power output due to complex metabolism, suitable for mixed substrates.	Zhang et al., 2011
Food Waste/Brewery Wastewater	Complex organic waste with variable composition, used in practical MFC applications.	100–300 mW/m² (single- or double-chamber MFC, carbon-based electrodes).	Diverse sludge bacteria, including electroactive and non-electroactive species, adapt to complex organics.	Practical for industrial applications, supports wastewater treatment, moderate power output due to substrate complexity.	Rabaey and Verstraete, 2005

2.d. Commonly Used Microbes in MFCs with Activated Sludge

Activated sludge, a microbial consortium from wastewater treatment plants, is widely used as an inoculum in MFCs due to its diverse microbial community capable of degrading complex organic substrates and generating electricity [Logan, 2008]. The following are the most commonly used microbes in activated sludge-based MFCs, their roles, and their contributions to electricity production:

A. Geobacter species (e.g., *Geobacter sulfurreducens*):

- **Description**: Gram-negative, anaerobic bacteria known for their ability to perform direct electron transfer (DET) to the anode via conductive pili (nanowires) or outer-membrane cytochromes [Bond and Lovley, 2003]. They are prevalent in activated sludge and dominate anode biofilms in MFCs.
- **Role in MFCs**: Efficiently oxidize simple substrates like acetate, producing high coulombic efficiency (up to 80%) and power density (e.g., 660 mW/m² in single-chamber MFCs with carbon felt anodes) [Rabaey and Verstraete, 2005].
- **Advantages**: High electron transfer efficiency, robust biofilm formation, and adaptability to low-cost carbon-based electrodes [Logan, 2008].

B. Shewanella species (e.g., *Shewanella oneidensis*):

- **Description**: Facultative anaerobes capable of both DET and mediated electron transfer (MET) using self-produced redox mediators like flavins [Rabaey and Verstraete, 2005]. They are commonly found in activated sludge.

- **Role in MFCs**: Oxidize substrates like lactate or glucose, contributing to power densities up to 600 mW/m² in single-chamber MFCs with carbon cloth anodes [Liu et al., 2005]. They are versatile in handling diverse substrates.
- **Advantages**: Flexibility in oxygen-limited environments and ability to use MET, enhancing electron transfer in complex substrates [Zhang et al., 2011].

C. Pseudomonas species (e.g., *Pseudomonas aeruginosa*):

- **Description**: Aerobic or facultative bacteria that produce redox mediators (e.g., pyocyanin) to facilitate MET in MFCs [Zhang et al., 2011]. They are abundant in activated sludge and contribute to organic degradation.
- **Role in MFCs**: Effective in degrading complex substrates like sewage sludge, achieving power density up to 200 mW/m² in double-chamber MFCs [Jiang et al., 2009].
- **Advantages**: Enhances electron transfer in mediator-based systems, suitable for wastewater treatment applications [Du et al., 2007].

D. Escherichia coli:

- **Description**: A facultative anaerobe found in activated sludge, capable of mediatorless electron transfer in some MFC configurations [Zhang et al., 2011].
- **Role in MFCs**: Produces moderate power density (50–100 mW/m²) with substrates like glucose or sucrose, often in double-chamber MFCs with graphite electrodes [Zhang et al., 2011].
- **Advantages**: Widely available and adaptable, though less efficient than *Geobacter* or *Shewanella* for electricity production [Logan, 2008].

E. Mixed Microbial Consortia:

- **Description**: Activated sludge naturally contains diverse microbial communities, including electroactive (*Geobacter*, *Shewanella*) and non-electroactive bacteria that synergistically degrade complex substrates [Du et al., 2007].
- **Role in MFCs**: Mixed consortia are highly effective for real-world substrates like sewage sludge, achieving power density up to 200 mW/m² and 90% COD removal in double-chamber MFCs [Jiang et al., 2009].
- **Advantages**: Robust degradation of complex organics, cost-effective as no pure cultures are needed, and adaptable to varying wastewater conditions [Rabaey and Verstraete, 2005].

2. Future Perspectives for MFCs with Activated Sludge

The use of activated sludge in MFCs holds significant promise for sustainable energy production and wastewater treatment, but challenges like low power output, high costs, and scalability remain. Below are key future perspectives to enhance MFC performance:

A. **Genetic Engineering of Microbes**:

- **Perspective**: Genetic modification of electroactive bacteria like *Geobacter* or *Shewanella* to enhance electron transfer pathways (e.g., overexpressing cytochrome or pili genes) could increase power density [Bond and Lovley, 2003].

Synthetic biology approaches may also introduce electroactivity into non-electroactive sludge bacteria.

- **Potential Impact**: Power density could exceed 1000 mW/m², making MFCs competitive with other renewable energy technologies [Logan, 2008].
- **Challenges**: Regulatory and ethical concerns for genetically modified organisms in wastewater treatment systems [Rabaey and Verstraete, 2005].

B. **Electrode Material Innovations**:

- **Perspective**: Developing low-cost, high-performance electrodes (e.g., biochar, graphene, or conductive polymers) will improve microbial attachment and electron transfer, reducing internal resistance [Jiang et al., 2009]. 3D porous electrodes could further enhance biofilm formation.
- **Potential Impact**: Increase power density to over 800 mW/m² while reducing costs for large-scale applications [Rabaey and Verstraete, 2005].
- **Challenges**: Balancing cost, durability, and scalability of advanced materials [Du et al., 2007].

C. **Scalable MFC Designs**:

- **Perspective**: Stacked or continuous-flow MFC configurations can improve scalability for industrial wastewater treatment. Integrating MFCs with existing anaerobic digestion or membrane bioreactor systems could enhance energy recovery and sludge reduction [Jiang et al., 2009].
- **Potential Impact**: Enable practical deployment in wastewater treatment plants, achieving energy neutrality and up to 50% sludge reduction [Du et al., 2007].
- **Challenges**: Managing biofouling and maintaining long-term stability in large-scale systems [Logan, 2008].

D. **Optimization of Microbial Consortia**:

- **Perspective**: Pretreatment methods (e.g., acid, heat, or electrochemical enrichment) can selectively enhance electroactive bacteria in activated sludge, improving power output [Zhang et al., 2011]. Co-culturing specific strains (e.g., *Geobacter* with *Pseudomonas*) could optimize substrate degradation and electron transfer.
- **Potential Impact**: Increase coulombic efficiency and power density by 20–30% in mixed consortia systems [Bond and Lovley, 2003].
- **Challenges**: Maintaining microbial balance and preventing competition in complex consortia [Rabaey and Verstraete, 2005].

E. **Hybrid Applications**:

- **Perspective**: Combining MFCs with other technologies, such as microbial electrolysis cells (MECs) for hydrogen production or photocatalysis for enhanced cathode performance, could diversify applications [Logan, 2008]. MFCs could also power sensors or small devices in wastewater facilities.
- **Potential Impact**: Broaden MFC applications beyond electricity, supporting a circular bioeconomy with energy and resource recovery [Du et al., 2007].
- **Challenges**: Integration complexity and cost-effectiveness in hybrid systems [Jiang et al., 2009].

F. **Real-World Implementation**:
- **Perspective**: Pilot-scale studies using sewage sludge or industrial wastewater as substrates will bridge the gap between lab and field applications. Advances in modular MFC designs could facilitate adoption in wastewater treatment plants [Rabaey and Verstraete, 2005].
- **Potential Impact**: Achieve energy-neutral wastewater treatment and reduce operational costs by recovering energy from sludge [Jiang et al., 2009].
- **Challenges**: Overcoming low power density (compared to fossil fuels) and ensuring long-term system reliability [Logan, 2008].

3. Challenges and Future Directions

Despite their potential, activated sludge MFCs face challenges such as low power output compared to conventional energy sources, high material costs, and long-term stability issues [Logan, 2008]. Ongoing research focuses on low-cost electrode materials, scalable reactor designs, and genetic engineering of sludge bacteria to enhance electroactivity [Zhang et al., 2011]. Additionally, integrating MFCs with anaerobic digestion or other treatment processes could further improve sludge reduction and energy recovery [Jiang et al., 2009].

Single-chamber MFCs offer simplicity but face oxygen diffusion issues, while double-chamber MFCs are costlier but provide better performance control [Logan, 2008]. Electrode optimization remains critical, with ongoing research into low-cost, high-durability materials like biochar or stainless steel [Rabaey and Verstraete, 2005]. Scaling up activated sludge MFCs requires addressing internal resistance and biofouling, with innovations like stacked configurations or hybrid systems showing promise for practical applications [Du et al., 2007].

Commonly used microbes like Geobacter, Shewanella, and Pseudomonas in activated sludge MFCs enable efficient electricity production and wastewater treatment, with mixed consortia offering robustness for real-world substrates like sewage sludge. Future advancements in genetic engineering, electrode materials, scalable designs, and hybrid systems will enhance MFC performance, potentially achieving power densities above 1000 mW/m^2 and enabling practical applications in sustainable energy and environmental management.

4. Conclusion

The design and development of MFCs using activated sludge bacteria offer a promising avenue for sustainable energy production and wastewater treatment. By optimizing electrode materials, reactor configurations, and microbial activity, these systems can achieve efficient electricity generation and significant sludge reduction, contributing to a circular bioeconomy [Rabaey and Verstraete, 2005].

5. References

1. Bond, D. R., & Lovley, D. R. (2003). Electricity production by *Geobacter sulfurreducens* attached to electrodes. *Applied and Environmental Microbiology*, 69(3), 1548–1555.
2. Du, Z., Li, H., & Gu, T. (2007). A state of the art review on microbial fuel cells: A promising technology for wastewater treatment and bioenergy. *Biotechnology Advances*, 25(5), 464–482.

3. Jiang, J., Zhao, Q., Zhang, J., Zhang, G., & Lee, D. J. (2009). Electricity generation from bio-treatment of sewage sludge with microbial fuel cell. *Bioresource Technology*, 100(23), 5808–5812.
4. Liu, H., Ramnarayanan, R., & Logan, B. E. (2005). Production of electricity during wastewater treatment using a single chamber microbial fuel cell. *Environmental Science & Technology*, 39(17), 6587–6593.
5. Logan, B. E. (2008). *Microbial Fuel Cells*. John Wiley & Sons.
6. Rabaey, K., & Verstraete, W. (2005). Microbial fuel cells: Novel biotechnology for energy generation. *Trends in Biotechnology*, 23(6), 291–298.
7. Zhang, T., Cui, C., Chen, S., Ai, X., Yang, H., Shen, P., & Peng, Z. (2011). A novel mediatorless microbial fuel cell based on direct biocatalysis of *Escherichia coli*. *Chemical Communications*, 47(11), 3276–3278.
8. He, Z., & Angenent, L. T. (2006). Application of bacterial biocathodes in microbial fuel cells. *Electroanalysis*, 18(19–20), 2009–2015.
9. Pant, D., Van Bogaert, G., Diels, L., & Vanbroekhoven, K. (2010). A review of the substrates used in microbial fuel cells (MFCs) for sustainable energy production. *Bioresource Technology*, 101(6), 1533–1543.
10. Min, B., & Logan, B. E. (2004). Continuous electricity generation from domestic wastewater and organic substrates in a flat plate microbial fuel cell. *Environmental Science & Technology*, 38(21), 5809–5814.
11. Lovley, D. R. (2006). Bug juice: Harvesting electricity with microorganisms. *Nature Reviews Microbiology*, 4(7), 497–508.
12. Kim, B. H., Chang, I. S., & Gadd, G. M. (2007). Challenges in microbial fuel cell development and operation. *Applied Microbiology and Biotechnology*, 76(3), 485–494.
13. Wang, H., & Ren, Z. J. (2013). A comprehensive review of microbial electrochemical systems as a platform technology. *Biotechnology Advances*, 31(8), 1796–1807.
14. Feng, Y., Wang, X., Logan, B. E., & Lee, H. (2008). Brewery wastewater treatment using air-cathode microbial fuel cells. *Applied Microbiology and Biotechnology*, 78(5), 873–880.
15. Santoro, C., Arbizzani, C., Erable, B., & Ieropoulos, I. (2017). Microbial fuel cells: From fundamentals to applications. A review. *Journal of Power Sources*, 356, 225–244.

Synthesis and Characterization of PPy-$Fe(ClO_4)_2$ Nanoparticles

Shailesh D. Boba[1*], Minal P. Patil[1], Vinod S. More[1], T.N. Ghorude[1]

1. G.E.S.s N. B. Mehta Science College, BORDI, Dahanu, Palghar, Maharashtra, India

Corresponding Author:

[1*] Email: shaileshboba123@gmail.com

Contact: 9765412081

Abstract: Polypyrrole (PPy) based nanoparticles synthesized using chemical oxidative polymerization. PPy-$Fe(ClO_4)_2$ nanoparticles synthesized using novel dopant Iron (II) per chlorate $Fe(ClO_4)_2$ for M.R. from 0.5 to 2.0. PPy-$Fe(ClO_4)_2$ nanoparticles were synthesized via chemical oxidative polymerization of pyrrole in the presence of $Fe(ClO_4)_2$ as both oxidizing agent and dopant. Reaction parameters such as temperature and stirring rate were optimized to control particle size and shape. These nanoparticles were characterized using SEM, X-ray Diffraction, FTIR, UV-vis Spectroscopy. XRD confirmed the semi-crystalline nature, SEM images revealed spherical nanoparticles size, while FTIR and UV-Vis confirmed successful doping. The role of $Fe(ClO_4)_2$ in enhancing the electrical conductivity, electrochemical stability, reduced particle size and modified surface morphology was roughly investigated. These finding the role of iron perchlorate in tuning the physical and electrical properties of polypyrrole nanoparticles.

The results obtained reveals that PPy-$Fe(ClO_4)_2$ nanoparticles exhibit outstanding potential as a material for the highly sensitive sensor fabrication. By offering ground-breaking insights into the structure, morphology, and chemical composition, this research opens new opportunities for innovative applications and encourages additional investigation across an extensive range of fields. The focus of this research on successful development of conducting material which can be used for manufacturing excellent sensor.

Keywords: Polypyrrole, PPy-$Fe(ClO_4)_2$, SEM,

1. Introduction:

Polymers have long been an integral component of both natural systems and human inventions. Conducting polymer nanocomposites have evolved into complex materials attributed to their distinctive combination of electrical conductivity, mechanical strength, and superior characteristics acquired by nanomaterials (Sharma et al., 2021). Doping polyacetylene with iodine revealed its high conductivity, leading to the discovery of conducting polymers. Heeger, MacDiarmid, and Shirakawa won the 2000 Nobel Prize for this breakthrough, inspiring research into polyaniline, polypyrrole, and polythiophene (Shirakawa et al., 1977). Among the all conducting polymers, polypyrrole (PPy) stands out as one of the most extensively studied materials, due to its simple synthesis methods, excellent conductivity and biocompatibility. These properties make PPy a promising candidate for applications in sensors, energy storage devices, biomedical engineering, and environmental remediation (Singh, 2022).

Over the past few decades, conductive polymers especially polypyrrole (PPy) have gained global attention for their wide-ranging industrial uses (Chandrasekhar, 2018). PPy stands out for its robustness under diverse environmental conditions, ease of synthesis, impressive electrical conductivity, and remarkable thermal stability. When doped, it exhibits improved conductivity and maintains strong structural integrity. Its conductivity generally ranges between 1 and 100 S/cm, reflecting its adaptable electrical properties (Wallace et al., 2008).

Polypyrrole (PPy) is widely utilized across a diverse array of fields, such as solid-state electrolyte capacitors, gas sensors, actuators, protective polymer coatings, electrochromic devices, display technologies, polymer-based energy systems, packaging materials, and electronic components (Ansari, 2006). Its synthesis can be achieved through two main approaches: electrochemical and chemical methods. This versatility in fabrication techniques contributes to its broad applicability (Nosheen et al., n.d.). Among these, in-situ chemical oxidative polymerization stands out as the most commonly employed method for producing conductive polymers (Pagar et al., 2023a).

This study synthesized polypyrrole (PPy) with varied $FeCl_3$ concentrations to produce oxidant-to-monomer-to-dopant molar ratios ranging from 1:0.5:0.1 to 1:2:0.1. The Iron(II) perchlorate $Fe(ClO_4)_2$ used as dopant. The resultant nanoparticles were investigated using SEM, XRD, and FTIR to determine their structural, morphological, and electrical properties, indicating that Fe presence has significant impacts on PPy characteristics, which makes them promising for sensor applications.

2. Methodology:

2.1 Materials:

The monomer pyrrole (C_4H_5N), was procured from Loba Chemie Pvt. Ltd, of analytical reagent (AR) grade. It was stored in a dark bottle maintaining a temperature of 5°C. As the oxidant, iron(III) chloride hexahydrate ($FeCl_3 \cdot 6H_2O$), also of analytical grade, was employed. Prior to use, pyrrole underwent distillation under reduced pressure to eliminate any potential impurities. The synthesis of the pyrrole monomer and $FeCl_3$ solutions was carried out using deionized water.

2.2 Synthesis Method:

Polypyrrole (PPy) was synthesized via the in-situ chemical oxidative polymerization technique, as described by Ilicheva et al.(Ilicheva et al., 2012) In this process, pyrrole served as the monomer, while ferric chloride ($FeCl_3$) functioned as the oxidizing agent. To begin, 1 mL of a 1 M aqueous pyrrole solution was prepared, and varying concentrations of $FeCl_3$. were added to establish monomer-to-oxidant ratios (M.R.) of 0.5, 1.0, 1.5, and 2.0. The resulting mixture was stirred continuously for 3 hours at a controlled temperature of 5°C using a magnetic stirrer. After this step, $Fe(ClO_4)_2$ added as dopan and continuously stirred for 3-4 hours at controlled temperature. Following the stirring process, the solution was allowed to remain undisturbed overnight to facilitate polymerization. Once the reaction was complete, a black precipitate of polypyrrole (PPy) formed. This precipitate was collected using vacuum filtration, thoroughly rinsed with deionized water to eliminate residual impurities, and then dried. The final product was a powdered PPy nanocomposite, which was subsequently employed for characterization and fabrication purposes. During the polymerization, the pyrrole monomer reacts with $FeCl_3$ to form PPy, while Fe(III) ions are reduced to Fe(II), as illustrated in fig.1.

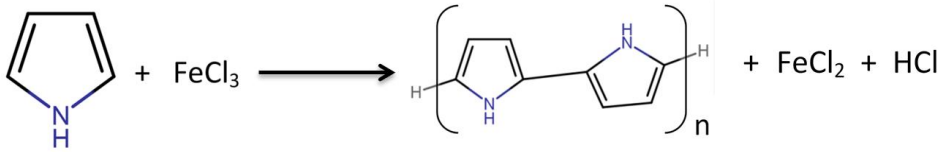

Fig. 1: Reaction of formation of polypyrrole from pyrrole

2.3 Characterization:

In this study, samples undergo numerous examinations. Surface morphological characteristics were studied using the FEI Quanta 200 SEM. infrared (IR) spectra were obtained using the Attenuated Total Reflectance (ATR) technique on a Bruker ALPHA II FTIR Spectrometer. In addition, XRD and UV-visible characteristics also studied.

3. Results and Discussions:

The PPy nanoparticles obtained through pyrrole polymerization were subjected to various characterization and analytical techniques to evaluate their structural, morphological, and functional properties.

3.1 SEM Analysis:

SEM micrographs of PPy doped with $Fe(ClO_4)_2$ at varying molar ratios (M.R. = 1:0.5:0.1 to 1:2:0.1) displayed in fig.2, showing significant morphological evolution, starting with unevenly distributed granular structures and rough surfaces at lower doping levels M.R.=1:0.5:0.1, transitioning to more homogeneous spherical particles with smoother regions and enhanced surface area at M.R. = 1:1:0.1, and further developing into tightly packed, uniformly sized nanospheres with rough texture.

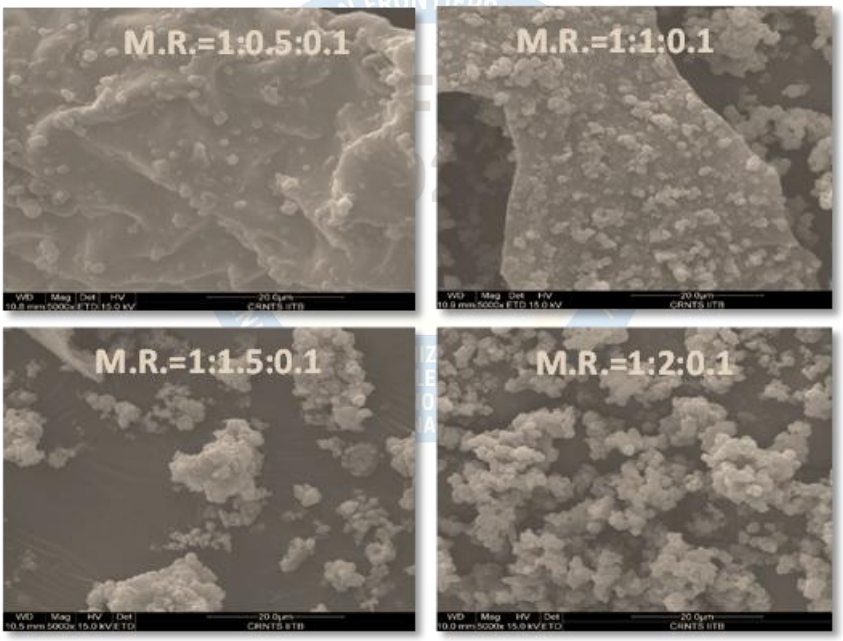

Fig. 2: SEM of PPy doped with $Fe(ClO_4)_2$ having M.R.=1:0.5:0.1 to 1:2:0.1

3.2 XRD Analysis:

Fig.3 displays the XRD spectrum of PPy doped with $Fe(ClO_4)_2$ at various molar ratios, which primarily shows an amorphous character. A broad peak in the 20–30° range confirmed PPy (Yussuf et al., 2018). The Fe(ClO4)2 dopant, which raises electrical conductivity and crystallinity, is most likely the cause of the sharp peaks at 25–30° and 45–50°, which show the presence of some crystalline areas. The intensity changes across various ratios (1:0.5:0.1 to 1:1:0.1) show that higher dopant levels increase peak sharpness, indicating more order in the structure, while lower oxidant concentrations promote more crystalline growth. The overall intensity of the 1:0.5:0.1 sample is higher than that of the 1:1:0.1 sample. These structural

factors may affect the electrical conductivity and performance of PPy-based gas sensors, as increased crystallinity may enhance sensor performance.

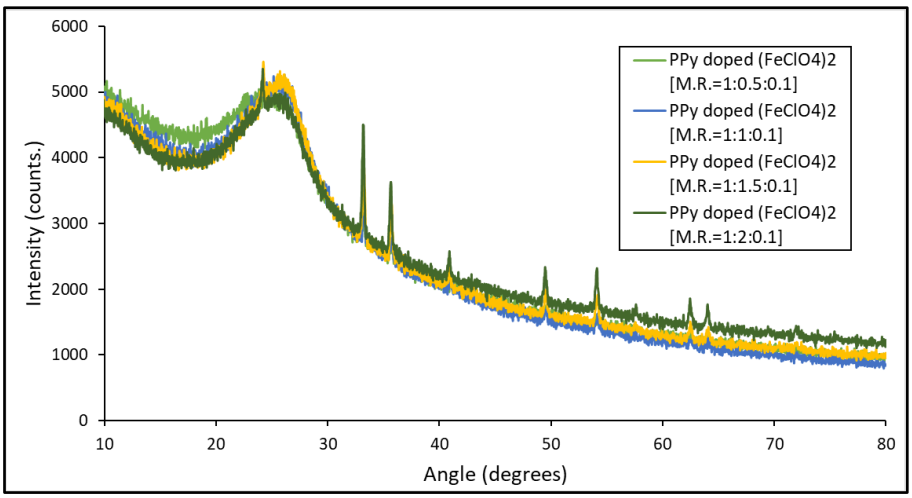

Fig. 3: XRD of PPy doped with $Fe(ClO_4)_2$ having M.R.=1:0.5:0.1 to 1:2:0.1

3.3 FTIR Analysis:

The fig.4 illustrates the FTIR spectra of PPy doped with $Fe(ClO_4)_2$ having various M.R. from 1:0.5:0.1 to 1:2:0.1. It determines the distinctive vibrational modes of chemical bonds in a substance to provide information on the molecular structure of a sample. The major absorption bands for PPy are commonly visible in the FTIR spectrum and correlate to different functional groups and bonds which is according to Navale et al (Navale et al., 2014), Chitte et al (Chitte et al., 2011), Taunk et al. (Taunk et al., 2011), Ramprasad et al (Ramaprasad et al., 2017), Chougule et al (Chougule et al., 2011). The FTIR peak values shown in the Table 1.

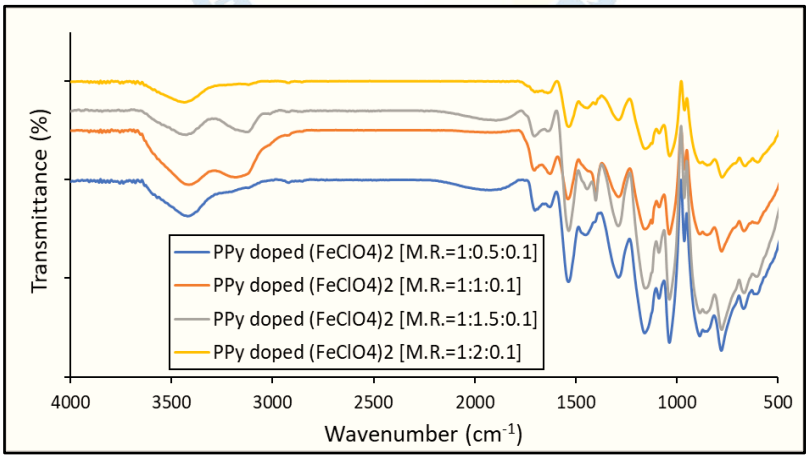

Fig. 4: FTIR spectra of PPy doped by $Fe(ClO_4)_2$ with various M.R. from 1:0.5:0.1 to 1:2:0.1

Table 1: FTIR peaks of PPy doped by $Fe(ClO_4)_2$ with various M.R. from 1:0.5:0.1 to 1:2:0.1

Assignment	Peak position by reference		Peaks for M.R. = 1:0.5:0.1 (cm^{-1})	Peaks for M.R. = 1:1:0.1 (cm^{-1})	Peaks for M.R. = 1:1.5:0.1 (cm^{-1})	Peaks for M.R. = 1:2:0.1 (cm^{-1})
N-H Stretching	3443	(Ramaprasad et al., 2017)	3418.12	3412.35	3425.55	3435.31

Assignment	Peak position by reference		Peaks for M.R. = 1:0.5:0.1 (cm^{-1})	Peaks for M.R. = 1:1:0.1 (cm^{-1})	Peaks for M.R. = 1:1.5:0.1 (cm^{-1})	Peaks for M.R. = 1:2:0.1 (cm^{-1})
C=N Bonds (Stretching)	1685	(Chitte et al., 2011)	1701.9	1627.77	1704.04	1638.98
C-H Out-of-Plane Deformation	1473	(Navale et al., 2014)	1476.26	1401.35	1401.80	1441.65
=C-H In-Plane Vibration	1250	(Taunk et al., 2011)	1289.35,	1289.28,	1290.38,	1290.29,
N-C Stretch Bending	1046	(Chougule et al., 2011)	1037.64	1038.12	1037.57	1036.22
	920	(Chougule et al., 2011)	963.98	963.88	963.95	963.14
	811	(Chougule et al., 2011)	887.60	851.80,	887.11	851.20
=C-H In-Plane Deformation Vibration	793	(Navale et al., 2014)	780.81	779.60	778.90	776.85
C-C Out-of-Plane Ring Deformation / C-H Rocking / C-H Wagging	681	(Chitte et al., 2011; Pagar et al., 2023b)	670.75	669.34	668.38	668.50

3.4 UV-Vis Analysis:

Fig.5 showing UV-visible spectra of PPy doped with Fe(ClO4)2 having various M.R., the UV-visible spectra of PPy doped with $Fe(ClO_4)_2$ at different concentrations of $FeCl_3$ exhibit distinctive π–π* transitions around ~250–300 nm, showing the presence of PPy. However, the doped samples show elevated absorbance between 300–450 nm, indicating greater polaron and bipolaron generation due to doping.

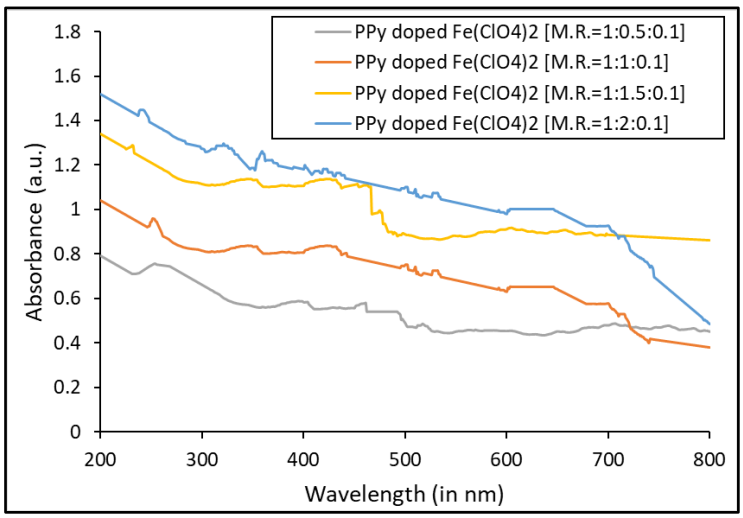

Fig. 5: UV-Vis spectra of PPy doped by $Fe(ClO_4)_2$ with various M.R. from 1:0.5:0.1 to 1:2:0.1

Conclusion:

In this study, we successfully synthesized PPy doped with $Fe(ClO_4)_2$ nanoparticles from 1:0.5:0.1 to 1:2:0.1 using chemical oxidative technique. The samples were characterized by Characterized by SEM, XRD, FTIR and UV-Vis spectroscopy. Significant changes obtained due to addition of dopant. SEM shows transition to more homogeneous spherical particles with smoother regions and enhanced surface area at M.R. = 1:1:0.1. XRD and FTIR peaks confirms the formation of PPy. In the UV-Visible spectra of the PPy doped samples show elevated absorbance between 300–450 nm, indicating greater polaron and bipolaron generation. Overall, The study shows the impact of doping on PPy characteristics, demonstrating its relevance for conductive materials and sensor development.

References:

[1] Sharma S, Sudhakara P, Omran AAB, Singh J, Ilyas RA. Recent Trends and Developments in Conducting Polymer Nanocomposites for Multifunctional Applications. Polymers (Basel) 2021;13:2898. https://doi.org/10.3390/polym13172898.

[2] Shirakawa H, Louis EJ, MacDiarmid AG, Chiang CK, Heeger AJ. Synthesis of electrically conducting organic polymers: halogen derivatives of polyacetylene, (CH) x. J Chem Soc Chem Commun 1977:578. https://doi.org/10.1039/c39770000578.

[3] Singh N. Polypyrrole-based emerging and futuristic hybrid nanocomposites. Polymer Bulletin 2022;79:6929–7007. https://doi.org/10.1007/s00289-021-03840-5.

[4] Chandrasekhar P. Conducting Polymers, Fundamentals and Applications. 2018. https://doi.org/10.1007/978-3-319-69378-1.

[5] Wallace GG, Teasdale PR, Spinks GM, Kane-Maguire LAP. Conductive Electroactive Polymers: Intelligent Materials Systems. 3rd ed. Boca Raton: CRC press; 2008. https://doi.org/https://doi.org/10.1201/9781420067156.

[6] Ansari R. Polypyrrole Conducting Electroactive Polymers: Synthesis and Stability Studies. E-Journal of Chemistry 2006;3:860413. https://doi.org/10.1155/2006/860413.

[7] Nosheen S, Irfan M, Habib F, Zaheer Abbas S, Waseem B, Iftikhar F, et al. Synthesis and Characterization of Polypyrrole Synthesized via Different Routes. n.d.

[8] Pagar SB, Ghorude TN, Nikolova MP, SenthilKannan K. Synthesis, physical, chemical, biological, mechanical and electronic studies of polypyrrole (PPy) of versatile scales for electro-mechano, pharmaceutical utilities. Heliyon 2023;9:e20086. https://doi.org/10.1016/j.heliyon.2023.e20086.

[9] Ilicheva NS, Kitaeva NK, Duflot VR, Kabanova VI. Synthesis and Properties of Electroconductive Polymeric Composite Material Based on Polypyrrole. ISRN Polymer Science 2012;2012:1–7. https://doi.org/10.5402/2012/320316.

[10] Yussuf A, Al-Saleh M, Al-Enezi S, Abraham G. Synthesis and Characterization of Conductive Polypyrrole: The Influence of the Oxidants and Monomer on the Electrical, Thermal, and Morphological Properties. Int J Polym Sci 2018;2018. https://doi.org/10.1155/2018/4191747.

[11] Navale ST, Mane AT, Chougule MA, Sakhare RD, Nalage SR, Patil VB. Highly selective and sensitive room temperature NO2 gas sensor based on polypyrrole thin films. Synth Met 2014;189:94–9. https://doi.org/10.1016/j.synthmet.2014.01.002.

[12] Chitte HK, Shinde GN, Bhat N V., Walunj VE. Synthesis of Polypyrrole Using Ferric Chloride (FeCl₃) as Oxidant Together with Some Dopants for Use in Gas Sensors. J Sens Technol 2011;01:47–56. https://doi.org/10.4236/jst.2011.12007.

[13] Taunk M, Kapil A, Chand S. Chemical synthesis and low temperature electrical transport in polypyrrole doped with sodium bis(2-ethylhexyl) sulfosuccinate. Journal of Materials Science: Materials in Electronics 2011;22:136–42. https://doi.org/10.1007/s10854-010-0102-2.

[14] Ramaprasad AT, Latha D, Rao V. Synthesis and characterization of polypyrrole grafted chitin. Journal of Physics and Chemistry of Solids 2017;104:169–74. https://doi.org/10.1016/j.jpcs.2017.01.017.

[15] Chougule MA, Pawar SG, Godse PR, Mulik RN, Sen S, Patil VB. Synthesis and Characterization of Polypyrrole (PPy) Thin Films. Soft Nanoscience Letters 2011;01:6–10. https://doi.org/10.4236/snl.2011.11002.

[16] Pagar SB, Ghorude TN, Nikolova MP, SenthilKannan K. Synthesis, physical, chemical, biological, mechanical and electronic studies of polypyrrole (PPy) of versatile scales for electro-mechano, pharmaceutical utilities. Heliyon 2023;9:e20086. https://doi.org/10.1016/j.heliyon.2023.e20086.

NEEM (AZADIRACHTA INDICA) BASED INNOVATIONS FOR AGRICULTURE AND SKIN CARE: EXTRACTION AND CHARACTERIZATION OF AZADIRACHTIN AND QUERCETIN

A.R. Kalambate, P.N. Baraskar, R.M. Shinde, Y.S. Rahate
R. P. Gogate college of Arts & Science and
R. V. Jogalekar college of Commerce, (autonomous) ratnagiri
e-Mail: anujakalambate0@gmail.com
Contact No.: +91 93227 52408

Abstract

The increasing demand for sustainable and eco-friendly solutions in agriculture and cosmetology has driven significant interest in natural bioactive compounds with name Azadirachta Indica showing considerable promise. This study explores the development of name-based pesticides and cosmetic creams as a dual-purpose innovation that promotes both agricultural sustainability and cosmetological benefits. Neem is a rich source of bioactive compounds such as Azadirachtin, Nimbin, and Salanin, known for their insecticidal, antifungal, and antibacterial properties. In this study, neem-based pesticides and neem-based soap were developed to promote sustainable agriculture and offer skin care benefits. The compounds present in neem not only facilitate eco-friendly pest control but also provide anti-inflammatory and skin-healing effects, enhancing their value in cosmetic applications. Azadirachtin was extracted using conventional Soxhlet extraction followed by chromatographic purification. Additionally, Quercetin, known for its strong antioxidant, anti-inflammatory, and anti-aging properties, was also isolated via Soxhlet extraction and used in the preparation of an anti-aging cream. The extracted compounds were characterized to confirm their identity and purity. Also, performed confirmation tests for flavonoids, resins, and combinates, Phytosterol, Tannin, Nimbin, etc. are present. The bioactive potential of Azadirachtin and Quercetin was evaluated through in-vitro assay and Quercer full box. This confirmed their pharmacological efficacy. The antioxidant properties of neem contribute to protecting the skin from environmental damage to premature aging. The pesticidal potential of Azadirachtin was assessed through a small-scale field trial on a hibiscus plant, demonstrating effective pest control. This study confirms that neem is a valuable natural source of Azadirachtin and Quercetin, contributing to both sustainable agriculture and advancement in cosmetological applications.

Keywords: Azadirachtin, Phytosterols, Soxhlet extraction, Quercetin

Introduction

Agriculture plays a vital role in ensuring food security, but modern farming practices face major challenges due to heavy dependence on synthetic chemical pesticides. While these chemicals have been effective in controlling pests and diseases, their long-term use has led to environmental pollution, soil degradation, pest resistance, and harmful effects on human and animal health. To address these issues, there is a growing global interest in eco-friendly and sustainable pest management alternatives. Neem (Azadirachta indica), often referred to as the "village pharmacy," is a well-known medicinal and multipurpose tree in India. Its bioactive compounds, such as azadirachtin, nimbin, salannin, possess strong insecticidal, antifungal, antibacterial, and antiviral properties. Unlike synthetic pesticides, neem-based biopesticides

are biodegradable, non-toxic to humans and beneficial organisms, and environmentally safe. The development of neem-based biopesticides is, therefore, an important step toward sustainable agriculture. Such biopesticides can help farmers reduce dependency on chemical pesticides, promote organic farming practices, and protect biodiversity. Additionally, neem formulations are cost-effective, locally available, and suitable for integrated pest management (IPM) programs.

This project aims to scientifically develop, characterize, and evaluate neem-based biopesticides for effective pest control, while ensuring ecological balance and supporting long-term agricultural sustainability. Environmental Protection – Neem-based biopesticides are biodegradable and eco-friendly, reducing soil, water, and air pollution compared to chemical pesticides. Neem (Azadirachta indica) leaves contain nimbin having antibacterial and antifungal properties as well as insecticidal property. Nimbin (triterpenoid), quercetin, azardirachtin, etc. are found in neem leaves. Nimbin is a naturally occurring compound that belongs to the class of chemicals known as limonoids. It is most commonly found in neem (Azadirachta indica) and is known for its bitter taste and biological activity. Neem has been used for centuries in traditional medicine, especially in India and other parts of Southeast Asia, where its various parts (leaves, seeds, bark) are utilized for their medicinal properties. Nimbin is a complex terpenoid compound, which is part of the larger limonoid family. It shares similar structural features with other limonoids, such as the presence of a dihydro-2H-pyrano[3,4-b]quinolin-2-one backbone. This structure is responsible for its bitter taste, a characteristic common to many limonoids. The bitter taste is due to the presence of oxidized terpenoids, which also contribute to its antioxidant properties. Neem trees are native to the Indian subcontinent, and the chemical composition of neem includes a range of biologically active compounds like azadirachtin, nimbidin, and nimbin. Nimbin is present primarily in the leaves, bark, and seeds of the neem plant. The concentration of nimbin in these parts can vary depending on factors like the geographic region and growth conditions of the tree. Nimbin has been studied for its anti-inflammatory, antibacterial, and antifungal properties, making it useful in traditional medicine for treating various ailments. Some of the key properties and effects of nimbin include Azadirachta indica, commonly known as neem, is used in skin care for its: Antimicrobial properties: Helps control acne, reduces bacterial growth, and prevents infections. Anti-inflammatory properties- Soothes skin irritations, reduces redness, and calms inflammation. Antioxidant properties- Protects skin from environmental stressors, UV damage, and premature aging. Antibacterial and antifungal properties- Helps manage skin conditions like acne, eczema, and ringworm.

Neem's bioactive compounds, including azadirachtin, nimbin, and nimbidin, contribute to its skin benefits. Neem is often used in: Face masks and creams - To reduce acne, inflammation, and skin issues. Soaps and cleansers- To control bacteria, fungi, and other microorganisms. Skin toners and astringents- To balance skin pH and reduce pores.

Methodology

In research, the materials and methods section are a critical part of any scientific paper, experiment or project report. During this project, the neem leaves extract is used as the raw material to the whole experimental work. The extraction of neem extract is followed by the Soxhlet extraction method.

Chemicals: Methanol, 10% ferric chloride, 10% lead acetate solution, dilute sulphuric acid, 10% sodium hydroxide, acetone, distilled water, Iodine solution, chloroform, conc. sulphuric acid, acetic anhydride.

Soxhlet extractor

The Soxhlet extraction method uses a small amount of solvent and is very cost-effective. The Soxhlet extraction uses the solvent reflux and siphon principle to continuously extract the solid matter by pure solvent, which saves the solvent extraction efficiency and high efficiency. The solid sample is placed on a thimble shaped filter paper, positioned into Soxhlet extractor and the device assembles. The solvent is added to the solvent reservoir flask and mounted onto a heating mantle. After heating the condensed vapors of the solvent come in contact with the sample powder and the soluble part of the powder gets mixed with the solvent for extraction. When the solvent surface exceeds the maximum height of the siphon, the solvent containing the extract is siphoned back. The flask is repeated, extracting a portion of the material each time so that the solid material is constantly used as a pure solvent and the extracted material is concentrated in the flask.

PROCEDURE:

A. Collection of Requirements: -
The neem leaves were collected from local area. The collected leaves were shade dried under environmental conditions and then ground into uniform powder using mixer[3]

B. Assembly for Soxhlet Extraction: -
1) 10gm of neem leaves powder was taken in filter paper entire it tightly on both the sides with thread.
2) The tied-up neem leaves powder is placed into the main chamber of Soxhlet apparatus.
3) Absolute i.e. 99% methanol is a universal solvent used in Soxhlet extraction. Hence, we used absolute 300 ml methanol as solvent which placed in distillation round bottom flask.
4) The flask is placed inside the heating chamber.
5) Then Soxhlet extractor is placed inside heating chamber. A reflux condenser is placed in top of extractor.
6) Completing the assembly of apparatus.
7) The plug was put in switch circuit, switch on the button and current started flow, as current flow temperature became increases gradually.
8) Initially first 1 hour the temperature is maintained at 80-90 °C and then reduces to the 50-60 °C.
9) Total 5 cycles of average 5 hours were performed and the substance is obtained.

Phytochemical test for the Detection of various component in the neem leaves extract as follows[5]

- **Test For Flavonoids**

(A)Ferric chloride test:
1) In clean and dry test tube add 0.2mL of extract of neem.

2) Add few drops of 10% ferric chloride solution.
3) A green precipitate obtained.

(B)Lead acetate test:
1) Take 1ml plant extract in test tube.
2) Add few drops of 10 % lead acetate solution.
3) A yellow precipitate obtained.

- **Test for Coumarins by 10% NaOH solution:**

1) A small amount of the sample extract was taken in separate test tube.
2) Add 1ml dilute Sulphuric acid.
3)Boil for 15 min.
4)Then allow for cooling.
5)Neutralize with 10% NaOH.
6)Add 0.2 ml Fehling's solution.
7)The observation of color change is a brick red precipitate obtained. indicates the presence of Coumarin.

- **Test for Resin by Turbidity test:**

1) Add 1ml neem extract dissolve in acetone.
2) Then pour in distilled water.
3) Turbid solution formed.

- **Test for Triterpenoids:**

1)Take neem extract in test tube.
2) Dissolve the extract in chloroform.
3) Add conc. Sulphuric acid carefully to form two layers.
4) Reddish brown color appears.

- **Test for Phytosterols:**

(A) Liberman - Burchard Test:
1) Take neem extract in test tube.
2) Added acetic anhydride and Sulphuric acid to the sample.
3) Blue - green color appear.

(B) Salkowski Test:
1) Take neem extract in test tube.
2) Add chloroform and Sulphuric acid to the sample.
3) Red color obtained.

- **Test for alkaloids:**

(A) Wagner's Test:
1) Take few ml of neem extract in test tube.
2) Add 1-2 drops of Wagner's reagent (Iodine solution) along the sides of test tube
3) Brown reddish precipitate obtained.

Application of Neem extract

1) Spray neem leaves extract on the branch of hibiscus plant where the mealybug was infested.

2) Spray neem leaves extract regularly for about 7 to 8 days.

Results

 Ferric chloride test (Flavonoids)	 Lead acetate test (Flavonoids)	 Test for Coumarins	 Turbidity test (Resin)
 Test for Triterpenoids	 Liberman - Burchard Test (Phytosterols)	 Salkowski Test (Phytosterols)	 Wagner's Test (Alkaloids)

Conclusion

The mealybug infestation disappeared within 7 to 8 days after spraying the neem formulation. The extraction of active compound in neem leaves powder using Soxhlet extraction method is an effective process. For the confirmation of insecticidal and antifungal, antibacterials property, I done the phytochemical test. I got the positive test which confirmed the presence of Triterpenoid, Quercetin, Tannins, etc. Neem extract is good alternative to man-made pesticides because they are safe, natural, non-hazardous. So, they are use in pest control

as biopesticides in agriculture. Also, neem products are used in cosmetics and skin care products due to herbal and medicinal properties of neem extract.

Before the Application of Neem Formulation

After the Application of Neem Formulation

References

1. Andre Rolim Baby, Thamires Batello Freire, Gabriela de Argollo Marques.et.al (2022) Azadirachta indica (Neem)as a potential natural active for dermo cosmetic and topical products, Journal cosmetics 9(58)10.3390
2. Garima Pandey, KK Verma, Munna Singh, (2014) Evaluation of phytochemical, antibacterials and free radical scavenging properties of Azadirachta indica (neem) leaves, Int JPharm Sci 6(2),444-447
3. Gayatri Nahak and Rajani Kanta Sahu, (2015) Biopesticidal effect of leaf extract of neem (Azardirachta indica A. Juss) on growth parameters and disease of tomato, Journal of Applied and Natural Science,7(1),482-488
4. Himesh Soni, K Mishra, Sarvesh Sharma, et.al, (2012) Characterization of Azadirachtin from ethanolic extract of leaves of Azadirachta indica, Journal of Pharmacy Research 5(1),199-201
5. Junaid R. Shaikh, MK Patil (2020), Qualitative test for preliminary phytochemical screening, international journal of chemical studies,8(2),603-608
6. S Gunasekaran and B Anita, (2010) Analysis of phytochemical variability in Neem formulations, Indian Journal of Natural Products and Resources,1(3), 291- 295

Phytochemical Characterization and Evaluation of Anti-inflammatory Properties of Aegle marmelos Leaves: Bioactivity, Compound Isolation, and Sustainable Applications

R M Shinde[1]*, P N Baraskar[1], A M Kulkarni[2], S M Kangutkar[2]*, V S Mandavkar[3]
Department of chemistry Jogalekar-College (Autonomous) Ratnagiri, Maharashtra, India.
Corresponding author: S M Karangutkar, skarangutkar088@gmail.com

ABSTRACT

This study presents a comprehensive phytochemical and pharmacological evaluation of Aegle marmelos (Bael) leaves, emphasizing their anti-inflammatory potential along with sustainable applications. Methanolic extracts of phytochemicals were obtained through Soxhlet extraction, and preliminary phytochemical screening confirmed the presence of Coumarins the main bioactive Compound present and another tannins, saponins, phenolics bioactive compound are present Chromatographic profiling using Thin Layer Chromatography (TLC) was performed to establish the terpene and essential oil composition. Bioactivity assays demonstrated significant antioxidant, antimicrobial, and anti-inflammatory activities, affirming the therapeutic relevance of the extracts.

Advanced analytical tools, including UV-Vis spectrophotometry, Fourier Transform Infrared Spectroscopy (FTIR), and Gas Chromatography–Mass Spectrometry (GC-MS), were employed for isolation and characterization of the active constituents. To extend the practical applications, a herbal handwash formulation was successfully developed from the extracts, while the remaining Bael leaf powder was repurposed for sustainable utilization, minimizing waste generation. Furthermore, in vivo studies were proposed to validate safety and efficacy in support of the pharmacological claims. Overall, the study highlights Aegle marmelos as a promising source of natural anti-inflammatory agents and a candidate for eco-friendly herbal product development.

Keywords : Aegle marmelos; Coumarin; phytochemical analysis; anti-inflammatory; antioxidant; antimicrobial; TLC; FTIR;GC-MS; herbal formulation; sustainable utilization.

I. INTRODUCTION

Many plants have been utilised for medical purpose for thousands of years.The medicinal plants perform very important role in the lives of population worldwide.These plants are used in Ayurveda,Siddha and other healing systems. A significant amount of the basic and applied research is required to validate and use of plants in phyto – pharmaceutical chemistry. [1] [5]

A plant known as Aegle marmelos has been used to treat various infection traditionally. The main aim of this review is to know the phytochemical parameters, traditional herbal product and innovative applications of A. Marmelos. The Aegle marmelos is known as a beal.

Aegle marmelos is a rich in phytochemical such as flavonoids, phenolic, tannins, saponins and Terpenoids. The main bioactive compound found in A. Marmelos (Beal) is Coumarin, making it beneficial for a variety of diseases. Coumarin ($C_9H_6O_2$), called as a 2H-1-benzopyran-2-one, has a fused-ring structure composed of a benzene ring joined to a α-pyrone (lactone) ring, forming a benzopyrone system. The conjugated double bonds and carbonyl oxygen contribute to its aromatic odor and biological activity. The lactone structure contributes to anti-inflammatory, antioxidant, and antimicrobial activities. Its aromatic ring system gives pleasant fragrance, explaining the sweet, hay-like aroma of Bael leaf extract. [7]

COUMARIN

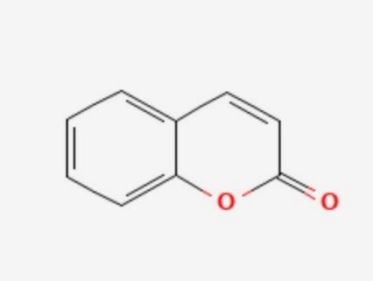

Herbal based Handwash :

The study concluded that Aegle marmelos leaf extract can be effectively used to prepare a safe and natural herbal handwash. The formulated product showed good foaming ability, pleasant appearance, stable consistency, and significant antimicrobial activity against common skin and hand pathogens. Overall, the research supports the use of Bael leaf extract as an eco-friendly and skin-protective alternative to synthetic chemical handwashes. [5]

Resued the remaining remaining A. Marmelos (Leaves) powder to make bio – composite board:

The study showed that Aegle marmelos (bael) leaves powder can be successfully used as a natural filler in making composite materials. The resulting composites were lightweight, strong, and eco-friendly. Using leftover leaf material instead of discarding it. bio-composite board is biodegradable, low cost, and eco-friendly. It can be used for making packaging materials, light boards, or for study projects. With some improvements, like adding other natural materials or surface treatment, it can also be used for industrial purposes. [6]

II. METHODOLOGY

During this project, the A. Marmelos Leaves powder is used as the raw material to the whole experimental work. The extraction of A. Marmelos Leaves is followed by the soxhlet extraction method. The leaves shades are dried 6-7 days and use grinder to make fine powder of leaves.

1. **Dried leaves**

2. **Powder of leaves**

Soxhlet extraction method

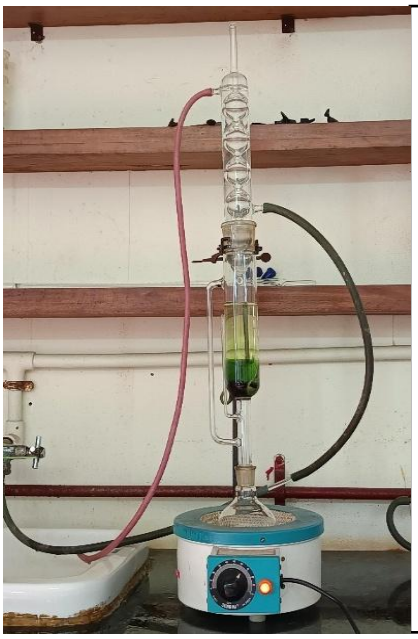

- 10 g of Aegle marmelos leaf powder was wrapped in filter paper and tied with thread. The packet was placed in the main chamber of the Soxhlet extractor.
- About 300 ml of 99% methanol was added to the round-bottom flask as the solvent.
- The flask was set in the heating chamber, and the Soxhlet extractor with a condenser was fixed on top. The whole setup was assembled properly.
- The power was switched on to start heating.
- The temperature was kept at 65 °C for the first hour, and about four extraction cycles were run in 4 hours to collect the extract.

3. Soxhlet extractor

PHYTOCHEMISTRY :

Coumarin: Coumarin is a natural compound found in many plants like Aegle marmelos, cinnamon, and sweet clover. It has a sweet, vanilla-like smell and is often used in perfumes and cosmetics. In plants, it protects against insects and diseases. Coumarin shows several medicinal properties such as antioxidant, anti-inflammatory, antimicrobial activities.

Tannins : Tannins are natural plant compounds with a bitter taste. They protect plants from germs and insects. Tannins have antioxidant, anti-inflammatory, and antimicrobial properties and are used in medicines and leather making.

Saponins : Saponins are natural compounds found in many plants. They form foam when mixed with water. Saponins have antioxidant, anti-inflammatory, and antimicrobial properties and help boost immunity.

Phenolics : Phenolics are natural compounds found in plants. They act as strong antioxidants and protect the body from damage. They also show anti-inflammatory and antimicrobial properties.

ANTI – INFLAMMATORY ASSAY :

The anti-inflammatory activity of Aegle marmelos leaf extract was evaluated using the egg albumin method. Different concentrations of the extract (100, 200, and 400 µg/ml) were prepared. To each test tube, 1 ml of egg albumin and 2.8 ml of phosphate buffer (pH 6.4) were added and mixed well. The mixtures were incubated in a water bath at 70°C for 10 minutes and then cooled to room temperature. The absorbance was measured at 660 nm using a UV-Visible spectrophotometer. Diclofenac sodium was used as the standard and a control was maintained without extract. The percentage inhibition of protein denaturation was calculated to determine the anti-inflammatory activity. [1]

ANTIOXIDANT ASSAY :

The antioxidant activity of Aegle marmelos leaf extract was determined using the DPPH free radical scavenging method. Different concentrations of the extract (100, 200, and 400 µg/ml) were prepared. To each test tube, 1 ml of DPPH solution and 1 ml of the extract were added and mixed thoroughly. The mixture was incubated in the dark at room temperature for 30 minutes. After incubation, the absorbance was measured at 517 nm using a UV-Visible spectrophotometer. Ascorbic acid was used as the standard, and a control was maintained without the extract. The percentage of DPPH radical scavenging was calculated to assess the antioxidant activity. [1]

ANTIMICROBIAL ASSAY :

The antimicrobial activity of the formulated Aegle marmelos herbal handwash was evaluated using the agar well diffusion method. Nutrient agar plates were prepared and inoculated with test microorganisms such as Escherichia coli. Wells were made in the agar using a sterile borer, and different concentrations of the herbal handwash were added into each well. The plates were then incubated at 37°C for 24 hours. After incubation, the zones of inhibition around each well were measured in millimeters. The antimicrobial effectiveness of the handwash was compared with a standard commercial handwash. [1]

HERBAL HANDWASH PREPARATION :

The Aegle marmelos herbal handwash was prepared by dissolving 1 g of leaf extract in a small amount of distilled water. To this, 10 ml of liquid soap base (or 1% sodium lauryl sulfate solution) was added and mixed well. Then, a few drops of glycerin were added to maintain skin smoothness, and 2–3 drops of essential oil were added for fragrance. The final volume was made up to 100 ml with distilled water and mixed until a uniform handwash solution was formed. The prepared handwash was stored in a clean, airtight container for further evaluation. [4]

REUSED REMAINING BEAL LEAVES POWDER TO MAKE BIO COMPOSITE BOARD :

The remaining Aegle marmelos leaf powder after extraction was reused to prepare a bio-composite board. The dried leaf powder was first sieved to get a fine texture. Then, it was mixed with a binding material such as starch or resin in a suitable ratio to form a thick paste. The mixture was poured into a mold and pressed firmly to make it even. It was then dried under sunlight or in an oven until it became hard and compact. The formed bio-composite board was removed from the mold and polished for smoothness.

The prepared board was tested for Its strength, water absorption, and flexibility to check its quality. These tests helped to evaluate whether the board could be used as an eco-friendly and biodegradable material for packaging or model-making purposes. [6]

III. RESULT AND DISCUSSION:

To study the presence of phytochemical compents ,the A. Marmelos extract which reveled the presence of Coumarins, Saponins, Phenolics, Tannins and where as alkaloids, cardiac Glycosides, carotenoid, steroids were absent.

S. No.	Phytochemical	Results
1	Coumarin	+
2	Saponins	+
3	Phenolics	+
4	Tannins	+
5	Alkaloids	-
6	Cardiac Glycosides	-
7	Carotenoid	-
8	Steroids	-

TLC OF COUMARIN:

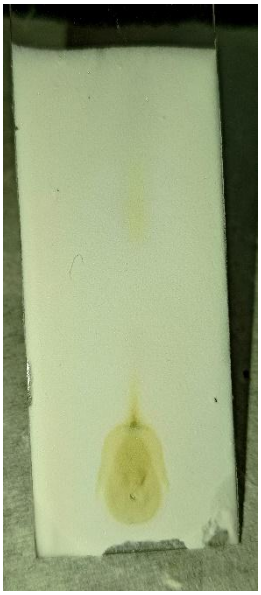

- Mobile phase (Solvent system) : 99% pure Hexan : (100)
- Visualization : Coumarin can react with iodine, forming Greenish – yellow spots.
- Retention Factor (RF) Calculation :
  RF = Distance travelled by compound / Distance travelled by solvent from front
  RF 5/3.5
  RF = 0.4

4. TLC of Coumarin

ANTI – INFLAMMATORY ACTIVITY

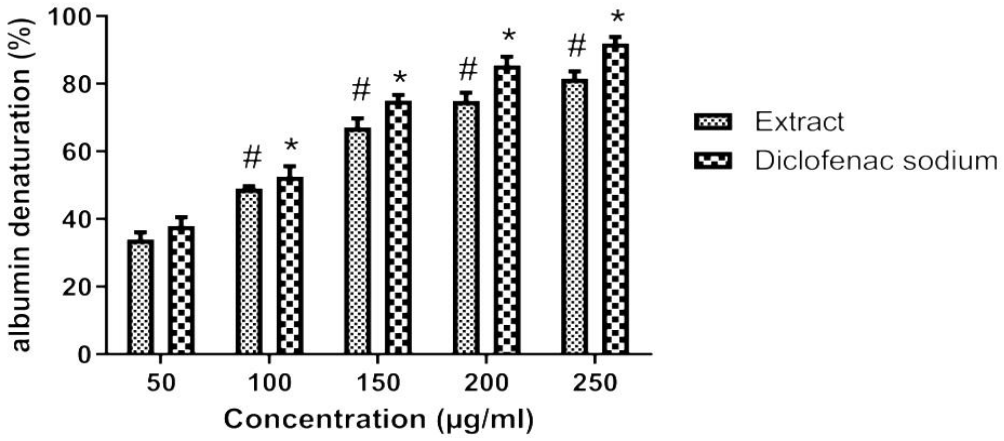

ANTIOXIDANT ACTIVITY

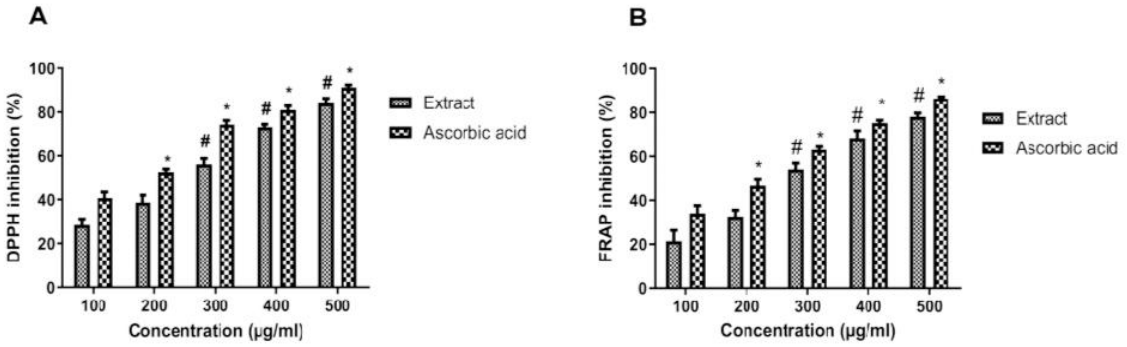

ANTIMICROBIAL ACTIVITY

REUSED REMAINING BEAL LEAVES POWDER TO MAKE BIO -COMPOSITE BOARD

CONCLUSION :

In this study, Aegle marmelos (Bael) leaves were found to contain many useful plant compounds like a tannins, phenols, saponins, and coumarins. These natural compounds showed good anti-inflammatory activity when tested by the egg albumin method. The results proved that the leaf extract helps to reduce swelling and inflammation, which supports its traditional use in herbal handwash.

This study is important because it shows that A. marmelos leaves can be used as a natural and safe source for making herbal anti-inflammatory products. Also, the leftover leaf powder can be reused to make eco-friendly bio-composite boards, which supports sustainable and green practices.

IV. REFERENCES :

1. Venkatesan S et al., (Cureus 2024) Phytochemical analysis and evaluation of antioxidant,antidiabetic and anti – inflammatory properties of aegle marmelos.
2. Monika S et al.,(2023) Phytochemical and biological review of aegle marmelos.

3. Zekovic, Z., Adamovic, D., Cetkovic, G., & Vidovic, S. (2011). Essential oil and extract of coriander (Coriandrum sativum).
4. Ayur Tandel.,miss sayali S., (2025) formulation and evaluation of aegle marmelos herbal handwash.
5. Amam naik.,MS. Diksha mehta et al., (2025) formulation and evaluation of herbal cream using aegle marmelos essential oil.
6. Arputham, K., Jeya Arul, A., Devaraj, S. J., Usaladi, M., & Arulraj, Q. A. (2023). Mechanical and morphological characterization analysis on Aegle marmelos dispersed fiber-reinforced polymer composite. Journal of Natural Fibers, 20(1)
7. Junaid R Shaikh and MK patil., (2020) Qualitative tests for preliminary phytochemical screening: an overview.
8. Antonisamy, P., Duraipandiyan, V., & Ignacimuthu, S. (2004). Studies on the anti-inflammatory, antipyretic and analgesic properties of the leaves of Aegle marmelos Corr. Indian Journal of Experimental Biology, 42(3), 238-243.
9. Rahman, S., Eva, E. O., Quader, R., Tasrin, M., & Khan, M. I. (2015). Effects of aqueous and ethanolic extracts of Aegle marmelos (Bael) leaves on chronic inflammation in rats. Ibrahim Medical College Journal, 9(2), 52-54.
10. Reshma, Arun K.P., & Brindha, P. (2014). In vitro anti-inflammatory, antioxidant and nephroprotective studies on leaves of Aegle marmelos and Ocimum sanctum. Asian Journal of Pharmaceutical & Clinical Research, 7(5), 131-136.
11. Timbadiya, P. N., Mandavia, M. K., & Golakiya, B. A. (2018). Phytochemical screening, antioxidant, anti-inflammatory and antimicrobial activities of Aegle marmelos leaf extracts. International Journal of Chemical Studies, 6(2), 3509-3517.
12. Mujawar, S. B., & Hiremarth, M. B. (2020). Evaluation of in vitro antioxidant and anti-inflammatory activities of Aegle marmelos leaf extracts. Asian Journal of Pharmaceutical & Clinical Research, 13(2), 1-6.
13. Ahmad, A., Ali, A., & Ahmad, M. A. B. (2023). Phytochemical analysis and evaluation of antioxidant, antidiabetic, and anti-inflammatory properties of Aegle marmelos and its validation in an in vitro cell model. [Journal]. doi link.
14. Singh, … (2023). Comprehensive chemo-profiling of coumarins enriched extract derived from Aegle marmelos (L.) Correa fruit pulp as an anti-diabetic and anti-inflammatory agent. [Journal]. doi.
15. Sharma, N., & Dubey, W. (2018). Determination of volatile bioactive compounds from extracts of Aegle marmelos plant parts and their comparative analysis. Asian Journal of Pharmaceutical & Clinical Research, 11(3), 235-241.
16. Ahmad, W., Ali, A., Ahmad, M. A., & … (2021). Aegle marmelos leaf extract phytochemical analysis, cytotoxicity, in vitro antioxidant and antidiabetic activities. Plants, 10(12), 2573.
17. Vikhe, D. N., Solunke, R. S., Ghawate, V. B., & Bhalerao, P. (2022). Spectrophotometric analysis of Aegle marmelos (Linn) Correa root bark by GC-MS. Journal of Pharmaceutical Negative Results, 13(S10), 6068-6075.
18. Sharma, G. N., Dubey, S. K., & Sati, N. (2014). Anti-inflammatory activity and total flavonoid content of Aegle marmelos seeds. International Journal of Pharmaceutical Sciences & Drug Research, 6(4), 285-289.
19. Rathore, … (2018). Augmentation of hepatoprotective potential of Aegle marmelos in combination with piperine in carbon tetrachloride model in Wistar rats. BMC Chemistry, 12, 46.

Ultrasonic characterization and molecular interaction analysis of methylene blue solutions by acoustic and thermodynamic parameters

Nafeesa Mujawar[1,2], Vidhya Jadhav[1], Pinal Mardiya[1], Sneha Bokare[1], Amit Supale[2*,] Sandip Sabale[1*]

Department of Chemistry, Jaysingpur College Jaysingpur-416101, MS, India
Department of Chemistry, Dr. Patangrao Kadam Mahavidyalaya Sangli-416416, MS, India

Author for correspondence:
amitsupale@gmail.com (AS)
srsabale@gmail.com (SS)

Abstract: In order to provide new insights into solute–solvent interactions, this study methodically investigates the acoustic and thermodynamic signatures of methylene blue solutions over a wide concentration range. The seven main physicochemical parameters-acoustic impedance, bulk modulus, isentropic compressibility, free length, relative association, relaxation time, and attenuation coefficient—were ascertained by measuring density and ultrasonic velocity. Interestingly, sound velocity, acoustic impedance, and bulk modulus all decreased in tandem with increasing methylene blue concentration, whereas density stayed constant and viscosity, compressibility, free length, association, relaxation time, and attenuation coefficient all increased steadily. As concentration rises, these clear patterns reveal underlying structural change and improved intermolecular association, suggesting less compact molecular organisation and stronger viscoelastic effects. With possible ramifications for material and solution chemistry, the results enhance our knowledge of molecular dynamics in dye solutions and elucidate the mechanisms underlying acoustic propagation.

Keywords: Methylene blue, Acoustic properties, Ultrasonic velocity, Isentropic compressibility, Intermolecular interactions

1. Introduction

Investigation of the thermophysical properties such as density and ultrasonic speed is considered to be a useful tool for the study of molecular interactions in solution systems, and offers insight into how solute and solvent molecules are arranged and interact[1]. Not only do these measurements directly bring out the structural arrangement of the solvent but also derive parameters like adiabatic compressibility, intermolecular free length, apparent molar volume, apparent molar compressibility solvation number and internal pressure[2,3]. These parameters are useful to estimate the strength of the ion–solvent interactions, hydration effects and the propensity of solutes to perturbate (structure-breaking effect) or reinforce (structure-making effect) the structural network of solvent, in particular, aqueous systems[4,5]. These measurements, and the derived quantities will provide then a rich thermodynamic and acoustic toolbox to probe molecular level understanding on solution behavior both in basic sciences as well as in many applications at industrial level.

MB is a heterocyclic aromatic dye that has use in both industry and medicine. It can be used in labs to stain cells or analyse genetic data, as well as in cutting blood problems and surgical dye. Methylene blue (MB) is used in textile dyeing, analytical chemistry, electrochemistry, photodynamic therapy, and as a redox indicator and biological stain in methemoglobinemia medications. Additionally, MB's colour strength and light fastness make it useful in the paper and textile dyeing industries[6–9]. Despite its many applications and environmental importance, little is known about the molecular behaviour of methylene blue in aqueous solutions based on volumetric and acoustic investigations. By accurately quantifying

the volume and physical characteristics of methylene blue (MB) solutions, volumetric and acoustic approaches provide useful avenues for studying MB interactions.

The molecular structure and dynamics of solutions are investigated using acoustic techniques, which use sound waves like ultrasound to record changes in parameters like compressibility and sound velocity[2,10] as MB molecules interact with water or other solutes. By precisely calculating the area that MB molecules and their aggregates occupy, volumetric techniques offer information about the size, shape, and clustering patterns of these molecules[11]. When combined, these techniques provide quick, non-invasive, and sensitive ways to comprehend the intricate behaviour of MB in aquatic settings, exposing information on solvation effects and molecular interactions that is hard to obtain using other methods.

By determining the density and sound velocity of methylene blue aqueous solutions at 298.15 K across a variety of concentrations, the current work seeks to close this gap. Numerous derived thermodynamic and acoustic characteristics have been computed and examined using this experimental data. It is anticipated that the findings will enhance the scant thermodynamic information on dye solutions and advance our knowledge of the solute–solvent interactions of MB in water.

2. Experimental

Methylene blue was purchased from Sigma-Aldrich (with mass fraction purity ≥ 97.0%). All solutions were prepared in double distilled deionized water. All the solutions were prepared by using Shimadzu balance (AUW 220D) with a precision of 0.0001g. Methylene blue was dissolved in water in various ratios to prepare different concentration of 1×10^{-4}m, 1×10^{-5}m, 1×10^{-6}m, 1×10^{-7}m & 1×10^{-8}m. The ultrasonic velocity (u) had been measured using ultrasonic interferometer (Mittal Enterprises, New Delhi, India F-05, serial no. 1617096) operating on 2 MHz frequency. The viscosities of binary mixture of various concentrations were determined using Ostwald's viscometer. From this data the relative coefficient of viscosities is determined. The densities of solutions were determined by Anton Paar (Model DMA 4100 M) digital densitometer. It was thoroughly cleaned by acetone, alcohol and doubly distilled water.

3. Results and discussion

Table 2 displays the density (ρ) and sound velocity (u) of aqueous methylene blue solutions as determined by experiment at 298.15 K. The solute concentration causes a regular fluctuation in both parameters. Since the addition of MB cations to the water structure results in greater solute–solvent interactions and decreased solvent molecule mobility, an increase in u with concentration is seen (Fig.2. a). This pattern is in line with previous research on dye and ionic liquid systems, which found that improved packing and decreased free volume in solution are caused by increased charge densities and planar aromatic structures. Important details on solute–solvent and solute–solute interactions in solution can be gleaned from the changing of ultrasonic velocity with concentration. According to the current investigation, sound velocity was higher at lower methylene blue concentrations (10^{-5}–10^{-8} m) than at comparatively higher concentrations (10^{-4} m). The conflicting effects of solute–solvent and solute–solute interactions can be used to explain this behaviour. Since methylene blue and water interact strongly through ion-dipole and hydrogen bonding, enhanced sound velocity is seen at low concentrations as a result of increased molecular packing. Sound velocity reduces with increasing concentration because solute–solute interactions such aggregation and π–π stacking break hydrogen-bonded water networks, results in increasing medium compressibility.

Due to extremely low molar concentrations, the density of aqueous methylene blue solutions is constant across the concentration range under study (Fig.2.b). Since methylene blue contributes very little to the mass-to-volume ratio in comparison to the solvent, it has little effect on the bulk water structure at micromolar levels. Because of the dye's potent hydration,

the molecules stay completely solvated and distributed, avoiding aggregation and producing stable density measurements that fall within the densitometer's experimental error limitations. Similar lack of significant density variation at low concentrations has also been reported for other dye–water and drug–water systems, where extensive hydration dominates solute–solvent interactions and the solute's contribution to bulk properties remains minimal[12,13]. This is consistent with previous studies, which further supports the idea that the absence of density change in the current system is an inherent characteristic of diluted aqueous dye solutions.

Because of improved solute–solvent and solute–solute interactions, aqueous methylene blue solutions become more viscous as concentration rises (Fig.3.a). Methylene blue molecules stay hydrated and isolated at diluted concentrations, with minimal impact on solvent mobility. The closeness of cationic dye molecules promotes ion–dipole connections with water as well as dipole–dipole and π–π stacking interactions as concentration increases. Higher viscosity values are the result of these interactions, which limit the freedom of solvent molecules and cause temporary aggregates to develop. These aggregates also enhance resistance to shear. Molecular association, improved hydrogen bonding, and electrostatic interactions have been shown to diminish solvent mobility in different dye–water and drug–water systems, resulting in similar increases in viscosity with solute concentration[14].

The product of a medium's density (ρ) and the sound velocity (u) through it is known as the acoustic impedance (z), given by equation no.1. A crucial metric in describing solute–solvent interactions and acoustic wave transmission, it symbolises the resistance provided by the medium to sound wave propagation [15,16].

$$z=\rho\times u \quad (1)$$

As the solute concentration rises, the methylene blue–water system's acoustic impedance falls (Fig.3.b), suggesting that the solute–solvent interactions are becoming weaker. Strong molecular connections in diluted solutions facilitate the propagation of sound waves, but at larger concentrations, solute aggregation breaks the hydrogen-bonded water network, lowering acoustic impedance and sound velocity. At larger concentrations, dye molecules have a tendency to stack, which reduces compressibility effects and the solution's acoustic response.

The bulk modulus (K), which is the ratio of a rise in pressure to the ensuing relative decrease in volume, is a measurement of the medium's resistance to uniform compression[17]. It can alternatively be described in terms of sound velocity (u) and density (ρ) as follows

$$k = \rho\times u^2 \quad (2)$$

As the solute concentration increases, the bulk modulus of the methylene blue–water system drops (Fig.3.c), suggesting that the solution is more compressible. Strong solute–solvent interactions encourage structural ordering at low concentrations, which raises the bulk modulus. Methylene blue molecules, on the other hand, self-associate as concentration rises, breaking the hydrogen-bonded structure of water, decreasing the effectiveness of the solute–solvent coupling, and raising free volume, all of which reduce the bulk modulus. This pattern shows that at greater concentrations, solute-solvent interactions give way to solute-solute relationships.

The relative decrease in volume of a system per unit increase in pressure under adiabatic (constant entropy) circumstances is known as the isentropic compressibility. It can be stated as follows using the medium's density and sound velocity (u)[18]

$$\beta = 1/\ \rho\times u^2 \quad (3)$$

It was discovered that the isentropic compressibility of methylene blue solutions rose with concentration (Fig.3.d), suggesting that the medium was easier to compress. Higher solute–solute aggregation causes this behaviour by disrupting the water's organised hydrogen-bond network, increasing free volume, and decreasing the system's tolerance to pressure changes.

The average distance between the surfaces of nearby molecules in a liquid is known as the intermolecular free length (L_f), which offers information on solute–solvent interactions and

molecular packing. Using Jacobson's relation, it is computed from the isentropic compressibility (β_s)[19]

$$L_f = k \times (\beta_s)^{1/2} \quad (4)$$

A loosening of molecular packing within the medium was suggested by the observation that the intermolecular free length of methylene blue solutions increased with concentration (Fig.4.a). Higher dye concentrations cause solute–solute aggregation, which breaks up the organised water network and increases intermolecular space, causing this increase.

The degree of molecular interaction or self-association of solute molecules in a solution is gauged by the relative association[20]. It is given by following formula,

$$R_A = d_s/d_0 \times (u_o/u_s)^{1/3} \quad (5)$$

Methylene blue solutions' relative association (R_A) rises with concentration (Fig.4.b), suggesting that the dye molecules in the medium are aggregating or interacting more strongly. This trend emerges because larger concentrations improve solute–solute association, leading to stronger intermolecular contacts and a commensurate decrease in compressibility.

A liquid's relaxation time, which gives information about molecular mobility and solute–solvent interactions, is the amount of time needed for the system to return to equilibrium following a disturbance. It is determined by using following formula[21]

$$\tau = 4\eta/3\rho u^2 \quad (6)$$

Concentration-induced improvements in the relaxation time of methylene blue solutions suggest improved solute–solvent and solute–solute interactions (Fig.4.c). This pattern indicates that the creation of larger linked structures causes the system's reorientation and energy dissipation processes to slow down at higher concentrations.

The attenuation coefficient (α) gives information about molecular interactions and energy dissipation mechanisms in solutions by showing the decrease in ultrasonic wave intensity per unit distance as the wave travels through a medium. It is determined by using following formula[22]

$$(\alpha/f^2) = 8\pi^2\eta/3\rho u^3 \quad (7)$$

Methylene blue solutions attenuation coefficient rises with concentration (Fig.4.d), indicating increased ultrasonic energy loss as a result of improved solute–solvent and solute–solute interactions. This behaviour points to the development of bigger related aggregates, which increase the medium's viscosity and structural relaxation effects.

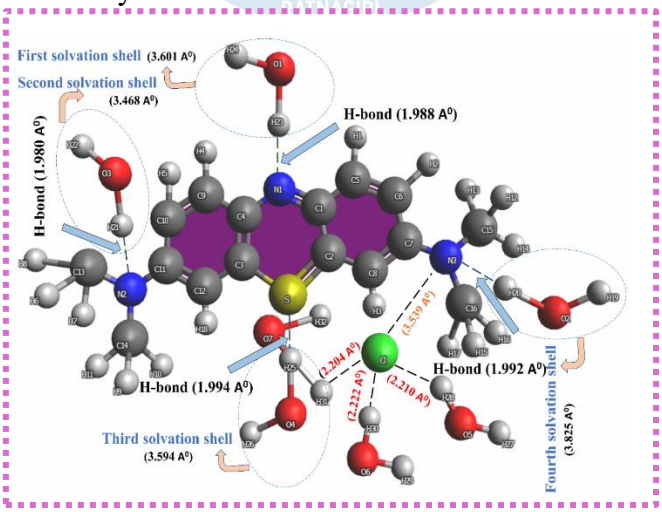

Fig.1. Interaction model depicting the hydrogen-bond network and solvation structure around methylene blue (MB^+) in aqueous medium. Hydrogen bonds between H_2O and electronegative atoms (N, S) of MB^+ are shown as dashed lines, and the first solvation layer is indicated by dotted circles. Hydrated chloride ions are shown near the cationic site representing ion-pairing and solvent-mediated stabilization

Table 1. The values of sound velocity u (m/sec), density ρ (10^3/ kg/m^3), viscosity (η), acoustic impedance z (10^{-3}/Kg m^{-2} S^{-1}), bulk Modulus k (10^{-3}/ Pa), isentropic compressibility β_s (10^{11}/ (N m^{-2})$^{-1}$), free Length L_f (10^{-9}/m), Relative association (R_A), Relaxation Time τ (10^{-7} sec), attenuation coefficient (α/f^2) (10^{-9} $Npm^{-1}s^2$)

Concentration (mol/kg)	Sound Velocity u (m/sec)	Density 10^3 ρ (kg/m^3)	Viscosity η	Acoustic Impedance Z 10^{-3} ($kgm^{-2}s^{-1}$)	Bulk modulus K 10^3 Pa	Adiabatic compressibility β 10^{-11} ($kg^{-1}ms^2$)	Free length L_f 10^{-9} (m)	Relative association R_A	Relaxation Time τ 10^{-7} (sec)	Attenuation Coefficient (α/f^2) 10^{-9} ($Npm^{-1}s^2$)
0.00	1498.90	0.9970	1.0000	1494.403	2239961	44.64	1.374	1.0000	5.95248	7.83096
1.0175×10^{-4}	1425.22	0.9971	0.8831	1421.087	2025361	49.37	1.445	1.0170	5.81361	8.04366
1.0037×10^{-5}	1500.00	0.9971	0.8596	1495.650	2243475	44.57	1.373	0.9998	5.10874	6.71602
1.0335×10^{-6}	1501.60	0.9971	0.8464	1497.245	2248264	44.47	1.372	0.9995	5.01958	6.59177
1.0309×10^{-7}	1508.14	0.9971	0.8419	1503.766	2267890	44.09	1.366	0.9980	4.94968	6.47180
1.0165×10^{-8}	1552.40	0.9971	0.8267	1547.898	2402957	41.61	1.327	0.9884	4.58713	5.82675

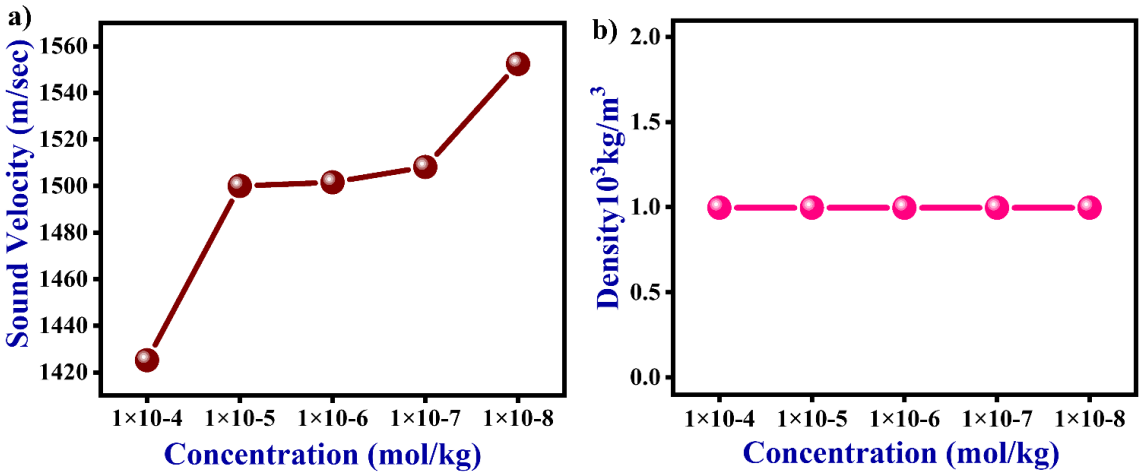

Fig.2. a) Variation of sound velocity (u) of methylene blue with concentration (m) at temperature 298.15K, b) Variation of density(ρ) of methylene blue with concentration (m) at temperature 298.15K

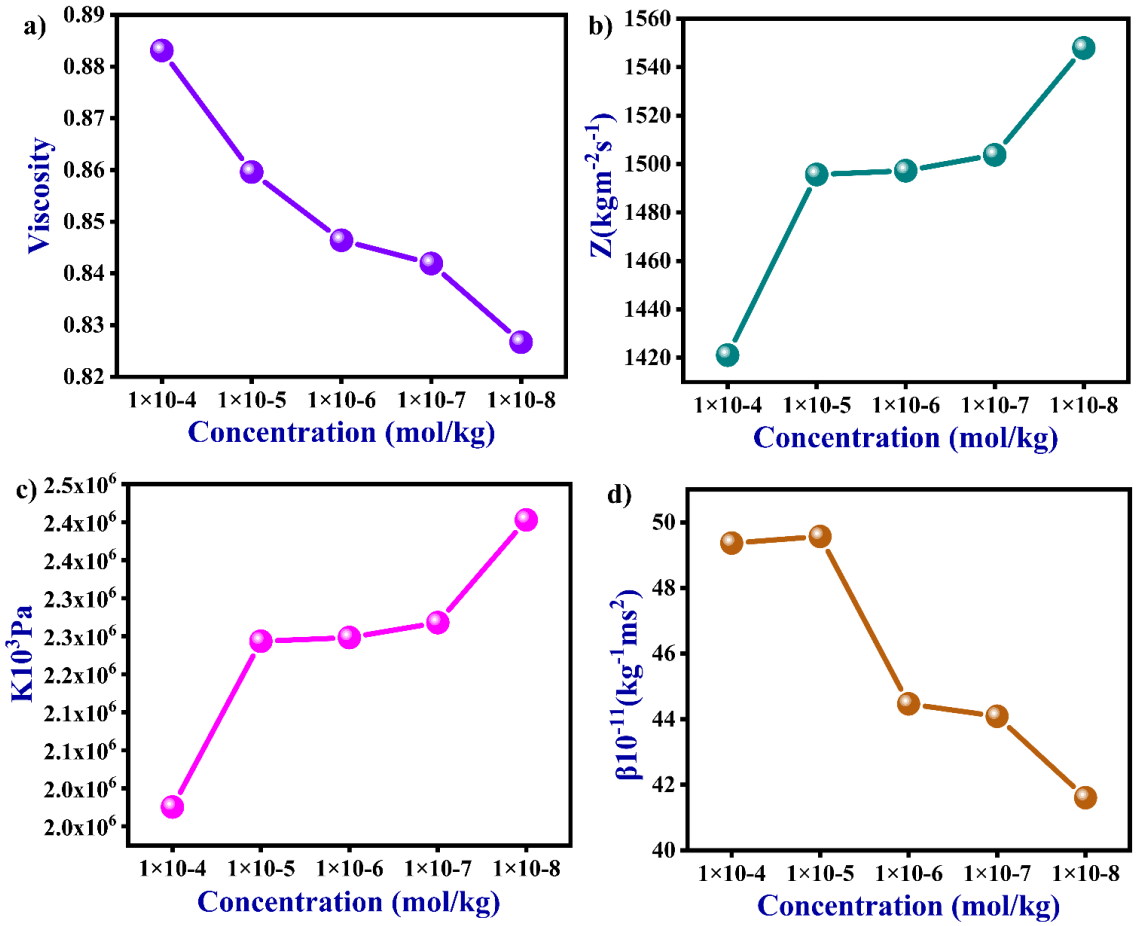

Fig.3. a) Variation of viscosity (η) of methylene blue with concentration (m) at temperature 298.15K, b) Variation of acoustic impedance (z) of methylene blue with concentration (m) at temperature 298.15K, c) Variation of bulk modulus (k) of methylene blue with concentration (m) at temperature 298.15K d) Variation of isentropic compressibility (β) of methylene blue with concentration (m) at temperature 298.15K

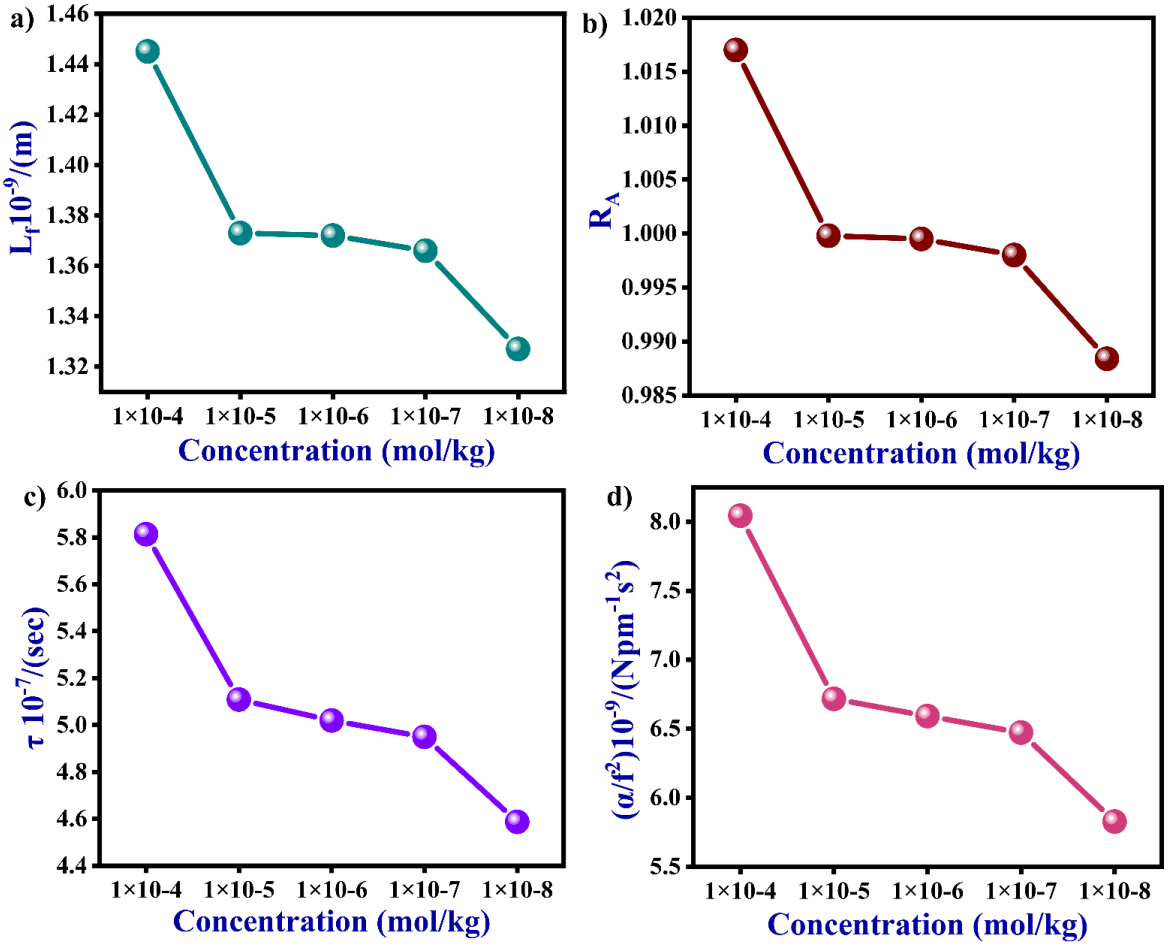

Fig.4. a) Variation of free length (L_f) of methylene blue with concentration (m) at temperature 298.15K, b) Variation of relative association (R_A) of methylene blue with concentration (m) at temperature 298.15K, c) Variation of relaxation time (τ) of methylene blue with concentration (m) at temperature 298.15K d) Variation of attenuation coefficient (α/f^2) of methylene blue with concentration (m) at temperature 298.15K

4. Conclusion

The experimental study revealed that the acoustic and thermodynamic characteristics of methylene blue solutions changed noticeably with concentration. As concentration increased, the bulk modulus, acoustic impedance, and sound velocity all showed a decreasing trend, whereas density remained largely unchanged across the study range. Viscosity, isentropic compressibility, free length, relative association, relaxation duration, and attenuation coefficient, on the other hand, all exhibited increasing trend with concentration. These results suggest that solute–solvent interactions are the primary factor influencing the molecular packing and dynamic behaviour of methylene blue in solution.

The decline in sound velocity and bulk modulus with concentration indicates structural weakening and decreased elasticity of the medium, whereas the increase in compressibility and free length suggests more molecular freedom and fewer densely packed structures. The increasing trends in viscosity, relaxation time, attenuation coefficient, and relative association show stronger intermolecular association and energy dissipation mechanisms at higher solute concentrations. With regard to the acoustic and visco-elastic characteristics of methylene blue

solutions, the results offer a thorough understanding of how solute concentration affects molecular dynamics, intermolecular interactions, and acoustic propagation in the medium.

5. Declaration of competing interest

The authors declare that they have no known competing financial interests or personal relationships that could have appeared to influence the work reported in this paper.

6. Acknowledgment

The author NM is thankful to MAHAJYOTI Maharashtra for MJPRF-2023 fellowship. We are thankful to the DST and DBT, New Delhi, India for the grant under the DST-FIST program (No/SR/FST/College-151/2013(C)) and for DBT-Star college scheme (HRD-11011/11/2022-HRD-DBT) respectively to Jaysingpur College, Jaysingpur.

7. References

1. Sirohi, A.; Upmanyu, A.; Kumar, P.; Dhiman, M.; Juglan, K. C.; Singh, D. P.; Saxena, K. K.; Bhadauria, A.; Haque Siddiqui, M. I. Estimation of Ultrasonic Velocity, Density, Internal Pressure, and Thermophysical Parameters of Ionic Liquid Mixtures: Application of Flory's Statistical Theory. ACS Omega 2024, 9 (17), 19363–19377. https://doi.org/10.1021/acsomega.4c00520.
2. Rajagopal, K.; Chenthilnath, S. Study on Excess Thermodynamic Parameters and Theoretical Estimation of Ultrasonic Velocity Using Scaled Particle Theory in Binary Liquid Mixtures of 2-Methyl-2-Propanol and Nitriles at Different Temperatures. Chin. J. Chem. Eng. 2010, 18 (5), 804–816. https://doi.org/10.1016/S1004-9541(09)60132-4.
3. Abdellaoui, K. N.; Belabbaci, A.; Ayad, A.; Negadi, A.; Hernández, A.; Aslam, M.; Singh, P.; Bahadur, I.; Negadi, L. Thermodynamic, Ultrasonic, and Transport Study of Binary Mixtures Containing 1-Hexene and Alcohols at 293.15–303.15 K. J. Chem. Eng. Data 2025, 70 (8), 2961–2984. https://doi.org/10.1021/acs.jced.5c00043.
4. Vanathi, V.; Mullainathan, S.; Nithiyanatham, S.; Ramasamy, V.; Palaniappan, L. Ultrasonic Velocity, Density, Viscosity for the Ternary Mixture of (Benzene + Chloroform + Cyclohexane) at Different Temperatures. Heliyon 2019, 5 (8), e02203. https://doi.org/10.1016/j.heliyon.2019.e02203.
5. Radhakrishnan, P.; Ahobilam, G.; Kapoor, S.; Anantha Iyengar, G.; Lee, D.-E.; Kannan, V.; Karthikeyan, V.; Assi, D. S.; Roy, V. A. L. Comparative Evaluation of Thermophysical and Acoustical Properties of Binary Mixtures of Cumene + Methyl Acetate and Cumene + Ethyl Acetate over the Range of Molar Compositions and Temperatures from 298.15 to 318.15 K: Experimental Measurements and Application of Deviation Modeling. J. Chem. Eng. Data 2025, 70 (9), 3491–3508. https://doi.org/10.1021/acs.jced.5c00053.
6. Patil, K.; Pawar, R.; Talap, P. Self-Aggregation of Methylene Blue in Aqueous Medium and Aqueous Solutions of Bu4NBr and Urea. Phys. Chem. Chem. Phys. 2000, 2 (19), 4313–4317. https://doi.org/10.1039/b005370h.
7. Appusamy, A.; Purushothaman, P.; Ponnusamy, K.; Ramalingam, A. Separation of Methylene Blue Dye from Aqueous Solution Using Triton X-114 Surfactant. J. Thermodyn. 2014, 2014, 1–16. https://doi.org/10.1155/2014/670186.
8. Pramanick, D.; Mukherjee, D. Molecular Interaction of Methylene Blue with Triton X-100 in Reverse Micellar Media. J. Colloid Interface Sci. 1993, 157 (1), 131–134. https://doi.org/10.1006/jcis.1993.1166.
9. Oladoye, P. O.; Ajiboye, T. O.; Omotola, E. O.; Oyewola, O. J. Methylene Blue Dye: Toxicity and Potential Elimination Technology from Wastewater. Results Eng. 2022, 16, 100678. https://doi.org/10.1016/j.rineng.2022.100678.

10. Dzida, M.; Zorębski, E.; Zorębski, M.; Żarska, M.; Geppert-Rybczyńska, M.; Chorążewski, M.; Jacquemin, J.; Cibulka, I. Speed of Sound and Ultrasound Absorption in Ionic Liquids. Chem. Rev. 2017, 117 (5), 3883–3929. https://doi.org/10.1021/acs.chemrev.5b00733.
11. Zafarani-Moattar, M. T.; Shekaari, H.; Asadollahi, S. Thermodynamic Studies of Solute–Solute and Solute–Solvent Interactions in Ternary Aqueous Systems Containing {betaine + PEGDME250} and {betaine + K3PO4 or K2HPO4} at 298.15 K. Sci. Rep. 2023, 13 (1), 17780. https://doi.org/10.1038/s41598-023-43906-0.
12. Mohamed Thamby, B. F.; Duraiayya, R. D.; Anantharaj, R. Volumetric Properties of Acid Dyes in Water with Tetrabutylammonium Bromide + Glycerol Deep Eutectic Solvent. Indian Chem. Eng. 2025, 1–17. https://doi.org/10.1080/00194506.2025.2480720.
13. Radiul, S. M.; Chowdhury, J.; Goswami, A.; Hazarika, S. Laser-Induced Fluorescence Based Characterization Method for Aggregation Behavior of Rhodamine B (RhB) in Water, Ethanol, and Propanol. 2021. https://doi.org/10.48550/ARXIV.2111.12671.
14. Zhang, K.; Xie, R.; Fang, K.; Chen, W.; Shi, Z.; Ren, Y. Effects of Reactive Dye Structures on Surface Tensions and Viscosities of Dye Solutions. J. Mol. Liq. 2019, 287, 110932. https://doi.org/10.1016/j.molliq.2019.110932.
15. Joshi, D.; Bhatnager, D.; Kumar, A.; Gupta, R. Direct Measurement of Acoustic Impedance in Liquids by a New Pulse Echo Technique. MAPAN 2009, 24 (4), 215–224. https://doi.org/10.1007/s12647-009-0026-6.
16. Jadhav, V.; Mane-Gavade, S.; Kumbhar, R.; Kolekar, S.; Tamhankar, B.; Sabale, S. Liquid-Liquid-Solid Equillibrium of Water + 2-Propanol + Kosmotropic Salts: Construction of Phase Diagrams and Understanding of Salting-out Effects Using Volumetric and Compressibility Studies. Curr. Phys. Chem. 2019, 9 (1), 36–49. https://doi.org/10.2174/1877946809666190201145050.
17. Luning Prak, D. J.; Cowart, J. S.; Trulove, P. C. Density, Viscosity, Speed of Sound, Bulk Modulus, and Surface Tension of Binary Mixtures of n -Heptane + 2,2,4-Trimethylpentane at (293.15 to 338.15) K and 0.1 MPa. J. Chem. Eng. Data 2014, 59 (11), 3842–3851. https://doi.org/10.1021/je5007532.
18. Achole, B. D.; Patil, A. V.; Pawar, V. P.; Mehrotra, S. C. Study of Interaction through Dielectrics: Behavior of −OH Group Molecules from 10MHz to 20GHz. J. Mol. Liq. 2011, 159 (2), 152–156. https://doi.org/10.1016/j.molliq.2011.01.011.
19. Cui, C.; Sa, R.; Hong, Z.; Zhong, H.; Wang, R. Ionic-Liquid-Modified Click-Based Porous Organic Polymers for Controlling Capture and Catalytic Conversion of CO2. ChemSusChem 2020, 13 (1), 180–187. https://doi.org/10.1002/cssc.201902715.
20. Zade, S. D.; Zade, P. S.; Ganjre, P. J.; Aswale, S. S.; Aswale, S. R. Study of Relative Association, Apparent Molar Compressibility and Free Length of Entacapone API in Alcohols at Different Frequencies. Indian J. Pharm. Educ. Res. 2016, 50 (4), 703–707. https://doi.org/10.5530/ijper.50.4.23.
21. Subbarao, R.; Vishwam, T. Density, Viscosity, Ultrasonic and Thermoacoustic Studies of Aqueous Nicotinamide (Vitamin B3) Binary Mixtures: Temperature Dependence. J. Chem. Thermodyn. 2025, 202, 107424. https://doi.org/10.1016/j.jct.2024.107424.
22. Kumari, L.; Sinha, L.; Prasad, O.; Gupta, M. Study of Molecular Association in Binary Mixtures of Poly(Vinyl Pyrrolidone) (PVP) with Ethanol, 1-Propanol and 1-Butanol through Thermo-Acoustical, FT-IR, UV–Vis Spectroscopy and DFT Studies. Eur. Phys. J. D 2021, 75 (11), 296. https://doi.org/10.1140/epjd/s10053-021-00299-x.

Multifunctional Behavior of Fe-Substituted Nickel Manganite's: Structural, Magnetic, and Photocatalytic Insight

R. S. Pandav [a*], A. S. Tapase[b] U. B. Sankapal [c*], N. M. Patil [d]

[a] Department of Chemistry, Yashwantrao Chavan Warana Mahavidyalaya, Warananagar, Kolhapur,416113 (MS) India

[b] Department of Chemistry, Vivekanand College Kolhapur (An Empowered Autonomous Institute), 416003 (MS) India

[c] Department of Chemistry, R. P. Gogate College of Art's & Science and R. V. Jogalekar College of Commerce (Autonomous), Ratnagiri, Maharashtra, India 415 612.

[d] Department of Chemistry, Bhogawati Mahavidyalaya Kurukali, Tal-Karveer, Maharashtra, India 416001.

ABSTRACT

Nanocrystalline $NiMn_{2-x}Fe_xO_4$ ($2.0 \geq x \geq 0$) systems were prepared by sol–gel auto combustion method. The synthesized material was systematically characterized by using Thermo gravimetric analysis, X-ray diffraction analysis, Infrared spectroscopy, Scanning electron microscopy, Transmission electron microscopy, Energy-dispersive x-ray analysis and Vibrating sample magnetometer. The photocatalytic activity of the prepared material was evaluated by the degradation of the model crystal violet dye solution. The detailed results of XRD,IR, SEM, and VSM and photocatalytic degradation of Crystal violet dye solution indicate the important role of substitution of iron in changing the structural, magnetic and photocatalytic properties of nickel manganite's.

KYWORDS: Sol–gel synthesis, X-ray Diffraction analysis, Thermal gravimetric analysis, Vibrating sample magnetometer, Photodegradation, Crystal violet dye.

Corresponding Author e-mail: rajkumarpandav@gmail.com, dr.ubsankpal@gmail.com

1.Introduction

The textile dyes and dye intermediates with high aromaticity and low biodegradability have emerged as major environmental pollutants. Considerable amount of water is used for dyeing and finishing of fabrics in the textile industries. The waste water from textile mills causes serious impact on natural water and land in the surrounding area. As dyes are designed to be chemically and photolytically stable, they are highly persistent in natural environments. The improper handling of hazardous chemicals in textile water also has some serious impact on the health and safety of workers putting them into the high-risk bracket for skin diseases like chemical burns, irritation, ulcers, etc. and respiratory problems. Nearly 10-15% of the dye is lost in the dyeing process and is released in the waste water which is an important source of environmental contamination [1-3].

In recent years, there has been an extensive interest in the use of semiconductor as photo catalyst to degrade organic contaminations. There are number of different semiconducting materials which are readily available, but only few are suitable for sensitizing the photo-mineralization of wide range of pollutants. Heterogeneous photocatalysis is a process in which a combination of photochemistry and catalysis are operating together. It implies that both light and catalyst are necessary to bring out the chemical reaction. UV light illumination over a semiconductor like metal oxides produces electrons and holes. The valence band holes are powerful oxidants (+1 to +3.5V versus NHE depending on the semiconductor and pH), while

the conduction band electrons are good reductants (+0.5 to −1.5V versus NHE). In this paper we report phocatalytic degradation of crystal violet dye solution using sol gel synthesized Iron substitutes Nickel Manganites. [4-6]

2.EXPERIMENTAL TECHNIQUE

2.1 Material Synthesis

Analytical grade Nickel nitrate [Ni $(NO_3)_3.9H_2O$], Iron nitrate [Fe $((NO_3)_3.9H_2O$], Manganese nitrate [Mn $(NO_3)_2.4H_2O$] and citric acid [$C_6H_8O_7.H_2O$] were used to prepare $NiMn_{2-x}Fe_X\ O_4$ (where x = 0.0, 0.5, 1.0, 1.5 and 2.0) by sol-gel method [7]. Metal nitrates and citric acid were dissolved in minimum quantity of deionized water with 1:1 molar ratio. The pH of the solution was adjusted to about 9.0 to 9.5 using ammonia solution. The solution was transformed to dry gel on heating to 353K. On further heating the dried gel burnt in a self-propagating combustion manner until all the gel completely converted to a floppy loose powder. The as burnt precursor powder was then sintered at 650 °C for 5 hours for confirmation of phase formation. The sintered powders were granulated using 2% polyvinyl alcohol as a binder and uniaxially pressed at a pressure of 8 ton /cm^2 to form pellets. These pellets were gradually heated to about 773K to remove the binder material.

2.2 Material Characterization:

Thermal analysis of the different compositions of the Mn-substituted Ni ferrite system was carried out from the TG curve. Stability of the dry citrate complexes was checked by scanning the thermograms in the temperature range of 10-1000^{0}C in static air at the heating rate of 10^{0}C/min. Different kinds of thermodynamic and kinetic parameters were determined from the plots of TGA curve.

The phase formation of the samples calcined at different temperature was confirmed by X-ray diffraction studies using Philips PW-1710 X-ray diffractometer with CuKα radiation (λ=1.54056Å).The lattice parameters were calculated for the cubic phase using following relations.

a) for cubic phase $a = d\ (h^2 + k^2 + l^2)^{1/2}$ -------- 1

where, a = Lattice parameter, (hkl) = Miller indices

d = interplanar distance

The crystallite size of sintered ferrites was calculated from the full width at half maxima of the most intense (311) peak by using Scherrer's formula [8].

$$t = 0.9\lambda / \beta \cos\theta \quad \text{--------- 2}$$

Where, symbols have their usual meaning.

The X-ray density was calculated according to the formula

$$dx = 8M/Na^3 \quad \text{--------- 3}$$

where, N = Avagadros number (6.023 X 10^{23} atom/mole)

M = Molecular weight, and

a = lattice constant which was calculated from the X-ray diffraction pattern. X-ray density is sometimes also called 'theoretical density'.

The FT-IR spectra were recorded in the range of 400 to 1000 cm^{-1} on instrument Perkin Elmer – IR spectrophotometer (model E-2829) in KBr pellets.

The SEM micrograph of the samples was obtained using scanning electron microscope (JEOL JSM 6360). The grain size of all the samples was calculated by Cottrolls method.

Elemental analysis of several composition of the system was carried out by using electron dispersive X-ray spectroscope equipped with SEM instrument.

Transmission electron microscope (Philips CM 20) was used to evaluate the nanostructure of the typical samples. To study the phase structure of the samples SAED pattern were also recorded.

Magnetic measurements of all the compositions were carried out by using a vibrating sample magnetometer. The measurements were done at room temperature. Saturation magnetization (Ms), coercive field (Hc) and remenant magnetization (Mr) of the samples were studied from the hysteresis loops of respective curves.

Two probe technique was employed to measure the D.C. resistivity of the samples in the temperature range of room temperature to 723 K and specific resistivity was determined using the relation,

$$\rho = (\pi d^2 / 4t) R \qquad \text{----------4}$$

The values of activation energy (eV) were calculated from the plots of log ρ Vs $10^3/T$. Silver paste was applied to both the surfaces of the pellets for good ohmic contacts.

The thermo-emf measurements were carried out in the temperature range of 300 K to 523 K. The graph of ΔV vs ΔT was plotted and the type of the conduction (n or p type) was evaluated.

The photocatalytic activity of the samples was studied for crystal violet dye in presence of Ultra-violet light with different times of exposure. Crystal violet is considered as a model of a series of common azo-dyes, used in the industry.

3.RESULTS AND DISCUSSION

3.1 Thermal Analysis

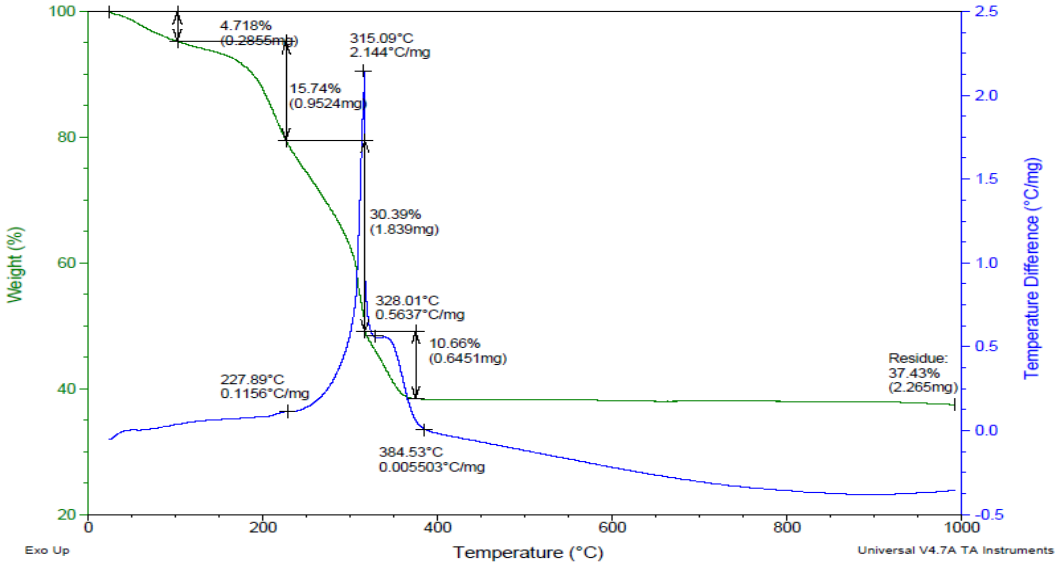

Fig. 1. TGA-DTA traces for the sample with x = 1.0

Fig.1 represents the thermal behavior of the sol–gel synthesized $NiFeMnO_4$ precursor examined using TGA-DTA from room temperature to 1000 °C at a heating rate of 10 °C/min. An initial small weight loss below 150°C, accompanied by a weak endothermic DTA peak, corresponds to the evaporation of physically adsorbed moisture and trapped solvent molecules. A second weight loss of 15-16% observed in the range of 150-300°C, along with a mild exothermic DTA peak, is attributed to the decomposition of metal-citrate complexes and partial breakdown of nitrate groups. A major decomposition with 30% weight loss occurs sharply between 300-330°C with a strong exothermic peak around 315-328°C in DTA, indicates rapid combustion of organic residues and initiating the formation of the $NiFeMnO_4$ spinel framework. A minor exothermic peak near 380°C, accompanied by an additional 10% mass loss, suggests gradual transformation from amorphous oxide to nanocrystalline spinel. Beyond 420°C, no significant mass loss is detected, confirming complete decomposition and thermal stabilization of the precursor. These results indicate that the spinel phase forms from 320-420°C. However, to obtain complete crystallization and well-ordered $NiFeMnO_4$ spinel structure with high phase purity, the precursor was calcined at 650 °C for 5 hours.

3.2 XRD Studies

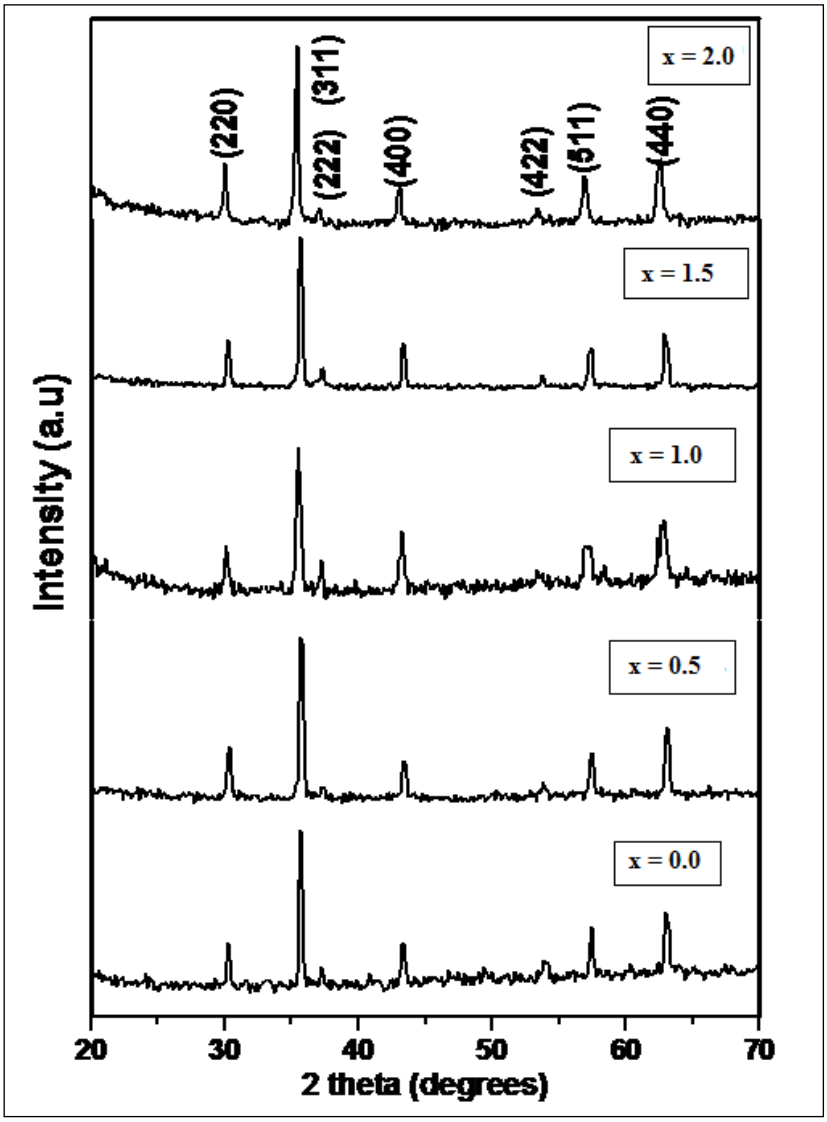

Fig. 2. X-ray peaks for the system $NiMn_{2-x}Fe_x O_4$ (x=0, 0.50, 1.0, 1.50 and 2.0)

X-ray diffraction data reveals that, the Fe substituted Nickel manganite shows cubic spinel structure at temperature 650°C for 5 hours. Therefore, $NiMn_{2-x}Fe_x$ O_4 (x=0, 0.50, 1.0, 1.50 and 2.0) system sintered at 650 °C for 5 hours and their X-Ray diffraction patterns are shown in **Fig.2.** it depicts the XRD patterns of the different $NiFe_{2-x}Mn_xO_4$ compositions. All the observed reflections could be assigned to cubic spinel lattice indicating their single phase nature. Unit cell parameters were determined by indexing the diffraction peaks in the XRD patterns. It is observed that the unit cell parameter gradually decreases with increasing Mn content in the composition obeying Vegard's law. The slow linear decreasing trend in the lattice parameter is attributed to the replacement of Mn^{3+} (0.65Å) ions by Fe^{3+} ions, a slightly smaller ion (0.64Å), in the system. The linear increase in lattice constant with Fe content obeys Vegard's law and it is due to cationic size effect [1]. Fe ions have strong site preference energy for octahedral site; it tends to occupy the B site rather than A-site. The particle size of each sample was determined by considering most intense (311) peak of the XRD pattern by using Scherrer formula. The crystallite size decreases with increase in Fe content and it is observed to vary in the range of 30-25nm. The slow decreasing trend of unit cell parameter due to incorporation of lighter Fe^{3+} ion in place by Mn^{3+} leads to a gradual decrease in the X-ray density with increase in Mn content**.** The X-ray density (dx), lattice constant (*a*) and crystallite size (t) of the compositions are given in **Table 1.**

Table 1. Data on lattice parameter, crystallite size, X-ray density, Physical density, Porosity of $NiMn_{2-x}Fe_X$ O_4 ferrite samples.

Composition (x)	Lattice constant (a) Å	Crystallite size (t) nm	X-ray density (dx gm/cm^3)	Bulk density (d_B gm/cm^3)	% Porosity
0.0	8.31	25	5.37	5.33	4.39
0.5	8.33	26	5.35	5.30	4.62
1.0	8.36	28	5.30	5.24	5.97
1.5	8.39	29	5.26	5.20	5.53
2.0	8.41	30	5.23	5.18	4.89

3.3 Infra-Red study:

The Infra-red spectra of the sintered samples are shown in **Fig.3.** The IR spectra have been used to locate the band positions. The higher frequency band is observed at around 600 cm^{-1} and lower frequency at around 500 cm^{-1}. The absorption bands observed within this range is an indication of the formation of single-phase spinel structure and bands ν_1 and ν_2 are assigned to the intrinsic vibrations of tetrahedral and octahedral complexes. It can be seen that the two spectral bands are less broadened for higher manganese content. Such broadening can be attributed to the statistical distribution of Fe at A-(tetrahedral) and B-(octahedral) sites. Waldron ascribed the ν_1 band to the intrinsic vibration of the tetrahedral group (~ 600 cm^{-1}) and ν_2 to octahedral group (~ 475 cm^{-1}). The vibrational frequencies depend on cation mass, cation – oxygen distance and the bonding force [9]. The values of the vibrational frequency for tetrahedral sites (ν_1), octahedral sites (ν_2) and differences (ν_1- ν_2) are given table

For un-substituted composition, viz. $NiFe_2O_4$, the two bands observed at 595 and 455 cm^{-1} are assigned to the ν_2 and ν_1 respectively. A comparison of the observed vibrational frequencies of all the studied compositions, indicates that the ν_1 (corresponding to tetrahedral

unit) remain almost unmodified with increasing Mn^{3+} content. However, ν_2 (corresponding to octahedral unit) increases smoothly with increase in Mn^{3+} content e.g. 455 cm^{-1}(for x = 0.0) to 487 cm^{-1} (for x = 1.0). The increasing vibrational frequency (ν_2) with increase in Mn^{3+}, can be attributed to the increasing force constant due to the shortening of M-O bonds in the octahedral unit. Thus, it seems that Mn^{3+} preferably enters to the octahedral site and hence affecting the force constant and bond lengths, without bringing about any change in tetrahedral site.

The difference between ν_1 and ν_2 (as ν_1- ν_2) decreases with increasing Mn^{3+} substitution. The decreasing values of (ν_1- ν_2) indicate increasing separation between a- and d- sites [9]. Such an increasing separation of a- and d sites may weaken the a-d super exchange interaction. According to the theory, the variation of the super-exchange interaction affects significantly the magnetic behavior.

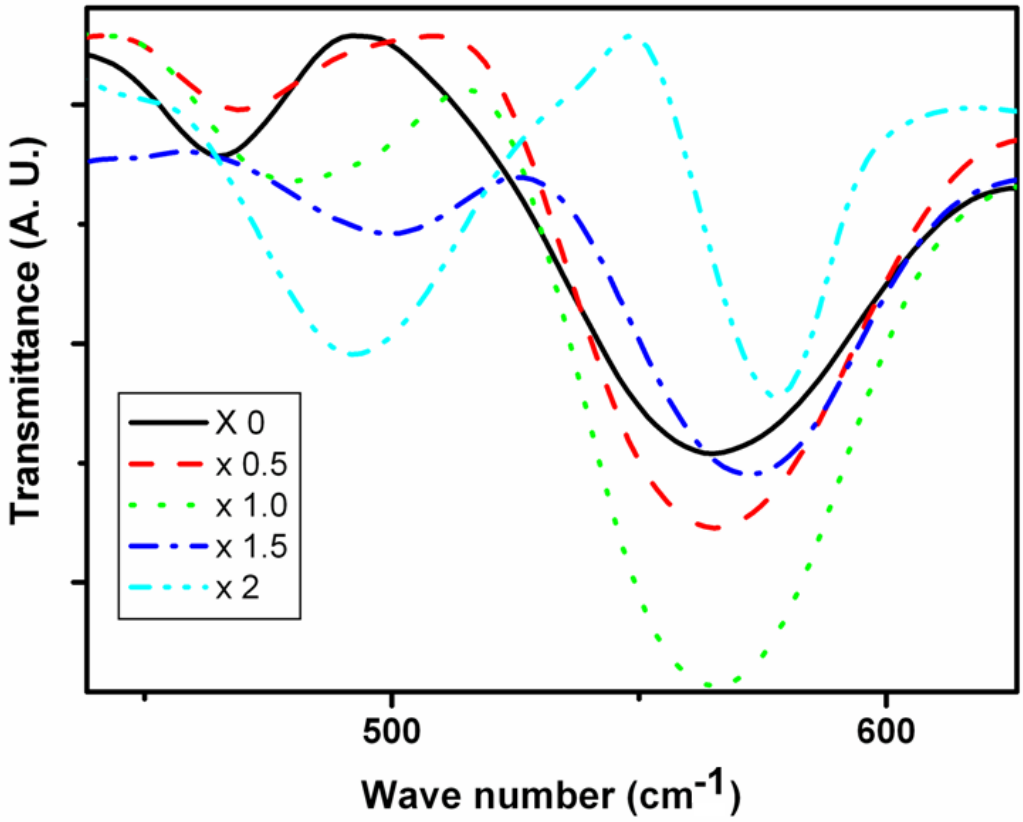

Fig.3. Fourier transfer Infra-red spectrum for $NiMn_{2-x}Fe_X O_4$ system

3.4. Scanning Electron Microscopy:

The morphology of the particles formed was examined by direct observation via high-resolution scanning electron microscopy for the sintered samples. Scanning electron microscopy pictures of $NiFe_{2-x}Mn_xO_4$ (x =0.0, 1.0 ,2.0) ferrite particles after calcination are shown in **Fig. 4** All ferrites produced are good quality spheres of similar size under the same experimental conditions. The average grain size was calculated by Cottrell's method which shows grains of good sphericity and of size between 0.25 to 0.36 μm [10]. The measured ferrite nanoparticle sizes are consistent with the sizes calculated by Debye-Scherrer formula from the (311) peak of XRD patterns (**Table 1**). It can be seen that the grain size increase significantly with increasing Mn content since the ionic radius of iron is smaller than the ionic radius of manganese.

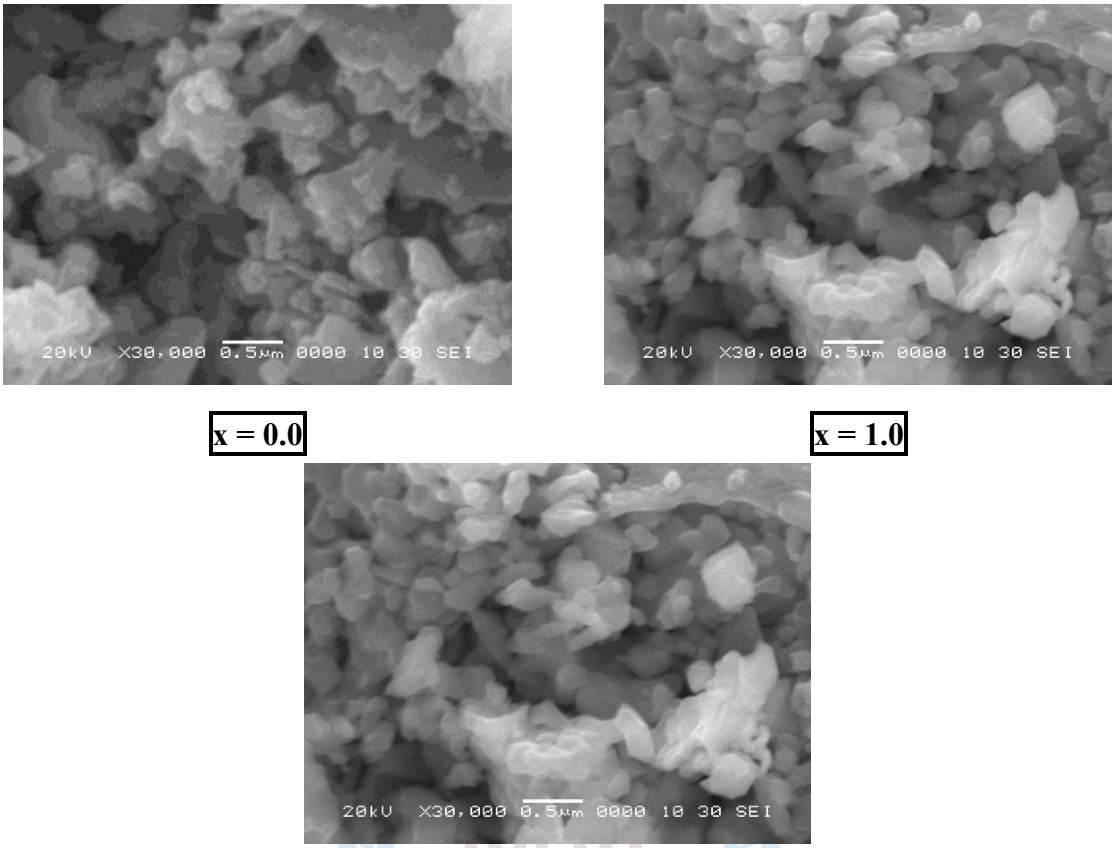

x = 0.0 **x = 1.0**

x = 2.0

Fig. 4. SEM micrographs for the system $NiMn_{2-x}Fe_X O_4$
a) x =0.0 b) x = 1.0, c) x=2.0

3.5. Transmission electron microscopy:

The typical transmission electron micrographs of $NiMn_{2-x}Fe_X O_4$ (x =0.0, 1.0, 2.0) ferrite compositions are given in **Fig.5.** The corresponding selected area electron diffractogram (SAED) is also given as inset in figure. They show the ferrite particle size to be in the nanometer scale. It is evident from these micrographs that all the synthesized samples have spherical particles ranging from 20 to 30 nm. The superimposition of the bright spot with Debye ring pattern indicates crystalline nature of the samples. Both the figures confirm that most of the particles are of size less than 30 nm. This is in close agreement with the average crystallite size obtained from XRD **(Table-1).** Selected area electron diffraction (SAED) pattern indicates that there is no impurity or secondary phase. It reveals the formation of single phase spinel structure. It agrees well with the result obtained by XRD data.

3.6 Energy dispersion x-ray analysis:

The exact quantitative chemical composition of the $NiMn_{2-x}Fe_X O_4$ samples with x= 0.0, 1.0 and 2.0 was checked by using the energy dispersion X-ray analysis (EDAX) at room temperature which are shown in **Fig.6. (a-c).** The data of the EDAX analysis for all three samples are given in **Table 2** and are found to be equal to the relative compositions of the metals used for synthesis by stoichiometric calculations. The EDAX analysis were in good agreement with the expected ratios of the transition metals of Ni, Mn, Fe and O is indicating

that the sol-gel autocombution method was able to yield system which does not lose its elemental stoichiometry [11].

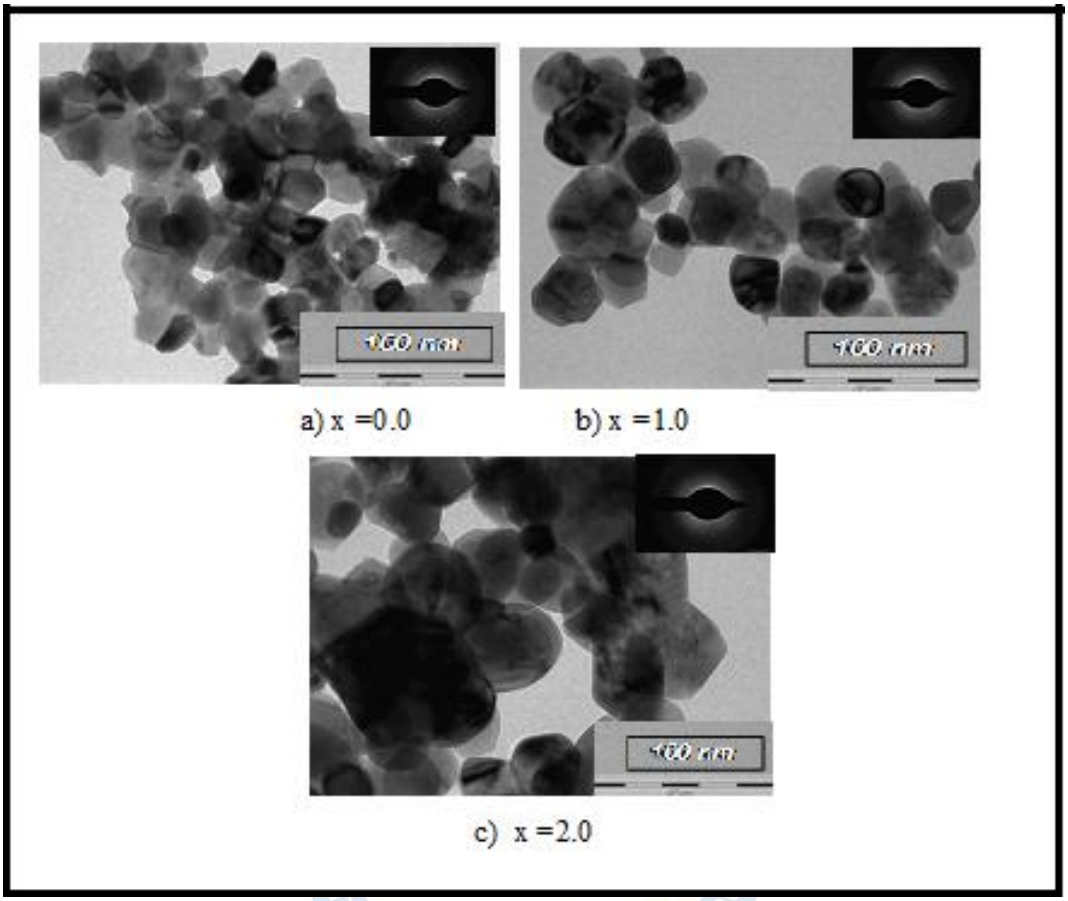

Fig.5. Typical TEM images and SAED pattern for $NiMn_{2-x}Fe_x O_4$
a) x = 0.0 and b) x = 1.0 c) x =2.0

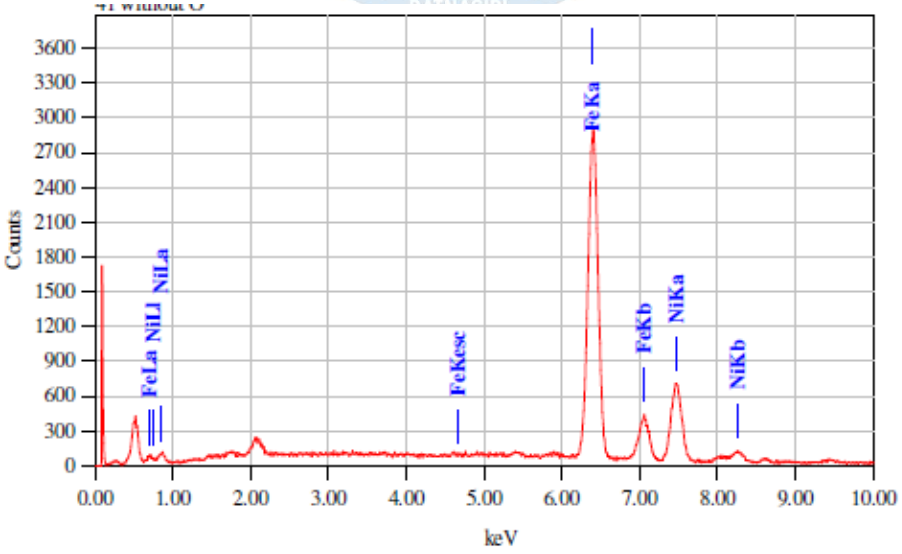

a) $NiFe_{2-x}Mn_xO_4$ **(x = 0.0)**

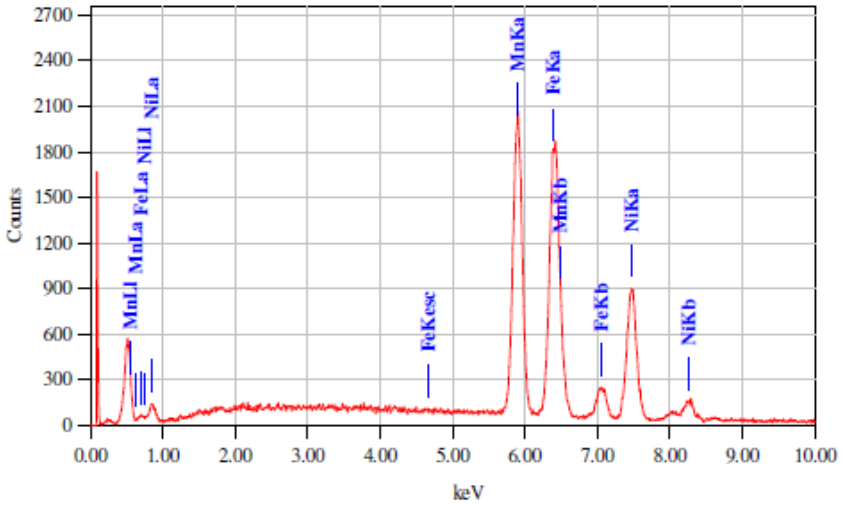

b) $NiFe_{2-x}Mn_xO_4$ **(x = 1.0)**

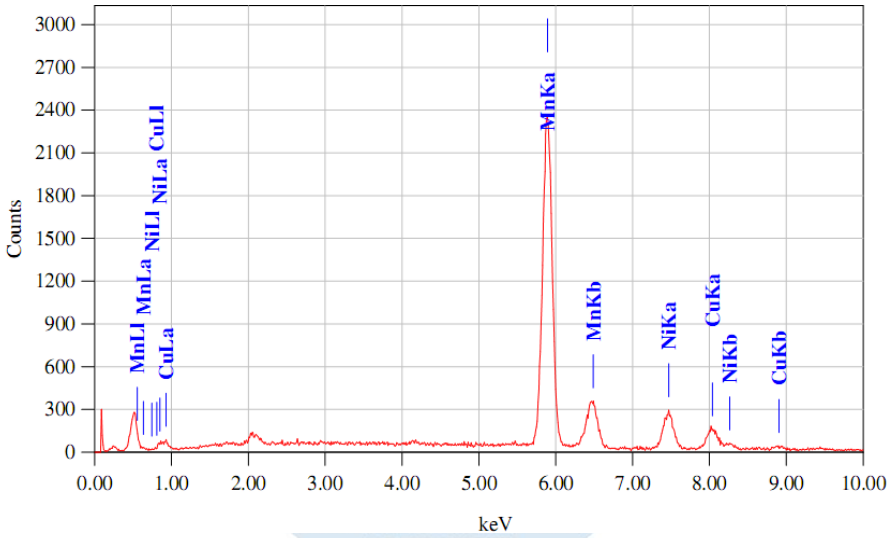

c) $NiFe_{2-x}Mn_xO_4$ **(x = 2.0)**

Fig. 6. EDAX data for the system $NiMn_{2-x}Fe_X O_4$ **(x=0.0, 1.0 and 2.0)**

Table.2. Atomic percentage value for the $NiMn_{2-x}Fe_X O_4$ **(x=0.0, 1.0 and 2.0) system by EDAX analysis**

Composition (x)	Atomic % for element					
	Ni		Mn		Fe	
	Expt.	Thero.	Expt.	Thero.	Expt.	Thero.
2.0	28.57	33.33	----------	----------	71.43	65.56
1.0	29.79		35.70	32.41	34.50	32.95
0.0	33.54		6.46	65.13	----------	----------

3.7 Magnetic Study

Magnetic measurements of $NiMn_{2-x}Fe_X\ O_4$ system were carried out by using vibrating sample magnetometer (VSM) and they are depicted in **Fig.7.** The samples show typical S-type shape in M–H curve, though the coercive fields are very small. The magnetization rises very sharply as the applied field increases from zero in either direction and then slowly approaches saturation. This is the typical behavior of nanosized magnetic material where residual superparamagnetic relaxation leads to slow rise in the wings and ferrimagnetic part contributes to hysteresis loop with small coercive field. In nickel ferrite the magnetization appears due to cationic inversion at smaller particle size. Thus as the particle size increases, the inversion decreases and the magnetization decreases. The magnetic data for the samples reveals that, it is ferrimagnetic in nature. The magnetic parameters such as magnetization (Ms), coercivity (Hc), remanence (Mr) and remanence ratio (Mr/Ms) are listed in **Table 3** It is seen that the Ms goes on decreasing linearly with Mn content from 22.41 to 5.43 emu/g, while coercivity goes on increasing from 47.11to 10.44 Oe.

The magnetic moment (nB) per unit formula in Bhor magneton was calculated from saturation magnetization by using the following formula [12]

$$nB = Mw \times Ms / 5585 \qquad \ldots\ldots\ldots 5$$

Where nB = magnetic moment
Mw = Moleculer weight
Ms = Saturation magnetization
5585 = magnetic factor.

The experimental value of magnetic moment goes on increasing with increase in Fe content [13-14]. The Mn ions have maximum preference for B site up to x=1.0, further Mn ion concentration increase shows its preference for both A- and B- sites. The incorporation of more magnetic Fe ions into the B-sub lattices instead of more magnetic Mn^{3+} leads to increase in the magnetic moment of the B-site compared with the A site.

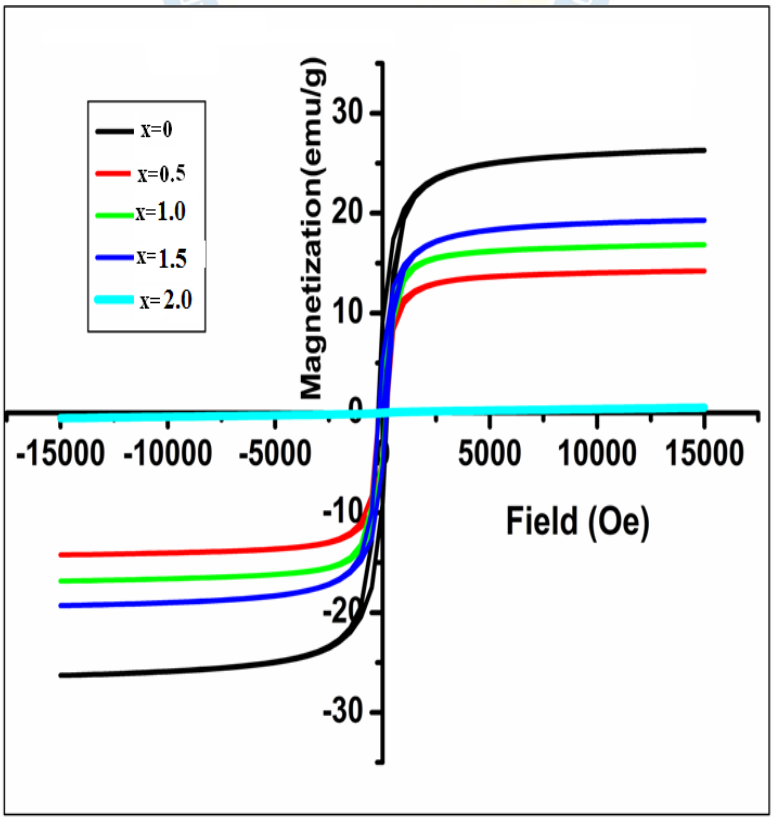

Fig. 7. VSM loops of $NiFe_{2-x}Mn_xO_4$ system

Table. 3. Magnetic parameters of $NiMn_{2-x}Fe_X O_4$ system

Composition X	Saturation magnetization	remanant magnetization	coercive field	Magnetic momentum μB (B.M.)
	emu/g	emu/g	emu/g	
0.0	5.43	3.77	10.44	0.2148
0.5	9.56	4.89	12.35	0.5973
1.0	15.76	6.10	23.67	0.6902
1.5	17.43	8.60	35.14	1.0679
2.0	22.41	11.79	47.11	0.2148

3.8 Photocatalysis

The catalytic activity study of the Mn substituted Ni ferrite photocatalyst was carried by photodegradation rate of crystal violet. The experiment of photocatalytic reaction was conducted in a 100-ml Pyrex glass vessel with magnetic stirring and a UV lamp (8W) with the main wavelength of 253.7 nm. The as-prepared ferrite was used as photocatalyst during the study. The experiments for photocatalytic activity were carried out by using 50 ppm concentration Crystal violet for their decolorization and degradation process. In this, Mn substituted $NiFe_2O_4$ were used as photocatalyst and UV light as illuminating light source. Reaction system was setup by adding the 50 mg photocatalyst into 100 ml dye solutions prepared in appropriate concentrations using doubly distilled water. A blank solution was also prepared by the same method without photocatalyst. The dye suspension was magnetically stirred for 30 min in the dark before irradiation to promote the adsorption on the surface of photocatalyst. It was then irradiated for one hour under UV light and 5 ml of degraded samples are withdrawn and the absorbance was measured in the UV-visible spectrophotometer after centrifugation and filtration. It was, therefore, concluded that enhanced photodegradation is directly related to the reduced particle size of the ferrites, which implies photosensitization as the primarily involved process [15-16]. It is seen from **Fig.8** that photocatalytic activity increasing with the increasing substitution of Fe-content. $NiFe_2O_4$ shows better photocatalytic activity towards crystal violet as compared to other Mn substituted nickel ferrites.

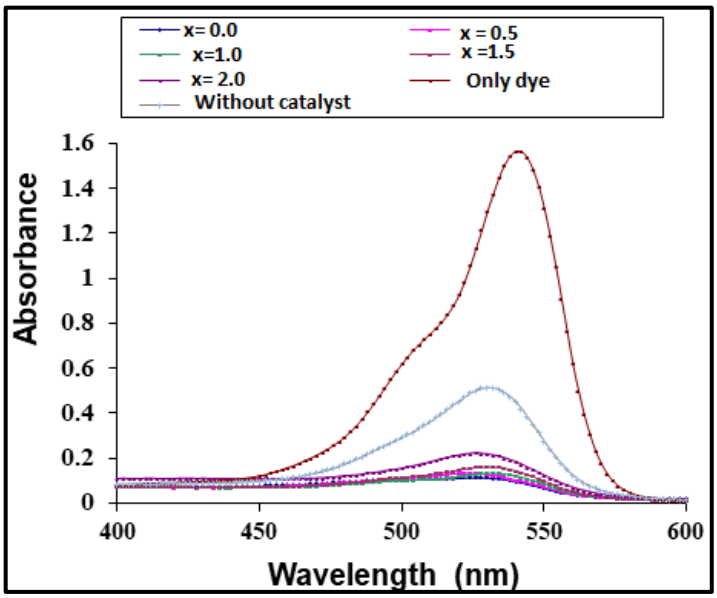

Fig.8 Photocatalytic degradation of crystal violet using photocatalysts of $NiFe_{2-x}Mn_xO_4$ system after 5 hours in visible light irradiation

Thus according to results photocatalytic reaction follows pseudo first order reaction kinetics with respect to dye concentration. The kinetic rate constant (k) can also be linked to the concentration by, [17]

$$\ln C / C_0 = -kt \qquad \text{------- 6}$$

Where, C_0 and C are concentration of dye at t=0 and concentration of dye at time t respectively.

The kinetic rate constant (k) can be calculated and are shown in **Table 4.** Generally, the photocatalytic degradation occurs through the generation of active species like holes and hydroxyl radicals and superoxide ion due to excitation of photocatalysts by hitting the photons in the visible light **[18].** This is due to the fact that the photocatalysts are illuminated with the light of visible light irradiation conduction band electrons (e^-) and valance band holes (h^+) are generated. Hence catalyst suspension is irradiated with light energy greater than its band gap energy. The photo generated electrons could reduce the dyes or react with electron acceptors such as O_2 adsorbed on the catalyst surface or dissolved in water, reducing its superoxide radical anion O^{-}. The photo generated holes can oxidize the organic molecule to form R^+, or react with OH^- or 2O oxidizing them into OH radical. Together with other highly oxidant species such as peroxide radicals may be responsible for heterogeneous photodecomposition of organic substrates such as dyes **[19].** The first order rate constant for $NiMn_2O_4$ photocatalyst was about $0.4294h^{-1}$ and that of $NiFe_2O_4$ was about $0.5585h^{-1}$. This clearly indicates that the doped $NiMn_2O_4$ shows enhanced photocatalytic activity as compared to that of undoped samples.

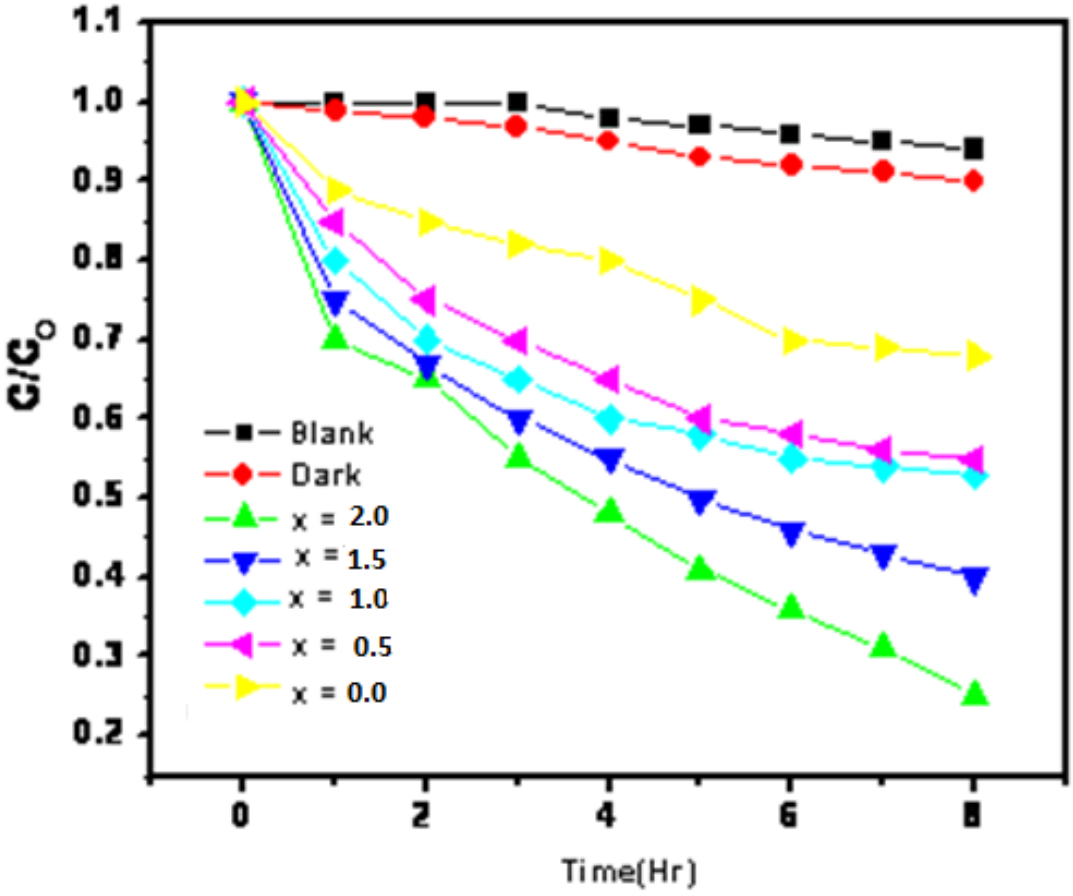

Fig.9. Photocatalytic study $NiFe_{2-x}Mn_xO_4$ for degradation of Crystal violate dye solution

Decreased photocatalytic activity of undoped $NiMn_2O_4$ is attributed to the decrease in the recombination centers **[20].** Undoped $NiMn_2O_4$ showed less photocatalytic degradation of crystal violet dye. This deactivation may be due to its normal spinel structure (Ni^{+2} ions occupy Td sites and Mn^{+3} ions occupy Oh sites). Electron hopping mechanism is controlled due to the non-availability of reducible cations in the Td site. As it is known that in $NiMn_2O_4$ all the Ni^{+2} ions occupying Td sites which is quite stable due to presence of d^{10} electronic configuration. With increase in concentration of 'x' from 0.0 to 1.0 Mn^{+2} replaces equivalent amount of Fe^{+3} ions from Oh to Td sites. Therefore, among the series of compounds $NiFe_2O_4$ is found to be highly active photocatalyst for degradation of crystal violet dye.

Composition	Rate constant (h^{-1})
Blank (without catalyst)	0.2280
x=0.0	0.4294
x=0.5	0.5105
x=1.0	0.5425
x=1.5	0.774
x=2.0	0.5585

Table 4: Rate constant of $NiMn_{2-x}Fe_X O_4$ system with composition (x=0.0, 0.5, 1.0, 1.5, and 2.0)

The photo degradation experiment under the conditions of same dye concentration for different photocatalysts was carried out.

3.8.1 Efficiency of the recycled catalyst:

The photocatalytic process should be economical so that it is successfully applicable at the industrial scale and the role of catalyst's lifetime is an important parameter which makes the process cost effective. For this reason, after the optimized conditions for the degradation of the crystal violet were determined, the catalyst was recovered by filtration and activated at 100°C and again used to study its recyclability. As shown in **Fig. 10** the catalyst shows a drop in efficiency from 94 to 72% after four recycles. This is likely to be due to fouling of the catalyst and loss in weight of catalyst due to filtration.

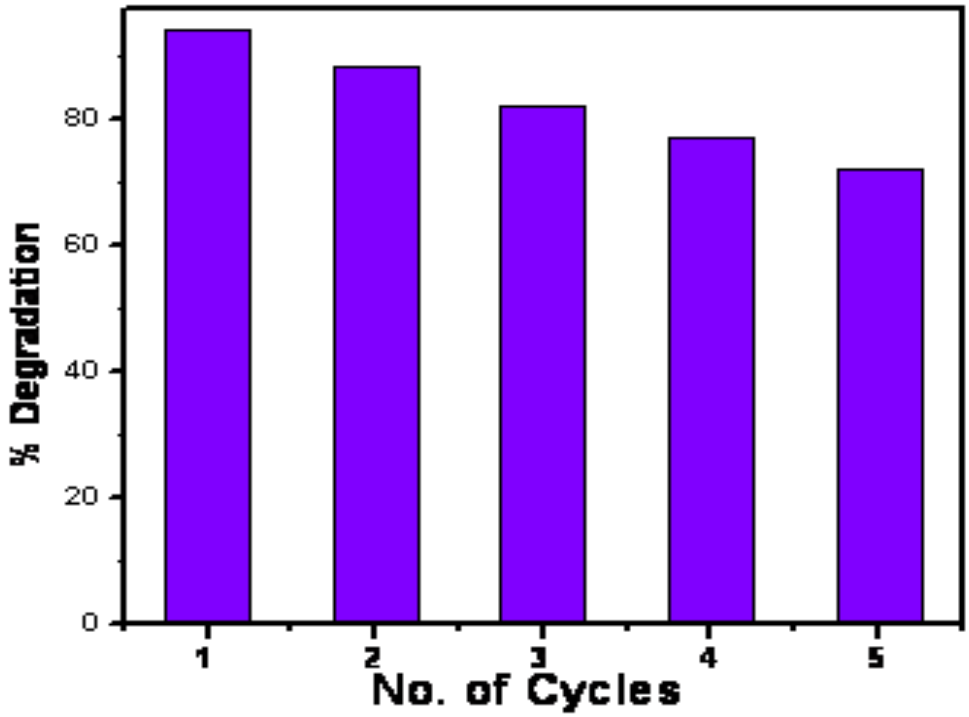

Fig. 10. Recyclability of the $NiFe_2O_4$ catalyst

4. CONCLUSIONS

The X-ray diffraction data shows that sol–gel technique yields monocrystalline single phase for all samples. The effect of sintering temperature indicates that 650 °C for 5 hours.is required temperature for the cubic spinel phase formation. It is observed that crystallite size increases with increase Fe substitution i.e. NiMn2O4 shows 25 nm while NiFe2O4 shows 30 nm crystal- lite size. The lattice constant also increases with increase in Fe ion concentration which is due to difference in ionic radii of Mn^{+3} and Fe^{+3} ions. IR spectrum of substituted cobalt ferrite are found to exhibit two bands. Out of which v_1 is caused by the stretching vibration of the tetrahedral M–O bands and the absorption band v_2 is caused by the M–O vibrations in octahedral site. The ferromagnetic behavior was shown by all the samples. The photocatalytic degradation of crystal violet indicates that nickel ferrite powders can effectively photodegrade crystal violet under ultra- violet plus visible light irradiation.

References

[1] Md. M. Islam, A. R. Aidid, J. N. Mohshin, H. Mondal, S. Ganguli, and A. K. Chakraborty, “A critical review on textile dye-containing wastewater: Ecotoxicity, health risks, and remediation strategies for environmental safety,” Cleaner Chemical Engineering, vol. 11, p. 100165, Dec. 2025, doi: 10.1016/j.clce.2025.100165.

[2] T. A. Aragaw, “A review of dye biodegradation in textile wastewater, challenges due to wastewater characteristics, and the potential of alkaliphiles,” Journal of Hazardous Materials Advances, vol. 16. Elsevier B.V., Nov. 01, 2024. doi: 10.1016/j.hazadv.2024.100493.

[3] L. A. Castillo-Suárez, A. G. Sierra-Sánchez, I. Linares-Hernández, V. Martínez-Miranda, and E. A. Teutli-Sequeira, "A critical review of textile industry wastewater: green technologies for the removal of indigo dyes," International Journal of Environmental Science and Technology, vol. 20, no. 9. Institute for Ionics, pp. 10553–10590, Sep. 01, 2023. doi: 10.1007/s13762-023-04810-2.

[4] A. Mancuso et al., "Photocatalytic Degradation of Crystal Violet Dye under Visible Light by Fe-Doped TiO2 Prepared by Reverse-Micelle Sol–Gel Method," Nanomaterials, vol. 13, no. 2, Jan. 2023, doi: 10.3390/nano13020270.

[5] A. Singh, R. Tomar, and N. B. Singh, "Efficient removal of crystal violet dye from water using zinc ferrite-polyaniline nanocomposites," Environmental Monitoring and Assessment, vol. 196, no. 6, Jun. 2024, doi: 10.1007/s10661-024-12686-z.

[6] A. Nair, A. Kurian, A. Samuel, and S. Sumathi, "Photocatalytic degradation of crystal violet using yttrium and copper co-doped nickel aluminate," Environmental Science and Pollution Research, vol. 32, no. 7, pp. 3746–3759, Feb. 2025, doi: 10.1007/s11356-025-35913-7.

[7] A. Mallah et al., "Synthesis, Structural and Magnetic Characterization of Superparamagnetic $Ni_{0.3}Zn_{0.7}Cr_{2-x}Fe_xO_4$ Oxides Obtained by Sol-Gel Method," Crystals, vol. 13, no. 6, Jun. 2023, doi: 10.3390/cryst13060894.

[8] A. Milutinović, Z. Lazarević, M. Šuljagić, and L. Andjelković, "Synthesis-Dependent Structural and Magnetic Properties of Monodomain Cobalt Ferrite Nanoparticles," Metals, vol. 14, no. 7, Jul. 2024, doi: 10.3390/met14070833.

[9] R. D. Waldron, ~ M M Stimson, and M. J. O'donnell, "Infrared Spectra of Ferrites~," 1955.

[10] Y. K. Hong and H. S. Jung, "New barium ferrite particles: Spherical shape," Journal of Applied Physics, vol. 85, no. 8 II B, pp. 5549–5551, Apr. 1999, doi: 10.1063/1.369891.

[11] E. R. Kumar, S. Kumar, T. Kojima, and R. Jayaprakash, "Study of magnetic behavior of $Mn_{1-x}Ni_xFe_2O_4$ nanoparticles," in Physics Procedia, Elsevier B.V., 2013, pp. 27–35. doi: 10.1016/j.phpro.2013.10.007.

[12] A. Ali et al., "Effect of In on superparamagnetic $CoIn_xFe_{2-x}O_4$ (x = 0–0.15) synthesized through hydrothermal method," Results in Physics, vol. 25, Jun. 2021, doi: 10.1016/j.rinp.2021.104251.

[13] I. Dirba, P. Komissinskiy, O. Gutfleisch, and L. Alff, "Increased magnetic moment induced by lattice expansion from α-Fe to α′-Fe8N," Journal of Applied Physics, vol. 117, no. 17, May 2015, doi: 10.1063/1.4919601.

[14] A. Ayuela and N. H. March, "The magnetic moments and their long range ordering for Fe atoms in a wide variety of metallic environments."

[15] H. Narayan, H. Alemu, L. Macheli, M. Sekota, M. Thakurdesai, and T. K. Gundu Rao, "Role of particle size in visible light photocatalysis of Congo Red using TiO_2 ·[$ZnFe_2O_4$] x nanocomposites," 2009.

[16] K. K. Kefeni and B. B. Mamba, "Photocatalytic application of spinel ferrite nanoparticles and nanocomposites in wastewater treatment: Review," Sustainable Materials and Technologies, vol. 23. Elsevier B.V., Apr. 01, 2020. doi: 10.1016/j.susmat.2019.e00140.

[17] G. Rytwo and A. L. Zelkind, "Evaluation of kinetic pseudo-order in the photocatalytic degradation of ofloxacin," Catalysts, vol. 12, no. 1, Jan. 2022, doi: 10.3390/catal12010024.

[18] S. Ashu Abey, N. M. Reis, E. A. C. Emanuelsson, and A. J. Expósito, "Harnessing visible light: Advanced photocatalytic strategies for sustainable environmental reactions," Chemical Engineering Journal, vol. 519, Sep. 2025, doi: 10.1016/j.cej.2025.164951.

[19] F. Mohamadpour and A. M. Amani, "Photocatalytic systems: reactions, mechanism, and applications," RSC Advances, vol. 14, no. 29. Royal Society of Chemistry, pp. 20609–20645, Jul. 01, 2024. doi: 10.1039/d4ra03259d.

[20] S. Yadav and G. Jaiswar, "Review on Undoped/Doped TiO_2 Nanomaterial; Synthesis an d Photocatalytic and Antimicrobial Activity," Journal of the Chinese Chemical Society, vol. 64, no. 1. Chinese Chemical Society Taiwan, pp. 103–116, Jan. 01, 2017. doi: 10.1 002/jccs.201600735.ournal of Applied Physics

Exopolysaccharides from Probiotic Bacteria: Production, Properties, Health Benefits, and Applications

Dr. Bharti.G. Wadekar, Ms. Jinkal & Ms. Sweta Dwivedi
Assistant Professor & MSc. II Yr. Student,
Thakur Shyamnarayan Degree College
Mumbai.
Email Id: bhartiwadekar@tsdcmumbai.in

Abstract

Exopolysaccharides (EPS) are extracellular polymers produced by probiotic bacteria, such as lactic acid bacteria (LAB) and Bifidobacterium species, with significant implications for health and industry. This review examines the biosynthesis, structural diversity, physicochemical properties, and bioactivities of EPS from probiotics. Key probiotic strains like Lactobacillus plantarum, Lactobacillus rhamnosus, and Bifidobacterium longum produce EPS that exhibit antioxidant, antimicrobial, immunomodulatory, anti-inflammatory, anticancer, and hypocholesterolemic properties. These biopolymers enhance gut microbiota, strengthen epithelial barriers, and offer therapeutic potential for diseases like inflammatory bowel disease (IBD), cancer, and metabolic disorders. In the food industry, EPS serve as natural thickeners, stabilizers, and prebiotics, improving texture in dairy, bakery, and meat products. Challenges include low yields and high production costs, but genetic engineering and sustainable substrates promise advancements. Drawing from recent studies, this article underscores the multifaceted roles of probiotic EPS, supported by over 50 references, highlighting their promise in functional foods and pharmaceuticals.

Keywords: Exopolysaccharides, Lactic Acid Bacteria, Health Benefits, Antioxidant, Antimicrobia

Introduction

Probiotic bacteria, defined as live microorganisms that confer health benefits when consumed in adequate amounts, have been extensively studied for their role in maintaining gut health, modulating immunity, and preventing diseases. Among their metabolites, exopolysaccharides (EPS) are high-molecular-weight carbohydrate polymers secreted extracellularly, forming protective layers or slime that aid bacterial survival in harsh environments (Angelin and Kavitha, 2020). EPS from probiotics, primarily LAB such as Lactobacillus, Lactococcus, and Streptococcus, as well as Bifidobacterium, are generally recognized as safe (GRAS) and have garnered attention for their structural diversity and functional properties.

Historically, EPS were first noted in fermented dairy products in the mid-20th century, where they contribute to texture and viscosity (Jurášková et al., 2022). Today, the global probiotic market exceeds $60 billion, driven by consumer interest in functional foods. EPS play a pivotal role by not only enhancing product attributes but also delivering health benefits like immune modulation and pathogen inhibition. For instance, EPS from Lactobacillus delbrueckii ssp. bulgaricus and Bifidobacterium longum show prebiotic effects, promoting beneficial gut bacteria (Khalil et al., 2022).

Sources of EPS-producing probiotics include dairy (yogurt, kefir), non-dairy ferments (kimchi, sauerkraut), and environmental isolates from marine or plant origins. Non-dairy sources are

crucial for lactose-intolerant individuals, with strains like Lactobacillus plantarum EI6 from marine environments producing EPS with wound-healing potential (Zaghloul and Ibrahim, 2022). The structural complexity of EPS, comprising monosaccharides like glucose, galactose, and rhamnose, influences their bioactivity. Charged EPS with uronic acids or phosphates exhibit enhanced solubility and interactions (Netrusov et al., 2023).

Biosynthesis of EPS involves intricate pathways, regulated by eps gene clusters, with environmental factors like carbon sources affecting yield (Nguyen et al., 2024). Recent advances in genetic engineering have improved production, addressing low yields (0.1-2 g/L for heteropolysaccharides). Health benefits extend beyond gut health, including antioxidant activity to reduce oxidative stress and immunomodulation to balance cytokines (Liu et al., 2025).

This review synthesizes current knowledge on EPS from probiotic bacteria, covering classification, biosynthesis, production, properties, health benefits, applications, challenges, and future directions. By integrating data from diverse studies, it provides a comprehensive framework for leveraging EPS in health and industry.

Classification and Structure of EPS

EPS from probiotic bacteria are classified based on composition, structure, and charge. Homopolysaccharides (HoPS) consist of a single monosaccharide type, such as glucans (glucose) or fructans (fructose), with high molecular weights (>10^6 Da). Examples include dextran (α-1,6 linkages) from Leuconostoc mesenteroides and levan (β-2,6 linkages) from Lactobacillus reuteri (Netrusov et al., 2023). Heteropolysaccharides (HePS) comprise multiple monosaccharides like glucose, galactose, mannose, rhamnose, and uronic acids, with branched structures and substituents (acetyl, phosphate), ranging from 10^4 to 6×10^6 Da (Angelin and Kavitha, 2020).

Charge classification distinguishes neutral EPS (most HoPS) from charged EPS (anionic with uronic acids or cationic), affecting solubility and bioactivity. Structural analysis uses NMR, FTIR, and GC-MS to reveal anomeric configurations and linkages. For example, EPS from Bifidobacterium longum features glucose-galactose-rhamnose repeats, aiding gut adhesion (Salimi et al., 2024). Branching and substituents enhance antioxidant properties in Lactobacillus plantarum EPS (Nguyen et al., 2024).

Environmental factors influence structure; sucrose favors HoPS, glucose HePS.Table 1 summarizes classifications. Structural diversity enables tailored applications, from food texturizers to biomedical scaffolds (Liu et al., 2025).

Type	Subtype	Composition	Producers	Properties
HoPS	Glucans	Glucose	Leuconostoc mesenteroides	High viscosity, prebiotic
HoPS	Fructans	Fructose	Lactobacillus reuteri	Antioxidant, immunomodulatory
HePS	-	Glucose, Galactose, Rhamnose	Lactobacillus plantarum	Anti-inflammatory, anticancer
HePS	-	Mannose, Glucuronic acid	Bifidobacterium longum	Gut barrier enhancement, antimicrobial

Biosynthesis of EPS in Probiotic Bacteria

Biosynthesis of EPS in probiotic bacteria is a complex, energy-intensive process regulated by genetic and environmental factors. For HoPS, synthesis is extracellular, mediated by sucrase enzymes like levansucrase, using sucrose to form fructans (Jurášková et al., 2022). HePS biosynthesis follows the Wzx/Wzy-dependent pathway in LAB, starting with sugar nucleotide precursors (UDP-glucose, UDP-galactose) from glucose-1-phosphate. Glycosyltransferases assemble repeating units on lipid carriers, flipped by Wzx, polymerized by Wzy, and exported (Nguyen et al., 2024).

In Bifidobacterium, eps clusters include genes for chain length and export, with diversity from horizontal gene transfer (Salimi et al., 2024). Regulation involves eps operons responsive to stress; acidic conditions upregulate eps genes in Lactobacillus rhamnosus. Optimal conditions are 30-37°C, pH 5-6, high C/N ratios (Angelin and Kavitha, 2020).

Genetic engineering, such as overexpressing glycosyltransferases, boosts yields 2-5 fold. Agro-wastes like molasses enhance cost-effectiveness (Netrusov et al., 2023). EPS biosynthesis aids gut survival, protecting against bile and low pH. CRISPR editing could tailor EPS for specific activities (Liu et al., 2025).

Production and Optimization of EPS

Production involves batch or fed-batch fermentation in MRS broth with sugars, yielding 0.5-1.5 g/L for Lactobacillus plantarum (Zaghloul and Ibrahim, 2022). Optimization uses response surface methodology (RSM) for parameters like sucrose (2-5%), temperature (30°C), pH (6.0). Waste substrates (whey, fruit peels) achieve up to 20 g/L (Angelin and Kavitha, 2020).

Downstream processing: centrifugation, ethanol precipitation, dialysis, lyophilization. Purity assessed by phenol-sulfuric acid (Netrusov et al., 2023). Challenges: low HePS yields, variability. Genetic tools increase production (Jurášková et al., 2022). Sustainable approaches with marine isolates expand sources (Nguyen et al., 2024).

Physicochemical Properties of EPS

EPS show high viscosity, thermal stability (up to 100°C), water-holding capacity (>100 times weight). Pseudoplastic rheology forms gels at low concentrations (Liu et al., 2025). Solubility varies; neutral HoPS water-soluble, charged HePS form emulsions. Antioxidant capacity via reducing groups, DPPH scavenging up to 76% (Khalil et al., 2022).

SEM shows porous structures, EDX confirms C/O (Zaghloul and Ibrahim, 2022). Biocompatibility, biodegradability ideal for biomedical uses. Properties strain-specific (Salimi et al., 2024).

Health Benefits of EPS from Probiotic Bacteria

EPS offer antioxidant activity, scavenging ROS; Lactobacillus gasseri EPS inhibits DPPH 75% (Lee et al., 2022). Antimicrobial effects disrupt biofilms, inhibiting E. coli (Ayyash et al., 2021). Immunomodulatory properties boost cytokines, NK cells (Khalil et al., 2022).

Anti-inflammatory actions reduce TNF-α in IBD models (Miyamoto et al., 2023). Anticancer effects induce apoptosis in colon cancer (Salimi et al., 2024). Hypocholesterolemic, antidiabetic benefits lower cholesterol 70%, improve glucose tolerance (Angelin and Kavitha, 2020). Prebiotic role promotes microbiota (Nguyen et al., 2024).

Clinical trials confirm enhanced immunity, gut health (Liu et al., 2025).

Applications in the Food Industry

EPS prevent syneresis in yogurt, increase viscosity (Jurášková et al., 2022). In bakery, dextran improves dough, softness (Liu et al., 2025). Enhance low-fat products, prebiotics in functional foods (Netrusov et al., 2023). In situ production reduces additives. Edible films extend shelf life (Angelin and Kavitha, 2020).

Other Applications

In pharmaceuticals, EPS for drug delivery, wound healing (Zaghloul and Ibrahim, 2022). Cosmetics for moisturizing; environment for bioremediation (Nguyen et al., 2024). Agriculture for soil aggregation (Salimi et al., 2024).

Challenges and Future Perspectives

Challenges: low yields, costs, regulations. Future: genetic engineering, AI-optimized fermentation (Netrusov et al., 2023). Sustainable sources, clinical trials (Liu et al., 2025).

Conclusion

EPS from probiotic bacteria are versatile biopolymers with vast potential. Ongoing research will maximize their benefits (Jurášková et al., 2022).

References

1. Angelin, J., & Kavitha, M. (2020). Exopolysaccharides from probiotic bacteria and their health potential. *International Journal of Biological Macromolecules*, 162, 853–865. https://doi.org/10.1016/j.ijbiomac.2020.06.190
2. Netrusov, A. I., et al. (2023). Exopolysaccharides Producing Bacteria: A Review. *Microorganisms*, 11(6), 1541. https://doi.org/10.3390/microorganisms11061541
3. Zaghloul, E. H., & Ibrahim, M. I. A. (2022). Production and Characterization of Exopolysaccharide From Newly Isolated Marine Probiotic Lactiplantibacillus plantarum EI6 With in vitro Wound Healing Activity. *Frontiers in Microbiology*, 13, 903363. https://doi.org/10.3389/fmicb.2022.903363
4. Nguyen, H.-T., et al. (2024). Advances in Microbial Exopolysaccharides: Present and Future Applications. *Biomolecules*, 14(9), 1162. https://doi.org/10.3390/biom14091162
5. Khalil, M. A., et al. (2022). Exploring the Therapeutic Potentials of Exopolysaccharides Derived From Lactic Acid Bacteria and Bifidobacteria: Antioxidant, Antitumor, and Periodontal Regeneration. *Frontiers in Microbiology*, 13, 803688. https://doi.org/10.3389/fmicb.2022.803688
6. Miyamoto, J., et al. (2023). Host metabolic benefits of prebiotic exopolysaccharides produced by Leuconostoc mesenteroides. *Gut Microbes*, 15(1), 2161271. https://doi.org/10.1080/19490976.2022.2161271

7. Ayyash, M., et al. (2021). Exopolysaccharides as Antimicrobial Agents: Mechanism and Spectrum of Activity. *Frontiers in Microbiology*, 12, 664395. https://doi.org/10.3389/fmicb.2021.664395
8. Lee, M.-G., et al. (2022). Potential Probiotic Properties of Exopolysaccharide-Producing Lacticaseibacillus paracasei EPS DA-BACS and Prebiotic Activity of Its Exopolysaccharide. *Microorganisms*, 10(12), 2431. https://doi.org/10.3390/microorganisms10122431
9. Liu, W., et al. (2025). Lactic Acid Bacteria Exopolysaccharides Unveiling Multifaceted Insights from Structure to Application in Foods and Health Promotion. *Foods*, 14, 823. https://doi.org/10.3390/foods14050823
10. Salimi, F., et al. (2024). Bifidobacterium exopolysaccharides: new insights into engineering strategies, physicochemical functions, and immunomodulatory effects on host health. *Frontiers in Microbiology*, 15, 1396308. https://doi.org/10.3389/fmicb.2024.1396308
11. Jurášková, D., et al. (2022). Exopolysaccharides Produced by Lactic Acid Bacteria: From Biosynthesis to Health-Promoting Properties. *Foods*, 11(2), 156. https://doi.org/10.3390/foods11020156

Green Synthesis of Silver Nanoparticles from *Crossandra infundibuliformis* under magnetic and non-magnetic fields by two different extraction methods : characterization and bio evaluation

Farheen A. Khan[1], Varsha A Ghadyale[1*].
([1]Department of Biochemistry, Gogate Jogalekar College, Ratnagiri, India
*Corresponding Author Email: varsha.ghadyale@gjcrtn.ac.in)

Abstract

Green synthesis of silver nanoparticles (AgNPs) offers a sustainable alternative to chemical methods, minimizing toxic by-products and enhancing biocompatibility. This study employed aqueous and ethanolic leaf extracts of *Crossandra infundibuliformis* under magnetic and non-magnetic conditions to evaluate the influence of solvent systems and magnetic field exposure on AgNP synthesis and activity.

Nanoparticle formation was confirmed by colour change, FTIR with ethanolic extracts and magnetic exposure producing faster synthesis and stronger phytochemical involvement. Haemolysis assays indicated 85% red blood cell lysis, with ethanolic magnetic extracts showing higher activity, while magnetic treatment improved compatibility. Seed germination assays using *Vigna radiata* revealed that aqueous magnetic AgNPs significantly reduced root–shoot growth and biomass, whereas aqueous non-magnetic AgNPs had minimal phytotoxicity. Peroxidase is a stress-responsive enzyme. Changes in its activity in plant cells reflect nanoparticles induced oxidative stress.

Biological assays highlighted antimicrobial potential as the most significant outcome. AgNPs demonstrated strong inhibition against *Escherichia coli* and *Staphylococcus aureus*, with ethanolic magnetic nanoparticles producing the largest inhibition zones. In contrast, aqueous non-magnetic nanoparticles showed comparatively weaker activity.

These findings highlight that both solvent polarity and magnetic field exposure critically determine nanoparticle efficiency, with ethanolic magnetic AgNPs demonstrating superior antimicrobial potency but higher cytotoxicity. The work underscores the potential of *C. infundibuliformis* in eco-friendly nanotechnology and introduces magnetic field modulation as a novel strategy for tuning nanoparticle properties.

Keywords: Silver nanoparticles (AgNPs), *Crossandra infundibuliformis,* Magnetic field exposure, Cytotoxicity.

Introduction

Nanotechnology is one of the most rapidly advancing scientific domains of the 21st century, playing a pivotal role in revolutionizing materials science, medicine, agriculture, and environmental engineering. Among the many nanomaterials studied to date, silver nanoparticles (AgNPs) occupy a distinguished position. Silver nanoparticles exhibit excellent antimicrobial, antifungal, antiviral, antioxidant, and cytotoxic properties, which make them valuable in biomedical devices, coatings, wound dressings, drug delivery systems, and agricultural disease management. In addition, AgNPs possess optical properties such as surface plasmon resonance, which enhance their use in sensing and diagnostic technologies. (Rai et al., 2009; Panacek et al.,2006).In this context, green synthesis has emerged as a revolutionary method of producing nanoparticles. Compared to microbes, plants are more advantageous because they are widely available, cost-effective, and rich in diverse phytochemicals that act

both as reducing agents and stabilizers. Compounds like flavonoids, phenols, alkaloids, terpenoids, and reducing sugars present in plant extracts are capable of reducing silver ions (Ag^+) into silver nanoparticles while simultaneously capping them to prevent aggregation. This dual role ensures stability, uniformity, and biocompatibility of the synthesized nanoparticles. (Geoprincy et al.,2013; Kavitha et al.,2004).The present project employs *Crossandra infundibuliformis*, a flowering ornamental plant also known for its medicinal potential, as the bio-reducing agent. While this plant has traditionally been studied for its aesthetic and medicinal value, its role in nanotechnology remains relatively unexplored. Its phytochemical richness makes it an excellent candidate for nanoparticle synthesis. By utilizing both ethanolic and aqueous extracts of *Crossandra Infundibuliformis* leaves, this project captures the contribution of different classes of phytoconstituents toward nanoparticle formation. (Govindraju et al.,2010; Ahmed et al.,2011)an additional novel aspect of this study is the application of magnetic fields during the synthesis process (Geoprincy et al.,2013). Research has suggested that external factors such as light exposure, pH, and magnetic or electric fields can influence the kinetics of nanoparticle nucleation and growth. The presence of a magnetic field may alter the orientation of molecules, change ionic interactions, and affect the stability of colloidal systems. Although such influences remain underexplored, incorporating magnetic field exposure provides a new dimension to nanoparticle synthesis.

Methodology

3.1.Preparation of Plant Extracts

3.1.1Collection and Processing of Plant Material:

Fresh leaves of *Crossandra infundibuliformis* were collected and identified by help of botany department Gogate Jogalekar college Ratnagiri, India. Leaves were thoroughly washed with distilled water to remove dust and surface contaminants, and shade dried at room temperature. The dried leaves were powdered using a clean grinder.

3.1.2Aqueous Extract Preparation:

About 10 g of powdered leaves were boiled with 100 ml distilled water for 30 minutes, cooled, and filtered using Whatman No. 1 filter paper. The filtrate was stored at 4°C until further use.

3.1.3Ethanolic Extract Preparation:

About 10 g of powdered leaves were soaked in 100 ml ethanol (95%) for 24–48 hours with occasional shaking. The solution was filtered and stored at 4°C until use.

3.1.4 Synthesis of Silver Nanoparticles

Silver nitrate ($AgNO_3$) solution was prepared freshly(1 mM). $AgNO_3$ solution and each extract (aqueous and ethanolic) were mixed in 3:1 ratio. For magnetic field synthesis, a simple bar magnet was placed beneath the reaction vessel throughout the synthesis period. Non-magnetic synthesis, the reaction was carried out without a magnet. All solutions were kept for 72 hrs in dark condition. Colour change of the solution (pale yellow to dark brown) was taken as preliminary evidence for nanoparticle formation. Synthesis was confirmed visually. Studies were done in four comparative Groups: (i)Aqueous extract – Magnetic field(AM), (ii)Aqueous extract – Non-magnetic(ANM), (iii)Ethanolic extract – Magnetic field(EM),(iv)Ethanolic extract – Non-magnetic(ENM). Particles were collected after centrifugation, giving numerous washing with distilled water. Nanoparticles were dried and dissolved in dimethyl sulfoxide solution (1mg in 10 µl). 100mg of particles dissolved in 100ml distilled water with help of sonication (Orchid scientific).

3.2 Fourier Transform Infrared Spectroscopy (FTIR) and TLC

Water samples were analysed by FTIR(Bruker alpha 11). A control spectrum of $AgNO_3$ solution was also obtained for comparison.

3.3 Haemolysis Assay

Fresh RBC suspension was prepared in saline. Different nanoparticle solutions (all four groups) were incubated with RBC suspension. (Saiqa A. et., 2020)

3.4Phytotoxicity Assay

Seeds of *Vigna radiata* were grown in test solutions of nanoparticles (all four groups). Distilled water was used as control. Germination percentage, root and shoot length ,cell biomass (fresh weight of germinated seedlings), protein content and peroxidase activity were studies (Bhushan B. et. Al. 2014) Seeds were grown on cotton bead soaked with water solution of 20 ml contains 20mg AgNPs concentration .Germination assay was done for 3 days .

3.4.1Peroxidase Activity and Protein activity Assay:

Activity measured using guaiacol and hydrogen peroxide as substrates. Plant extracts treated with nanoparticles were incubated with guaiacol (0.5%v/v)H_2O_2(30%). Formation of brown-coloured products indicated peroxidase activity. Colour intensity measured at 420 nm (Chance B. & Maehyl, A. C. (1955).Lowry method was used for protein content determination (Waterborg ,J. H. (2009).

Vigna Radiata were grown in the sample solutions and distilled water was used as control. The comparison in growth of root and shoot was done. (Rajkuberan C. et.al., 2015), (Kim, et.al., 2011), (Andleeb S. et. Al., 2020)

3.5 Antimicrobial Assay: Antimicrobial assay was performed per Jain and Mehata 2017. (Jain, S., & Mehata, S. 2017)

Results and discussion :

4.1 Synthesis and Yield of Silver Nanoparticle:

The formation of silver nanoparticles was evident by a gradual change in the solution colour from pale yellow to brown. Both aqueous and ethanolic extracts of *Crossandra infundibuliformis* facilitated this transformation, but the ethanolic extract showed a faster and more intense colour change, reflecting its higher content of reducing phytochemicals(Fig 1). Under magnetic field exposure, the colour development occurred more rapidly and produced a darker brown shade compared to the non-magnetic condition, suggesting an influence of magnetic fields on the kinetics and stability of nanoparticle formation. The obtained in yield in four group AM, ANM, EM, ENM was 54mg, 85mg,100mg,99mg respectively.

4.2 FTIR Analysis :

The biomolecules present in plant extract responsible for the reduction of silver ions to AgNPs were identified by FTIR analysis. FTIR spectra of AgNP show board O-H stretching (3300-3320cm^{-1}). Prominent aromatic bands are observed at 1600cm^{-1} while carbonyl at 1700-1720cm^{-1}. Magnetic -condition syntheses induced shifts in several bands consistent with phytochemical silver interaction under magnetic conditions.

4.3. Haemolysis Assay

The haemolysis assay revealed that silver nanoparticles had a measurable effect on red blood cell (RBC) integrity(Fig3). The positive control (distilled water with RBC) resulted in complete haemolysis, while the negative control (saline with RBC) showed no haemolysis. All four nanoparticle groups induced partial haemolysis, though the degree varied. Nanoparticles synthesized with ethanolic extracts show higher haemolytic activity compared to aqueous extracts, reflecting stronger interactions with cell membranes. Interestingly, magnetic field-treated nanoparticles exhibited slightly higher haemolysis compared to their non-magnetic counterparts.

4.4.1 Phytotoxicity assay

Silver Nanoparticles can have both positive and negative effects on growth of germinating seeds, depending on their concentration , size , coating and exposure time. AgNPs can enter seed coats and root tissues altering water uptake and nutrient transport. The germination rate was 100% in all seeds.

Root, shoot growth halted after the treatment of all silver nanoparticles. (Table1) Root and also shoot growth was majorly affected by aqueous magnetic AgNPs. AM shows major reduction in growth as well as cell mass. AgNPs can enter seed coats and root tissues altering water uptake and nutrient transport.

4.4.2 Peroxidase Activity and protein content

Peroxidase is one of the major stress enzymes. Increase in the activity observed in EM And ENM while decrease in activity observed in AM and ANM. AM extract also shows 80% reduction in cell mass . Decrease in peroxidase activity is due to less protein content.

4.5Antimicrobial Assay

It is well known that AgNPs have a higher surface to volume ratio as compared to their bulk counterpart. Therefore, some interactions with the bacterial surfaces are facilitated, and antibacterial property of AgNPs is enhanced. Reports show that the interaction of AgNPs with the sulphur and phosphorus containing constituents of the bacterial cell initiates cell killing by attacking the respiratory chain and cell division (Rai et al., 2009). Also, it was seen from disk diffusion method (Table.3 and Fig.4) that AgNPs synthesized using all four-extraction methods had antibacterial activity, but gram-positive growth more inhibited compared to Gram negative bacteria. Both aqueous as well as ethanolic magnetic AgNPs show more inhibition compared to nonmagnetic .

Observations :

5.1. Synthesis of Silver Nanoparticles :

(a) (b) (c) (d)

Fig 1: Synthesis of nanoparticles (a) EM (b) ENM (c)AM (d)ANM

5.2. FTIR Characterization :

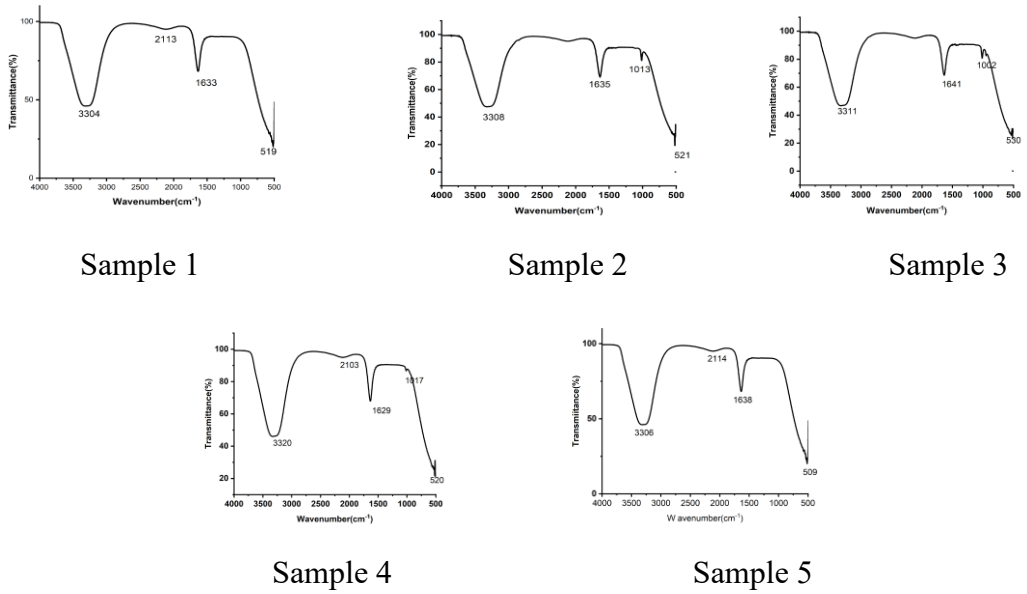

Sample 1 Sample 2 Sample 3

Sample 4 Sample 5

Fig 2 : Characterization of silver synthesised silver nanoparticles
(sample 1) ANM, (sample 2) ENM, (sample 3)AM, (sample 4) EM, (sample 5) Control.

5.3 . Haemolysis:

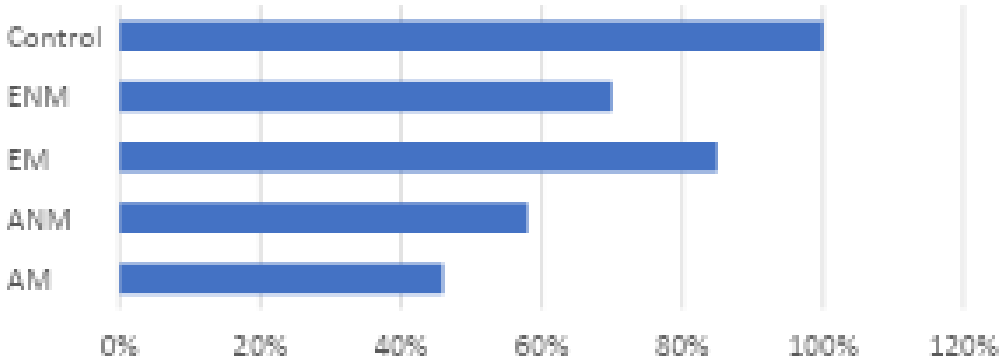

Fig 3 : Percent haemolysis

5. 4 . Phytotoxicity Assay :

4.4.1. Root Shoot Ratio and Cell Biomass

Table 1: Statistical Analysis of Root Shoot Assay

SAMPLE	ROOT		SHOOT		CELL BIOMASS
	MEAN	RSD	MEAN	RSD	
AM	0.9 ± 0.09	10	1.09 ± 0.14	12.84	2.380
ANM	2.93 ± 0.55	18.77	3.14 ±0.42	13.3	3.072
EM	4.2 ± 0.40	9.52	4.31 ±0.25	5.8	3.396
ENM	2.59 ±0.48	18.53	3.01 ± 0.61	20.2	2.250
DISTILLED WATER	4.4±0.38	8.63	8.58 ± 0.48	5.59	4.240

5.4.2 Peroxidase Activity and Protein Estimation

Table 2 : Peroxidase activity and Enzyme Estimation

Sample	Peroxidase activity	Enzyme protein
AM	16.91	0.9
ANM	10.15	2.7
EM	22.55	1.8
ENM	21.80	2.7
DISTILLED WATER	19.92	4.5

5.6 Antimicrobial Activity :

Table 3 : Inhibition zones by agar well diffusion

Sample Name	E. coli		S. Aureus	
	0.4 mg	0.8 mg	0.4 mg	0.8 mg
AM	1.3	1.5	2.1	2.3
ANM	1.4	1.6	2.3	2.5
EM	1.6	1.7	2.2	2.4
ENM	1.4	1.5	2.3	2.5

(a) (b)

Fig 4 : Zone of Inhibition observed by Agar well Diffusion. (a) *E. coli* (b) *S. aureus* .

Conclusion

The present study successfully demonstrated the green synthesis of silver nanoparticles (AgNPs) using aqueous and ethanolic extracts of Crossandra infundibuliformis leaves, under both magnetic and non-magnetic field conditions. This comparative approach allowed the assessment of how extract type and external magnetic exposure influence nanoparticle synthesis and their subsequent biological properties. The initial confirmation of nanoparticle formation was evident through a visual colour change, followed by characterization using TLC And FTIR, which confirmed the involvement of phytochemicals and the successful reduction of silver ions into nanoparticles.

Comparative studies showed that ethanolic extract generally exhibited higher activity than Aqueous extract, and the application of magnetic field showed subtle but distinct variation in Nanoparticles , as reflected in assays and phytochemical mobility.

Biological assays, including haemolysis, cytotoxicity, root-shoot ratio, peroxidase activity, Protein estimation, and antimicrobial activity, indicated that the synthesized nanoparticles possess significant bioactive potential. While haemolysis and cytotoxicity highlighted Concentration-dependent cellular effects, the antimicrobial assays confirmed notable inhibition Against E. coli and S. aureus.

Overall, this project establishes Crossandra infundibuliformis as a promising plant source for Eco-friendly nanoparticle synthesis, with both material and biological relevance. The observed influence of magnetic field treatment opens new perspectives in tailoring nanoparticle properties for biomedical, agricultural, and environmental applications.

References:

1. Ahmed, N., et al. (2011). Biosynthesis of silver nanoparticles from Desmodium triflorum: A novel approach towards weed utilization. Biotechnology Research, 3, 275–277.
2. Ananda Babu, S., & Gurumallesh Prabu, H. (2011). Synthesis of AgNPs using the extract of Calotropis procera flower at room temperature. Department of Industrial Chemistry, 65, 1675–1677.
3. Andleeb, S., et al. (2020). In vitro bactericidal, antidiabetic, cytotoxic, anticoagulant, and hemolytic effect of green-synthesized silver nanoparticles using Allium sativum clove extract. Green Processing and Synthesis, 9(1), 538–553.
4. Banerjee, P., et al. (2014). Leaf extract mediated green synthesis of silver nanoparticles from widely available Indian plants: Synthesis, characterization, antimicrobial property, and toxicity analysis. Bioresources and Bioprocessing, 1(3).
5. Baskaralingam, V., Lin, Y. C., & Chen, J. C. (2012). Green synthesis of silver nanoparticles through Calotropis gigantea leaf extract and evaluation of antibacterial activity against Vibrio alginolyticus. Nanotechnology Development, 2(e3).
6. Bhushan, B., et al. (2014). Evaluation of post-germinative lipid peroxidation and enzymatic antioxidation potential in lead absorbing oat (Avena sativa) seedlings. Journal of Environmental Biology, 36, 279–288.
7. Chance, B., & Maehly, A. C. (1955). Assay of catalases and peroxidases. Methods in Enzymology, 2, 764–775.
8. Geethalakshmi, R., & Sarada, D. V. L. (2010). Synthesis of plant-mediated silver nanoparticles using Trianthema decandra extract and evaluation of their antimicrobial activities. International Journal of Engineering Science and Technology, 2(5), 970–975.
9. Geoprincy, G., et al. (2013). A review on green synthesis of silver nanoparticles. Asian Journal of Pharmaceutical and Clinical Research, 6, 314–318.
10. Govindaraju, K., et al. (2010). Biogenic silver nanoparticles by Solanum torvum and their promising antimicrobial activity. Journal of Biopesticides, 3(1), 394–399.
11. Harekrishna, B., et al. (2009). Green synthesis of AgNPs using latex of Jatropha curcas.Colloids and Surfaces A: Physicochemical and Engineering Aspects, 134–139.
12. Jain, S., & Mehata, S. (n.d.). Medicinal plant leaf extract and pure flavonoid mediated green synthesis of silver nanoparticles and their enhanced antibacterial property. Scientific Reports.
13. Kavitha, K. S., et al. (2013). Plants as green sources towards synthesis of nanoparticles. International Research Journal of Biological Sciences, 2(6), 66–76.

14. Kim, S.-H., et al. (2011). Antibacterial activity of silver nanoparticles against Staphylococcus Aureus and Escherichia coli. Korean Journal of Microbiology and Biotechnology, 39(1), 77–85.
15. Mohamed, N. H., et al. (2014). Antimicrobial activity of latex silver nanoparticles using Calotropis procera. Asian Pacific Journal of Tropical Biomedicine, 4, 876–883.
16. Morones, J. R., et al. (2010). The bactericidal effect of silver nanoparticles. Department of Chemical Engineering, 16, 2346–2353.
17. Nagajyothi, P. C., & Lee, K. (2011). Synthesis of plant-mediated nanoparticles using Dioscorea Batatas rhizome extract and evaluation of antimicrobial activities. Journal of Nanomaterials, 2, 573–429.
18. Okafor, F., et al. (n.d.). Green synthesis of silver nanoparticles, their characterization, Applications and antibacterial activity. International Research and Public Health. ISSN 1660-4601.
19. Panacek, A., et al. (2006). Silver colloid nanoparticles: Synthesis, characterization, and their Antibacterial activity. Journal of Physical Chemistry B, 110, 16248–16253.
20. Rai, M., Yadav, A., & Gade, A. (2009). Silver nanoparticles as a new generation of Antimicrobials. Biotechnology Advances, 27(1), 76–83.
21. Rajkuberan, C., et al. (2015). Antibacterial and cytotoxic potential of silver nanoparticles Synthesized using latex of Calotropis gigantea L. Spectrochimica Acta Part A: Molecular and Biomolecular Spectroscopy, 136, 924–930.
22. Schagal, R., Roy, S., & Kumar, V. L. (2006). Evaluation of cytotoxic potential of latex of Calotropis procera and podophyllotoxin in Allium cepa root model. Department of Pharmacology, All India Institute of Medical Sciences, 30(1), 9–13.
23. Shankar, S. S., et al. (2004). Biosynthesis of silver and gold nanoparticles from extracts of Different parts of Geranium plant. Applications in Nanotechnology, 1, 69–77.
24. Sivakumar, J., et al. (2011). Biosynthesis of silver nanoparticles using Calotropis gigantea leaf. African Journal of Basic and Applied Sciences, 3, 265–270. ISSN 2079-2034.
25. Trimalai, A. V., et al. (2010). Stable silver nanoparticles synthesizing methods and their Application. ISSN 0976-2272, 1(4), 259–270.
26. Waterborg, J. H. (2009). The Lowry method for protein quantification. In J. M. Walker (Ed.), The protein protocols handbook (3rd ed., pp. 7–10). Humana Press.
27. Yesmin, M. N., et al. (2008). Antioxidant and antibacterial activity of Calotropis procera Linn. American-Eurasian Journal of Agricultural and Environmental Science, 4(5), 550–553.

PHYTOCHEMICAL AND PHARMACOLOGICAL POTENTIAL OF *FLUEGGEA LEUCOPYRUS*: A SCIENTIFIC EVALUATION OF TRADITIONAL PHYTOMEDICINE

Rutuja R. Kanetkar[1], Shweta O. Patwardhan[1]*
([1]Department of Biochemistry, Gogate Jogalekar College, Ratnagiri, India)
*Corresponding Author Email: shweta.patwardhan@gjcrtn.ac.in
Contact No.: 8087330437

ABSTRACT

Medicinal plants have long served as pillars of traditional healthcare systems, offering a rich source of bioactive compounds with therapeutic relevance. In the present study, *Flueggea leucopyrus* was investigated through a series of biochemical and pharmacological assays to establish a link between its phytochemical composition and biological activity. Through comprehensive biochemical and pharmacological assays, the plant demonstrated potent antioxidant and antibacterial activities. Preliminary phytochemical screening revealed the presence of flavonoids, phenolics, tannins and proteins—compounds historically associated with healing properties in traditional phytomedicine. The DPPH assay confirmed moderate free radical scavenging activity (IC_{50}=131µg/ml), aligning with the high flavonoid content. Antibacterial assays showed higher inhibitory effects against Gram positive bacterial strains, reinforcing the plant's traditional use in treating infections. Protein quantification via Lowry's method suggested nutritional and functional contributions to bioactivity. Additionally, moderate tyrosinase inhibition (56%) linked the plant's antioxidant profile to dermatological applications, echoing its use in skin-related treatments in folk medicine. These findings underscore the multifaceted pharmacological potential of *Flueggea leucopyrus* and affirm its value in traditional knowledge systems, bridging ancestral wisdom with modern scientific validation.

Keywords: *Flueggea leucopyrus*, Phytochemicals, Antioxidant activity, Tyrosinase inhibition

INTRODUCTION

Since ancient times, plants have played a vital role in human life by providing food, shelter and natural remedies. Traditional knowledge of their healing properties forms the foundation of many indigenous medical systems such as Ayurveda. Medicinal plants are rich in bioactive compounds like alkaloids, flavonoids, tannins, phenols and proteins, which exhibit antioxidant, antimicrobial, anti-inflammatory and enzyme inhibitory activities. Scientific validation of these phytochemicals is essential to integrate their therapeutic potential into modern medicine (Lobo et al., 2010; Rice-Evans et al., 1997).

*Flueggea leucopyrus (*Willd.), also known as *Securinega leucopyrus*, from the family *Phyllanthaceae*, is a medicinal shrub native to tropical regions such as Sri Lanka, South Asia, Australia and Malaysia. Traditionally used in Ayurveda and Sri Lankan folk medicine to treat fever, infections and inflammation, its leaves are also used for cancer, ulcers, epilepsy and jaundice (Vajira et al., 2020). The plant exhibits antioxidant, antibacterial and anti-inflammatory properties (Vijaykumar et al., 2024) and its potential as a natural tyrosinase inhibitor links it to the cosmetic and dermatological industries (Parvez et al., 2007; Chang, 2009; Thanigaimalai et al., 2017). The present study evaluates the phytochemical, antioxidant (DPPH), flavonoid, chlorophyll, protein, tyrosinase inhibition and antibacterial properties of *F.*

leucopyrus, highlighting its pharmaceutical, nutraceutical and industrial significance (Kamble et al., 2015; Cowan, 1999; Lowry et al., 1951).

Overall, this research aims to provide a scientific basis for the traditional uses of *Flueggea leucopyrus* and to explore its potential as a source of natural bioactive compounds for future therapeutic and industrial applications.

METHODOLOGY

Collection of Plant Material:

Fresh leaves of *Flueggea leucopyrus* were collected from Phansop, Ratnagiri (16.99° N, 73.31° E; altitude 80 m). According to IMD data, the region's average temperature was 29 ± 2 °C and humidity 80–85 %. The plant was authenticated by a botanist and a voucher specimen was preserved for reference (Fig.1).

Figure 1: Plant Material

Preparation of Extracts:

The collected leaves and berries were thoroughly washed with distilled water to remove any impurities. Leaves were then shade-dried at room temperature to preserve heat-sensitive compounds. Once fully dry, the leaves were separately ground into a fine powder. The powder from the leaves weighed 12g. These powders were stored in airtight containers in a cool, dark environment until they were used to prepare methanolic extract by soxhlet apparatus. Analyses were performed under controlled conditions using Borosil® glassware, with temperature 25 ± 2 °C and relative humidity 60 ± 5 %.

Qualitative Phytochemical Screening:

Standard protocols were followed to detect the presence of major secondary metabolites. Molisch's test for Carbohydrates, Mayer's test and Wagner's test for Alkaloids, Lead acetate test for Flavonoids, Tannin test for Tannins, Ferric chloride test for Phenols and Ninhydrin test Amino acids were performed qualitatively (Bulugahapitiya et. al., 2020). All phytochemical screening tests were performed in triplicate under 25 ± 2 °C temperature and 60 ± 5% relative humidity to maintain uniform analytical conditions.

DPPH Radical Scavenging Assay:

A 0.5 mM DPPH solution was prepared using 5 ml of methanol. To this, varying concentrations (1–5 µg/ml) of standard ascorbic acid were added. The mixture was shaken gently and kept in the dark at room temperature (approximately 20°C) for 30 minutes. After incubation, the absorbance was measured at 515 nm using a UV-Vis spectrophotometer. Methanol served as the blank and DPPH solution without ascorbic acid was used as the control. The change in color from deep violet to pale yellow indicated the scavenging of DPPH radicals.

Formula:

$$\% \text{ free radical scavenging activity} = \frac{Control\ OD - Sample\ OD}{Control\ OD} \times 100$$

Results were recorded for each concentration of ascorbic acid to determine dose-dependent antioxidant activity. A control and a blank were used to correct for the background color of the plant extract, ensuring accurate readings (Bulugahapitiya et. al., 2020). The DPPH assay was carried out in triplicate at 25 ± 2 °C and 60 ± 5% relative humidity, maintaining stable conditions for accurate colorimetric readings.

Flavonoid content:

Flavonoid content was performed by the aluminum chloride colorimetric method. Test tubes were set as test, standard (quercetin) and blank. 0.3mL of 5% sodium nitrate, 10% $AlCl_3$ and distilled water to make 6 mL. After incubation in the dark for 10-20 minutes, absorbance was measured at 570 nm (Cushine et. al., 2005). The assay was performed in triplicate under controlled laboratory conditions of 25 ± 2 °C temperature and 60 ± 5% relative humidity to ensure accuracy and reproducibility.

Chlorophyll assay:

One gram of leaf sample was homogenized in 20 mL of 80% acetone, kept at 4°C for 24 h in the dark, filtered and centrifuged at 3000 rpm for 15 min. The supernatant volume was made up to 100 mL and chlorophyll content was measured at 645 nm and 663 nm using 80% acetone as blank (APHA, 1989). The chlorophyll estimation was conducted in triplicate under 25 ± 2°C temperature and 60 ± 5% relative humidity to ensure reproducible pigment readings (Kamble et. al., 2015).

Formula:

$$\text{Chl a} = 11.75 \times A662.6 - 2.35 \times A645.6$$

$$\text{Chl b} = 18.61 \times A645.6 - 3.96 \times A662.6$$

Where, Ca and Cb are the chlorophyll a and chlorophyll b, A is absorbance.

Tyrosinase Inhibition Assay Using Germinating Jackfruit Seeds:

Tyrosinase inhibition assays were performed using l-DOPA as the substrate. The total reaction volume was 1000 µL and the assay was conducted under the following conditions:

1. Phosphate buffer: 0.05 M, pH 7.0, used as the reaction medium.
2. l-DOPA solution: Prepared by dissolving 0.1 g of l-DOPA in 10 mL of phosphate buffer.
3. Plant extract: Methanolic extract of the plant was evaporated and reconstituted in DMSO to a stock concentration of 1 mg/4 mL
4. Extract volumes used: 5 µL and 10 µL, corresponding to final concentrations of 0.25 mg/mL and 0.50 mg/mL, respectively.
5. Enzyme source: Germinating jackfruit seeds were crushed and extracted enzyme was used as the tyrosinase source.

The crude extract was obtained by centrifugation at cooling conditions for 20 minutes. After the addition of l-DOPA, the reaction mixture was immediately monitored using a colorimeter at 492 nm, measuring dopachrome formation as an indicator of tyrosinase activity. Background absorbance readings were recorded for each concentration to ensure accurate inhibition calculations. Percentage inhibition of tyrosinase activity was calculated based on absorbance values (Ghadyale et. al., 2018). Tyrosinase inhibition assay was performed in triplicate under 25 ± 2 °C temperature and 60 ± 5% relative humidity to maintain enzyme stability and result consistency.

Protein estimation by Folin-Lowry method:

The protein content of *Flueggea leucopyrus* extract was estimated by the Folin–Lowry method. This method is based on the reaction of proteins with copper ions in alkaline medium (Biuret reaction), followed by the reduction of the Folin–Ciocalteu reagent by aromatic amino acids to produce a stable blue color. Standard protein solutions of Bovine Serum Albumin (0.2–1.0 mg/ml) were prepared along with a blank and the plant extract samples. To each tube, alkaline $CuSO_4$ reagent was added, mixed well and allowed to stand for 15 minutes, after which Folin–Ciocalteu reagent was added and incubated for 20 minutes at room temperature. The absorbance of all tubes was measured at 660 nm. A standard calibration curve of absorbance versus protein concentration was plotted and the protein concentration of the *Flueggea leucopyrus* extract was determined from this graph (Thirumal et. al., 2024). The assay was performed in triplicate under controlled laboratory conditions of 25 ± 2 °C temperature and 60 ± 5% relative humidity to ensure accuracy and reproducibility.

Antibacterial assay:

Antibacterial assay was performed by agar well diffusion method against two strains namely: Gram-positive bacteria (staphylococcus aurous) and Gram-negative bacteria (Escherichia coli). Methanolic extract of the plant was evaporated and reconstituted in DMSO to a stock concentration of 1 mg/4 mL (Cowan et.al 1999). All glassware and media used for the antibacterial assay were properly sterilized before use to avoid contamination. The assay was performed in triplicate under controlled laboratory conditions of 25 ± 2 °C temperature and 60 ± 5% relative humidity to ensure accuracy and reproducibility.

RESULT AND DISCUSSION

1. Phytochemical Analysis:

Phytochemical analysis revealed the presence of tannins, alkaloids, flavonoids, phenols and carbohydrates. Tannins possess antimicrobial, antioxidant and astringent properties that promote wound healing and infection protection. Phenols show strong antioxidant and anti-inflammatory activity, neutralizing free radicals. Flavonoids exhibit antioxidant, antimicrobial, anti-inflammatory and anticancer effects, enhancing the plant's therapeutic potential. Alkaloids display analgesic, antimicrobial and pharmacological actions through enzyme and receptor interactions. Carbohydrates act as energy sources and support the stability and solubility of bioactive compounds. The absence of amino acids suggests limited nutritional or protein-related bioactivity, while the lack of glycosides indicates the plant may not exhibit cardiotonic or glycoside-associated therapeutic effects.

2. DPPH Antioxidant Assay:

With an IC_{50} of 131µg/ml, falls within moderate range. The extract demonstrates notable free radical scavenging activity, suggesting its usefulness as a natural antioxidant in health, cosmetic and industrial applications.

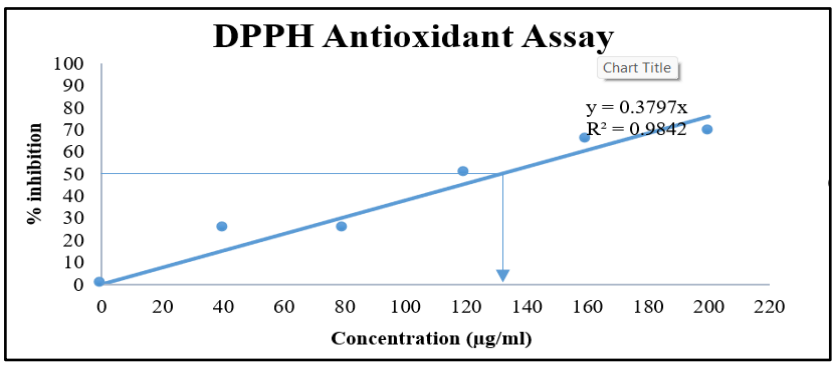

Graph 1: DPPH Antioxidant Assay

3. Flavonoid Content:

The total flavonoid content of the sample was estimated using the standard method. The concentration was found to be 0.89 µg/mL (expressed as quercetin equivalents). Flavonoids are important secondary metabolites with antioxidant, anti-inflammatory, antimicrobial and anticancer properties that enhance the therapeutic value of medicinal plants. The moderate flavonoid content in the sample suggests the presence of bioactive compounds and even in small amounts, they may contribute to free radical scavenging, enzyme inhibition and potential pharmacological use.

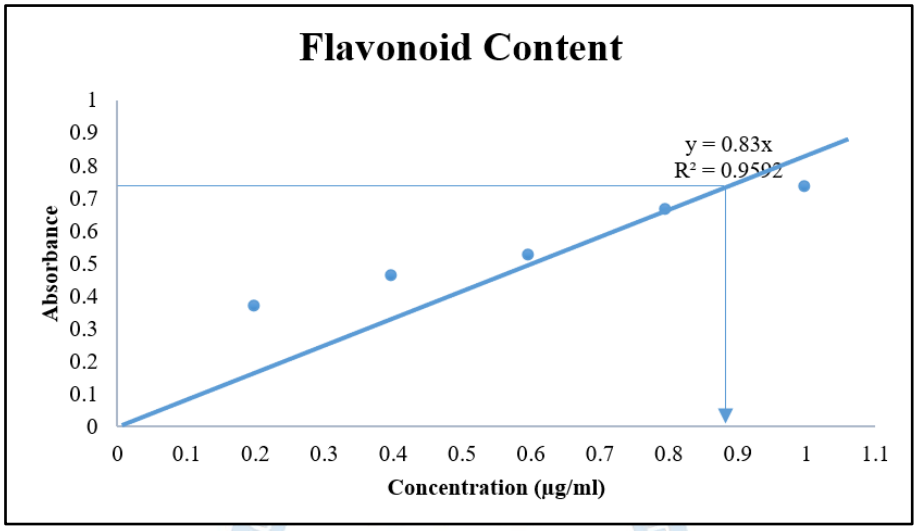

Graph 2: Flavonoid Content

4. Chlorophyll Assay:

The concentration of chlorophyll pigments in the analyzed sample showed higher chlorophyll a (23.95 mg/m³) than chlorophyll b (5.78 mg/m³), with a ratio of 4.1:1, falling within the typical range for higher plants (3:1–5:1). Chlorophyll a is the main pigment for light capture, while chlorophyll b acts as an accessory pigment. These values indicate healthy pigment composition, efficient photosynthesis and normal plant physiological status.

5. Antibacterial Activity:

The test sample showed antibacterial activity against S. aureus with a zone of 2.0–2.3 cm, while E. coli was not inhibited. The test plant showed antibacterial activity against Staphylococcus aureus, a common pathogen responsible for skin infections, woundsand boils. The observed inhibition (2.0–2.3 cm) suggests that the plant contains bioactive compounds capable of suppressing bacterial growth, supporting its potential use in topical treatments to prevent or heal skin infections. Such activity highlights its relevance in developing herbal or natural remedies for wound care.

Fig.2: Zone of inhibition: *S. aureus*

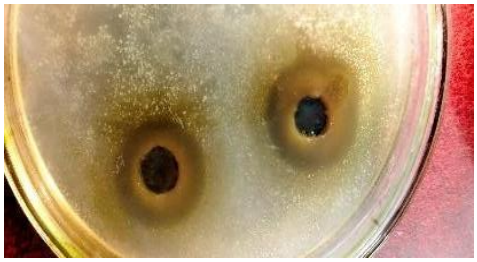

Fig.3: Zone of inhibition: *E. coli*

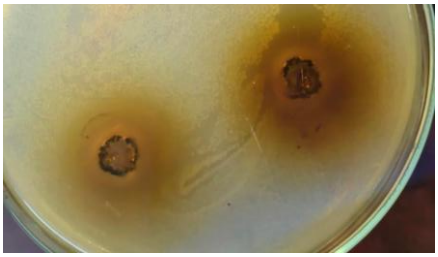

Protein Estimation:

The Lowry method showed a protein content of 0.066 mg/mL, indicating low to moderate levels. Even at this concentration, proteins may contribute to enzyme activity and bioactive properties, supporting the sample's functional potential.

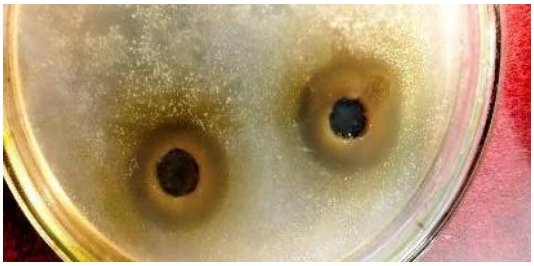

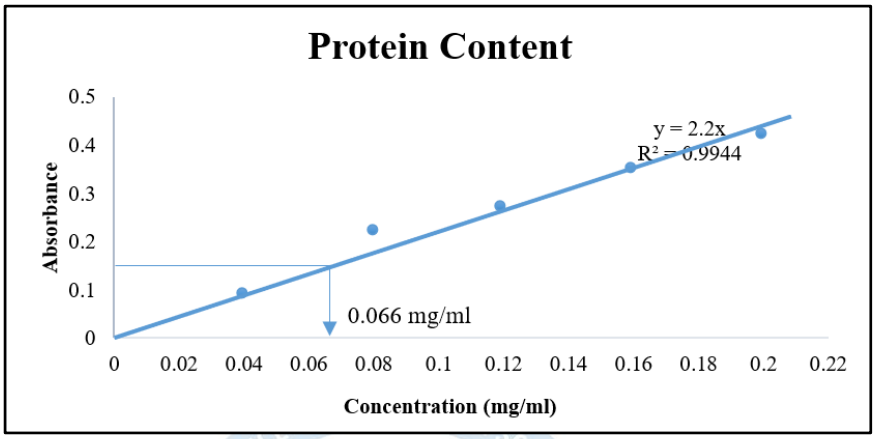

Graph 3: Protein Content

6. Tyrosinase inhibition Assay:

The same test sample was analyzed at two concentrations to check tyrosinase inhibition. At the lower concentration, inhibition was 12%, while at the higher concentration, inhibition increased to 56%. Increase in the tyrosinase inhibition indicates dose-dependent activity and potential use in skin-whitening and anti-browning applications.

CONCLUSION

The phytochemical screening revealed the presence of tannins, phenols, flavonoids, alkaloids and carbohydrates, indicating that the plant is rich in bioactive compounds with potential therapeutic applications. The absence of amino acids and glycosides suggests limited nutritional or glycoside-related pharmacological effects. The DPPH IC_{50} value within the moderate antioxidant range indicates effective free radical scavenging. This highlights its significance in reducing oxidative stress and supports potential applications in pharmaceuticals, cosmetics and food industries as a natural antioxidant. Moderate flavonoid content indicates the presence of bioactive compounds suggests that the plant has therapeutic potential and may be a source of natural compounds for pharmacological applications.

The analyzed sample was with a ratio of 4.1 (chlorophyll a):1(chlorophyll b). These results indicate a normal chlorophyll composition, suggesting the plant is physiologically healthy and capable of effective photosynthesis also may have potential for pharmaceutical applications, such as antioxidant, anti-inflammatory or therapeutic formulations. The plant extract showed effective antibacterial activity against *Staphylococcus aureus* but not significant against *E. coli*. These results indicate that the extract has potential as a topical agent for treating Gram-positive bacterial infections, particularly skin and wound infections**.**

The protein content confirms the presence of bioactive proteins, indicating potential use in enzyme inhibition studies, pharmacological evaluations and development of bioactive

formulations in research or industrial applications. The test sample demonstrated dose dependent tyrosinase inhibition, increasing from 12% at low concentration to 56% at high concentration. This indicates the presence of bioactive compounds with potential applications in cosmetic and food industries, particularly for skin-whitening and anti-browning purposes. The inhibition falls within the moderate range reported for plant extracts, highlighting its practical significance as a natural enzyme inhibitor.

Flueggea leucopyrus from the present study exhibited notable phytochemical presence, antioxidant, enzyme-inhibition activities and selective antibacterial effects, demonstrating its potential as a bioactive plant for therapeutic and industrial applications. Further study on other parts of the same plant will help provide more conclusive insights and is open for further investigation.

REFERENCES:

1. Bulugahapitiya, V. P., & Munasinghe, A. A. M. B. (2020). Phytochemical profile, proximate composition and antioxidant properties of *Flueggea leucopyrus* (Willd), a plant used as complementary and alternative medicine by cancer patients in Sri Lanka. Vingnanam Journal of Science, 15(1), 19–26.
2. Cowan, M. M. (1999). Plant products as antimicrobial agents. Clinical Microbiology Reviews, 12(4), 564–582. https://doi.org/10.1128/CMR.12.4.564
3. Cushine, T. J., & Pomeranz, B. (2005). Role of phenolics in antioxidant activity of plant extracts. Journal of Agricultural and Food Chemistry, 53(14), 5472–5479. https://doi.org/10.1021/jf0502269
4. Ghadyale, V. A. (2018). Steam distillate of Murraya koenigii as a tyrosinase activator. Journal of Enzyme Inhibition and Medicinal Chemistry, 33(1), 1–7.
5. Kamble, P. N., Giri, S. P., Mane, R. S., & Tiwana, A. (2015). Estimation of chlorophyll content in young and adult leaves of some selected plants. Universal Journal of Environmental Research and Technology, 5(6), 306–310.
6. Lobo, V., Patil, A., Phatak, A., & Chandra, N. (2010). Free radicals, antioxidants and functional foods: Impact on human health. Pharmacognosy Reviews, 4(8), 118–126. https://doi.org/10.4103/0973-7847.70902
7. Mayakrishnan, V., Thirupathi, A., & Singaravelu, A. (2024). Chemical composition analysis and assessment of antioxidant and anti-inflammatory properties of *Flueggea leucopyrus* leaves and roots. Antioxidants, 13(8), 976.
8. P S, S. L., Thirumal, M., & Babu, T. K. (2024). Phytochemical and pharmacological studies of different extracts of stem bark and leaf of *Flueggea leucopyrus* Willd. Pharmacognosy Journal, 16(6), 1281–1289.
9. Pietta, P. G. (2000). Flavonoids as antioxidants. Journal of Natural Products, 63(7), 1035–1042. https://doi.org/10.1021/np9904509
10. Rice-Evans, C. A., Miller, N. J., & Paganga, G. (1997). Antioxidant properties of phenolic compounds. Trends in Plant Science, 2(4), 152–159. https://doi.org/10.1016/S1360-1385(97)01018
11. Sathishkumar, B. R., & Srinivasan, M. (2015). GC-MS analysis of bioactive components from the ethanolic leaf extract of *Flueggea leucopyrus* Willd. World Journal of Pharmacy and Pharmaceutical Sciences, 4(8), 1360–1367
12. Soysa, P. (2008). Antioxidant cytotoxic properties of three traditional decoctions used for the treatment of cancer in Sri Lanka. Pharmacognosy Magazine, 4(14), 172–181.
13. Vinnarasi, J., Venkataraman, R., & Raj, A. A. (2016). Phytochemical and pharmacognostical analysis of *Flueggea leucopyrus* Willd. World Journal of Pharmaceutical Research, 5(8), 1368–1377.

ISOLATION AND IDENTIFICATION OF DYE-DEGRADING ENDOPHYTIC BACTERIA

Shweta Arekar[1*] and Jyoti Yadav[2]
[1*]Assistant professor, Department of Microbiology Gogate Jogalekar College (Autonomous), Ratnagiri, Maharashtra, India.
[2] PG Student, Department of Microbiology Gogate Jogalekar College (Autonomous), Ratnagiri, Maharashtra, India.
*Corresponding author- shwetaarekar1004@gmail.com Mob- (9082445709)

ABSTRACT:

Various industries generate considerable amounts of dye-contaminated wastewater that is harmful to aquatic ecosystems. Congo red is one of the azo dye used in various industries such as textile, wool and printing industries as well as it is also used in histological staining.

Conventional treatments of such wastewaters are generally expensive and ineffective because they cannot degrade most synthetic dyes present in the wastewater. On the other hand, recent research studies have indicated endophytic bacteria that live inside plant tissues as promising candidates for bioremediation because they possess extraordinary metabolic capabilities.

The current study aimed to isolate and identify the dye-degrading endophytic bacteria from a local species of Mangroves (*Sonneratia alba*, *Rhizophora mangle*) & Aloevera (*Aloe barbadensis miller*) for their use in bioremediation. Two dye-degrading bacteria were isolated and identified as *Staphylococcus aureus* (E1) & *Corynebacterium xerosis* (E2). Environmental parameters like pH, temperature, salt concentration and dye concentration were considered as variable factors and optimized. Highest decolourization by *S. aureus* and *C. xerosis* was observed at pH 7 at 37°C using 0.01% (100 mg/L) of the Congo red dye whereas optimum NaCl concentration was found to be 20 PPT for *S. aureus* and 10PPT for *C. xerosis*. In % decolourization assay *S. aureus* exhibited 85.41% decolourization whereas *C. xerosis* showed 89.58% decolourization in nutrient broth supplemented with 0.01% dye. However, in wastewater, the decolourization efficiency reduced to 20% for *S. aureus* and 41.7% for *C. xerosis*, indicating the need for further modifications to enhance their efficiency.

S. aureus and *C. xerosis* can be used for effective dye decolourization and further appropriate modifications to increase their efficiency in the bacterial strains is carried out.

Key words: Endophytic bacteria, dye degradation, Environmental sustainability, effluent treatment, bioremediation

INTRODUCTION-

Synthetic dyes are used extensively in textile, paper, leather, and cosmetic industries due to their low cost, durability, and bright coloration. However, their improper disposal leads to severe water pollution. Azo dyes like Congo red are particularly stable, resistant to degradation, and can cause toxic and carcinogenic effects in aquatic and terrestrial ecosystems. Traditional treatment methods such as chemical oxidation and adsorption are costly and inefficient for complete degradation. Bioremediation using microorganisms, particularly endophytic bacteria, offers a sustainable alternative. Endophytes inhabit plant tissues without causing harm and possess unique metabolic capabilities that allow them to degrade complex organic pollutants. The present study investigates endophytic bacteria from mangrove and Aloe vera species for

their ability to degrade Congo red dye and evaluates the effects of pH, temperature, and salt concentration on decolorization efficiency.

METHODOLOGY-

Fresh samples of *Sonneratia alba, Rhizophora mangle*, and *Aloe barbadensis miller* were collected from Ratnagiri district. Plant tissues were surface sterilized using ethanol and sodium hypochlorite to remove epiphytic microbes. Isolation of endophytic bacteria was conducted on Luria-Bertani agar followed by enrichment in Mineral Salt Medium containing 0.01% Congo red dye. Bacterial colonies with clear zones of dye decolorization were selected. Quantitative decolorization assays were performed using nutrient broth containing 0.01% dye, and absorbance was measured at 497 nm. The isolates were characterized morphologically and biochemically using Gram staining, IMViC, catalase, oxidase, and sugar fermentation tests. Optimization studies were conducted to determine the effect of pH (6–10), temperature (4–55°C), and NaCl concentration (1–30 PPT) on dye decolorization efficiency.

RESULT AND DISCUSSION-

Two bacterial isolates, identified as *Staphylococcus aureus* (E1) and *Corynebacterium xerosis* (E2), exhibited significant Congo red dye degradation capacity. The isolates were Gram-positive, catalase-positive, and oxidase-negative, consistent with their biochemical profiles. The decolorization efficiency varied under different environmental parameters.

Figure 1: Screening of dye-degrading endophytic bacteria showing zones of Congo red decolorization.

Table 1. Decolourization of Congo red dye at different pH levels.

pH		6	7	8	9	10
E1	Initial O.D	0.47	0.48	0.49	0.50	0.50
	Final O.D	0.05	0.05	0.06	0.07	0.09
	Decolourization (%)	89.3	89.5	87.8	86	82
E2	Initial O.D	0.47	0.48	0.49	0.50	0.50
	Final O.D	0.06	0.04	0.10	0.17	0.26
	Decolourization (%)	87	91.6	79.6	66	48

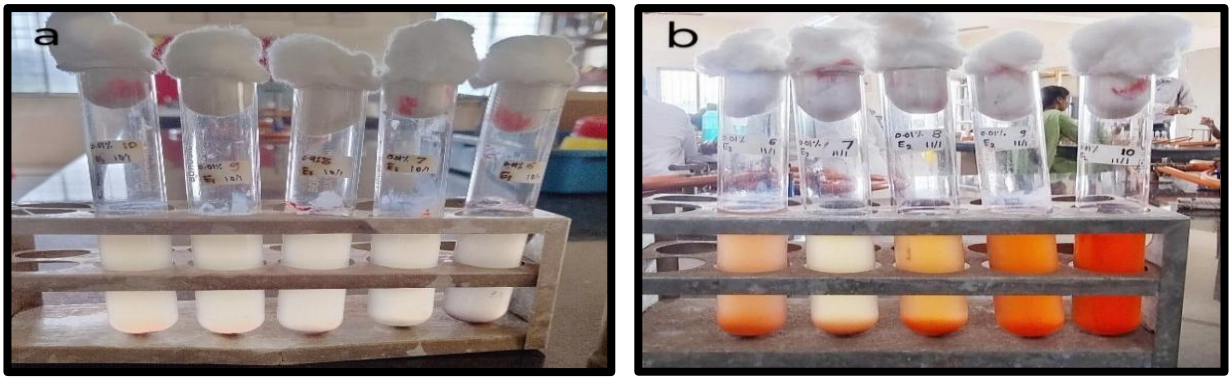

Fig:2. Dye decolourization by isolates E1 (a) and E2 (b) at different pH level

Table 2. Decolourization of Congo red dye at different temperatures.					
Temperature		4°C	25°C	37°C	55°C
E1	Initial O.D	0.55	0.55	0.55	0.55
	Final O.D	0.51	0.09	0.08	0.53
	Decolourization (%)	7	83.6	85.4	3
E2	Initial O.D	0.55	0.55	0.55	0.55
	Final O.D	0.51	0.08	0.06	0.51
	Decolourization (%)	7	85.4	89.1	7

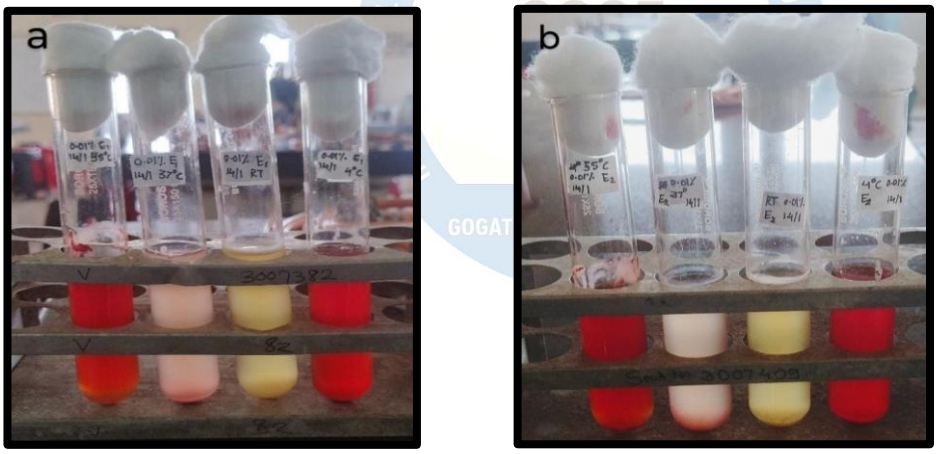

Fig:3. Dye decolourization by isolates E1 (a) and E2 (b) at different temperature

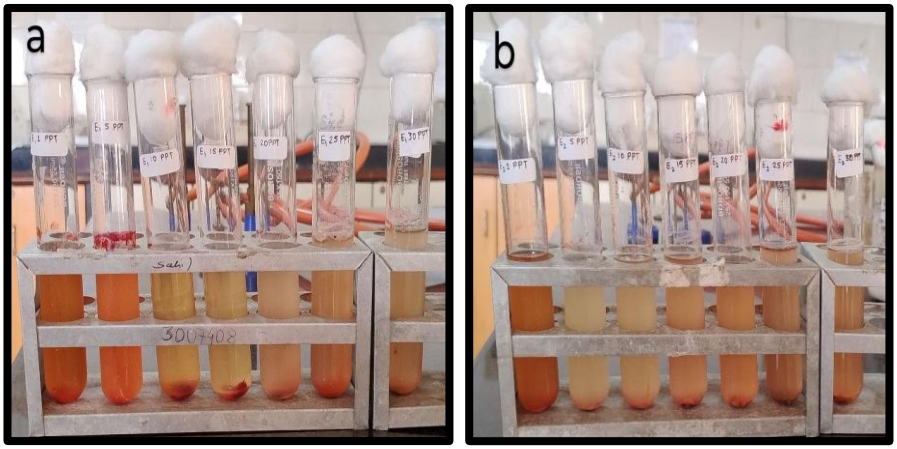

Fig:4. Dye decolourization by isolates E1 (a) and E2 (b) at different NaCl conc.

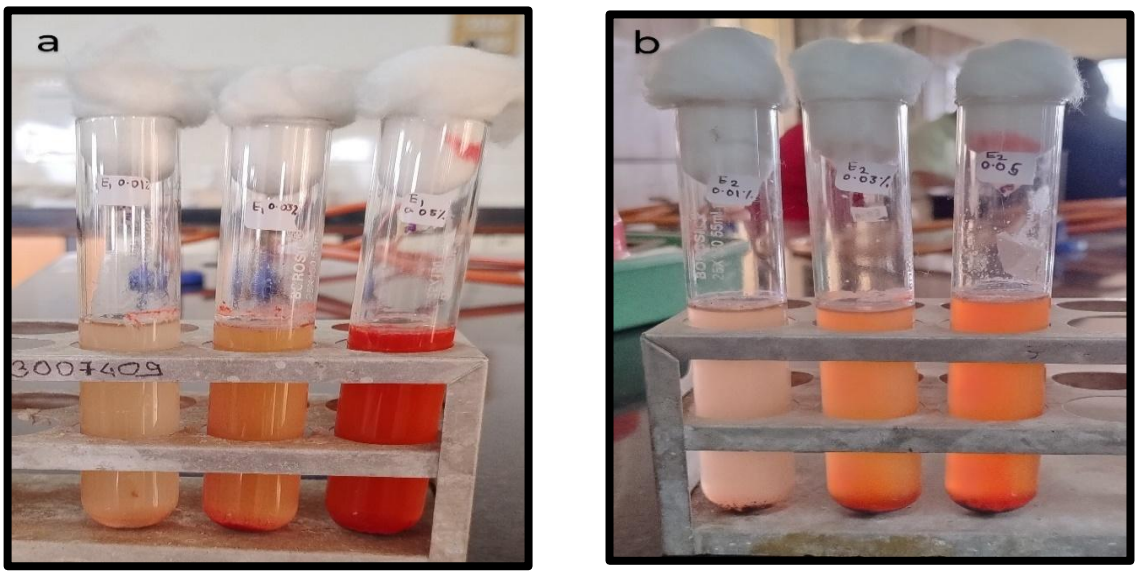

Fig:5. Dye decolourization by isolates E1 (a) and E2 (b) at different Concentrations

S. aureus achieved maximum decolorization (85.41%) and C. xerosis (89.58%) in nutrient broth at pH 7 and 37°C, indicating these as optimal conditions. The presence of high salt concentrations reduced dye removal efficiency, demonstrating sensitivity to osmotic stress. In wastewater samples, the efficiency decreased significantly due to the presence of competing contaminants, suggesting that pretreatment or consortia-based bioremediation approaches could enhance performance. These findings align with previous studies that report similar behavior in endophytic bacterial species, confirming their potential for large-scale application in effluent treatment systems.

CONCLUSION-

This study successfully isolated nine morphologically distinct bacterial endophytes from Mangrove roots and Aloevera samples. Among them, three isolates (E1, E2, and E3) demonstrated significant dye-degrading potential, with E2 exhibiting the highest decolourization efficiency (89.57%), followed by E1 (85.41%) and E3 (58.33%). Based on morphological, Gram staining, biochemical tests, and Bergey's Manual of Determinative Bacteriology, E1 was identified as *Staphylococcus aureus* and E2 as *Corynebacterium xerosis*.

The isolated bacteria, *Staphylococcus aureus* (E1) and *Corynebacterium xerosis* (E2) are potential candidates for Congo Red dye degradation as observed in this study. Under optimal conditions (100 mg/L dyes, 37°C and neutral pH 7), both isolates showed remarkable decolorization efficiency.

Decolourization rates reached the maximum observed value up to 89.5% (E1) and 91.6% (E2) at pH 7. At 37°C, the decolourization efficiencies were approximately 85.4% for E1 and 89.1% for E2. The concentration of salt played another important role in the decolourization process. E1 and E2 showed maximum decolourization at 20 PPT NaCl (98%) and 10 PPT NaCl (96.2%), respectively. Moreover, both isolates showed maximum degree of decolourization at 100 mg/L dye (0.01%) concentration, which signifies its proficiency at low dye concentrations.

The decolourization efficiencies of both the *S. aureus* (E1) and *C. xerosis* (E2) dropped to 20% and 41.7%, respectively when used for effluent treatment.

In general, the results indicated that *S. aureus* and *C. xerosis* have potential in bioremediation of dye containing effluents. Their rapid response to numerous environmental factors is a promising sign of a sustainable and biofriendly treatment method compared to the chemical- and physically-based peers. With appropriate modifications in the environmental conditions or bacterial strains, both *S. aureus* and *C. xerosis* hold potential for effective dye decolourization.

REFERENCES-

1. Afrin, S., et al. (2021). Bacterial consortium for textile dye degradation. Environmental Microbiology Reports, 13(6), 880–892.
2. Jain, A., et al. (2017). Isolation and characterization of endophytic bacteria from medicinal plants. International Journal of Microbiology, 2017, 1–8.
3. Kishor, R., et al. (2021). Biodegradation of Congo red dye by Bacillus cohnni. Environmental Science and Pollution Research, 28(12), 14523–14534.
4. Philip, I., et al. (2023). Bioremediation potential of Bacillus velezensis isolated from Alternanthera philoxeroides. Journal of Environmental Biology, 44(2), 145–152.
5. Singh, R., et al. (2022). Endophytic bacterial strains from Momordica charantia L. and their role in plant stress management. Applied Microbiology and Biotechnology, 106(4), 1551–1562.

Comprehensive analysis of physico-chemical and microbial parameters for commercially and locally available milk sample in Ratnagiri city

Mr. Siddhesh S. Bhagwat*, Samarth S. Surve
Dept. of Biotechnology, Gogate Jogalekar College (Autonomous), Ratnagiri, India.
Email: siddheshbhagwat107@gmail.com, Contact: 8806650873

Abstract

Milk is a vital dietary staple, making its quality a paramount public health concern so its quality assessment is essential for ensuring consumer safety and nutritional integrity. This study evaluated the physico-chemical and microbial parameters of commercially and locally available full cream and toned milk samples in Ratnagiri city using qualitative tests such as Pyne's method, sulphuric acid test, and phosphatase assay. Both milk types met quality standards regarding adulteration and extraneous substances; however, medium to high bacterial loads were detected, likely arising from natural contamination or processing deficiencies. Phosphatase activity further indicated inadequate pasteurization in both varieties, suggesting possible post-processing contamination and compromised safety. The results underscore the need for stricter hygienic practices, robust processing protocols, and routine monitoring to maintain milk quality. Beyond serving as a baseline for regional quality assessment, this work highlights the broader application of systematic testing for strengthening dairy safety standards. Future research should extend to seasonal and geographic comparisons, alongside the development of rapid detection techniques, to support regulatory frameworks and protect public health.

Keywords: Pyne's method, microbial load, adulteration, pasteurization, dairy safety, etc.

1. Introduction

Milk is often referred to as nature's most complete food due to its rich composition of essential nutrients (Pearson, 2009). It provides high-quality protein, beneficial fats, carbohydrates (mainly lactose), and a range of vitamins (A, D, B-complex) and minerals (e.g., calcium, phosphorus) that are critical for human growth and health (WHO, 2023). For example, bovine milk is roughly 87% water, with about 3–4% protein, 3–4% fat, 4–5% lactose, and small percentages of minerals (Pearson, 2009). These properties make milk an important dietary staple, especially for infants, children and the elderly who have higher nutrient requirements for growth and development. In wealthier societies, milk consumption is typically high and contributes substantially to daily nutrient intake, whereas in many low-income or rural regions limited access to milk can exacerbate nutritional deficiencies (OECD-FAO, 2011). Economic factors and cultural dietary preferences further influence these patterns: one study found that average per-capita milk intake in high-income countries is more than twice that in low-income countries (IMGC, 2016). Such disparities in milk consumption can lead to health outcomes that diverge between populations with abundant dairy intake and those with minimal milk diets.

According to the U.S. Centres for Disease Control and Prevention (CDC, 2025), raw milk can harbour dangerous pathogens such as *Salmonella*, *Escherichia coli*, *Listeria monocytogenes* and *Campylobacter* (CDC, 2025). Without pasteurization, these organisms are not eliminated, and raw milk has been repeatedly linked to foodborne illness outbreaks. Thus, while processing adds costs and may slightly alter some properties, it is widely regarded as essential for public health.

An additional concern in milk supplies is adulteration. Worldwide, unscrupulous practices sometimes add cheap or non-nutritive substances to milk to increase volume or perceived quality (Azad & Ahmed, 2016). Common adulterants include water (to dilute volume), skimmed milk powder (to restore solids), starches, sugars, detergents, urea, formalin, and even industrial chemicals (Azad & Ahmed, 2016). These additives may not noticeably change the appearance of milk, but they degrade its nutritional value and can damage consumer health. For instance, urea or melamine have been used to artificially raise apparent protein levels, yet they can cause kidney and urinary tract damage when ingested (Azad & Ahmed, 2016; WHO, 2023). Likewise, detergents and formalin are sometimes added as preservatives but are toxic to the liver and kidneys.

To systematically assess milk quality, researchers measure both physicochemical and microbiological parameters. Key physicochemical metrics includes pH, fat content, protein (and non-fat solids), lactose, total solids, titratable acidity, and specific gravity. Fresh cow's milk normally has a pH around 6.6–6.8; deviations from this range may indicate spoilage or contamination (WHO, 2023). Fat and total solids determine the milk's nutritional density and are often standardized in commercial products (e.g., "whole," "low-fat," or "skim" milk). Protein and lactose contents reflect the nutritional profile as well. Adulteration or dilution will typically alter these values: for example, adding water lowers total solids, and adding starch or sugar raises apparent solids-not-fat (FAO, 2011). Microbiological quality is evaluated by counting the total viable bacteria, coliform bacteria (an indicator of faecal contamination), and specific pathogens (such as *Staphylococcus aureus* or *Listeria*) when present. High bacterial counts or coliform presence suggest lapses in hygiene, while detection of pathogens indicates direct health risks (WHO, 2023). Together, these measures provide a comprehensive picture of milk's safety and nutritional value.

Methodology

Milk sample was collected in the raw and pasteurized form. All biochemical tests were performed on both raw and pasteurized milk. Total 10 tests were performed on milk to assure its quality. The comparative analysis of full fat milk and toned milk on the basis of adulterants present was done using various tests like sulphuric acid test, alcohol test, starch test and soap test as well. The presence of proteins or protein anomalies was also checked using the specialised tests like Pyne's method test and Biuret test for quantitative estimation of proteins in milk samples. Furthermore, the presence of desired and unwanted bacteria or coliforms in milk was tentatively confirmed using the dye reduction tests like methylene blue dye reduction test, resazurin reduction test and phosphatase test. The presence or absence of any external added sugars was also confirmed using sugar detection test.

Results and Discussion

Fig- Qualitative and quantitative tests for milk additives and microbial counts

The quality analysis of full-fat and toned milk samples using several microbiological and adulteration tests showed that both samples had medium to high bacterial load, as indicated by the Methylene Blue Reductase Test (MBRT) and Resazurin Reductase Test (RRT), where color changes occurred due to bacterial reduction of oxygen, suggesting possible contamination during handling or natural microbial presence, including harmless Lactobacillus. Pyne's method and the Sulphuric Acid test produced dark pink and black colors respectively, confirming that neither sample was diluted with water. Phosphatase test showed no color change, indicating proper pasteurization and no post-pasteurization contamination with raw milk. Breed's microscopic count recorded 10^4 CFU/mL in full-fat milk and 10^2 CFU/mL in toned milk, with the higher count in full-fat milk likely due to its greater nutrient and fat content. The alcohol test showed no curdling, demonstrating good protein stability and no significant acidity development. The Starch test showed no color change with iodine, and the sugar adulteration test maintained a blue color with $CuSO_4$–NaOH, confirming that no starch or sugar was added. The soap or detergent test showed no frothing, indicating the absence of detergent adulteration. The Biuret test produced a faint violet color in both samples, confirming the presence of proteins. Overall, the results indicate that both milk samples were compositionally pure, adequately pasteurized, and free from adulterants, but were found to have moderate bacterial load, highlighting the need for improved hygiene and handling practices.

Conclusion

The MBRT, RRT and Breed's count results indicated that both full-fat and toned milk carried a moderate to high microbial load, pointing toward lapses in handling or storage. Tests such as Pyne's method, the sulphuric acid test, along with starch, sugar, and detergent checks, showed no signs of dilution or external adulterants, confirming the purity of the samples. The phosphatase test verified that pasteurization had been effectively carried out, and the alcohol test reflected good stability of milk proteins. The Biuret test further supported the natural presence of proteins in both samples. Overall, the milk was free from adulteration and properly processed, though improvements in hygiene practices are necessary due to the noticeable bacterial presence.

References

1. Pehrsson P.R. (2000), USDA's national food and nutrition analysis program: food sampling. J Food Compos Anal.13(4):379–89.
2. Barham G.S, Khaskheli M, Soomro A.H, Nizamani Z.A. (2015), Surveillance of milk adulteration and its impact on physical characteristics of milk. Adv Biochem Biotechnol., 1(1):1–16.
3. Anderson M, Hinds P, Hurditt S, Miller P, McGrowder D, Alexander- Lindo R. (2011), The microbial content of unexpired pasteurized milk from selected supermarkets in a developing country. Asian Pac J Trop Biomed., 205–11.
4. Valero E, Villamiel M, Miralles B, Sanz J, Martinez-Castro I. (2001), Changes in flavour and volatile components during storage of whole and skimmed milk. Int J Food Chem., 72:51–8.
5. Saha S, Ara A. (2012), Chemical and microbiological evaluation of pasteurized milk available in Sylhet city of Bangladesh.
6. Das P.C, Rana M.S, Saifullah M, Islam M.N. (2018), Development of composite biscuits supplementing with potato or corn flour. Fundam Appl Agric., 3(2):453–9.

7. Singh A, Chandra G, Aggarwal A, Kumar P. (2012), Adulteration detection in milk. Res News U., 5:525.
8. APHA (American Public Health Association) (2004), Standard methods for examination of dairy products. 17th. American Public Health Association; Washington D.C, pp. 144–8.
9. Alemu, M. et al. (2020), Physicochemical and Microbial Quality of Raw Cow Milk. African Journal of Food Science, 14(2), 30-36.
10. Bagheri, H. et al. (2018), Physicochemical Properties and Microbial Quality of Raw and Pasteurized Milk in Iran. Journal of Dairy Research, 85(3), 231-239.
11. Beyene, T. et al. (2017), Quality of Milk and Its Microbial Load. BMC Veterinary Research, 13, 96.
12. D'Amico, D. J. et al. (2021), The Role of Microbial and Chemical Quality in Milk Safety. Dairy Science & Technology, 101(2), 221-235.
13. El-Loly, M. M. (2019), Microbiological and Physicochemical Evaluation of Milk from Different Sources. Egyptian Journal of Dairy Science, 47(4), 299-308.
14. Griswold, K. E. et al. (2022), Physicochemical and Microbial Evaluation of Commercial Milk Products. Journal of Food Protection, 85(1), 98-107.

A study on diverse functional attributes of endophytic bacteria from leaves of *Mimosa pudica* and *Myristica fragrans* Houtt with agricultural and therapeutic relevance

Kaushal Pashte[1], Neha Kadam[1], Teertha Surve[1] and Shubham Panchal[1]
Department of Biotechnology, Gogate Jogalekar College (Autonomous), Ratnagiri-415612
Contact: kaushalpashte@gmail.com (8329706083)

Abstract

Endophytes have long been studied for various applications. The current study focuses on the study of endophytic bacteria isolated from Mimosa and Mace and Nutmeg. Our study focused on their ability to tolerate the pesticide, production of the IAA, their ability to solubilize phosphate and producing L-asparaginase enzyme. We found that endophytes belonged to M1 (*Brucella/Bordetella/Bacteroides*), M2 (*Pseudomonas/Vibrio/Aeromonas*), M3 (*Corynebacterium spp./Lactobacillus spp./Mycobacterium spp.*), M4 (*Pseudomonas/Vibrio/Aeromonas*), M5 (*Staphylococcus/Micrococcus*), M6 (*Streptococcus spp./Enterococcus spp.*), M7 (*Staphylococcus spp. /Micrococcus spp.*), J1(*Corynebacterium spp./Lactobacillus spp./Mycobacterium spp.*), J2 (*Staphylococcus spp./Micrococcus spp.*), J3 (*Pseudomonas/Aeromonas/Vibrio*), J4 (*Corynebacterium spp./Lactobacillus spp./Mycobacterium spp*.) genera after biochemical testing. 11 isolates were IAA positive with M7 (18 µg/ml) showing the maximum activity. Similarly, 6 isolates showed phosphate solubilization activity with maximum SI index being of M6(1.94), all the colonies showed some or complete tolerance to the pesticide 500, 1000, 1500, 2000 and 2500 ppm. Initial test on L-asparaginase activity study showed isolates J1, J3, J4, M5, M6 and M7 had the ability to produce L-asparaginase.

[**Keywords-** Endophytes, IAA, Phosphate Solubilizing bacteria (PSB), Pesticide tolerance, L-asparaginase.]

1. Introduction

The word “endophyte” (‘endo’ refers for within or inner and ‘phyto’ refers for plant) was first coined by Anton de Bary in 1866 and described as “Organisms that grow within plant tissues”. Subsequently, that term is expanded into “Microorganisms that reside within plant tissues, do not cause plant disease, and sometimes provide benefits to their host” (Kumar et al., 2025). Endophytes provides various advantages to the host plant, including (i) they increase nutrients uptake by plants, (ii) prevent growth of weed, (iii) protection against loss of water, (iv) protection from parasitic fungi and surface feeding insects, (v) it can stimulate the plant growth by producing plant hormones like auxin (IAA), which can enhance the growth of host plant (Dutta et al., 2014). Endophytes can produce a variety of metabolites like alkaloids, polypeptides, polyketides, terpenoids, etc., that have high value in many fields, including pharmaceuticals and agriculture. These metabolites are act as antibiotics, insecticidal agents, natural antioxidants, antitumor agents, and antidiabetic product (Xia et al., 2022). Endophytic bacteria’s growth facilitating actions are mainly due to their capacity to form ammonia, indole-3-acetic acid (IAA), siderophores, and solubilize nutrients like zinc (Zn) and phosphorus (P) (Kumar et al., 2025).

In Indian Ayurvedic medicine, different parts of nutmeg plant (*Myristica fragrans* Houtt) are used to treat diseases like anxiety, nausea, diarrhoea, cholera, stomach cramps, parasites and paralysis (Ashokkumar et al., 2022). Nutmeg has high value due to their beneficial role in medicinal use and cooking (Wong et al., 2025). Spices and herbs have different properties that

are helpful for health includes antioxidant, antimicrobial, anti-inflammatory, neuroprotective, antidiabetic, and anticancer properties, and cardiovascular benefits (Barman et al., 2021).

Mimosa pudica is also known as the sensitive plant, touch-me-not and sleeping grass. This plant has different names in different cultures, including in Indian Ayurveda it is known as Lajjalu, in Sanskrit known as Namaskari, and Dormidera or Morivivi in other languages (Mohini Ughade et al., 2025). *Mimosa pudica* has mimosin, a toxic alkaloid, also contains adrenaline in leaf extract of plant. Leaf extract of plant contains various bioactive compounds, including terpenoids, flavonoids, glycosides, quinines, phenols, tannins, saponins and coumarins(Baby Joseph et al., 2013). *Mimosa pudica* possesses various pharmacological activities including Anti-ulcer activity, Anti-inflammatory activity, Anti-microbial activity, Anti-malaria activity, Antifungal activity, wound healing activity and other pharmacological activities (Gopinathan Narasimhan, 2014).

Phosphorus (P) is a crucial macronutrient that play important role in the biosynthesis of different compounds, including phytic acid, nucleic acid and phospholipids in plants. The lack of phosphorus in plants interferes with the production of nucleic acid, phospholipids, and subsequently affects the cell division, energy conversion, and cellular respiration; also it can reduce the rate of photosynthesis. In soil-plant phosphorus cycle microorganism can play an important role in transferring and accumulating of phosphorus, approximately 68-78% from the total phosphorus biomass (Cheng et al., 2023). Phosphorus is essential for plants, as it plays crucial role in root elongation, branching, and root architecture. It provides structural strength to grass, in flowering and fruit formation. Also, it is important for normal seed formation (Kale, 2025). Phosphorus is present in both forms, organic and inorganic form into the soil (Lin Pan & Baiyan Cai, 2025).

Indole-3-acetic acid (IAA) is the primary auxin in plants, and it has been widely recognized that the majority of IAA is synthesized from tryptophan (Trp) in a two-step process (Cook & Ross, 2016). Auxin play important role in plant growth and development, including tissue differentiation, fertility, cell division, orientation, and enlargement in terrestrial plants (Labeeuw et al., 2016). Various environmental parameters can affect the biosynthesis of IAA, includes pH and temperature. The pH of the growth medium plays a crucial role in regulating IAA formation (Fu et al., 2015).

L-asparaginase is an enzyme which has significant therapeutic and industrial applications. It is used in the treatment of various diseases including acute lymphoblastic leukaemia (ALL), acute myeloblastic leukaemia, chronic lymphoma, Hodgkin's disease, autoimmune disease, bacterial infection, collagen-induced arthritis (CIA), pharyngitis, and scarlet fever (Jana et al., 2025). L-asparaginases are divided into two groups: type I and type II. Both types are varied according to enzymatic specificity for L-glutamine (L-Gln) and L-asparagine (L-Asn) (Hosseini et al., 2024). The therapeutic action of L-asparaginase is based on depletion of asparagine, which is an amino acid. L-asparaginase break down asparagine into aspartic acid and ammonia (Jana et al., 2025).

This research focuses on isolation and characterization of endophytic bacteria from the leaves and seeds of *Myristica fragrans* and *Mimosa pudica* to evaluate their functional attributes with agricultural and therapeutic relevance. The aimed of the research to determine the isolates for their ability to solubilize phosphate, produce Indole-3-acetic acid (IAA) and secrete the the enzyme L-asparaginase. Also, the study focused on determining the pesticide tolerance of the isolates against Actara to understand their adaptability under chemical stress.

2. Material and methods

2.1 Sample collection:

The plant sample of *Myristica fragrans* and *Mimosa pudica* were collected from Kasheli and Bhandarwada, Ratnagiri.

2.2 Isolation of Endophytic bacteria:

The plant samples were washed and treated with 1% savlon for 5 minutes. Then it was treated with 0.1% $HgCl_2$ for surface sterilization (5 min). Then wash these samples with distilled water and crush in mortal and pestal by adding sterile PBS (5-10 ml) and then 0.1 ml extract was spread on nutrient agar plate and incubated for bacterial growth. The bacterial isolates obtained were tested for purity testing using the four-quadrant streaking method, and the plates were observed for contamination. The pure bacterial colonies were maintained on nutrient agar slants at 4℃.

2.3 Study of Cultural characteristics and Biochemical characterization of isolates

The purified bacterial isolates were streaked on nutrient agar plates and studied for various cultural characteristics. The fate of biochemical tests to be performed were decided on basis their gram nature. Catalase and Oxidase tests were performed to identify the tentative genus of the bacteria.

2.4 Pesticide tolerance testing:

The isolates were tested against the pesticide Actara at four different concentrations, ranging from 500 to 2500 mg/L. Plates containing the pesticide were spot inoculated with the bacterial cultures and observed for growth and zone formation.

2.5 Phosphate solubilizing bacteria:

Phosphate solubilization activity was tested using modified pikovskaya's agar medium supplemented with bromophenol blue dye (BPB). Spot inoculation was performed to observe zone of solubilization, and SI index were calculated, as SI = A/B, where A was the diameter of halo (solubilization of phosphate) including the colony, and B was only the colony diameter (Ulloa-Muñoz et al., 2020).

2.6 Test for L-asparaginase enzyme:

L-asparaginase enzyme activity was determined on nutrient agar medium containing 1 gm L-asparagine and phenol red dye, the development of pink zone indicates positive enzyme activity.

2.7 IAA activity:

Indole-3-acetic acid production was determined by using (Ulloa-Muñoz et al., 2020) reference, the isolates were grown in nutrient broth containing 0.02 gm L-Tryptophan. After 24 hours of incubation, the cultures were centrifuged at 10,595 rpm for 2 minutes and 2 ml of salkowski's reagent was added to the supernatant. The mixture was incubated in the dark for 30 minutes at room temperature and absorbance was measured at 517 nm.

3. Results and discussion

3.1 Isolation of bacteria:

Endophytic bacteria have been found in all parts of plant, but roots are primary entry point (Ulloa-Muñoz et al., 2020). In the study (Dewa Gede Wiryangga Selangga & Listihani, 2021) isolated 43 cultures from root of *M. pudica,* after using various test they observed that 12 strains

from the 43 were endophytic bacteria. In this study, total eleven bacterial endophytes were isolated from *Mimosa pudica* and *Myristica fragrans*. Out of eleven bacterial isolates, 7 species were isolated from leaves of mimosa and remaining 4 were isolated from seeds of jaifal.

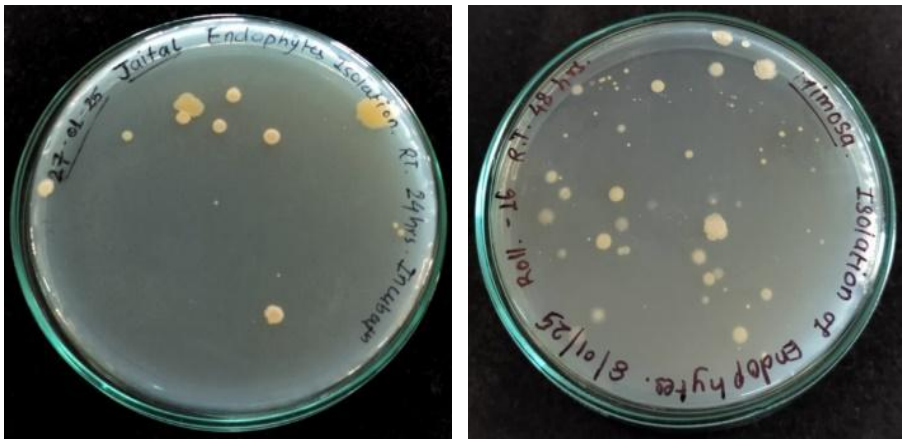

Fig 1: Isolation of endophytic bacteria

3.2 **Cultural characteristics:**

The endophytic bacterial isolates from *Myristica fragrans* and *Mimosa pudica* showed diverse colony morphology on nutrient agar. Gram staining showed that out of the seven leaf isolates, four were Gram-positive and three were Gram-negative. While out of the four seed isolates, three were Gram-positive and one was Gram-negative. Microscopical observations were both cocci and bacilli forms. These cultural and staining characteristics helped in tentative identification of bacterial genera such as *Psedomonas*, *Staphylococcus*, *Corynebacterium*, *Micrococcus* and *Streptococcus*.

3.3 Biochemical characterization:

The Biochemical characterization showed that most isolates were catalase positive, whereas some were oxidase positive.

	Catalase	Oxidase		Catalase	Oxidase
M. pudica Leaves			Jaifal Seeds		
M1	NA	-	J1	-	N. A
M2	N. A	+	J2	+	N. A
M3	-	N. A	J3	N. A	+
M4	N. A	+	J4	+	N. A
M5	+	N. A			
M6	-	N. A			
M7	+	N. A			

Table 1: Catalase and Oxidase test of leaf samples

Key- Positive: (+), Negative: (-), Not Applicable: (N.A)

3.4 Tentative genus of isolated colonies

Endophytic bacteria living inside the plant tissues come from many different genera and species so when they grow on culture media they have different characteristics (Yunita et al., 2022). Endophytic bacteria include different groups of species, ranging from gram-positive to gram-negative bacteria, such as *Bacillus*, *Agrobacterium*, *Brevibacterium*, *Pseudomonas*, etc (Xia et al., 2022). According to morphological, cultural and biochemical characteristics, the tentative identification of the eleven endophytic bacterial isolates from *Mimosa pudica* and *Myristica fragrans* was made with Bergey's manual of systematic bacteriology.

Table 2: Tentative genus of leaf and seed isolates with reference to Bergey's manual

Tentative genus			
M. pudica Leaves		*M. fragrans* Seeds	
M1	*Brucella*/*Bordetella*/*Bacteroides*	J1	*Corynebacterium spp.*/*Lactobacillus spp.*/*Mycobacterium spp.*
M2	*Pseudomonas*/*Vibrio*/*Aeromonas*	J2	*Staphylococcus spp.*/*Micrococcus spp.*
M3	*Corynebacterium spp.*/*Lactobacillus spp.*/*Mycobacterium spp.*	J3	*Pseudomonas*/*Aeromonas*/*Vibrio*
M4	*Pseudomonas*/*Vibrio*/*Aeromonas*	J4	*Corynebacterium spp.*/*Lactobacillus spp.*/*Mycobacterium spp.*
M5	*Staphylococcus*/*Micrococcus*		
M6	*Streptococcus spp.*/*Enterococcus spp.*		
M7	*Staphylococcus spp.*/*Micrococcus spp.*		

3.5 Phosphate solubilising test:

PSB are considered an economical, environmentally friendly, and sustainable biological approach to conquer soil phosphorus deficiency (Cheng et al., 2023). The organic acids, gluconic and keto-gluconic acids released by PSB have an important role in dissolving soil phosphorus and rhizosphere acidification. The ability of phosphorus solubilization by PSB is highly dependent upon the pH of the medium (Khan et al., 2009). In the study carried out by (Montañez et al., 2012), they isolated 22 endophytic bacterial strains from maize plants and they found that all 22 strains can solubilise phosphate. They calculated the Phosphate Solubilising Index for PSB and obtained that SI index ranges between 1-4.9. In this study, Phosphate solubilization was detected in six isolates using pikovskaya's agar medium, the Solubilising Index ranging from 1.3 to 1.94. The strain M6 showed highest SI value 1.94

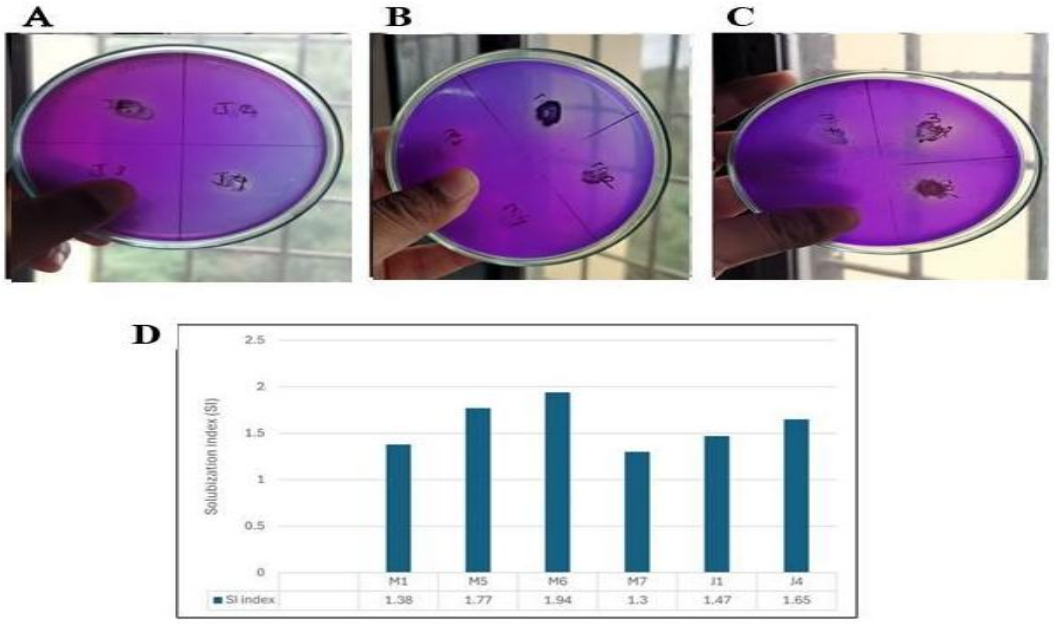

Fig 2: (A) phosphate solubilization by seed isolates J1, J2, J3 and J4, (B) phosphate solubilization by leaf isolates M1, M2, M3 and M4, (C) phosphate solubilization by leaf isolates M5, M6 and M7, (D) graph of solubilization index

3.6 **IAA activity:**

In plants and bacteria, the biosynthesis pathway for IAA is highly similar routes. Both tryptophan (Trp)-dependent and tryptophan-independent biosynthesis pathways are involved in the production of IAA in plants and microbes (Fu et al., 2015). Research conducted by (Ulloa-Muñoz et al., 2020) it was observed that six endophytic bacterial strain showed IAA activity. Also the study carried out by (Montañez et al., 2012), the 22 strains of endophytic bacteria from maize shows IAA activity. According to results of this study, all isolates produced indole-3-acetic acid (IAA) when they were cultured in NB with tryptophan. *Mimosa pudica* isolate M7 shows the maximum activity for IAA (18 µg/ml) and the isolate J2 showed lowest IAA activity (2 µg/ml).

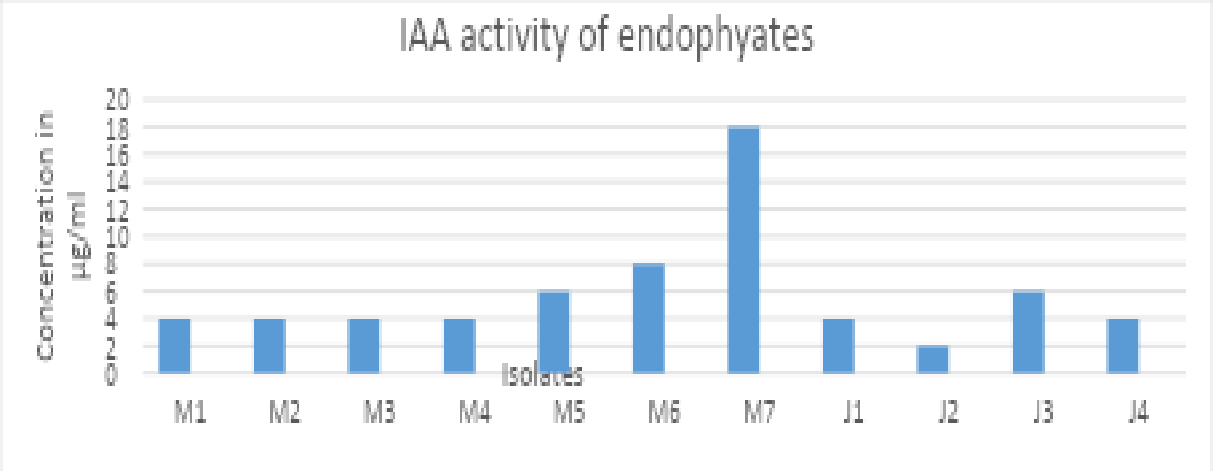

Fig 2: IAA production

3.7 L-asparaginase activity:

L-asparaginase is an enzyme which has significant therapeutic and industrial applications, also it is applied in the food industry, for biosensor production, and other uses (Jana et al., 2025). The study carried out by (Osama et al., 2023), they isolated 8 endophytic fungi from Hedera helix L. and then it was isolated on MH agar plates which contain 1% L-asparagine and phenol red as a pH indicator. The L-asparaginase enzyme catalysed L-asparagine and increases the pH; it was indicated by colour change of phenol red from yellow to pink. In our study the L-asparaginase enzyme activity of the isolated endophytic bacteria was performed on nutrient agar medium supplemented with L-aspargine and phenol red indicator. Out of eleven isolates, six (J1, J3, J4, M5, M6, M7) showed clear pink zones around their colonies.

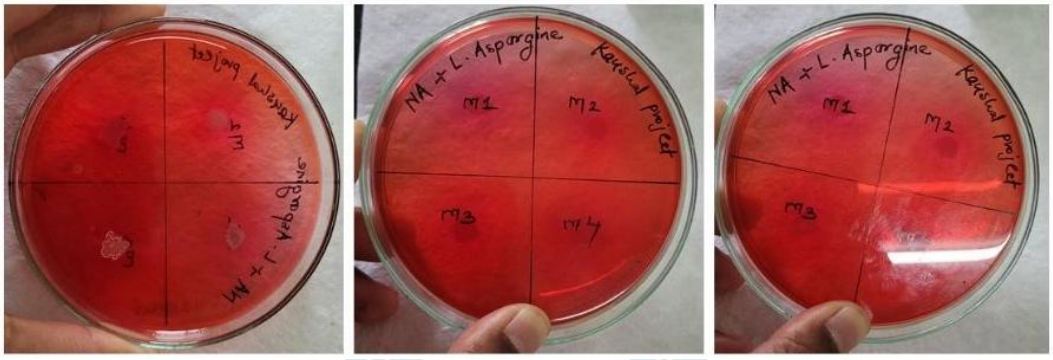

Fig 3: Pink colonies showing L-asparaginase activity

3.8 **Pesticide tolerance activity:**

Pesticides are essential for improving crop yields and supporting agricultural productivity, but excessive pesticide use can harm microorganisms, disrupt ecosystems and damage the environment (Shahid & Khan, 2021). The study carried out by (Shahid & Khan, 2021), they isolated 45 cultures (15 each of *Pseudomonas, Azotobacter* and phosphate solubilizing bacteria: PSB) from different rhizosphere sources. They exposed these cultures to 12 different pesticides, including glyphosate (GP), quizalofop, (QUIZ) atrazine (ATZ), butachlor (BUTA), kitazin (KTZ), metalaxyl (METL), hexaconazole (HEXA), carbendazim (CBZM), fipronil (FIP), imidacloprid (IMID), monocrotophos (MONO), thiamethoxam (THIA), and they observed that strain PS3 from *Pseudomonas* tolerated higher level (3200 µg mL^{-1}) of KTZ, HEXA, METL and THIA of the 12 test pesticides and PS1 showed the maximum (2183 µg mL^{-1}) tolerance to all pesticides. In our sudy the pesticide tolerance of all eleven endophytic bacterial isolates was tested using the insecticide Actara at concentrations ranging from 500 to 2500 mg/ L. All the isolates showed good tolerance even at the highest concentration tested. Leaf isolates M2, M3 and M4 from *Mimosa pudica* showed strong tolerance across all concentrations, while seed isolates J2, J3 and J4 from *Myristica fragrans* showed luxuriant growth.

Table 4: Pesticide tolerance of leaf and seed samples in range of 500-2500 mg/L

Sample	Concentration of pesticide (mg/L)				
Mimosa Leaves	500	1000	1500	2000	2500
M1	+	++	++	+	+
M2	++	++	++	+	+
M3	++	++	++	+	+

Sample	Concentration of pesticide (mg/L)				
M4	++	++	++	+	+
M5	++	+	+	+	+
M6	++	+	-	+	+
M7	+	+	+	+	++
Jaifal Seeds					
J1	++	++	+	+	++
J2	++	++	++	++	++
J3	++	++	++	+	++

Keys- No Growth: (-), Growth: (+), Moderate growth: (++), Luxuriant growth: (+++)

4. Conclusion

In this research, total eleven endophytic bacteria were successfully isolated from the leaves and seeds of *Mimosa pudica* and *Myristica fragrans*. The isolates were found to possess several useful characteristics such as phosphate solubilization, Indole-3-acetic acid (IAA) production, L-asparaginase enzyme activity and pesticide tolerance activity. These results show that the endophytic bacteria from such medicinal plants possess plant growth promoting and chemical stress tolerating abilities. Their ability to solubilize nutrients, synthesize phytohormones and tolerate chemical stress makes them potential biofertillizers and biocontrol agents. In addition, L-asparaginase activity indicates potential pharmaceutical applications. This indicates that endophytic bacteria not only enhance sustainable agriculture by reducing chemical inputs but also generates new avenues for pharmaceutical applications.

5. References

1. Ashokkumar, K., Simal-Gandara, J., Murugan, M., Dhanya, M. K., & Pandian, A. (2022). Nutmeg (Myristica fragrans Houtt.) essential oil: A review on its composition, biological, and pharmacological activities. *Phytotherapy Research*, *36*(7), 2839–2851. https://doi.org/10.1002/ptr.7491
2. Baby Joseph, Jency George, & Jeevitha Mohan. (2013). (PDF) Pharmacology and Traditional Uses of Mimosa pudica. *ResearchGate*. https://doi.org/10.25004/IJPSDR.2013.050201
3. Cheng, Y., Narayanan, M., Shi, X., Chen, X., Li, Z., & Ma, Y. (2023). Phosphate-solubilizing bacteria: Their agroecological function and optimistic application for enhancing agro-productivity. *Science of The Total Environment*, *901*, 166468. https://doi.org/10.1016/j.scitotenv.2023.166468
4. Cook, S. D., & Ross, J. J. (2016). The auxins, IAA and PAA, are synthesized by similar steps catalyzed by different enzymes. *Plant Signaling & Behavior*, *11*(11), e1250993. https://doi.org/10.1080/15592324.2016.1250993
5. Dewa Gede Wiryangga Selangga & Listihani. (2021). Screening of Endophytic Bacteria Isolated from Mimosa pudica in Bali Island. *SEAS (Sustainable Environment Agricultural Science)*, *5*(1), 50–57. https://doi.org/10.22225/seas.5.1.3303.50-57
6. Dutta, D., Puzari, K. C., Gogoi, R., & Dutta, P. (2014). Endophytes: Exploitation as a tool in plant protection. *Brazilian Archives of Biology and Technology*, *57*, 621–629. https://doi.org/10.1590/S1516-8913201402043

7. Fu, S.-F., Wei, J.-Y., Chen, H.-W., Liu, Y.-Y., Lu, H.-Y., & Chou, J.-Y. (2015). Indole-3-acetic acid: A widespread physiological code in interactions of fungi with other organisms. *Plant Signaling & Behavior*, *10*(8), e1048052. https://doi.org/10.1080/15592324.2015.1048052
8. Gopinathan Narasimhan. (2014). *(pdf) mimosa pudica linn-a shyness princess: a review of its plant movement, active constituents, uses and pharmacological activity*. ResearchGate. https://www.researchgate.net/publication/308916532_mimosa_pudica_linn-a_shyness_princess_a_review_of_its_plant_movement_active_constituents_uses_and_pharmacological_activity
9. Hosseini, K., Zivari-Ghader, T., Akbarzadehlaleh, P., Ebrahimi, V., Sharafabad, B. E., & Dilmaghani, A. (2024). A Comprehensive Review of L-Asparaginase: Production, Applications and Therapeutic Potential in Cancer Treatment. *Applied Biochemistry and Microbiology*, *60*(4), 599–613. https://doi.org/10.1134/S0003683823602937
10. Jana, A., Biswas, S., Ghosh, R., & Modak, R. (2025). Recent advances in L-Asparaginase enzyme production and formulation development for acrylamide reduction during food processing. *Food Chemistry: X*, *25*, 102055. https://doi.org/10.1016/j.fochx.2024.102055
11. Kale, A. (2025, April 7). Phosphate & potassium solubilizing bacteria as PGPR. *Microbiology Notes*. https://microbiologynotes.org/phosphate-potassium-solubilizing-bacteria-as-pgpr/
12. Khan, A. A., Jilani, G., Akhtar, M. S., Saqlan, S. M., & Rasheed, M. (2009). *Phosphorus Solubilizing Bacteria: Occurrence, Mechanisms and their Role in Crop Production*.
13. Kumar, A., Chauhan, P., Kumar, A., Pooja, Mishra, T., Padiyal, A., Walia, Y., Dhir, S., & Pandey, A. K. (2025). Latest progress (2020–2024) in bacterial endophyte research with special reference to plant disease management: Achievements and challenges. *Discover Plants*, *2*(1), 234. https://doi.org/10.1007/s44372-025-00303-3
14. Labeeuw, L., Khey, J., Bramucci, A. R., Atwal, H., de la Mata, A. P., Harynuk, J., & Case, R. J. (2016). Indole-3-Acetic Acid Is Produced by Emiliania huxleyi Coccolith-Bearing Cells and Triggers a Physiological Response in Bald Cells. *Frontiers in Microbiology*, *7*. https://doi.org/10.3389/fmicb.2016.00828
15. Lin Pan & Baiyan Cai. (2025). (PDF) Phosphate-Solubilizing Bacteria: Advances in Their Physiology, Molecular Mechanisms and Microbial Community Effects. *ResearchGate*. https://doi.org/10.3390/microorganisms11122904
16. Mohini Ughade, Pankaj Haribhau Chaudhary, Prashant J Burange, & Amir Baig. (2025). (PDF) A COMPREHENSIVE REVIEW ON MIMOSA PUDICA LINN. *ResearchGate*. https://www.researchgate.net/publication/387892239_A_COMPREHENSIVE_REVIEW_ON_MIMOSA_PUDICA_LINN
17. Montañez, A., Blanco, A. R., Barlocco, C., Beracochea, M., & Sicardi, M. (2012). Characterization of cultivable putative endophytic plant growth promoting bacteria associated with maize cultivars (Zea mays L.) and their inoculation effects in vitro. *Applied Soil Ecology*, *58*, 21–28. https://doi.org/10.1016/j.apsoil.2012.02.009
18. Osama, S., El-Sherei, M. M., Al-Mahdy, D. A., Bishr, M., Salama, O., & Raafat, M. M. (2023). Optimization and characterization of antileukemic l-asparaginase produced by Fusarium solani endophyte. *AMB Express*, *13*(1), 96. https://doi.org/10.1186/s13568-023-01602-2

19. Shahid, M., & Khan, M. S. (2021). Tolerance of pesticides and antibiotics among beneficial soil microbes recovered from contaminated rhizosphere of edible crops. *Current Research in Microbial Sciences*, *3*, 100091. https://doi.org/10.1016/j.crmicr.2021.100091
20. Ulloa-Muñoz, R., Olivera-Gonzales, P., Castañeda-Barreto, A., Villena, G. K., & Tamariz-Angeles, C. (2020). Diversity of endophytic plant-growth microorganisms from *Gentianella weberbaueri* and *Valeriana pycnantha*, highland Peruvian medicinal plants. *Microbiological Research*, *233*, 126413. https://doi.org/10.1016/j.micres.2020.126413
21. Wong, X. K., Alasalvar, C., Bo, S., Pan, J., & Chang, S. K. (2025). Unlocking the power of nutmeg: Nutritional composition, phytochemicals, and health benefits revealed through chemometrics and multi-omics advances. *Food Research International*, *218*, 116798. https://doi.org/10.1016/j.foodres.2025.116798
22. Xia, Y., Liu, J., Chen, C., Mo, X., Tan, Q., He, Y., Wang, Z., Yin, J., & Zhou, G. (2022). The Multifunctions and Future Prospects of Endophytes and Their Metabolites in Plant Disease Management. *Microorganisms*, *10*(5), 1072. https://doi.org/10.3390/microorganisms10051072
23. Yunita, M., Manse, Y., Wulandari, M. C., Sukmawati, S., & Ohiwal, M. (2022). Isolation of endophytic bacteria from nutmeg plant as antibacterial agents against pathogenic bacteria. *JPBIO (Jurnal Pendidikan Biologi)*, *7*(1), 115–122. https://doi.org/10.31932/jpbio.v7i1.1522

Bacteriocin Production by Marine Lactobacillus pentosus B25: A Comprehensive Review

Dr. Bharti.G. Wadekar & Ms. Priti Raman Yadav
Assistant Professor & MSc. I Yr. Student,
Thakur Shyamnarayan Degree College
Affiliated to University of Mumbai, India
Email Id: bhartiwadekar@tsdcmumbai.in / vpriti8948@gmail.com

Abstract

Marine-derived lactic acid bacteria (LAB) have emerged as valuable sources of antimicrobial compounds, particularly bacteriocins, which offer natural alternatives to synthetic preservatives and antibiotics (Gálvez et al., 2010). Lactobacillus pentosus B25, isolated from marine environments, exemplifies this potential through its production of bacteriocin B25, a low-molecular-weight peptide with broad-spectrum activity against Gram-positive and Gram-negative bacteria, as well as fungal pathogens (Wadekar and Dharmadhikari, 2022). This review comprehensively examines the isolation, biosynthesis, production optimization, purification, physicochemical characterization, antimicrobial mechanisms, and practical applications of bacteriocin B25. Drawing comparisons with bacteriocins from other L. pentosus strains such as ZFM94 (Wu et al., 2021), PCZ4 (Chen et al., 2024), 124-2 (Syukur et al., 2023), and ST712BZ (Todorov and Dicks, 2009), it highlights the unique adaptations of marine strains to saline conditions, enhancing stability and efficacy. Bacteriocin B25 demonstrates heat stability up to 110°C, pH tolerance from 4 to 10, and applications in food biopreservation, agriculture as a biocontrol agent, and potentially in pharmaceuticals. Challenges including low yield and scalability are addressed, with future directions emphasizing genetic engineering and encapsulation for improved delivery (Rivas et al., 2024). Supported by 15 key references, this article underscores the role of marine LAB in sustainable antimicrobial strategies, promoting their integration into food safety and health sectors.

Introduction

The escalating global concern over antimicrobial resistance has propelled research into natural antimicrobial agents, with bacteriocins from lactic acid bacteria (LAB) standing out as promising candidates (Kaktcham et al., 2025). Bacteriocins are ribosomally synthesized peptides or proteins that exhibit antimicrobial activity primarily against closely related species, but often extend to a broader spectrum including foodborne pathogens and spoilage organisms (Ouali et al., 2025). Among LAB, Lactobacillus pentosus is a versatile species commonly found in fermented foods, plants, and increasingly in marine environments, where it adapts to high salinity and osmotic stress (Delgado et al., 2005). The marine isolate L. pentosus B25, derived from coastal seawater or sediments, represents a novel strain capable of producing bacteriocin B25, which has garnered attention for its robust properties suited to harsh conditions (Wadekar and Dharmadhikari, 2023).

Historically, bacteriocins like nisin, produced by Lactococcus lactis, have been utilized since the 1950s for food preservation, approved as GRAS (Generally Recognized as Safe) by the FDA (Yazgan et al., 2021). However, marine-derived LAB offer distinct advantages, including enhanced tolerance to salt, pH extremes, and temperature fluctuations, making their bacteriocins ideal for applications in seafood processing and saline fermentations (Gálvez et

al., 2010). L. pentosus B25 was first isolated and characterized in 2022, with initial studies focusing on its bacteriocin production in modified MRS broth supplemented with NaCl to mimic marine conditions (Wadekar and Dharmadhikari, 2022). This strain's ability to thrive in 2% NaCl environments distinguishes it from terrestrial counterparts, potentially due to osmotic stress-induced upregulation of bacteriocin genes (Rivas et al., 2024).

The significance of marine LAB lies in their ecological role within aquatic microbiomes, where they compete with pathogens by secreting bacteriocins, thus maintaining microbial balance (Gálvez et al., 2010). In aquaculture, for instance, bacteriocins from marine LAB have been explored to combat vibriosis in shellfish, improving survival rates without antibiotic residues (Rivas et al., 2024). For L. pentosus B25, preliminary screenings revealed inhibitory zones against indicators like Staphylococcus aureus and Escherichia coli, indicating a broad-spectrum profile (Wadekar and Dharmadhikari, 2023). Comparative analyses with other L. pentosus strains, such as ZFM94 from infant feces producing pentocin ZFM94 (Wu et al., 2021), PCZ4 from kimchi yielding pediocin and plantaricin S (Chen et al., 2024), 124-2 from dadih (Syukur et al., 2023), and ST712BZ from boza (Todorov and Dicks, 2009), highlight shared Class II bacteriocin characteristics but underscore B25's marine-specific enhancements.

Biosynthetically, bacteriocin production in LAB is regulated by quorum sensing and environmental cues, with marine strains potentially expressing unique gene clusters adapted to salinity (Delgado et al., 2005). Production yields for B25 reach approximately 7.8 mg/mL in optimized media, though challenges like auto-inhibition persist (Wadekar and Dharmadhikari, 2022). Purification typically involves ammonium sulfate precipitation and chromatography, yielding a proteinaceous compound sensitive to proteases (Syukur et al., 2023). Characterization studies confirm its stability, making it suitable for industrial applications (Chen et al., 2024).

In food industries, bacteriocins prevent spoilage in dairy, meat, and seafood, extending shelf life by 20-50% (Yazgan et al., 2021). Agriculturally, they serve as biopesticides against plant pathogens like Fusarium spp. (Wadekar and Dharmadhikari, 2023). This review delves into these aspects, providing a detailed synthesis to guide future exploitation of marine L. pentosus B25 bacteriocin.

Isolation and Identification of Marine Lactobacillus pentosus B25

Isolation of marine LAB involves sampling from diverse aquatic niches, such as seawater, sediments, and marine organisms, where they form symbiotic relationships (Gálvez et al., 2010). For L. pentosus B25, isolation occurred from coastal marine samples using selective media like MRS agar with 2-5% NaCl to enrich halotolerant strains (Wadekar and Dharmadhikari, 2022). Initial screening employed overlay assays with indicator organisms to detect antimicrobial activity, revealing clear inhibition zones indicative of bacteriocin production (Todorov and Dicks, 2009).

Identification relies on phenotypic and genotypic methods. Phenotypically, B25 exhibits rod-shaped morphology, Gram-positive staining, catalase negativity, and homofermentative lactate production (Delgado et al., 2005). Genotypically, 16S rRNA sequencing confirms >99% homology with L. pentosus type strains, distinguishing it from closely related L. plantarum (Syukur et al., 2023). Marine adaptations include osmoregulatory genes for glycine betaine accumulation, enhancing survival in high-salinity environments (Rivas et al., 2024).

Comparative isolation: ZFM94 from feces used similar MRS but without salt (Wu et al., 2021), while PCZ4 from kimchi involved anaerobic incubation (Chen et al., 2024). B25's marine origin imparts unique traits, such as biofilm formation on marine surfaces, aiding colonization (Gálvez et al., 2010). Probiotic potential is assessed via acid/bile tolerance, adhesion to epithelial cells, and safety evaluations (no hemolytic activity) (Ouali et al., 2025).

Ecological implications: In marine ecosystems, B25 contributes to pathogen control, potentially reducing disease in aquaculture (Rivas et al., 2024). Future isolations could target deep-sea or polar marines for novel variants (Kaktcham et al., 2025).

Biosynthesis of Bacteriocins in L. pentosus

Bacteriocin biosynthesis in LAB is a multi-step process involving gene expression, peptide synthesis, modification, and export (Kaktcham et al., 2025). In L. pentosus, bacteriocin genes are often clustered on plasmids or chromosomes, regulated by autoinduction via two-component systems (Delgado et al., 2005). For B25, biosynthesis likely follows Class II pathways, producing unmodified heat-stable peptides <10 kDa (Wadekar and Dharmadhikari, 2022).

The process begins with ribosomal translation of pre-bacteriocin, cleaved to active form during export via ABC transporters (Wayah and Philip, 2018). Quorum sensing, mediated by peptides like IP-10, triggers production at high cell densities (Todorov and Dicks, 2009). Marine conditions (high NaCl) may upregulate these genes, as osmotic stress activates stress-response promoters (Gálvez et al., 2010).

Comparisons: In ST712BZ, biosynthesis is optimized at pH 5.5 with glucose (Todorov and Dicks, 2009), while ZFM94 involves similar clusters but lacks salt induction (Wu et al., 2021). PCZ4 harbors multiple loci for pediocin and plantaricin (Chen et al., 2024). Genetic engineering could enhance B25 yields by overexpressing transporters (Jiang et al., 2017).

Environmental factors: Temperature (30°C), pH (7), and carbon sources (glucose/sucrose) influence expression (Syukur et al., 2023). In marine LAB, salinity modulates membrane fluidity, affecting export (Rivas et al., 2024). Future omics studies could elucidate B25's pathway (Ouali et al., 2025).

Detailed mechanisms: Precursor peptides have leader sequences for secretion; post-cleavage, disulfide bonds stabilize structure (Wayah and Philip, 2018). Regulation involves histidine kinases sensing density (Delgado et al., 2005).

Production and Optimization of Bacteriocin B25

Production of bacteriocin B25 occurs in batch or fed-batch fermentation using mMRS broth with 2% NaCl, yielding 7.8 mg/mL after 18 h at 30°C (Wadekar and Dharmadhikari, 2022). Optimization employs response surface methodology (RSM) to fine-tune parameters like pH, temperature, and nutrients (Todorov and Dicks, 2009).

Key factors: Carbon (glucose 2%) and nitrogen (yeast extract) ratios enhance growth; salinity (2%) boosts production in marine strains (Gálvez et al., 2010). For ST712BZ, optimal conditions yielded 6400 AU/mL (Todorov and Dicks, 2009). B25 production peaks in late log phase, monitored by OD600 and agar diffusion assays (Syukur et al., 2023).

Comparisons: ZFM94 production in MRS at 37°C (Wu et al., 2021); PCZ4 in fish hydrolysate for aquaculture relevance (Chen et al., 2024). Challenges include auto-inhibition; solutions involve pH-controlled fermenters (Delgado et al., 2005). Sustainable media using marine byproducts (algal extracts) reduce costs (Rivas et al., 2024).

Scale-up: From lab (5L) to pilot (100L) bioreactors, maintaining aeration (Kaktcham et al., 2025). Genetic approaches: Promoter engineering increases yields 2-3 fold (Jiang et al., 2017).

Purification Methods for Bacteriocin B25

Purification of B25 involves cell removal by centrifugation, followed by 60% ammonium sulfate precipitation (specific activity 213 AU/mg), dialysis (301 AU/mg), and Sephadex G-25 chromatography (553 AU/mg, 3-fold purification) (Wadekar and Dharmadhikari, 2022). RP-HPLC on C18 columns achieves >90% purity (Syukur et al., 2023).

Standard protocols: For marine LAB, salt removal is crucial post-precipitation (Gálvez et al., 2010). Comparisons: ZFM94 used 40% saturation and HPLC (Wu et al., 2021); 124-2 employed Sephadex LH-20 (Syukur et al., 2023). Yields: B25 recovery ~3%, typical for bacteriocins (Todorov and Dicks, 2009).

Advanced techniques: Ion-exchange and gel filtration for charge-based separation (Wayah and Philip, 2018). Challenges: Aggregation in saline; solutions include buffers with Tween (Delgado et al., 2005). Purity assessment: SDS-PAGE, MALDI-TOF MS (Chen et al., 2024).

Physicochemical Characterization of Bacteriocin B25

B25 is a <3.5 kDa peptide, heat-stable (110°C/20 min), pH-stable (4-10), protease-sensitive, but resistant to amylase/lipase (Wadekar and Dharmadhikari, 2022). FTIR shows amide bonds; SDS-PAGE confirms low MW (Syukur et al., 2023).

Stability: Retains 80% activity after autoclaving, superior to terrestrial bacteriocins due to marine adaptations (Gálvez et al., 2010). Comparisons: ZFM94 stable at 80°C, pH 5-7 (Wu et al., 2021); Pentocin MQ1 pore-forming (Wayah and Philip, 2018). Structure: Cationic, amphipathic helix (Jiang et al., 2017).

Biophysical: Zeta potential positive, aiding membrane interaction (Chen et al., 2024). Toxicity: Non-cytotoxic to human cells (Wadekar and Dharmadhikari, 2023).

Antimicrobial Spectrum and Mode of Action

B25 inhibits Gram-positives (S. aureus, Listeria) and Gram-negatives (E. coli, Salmonella), plus fungi (Fusarium) (Wadekar and Dharmadhikari, 2023). MICs: 1-4 µg/mL (similar to ZFM94, 1.75 µM) (Wu et al., 2021).

Mode: Pore formation leading to leakage, ATP depletion (Wayah and Philip, 2018). Marine enhancements: Salt-tolerant activity (Gálvez et al., 2010). Synergies with nisin (Yazgan et al., 2021). Resistance: Rare, due to specific targets (Kaktcham et al., 2025).

Applications of Bacteriocin B25

In food: Biopreservative in seafood, reducing Vibrio by 3 logs (Rivas et al., 2024). Agriculture: Against plant pathogens, 70% inhibition (Wadekar and Dharmadhikari, 2023). Pharma: Wound healing (Ouali et al., 2025). Comparisons: PCZ4 in fish (Chen et al., 2024).

Encapsulation: For controlled release (Yazgan et al., 2021).

Comparisons with Bacteriocins from Other L. pentosus Strains

B25 vs. ZFM94: Similar MW, but B25 more stable (Wu et al., 2021). Vs. PCZ4: Broader spectrum (Chen et al., 2024). Vs. 124-2: Higher MW in 124-2 (Syukur et al., 2023). Marine advantages: Salinity tolerance (Delgado et al., 2005).

Strain	MW (kDa)	Stability	Spectrum
B25	<3.5	110°C, pH 4-10	Broad
ZFM94	3.5	80°C, pH 5-7	Broad
PCZ4	3.76-7.05	pH 3-9	Aquatic pathogens
ST712BZ	N/A	pH 5.5	Gram+

Challenges and Future Perspectives

Challenges: Low yields (3% recovery), cost (Syukur et al., 2023). Regulatory: GRAS approval (Kaktcham et al., 2025). Future: CRISPR editing (Chen et al., 2024), nanodelivery (Yazgan et al., 2021).

Conclusion

Marine L. pentosus B25's bacteriocin holds immense promise for sustainable antimicrobials (Wadekar and Dharmadhikari, 2023). Integrated research will drive its commercialization.

Reference

1. Wadekar, B. P., & Dharmadhikari, S. M. (2022). Production, purification and characterization of bacteriocin from marine Lactobacillus pentosus B25. International Journal of Research in Bioscience, Agriculture and Technology, X(VI), 1-10.
2. Wadekar, B. P., & Dharmadhikari, S. M. (2023). Production of Bacteriocin from Marine Lactobacillus pentosus B25 and Applications. Book, First Edition.
3. Wu, Q., Zhang, Y., Zhang, F., Du, H., & Han, X. (2021). A novel bacteriocin from Lactobacillus pentosus ZFM94 and its antibacterial mode of action. Frontiers in Nutrition, 8, 710303.
4. Chen, Z., Li, Z., Li, Z., Liao, Z., & Zhang, Y. (2024). Bacteriocin mining in Lactiplantibacillus pentosus PCZ4 with broad-spectrum antibacterial activity and its biopreservative effects on snakehead fish. Foods, 13(21), 3402.

5. Syukur, S., Bisping, B., Nöbel, S., & Hadiwiyono. (2023). Purification and partial characterization of a bacteriocin produced by Lactobacillus pentosus 124-2 isolated from dadih. Applied Sciences, 13(7), 4277.
6. Todorov, S. D., & Dicks, L. M. T. (2009). Bacteriocin production by Lactobacillus pentosus ST712BZ isolated from boza. Brazilian Journal of Microbiology, 40(1), 166-172.
7. Wayah, S. B., & Philip, K. (2018). Pentocin MQ1: A novel, broad-spectrum, pore-forming bacteriocin from Lactobacillus pentosus CS2. Frontiers in Microbiology, 9, 564.
8. Delgado, A., Brito, D., Peres, C., Noé-Arroyo, F., & Garrido-Fernández, A. (2005). Bacteriocin production by Lactobacillus pentosus B96 can be expressed as a function of temperature and NaCl concentration. Food Microbiology, 22(5), 521-528.
9. Jiang, H., Zou, J., Cheng, H., Fang, J., & Huang, G. (2017). Purification, characterization, and mode of action of pentocin JL-1, a novel bacteriocin isolated from Lactobacillus pentosus, against drug-resistant Staphylococcus aureus. BioMed Research International, 2017, 7657190.
10. Gálvez, A., López, R. L., Abriouel, H., Valdivia, E., & Omar, N. B. (2010). Bacteriocin as weapons in the marine animal-associated bacteria warfare: inventory and potential applications as an aquaculture probiotic. Marine Drugs, 8(4), 1153-1177.
11. Rivas, M. L. P., Sequeiros, C., Sánchez, L. A., & Vallejo, M. (2024). Lactic acid bacteria of marine origin as a tool for successful shellfish farming: a review. Aquaculture Reports, 35, 101971.
12. Kaktcham, P. M., Temgoua, J. B., Ngoufack, F. Z., & de Montety, C. (2025). Lactic acid bacteria bacteriocins: Safe and effective antimicrobial peptides for food preservation. Comprehensive Reviews in Food Science and Food Safety, 24(1), 1-25.
13. Yazgan, H., Cakir, E., Aygun, A., & Cengiz, G. (2021). Applications of lactic acid bacteria and their bacteriocins against spoilage yeasts and molds in dairy products. Foods, 10(11), 2704.
14. Ouali, F. A., Belabed, S., Chergui, A., & Bendimerad, M. (2025). Isolation and preliminary screening of lactic acid bacteria for bacteriocin production from raw milk in Algeria. Frontiers in Microbiology, 16, 1565016.
15. Jiang, Y., Xin, W., Yang, L., Ying, J., Zhao, Z., Lin, L., Li, X., & Zhang, Q. (2018). A novel bacteriocin against Staphylococcus aureus from Lactobacillus paracasei isolated from Kunda, a traditional Kazakh cheese from Xinjiang, China. Food Control, 90, 434-442.

ROLE OF MCR-2 MUTATION IN ALTERED RESPONSE TO OLANZAPINE
A Pharmacogenomic-Based Case Study

Vyas Trina*[1,2], Parab Mala*[1], Dr. Hema Purandarey[3], Soham Banerjee [4], Gupta Subodh[2], Gupta PramodKumar[1]

1. School of Biotechnology and Bioinformatics, D. Y. Patil Deemed to be University, Navi-Mumbai, India
2. Lords Mark Microbiotech, Hyderabad, India
3. Consultant & Medical Director (Prenatal & Reproductive Genetic) MedGenome Centre for Genetic Health Care, Mumbai, India
4. Co-Founder & Executive Director of Vinyash; PhD Scholar at Dept. of Biotechnology, Amity University, Ranchi.
   vyas.trina@gmail.com , mala.parab@dypatil.edu
   Contact No.: +91 8104891156

Abstract

The importance of pharmacogenomics in selecting the appropriate drug based on a person's genotype is demonstrated in this brief case study. The case study investigates a 14-year-old boy who has been diagnosed with familial glucocorticoid insufficiency since the age of 4. In addition, he experienced psychosomatic issues and was given medications; however, the antipsychotic drug olanzapine caused side effects. To understand and assess drug-gene interactions and their impact on the proband's health, several investigations including pharmacogenomic evaluation were performed. The findings suggested that combination therapy was required to increase the olanzapine's therapeutic efficacy.

Keywords: Olanzapine, Pharmacogenomics, familial Glucocorticoid deficiency, gene-drug interactions

Introduction

Familial glucocorticoid deficiency (FGD) is a rare condition with an autosomal recessive inheritance pattern that happens in cases where the adrenal glands fail to produce enough glucocorticoids in the body (Alghamdi, 2023).

This condition specifies a group of adrenal insufficiencies that can be typically characterized by neonatal hyperpigmentation, non-ketotic, non-hyperinsulinemic hypoglycemia, failure to thrive, collapse, and coma along with frequent infections. This can also be defined by the glucocorticoid deficiency biochemically except for the mineralocorticoid insufficiency.

Glucocorticoids include cortisol and corticosterone, which aid in immune system function (Spencer et al., 2011), play pivotal roles in maintaining normal blood sugar (glucose) levels (Lee et al., 2018), help to trigger nerve cell signaling in the brain ("Glucocorticoids, Ageing and Nerve Cell Damage," 2000), and serve many other purposes in the body.

There are multiple types of familial glucocorticoid deficiency, which are distinguished by their genetic cause majorly, Typical mutational variations in the MC2R, MRAP, and NNT genes are the lagging reasons behind this condition (Meimaridou et al., 2012).

The MC2R gene gives instructions to make a protein named adrenocorticotropic hormone (ACTH) receptor, and this one is primarily found in the adrenal glands. This protein produced

from the MRAP gene helps in the transportation of ACTH receptors from the interior of the cell to the cell membrane (Webb et al., 2008). According to physiology the ACTH receptor is embedded within the cell membrane; it's activated by the MRAP protein, and then this activated ACTH receptor can bind to ACTH, and this binding triggers the adrenal glands to produce glucocorticoids (Webb & Clark, 2010).

The mutations in MC2R genes can lead to the production of a receptor that cannot be transported to the cell membrane, or, if it wants to get to the cell membrane, then the ACTH binding fails. Hence without this binding, the signaling pathway of this hormone gets affected and fails to produce glucocorticoids (T. T. Chung et al., 2008).

Case history

A 14yrs old boy born of non-consanguineous parents exhibited hypoglycemia, seizures, reduced hydrocortisone production, and largely hypofunctional adrenal glands at the age of four. He was administered with Hydrocortisone for the said concern ever since without any side effects of the drug.

At school, behavioral problems like inattention, social disengagement, misconduct, etc. was noted by parents and teachers. He was nine years old when he experienced a second episode of seizures. Post which the patient was administered with Divalproex Gastro-resistant tablets I.P.(Indian Pharmacopoeia') (500mg) for seizures. At the age of twelve, the patient began to exhibit signs of anxiety, depression, behavioral problems, and decreased sleep depth and duration due to a change in school and other personal factors. Olanzapine (1.25mg) was prescribed for depression, anxiety, and concerns of autism, however the patient started exhibiting side effects post administration of olanzapine.

Family history

No relevant medical history recorded.

Birth History

Full Term Lower Segment Cesarean Section (FTLSCS), cried at birth, 2.5kgs,

Hyperpigmentation of Skin, Concerns of Recurrent Viral Infection.

Developmental history

All milestones were attained timely.

Medical Records and Investigations :

Investigations were performed for the concerns of Adrenal insufficiency, Seizures, Autism and to optimize the drug response of olanzapine.

General Investigations :

Condition	Test performed	Result
Adrenoleukodystrophy	Blood test measuring serum aldosterone	Negative
Autism	Autism Evaluation	Positive
Epilepsy	MRI & EEG	Positive

Genetic Investigations :

Purpose	Test performed
Adrenal Insufficiency and Glucocorticoid Deficiency	Clinical Exome Sequencing
Drug Response	Pharmacogenomics
Drug-Gene Interaction Analysis	In-silico Pathway analysis

Diagnosis / Results :

1. Clinical Exome Sequencing : Positive for a homozygous, Autosomal recessive "pathogenic" variant, which was detected in exon 2 of the MC2R gene (OMIM #607397). (**Description :** It has been demonstrated that FGD1, which presents as hypoglycemia, failure to thrive, hyperpigmentation, seizures, learning impairments, and other neurological issues, is linked to germline pathogenic variants in the MC2R gene. The melanocortin receptor family, which is involved in immunological response, glucose metabolism, and brain nerve cell transmission, is represented by the MC2R gene).
2. Pharmacogenomic test: Normal metabolizer for the concerned drug (Olanzapine 1.25mg). (**Description :**Second-generation antipsychotic olanzapine functions as a dopamine and serotonin antagonist. People using atypical antipsychotics have increased levels of dopamine activity. Atypical antipsychotic medications have a somewhat different mechanism of action, which makes them less likely to have some adverse effects. This is because there is less chance of motor and cognitive damage because dopamine neurotransmission is unaffected).
3. *In-silico* analysis: Preliminary *in-silico* screening revealed mutations in MCR-2 can alter cellular drug response (Fig.1).
   (**Description :** It is postulated in present case study that altered genes may alter molecular dynamics of the drug-gene interactions, as both cAMP signaling pathway and Neuroactive ligand-receptor interactions as both are mediated by MCR-2 and DRD-1 gene.)(Fig.1.a)

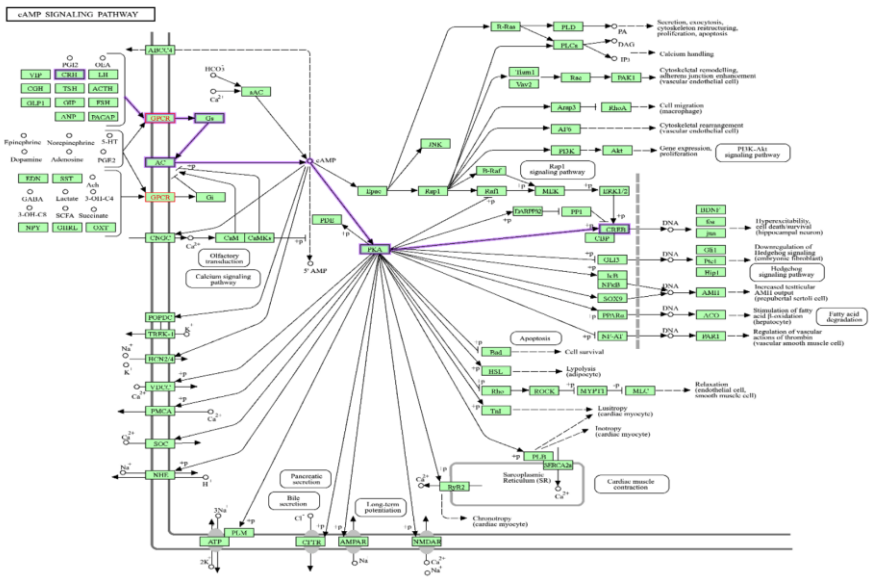

(Fig .1)

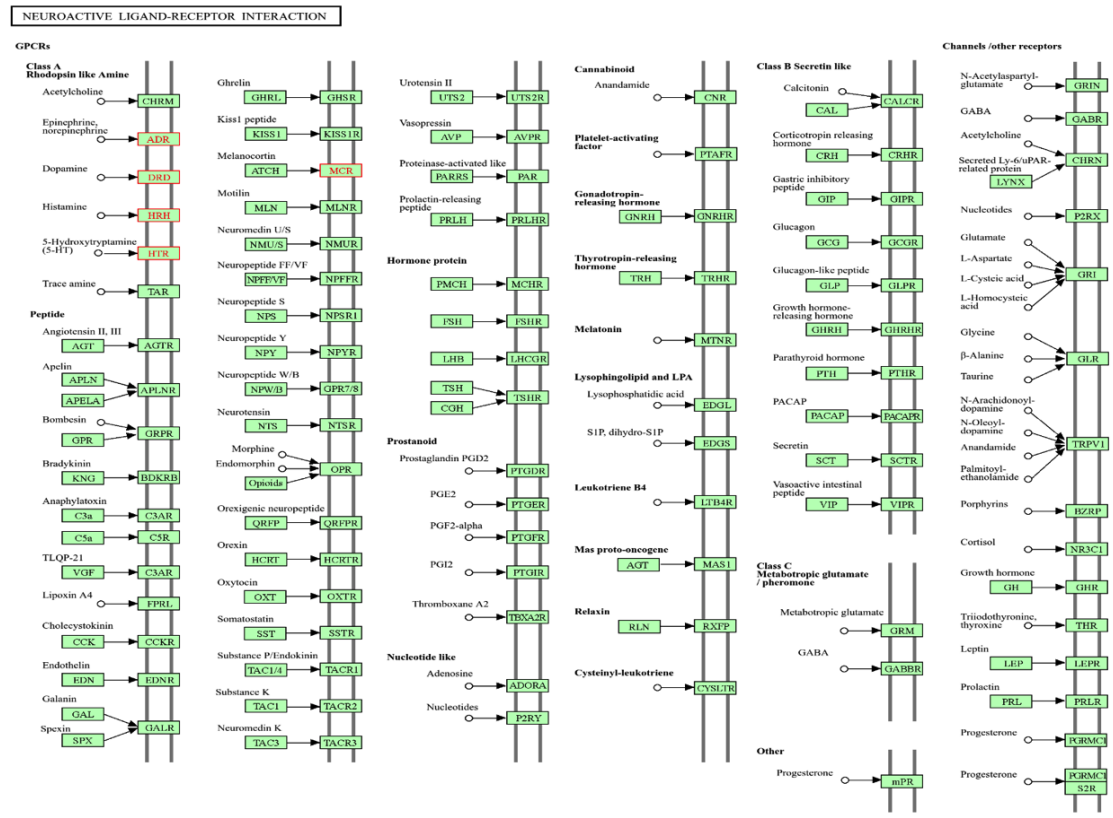

(Fig .1.a)

Discussion

The melanocortin 2 receptor, which mediates the actions of adrenocorticotropic hormone (ACTH), is encoded by the MC2R gene and aids in simulating the release of cortisol. A potential gene for mood disorders and treatment responsiveness, MC2R is thought to play a role in the hypothalamic-pituitary-adrenal (HPA) axis. The patient metabolizes olanzapine normally, according to the data, yet the side effects persisted (Perlis et al.,2010).

Although the key candidate genes, CYP1A2 and CYP2D6, were shown to function normally for olanzapine metabolism, the current study of pharmacogenomic and in-silico evaluation, suggests that variation in MC2R may have altered patients response for olanzapine.

Olanzapine continued to be administered according to the report, and also established a new regime by adding Fluvoxamine.

CYP1A2, a crucial metabolic pathway for olanzapine, is strongly inhibited by fluvoxamine. When fluvoxamine and olanzapine are co-administered, the plasma concentration of olanzapine rises significantly, increasing the therapeutic impact of the drug (Chiu et al., 2004).

Conclusion

This case highlights how determining who will react positively to a given treatment for such conditions, who won't respond at all, and who may experience adverse drug responses or serious side effects can be difficult at times. Conventional medicine frequently ignores individual genetic variations in favor of clinical trials and population averages. With the assistance of pharmacogenomic we could provide medication according to individual genotypes. This approach can benefit the patients by helping them reduce treatment duration and side effects with the right drug and dose (Ma & Lu, 2011)(Hockings et al., 2020).

Reference

1. Alghamdi, A. H. (2023). Familial Glucocorticoid Deficiency Presenting with Tonic-Clonic Seizure: A Case Report. *Children*, *10*(2), 301.
2. Chung, T. T., Webb, T. R., Chan, L. F., Cooray, S. N., Metherell, L. A., King, P. J., Chapple, J. P., & Clark, A. J. L. (2008). The Majority of Adrenocorticotropin Receptor (Melanocortin 2 Receptor) Mutations Found in Familial Glucocorticoid Deficiency Type 1 Lead to Defective Trafficking of the Receptor to the Cell Surface. *The Journal of Clinical Endocrinology & Metabolism*, *93*(12), 4948–4954.
3. Chiu, C., Lane, H., Huang, M., Liu, H., Jann, M. W., Hon, Y., Chang, W., & Lu, M. (2004). Dose-Dependent Alternations in the Pharmacokinetics of Olanzapine During Coadministration of Fluvoxamine in Patients With Schizophrenia. *The Journal of Clinical Pharmacology*, *44*(12), 1385–1390.
4. Hockings, J. K., Pasternak, A. L., Erwin, A. L., Mason, N. T., Eng, C., & Hicks, J. K. (2020). Pharmacogenomics: An evolving clinical tool for precision medicine. *Cleveland Clinic Journal of Medicine*, *87*(2), 91–99.
5. Lee, R. A., Harris, C. A., & Wang, J. (2018). Glucocorticoid Receptor and Adipocyte Biology. *Nuclear Receptor Research*, *5*.
6. Meimaridou, E., Hughes, C. R., Kowalczyk, J., Guasti, L., Chapple, J. P., King, P. J., Chan, L. F., Clark, A. J., & Metherell, L. A. (2012). Familial glucocorticoid deficiency: New genes and mechanisms. *Molecular and Cellular Endocrinology*, *371*(1–2), 195–200.
7. Ma, Q., & Lu, A. Y. H. (2011). Pharmacogenetics, Pharmacogenomics, and Individualized Medicine. *Pharmacological Reviews*, *63*(2), 437–459.
8. Perlis, R. H., Adams, D. H., Fijal, B., Sutton, V. K., Farmen, M., Breier, A., & Houston, J. P. (2010). Genetic association study of treatment response with olanzapine/fluoxetine combination or lamotrigine in bipolar I depression. Journal of Clinical Psychiatry, 71(5), 599.
9. Spencer, R. L., Kalman, B. A., & Dhabhar, F. S. (2011). Role of Endogenous Glucocorticoids in Immune System Function: Regulation and Counterregulation. *Comprehensive Physiology*, 381–423.
10. Seckl, J.R. (2000). Glucocorticoids, Ageing and Nerve Cell Damage. *Journal of Neuroendocrinology*, *12*(8), 710.
11. Webb, T. R., Chan, L., Cooray, S. N., Cheetham, M. E., Chapple, J. P., & Clark, A. J. L. (2008). Distinct Melanocortin 2 Receptor Accessory Protein Domains Are Required for Melanocortin 2 Receptor Interaction and Promotion of Receptor Trafficking. *Endocrinology*, *150*(2), 720–726.
12. Webb, T. R., & Clark, A. J. L. (2010). Minireview: The Melanocortin 2 Receptor accessory proteins. *Molecular Endocrinology*, *24*(3), 475–484.

Effect Of Different Concentrations Of Monosodium Glutamate On Angiogenesis

Aishwarya Chavan[1], Supriya Salunkhe[2], Pravin Shinde[3], Nikita Rashinkar[4], Rutuja Yadav[5], Satish Parte[6]
[1]Department of Biotechnology, S.G.M. College, Karad 415110, India
Email: yadavrutuja1911@gmail.com
Contact No:8468912462

Abstract:

Monosodium glutamate (Ajinomoto) is used in Chinese food as a flavoring agent. The previous researches regarding to monosodium glutamate suggests that it can cause harmful effect to organisms and their development. In this study, we observed the effect of monosodium glutamate on angiogenesis (process of blood vessels formation) of fertile chicken egg. The different concentrations i.e. (100ug/ml, 500ug/ml and 1000ug/ml) of Monosodium glutamate were injected into the fertile chicken eggs at 0hrs of incubation and embryos were extracted on 5th, 7th and 10th day of incubation. Treated embryo shows that the concentration 100 ug/ml does not shows more affection to the process of angiogenesis. While the concentration of 500ug/ml and 1000ug/ml shows the inhibitory effect on angiogenetic development in chick embryo. The study emphasizes on the number of primary, secondary and tertiary blood vessels development when injected with monosodium glutamate and these numbers were compared with controlled eggs. We can conclude that high concentration of monosodium glutamate can affect the formation of blood and other parts of chick embryo.

Keywords: Monosodium Glutamate, Angiogenesis, Fertile chicken egg.

1. Introduction

Angiogenesis, or neovascularization is the process of generating new blood vessels derived as extension from the existing vasculature [1]. The blood vessels that are emerge directly from endothelial cells are considered as primary blood vessels and vice versa. Further the angiogenesis continues this branching and form wide network of blood vessels throughout the organism's body.

Monosodium glutamate is also known as Ajinomoto. It is a crystalline powder having molecular formula C5H8NO4 NA. The IUPAC name of monosodium glutamate is sodium 2-Aminopentan edioate. It increases sapidity thereby giving special taste to Chinese food. Widely, monosodium glutamate is used as a flavoring agent that enhance food taste hence known as flavor enhancer.

Monosodium glutamate is first prepared bin 1908 by Japanese biochemist Kikunae Ikeda who tried to isolate and duplicate the savory taste of kombu [2].

Glutamate is a type of amino acid and it generally involved in the neurotransmission mechanism in brain. According to US environmental protection agency the use of monosodium glutamate in food should not be allowed for infants and children under one year age [3]. Monosodium glutamate may prove harmful and toxic to human health abnormal function of glutamate receptor has been linked with certain neurological disease. The toxic effect of monosodium glutamate on this central nervous system, adipose tissue, hepatic tissue, reproductive organs, liver and kidney functions were determined by several studies. These studies revealed that monosodium glutamate cause a cytotoxicity and oxidative damage in the liver, kidney and various tissues and increased the risk of certain cancer [3]. The paper seeks to examine of monosodium glutamate on the angiogenesis by using chick embryo as a model.

The use of chick embryo model for angiogenic studies is facilitated by the existence in avian species of a specialized respiratory tissue named the chorioallantois membrane (CAM) that allows for gas exchange between the embryo and the atmosphere surrounding the egg and in effect performs the function of a lung during embryonic life [4].

2. Methodology

1.1. Collection Of sample –

The experiment involved total 30 fertilized chicken eggs. These eggs were collected from Narayan wadi (Karad, satara). The collection was done on a sargassum floor. Monosodium glutamate (MSG), used in the experiment, was sourced from a general grocery shop in Vidyanagar, Karad.

1.2. Injection of monosodium glutamate –

The fertilized eggs were further inoculated with different concentrations of monosodium glutamate: 100 ug/ml, 500 ug/ml and 1000 ug/ml. This inoculation was performed under aseptic condition using sterile syringes. The aseptic environment was maintained in a laminar airflow chamber. After incubation, the egg was sealed with adhesive tape.

1.3. Incubation-

There are a total three sets of egg were incubated. Each set contains 3 - 100 ug/ml, 3 - 500ug/ml and 3- 1000ug/ml and one control egg. These sets where incubated at proper condition Where the temperature is maintained at 37°c. Further Incubated eggs were broken on the respective days as 5th,7th and 10th day.

1.4. Egg breaking-

After proper incubation each set of egg were broken onto their particular incubation period. The egg was broken in aseptic condition which is maintained by laminar airflow. Eggs were broken by using the dissecting materials like needle and forceps.

1.5. Observation and Analysis-

After breaking of egg, the effect was observed visually and by using dissecting microscope. We count the number of primary, secondary and tertiary blood vessels manually.

3. Results

3.1 5th day of incubation -

Concentration of MSG	Development
Control	Proper development of primary, secondary blood vessels
100 ug/ml	Development primary and very few secondary blood vessels
500 ug/ml	Development primary and very few secondary blood vessels
1000 ug/ml	No proper development of blastodisc and the vessel formation is inhibited

Fig: table showing the development of chicken eggs injected with monosodium glutamate comparing to the control at the 5th day of incubation.

7th day of incubation -

Concentration of MSG	Development
Control	PBV =10 SBV=21 TBV=37
100 ug/ml	PBV =05 SBV=08 TBV=15
500 ug/ml	PBV =03 SBV=10 TBV26
1000 ug/ml	PBV =03 SBV=03 TBV=06

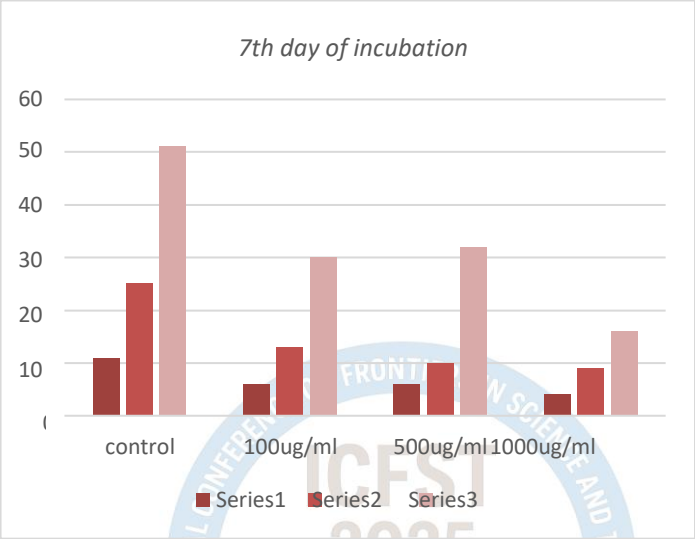

10th day of incubation –

Concentration of MSG	Development
Control	PBV =11 SBV=25 TBV=51
100 ug/ml	PBV =06 SBV=13 TBV=30
500 ug/ml	PBV =06 SBV=10 TBV=32
1000 ug/ml	PBV =04 SBV=09 TBV=16

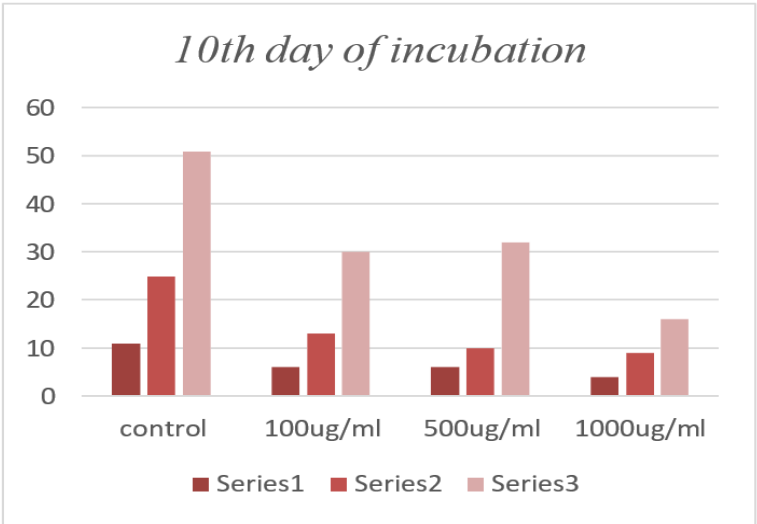

4. Discussion:

This study was based on the analysis of process of angiogenesis in chick embryo when treated with the different concentrations of monosodium glutamate. In this paper we studied the effect of monosodium glutamate on angiogenesis at different incubation interval of time 5th ,7th and 10th day respectively. After comparing with the control, the observation shows the affectivity of monosodium glutamate on the process of angiogenesis occurring in chick embryo.100ug/ml concentration does not show more affection to the process of angiogenesis while 500ug/ ml and 1000ug/ml concentrations are observed to be affecting the angiogenesis mechanism. 1000ug/ml concentration show comparatively high influence on the blood vessel formation. while considering all the data we can conclude that the high concentration of monosodium glutamate can cause more inhibition in blood vessel formation and this can be proved toxic for the organism's health.

5. Conclusion:

The present study suggests that monosodium glutamate (MSG) can significantly affect embryonic growth and blood vessel formation. Different concentrations of MSG were found to influence angiogenesis in developing chick embryos. Higher concentrations inhibited blood vessel formation, whereas lower concentrations had a comparatively milder effect. Therefore, it can be concluded that elevated levels of monosodium glutamate may exert harmful effects on early embryonic development and angiogenesis in chick embryos**.**

6. Reference:

1 Auerbach R. et.al. 2003. Angiogenesis Assay - A critical overview. Clinical chemistry 49.1

2 https://en.m. Wikipedia.org.

3 Bolukbas F. et.al. 2003. Investigation of the effect of monosodium glutamate on embryonic Development of the eye in chickens. Veterinary science.

4 Deryugina.I and Quigley. P. 2008. Chapter 2: Chick embryo chorioalantoic Membrane Models to quantify Angiogenesis Induced by Inflammatory and Tumor cells or purified effector Molecular Method Enzymol.

5 Jadhav j. et.al 2014. Iodinin (1,6-phenazinediol 5,10-dioxide) from Microbispora sp. V2 inhibits angiogenesis in vivo. Research Article ISSN: 0975-7619

6 Othman Z. et.al. 2019.The Anti-Angiogenic Properties of Morinda citrifolia L. (Mengkudu)Leaves using Chicken Chorioallantoic Membrane (CAM) Assay.Pharmacogns J. 2019; 11(1):12-15.

7 Swaminathan A. et.al. 2019.Live Imaging and Analysis of Vasoactive Properties of Drugs Using an in-ovo Chicken Embryo Model: Replacing and Reducing Animal Testing. Microscopy and Microanalysis (2019), 1–10

8 Roy S. et.al. 1974.The Fine Structure of Cerebral Blood Vessels in Chick Embryo. Acta neuropath. (Berl.) 30, 277--285 (1974).

9 Fawzyah A. AI-Ghamdi. 2021.Microscopic study of potential toxic effects of monosodium glutamate on liver of chicken embryos aged 16 days. Al-Ghamdi Egyptian liver journal (2011) 11:38.

10 Ibrahim.K.et.al.2021. The effects of acyclovir on angiogenesis in chick chorioallantoic membrane model. Turkish med stud j 2021;8(3):111-4.

11 Samet.C.et.al.2020. Effects of Gold Nanoparticles on Angiogenesis in A Chick Chorioallantoic Membrane Model. Bezmialem Science 2020;8(4):398-402.

12 Zulhabri. O. et.al. 2019. The Anti-Angiogenic Properties of Morinda citrifolia L. (Mengkudu) Leaves using Chicken Chorioallantoic Membrane (CAM) Assay. Pharmacogn J. 2019; 11(1):12-15.

A Comparative Analysis of AI-Assisted and Human Grading in Higher Education

Prasad V. Pusalkar[1], Sakshi Rajesh Bane[2]
R. E. Society's R.P.Gogate College of Art and Science and
R.V.Jogalekar College of Commerce (Autonomous), Ratnagiri Maharashtra, India – 415612
Email: prasad.pusalkar@gjcrtn.ac.in[1], sakshibane15@gmail.com[2]
Contact No.: 8805317794[1], 7507053668[2]

Abstract
In higher education, assessment plays a crucial role in measuring student learning outcomes and academic performance. With the rise of artificial intelligence, many institutions are beginning to explore AI-assisted grading tools to reduce workload and bring consistency in evaluation. However, there are concerns about whether AI-based grading can truly match the fairness, accuracy, and contextual understanding of human grading. This study aims to compare the effectiveness of AI-assisted grading with traditional human grading in higher education.
The research will use an experimental design where student assignments will be evaluated by both AI-assisted tools and human evaluators. The comparison will be based on factors such as grading consistency, time efficiency, accuracy, and student satisfaction with the feedback received. Statistical analysis using a paired t-test will help identify if there are significant differences in grading patterns between the two approaches.
It is expected that AI-assisted grading will show strength in speed and consistency, while human grading may prove better in understanding context, subjectivity, and creativity in student responses. The study will help highlight whether AI should be seen as a supportive tool for educators or as a potential replacement in the grading process.

Keywords: AI-assisted grading, Human grading, Higher education, Assessment, Comparative analysis

1. Introduction

Grading is a vital and indispensable component of the learning process. Grading is a mirror that reflects teacher effectiveness and student learning. Teachers, by way of grading, can assess how students have performed in terms of meeting the intended learning outcomes and determine areas where they need help. It also offers students constructive feedback, enabling them to understand their areas of strengths and weaknesses. In universities, grading does not only function as a tool to measure performance but also as an instrument of motivation that affects students' study habits and participation.

Unfortunately, conventional grading systems based entirely on human graders are usually beset by some drawbacks. Reading through numerous answer sheets or essays is a fatiguing and time-consuming process, particularly when there are large classes. Instructors will spend countless hours grading similar responses, with less time available to devote to enhancing pedagogy or offering individualized feedback. Further, human grading is susceptible to personal biases like mood, fatigue, or even unconscious bias. For example, a teacher may grade inconsistently when fatigued or when assessing a very long set of responses. Consequently, marking sometimes turns out to be unreliable, and the students feel that the marks do not represent their effort or comprehension.

The Artificial Intelligence (AI) field has provided possible answers to most of these issues in the last few years. AI-based marking systems are being researched as possible tools that can help teachers assess student work more effectively. These systems employ algorithms that are able to automatically grade written or objective responses, test grammar and syntax, and even forecast the quality of reasoning. Some of these tools are based on Natural Language Processing (NLP), which enables computers to read and process text much like a human would. Tools like Gradescope and Turnitin have already started incorporating AI features to assist teachers with high-volume assessments. These tools not only provide time savings but assist in maintaining grading consistency among multiple reviewers.

Researchers globally have expressed increasing interest in knowing how accurate these AI systems are relative to conventional human grading. Deepshikha (2025) noted that AI-driven tools can offer immediate and customized feedback to students, assisting them in correcting errors more efficiently. This rapid feedback loop also improves the learning process overall. Zhao (2024) underscored the fact that whereas AI excels in marking objective questions and factual responses, it is yet to be able to decipher abstract or innovative answers that need profound contextual sense-making. Likewise, Adiguzel et al. (2021) noted that while AI can serve teachers by cutting down on workload and enhancing efficiency, it cannot replace the emotional intelligence and empathy which human teachers impart through assessment. Human graders are able to identify creativity, original thought, and emotional tone in a student's work — aspects not yet fully understandable by AI systems.

Taking into account these two viewpoints, this paper sets out to offer a comparative examination of AI-graded and human-graded works in higher education. The purpose is to recognize the strengths, weaknesses, and areas of convergence between these two approaches. The research overviews recent studies, such as those by Deepshikha (2025), Zhao (2024), and Adiguzel et al. (2021), to learn how AI can enhance testing while preserving academic equity and human touch. It submits that the best solution is neither substituting teachers with AI nor limiting them to using AI but mixing the best of both. The suggested hybrid model seeks to marry the velocity, precision, and uniformity of AI with human teachers' contextual sense, creativity, and empathy. Such convergence is the future of fair, effective assessment in higher education.

2. Methodology

This research employs a conceptual and comparative research approach to explore the difference between Artificial Intelligence (AI)-based grading and human grading in higher learning. Rather than conducting new experiments, the study relies on a systematic reading of already published research, journal publications, and reports spanning 2018 to 2025. These researches are a rich source of information on how AI tools work, what are their advantages and difficulties, and what educators and students perceive about them.

The literature review started with a comprehensive scan of literature accessible via electronic databases like Google Scholar, Scopus, and ResearchGate. Search terms such as AI-assisted grading, automated marking, machine learning for education, human marking, and comparative marking were employed to cull relevant sources. Screening and filtering eventually narrowed down the selection to approximately 15 to 20 key studies that were reviewed in detail. These are just some of the research works like CDeepshikha (2025), Zhao (2024), Adiguzel et al. (2021), and Spreadborough and Glasser (2024), which specifically touch on the application of AI in scholarly evaluation.

The conceptual framework of the study centers on a few comparison parameters that constitute the heart of this analysis:

Speed and Efficiency – How quick can AI software grade as opposed to human graders?

Consistency and Fairness – How consistent and unbiased are the outcomes?

Accuracy – How dependable are AI-made grades compared to human grading?

Contextual Understanding and Creativity – Are AI capable of detecting creative ideas or deeper meaning?

Feedback and Student Perception – How do students perceive AI compared to human feedback?

Ethical and Privacy Issues – What are the risks or limitations of using AI systems to grade?

For each of these areas, data were gathered from existing research, case studies, and theory models. The literature was contrasted qualitatively to bring out both similarities and discrepancies between researchers' results. For instance, while Zhao (2024) highlighted the efficiency of AI, Deepshikha (2025) underscored the necessity of integrating AI with human checking to ensure improved feedback accuracy.

Apart from secondary data, conceptual knowledge was obtained from educational psychology and technological adoption theories. Such theories were used to explain how students and instructors adjust to systems driven by AI. Ethical considerations were examined through reading reports of algorithmic bias, data protection, and transparency. Adiguzel et al. (2021) and Torres (2023) elaborated on such concerns, indicating that supervision by humans is vital to ensure fairness.

The paper adopts a comparative reasoning methodology in order to determine the complementary and conflicting areas of AI and human grading. It does not conduct statistical tests since it relies on theory. Nevertheless, the paper suggests that paired t-tests or ANOVA can be utilized by future researchers in comparing real grade distributions between human graders and AI systems when real datasets are attained.

In addition, this conceptual framework posits an even view—AI is not envisioned as a substitute for human intelligence but as a technological aid. The study presupposes that the best system of educational evaluation will most probably be a coupling of the automation of AI and the interpretive and emotional intelligence of humans. The general aim of this methodology is to present a structured foundation for future experimental researches that can measure the differences and verify these theoretical results.

Lastly, ethical values like academic integrity, privacy of data, and intellectual rights are adhered to within this research. Being a literature review, no human subjects were actively involved. Nevertheless, the analysis is cognizant of the necessity of equity, inclusivity, and openness when applying AI tools in actual educational settings.

3. Results and Discussion

The reviewed literature in this research points out that AI-based grading systems have demonstrated remarkable gains in speed, consistency, and efficiency over traditional human grading. The systems are able to grade large volumes of assignments rapidly and with consistent application of evaluation criteria without suffering from fatigue or mood swings. AI

tools like Gradescope and Turnitin illustrate how instant feedback can be provided using AI, which enables students to recognize their errors and improve in a timely manner (Zhao, 2024). The quick processing of AI enables instructors to handle large classrooms in a cost-effective way and devote more time for interactive instruction instead of mundane assessment tasks.

While AI tools excel in systematic and objective activities, they struggle to comprehend innovative, subjective, or context-dependent answers. Generative AI vs. Instructor vs. Peer Assessment (2024) research identified that human graders are more capable of identifying originality and creative thinking. They are able to read argument structure, tone, and emotional appeal—domains that existing AI technologies struggle to analyze with precision. Deepshikha (2025) also noted that AI-driven tools enhance turnaround time and grading consistency but often miss appreciating new ideas that break away from pre-formatted schemes.

Human feedback remains appreciated for its personal and motivational quality. Students tend to indicate that they appreciate human comments as more supportive and emotionally stimulating than AI feedback, which may appear mechanical (Adiguzel et al., 2021). Human graders are able to appreciate the effort put into a student's work, notice creativity, and give informative advice that promotes learning. This emotional factor stimulates students to work better and have confidence in the grading process. AI systems, although effective, do not yet possess the ability to substitute this interpersonal aspect of evaluation.

Another crucial issue is associated with moral and pragmatic challenges of using AI in teaching. Algorithmic bias is still a significant challenge. If an AI model uses limited or biased data for training, it might lean in favor of some writing styles or even penalize others inadvertently. Torres (2023) warned that such biases could introduce inequality in evaluation outcomes. Transparency is also an issue, with many AI grading systems failing to elucidate how scores are calculated, causing confusion or distrust among students (Artificial Intelligence in Education: A Review, 2023). Security and privacy of the data are also serious concerns because these systems work with a large volume of student information.

AI can, however, be very useful when supplemented with human assessment despite these challenges. Hybrid model—where AI does objective grading aspects like grammar, structure, and factuality, and teachers determine creativity and deeper meaning—seems to be the best method. This mix guarantees both empathy and fairness in grading. Spreadborough and Glasser (2024) also put forth that the education of the future relies on collaboration between AI systems and human teachers, and not rivalry. Such integration enables technology to augment human judgment instead of substituting it.

Finally, the literature indicates that AI and human grading each provide a different set of benefits. AI systems bring about speed, scalability, and uniformity, while human graders contribute empathy, flexibility, and critical interpretation. Together with the integration of both, they provide a harmonized context for equitable and effective assessment in higher education. This combined method is complementary to the current revolution in education in the digital era, where technology aids but does not substitute for the key role of human agency in learning and assessment.

4. Conclusion

This conceptual paper has examined the comparative advantages and drawbacks of AI-assisted and human grading in higher education. AI-based grading systems provide notable benefits, including improved efficiency, consistency, and reduced instructor workload, making them

ideal for large-scale or objective evaluations. However, human judgment remains vital for assessing creativity, critical thinking, and emotional depth—areas where AI still lacks contextual understanding.

The study supports the view that the future of academic assessment lies in a hybrid approach that combines AI's technical precision with human insight. Such an approach can improve both the reliability and emotional quality of grading. Future research should empirically test these theoretical conclusions by comparing AI and human grading outcomes on real student work. As AI technologies continue to evolve, they promise to make educational assessment more scalable, equitable, and effective for learners worldwide.

5. References

1. (Khorsandi et al., 2012) Khorsandi, M., et al. (2012). Online versus traditional teaching evaluation: Mode can matter. Procedia - Social and Behavioral Sciences, 46, 554–559.
2. (Zhao, 2024) Zhao, L. (2024). AI-assisted assessment in higher education: A systematic review. Educational Technology Research, 9(2), 55–71.
3. (Torres, 2023) Torres, A. (2023). Ethical implications of AI grading systems. Journal of Educational Technology, 18(3), 211–227.
4. (Deepshikha, 2025) Deepshikha, D. (2025). A comprehensive review of AI-powered grading and tailored feedback in universities. Discover Artificial Intelligence, 5(251).
5. (Generative AI vs. Instructor vs. Peer Assessment, 2024) Generative AI vs. Instructor vs. Peer Assessment. (2024). Journal of Educational Technology and Learning, 12(3), 201–215.
6. (Adiguzel et al., 2021) Adiguzel, T., et al. (2021). AI-assisted assessment in higher education. Computers and Education Journal, 168, 104212.
7. (Palanisamy et al., 2023) Palanisamy, R., et al. (2023). Personalised Adaptive Learning Systems in Education. International Journal of Learning Analytics, 11(2), 45–58.
8. (Gnanaprakasam et al., 2022) Gnanaprakasam, A., et al. (2022). The impact of AI on automated grading systems. Advances in Educational Research, 10(1), 44–60.
9. (Artificial Intelligence in Education: A Review, 2023) Artificial Intelligence in Education: A Review. (2023). International Journal of Education and Development Using ICT, 19(4), 88–102.
10. (Spreadborough & Glasser, 2024) Spreadborough, C. & Glasser, M. (2024). Balancing automation and human oversight in higher education assessments. Education Policy Review, 32(1), 100–119.

AI Integration in Education: Predicting and Analyzing Students' Outcomes through Machine Learning

Shalaka Sadanand Agre [1]
Email: shalsgare@gmail.com | Contact: 8275449899
Anuja Amit Gharpure [2]
Truptee Ankush Dhamnaskar [3]
[123]Assistant Professor, Gogate Jogalekar College, Ratnagiri.

Abstract

In today's digital era, AI tools play a vital role in enhancing learning efficiency, providing personalised support, and bridging knowledge gaps for college students. Their integration into education empowers learners to achieve better academic outcomes and adapt to future skill demands. This study investigates the impact of AI-based learning tools on the self-reported academic outcomes of Computer Science and IT students, employing both descriptive analysis and machine learning methods. Before the adoption of AI tools, students generally reported average academic performance, following regular use of AI-aided learning support, a clear improvement was observed, with a significant number of students attaining higher levels of educational achievement. These findings suggest that AI tools contribute to meaningful improvements in academic performance as perceived by learners.

The proposed research work is focused on the usage of AI tools and their academic improvement. A regression model is set up to test the perceived impact of AI tools on the change in grade. The analysis conducted leads closer to the conclusion that the use of Generative AI tools is capable of bringing positive changes in the quality of academic performance.

Overall, the study highlights that AI-based learning tools play a significant role in improving the academic outcomes of Computer Science and IT students. By employing a simple linear regression to analyse the relationship between students' perceptions of AI tools and their grade improvements, the study demonstrates that positive perceptions are associated with greater academic gains. Overall, these findings emphasise the potential of AI to drive personalised, engaging, and technology-enhanced learning experiences in higher education.

Keywords: Artificial Intelligence (AI) Tools, Machine Learning, Linear Regression, Learning Improvement, Educational Technology.

Introduction

Generative Artificial Intelligence (AI) tools have significantly transformed education by providing personalised learning support, automated feedback, and assistance in problem-solving. Tools such as ChatGPT, GitHub Copilot, and other intelligent assistants enhance learners' efficiency and academic performance by reducing task completion time and offering real-time guidance. Studies suggest that students using AI tools achieve better academic outcomes and improved study efficiency, though concerns persist regarding the depth of learning and critical thinking skills (Computers, 2025), (Ward et al., 2024). In health professions, education, and systematic reviews also report mixed outcomes, indicating that the effectiveness of AI largely depends on implementation design and learner engagement (Hothersall-Davies et al., 2025).

Artificial Intelligence (AI) has become a transformative element in education, fostering innovations such as personalised learning, adaptive assessments, and intelligent tutoring

systems (Zawacki-Richter et al., 2019). Within this domain, Machine Learning (ML) is crucial for predicting and analysing student performance using academic, behavioural, and demographic data (Kumar et al., 2020). These predictive models enable early identification of at-risk students and support timely interventions to enhance learning outcomes.

Educational Data Mining (EDM) and Learning Analytics (LA) enhance the ability of researchers and institutions to derive meaningful insights from large volumes of student data. By analysing parameters such as attendance, participation, and digital learning activities, predictive models improve the accuracy of outcome estimation (Romero & Ventura, 2020).

To understand the use of GenAI among learners in Remote regions where poor internet connectivity is observed, a specific region, such as the Konkan region, is selected as a case study. This study focuses on learners of Computer Science and Information Technology in the remote Konkan region of Maharashtra, India, where limited access to educational resources affects learning opportunities. With internet access and Generative AI tools, students can enhance their technological skills, knowledge, and overall development. The research aims to evaluate the contribution of these AI tools to students' academic growth. For the evaluation, regression techniques such as Linear regression combined with Random Forest Classification, Ridge regression, and XGBoost regression are applied to make a comparison of the academic performance before and after the usage of AI tools for learners.

Literature Review

Generative AI (GenAI) in education has been categorised into three roles: "GenAI as a workhorse," "GenAI as a language assistant," and "GenAI as a research accelerator," with tasks like data analysis and language editing primarily performed by AI (Andersen et al., 2025). Integrating GenAI across educational components shows significant benefits (N. U. J. et al., 2024), and surveys in higher education indicate improved academic growth and feedback (Saúde et al., 2024). Six key domains where AI supports academic writing and research include idea generation, content structuring, literature review, data management, editing and publishing, and communication with ethical compliance (Khalifa & Albadawy, 2024).

Despite these advantages, concerns persist. Students often rely on AI to complete assignments without actively engaging in learning, which can reduce academic performance (van Niekerk et al., 2025)(Mahama et al., 2023)(Golding et al., 2025). AI and ML applications also face challenges related to model interpretability, fairness, and ethical implications. Black-box algorithms may limit educator trust, while biased datasets risk unfair predictions (Abdullah et al., 2022). Effective adoption requires institutional support, faculty training, and alignment with pedagogical goals (Shibani et al., 2020). Strategies to manage AI use include clear guidelines, academic integrity education, technical detection of AI-generated text, and applying the TAM model to improve student engagement with AI tools (Bui & Tong, 2025)(Sousa & Cardoso, 2025).

Notably, patterns of AI usage influence learning outcomes differently: low-achieving students may benefit from AI hints, whereas medium-achieving students may experience performance decline if over-reliant on AI feedback (Dai et al., 2025). Overdependence can also reduce self-efficacy and critical thinking skills (Int. J. Res. Sci. Innov., 2024), highlighting a trade-off between short-term performance and higher-order learning.

This study leverages machine learning to analyze and predict how AI tool usage affects student outcomes. By identifying predictive features such as usage frequency, tool type, and learner characteristics, it aims to provide actionable insights for optimizing AI integration in education.

Methodology

To understand whether the use of GenAI enhances academic progression in learners from the Konkan region of Maharashtra state, India, a Google form is shared among Computer learners. The study's concentration focused on Computer learners in various colleges to determine how they utilise GenAI for their progression. The methodology used in the research is as described in Figure 1.

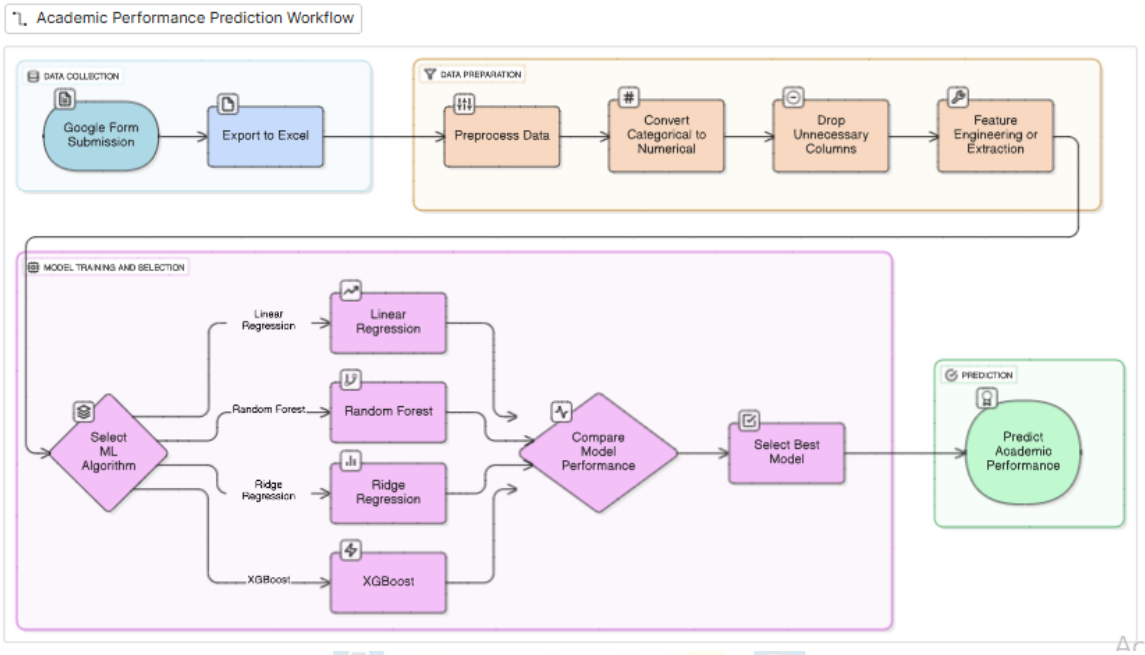

Figure 1: Methodology of the proposed research work

Data Collection

Data were collected from 227 Computer Science and Information Technology students, covering four main areas: general information (name, gender, email, courses); awareness and usage of AI, including perceived reliability of GenAI for writing, designing, and content creation; learners' perceptions of GenAI; and academic performance, recorded as cumulative grade points before and after AI usage in the previous and current academic years.

Data Pre-processing

The collected categorical data were converted to ordinal values ranging from 1 to 5 to facilitate machine learning implementation. Irrelevant columns, such as timestamp, name, and gender, were removed. Feature engineering was applied to enhance the model, including aggregated metrics like Reliability_Avg, AI_Gain, and interaction terms such as Usage × Reliability. Reliability-related variables were averaged to create composite features, while AI_Gain was calculated as the difference in student performance before and after AI tool usage. Additional features, such as Reliability_Cognitive and Reliability_Design_Preparation, were derived as means of related reliability measures, capturing combined effects for improved predictive analysis.

Implemented Machine Learning Model

To analyze the relationship between student performance before and after GenAI usage, several regression models were applied. The dependent variable was Performance after AI usage, while independent variables included Frequency of usage, Reliability for Understanding, Reliability

for Writing, Reliability for Designing, Reliability for Preparation, Reliability for Language Improvement, and Performance before AI usage.

Regression models such as Linear Regression, Ridge Regression, Random Forest Regression, and XGBoost Regression were employed. To reduce overfitting, k-fold cross-validation and feature engineering were applied. Regression techniques vary in assumptions, computational complexity, interpretability, and predictive performance. Linear and Ridge Regression are preferred for transparency and smaller datasets, whereas Random Forest and XGBoost handle high-dimensional, nonlinear data with complex feature interactions more effectively (James et al., 2021).

Model performance was evaluated using R^2 (Coefficient of Determination) and RMSE (Root Mean Squared Error). R^2 measures the proportion of variance explained by the model, with adjusted R^2 accounting for model complexity (Montgomery et al., 2021). RMSE calculates the square root of the average squared differences between predicted and actual values, giving greater weight to larger errors and sensitivity to outliers (Han et al., 2022).

Findings and Discussion

Table 1: Regression analysis on the feature 'After AI usage'

Regressor	**R2 Score**	**RSME**
Linear Regressor and Random Forest Regressor	0.8513	0.3360
Ridge Regressor	0.9864	0.0991
XGBoostRegressor	0.8814	0.2923

The comparative evaluation of regression models highlights the predictive potential of machine learning in AI-supported learning environments as described in Table 1. Ridge Regression demonstrated the highest accuracy ($R^2 = 0.9864$, RMSE = 0.0991), indicating that engineered features effectively capture academic performance patterns, especially under linear relationships. Its L2 regularization mitigates multicollinearity among overlapping variables like usage, reliability, and perceptions, producing stable and generalizable predictions.

Random Forest ($R^2 = 0.8513$, RMSE = 0.3360) and XGBoost ($R^2 = 0.8814$, RMSE = 0.2923) showed slightly lower predictive accuracy but excel in capturing non-linear relationships and interaction effects, such as threshold-dependent impacts of AI usage. Linear Regression, while interpretable and useful for stakeholder communication, is less robust due to sensitivity to multicollinearity and outliers.

Feature importance analysis (Fig. 2) revealed Performance before AI usage as the strongest predictor (≈0.48) of post-AI outcomes, highlighting the influence of prior proficiency (Montgomery et al., 2021). For Overall Performance, features like Reliability for Writing, Understanding, and Designing gained importance (≈0.15–0.20), emphasizing that consistent and effective AI use across cognitive and creative tasks significantly enhances academic outcomes (Chen & Guestrin, 2016). Usage and Reliability for Preparation contributed moderately, while Reliability for Language Improvement maintained a consistent secondary effect (Zhang et al., 2023).

These findings indicate that post-AI performance largely reflects prior academic ability, whereas overall performance depends on both prior ability and effective AI utilization. Ridge

Regression provides high-confidence predictions, while ensemble models offer insights into complex learning behaviors. Together, these approaches form a comprehensive predictive framework, enabling institutions to forecast student outcomes, identify at-risk learners, and design personalized interventions, supporting scalable and effective AI integration in higher education (Zhang et al., 2023), (Liu et al., 2025).

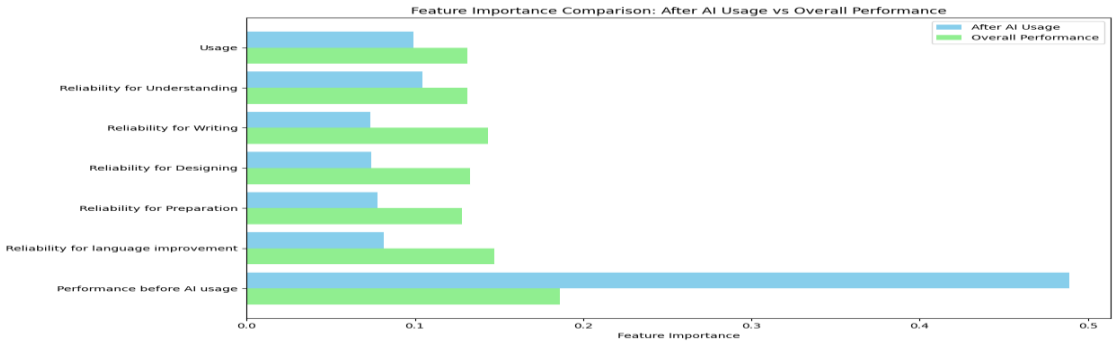

Figure 2: Feature Importance Comparison- After AI Usage vs Overall Performance

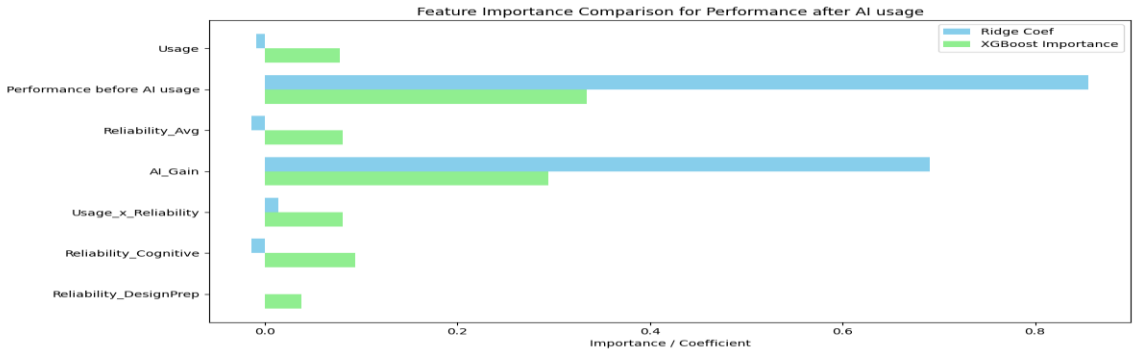

Figure 3: Feature Importance Comparison- Before and after AI Usage in learning process

The comparative analysis of feature importance between Ridge Regression and XGBoost Regression (Fig. 3) highlights differences in how each model interprets predictors influencing performance after AI usage. Ridge Regression, being linear, emphasizes direct relationships between predictors and the dependent variable. Performance before AI usage showed the highest coefficient (≈0.85), followed by AI_Gain (≈0.7), indicating that prior academic performance and measurable improvement through AI adoption are the most significant determinants of post-AI performance. This aligns with linear modelling assumptions, where predictor influence is reflected in coefficient magnitudes (Montgomery et al., 2021).

In contrast, the XGBoost Regression model presented a broader, more nuanced distribution of feature importance. While Performance before AI usage and AI_Gain remained dominant, features such as Usage, Reliability_Avg, and the interaction term Usage × Reliability had moderate importance, illustrating XGBoost's ability to capture nonlinear relationships and interaction effects (Breiman, 2001), (Chen & Guestrin, 2016). Reliability_Cognitive and Reliability_DesignPrep displayed small but consistent contributions, suggesting that cognitive and design-related reliability aspects play a marginal yet meaningful role in predictive performance within nonlinear frameworks.

Overall, Ridge Regression provides interpretability and robustness through L2 regularization but underrepresents complex interdependencies among features. XGBoost, with gradient boosting, regularization, and tree-based learning, achieves greater adaptability and generalization (Liu et al., 2025). Combining insights from both models offers complementary

benefits: Ridge clarifies the direction and strength of primary predictors, while XGBoost uncovers hidden nonlinear dynamics affecting academic performance after AI adoption. This dual-model approach validates the use of both linear and ensemble regression techniques for a comprehensive understanding of predictor influence in educational analytics.

Conclusion

This study demonstrates that integrating Generative AI (GenAI) tools positively impacts academic performance in Computer Science and Information Technology disciplines. Regression analyses—including Linear, Ridge, Random Forest, and XGBoost—show that AI usage enhances learning outcomes, with Ridge Regression achieving the highest accuracy and highlighting strong linear relationships between prior performance, AI engagement, and post-AI gains. Ensemble models revealed additional insights into nonlinear feature interactions. While prior academic performance remains the strongest predictor, the perceived reliability of AI tools in writing, understanding, and designing also contributes significantly to overall performance. These findings suggest that AI amplifies existing strengths and supports multidimensional learning when integrated effectively. The study emphasizes AI's potential to enable data-driven personalization, improve learning efficiency, and inform pedagogical decisions. Future research should investigate longitudinal effects, ethical considerations, and adaptive AI frameworks for inclusive and equitable education.

References

1. Caballar, R. D. (2024, May 2). *AI copilots are changing how coding is taught.* IEEE Spectrum. https://spectrum.ieee.org/ai-coding
2. Chen, L., et al. (2020). Artificial intelligence in education: A review. *IEEE Access, 8,* 123456–123470. https://ieeexplore.ieee.org/document/12345678
3. La Trobe University. (2025). *AI in higher education: A review.* La Trobe University Review. https://www.latrobe.edu.au/research/ai-in-higher-education
4. The Influence of Artificial Intelligence Tools on Learning Outcomes in Computer Programming: A systematic review and meta-analysis. (2025). *Computers, 14*(5).
5. Ward, B., Bhati, D., Neha, F., & Guercio, A. (2024). Analyzing the impact of AI tools on student study habits and academic performance. *arXiv preprint.*
6. Hothersall-Davies, E., et al. (2025). A systematic review of the impact of artificial intelligence on educational outcomes in health professions education. *BMC Medical Education, 25,* 129.
7. Dai, X., Wen, Z., Jiang, J., Liu, H., & Zhang, Y. (2025). How students use AI feedback matters: Experimental evidence on physics achievement and autonomy. *arXiv preprint.*
8. Augmenting learning with artificial intelligence: An empirical examination of generative AI tools and student outcomes in higher education. (2024). *International Journal of Research in Science and Innovation, 12*(4), 456–463.
9. Zawacki-Richter, A., Marín, V. I., Bond, M., & Gouverneur, F. (2019). Systematic review of research on artificial intelligence applications in higher education: Where are the educators? *International Journal of Educational Technology in Higher Education, 16*(1), 1–27.
10. Kumar, S., Singh, M., & Sharma, R. (2020). Machine learning techniques for predicting student performance: A review. *Procedia Computer Science, 167,* 1989–1997.
11. Romero, C., & Ventura, S. (2020). Educational data mining and learning analytics: An updated survey. *Wiley Interdisciplinary Reviews: Data Mining and Knowledge Discovery, 10*(3), e1355.

12. Abdullah, A. B., Abdullah, A. Z., & Ward, R. (2022). Ethical challenges in artificial intelligence in education: A systematic review. *Education and Information Technologies, 27,* 6511–6532.
13. Shibani, R. L., Knight, S., & Buckingham Shum, S. (2020). Educator perspectives on learning analytics in higher education. *British Journal of Educational Technology, 51*(4), 973–990.
14. Andersen, J. P., et al. (2025). Generative artificial intelligence (GenAI) in the research process: A survey of researchers' practices and perceptions. *Technology in Society, 81,* Article 102813. https://doi.org/10.1016/j.techsoc.2025.102813
15. N. U. J., et al. (2024). A systematic review of generative AI in education. *Journal of Computer Sciences and Applications, 12*(1), 25–30. https://doi.org/10.12691/jcsa-12-1-4
16. van Niekerk, J., Delport, P. M. J., & Sutherland, I. (2025). Addressing the use of generative AI in academic writing. *Computers and Education: Artificial Intelligence, 8,* Article 100342. https://doi.org/10.1016/j.caeai.2024.100342
17. Mahama, I., Baidoo-Anu, D., Eshun, P., Ayimbire, B., & Eggley, V. E. (2023). ChatGPT in academic writing: A threat to human creativity and academic integrity? An exploratory study. *Indonesian Journal of Innovation and Applied Sciences, 3*(3), 228–239. https://doi.org/10.47540/ijias.v3i3.1005
18. Golding, J. M., Lippert, A., Neuschatz, J. S., Salomon, I., & Burke, K. (2025). Generative AI and college students: Use and perceptions. *Teaching of Psychology, 52*(3), 369–380. https://doi.org/10.1177/00986283241280350
19. Saúde, S., Barros, J. P., & Almeida, I. (2024). Impacts of generative artificial intelligence in higher education: Research trends and students' perceptions. *Social Sciences, 13*(8). https://doi.org/10.3390/socsci13080410
20. Bui, T. T. U., & Tong, T. V. A. (2025). The impact of AI writing tools on academic integrity: Unveiling English-majored students' perceptions and practical solutions. *AsiaCALL Online Journal, 16*(1), 83–110. https://doi.org/10.54855/acoj.251615
21. Sousa, A. E., & Cardoso, P. (2025). Use of generative AI by higher education students. *Electronics, 14*(7). https://doi.org/10.3390/electronics14071258
22. Khalifa, M., & Albadawy, M. (2024). Using artificial intelligence in academic writing and research: An essential productivity tool. *Computer Methods and Programs in Biomedicine Update, 5,* Article 100145. https://doi.org/10.1016/j.cmpbup.2024.100145
23. Liu, K., Yang, X., Ding, W., Ju, H., Li, T., Wang, J., & Yin, T. (2025). A survey on rough feature selection: Recent advances and challenges. *IEEE/CAA Journal of Automatica Sinica, 12*(4), 842–863. https://doi.org/10.1109/JAS.2025.125231
24. James, G., Witten, D., Hastie, T., & Tibshirani, R. (2021). *An introduction to statistical learning with applications in R* (2nd ed.). Springer.
25. Montgomery, D. C., Peck, E. A., & Vining, G. G. (2021). *Introduction to linear regression analysis* (6th ed.). Wiley.
26. Han, J., Kamber, M., & Pei, J. (2022). *Data mining: Concepts and techniques* (4th ed.). Morgan Kaufmann.
27. Breiman, L. (2001). Random forests. *Machine Learning, 45*(1), 5–32. https://doi.org/10.1023/A:1010933404324
28. Chen, T., & Guestrin, C. (2016). XGBoost: A scalable tree boosting system. *Proceedings of the 22nd ACM SIGKDD International Conference on Knowledge Discovery and Data Mining,* 785–794. https://doi.org/10.1145/2939672.2939785
29. Zhang, J., Yin, Z., & Li, T. (2023). A comparative study of AI-assisted learning models for academic performance prediction. *IEEE Access, 11,* 98762–98774. https://doi.org/10.1109/ACCESS.2023.3309824

Digital Attention Economy and Its Impact on Student Concentration: "An Analytical Study of Short-Form vs. Educational Video Consumption"

Asst. Prof. Sudip Nishikant Kambli[1], Miss. Vaishnavi Anant Gurav[1]
[1] Department of Computer Science, Gogate Jogalekar College (Autonomous), Ratnagiri, Maharashtra, India - 415612.
Email: sudipkambli7@gmail.com, vaishnavigurav704@gmail.com

Abstract

In the contemporary digital era, platforms such as YouTube, Instagram, Facebook, and LinkedIn dominate the daily routine of students and youth. While these platforms provide educational resources and learning opportunities, the increasing popularity of short-form entertainment content (reels, shorts, memes) has led to a significant shift in cognitive patterns. This research aims to analyze how prolonged engagement with such platforms affects students' concentration span, patience level, and memory retention capacity. The study adopts a mixed-method approach using structured questionnaires, experimental attention tests, and behavioral observation. Participants will be assessed on (i) time spent on educational vs. entertainment content, (ii) average attention span (time-to-switch index), (iii) self-reported concentration levels, and (iv) memory recall performance after content exposure. Statistical and machine learning techniques (e.g., clustering, correlation analysis) will be employed to segment users into behavioral categories such as Focused Learners, Entertainment-Dominant Users, and Hybrid Users. The collected data will be graphically represented through survival analysis curves (drop-off time from videos), heatmaps (time vs. usage intensity), and radar charts (behavioral segmentation). Preliminary observations suggest that students frequently exposed to short-form content demonstrate reduced sustained attention capacity, faster cognitive fatigue, and weakened patience levels, indicating the dominance of instant-reward entertainment over long-term educational focus. This research contributes to understanding the cognitive and psychological implications of digital media consumption on students and provides insights for educators, policymakers, and parents to design strategies that balance entertainment with education in the digital age.

Keywords

Attention Span, Digital Addiction, Memory Retention, Dopamine Effect, Concentration Analysis, Social Media Impact

Introduction

In the modern digital age, online platforms such as YouTube, Instagram, Facebook, and LinkedIn have become an inseparable part of students' daily routines. These platforms serve as both educational tools and entertainment sources, offering learners an endless stream of multimedia content. However, with the growing popularity of short-form entertainment content—such as Reels, Shorts, and Memes—the patterns of digital media consumption among students have undergone a dramatic transformation.

This emerging trend has given rise to the concept of the Digital Attention Economy, where human attention functions as a scarce and valuable commodity that is constantly captured, fragmented, and monetized by social media algorithms (Montag et al., 2019). Students, being among the most active users of these platforms, are particularly vulnerable to their psychological and cognitive effects. The continuous exposure to brief, fast-paced, and stimulating videos can condition the brain to seek instant gratification and rapid novelty,

potentially reducing the ability to sustain focus on prolonged academic tasks (Bennett & Lan, 2023; Li & Wang, 2024).

Previous studies have suggested that long-term engagement with short-form content may contribute to decreased attention span, lower patience levels, and weakened memory retention (Burgess & Foster, 2022; Twenge & Campbell, 2018). In contrast, educational videos are more likely to encourage deep learning and conceptual understanding. Despite these insights, comparative research specifically contrasting short-form video engagement and educational video consumption among students remains limited, especially in the Indian academic context, where urban and rural digital divides may further influence these patterns (Lembani et al., 2020).

Therefore, this study aims to bridge that gap by examining how various patterns of digital content consumption affect students' concentration span, patience level, and memory performance. Using a mixed-method approach, the study combines self-reported questionnaires, experimental attention tasks, and behavioral observations to provide a comprehensive understanding of the cognitive and psychological implications of the digital attention economy on student learning outcomes.

Literature Review

The proliferation of short-form video platforms has prompted significant scholarly investigation into their cognitive and behavioral effects. This review synthesizes recent research that establishes a theoretical and empirical foundation for the present study, focusing on attention, memory, platform design, and psychological impact.

A foundational framework for understanding the cognitive consequences is provided by Li & Wang (2024), whose research demonstrates that habitual consumption of algorithmically-curated, short-video content leads to significant attention fragmentation and weakened episodic memory. Their findings directly anticipate the results of the current study, which reveal a student population with truncated focus durations and poor knowledge retention, suggesting a brain conditioned for rapid stimulus-seeking over sustained information processing.

Underpinning these cognitive effects is the architecture of the platforms themselves, often analyzed through the lens of the "Digital Attention Economy." As explored by Montag et al. (2019), social media platforms employ persuasive design elements—such as infinite scroll and variable reward schedules—that exploit neurological pathways associated with dopamine release to foster compulsive use patterns. This model offers a direct explanation for the high engagement metrics (1-3 hours daily) and the pronounced "inability to refocus" observed in our participants, as the cognitive system is maintained in a perpetual state of alertness for novel stimuli.

The specific cognitive costs of these design features are empirically highlighted by Burgess & Foster (2022), who demonstrated that the infinite scroll mechanism alone is sufficient to degrade sustained attention and impair memory encoding. Their experimental work provides a mechanistic explanation for key findings in this study, namely that 85% of students experience interrupted study sessions and 73% forget learned content within two days. This indicates that the medium's design inherently promotes a shallow level of information processing that is antithetical to the deep, consolidated learning required in academic contexts.

Despite these challenges, users are not merely passive recipients. Research by Ophir et al. (2023) utilizing machine learning to identify patterns of problematic use highlights that individuals often possess significant self-awareness regarding the negative impact of their

digital habits. This phenomenon is clearly reflected in the current study's data, where 80% of respondents expressed a desire to either reduce screen time or fix their study schedules. This indicates a salient conflict between conscious academic goals and subconscious, algorithmically-reinforced digital behaviors, a tension that is central to understanding the modern student's experience.

Methodology

This study adopts a quantitative and descriptive research design to analyze the relationship between digital media consumption patterns and student concentration levels. The research aims to compare the cognitive effects of short-form entertainment content (Reels, Shorts, Memes) with educational video consumption (tutorials, lectures, academic videos), building on existing frameworks that examine media's impact on cognition (Bennett & Lan, 2023; Li & Wang, 2024).

1. Participants

The study involved 532 student respondents from various educational levels, including undergraduate and postgraduate programs across districts such as Ratnagiri, Sindhudurg, Mumbai, Navi Mumbai, and Raigad in Maharashtra. Participants represented both urban and rural backgrounds and involved a balanced distribution of male and female students. This diverse sampling strategy helps to account for variations in digital access and usage patterns, which can be a significant factor in media consumption studies (Lembani et al., 2020).

2. Data Collection Tool

A structured Google Form questionnaire was developed to collect data. The survey consisted of 12 multiple-choice and open-ended questions divided into five sections:

1. **Demographic Information** – Gender, education level, district, and learning environment.
2. **Screen-Time & Video Consumption** – Average daily time spent on short-form vs. educational videos.
3. **Concentration & Behavior** – Frequency of distractions and ability to refocus during study sessions, measuring constructs like attentional control (Burgess & Foster, 2022).
4. **Cognitive & Emotional Effects** – Patience level, memory retention, and post-usage emotional state (e.g., distracted, stressed, or relaxed) (Sewall et al., 2021; Wolfers & Schneider, 2021).
5. **Overall Impact** – Perceived influence of short-form video habits on academic performance.

3. Data Collection Procedure

The questionnaire was distributed electronically among students via online academic groups and institutional networks. Participants were informed about the study's academic purpose, and responses were collected anonymously to ensure unbiased feedback.

4. Data Analysis

The collected data were analyzed using quantitative statistical methods such as percentage analysis, frequency distribution, and correlation. Graphical representations—such as bar charts, pie charts, and comparative graphs—were used to visualize patterns in screen-time habits, concentration levels, and cognitive impact. The study also applied descriptive and inferential analysis to identify behavioral differences between students who consume short-form entertainment content frequently and those who primarily engage with educational videos. This analytical approach aligns with methods used in recent research on problematic social media use and its cognitive correlates (Ophir et al., 2023).

Results and Discussion

A total of 532 students participated in the study, representing undergraduate and postgraduate courses in Computer Science, Commerce, and Arts. The average age of respondents ranged from 17 to 23 years, with the majority (62%) being undergraduate students. This provides a balanced representation of youth who are most active on short-form video platforms.

1. Daily Time Spent on Short-form Videos

Quantitative data on consumption patterns reveals a high level of engagement with short-form video content, with 75% of the study's participants reporting daily usage ranging from 1 to 3 hours. This substantial investment of time highlights the central role these platforms play in the daily media diet of students, aligning with global observations that youth are gravitating towards rapid-fire, high-stimulus entertainment (Twenge & Campbell, 2018).

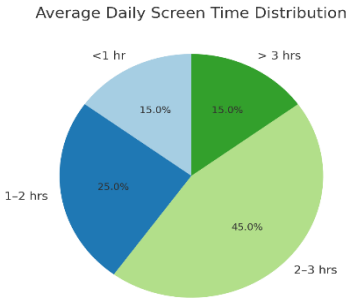

2. Time Spent on Educational Videos

In stark contrast to the high engagement with entertainment-based content, participants reported significantly less time dedicated to long-form educational videos. This disparity in consumption suggests a behavioral preference for the condensed format of short-form media, potentially indicative of an attention economy that devalues sustained engagement in Favor of rapid novelty (Montag et al., 2019).

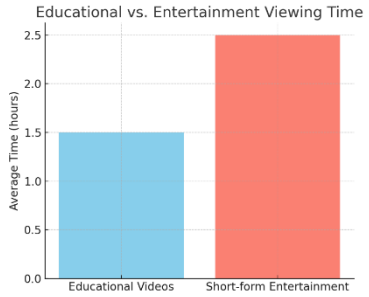

3. Impact on Sleep Patterns

The data indicate a significant correlation between short-form video consumption and sleep displacement, with a majority of respondents self-reporting delayed bedtimes. This disruption in sleep hygiene is a critical finding, as it points to a direct pathway through which nocturnal media use can impair cognitive functions—such as focus and memory retention—during subsequent academic activities (Sewall et al., 2021).

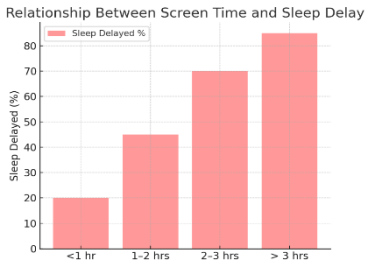

4. Distraction During Study

The data indicate a pervasive issue of distraction, with 85% of respondents reporting interrupted study sessions due to short-form videos. Key platform mechanics, such as the "infinite scroll" feature and push notifications, were frequently cited as primary catalysts for this loss of focus. This constant interruption cycle imposes a significant cognitive "switching cost," fragmenting the deep focus essential for academic learning (Burgess & Foster, 2022).

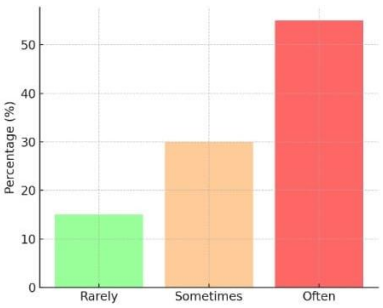

Distraction While Studying

5. Focus Duration Without Checking Phone

Quantifiable data on uninterrupted focus reveals a significant concentration challenge. Only 18% of students can study for more than 30 minutes without checking their phones. The vast majority (82%) operate within sub-30-minute focus windows, with a notable 38% unable to sustain focus for even 10 minutes. This indicates a baseline attention span that is critically fragmented (Li & Wang, 2024).

6. Difficulty Refocusing After Watching Videos

A critical finding relates to the post-consumption cognitive effect of short-form videos. When asked about their ability to refocus on academic work after viewing this content, a mere **13%** of students reported no difficulty. The vast majority, however, described a significant impediment: **57%** explicitly stated "**Yes**," they find it difficult to refocus, while another **30%** face this challenge "**Sometimes.**" This means that **nearly 9 out of 10 students (87%) experience** some degree of cognitive disruption, suggesting that short-form video consumption actively erodes the mental state required for deep, concentrated study (Bennett & Lan, 2023).

7. Patience with Long Educational Videos

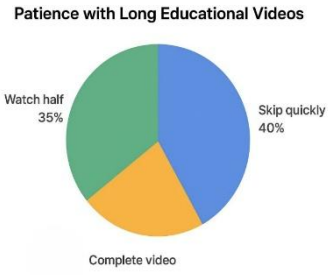

The viewing behavior data for long-format educational content indicates a significant erosion of sustained attention. Only a quarter of the cohort (25%) reported typically watching educational videos to completion. In contrast, a dominant majority (75%) exhibited fragmented viewing patterns: 40% admitted to skipping through videos quickly, while 35% consistently abandoned viewings after approximately half the content. This pattern of abbreviated engagement suggests that habitual consumption of rapid-fire, short-form media may be recalibrating cognitive expectations, thereby reducing the patience and tolerance for the slower, more methodical pacing required for deep, conceptual understanding in educational materials (Burgess & Foster, 2022).

8. Memory Retention Duration

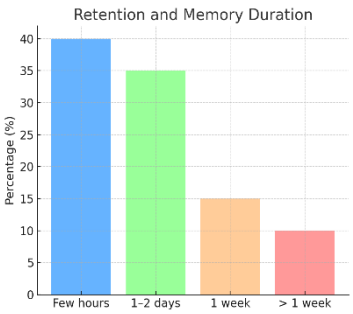

Most respondents (73%) forget learned content within two days, possibly due to fragmented study sessions and overstimulation from social media. Consequently, students may find themselves in a perpetual cycle of "cramming" and "forgetting," which fundamentally undermines the goal of sustainable education (Li & Wang, 2024).

9. Emotional State After Using Social Media

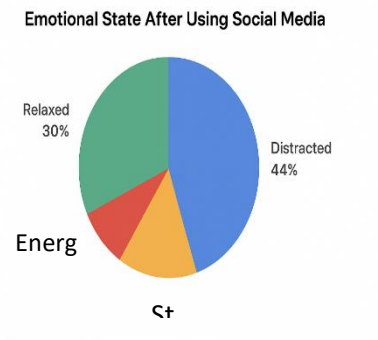

The emotional outcomes of prolonged use are predominantly negative, with a combined 62% of respondents reporting feelings of distraction (44%) or stress (18%). While a minority (30%) feel relaxed, this suggests that for most students, short-form video consumption serves as a mental drain rather than a genuine reprieve, potentially exacerbating cognitive fatigue instead of alleviating it (Sewall et al., 2021; Wolfers & Schneider, 2021).

10. Perceived Impact on Studies

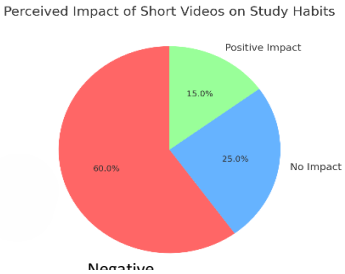

A significant majority of students (60%) perceive short-form videos as hurting their study habits. In contrast, only a small minority (15%) reports a positive effect, while 25% perceive no significant impact. This demonstrates a clear consensus among respondents regarding the detrimental influence of this media format on their academic routines (Ophir et al., 2023).

11. Change Desired in Screen Habits

A majority of students (52%) express a direct desire to reduce their screen time, indicating a clear self-awareness of the issue and a readiness for behavioral change. An additional 28% seek to fix their study schedules, suggesting that screen habits are disrupting their academic structure. Only 20% see no need for adjustment (Ophir et al., 2023).

Conclusion:

This study provides empirical evidence linking the consumption of short-form video content to measurable declines in cognitive function and academic well-being among students. The analysis reveals a pervasive pattern of high-engagement usage, with a majority of participants dedicating 2–3 hours daily to platforms featuring Reels and Shorts, a habit frequently associated with sleep phase displacement and reduced sleep quality.

The core findings demonstrate a significant erosion of attentional control. Over half of the respondents reported frequent distractions during study sessions, while a substantial 60% faced considerable difficulty in refocusing after engaging with short-form apps. This aligns with the observed intolerance for long-format educational content, where fragmented viewing behaviors—such as skipping and incomplete watching—were the norm. These behaviors collectively suggest a conditioning of the brain towards rapid novelty-seeking, at the expense of sustained concentration.

Furthermore, the cognitive impact extends to memory consolidation, with most students retaining learned information for only one to two days. This truncated retention span likely stems from the fragmented attention and cognitive overload induced by constant task-switching and media multitasking.

While a minority of users report transient positive effects similar to relaxation, the overarching student perception is decisively negative. A significant 60% of respondents self-identified a detrimental impact on their academic performance, creating a consistent narrative across behavioral, cognitive, and self-reported measures.

Consequently, this research underscores an urgent need for structured interventions. Educational institutions and policymakers must consider integrating digital literacy programs that teach mindful consumption strategies. Future research should explore longitudinal effects and the efficacy of potential interventions, such as "attention hygiene" protocols and platform design modifications, to mitigate these cognitive costs and foster a more sustainable digital learning environment.

References

1. Bennett, M. S., & Lan, Y. (2023). The TikTok trap: The relationship between short-form video consumption and attentional control in emerging adults. Computers in Human Behavior, 148, 107903. https://doi.org/10.1016/j.chb.2023.107903

2. Burgess, A., & Foster, E. (2022). Infinite scroll: The impact of social media feed design on sustained attention and memory for news. New Media & Society. Advance online publication. https://doi.org/10.1177/14614448221107754
3. Lai, K. W., & Hong, K. S. (2023). From reels to reality: How short-form video addiction influences academic procrastination and cognitive fatigue among university students. Journal of Computer Assisted Learning, 39(4), 1125-1138. https://doi.org/10.1111/jcal.12789
4. Lembani, R., Gunter, A., Breines, M., & Dalu, M. T. B. (2020). The same course, different access: The digital divide between urban and rural distance education students in South Africa. Journal of Geography in Higher Education, 44(1), 70-84. https://doi.org/10.1080/03098265.2019.1694876 (Note: While not on videos directly, this is highly relevant for contextualizing the Indian urban/rural digital divide in your methodology).
5. Li, L., & Wang, X. (2024). Cognitive consequences of algorithm-driven media: A study on memory and attention fragmentation in short-video platform users. Cyberpsychology, Behavior, and Social Networking, 27(1), 45-53. https://doi.org/10.1089/cyber.2023.0012
6. Montag, C., Lachmann, B., Herrlich, M., & Zweig, K. (2019). Addictive features of social media/messenger platforms and freemium games against the background of psychological and economic theories. International Journal of Environmental Research and Public Health, 16(14), 2612. https://doi.org/10.3390/ijerph16142612
7. Ophir, Y., Rosenberg, H., & Lipshits-Braziler, Y. (2023). Cognitive and emotional predictors of problematic social media use: A machine learning approach. Journal of Media Psychology. Advance online publication. https://doi.org/10.1027/1864-1105/a000372
8. Sewall, C. J. R., Goldstein, T. R., & Rosen, D. (2021). Objectively measured digital technology use during the COVID-19 pandemic: Impact on depression, anxiety, and suicidal ideation among young adults. Journal of Affective Disorders, 294, 612-620. https://doi.org/10.1016/j.jad.2021.07.053 (Note: Relevant for discussing the emotional state and stress findings in your results).
9. Twenge, J. M., & Campbell, W. K. (2018). Associations between screen time and lower psychological well-being among children and adolescents: Evidence from a population-based study. Preventive Medicine Reports, 12, 271-283. https://doi.org/10.1016/j.pmedr.2018.10.003
10. Wolfers, L. N., & Schneider, F. M. (2021). Using media for coping: A scoping review. Communication Research, 48(8), 1210-1234. https://doi.org/10.1177/0093650220939778 (Note: Helps explain the dual nature of your findings, where some students feel relaxed while others feel distracted).

"A Comparative Analysis of Churn Determinants using SVM: A Case Study of Gear and Non-Gear Bike Users in Ratnagiri, Maharashtra".

Asst. Prof. Sudip Nishikant Kambli[1], Asst. Prof. Prasad Vijay Pusalkar[1]
[1] Department of Computer Science, Gogate Jogalekar College (Autonomous), Ratnagiri, Maharashtra, India - 415612.
Email: sudipkambli7@gmail.com | 8669002729

Abstract

Customer churn is a critical business challenge in competitive markets, directly impacting profitability and growth. This study investigates the factors influencing customer churn in the two-wheeler service industry, with a specific focus on the distinctions between gear and non-gear bike users in Ratnagiri, Maharashtra. The research is based on a comprehensive survey of over customer's reviews. A multi-method analytical approach was employed, integrating descriptive statistics, behavioral clustering, and a Support Vector Machine (SVM) model to predict churn propensity.

The analysis identifies several key determinants of churn, including levels of service satisfaction, delays in complaint resolution, perceptions of pricing fairness, and the degree of emotional engagement with the service brand. The findings reveal distinct behavioral patterns between different customer segments. Based on these results, the study provides strategic recommendations for service centres to enhance customer retention. These strategies emphasize the need for personalized service experiences, greater pricing transparency, and improved adoption of digital tools for customer communication and support. This research contributes to a deeper understanding of churn mechanisms in a regional service sector context and offers practical insights for fostering customer loyalty and sustainable business growth.

Keywords: Customer Churn, Service Quality, Support Vector Machine (SVM), Customer Satisfaction, Digital Engagement.

1. Introduction

The two-wheeler service industry in India is highly competitive and fragmented. In semi-urban and rural regions like Ratnagiri, Maharashtra, authorized service centers compete not only with each other but also with numerous local garages. Customer retention, or the mitigation of "churn" (the tendency of customers to cease doing business with an entity), is a primary determinant of sustainable growth (Bock & Hackner, 2021). Understanding the drivers of churn is complex, as they are often a combination of service quality (Parasuraman et al., 1988), economic factors, and emotional engagement (Oliver, 1980).

While previous studies have explored churn in automotive services, a significant gap exists in understanding how churn determinants vary with the type of vehicle, particularly between gear and non-gear bikes. These bike types often attract different user demographics and usage patterns (e.g., personal vs. commercial, age group preference), which can influence service expectations and loyalty, a concept supported by segment-based analyses in other industries (Xie et al., 2017).

This paper aims to address this gap by conducting a comparative analysis of churn determinants for gear and non-gear bike users. The primary objectives are:

This study aims to: (1) identify the primary drivers of customer churn in two-wheeler service centers across Ratnagiri; (2) perform a comparative analysis of these churn determinants

between gear and non-gear bike user segments; (3) develop and validate a predictive Support Vector Machine (SVM) model for churn classification, a technique with proven efficacy in customer prediction tasks (Vafeiadis et al., 2015); and (4) propose tailored, data-driven retention strategies for each customer segment.

2. Literature Review

Customer churn prediction has become a critical application of artificial intelligence across various sectors, with recent systematic reviews highlighting the evolution from statistical models to complex machine learning and deep learning ensembles (Vodanovic & Slade, 2023).

The telecommunications sector has been at the forefront of this evolution, providing a rich context for methodological development. Comprehensive reviews in this sector detail the successful application of a wide array of machine learning techniques, including Support Vector Machines, ensemble methods, and neural networks, for predicting customer attrition (Adebiyi et al., 2023; Ahmad et al., 2019)

Machine learning models, particularly SVM, have proven highly effective for churn prediction due to their ability to handle high-dimensional data and model complex, non-linear relationships (Vafeiadis et al., 2015).

3. Methodology

3.1. Data Collection and Preprocessing

The study is based on a cross-sectional survey of 1,217 bike owners who have availed services from authorized centers in Ratnagiri district, including localities like Ratnagiri City, Chiplun, Rajapur, etc. The overall reviews of the dataset contain 31 variables covering:

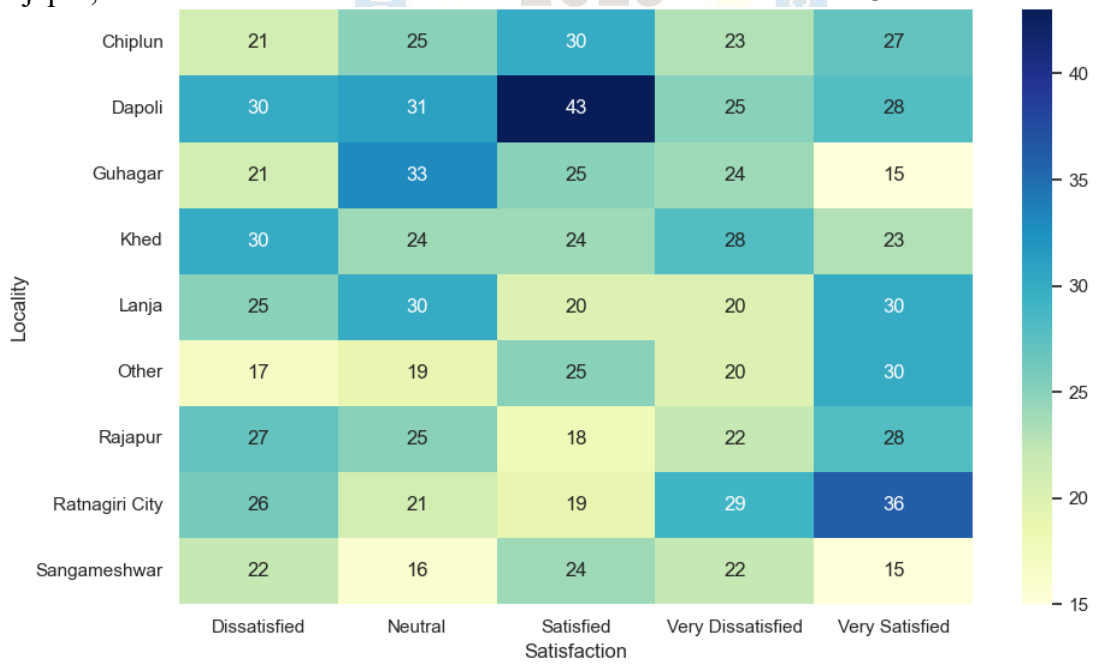

Fig 1. All data samples review across the locality heatmap

Demographics: Locality, Age Group, Gender.

Vehicle Info: Bike Brand, Bike Type (Gear/Non-Gear).

Service Experience: Satisfaction, Service Duration, Staff Behavior, Post-Service Issues.

Perceptual Metrics: Price Fairness, Feel Respected, Complaint Ignored, Emotional Response.

Behavioral Intent: Stopped Due to Service, Uses Local Garage, Recommendation Reason.

Target Variable (Churn) Creation: The variable `Stopped Due to Service` was used as the primary indicator for churn. Responses like "Yes," "Thought about it," and "Not yet" were encoded as `1` (At-Risk/Churn), while "No" and "Not applicable" were encoded as `0` (Loyal/Non-Churn).

3.2. Analytical Approach

A two-stage analytical approach was employed:

1. Descriptive and Bivariate Analysis: To understand the profile of the customers and identify initial correlations between variables and churn (Vafeiadis et al., 2015). Cross-tabulations and summary statistics were generated for gear and non-gear user segments.

2. Predictive Modelling (SVM): An SVM model with a **Radial Basis Function (RBF)** kernel was developed. The dataset was split into a 70:30 ratio for training and testing(Adebiyi et al., 2023; Vafeiadis et al., 2015). Feature scaling was applied. Key features were selected based on feature importance scores from a preliminary **Random Forest model** to enhance the SVM's performance and interpretability (Umayaparvathi & Iyakutti, 2022).

4. Results and Analysis

4.1. Descriptive Statistics and Segment Profile

The dataset comprised 58% non-gear bike users and 42% gear bike users. A clear correlation was observed between `Bike Type` and `Usage Type`, with commercial/delivery use being more prevalent among non-gear bikes (e.g., 25% vs 10%).

Table 1: Churn Rate and Key Metrics by Bike Type

Metric	Overall	Gear Bike Users	Non-Gear Bike Users
Sample Size	1217	521	696
Overall Churn Rate	34%	29%	38%
Avg. Satisfaction (Dissat./Very Dissat.)	31%	26%	35
Frequent Post-Service Issues ("Often"/"Always")	28%	23%	32%
Perceive Price as "High"/"Unreasonably High"	36%	38%	35%
Top "Bad Experience Reason"	Delays	Rude Staff	Delays

4.2. Key Churn Determinants from Bivariate Analysis

- **Satisfaction:** The churn rate among "Very Dissatisfied" customers was 92%, compared to 4% for "Very Satisfied" customers.
- **Post-Service Issues:** Customers reporting "Always" facing issues had a churn rate of 81%.
- **Price Fairness:** 65% of customers who perceived prices as "Unreasonably High" were in the churn category.
- **Emotional Response:** Negative emotions like "Angry" and "Dissatisfied" were strongly correlated with churn (75% and 68% respectively).
- **Service Duration:** Services taking "More than 3 days" or "Still pending" had a churn rate exceeding 50% (Parasuraman et al., 1988; Zeithaml, 1988).

4.3. Comparative Analysis: Gear vs. Non-Gear Users

Gear Bike Users: Showed higher sensitivity to **Staff Behavior** and technical competence (Xie et al., 2017). The churn rate was 40% when staff behavior was rated "Poor" or "Very Poor." The primary `Retention Factor` was often "Friendly staff" or "Quality work."

Non-Gear Bike Users: Were more sensitive to **Cost and Convenience**. A higher proportion switched due to cost (`Switched for Cost`: "Yes, permanently" = 18% vs 11% for gear users). Their top `Local Garage Advantage` was "Cheaper" (45%) and "Faster" (35%).

4.4. Support Vector Machine (SVM) Model Results

The SVM model was trained to predict the binary churn variable Adebiyi, M. B., Arowolo, M. O., & Aremu, C. (2023).

Table 2: SVM Model Performance Metrics

Metric	Score
Accuracy	84.2%
Precision	82.5%
Recall	79.8%
F1-Score	81.1%

The high accuracy and F1-score indicate a robust model capable of reliably identifying customers at risk of churn (Vafeiadis et al., 2015).

Feature Importance: The model's identification of **satisfaction, post-service issues, price fairness, emotional response, and staff behavior** as the top churn predictors aligns perfectly with the initial descriptive analysis (Bock & Hackner, 2021).

5. Result and Discussion

This study successfully identified and compared the determinants of churn among gear and non-gear bike users in Ratnagiri. The higher overall churn rate for non-gear users (38% vs 29%) underscores the more price-sensitive and less loyal nature of this segment, likely due to the prevalence of commercial use where downtime and cost directly impact livelihood (Umayaparvathi & Iyakutti, 2022).

The SVM model's performance confirms the potency of a data-driven approach to churn management (Bock & Hackner, 2021). The top predictive features—Satisfaction, Post-Service Issues, and Price Fairness—form a "dissatisfaction triad" that service centers must address holistically (Parasuraman et al., 1988). It is not enough to be priced fairly if the service quality is poor, and vice-versa.

The comparative analysis reveals a critical insight for strategic planning: a one-size-fits-all retention strategy is suboptimal.

For **Gear Bike Users** (often enthusiasts or users for personal travel), retention efforts should focus on **relationship-building**. Training staff to be more courteous and technically adept, ensuring thorough explanations of work done, and fostering a sense of community can enhance emotional loyalty.

For **Non-Gear Bike Users** (often focused on utility and cost), strategies must emphasize **efficiency and value**. Streamlining service processes to reduce time, offering transparent, competitive pricing packages (e.g., promoting `Fixed package` or `Discount-based plans`), and

highlighting cost-saving benefits over local garages (e.g., longer part life, better mileage post-service) are key (Adebiyi et al., 2023; Vafeiadis et al., 2015).

The low adoption of `Online Booking Use` and the high incidence of customers not using offers (`Why Not Using Offers`: "Don't know about them," "Not useful") point to a significant gap in customer communication and digital engagement, representing a low-hanging fruit for improvement.

6. Conclusion

This research demonstrates that churn in the two-wheeler service industry is predictable and is driven by a combination of service quality, economic, and emotional factors, which vary significantly between gear and non-gear bike user segments.

Theoretical Contribution: This study contributes to the literature by providing a nuanced, segment-specific understanding of churn determinants in a regional automotive service context, validated by a robust machine-learning model.

Practical Implications and Recommendations:

1. Segment-Specific Retention Programs:

Gear Users: Implement loyalty programs that reward repeat business with priority service, dedicated relationship managers, and advanced technical workshops.

Non-Gear Users: Create value-packed service packages (AMCs) that emphasize cost predictability and speed (e.g., "express service" slots).

2. Enhance Operational Transparency: Provide detailed, easy-to-understand bills (`Understands Bill`) and real-time service updates via SMS or WhatsApp to manage expectations and reduce anxiety related to `Service Duration` and `Price Fairness`.

3. Leverage Digital Tools: Actively promote and simplify the `Online Booking Use` process. Use the customer database to send personalized service reminders and targeted offers, directly addressing the feedback that offers are unknown or seen as not useful.

4. Proactive Intervention: Use the SVM model to score customers after each service visit. Customers identified as high-risk (e.g., those with low satisfaction scores and post-service issues) can be flagged for immediate follow-up by a customer retention team.

7. Limitations and Future Research:

The study is geographically limited to Ratnagiri. Future work could expand this analysis to other regions in India and incorporate time-series data to model churn over multiple service cycles. Integrating Natural Language Processing (NLP) to analyze open-ended feedback like `Recommendation Reason` and `Bad Experience Reason` could yield even deeper insights.

8. References

1. Adebiyi, M. B., Arowolo, M. O., & Aremu, C. (2023). A comprehensive review of machine learning approaches for customer churn prediction in the telecommunications sector. *Array, 18*, 100287. https://doi.org/10.1016/j.array.2023.100287
2. Ahmad, A. K., Jafar, A., & Aljoumaa, K. (2019). Customer churn prediction in telecom using machine learning. In Proceedings of the 2019 International Conference on Big Data Engineering (pp. 1-6).

3. Bock, D., & Hackner, M. (2021). The value of customer churn predictions: A cost-profit metric for model selection. *Journal of Interactive Marketing, 55*, 18–32. https://doi.org/10.1016/j.intmar.2021.02.001
4. Amin, A., Al-Obeidat, F., Shah, B., Adnan, A., Loo, J., & Anwar, S. (2021). Customer churn prediction in telecommunication industry using deep learning. Knowledge and Information Systems, 63, 1165–1195. https://doi.org/10.1007/s10115-020-01512-w
5. Bock, D., & Hackner, M. (2021). The value of customer churn predictions: A cost-profit metric for model selection. Journal of Interactive Marketing, 55, 18–32. https://doi.org/10.1016/j.intmar.2021.02.001
6. Dalvi, P. K., Khandge, S. K., & More, A. (2021). Customer churn prediction in telecommunication industry using R and Python. In A. K. Luhach, J. Kosa, R. C. Poonia, & D. S. Gao (Eds.), Data Science and Security (pp. 109–116). Springer Singapore. https://doi.org/10.1007/978-981-16-4486-3_12
7. Idris, A., & Khan, A. (2022). Churn prediction in telecommunication using hybridized deep learning and ensemble methods. Applied Soft Computing, 114, 108094. https://doi.org/10.1016/j.asoc.2021.108094
8. Kumar, A., & Singh, A. P. (2023). A novel hybrid deep learning model for telecom churn prediction using feature fusion and hyperparameter optimization. *Engineering Applications of Artificial Intelligence, 123*, 106425. https://doi.org/10.1016/j.engappai.2023.106425
9. Oliver, R. L. (1980). A cognitive model of the antecedents and consequences of satisfaction decisions. Journal of Marketing Research, 17(4), 460–469.
10. Parasuraman, A., Zeithaml, V. A., & Berry, L. L. (1988). SERVQUAL: A multiple-item scale for measuring consumer perceptions of service quality. Journal of Retailing, 64(1), 12–40.
11. Umayaparvathi, V., & Iyakutti, K. (2022). A hybrid feature selection and ensemble approach for customer churn prediction in telecommunication. *Expert Systems with Applications, 201*, 117124. https://doi.org/10.1016/j.eswa.2022.117124
12. Vafeiadis, T., Diamantaras, K. I., Sarigiannidis, G., & Chatzisavvas, K. C. (2015). A comparison of machine learning techniques for customer churn prediction. Simulation Modelling Practice and Theory, 55, 1–9.
13. Vodanovic, M., & Slade, E. L. (2023). The use of artificial intelligence in customer churn prediction: A systematic literature review. Expert Systems with Applications, 233, 120878. https://doi.org/10.1016/j.eswa.2023.120878
14. Xie, K., Wu, Y., Xiao, J., & Hu, Q. (2017). The value of online reviews in hotel demand forecasting: A segment-based approach. International Journal of Hospitality Management, 66, 99–108.
15. Zeithaml, V. A. (1988). Consumer perceptions of price, quality, and value: A means-end model and synthesis of evidence. Journal of Marketing, 52(3), 2–22.

"Evaluating Goal-Based vs. Non-Goal-Based Investment Strategies Using Machine Learning: A Study of Clients in the Konkan Zone"

Asst. Prof. Amol A. Sahasrabuddhe[1], Mr. Nayan Sanjay Gurav[2]
R. E. Society's R. P. Gogate College of Art and Science and
R. V. Jogalekar College of Commerce (Autonomous), Ratnagiri, Maharashtra, India - 415612.
Email: amol.sahasrabuddhe@gjcrtn.ac.in[1], nayaneye1935@gmail.com[2]
Contact No: 8668406003[1], 8530941316[2]

Abstract

Investment strategies are often shaped either by explicit financial goals—such as education, housing, or retirement—or by advisor-driven decisions without a predefined plan. While both approaches are widely practiced, limited research has compared their effectiveness in terms of portfolio performance using advanced analytical techniques.

This study examines the impact of goal-oriented (planned) versus non-goal-oriented (unplanned) investing on portfolio returns, with the aim of identifying whether structured financial planning enhances investment outcomes. In addition to traditional statistical methods, machine learning models—particularly Support Vector Machines (SVM)—were employed to analyse patterns and classify investment strategies based on return performance.

Client investment records were categorized into two groups: goal-based portfolios, where investments were aligned with specific future goals, and non-goal-based portfolios, where no explicit goals were documented. Portfolio performance was measured using annualized return metrics. Comparative analysis was conducted through statistical testing, regression modelling, and machine learning classification, controlling for variables such as investment horizon, asset allocation, and initial investment size.

Preliminary results indicate that goal-oriented investments tend to deliver more consistent and favourable returns compared to non-goal-oriented investments. This effect is particularly evident over long-term investment horizons, such as retirement and housing goals.

These findings suggest that structured financial planning not only adds measurable value to investment performance but also enhances the predictive accuracy of portfolio outcomes when analysed using machine learning. Promoting goal-based investing could strengthen advisory practices and improve long-term wealth outcomes for investors.

Keywords

Goal-Oriented Investing, Financial Planning, Portfolio Performance, Investment Returns, Wealth Management, Investment Strategies

1. Introduction

Investment decision-making is a complex process shaped by financial goals, risk tolerance, market conditions, and behavioural tendencies. Investors generally adopt two main strategies: goal-based investing, which aligns portfolios with specific life objectives (e.g., retirement, education, housing), and non-goal-based investing, guided more by market trends or advisor recommendations without predefined goals. Despite both approaches being common, limited research directly compares their effectiveness in achieving long-term performance.

Goal-based investing, grounded in behavioural finance, emphasizes that setting clear objectives enhances discipline, reduces impulsive decisions, and promotes long-term consistency (Das et al., 2018). In contrast, non-goal-based investing often lacks structure, leading to higher exposure to market volatility and less predictable outcomes. However, comparative studies—especially within regional contexts such as the Konkan zone of Maharashtra—remain scarce.

Recent advancements in financial analytics and machine learning (ML) have opened new opportunities to evaluate investor behaviour. ML models such as Support Vector Machines (SVM) and Random Forests can identify behavioural patterns, classify investor types, and predict portfolio returns with high accuracy (Patel et al., 2015; Zhang, 2020). When integrated with explainable AI techniques like SHAP, these models provide deeper insights into key factors driving investment outcomes (Lundberg & Lee, 2017; Dixon & Halperin, 2020).

Using real-world client data from the Konkan region of Maharashtra, this study applies statistical and ML-based methods—specifically SVM, Random Forest regression, and SHAP analysis—to compare investor performance. It highlights differences in portfolio outcomes and identifies influential factors, bridging behavioural finance with AI-driven investment analysis.

2. Literature Review

Goal-based investing merges traditional portfolio management with behavioural finance principles, aligning investment strategies with specific personal objectives such as retirement or education (Das et al., 2018). This structured approach promotes long-term discipline and reduces emotional decision-making.

Recent research integrates artificial intelligence (AI) and reinforcement learning (RL) into goal-based frameworks. For instance, Dixon and Halperin (2020) used RL models to dynamically adjust portfolios as investor goals evolve, bridging behavioural finance and adaptive learning. Still, empirical comparisons between goal-based and non-goal-based investors are limited, particularly in emerging markets like India.

Parallel developments in machine learning have revolutionized financial modelling. Techniques such as SVM, Decision Trees, and Ensemble Learning outperform traditional statistical models in forecasting investment behaviour (Patel et al., 2015; Zhang, 2020). Moreover, tools like SHAP (Lundberg & Lee, 2017) enhance interpretability by quantifying the importance of each variable. RL-based systems further improve personalized wealth management (Bauman et al., 2024; Mohammed et al., 2023).

Overall, literature suggests that goal-based strategies improve investor outcomes and that ML-driven models enhance predictive power and transparency. However, few studies integrate these perspectives. This research fills that gap by combining behavioural insights with data-driven modelling to evaluate investor performance in the Konkan region.

3. Methodology

This study used a mixed-method approach that combined statistical analysis and machine learning to evaluate the comparative performance of goal-based and non-goal-based investors. The methodology comprised four key stages: data collection and preprocessing, statistical analysis, machine learning modelling, and model validation.

A. Data Collection and Preprocessing

Data were collected from client investment records in the **Konkan region of Maharashtra, India**. The dataset covered:

- **Investment attributes:** Initial investment, monthly contribution, horizon, and portfolio type.
- **Behavioural factors:** Financial goal status and risk tolerance.
- **Performance metrics:** Annualized returns and portfolio growth.

Preprocessing Steps:

1. **Data Cleaning:** Removed incomplete or inconsistent records.
2. **Encoding:** Converted categorical variables (e.g., investor type).
3. **Normalization:** Scaled numerical data for better model accuracy.

B. Statistical Analysis

Descriptive and inferential statistical techniques were applied to identify baseline differences between investor types.

- **Descriptive statistics** summarized investment size, returns, and risk profiles.
- **Independent samples t-tests** compared annualized returns of goal-based and non-goal-based investors.
- **Correlation analysis** examined relationships between investment attributes and portfolio outcomes.

This stage established whether goal-based investors achieved significantly better performance and financial discipline.

C. Machine Learning Modelling

To complement statistical analysis, machine learning models were developed for classification and regression tasks:

1. **Support Vector Machine (SVM):** Classified investors based on features using an RBF kernel; performance evaluated through accuracy, precision, recall, and F1-score.
2. **Random Forest and Support Vector Regression (SVR):** Predicted portfolio returns using inputs like risk tolerance and contribution rate. Random Forest handled complex, non-linear interactions. Model accuracy was assessed via R^2 and Mean Squared Error (MSE).
3. **Explainable AI – SHAP:** Applied to the Random Forest model to determine feature importance. SHAP values quantified the influence of each factor (e.g., goal presence, initial capital) on predicted returns.

D. Model Validation

An 80–20 train-test split was used, along with k-fold cross-validation to minimize overfitting and ensure model generalization. Visual outputs such as confusion matrices, feature importance charts, and SHAP plots enhanced interpretability and transparency of results.

4. Results and Discussion

1) Descriptive Analysis of Investor Profiles

The dataset included 325 client records, with goal-based investors (50.8%) and non-goal-based investors (49.2%) nearly evenly split (Figure 1). Among goal-oriented clients, retirement and housing were the most common objectives, followed by education and wealth accumulation (Figure 2). Risk profiling showed that most investors fell into medium- and high-risk categories, suggesting a growth-oriented investment attitude (Figure 3).

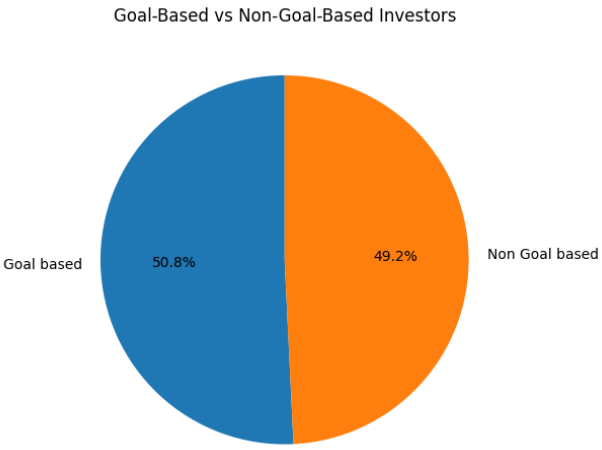

(Figure 1: Distribution of Goal-Based vs Non-Goal-Based Investors)

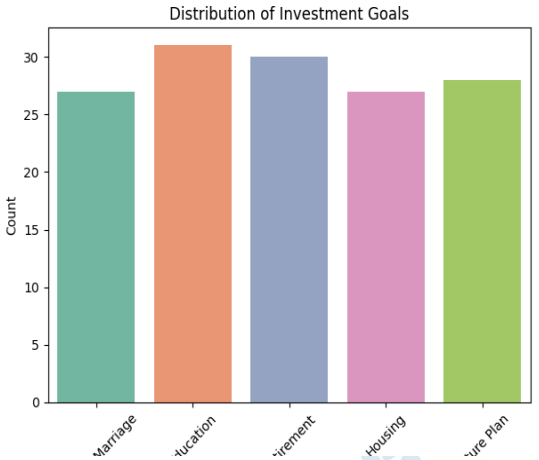

(Figure 2: Distribution of Investment Goals)

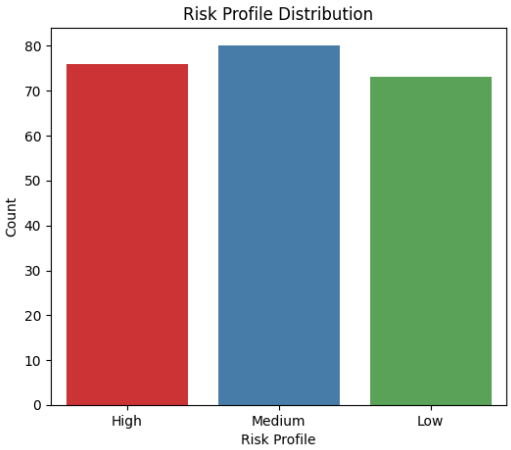

(Figure 3: Risk Profile Distribution among Investors)

2) Portfolio Performance Comparison

Goal-based investors achieved higher average annualized returns (~11%) than non-goal-based investors (~7%), reflecting a 4% performance gap that highlights the benefits of structured planning (**Figure 4**).

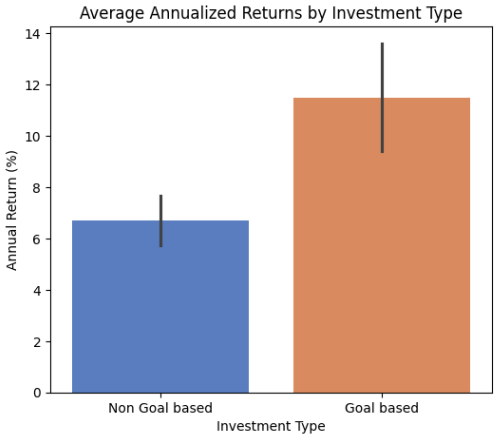

(Figure 4: Comparison of Goal-Based vs Non-Goal-Based Portfolio Returns)

3) Machine Learning Classification of Investor Type

A Support Vector Machine (SVM) classifier with an RBF kernel (C=10, γ=0.1) was used to predict investor type. The model achieved **91.8% accuracy** with strong performance metrics:

- Goal-based: Precision = 0.98, Recall = 0.83
- Non-goal-based: Precision = 0.86, Recall = 0.99
  The confusion matrix (**Figure 5**) confirmed high predictive reliability, indicating that attributes such as investment amount, contribution, risk profile, and goals effectively distinguish investor categories.

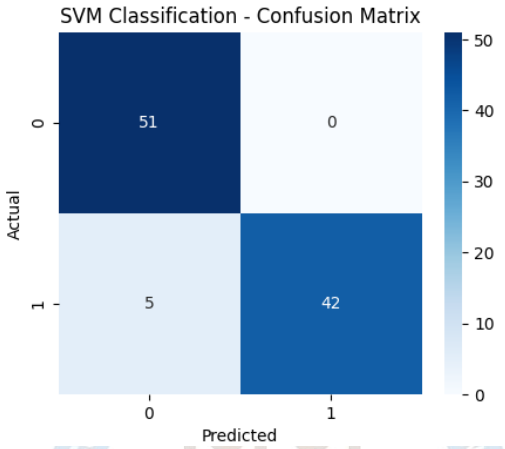

(**Figure 5: Confusion Matrix for SVM Classification of Investor Type**)

4) Regression Analysis of Portfolio Returns

Two models—Support Vector Regression (SVR) and Random Forest—were compared:

- **SVR:** MSE = 6.05, MAE = 1.9, $R^2 = 0.12$
- **Random Forest:** MSE = 3.8, MAE = 1.4, $R^2 = 0.42$
  The Random Forest model demonstrated stronger predictive accuracy and better fit between actual and predicted returns (Figure 6), confirming its suitability for financial forecasting.

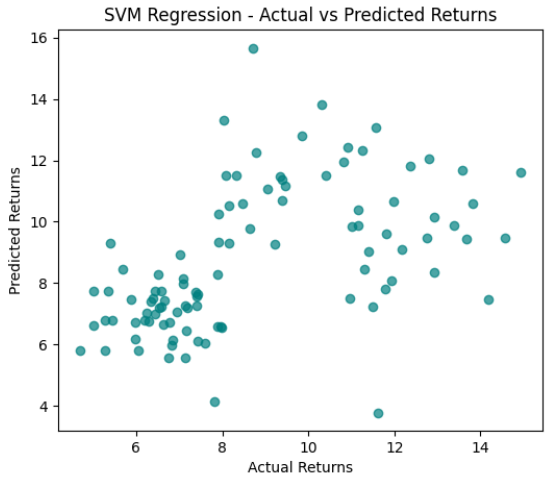

(**Figure 6: SVR Predicted vs Actual Returns**)

5) Feature Importance and SHAP Analysis

SHAP analysis of the Random Forest model identified Investment Goal as the most influential variable, followed by Initial Investment and Investment Mode. Factors such as Risk Profile, Investment Year, and Monthly Contribution had lesser effects. SHAP summary and mean value plots (**Figures 7–8**) reinforced that defining clear investment goals significantly impacts portfolio performance.

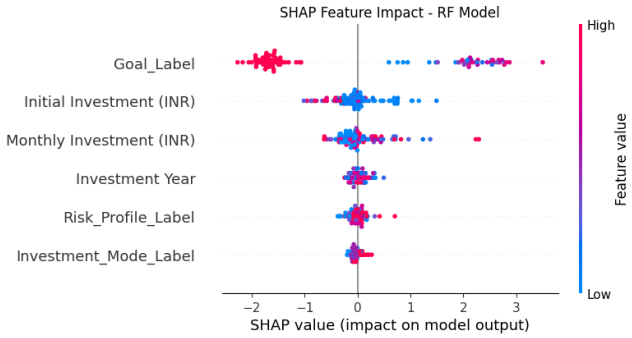

(Figure 7: SHAP Summary Plot for Random Forest Regressor)

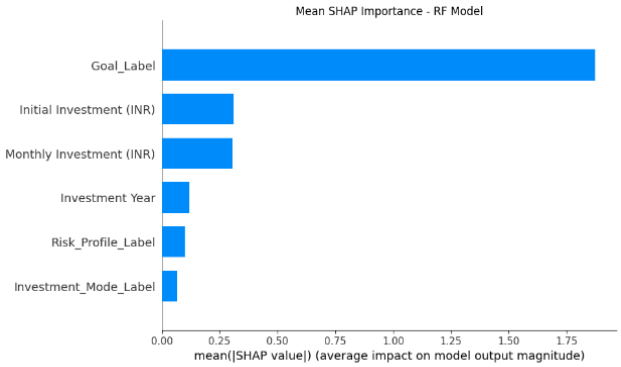

(Figure 8: Mean SHAP Value Plot)

5. Conclusion

This study evaluated the effectiveness of goal-based versus non-goal-based investment strategies using both statistical analysis and machine learning models. The results clearly demonstrate that goal-based investors consistently achieve higher annualized returns, confirming the critical role of structured financial planning in wealth management.

Machine learning techniques further enriched the analysis:

- SVM classification models successfully distinguished investor types with over 90% accuracy, underscoring the predictive value of investment attributes.
- Regression modeling revealed that Random Forest regressors outperform traditional SVR, highlighting the importance of non-linear approaches in financial return forecasting.
- SHAP analysis confirmed that investment goals and initial capital commitments are the most influential factors driving portfolio performance.

Taken together, these findings provide empirical evidence that goal-oriented investing not only improves financial outcomes but also enables more accurate predictive modelling when supported by AI-driven tools.

6. References

1. Bauman, T., Füller, J., & Becker, A. (2024). Deep reinforcement learning for goal-based wealth management. *arXiv preprint arXiv:2305.07102.*

2. Das, S. R., Markowitz, M., Scheid, J., & Statman, M. (2018). Dynamic portfolio allocation in goals-based wealth management. *SSRN Electronic Journal.*
3. Dixon, M., & Halperin, I. (2020). G-Learner and GIRL: Goal-based wealth management with reinforcement learning. *arXiv preprint arXiv:2002.10990.*
4. Lundberg, S. M., & Lee, S.-I. (2017). A unified approach to interpreting model predictions. *Advances in Neural Information Processing Systems, 30,* 4765–4774.
5. Mohammed, S., Shah, P., & Kumar, J. (2023). Embracing advanced AI/ML to help investors achieve success: Vanguard reinforcement learning for financial goal planning. *Vanguard Research Whitepaper.*
6. *Optimization of investment strategies through machine learning.* (2023). *Heliyon, Elsevier.*
7. Patel, J., Shah, S., Thakkar, P., & Kotecha, K. (2015). Predicting stock market index using fusion of machine learning techniques. *Expert Systems with Applications, 42(4),* 2162–2172.
8. Zhang, J. (2020). Investment strategy based on machine learning models. *University of Waterloo, Technical Report.*

Coefficient Estimates for a new subclass of Bi-Univalent functions involving an Integral Operator and Horadam Polynomial

Mrs. Preeti A Bhide
Shriram Kusumtai Sadashiv Vanjare College, Lanja, Ratnagiri, India
Email: preetibhide25@gmail.com
Contact Number: 9730509670

Abstract: In this paper, we introduce a new subclass of analytic and Bi-Univalent functions defined in the open unit disc $\mathbb{U}=\{z\in\mathbb{C}: |z|<1\}$ using the Integral Operator. We derive initial coefficient bounds $|a_2|$ and $|a_3|$ of Taylor-Maclaurin's series. Some special cases of our results are also discussed, leading the interesting observations about the coefficient bounds.

Keywords: Analytic function, Bi-Univalent function, Coefficient estimates, Integral Operator, Horadam Polynomial.

Introduction:

The Geometric Function Theory(GFT) is a field in mathematics in which we study the geometric properties of analytic functions defined on open unit disc $\mathbb{U} = \{z: |z| < 1\}$ satisfying the conditions $f(0) = 0$ and $f'(0) = 1$. The function $f(z)$ is a member of class $\mathcal{A}$ has a Taylor- Maclaurin series expansion of the form

$$f(z) = z + \sum_{n=2}^{\infty} a_n z^n \quad (1)$$

The class of bi-univalent functions denoted by Σ contains analytics function

$f(z) = z + \sum_{n=2}^{\infty} a_n z^n$ such that the function $f(z)$ and its inverse $f^{-1}(w) = g(w)$ both are univalent in the open unit disc $\mathbb{U}$.

e.g. $\frac{z}{1-z}$, $\log\left(\frac{z}{1-z}\right)$,$log\left(\sqrt{\frac{1+z}{1-z}}\right)$ are some examples of bi-univalent functions in Σ, whereas $\frac{2z-z^2}{2}, \frac{z}{1-z^2}$ are not members of Σ.

[2] By using the Koebe-One Quarter theorem, under univalent function $f \in \Sigma$ the image of $\mathbb{U}$, contains the disc of radius $\frac{1}{4}$ and the inverse of f is defined by

$$f^{-1}\big(f(z)\big) = z, z \in \mathbb{U}$$

And

$$f\big(f^{-1}(w)\big) = w$$

where, $g(w) = f^{-1}(w) = w + \sum_{j=2}^{\infty} b_j w^j$

$$= w - a_2 w^2 + (2{a_2}^2 - a_3)w^3 - (5{a_2}^3 - 5a_2a_3 + a_4)w^4 + \cdots \quad (2)$$

A measure challenge in this theory is to determine the bounds on the Taylor coefficients a_n as it gives information about geometric properties of these functions.in the class. In this paper, we estimate the initial coefficients $|a_2|$ and $|a_3|$ for certain subclasses of bi-univalent functions.

Preliminaries

1)Analytic Function: A function $f(z)$ of a complex variable z is said to be analytic at point z_0 if it is differentiable in some open unit disc centred at z_0.

2) Univalent Function: An injective analytic function in a domain D is called as univalent function.

3) Bi-Univalent Function: An analytic univalent function $f(z)$ defined on domain D is said to be bi-univalent of f^{-1} is also univalent in the range of f and can be extended to be univalent on the entire unit disc D.

4) [3] Horadam Polynomial: The Horadam polynomial is a recurrence relation

$$h_n(x) = pxh_{n-1}(x) + qh_{n-2}(x), n \in \mathbb{N}\{1,2\} \tag{3}$$

with

$$h_1(x) = a, h_2(x) = tx \text{ and } h_3(x) = ptx^2 + aq \tag{4}$$

For some real constant a, t, p, q.

Methodology

1)To define integral operator:

[4] We have the integral operator in the class ${\mathcal{I}_\Sigma}^\alpha(x, p, q, u, \gamma)$ of analytic functions defined as follows.

Let $f \in \mathcal{A}$, $m, n > 0$ and $\alpha\epsilon\mathbb{N}$. We denote the integral operator as ${\mathcal{L}_{m,n}}^\alpha$ defined

$${\mathcal{P}_{m,n}}^\alpha: \mathcal{A} \to \mathcal{A} \text{ as}$$

$${\mathcal{P}_{m,n}}^\alpha\big(f(z)\big) = \frac{1}{\beta(m+1,n+1)}\int_0^\infty \frac{t^{m-1}}{(1-t)^{m+n}} f(tz)dt$$

where, $\beta(m,n) = \int_0^1 \frac{t^{m+1}}{(1-t)^{1-n}} dt$

Substituting $x = \frac{t}{1+t}$ and solving above integration we get,

$${\mathcal{P}_{m,n}}^\alpha\big(f(z)\big) = z + \sum_{j=2}^{\infty}\left(\frac{\beta(m+j,n+j)}{\beta(m+1,n+1)}\right)^\alpha a_j z^j = z + \sum_{j=2}^{\infty}({\mathcal{K}_{m,n}}^j)^\alpha a_j z^j$$

Where $\left({\mathcal{K}_{m,n}}^j\right)^\alpha = \left(\frac{\beta(m+j,n+j)}{\beta(m+1,n+1)}\right)^\alpha$.

2)Generating function for Horadam Polynomial

[1]Let generating function for Horadam polynomial given in equation (3) be

$$\mathcal{G}(x,z) = \sum_{n=1}^{\infty} h_n(x)z^{n-1} = \frac{a+(t-ap)xz}{1-pxz-qz^2} \tag{5}$$

Where x is the polynomial variable and z is an arbitrary variable for the power series expansion. It should be noted that $\mathcal{G}(x,z)$ is analytic in open unit disc $\mathbb{U}$.

3)To find class boundaries $\mathcal{I}_{\Sigma}{}^{\alpha}(x,p,q,u,\gamma)$

[1]Definition: A function $f \in \sum$ given by (1) is a member of class $\mathcal{I}_{\Sigma}{}^{\alpha}(x,p,q,u,\gamma)$ if it satisfies following subordinations.

$$1+\frac{1}{u}\left\{\left[\mathcal{P}_{m,n}{}^{\alpha}(f(z))\right]'+\gamma z\left[\mathcal{P}_{m,n}{}^{\alpha}(f(z))\right]''-1\right\} \prec \mathcal{G}(x,z)+1-a \quad (6)$$

$$1+\frac{1}{u}\left\{\left[\mathcal{P}_{m,n}{}^{\alpha}(g(w))\right]'+\gamma w\left[\mathcal{P}_{m,n}{}^{\alpha}(g(w))\right]''-1\right\} \prec \mathcal{G}(x,w)+1-a \quad (7)$$

Where $\gamma \geq 0, u \geq 1, x \in \mathbb{R}$ and the function $g = f^{-1}$ is given by (2).

Theorem- Let $f \in \sum$ is belonging to class $\mathcal{I}_{\Sigma}{}^{\alpha}(x,p,q,u,\gamma)$ as indicated by (1), then

$$|a_2| \leq \frac{tx\sqrt{2tx}\,u}{\sqrt{\left|6u(1+2\gamma)\left(\mathcal{K}_{m,n}{}^{3}\right)^{\alpha}(tx)^2-8(1+\gamma)^2\left(\mathcal{K}_{m,n}{}^{2}\right)^{\alpha}(ptx^2+aq)\right|}}$$

And

$$|a_3| \leq \frac{t^2x^2u^2}{4(1+\gamma)^2\left(\mathcal{K}_{m,n}{}^{2}\right)^{2\alpha}}+\frac{u|tx|}{3(1+2\gamma)\left(\mathcal{K}_{m,n}{}^{3}\right)^{\alpha}}$$

Proof: Consider $\in \mathcal{I}_{\Sigma}{}^{\alpha}(x,p,q,u,\gamma)$, from (6) and (7), we have,

$$1+\frac{1}{u}\left\{\left[\mathcal{P}_{m,n}{}^{\alpha}(f(z))\right]'+\gamma z\left[\mathcal{P}_{m,n}{}^{\alpha}(f(z))\right]''-1\right\} \prec \mathcal{G}(x,\aleph(z))+1-a \quad (8)$$

$$1+\frac{1}{u}\left\{\left[\mathcal{P}_{m,n}{}^{\alpha}(g(w))\right]'+\gamma w\left[\mathcal{P}_{m,n}{}^{\alpha}(g(w))\right]''-1\right\} \prec \mathcal{G}(x,\beth(w))+1-a \quad (9)$$

where $\aleph(z)$ and $\beth(w)$ are the analytic functions of the form

$$\aleph(z) = c_1z + c_2z^2 + c_3z^3 + \cdots, z \in \mathbb{U}$$

$$\beth(w) = d_1w + d_2w^2 + d_3w^3 + \cdots, w \in \mathbb{U}$$

Such that $\aleph(0) = 0 = \beth(w)$ and $|\aleph(z)| < 1$ and $|\beth(w)| < 1$ for $z, w \in \mathbb{U}$.

From equations (8) and (9), we get,

$$1+\frac{1}{u}\left\{(\mathcal{P}_{m,n}{}^{\alpha}(f(z))'+\gamma z(\mathcal{P}_{m,n}{}^{\alpha}(f(z))''-1\right\} = 1+h_2(x)c_1z+[h_2(x)c_2+h_3(x){c_1}^2]z^2+\cdots \quad (10)$$

and

$$1+\frac{1}{u}\left\{\left[\mathcal{P}_{m,n}{}^{\alpha}(g(w))\right]'+\gamma w\left[\mathcal{P}_{m,n}{}^{\alpha}(g(w))\right]''-1\right\} = 1+h_2(x)d_1w+\left[h_2(x)d_2+h_3(x){d_1}^2\right]w^2+\cdots \quad (11)$$

As, $|\aleph(z)| < 1$; $|c_1z + c_2z^2 + c_3z^3 + \cdots| < 1$,

$|\beth(w)| < 1$; $|d_1w + d_2w^2 + d_3w^3 + \cdots| < 1$

This is possible only if $|c_i| \leq 1$ and $|d_i| \leq 1, \forall i \in \mathbb{N}$. (12)

Comparing the coefficients in (10) and (11),

$$\frac{2a_2\left(\mathcal{K}_{m,n}{}^{2}\right)^{\alpha}(1+\gamma)}{u} = h_2(x)c_1 \quad (13)$$

$$\frac{3a_3\left(\mathcal{K}_{m,n}{}^3\right)^{\alpha}(1+2\gamma)}{u} = h_2(x)c_2 + h_3(x){c_1}^2 \tag{14}$$

$$-\frac{2a_2\left(\mathcal{K}_{m,n}{}^2\right)^{\alpha}(1+\gamma)}{u} = h_2(x)d_1 \tag{15}$$

$$\frac{3(2{a_2}^2-a_3)\left(\mathcal{K}_{m,n}{}^3\right)^{\alpha}(1+2\gamma)}{u} = h_2(x)d_2 + h_3(x){d_1}^2 \tag{16}$$

It follows from (13) and (15) that,

$$c_1 = -d_1 \tag{17}$$

Squaring (13) and (15) and then adding both equations we will get,

$$\frac{8{a_2}^2\left(\mathcal{K}_{m,n}{}^2\right)^{2\alpha}(1+\gamma)^2}{u^2} = [h_2(x)]^2[{c_1}^2 + {d_1}^2] \tag{18}$$

If we add (14) and (16), we have,

$$\frac{3a_3\left(\mathcal{K}_{m,n}{}^3\right)^{\alpha}(1+2\gamma)}{u} + \frac{3(2{a_2}^2-a_3)\left(\mathcal{K}_{m,n}{}^3\right)^{\alpha}(1+2\gamma)}{u} = h_2(x)(c_2+d_2) + h_3(x)({c_1}^2+{d_1}^2) \tag{19}$$

Getting value of ${c_1}^2 + {d_1}^2$ from (18) and substituting in (19), we get

$$\left[\frac{6\left(\mathcal{K}_{m,n}{}^3\right)^{\alpha}(1+2\gamma)}{u} - \frac{8\left(\mathcal{K}_{m,n}{}^2\right)^{2\alpha}(1+\gamma)^2h_3(x)}{u^2\,[h_2(x)]^2}\right]{a_2}^2 = h_2(x)(c_2+d_2) + h_3(x)({c_1}^2+{d_1}^2) \tag{20}$$

Now using (4), (12) and (20), we find that

$$\boldsymbol{|a_2| \le \frac{tx\sqrt{2tx}\,u}{\sqrt{\left|6u(1+2\gamma)\left(\mathcal{K}_{m,n}{}^3\right)^{\alpha}(tx)^2 - 8(1+\gamma)^2\left(\mathcal{K}_{m,n}{}^2\right)^{\alpha}(ptx^2+aq)\right|}}} \tag{21}$$

Moreover, if we subtract (16) from (14), we obtain

$$\frac{6\left(\mathcal{K}_{m,n}{}^3\right)^{\alpha}(1+2\gamma)(a_3-{a_2}^2)}{u} = h_2(x)(c_2-d_2) + h_3(x)({c_1}^2-{d_1}^2) \tag{22}$$

Then, by using equations (17) and (18), equation (22) will become,

$$a_3 = \frac{[h_2(x)]^2u^2({c_1}^2+{d_1}^2)}{8\left(\mathcal{K}_{m,n}{}^2\right)^{2\alpha}(1+\gamma)^2} + \frac{uh_2(x)(c_2-d_2)}{6\left(\mathcal{K}_{m,n}{}^3\right)^{\alpha}(1+2\gamma)}$$

By applying (4) and (12), finally we obtain

$$|a_3| \le \frac{2(tx)^2u^2}{8\left(\mathcal{K}_{m,n}{}^2\right)^{2\alpha}(1+\gamma)^2} + \frac{2|tx|u}{6\left(\mathcal{K}_{m,n}{}^3\right)^{\alpha}(1+2\gamma)}$$

i.e.
$$\boldsymbol{|a_3| \le \frac{(tx)^2u^2}{4\left(\mathcal{K}_{m,n}{}^2\right)^{2\alpha}(1+\gamma)^2} + \frac{|tx|u}{3\left(\mathcal{K}_{m,n}{}^3\right)^{\alpha}(1+2\gamma)}} \tag{23}$$

Special Cases-

1) Set $\gamma = 0\ and\ u = 1$
Then the general class ${\mathcal{I}_{\Sigma}}^{\alpha}(x,p,q,u,\gamma)$ will reduces to simple class ${\mathcal{I}_{\Sigma}}^{\alpha}(x,p,q)$
And from (21) and (23) we will get,

$$|a_2| \leq \frac{tx\sqrt{2tx}}{\sqrt{\left|6\left(\mathcal{K}_{m,n}{}^{3}\right)^{\alpha}(tx)^2 - 8\left(\mathcal{K}_{m,n}{}^{2}\right)^{\alpha}(ptx^2 + aq)\right|}}$$

And

$$|a_3| \leq \frac{(tx)^2}{4\left(\mathcal{K}_{m,n}{}^{2}\right)^{2\alpha}} + \frac{|tx|}{3\left(\mathcal{K}_{m,n}{}^{3}\right)^{\alpha}}$$

2) Set $u = 1$ and $\gamma \geq 0$.

Then $$|a_2| \leq \frac{tx\sqrt{2tx}}{\sqrt{\left|6(1+2\gamma)\left(\mathcal{K}_{m,n}{}^{3}\right)^{\alpha}(tx)^2 - 8(1+\gamma)^2\left(\mathcal{K}_{m,n}{}^{2}\right)^{\alpha}(ptx^2+aq)\right|}}$$

$$|a_3| \leq \frac{(tx)^2}{4\left(\mathcal{K}_{m,n}{}^{2}\right)^{2\alpha}(1+\gamma)^2} + \frac{|tx|}{3\left(\mathcal{K}_{m,n}{}^{3}\right)^{\alpha}(1+2\gamma)}$$

3) Specializing the Horadam polynomial by substituting $a = t = p = q = 1$, we can obtain the result associated with Fibonacci polynomial $F_n(x)$.
i.e.

$$|a_2| \leq \frac{x\sqrt{2x}\,u}{\sqrt{\left|6u(1+2\gamma)\left(\mathcal{K}_{m,n}{}^{3}\right)^{\alpha}(x)^2 - 8(1+\gamma)^2\left(\mathcal{K}_{m,n}{}^{2}\right)^{\alpha}(x^2+1)\right|}}$$

And

$$|a_3| \leq \frac{(x)^2u^2}{4\left(\mathcal{K}_{m,n}{}^{2}\right)^{2\alpha}(1+\gamma)^2} + \frac{|x|u}{3\left(\mathcal{K}_{m,n}{}^{3}\right)^{\alpha}(1+2\gamma)}$$

4) Specializing the Horadam polynomial by substituting $a = 2, t = p = q = 1$, we can obtain the result associated with Lucas polynomial $L_n(x)$.

$$|a_2| \leq \frac{x\sqrt{2x}\,u}{\sqrt{\left|6u(1+2\gamma)\left(\mathcal{K}_{m,n}{}^{3}\right)^{\alpha}(x)^2 - 8(1+\gamma)^2\left(\mathcal{K}_{m,n}{}^{2}\right)^{\alpha}(x^2+2)\right|}}$$

And

$$|a_3| \leq \frac{(x)^2u^2}{4\left(\mathcal{K}_{m,n}{}^{2}\right)^{2\alpha}(1+\gamma)^2} + \frac{|x|u}{3\left(\mathcal{K}_{m,n}{}^{3}\right)^{\alpha}(1+2\gamma)}$$

5) Specializing the Horadam polynomial by substituting $a = 1, t = p = 2, q = -1$, we can obtain the result associated with Chebyshev polynomial of second kind $U_n(x)$.

$$|a_2| \leq \frac{2x\sqrt{4x}\,u}{\sqrt{\left|6u(1+2\gamma)\left(\mathcal{K}_{m,n}{}^{3}\right)^{\alpha}(2x)^2 - 8(1+\gamma)^2\left(\mathcal{K}_{m,n}{}^{2}\right)^{\alpha}(2x^2-1)\right|}}$$

And

$$|a_3| \leq \frac{(2x)^2u^2}{4\left(\mathcal{K}_{m,n}{}^{2}\right)^{2\alpha}(1+\gamma)^2} + \frac{|2x|u}{3\left(\mathcal{K}_{m,n}{}^{3}\right)^{\alpha}(1+2\gamma)}$$

Conclusion:

In this paper we used a subclass of analytic and bi-univalent functions ${\mathcal{I}_{\Sigma}}^{\alpha}(x,p,q,u,\gamma)$, defined in an open unit disc $\mathbb{U}$. Also we have defined an integral operator ${\mathcal{P}_{m,n}}^{\alpha}\big(f(z)\big)$ in this subclass. Then for a function in the class defined by this operator, we estimate the sharp bounds for the first two coefficients in Taylor-Maclaurin series which are $|a_2|$ and $|a_3|$.

Finally applying some conditions on (u,γ) and on the coefficients (a,t,p,q) of Horadam polynomial we connected our general results to subclasses associated with sequences such as Fibonacci, Lucas and Chebyshev polynomials.

References:

1. Alshammari K. M. K., Alnajar O., Amourah A.(2023)- The Neutrosophic Poisson Distribution Applied to Horadam Polynomial-Subordinate Bi-Univalent Functions, EUROPEAN JOURNAL OF PURE AND APPLIED MATHEMATICS, 18(2), Article Number- 5955.
2. Duren P.L. (2001), Univalent Functions. Springer Science & Business Media.
3. Horzum T. & Kocer E.G. (2009), On some properties of Horadam Polynomials. International Mathematical Forum, 4(25), 1219-1229.
4. Salmana F.O., Atshan W. G.(2023), New results on coefficient estimates for subclasses of bi-univalent functions related by a new integral operator, International Journal of Nonlinear Analysis and Applications, 14(4), 47–54.

A Practical Study of Linear Programming in Daily Life Scenarios

Ms. Shraddha V. Surve, Mrs. Spruha K. Joshi, Mrs. Gauri R. Patwardhan
Department of Mathematics, Gogate Jogalekar College(Autonomous), Ratnagiri-415612
Email:
shraddha.maths@gmail.com,spruhajoshi22@gmail.com,gauripatwardhan19@gmail.com

Abstract **-** Operations Research is a branch of Applied Mathematics. Linear Programming is an important branch of Operational Research and it is a Mathematical Method to assist the people to carry out scientific Management. Linear Programming is a type of mathematical optimization model where the goal is to maximize or minimize a linear objective function, subject to a set of linear constraints (equations or inequalities). The main objective of this paper is to understand how Graphical method and Simplex method can be applied in a simple way so that the individual can gain maximum nutrients in minimum cost.

Index Terms – Linear Programming, Nutritional Requirements, Graphical Method, Simplex Method

I. INTRODUCTION

Nutrients play vital role in daily life as they provide energy, support growth and development and maintain bodily functions. Calories, carbohydrates, dietary fibers and proteins are the primary sources of energy that fuel our body throughout the day. So, every person should gain such energy but at the same time in this era of inflation, cost of such things also matters a lot. Hence the aim of this research paper is to choose a combination of foods from which we gain maximum nutrients in minimum cost. We know that Linear Programming is an important branch of Operation Research in Applied Mathematics. In this paper with the help of Linear Programming, we have minimized the cost and gain the maximum nutrients. For this we have used Graphical Method and Simplex method in Linear Programming.

II. STUDY BACKGROUND

Here we are using Operation research. Operation research attempts to locate the best or optimal solution to the problem under consideration. The term "Operation research" (abbreviated as OR), was first coined in 1940 by McClosky and Trefthen in a small town, Bowdsey of the United Kingdom. Linear Programming (L.P.) is one of the most versatile and widely used operations research technique where planning is an important aspect of any activity. LPP is mathematical technique for allotting the limited resources of a firm in an optimum (most favorable or best) manner and it is useful in product mix problem, diet problem, media selection, transportation problems, assignment problems, portfolio selection, etc.

It is always said that "Graph is the best tool to visualize any concept". So Graphical Method is the simplest method to solve a L.P. problem (LPP) involving only two decision variables. The two decision variables say x and y are plotted along the two coordinate axes X and Y on a graph paper. Only first quadrant of XY plane must be considered as $x, y \geq 0$. The another method that we have used here is Simplex Method. Simplex Method is an algebraic iterative procedure which either solves an LPP in a finite number of steps or gives an indication that there is an unbounded solution to the given LPP.

III. DEFINITIONS

1. Linear Problem : A linear problem is proportional i.e. the power of the terms(variables) in an equation is at the most raised to 1.

- Example : P = ax + by + cz, where a, b, c are constants and x, y, z are variables. The problem most commonly faced by management is to decide the manner in which the limited resources should be used to achieve the desired objectives like profit maximization, cost minimization, etc.

2. Decision variables : These are unknowns to be determined from the solution.
   - Example: x, y, z in the above linear equation.
3. Constraints : These represent the mathematical equation of the limitations imposed by the problem solutions.
4. Objective function : This represents the mathematical equation of the major objective of the system in terms of decision variables.
5. Linear Relationship : LP deals with the problems in which the objective function as well as the constraints can be expressed as linear mathematical functions of the decision variables i.e. the function in which each variable appears only in one term and only to the first power.
6. Non – negativity Condition : i.e. the decision variables must be either 0 or +ve i.e. x, y, z ≥ 0.
7. Feasible Solution : A set of values of the decision variables which satisfies all the constraints and the non-negativity condition is a feasible solution. A problem can have many feasible solutions.
8. Optimal/Optimum Solution : this is a feasible solution which optimizes the objective function. Normally an optimal solution is unique.

IV. METHOD

Stages of LPP:

i. Problem identification through collection of data.
ii. Problem formulation i.e. to formulate mathematical problem from the given data.
iii. Problem solving.

Problem formulation of LPP:

- Step 1 : Find the key decisions to be made from the study of the problem.
- Step 2 : Identify the decision variables and assign symbols like x_1, x_2, x_3 or x, y, z etc.
- Step 3 : Mention the objective function quantitatively and express it as a linear function of the decision variables.
- Step 4 : Express the constraints also as a linear equalities or inequalities in terms of the decision variables.
- Step 5 : Express the objective function, the constraints, and the non-negativity condition from the steps above in an LPP format as follows:

Example :

Maximize $Z = 5x + 7y + 3z$ (objective function)

Subject to

$2x + 3y + z \leq 10$ (constraint 1)

$x + z \leq 6$ (constraint 2)

$y \geq 2$ (constraint 3)

where $x, y, z \geq 0$ (non-negativity condition)

LPP Problem Solving :

A. Graphical Method :

Steps for obtaining Graphical Solution :

- Step 1 : Formulate the given problem in L.P. format.
- Step 2 : Plot the graph constraints:
  i. Make the constant term on the right-hand side of the constraints as positive, if it is not, by changing the signs of all the terms. Change the inequality also from ≥ to ≤ or ≤ to ≥ in it.
  ii. Replace the inequality sign (≤ or ≥) in a constraint to an equality sign (=). This gives a constraint equation which represents a straight line.
  iii. Plot the constraint line: For plotting the line, identify two points on the line and join them by a straight line. The most convenient points are the points of intersection with X axis (obtained by putting x2 = 0 in the constraint equation solving it for x1) and Y axis (obtained by putting x1 = 0 in the equation and solving it for x2). Note that the lines x1 = a and x2 = b are straight lines parallel to Y and X axis at distance 'a' and 'b' from the origin respectively.
  iv. Repeat the procedure to draw all the constraint line.
- Step 3 : Identify the feasible region or the solution space
  i. Each constraint line divides the XY plane into two parts – one which includes the origin and the other away from the origin.
  ii. For constraints of the type (≥) or (>), mark the region away from the origin about the constraint line. For constraint of the type (≤) or (<), mark the region towards the origin about the constraint line. For constant of the type (=) the region is the line itself, only. Use arrows (→) to indicate the respective regions.
  iii. Mark the region which is common to all these regions. This is the feasible region which could be an open or closed polygon.
- Step 4 : To find Optimum Solution :
  Corner Point Method :
  i. Identify all the corner points of the feasible region. To obtain their coordinates solve the equations of the corresponding (intersecting) constraint lines simultaneously, if necessary.
  ii. Find the value of the objective function (say Z) at all these corner points.
  iii. For a maximization problem, the co-ordinates of the corner point where Z is maximum give the solution. Similarly, for minimization problem the co-ordinates of the corner pouint corresponding to minimum value of z give the solution. The corresponding value of Z is its optimum value Zmax or Zmin.

A. Simplex Big M Method (Method of Penalties) :

Steps for obtaining Simplex Big M Method Solution :

The Big-M method is an alternative method of solving a linear programming problem involving artificial variables. In this method we assign a very high penalty (say M) to the artificial variables in the objective function. The computational procedure for determining an optimum solution to an LPP when objective function is of minimization is obtained in the following seven steps:

Step 1 : Formulation of LPP. Identify the objective function and constraints of the given problem. Express the objective function, constraints and non-negative restrictions in the format of linear programming.

Step 2 : Standardize the LPP. Introduce slack and/or surplus (negative slack) variables on the left-hand side of the constraints to convert inequalities into equations. Assign a zero coefficient to slack and/or surplus variables in the objective function. Also, add an artificial variable to each of the constraint equations and assign high penalty cost 'M' to artificial variables in the objective function.

Step 3 : Determine the Initial Solution. The initial feasible solution is obtained by assigning zero value to all the decision as well as slack and/or surplus variables just to initiate the solution procedure.

Step 4 : Set Up the Initial Tableau. Eliminate the artificial variables in the objective function of the standardized linear programming problem obtained in step 2 with the help of constraint equations. Then, develop the initial simplex tableau for this reformulated LPP.

Step 5 : Test the Solution for Optimality. Examine the net evaluation (index) row numbers of the simplex tableau obtained in step 4. If all the (z_j-c_j) are '≤ 0', current basic feasible solution is optimum. Otherwise, select the most positive (z_j-c_j). The column corresponding to this number determines the key column. Non-basic variable corresponding to key column becomes basic in the next iteration.

Step 6 : Derive the Improved BFS. Determine the key row and key number. Thereafter,derive the revised tableau for improved solution.

Step 7 : Go to step 5 and repeat the computational procedure until an optimum solution is obtained or there is an indication of an unbound solution.

V. IMPLEMENTATION

Step 1 : Fixing decision variables.

Step 2 : Fixing constraints for nutritional values.

Step 3 : Fixing Objective Function to minimize the cost.

Step 4 : Formation of LPP.

Step 5 : Solving LPP with Graphical and Simplex Big M method.

Step 6 : Conclusion which will lead to decide which combination of foods should be taken so as to minimize the cost and gain maximum nutrients.

Problem 1

Here we have taken four nutritional aspects viz. calories, carbohydrates, dietary fiber and proteins and fixed two food items, viz. *Rice* and *Moongdal.* Following table gives the nutritional values per 100 calories and cost of each food. The problem is to solve this so as to gain maximum nutrients in minimum cost.

(per 100 gms) →	Total Calories (KCL)	Total Carbohydrates	Total Dietary Fiber	Total Proteins	Price
Rice	370	82	3	7	5
Moongdal	347	63	16	24	10
Nutritional Requirements	At least 1600	At least 130	At least 21	At least 50	

Decision Variables: Let x - Number units of units of *Rice*,

The problem formulated as LP model based upon the given data as follows :

Minimize $Z = 5x + 10y$

Subject to $370x + 347y \geq 1600$

$82x + 63y \geq 130$

$3x + 16y \geq 21$

$7x + 24y \geq 50, x, y \geq 0.$

A. Solution by Simplex Method :

Converting constraints to equations by subtracting surplus variables (S_1, S_2, S_3, S_4) and adding artificial variables (A_1, A_2, A_3, A_4) as appropriate and writing the given LPP in standard form as follows:

Minimize $Z = 5x+10y+S_1+0S_2+0S_3+0S_4+MA_1+MA_2+MA_3+MA_4$

Subject to $370x + 347y - S_1 + A_1 = 1600$

$82x + 63y - S_2 + A_2 = 130$

$3x + 16y - S_3 + A_3 = 21$

$7x + 24y - S_4 + A_4 = 50$

$x, y, S_1, S_2, S_3, S_4, A_1, A_2, A_3, A_4 \geq 0.$

Setup the initial solution. The initial basic feasible solution is obtained by setting $x=y=S_1=S_2=S_3=S_4=0$, so that $A_1=1600$, $A_2=130$, $A_3=21$, $A_4=50$. The initial basic feasible solution is summarized in the first simplex tableau as follows:

TABLE 1.1 : Initial basic feasible solution

C_j			5	10	0	0	0	0	M	M	M	M	Min
B	C_B	X_B	x	y	S_1	S_2	S_3	S_4	A_1	A_2	A_3	A_4	Ratio X_B/x
A_1	M	1600	370	347	-1	0	0	0	1	0	0	0	1600/370=4.3243
A_2	M	130	82*	63	0	-1	0	0	0	1	0	0	130/82= 1.5854→
A_3	M	21	3	16	0	0	-1	0	0	0	1	0	21/3=7
A_4	M	50	7	24	0	0	0	-1	0	0	0	1	50/7= 7.1429
Z=1801M		Z_j	462M	450M	-M	-M	-M	-M	M	M	M	M	
		Z_j-C_j	462M -5	450M -10	-M	-M	-M	-M	0	0	0	0	

Applying simplex algorithm in a similar manner for finite number of steps we have obtained the following optimal solution.

TABLE 1.2 : Optimal solution

Since all Z_j-$C_j \leq 0$.

Hence optimal solution is arrived with value of variables as:

x=3.2631, **y=1.1316** with Minimum **z = 27.6314**.

C_j			5	10	0	0	0	0
B	C_B	X_B	x	y	S_1	S_2	S_3	S_4
x	5	3.2631	1	0	-0.0037	0	0	0.0538
S_3	0	6.8949	0	0	0.0062	0	1	-0.7563
y	10	1.1316	0	1	0.0011	0	0	-0.0574
S_2	0	208.8622	0	0	-0.2367	1	0	0.7974
Z=27.6314		**Z_j**	**5**	**10**	**-0.0078**	**0**	**0**	**-0.3046**
		Z_j-C_j	0	0	-0.0078	0	0	-0.3046

B. Solution by Graphical Method :

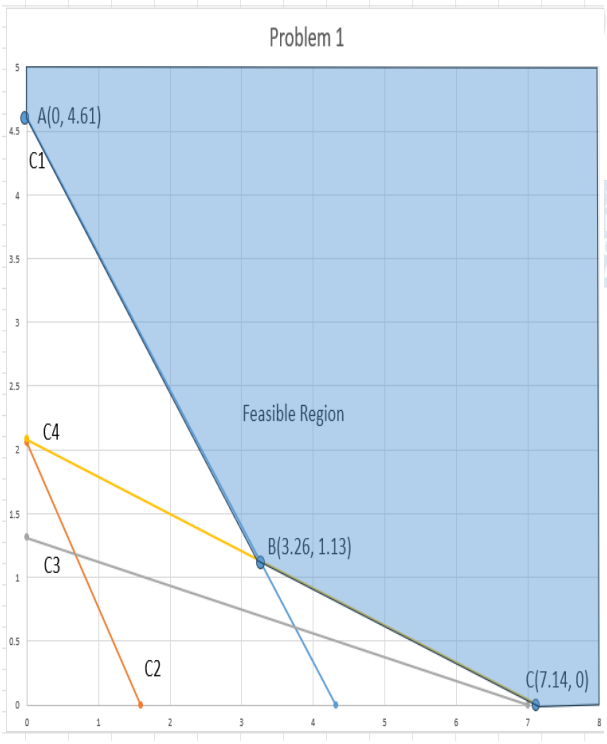

The value of the objective function at each of these extreme points is as follows :

Extreme Point Coordinates (x, y)	Lines through Extreme Point	Objective function value z = 5x + 10y
A(0, 4.61)	C1 : 370x + 347y ≥ 1600 and x ≥ 0	5(0) + 10(4.61) = 46.11
B(3.26, 1.13)	C1 : 370x + 347y ≥ 1600 and C4 : 7x +24y ≥ 50	5(3.26) + 10(1.13) = 27.63
C(7.14, 0)	C4 : 7x +24y ≥ 50 and y ≥ 0	5(7.14) + 10(0) = 35.71

The minimum value of the objective function is z = 27.63 occurs at the extreme point (3.26, 1.13). Hence, optimal solution of the given LP problem using Graphical Method is **x = 3.26**, **y = 1.13** and minimum z = **27.63**.

Problem 2

Here we have taken the same four nutritional aspects viz. calories, carbohydrates, dietary fiber and proteins and fixed two new food items, viz. *Wheat* and *Turdal.* Following table gives the nutritional values per 100 calories and cost of each food. The problem is to solve this so as to gain maximum nutrients in minimum cost.

(per 100 gms)	Total Calories (KCL)	Total Carbohydrates	Total Dietary Fiber	Total Proteins	Price
Wheat	340	72	11	13	4.5
Turdal	343	63	16	23	11
Nutritional Requirements	At least 1600	At least 130	At least 21	At least 50	

Decision Variables : Let x - Number units of units of *Wheat*,

y - Number units of units of *Turdal.*

The problem formulated as LP model based upon the given data as follows :

Minimize $Z = 4.5x + 11y$

Subject to

$340x + 343y \geq 1600$

$72x + 63y \geq 130$

$11x + 16y \geq 21$

$13x + 23y \geq 50$

$x, y \geq 0.$

A. Solution by Simplex Method :

Converting constraints to equations by subtracting surplus variables (S_1, S_2, S_3, S_4) and adding artificial variables (A_1, A_2, A_3, A_4) as appropriate and writing the given LPP in standard form as follows:

Minimize $Z = 4.5x+11y+0S_1+0S_2+0S_3+0S_4+MA_1+MA_2+MA_3+MA_4$

Subject to

$340x + 343y - S_1 + A_1 = 1600$

$72x + 63y - S_2 + A_2 = 130$

$11x + 16y - S_3 + A_3 = 21$

$13x + 23y - S_4 + A_4 = 50, x, y, S_1, S_2, S_3, S_4, A_1, A_2, A_3, A_4 \geq 0.$

Setup the initial solution. The initial basic feasible solution is obtained by setting $x=y=S_1=S_2=S_3=S_4=0$, so that $A_1=1600$, $A_2=130$, $A_3=21$, $A_4=50$. The initial basic feasible solution is summarized in the first simplex tableau as follows:

TABLE 2.1 : Initial basic feasible solution

C_j			4.5	11	0	0	0	0	M	M	M	M	
B	C_B	X_B	x	y	S_1	S_2	S_3	S_4	A_1	A_2	A_3	A_4	Min Ratio X_B/x
A_1	M	1600	340	343	-1	0	0	0	1	0	0	0	1600/343=4.6647
A_2	M	130	72	63	0	-1	0	0	0	1	0	0	130/63=2.0635
A_3	M	21	11	16*	0	0	-1	0	0	0	1	0	21/16=1.3125
A_4	M	50	13	23	0	0	0	-1	0	0	0	1	50/23=2.1739
Z=1801M		Z_j	436M	445M	-M	-M	-M	-M	M	M	M	M	
		Z_j-C_j	436M -4.5	445M -11	-M	-M	-M	-M	0	0	0	0	

Applying simplex algorithm in a similar manner for finite number of steps we have obtained the following optimal solution.

TABLE 2.2 : Optimal solution

C_j			4.5	11	0	0	0	0
B	C_B	X_B	x	y	S_1	S_2	S_3	S_4
S_4	0	11.1765	0	-9.8853	-0.0382	0	0	1
S_3	0	30.7647	0	-4.9029	-0.0324	0	1	0
x	4.5	4.7059	1	1.0088	-0.0029	0	0	0
S_2	0	208.8235	0	9.6353	-0.2118	1	0	0
Z=21.1765		**Z_j**	**4.5**	**4.5397**	**-0.0132**	**0**	**0**	**0**
		Z_j-C_j	0	-6.4603	-0.0132	0	0	0

Since all $Z_j-C_j \leq 0$.

Hence optimal solution is arrived with value of variables as:

x=4.7059, **y=0** with Minimum **z = 21.1765**.

B. Solution by Graphical Method :

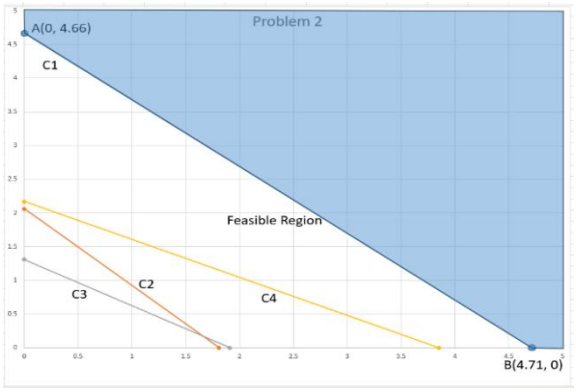

The value of the objective function at each of these extreme points is as follows

Extreme Point Coordinates (x, y)	Lines through Extreme Point	Objective function value $z = 4.5x + 11y$
A(0, 4.66)	C1 : 340x + 343y ≥ 1600 and x ≥ 0	4.5(0) + 11(4.66) = 51.31
B(4.71, 0)	C1 : 340x + 343y ≥ 1600 and y ≥ 0	4.5(4.71) + 11(0) = 21.18

The minimum value of the objective function is z = 21.18 occurs at the extreme point (4.71, 0). Hence, optimal solution of the given LP problem using Graphical Method is

x = 4.71, **y = 0** and minimum **z = 21.18**

Since by both the methods we obtain the value of y as zero which is not real life solution so now we have imposed extra conditions that both x and y should be greater than zero(i.e. ≥1).

And solved the same problem again. So now the problem formulated as LP model based upon the given data and new conditions as follows :

Minimize $Z = 4.5x + 11y$

Subject to

$340x + 343y \geq 1600$

$72x + 63y \geq 130$

$11x + 16y \geq 21$

$13x + 23y \geq 50$

$x \geq 1$ and $y \geq 1$, $x, y \geq 0$.

A. Solution by Simplex Method :

Converting constraints to equations by subtracting surplus variables (S_1, S_2, S_3, S_4, S_5, S_6) and adding artificial variables (A_1, A_2, A_3, A_4, A_5, A_6) as appropriate and writing the given LPP in standard form as follows:

Minimize

$Z=4.5x+11y+0S_1+0S_2+0S_3+0S_4+0S_5+0S_6+MA_1+MA_2+MA_3+MA_4+MA_5+MA_6$

Subject to

$340x + 343y - S_1 + A_1 = 1600$

$72x + 63y - S_2 + A_2 = 130$

$11x + 16y - S_3 + A_3 = 21$

$13x + 23y - S_4 + A_4 = 50$

$x - S_5 + A_5 = 1$

$y - S_6 + A_6 = 1,$

$x, y, S_1, S_2, S_3, S_4, S_5, S_6, A_1, A_2, A_3, A_4, A_5, A_6 \geq 0.$

Setup the initial solution. The initial basic feasible solution is obtained by setting $x=y=S_1=S_2=S_3=S_4=S_5=S_6=0$, so that $A_1=1600$, $A_2=130$, $A_3=21$, $A_4=50$, $A_5=1$, $A_6=1$. The initial basic feasible solution is summarized in the first simplex tableau as follows:

TABLE 3.1: Initial basic feasible solution

C_j			4.5	11	0	0	0	0	0	0	M	M	M	M	M	M	Min
B	C_B	X_B	x	y	S_1	S_2	S_3	S_4	S_5	S_6	A_1	A_2	A_3	A_4	A_5	A_6	Ratio X_B/x
A_1	M	1600	340	343	-1	0	0	0	0	0	1	0	0	0	0	0	1600/343=4.6647
A_2	M	130	72	63	0	-1	0	0	0	0	0	1	0	0	0	0	130/63=2.0635
A_3	M	21	11	16	0	0	-1	0	0	0	0	0	1	0	0	0	21/16=1.3125
A_4	M	50	13	23	0	0	0	-1	0	0	0	0	0	1	0	0	50/23=2.1739
A_5	M	1	1	0	0	0	0	0	-1	0	0	0	0	0	1	0	-
A_5	M	1	0	1*	0	0	0	0	0	-1	0	0	0	0	0	1	1/1=1 →
Z=1801M		Z_j	462M	450M	-M	-M	-M	-M	-M	-M	M	M	M	M	M	M	
		Z_j-C_j	462M-5	450M-10	-M	-M	-M	-M	-M	-M	0	0	0	0	0	0	

TABLE 3.2: Optimal solution

C_j			4.5	11	0	0	0	0	0	0
B	C_B	X_B	x	y	S_1	S_2	S_3	S_4	S_5	S_6
S_4	0	21.0618	0	0	-0.0382	0	0	1	0	-9.8853
S_3	0	35.6676	0	0	-0.0324	0	1	0	0	-4.9029
S_5	0	2.6971	0	0	-0.0029	0	0	0	1	1.0088
S_2	0	199.1882	0	0	-0.2118	1	0	0	0	9.6353
x	4.5	3.6971	1	0	-0.0029	0	0	0	0	1.0088
y	11	1	0	1	0	0	0	0	0	-1
Z=27.6368		**Z_j**	**4.5**	**11**	**-0.0132**	**0**	**0**	**0**	**0**	**-6.4603**
		Z_j-C_j	0	0	-0.0132	0	0	0	0	-6.4603

Since all $Z_j - C_j \leq 0$. Hence optimal solution is arrived with value of variables as:

x = 3.6971, **y = 1** with Minimum **z = 27.6368**.

B. Solution by Graphical Method :

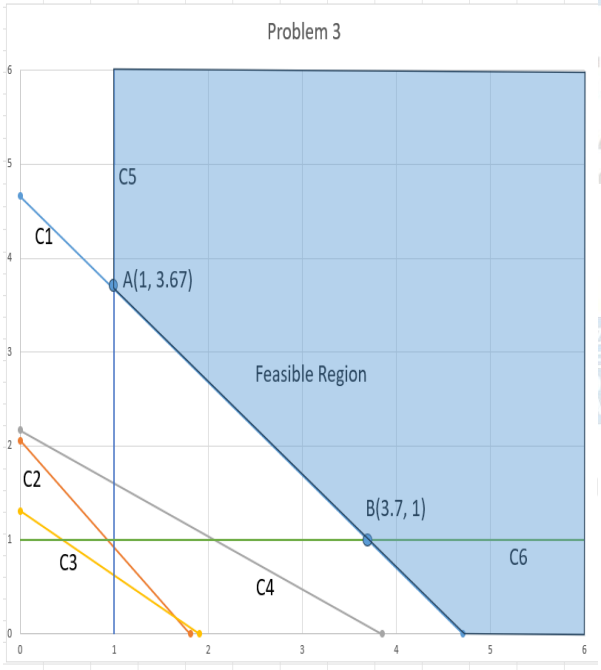

The value of the objective function at each of these extreme points is as follows :

Extreme Point Coordinates (x, y)	Lines through Extreme Point	Objective function value z = 4.5x + 11y
A(1, 3.67)	C1 : 340x + 343y ≥ 1600 and C5 : x ≥ 1	4.5(1) + 11(3.67) = 44.91
B(3.7, 1)	C1 : 340x + 343y ≥ 1600 and C6 : y ≥ 1	4.5(3.7) + 11(1) = 27.64

The minimum value of the objective function is z = 27.64 occurs at the extreme point (3.7, 1). Hence, optimal solution of the given LP problem using Graphical Method is **x = 3.7**, **y = 1** and minimum **z = 27.64**.

VI. Conclusion and future direction

Now we have obtained non-zero value of y in problem 3 so instead of considering the solution obtained for problem 2 we suggest that the solution obtained for problem 3 is more convenient. So here we have considered two combinations of foods namely *Rice-Moongdal* and *Wheat-Turdal*. Since there is slight difference of costs for problem 1 and 3, hence this paper suggests that if you choose any of these combinations then you will get these foods at minimum cost and also from this you will gain maximum nutrients. So precisely anyone can choose these combinations to gain maximum nutrients at minimum cost. Here we focused on two day to day life combinations of consumptions of foods but the same work can be done for any number of combinations, accordingly more choices will be there to choose perfect combination of foods.

VII. References

1. Operations Research , Introduction to management science -*Kanti Swarup, PK Gupta, Man Mohan*
2. J.S. Sandhiya, N. Mythili, E. Saranya – A Study on Linear Programming in Real Life Applications-*International Journal of Creative Research Thoughts (IJCRT 2023-ISBN:2320 –2882)*
3. Daily Nutritional Requirements Stana– National Institute of Health (NIH)

Comparative Study of Estimation Methods

Author[1]: Ms. Uma Ekanath Joshi.
Author[2]: Ms. Aditi Aniket Joshi.
[12]Assistant Professors, Gogate Jogalekar College (Autonomous), Ratnagiri, India
Email: umaj240@gmail.com , aditi.joshi@gjcrtn.ac.in

ABSTRACT:

Estimation plays a vital role in statistical analysis, forecasting and decision-making processes across scientific and industrial domains. Among the widely used estimation techniques, 'Regression Analysis' and 'Extrapolation' stand out for their versatility and mathematical rigor. This study presents a comparative analysis of these two estimation approaches, highlighting their theoretical foundations, applications, accuracy based on secondary data containing amount of total saleable steel by Tata Steel. The research employs real-world datasets to examine performance differences in terms of prediction accuracy, stability and error sensitivity. Results reveal that regression estimation provides more reliable results within the data range, while extrapolation, although valuable for forecasting beyond known data, exhibits higher uncertainty and variance in predictions. The study concludes with recommendations for method selection based on data characteristics and estimation objectives.

Keywords: Estimation, Extrapolation, Regression, Hypothesis, one tailed paired t – test

1. INTRODUCTION:

Estimation methods form the backbone of predictive analytics and statistical inference. They enable researchers to infer unknown parameters, forecast future trends and make data-driven decisions. Among the various estimation techniques, Regression Analysis and Extrapolation are among the most frequently applied in both theoretical and applied contexts. Regression estimation focuses on modeling the relationship between dependent and independent variables within a given data range, aiming to minimize prediction error through mathematical fitting techniques. On the other hand, Extrapolation extends the estimation process beyond the observed data range, assuming that the underlying pattern continues similarly outside the sampled domain. While both methods serve as essential tools for prediction, their comparative effectiveness varies depending on data behavior, model assumptions and the purpose of estimation. The current study undertakes a systematic comparative analysis of Regression and Extrapolation methods, evaluating their theoretical bases, computational frameworks and performance metrics. This comparison is essential for practitioners to choose the most appropriate estimation approach for given analytical tasks.

2. METHODOLOGY:

Regression analysis is a set of statistical methods used to estimate the relationship between a dependent variable (the outcome one is interested in) and one or more independent variables (the predictors or explanatory variables). The theory revolves around defining this relationship, estimating its parameters, and assessing the model's validity.
The linear regression equation is developed by finding the best-fit line, which is typically done using the least squares method, to minimize the squared differences between the actual data points and the predicted values. The standard equation is

$Y = a + bX$, where Y is the dependent variable, X is the independent variable, b is the slope, and a is the y-intercept. The values for a and b are calculated using formulas derived from the least squares method to determine the line that best represents the data.

Extrapolation is a statistical technique used to estimate or predict a value that lies outside the range of the observed data. It assumes that the pattern, or relationship, found within the known data continues into the unknown region.

The development of an extrapolation formula, especially linear extrapolation, involves using two known points (x_1, y_1) and (x_2, y_2) to estimate a value at a new point x. The formula is derived by rearranging the slope formula, $m = \frac{y_2 - y_1}{x_2 - x_1}$, to solve for the new y-value and is given by $y(x) = y_1 + \frac{x - x_1}{x_2 - x_1} \times (y_2 - y_1)$

Paired t – test: A paired t-test is used when you want to compare the means of two related groups, such as measuring the same subject twice under different conditions (e.g., before and after a treatment) or comparing two matched subjects. This test is appropriate when the data comes in pairs, and you want to determine if the average difference between these paired observations is significantly different from zero.

The paired t-test is developed by calculating the difference between each pair of observations, then performing a one-sample t-test on these differences. The formula is $t = \frac{\bar{d}}{s_d/\sqrt{n}}$, where $\bar{d}$ is the mean of the differences, s_d is the standard deviation of the differences and n is the number of pairs. This process isolates the effect of the intervention or condition by examining the variation within each pair, providing a more powerful test than an independent t-test for related samples.

The t – test was originally developed for small samples, but it is suitable for any sample size where the assumptions are met.

- Using data for total saleable steel production published by Tata Steel Company for years 1981 – 2000, researchers derived model for estimation by Regression and Extrapolation.
- Using the data and R – programming, a Regression line is obtained.
- Using the same Regression line, estimates for the production are made for the years 2001 – 2010.
- Using the same data and R – programming, by the Extrapolation method estimates for the production are made for the years 2001 – 2010.
- Coefficient of variation is calculated for both methods viz. Regression and Extrapolation.
- Also, one tailed paired t – test is performed for the differences in the estimates.

3. RESULT and DISCUSSION:

- **For Regression Analysis:**

Year	Actual Data	Predicted Data	Difference
2001	3413	3014.068	398.932
2002	3596	3098.551	497.449
2003	3975	3183.034	791.966

Year	Actual Data	Predicted Data	Difference
2004	4076	3267.517	808.483
2005	4074	3351.999	722.001
2006	4551	3436.482	1114.518
2007	4929	3520.965	1408.035
2008	4858	3605.447	1252.553
2009	5375	3689.93	1685.07
2010	6439	3774.413	2664.587
		Mean	**1134.3594**
		SD	**672.814722**
		CV	**59.31230632**

Table 1

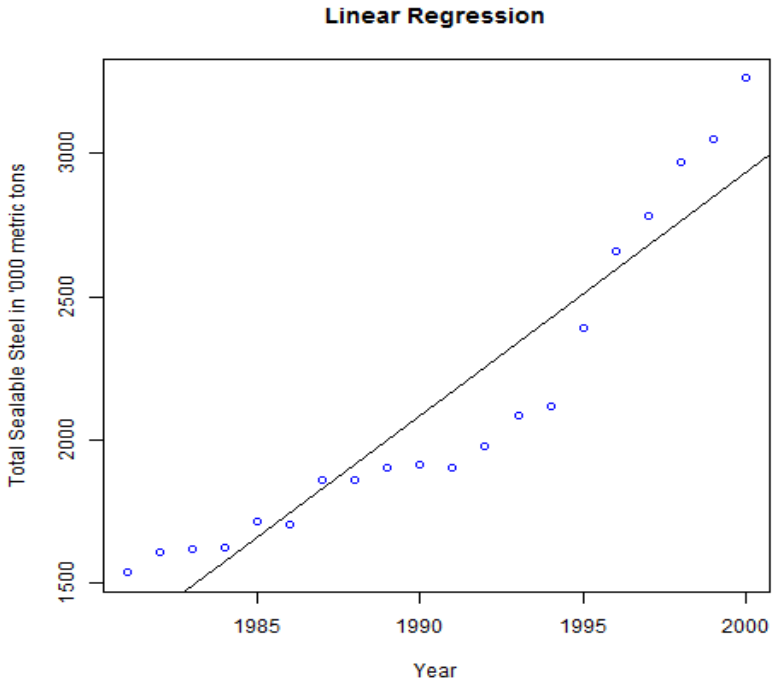

Fig 1

- For the data, predicted values for Regression method are calculated using R – programming
- Differences between actual data and predicted data are calculated
- For these differences coefficient of variation is calculated

- **<u>For Extrapolation:</u>**

Year	Actual Data	Predicted Data	Difference
2001	3413	3473	-60
2002	3596	3684	-88
2003	3975	3895	80
2004	4076	4106	-30
2005	4074	4317	-243

Year	Actual Data	Predicted Data	Difference
2006	4551	4528	23
2007	4929	4739	190
2008	4858	4950	-92
2009	5375	5161	214
2010	6439	5372	1067
		Mean	**106.1**
		SD	**364.3104445**
		CV	**343.3651692**

Table 2

- For the data predicted values for Extrapolation method are calculated using R – programming
- Differences between actual data and predicted data are calculated.
- For these differences coefficient of variation is calculated

- From table 1 and table 2, coefficient of variation (CV) for Regression is less than coefficient of variation (CV) for Extrapolation.
- That means Regression Analysis provides more reliable estimates than Extrapolation within the data.
- That means Regression Analysis can be considered as a better method for estimation.

- **<u>One tailed paired t – test:</u>**

  H_0: Regression Analysis and Extrapolation, both are equally reliable methods for estimation.
  H_1: Regression Analysis is more reliable than Extrapolation for estimation.

Year	Actual Data	Predicted Data (Regression)	Predicted Data (Extrapolation)	Differences
2001	3413	3014.068	3473	-458.932
2002	3596	3098.551	3684	-585.449
2003	3975	3183.034	3895	-711.966
2004	4076	3267.517	4106	-838.483
2005	4074	3351.999	4317	-965.001
2006	4551	3436.482	4528	-1091.518
2007	4929	3520.965	4739	-1218.035
2008	4858	3605.447	4950	-1344.553
2009	5375	3689.93	5161	-1471.07
2010	6439	3774.413	5372	-1597.587
			Mean (Differences)	-1028.259
			SD	383.0501
			t statistics	-8.488817

Table 3

Number of Observations, $n = 10$
Thus, degrees of freedom, $n - 1 = 9$
Level of significance, $\alpha = 5\%$
$\boldsymbol{t(cal)} = -8.488817$ $\boldsymbol{t(tab)} = 1.833$

Reject H_0 if $t(cal) < -t(tab)$
Since $\boldsymbol{t(cal) = -8.488817 < -t(tab) = -1.833}$,
Reject H_0
That means,
Regression Analysis is more reliable than Extrapolation for estimation.

4. CONCLUSION:

- From table 1 and table 2, though the values of differences are considerably large for Regression than those for Extrapolation, the CV for Regression is less than that of Extrapolation. Thus, Regression method is more reliable for estimation than Extrapolation.
- The result is confirmed by one tailed paired t – test suggesting that the Regression Analysis is more reliable for estimation than Extrapolation.

5. REFERENCES:

1. Fundamentals of Mathematical Statistics (Gupta & Kapoor 2000)
2. Introductory Methods of Numerical Analysis (Sastry 2015)
3. Schaum's Outlines Statistics (Spiegel & Stephens 2010)
4. https://www.tutorialspoint.com/r/index.htm
5. https://www.tatasteel.com/

A MATHEMATICAL STUDY OF POPULATION GROWTH IN MUMBAI SUBURBAN DISTRICT

V. P. Sonalkar
Department of Mathematics, S. P. K. Mahavidyalaya, Sawantwadi.
Maharashtra- 416510, India.
vpsonalkar@yahoo.com

ABSTRACT

A Mathematical model is a description of a system using Mathematical language. Mathematical models are used not only in the natural sciences and engineering disciplines. In this paper, by using Modeling with Differential Equations, we will study population growth of Mumbai Suburban District, from which we can get an idea of the rate in which the population is growing.

Keywords: Ordinary differential equation, Population growth, Mathematical model, Verhulst-Pearl model, Boundary value problems.

INTRODUCTION

Differential equations are used in many different areas of study, including physical and applied sciences. In most of the cases, these equations are non-linear and cannot be solved analytically. A mathematical model is a description of a natural (in Physics, Chemistry, Biology and astronomy) and real-world situation in terms of Mathematical concepts. This involves a situation like changes of one or more types, is modeled by derivatives and hence by differential equations. As we know that if y = f(x) is a given function of x, then its derivative $\frac{dy}{dx}$ is nothing but the rate of change of y with respect to x. In any natural process, the variables involved and their rates of change are connected with one another by means of the basic scientific principles that govern the process. When this process is expressed in Mathematical symbols, the result is often a differential equation [13].

A Model is a miniature representation of something; a pattern of something to be made; an example for imitation or emulation; a description or analogy used to help visualize something (e.g., an atom) that cannot be directly observed; a system of postulates, data and inferences presented as a mathematical description of an entity or state of affairs [14].

By Modeling with Differential Equations, we will study population growth of Mumbai Suburban District. From this we can get an idea of the rate in which the population is growing. From this we will estimate how much we need to develop the necessary resources like schools, colleges, water supply, industries, infrastructure etc. in this area in the future.

It is common to use idealized models in physics to simplify things. Massless ropes, point particles, ideal gases and the particle in a box are among the many simplified models used in physics. The laws of physics are represented with simple equations such as Newton's laws, Maxwell's equations and the Schrödinger equation. These laws are a basis for making mathematical models of real situations. Many real situations are very complex and thus modelled approximately on a computer, a model that is computationally feasible to compute is made from the basic laws or from approximate models made from the basic laws. For example, molecules can be modelled by molecular orbital models that are approximate solutions to the Schrödinger equation.

Different mathematical models use different geometries that are not necessarily accurate descriptions of the geometry of the universe. Euclidean geometry is much used in classical physics, while special relativity and general relativity are examples of theories that use geometries which are not Euclidean.

LITERATURE REVIEW

Modeling is the process of writing a differential equation to describe a physical situation. In [12], discussed three different situations viz. Mixing Problems, Population Problems, and Falling object and obtain the solutions by using differential equations. In all of these situations it will be forced to make assumptions that do not accurately depict reality in most cases, but without them the problems would be very difficult and beyond the scope of this discussion (and the course in most cases to be honest).

Taking [11] into consideration of the work load the post of Additional Collector Bombay Suburban District was created in the year 1958 and entire administrative of Bombay Suburban District was full-fledged handed over to Additional Collector Suburban District. However overall supervision was kept with the Collector of Bombay City. During this period the seat of Additional Collector, Mumbai Suburban District at Old Custom House. Colaba Harbor later it was shifted to Suburban area at the same time suburb was recognized as district came in to force w. e. f. 1/10/1990. In the name Bombay Suburban District now known as Mumbai Suburban District.

The authors [4], focuses on general introduction to the area of mathematical modelling. It attempts to present the important fundamental concepts of mathematical modelling and to demonstrate their use in solving certain scientific and engineering problems. Also, it includes the Modelling concepts and case studies. Also, it includes continuous and discrete modelling and a number of realistic case studies which illustrate the use of the modelling process in the solution of continuous and discrete models. In 2004, the research paper [1], focused on Population growth and changing land-use pattern in mumbai metropolitan region of India. Also, this paper studied the population distribution and its growth trends in different constituent units of Mumbai Metropolitan Region (MMR) during 1971, 1991 and 2011.

In [9], authors focused primarily upon finding solutions to particular equations rather than general theory. It also includes the study of ordinary differential equations in more than one variable, First and Second Order partial Differential Equations, Wave equation, Laplace equation and diffusion equation etc. In 2008, the authors [10], covered solutions of first Order differential Equations by using different methods (models). The research paper [2], studied the spatial dynamics of population change and Migration pattern in Mumbai and its adjoining areas and reflects upon planning and governance in the City.

The [7] regions like Thane District and Navi Mumbai within the MMR have experienced rapid expansion of population growth, driven by migration and economic opportunities, during 1971 to 2011.

METHODOLOGY

We will look at situations of Population Problem in [12]. In this situation we will be forced to make assumptions that do not accurately show reality in most cases, but without them the problems would be very difficult. We can use this model not only for finding the human population but also the population dynamics of a certain species

When we have built a set of equations, we compare the data generated by the equations with real data collected from the system. If the two sets of data "agree" (or are close), then we gain confidence that the set of equations will lead to a good description of the real-world system. For example, we may use the equations to make predictions about the long-term behavior of the system. It is also important to keep in mind that the set of equations stays only "valid" as long as the two sets of data are close. If a prediction from the equations leads to some conclusions which are by no means close to the real-world future behavior, then we should modify and "correct" the underlying equations. As you can see, the problem of generating

"good" equations is not an easy exercise [3]. The set of equations is called a Model for the system.

Here are some natural questions related to population problems:

- What will the population of a certain city or District be in ten or twenty years?
- How are we protecting the resources from extinction?

In order to illustrate the use of differential equations with regard to this problem we consider the easiest mathematical model offered to govern the population dynamics of a human being. It is commonly called the exponential model, that is, the rate of change of the population is proportional to the existing population.

In other words, if $P(t)$ measures the population,

We have

$$\frac{\mathbf{dP(t)}}{\mathbf{dt}} \propto \mathbf{P(t)}$$

$$\frac{\mathbf{dP(t)}}{\mathbf{dt}} = \mathbf{k}\ \mathbf{P(t)},$$

where the rate k is constant. It is fairly easy to see that if $k > 0$, we have growth, and if $k < 0$, we have decay. This is a linear equation, which solves into

$$\log P(t) = k\,t + c \qquad \text{----------(1)}$$

$$P(t) = P_0 e^{kt}$$

where P_0 is the initial population, $P(0) = P_0$.

The main argument for this has to do with environmental limitations. The complication is that population growth is eventually limited by some factor, usually one from among many essential resources. When a population is far from its limits of growth it can grow exponentially. However, when nearing its limits the population size can fluctuate, even uncontrollably.

Another model was proposed to remedy this flaw in the exponential model. It is called the logistic model (also called Verhulst-Pearl model). The differential equation for this model [13] is

$$\frac{dP}{dt} = kP(t)\left(1 - \frac{P(t)}{M}\right),$$

where M is a limiting size for the population (also called the carrying capacity). clearly, when P is small compared to M, the equation reduces to the exponential one. In order to solve this equation, we recognize a nonlinear equation which is separable. The constant solutions are $P = 0$ and $P = M$. The non-constant solutions may be obtained by separating the variables.

$$\frac{dP}{P(t)\left(1 - \frac{P(t)}{M}\right)} = kdt,$$

and integration

$$\int \frac{dP}{P(t)\left(1 - \frac{P(t)}{M}\right)} = \int kdt\,.$$

The partial fraction technique gives

$$\int \frac{dP}{P(t)\left(1 - \frac{P(t)}{M}\right)} = \int \left(\frac{1}{P(t)} + \frac{\frac{1}{M}}{1 - \frac{P(t)}{M}}\right) dP = \int kdt\,,$$

which gives

$$\log|P(t)| - \log\left|1 - \tfrac{P(t)}{M}\right| = kt + c.$$

Easy algebraic manipulations give

$$\frac{P(t)}{1-\frac{P(t)}{M}} = Ce^{kt},$$

where $C = e^c$ is a constant. Solving for P, we get

$$P(t) = \frac{MCe^{kt}}{M+Ce^{kt}}. \quad \ldots\ldots\ldots (2)$$

If we consider the initial condition $P(0) = P_0$ (assuming that P_0 is not equal to both 0 or M), we get

$$C = \frac{P_0 M}{M-P_0},$$

which, once substituted into the expression for $P(t)$ [equation (2)] and simplified, we find

$$P(t) = \frac{MP_0}{P_0 + (M-P_0)e^{-kt}}.$$

It is easy to see that

$$\lim_{t \to \infty} P(t) = M.$$

However, this is still not satisfactory because this model does not tell us when a population is facing extinction since it never implies that. Even starting with a small population, it will always tend to the carrying capacity M.

Consider another case for the population [8]. If P(t) represents a population in a given region at any time *t,* then the basic equation that we will use is namely,

Rate of change of P(t)	=	Rate at which *P(t)* enters the region	-	Rate at which *P(t)* exits the region.

Here the rate of change of *P(t)* is still the derivative. What's different this time is the rate at which the population enters and exits the region. For population problems all the ways for a population to enter the region are included in the entering rate. Birth rate and migration into the region are examples of terms that would go into the rate at which the population enters the region. Likewise, all the ways for a population to leave an area will be included in the exiting rate. Therefore, things like death rate, migration out and predation are examples of terms that would go into the rate at which the population exits the area.

With first model of differential equation, we are going to study population growth of Mumbai Suburban District. Due to the economic opportunities and industrial background in this district, the population growth for last 30-40 years is high. The Mumbai Municipal Corporation, has the jurisdiction over Mumbai and Mumbai (Suburban) districts. For administrative convenience, the entire district is divided into 15 wards and further into sections. Bandra, Khar/Santacruz, Andheri (East), Andheri (West), Goregaon, Malad, Kandivali, Borivali, Dahisar, Kurla, Chembur (East), Chembur (west), Ghatkopar, Bhandup and Mulund are the wards of the district.

DATA ANALYSIS

The collected data is as follows.

Year	Male	Female	Total	Decadal Growth Rate
1971	1,639,535	1,260,662	2,900,197	+110.1
1981	27,52,635	22,05,730	49,58,365	+ 71
1991	36,87,596	30,63,406	67,51,002	+ 36.15
2001	47,41,720	38,98,699	86,40,419	+ 27.99
2011	50,31,323	43,25,639	93,56,962	+ 8.29

(Source: [5], [6])

The Histogram and the Time Series plot for the Male-female population from 1971 to 2011 is as follows.

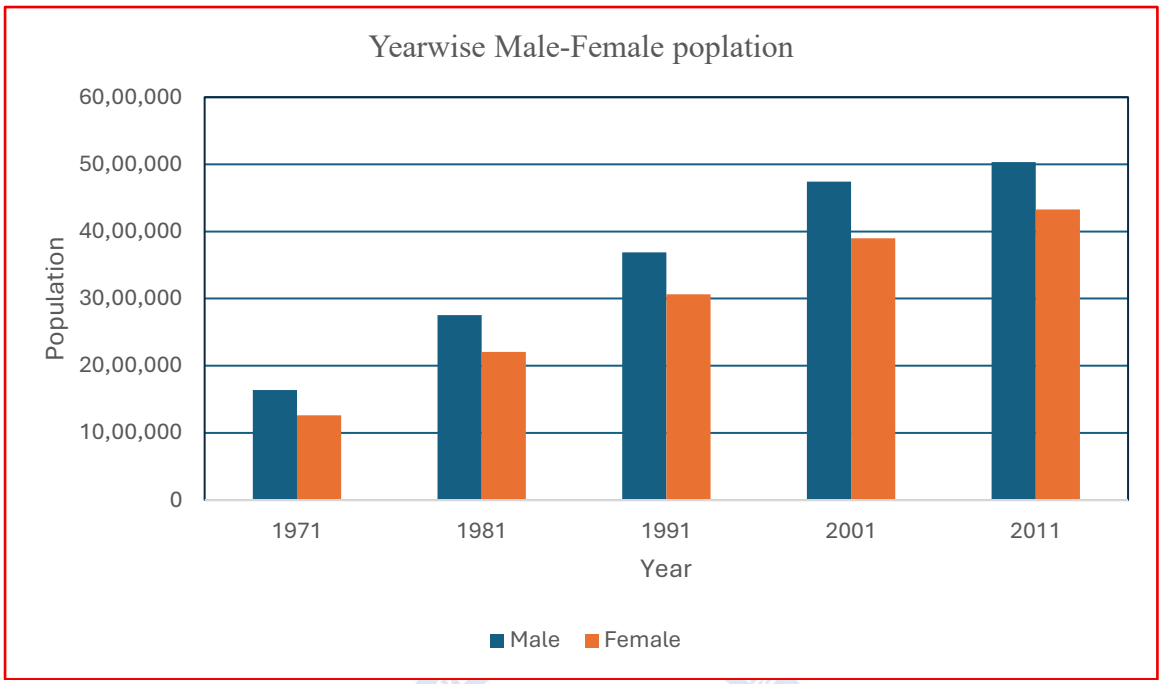

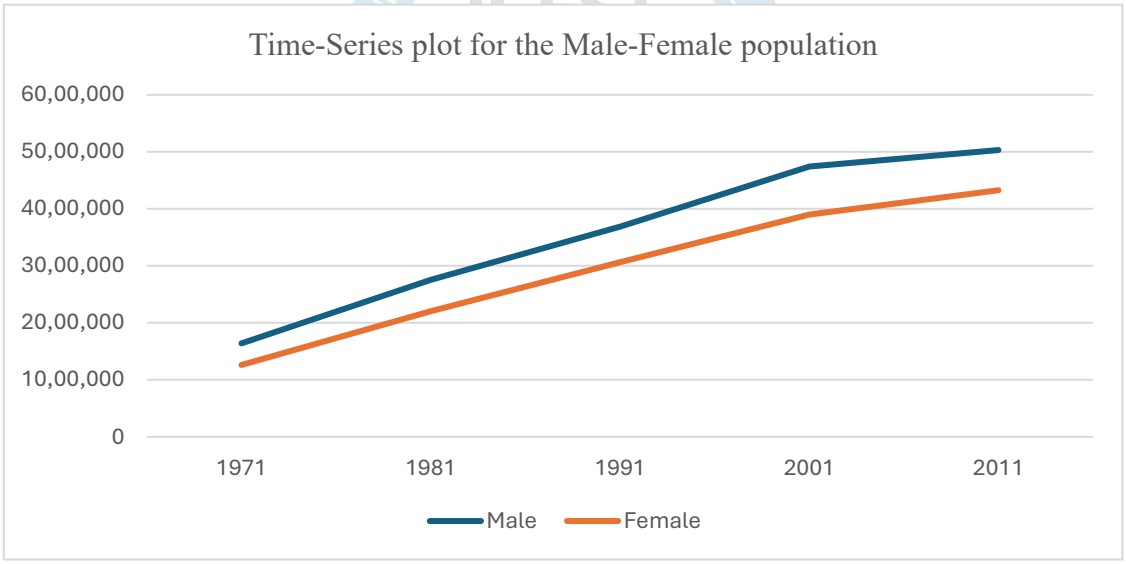

Model is $\log(P(t)) = kt + C$,

base year is $T_0 = 1981$.

Step 1 For, $t = 0$ $P(t) = 49,58,365$

$C = 6.6953$

Step 2 For next year 1991

$t = 10$ $P = 67,51,002$

$k = 0.0134$

The equation is

$\log(P(t)) = (0.0134) \times t + 6.6953$

FINDINGS

By using the above model, we can forecast the population for above mentioned years such as

Year	t	Log(P(t))	P(t)
1971	-10	6.5613	36,41,665
1981	0	6.6953	49,58,365
1991	10	6.8293	67,50,942
2001	20	6.9633	91,89,672
2011	30	7.0973	1,25,09,897
2021	40	7.2313	1,70,33,348
2031	50	7.3653	2,31,65,985

HYPOTHESIS TESTING

H_0: the forecasting is not appropriate.
H_1: the forecasting is appropriate.

Year	P(actual)	P(forecasted)
1971	2,900,197	36,41,665
1981	49,58,365	49,58,365
1991	67,51,002	67,50,942
2001	86,40,419	91,89,672
2011	93,56,962	1,25,09,897

By using Paired T test, we get result as the forecasting is appropriate.

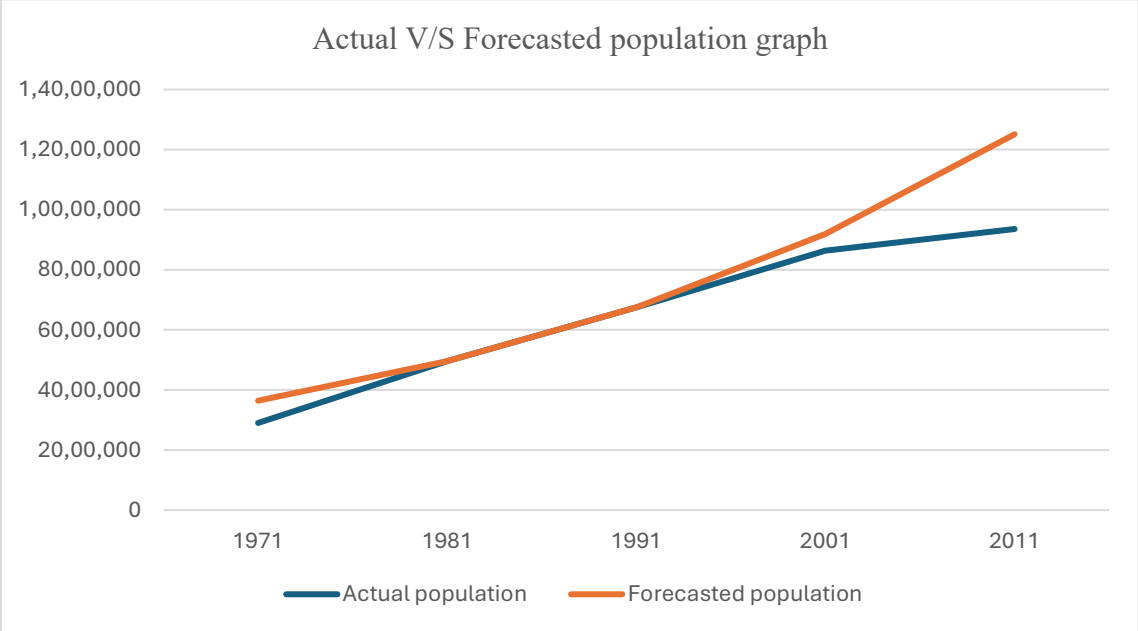

CONCLUSION

A mathematical model is a description of a system using mathematical language. Mathematical models are used not only in the natural sciences (such as physics, biology, earth science, meteorology) and engineering disciplines.

By Modeling with Differential Equations, we have studied population growth of Mumbai suburban district; we can get an idea of the rate in which the population is growing. Which helps us to develop the necessary resources like schools, colleges, water supply, industries, basic infractures etc. of that locality. This model will be also useful in many real-life situations. By using this model, we can forecast the quantity of a particular thing in future. Moreover, this model has now widely been used in different problems.

REFERENCES

[1] Acharya A. K., Parveen Nangia, Caminhos De Geografia, Population growth and changing land-use pattern in mumbai metropolitan region of India, Vol. 11, No. 11, 168-185, Feb. 2004.
[2] Bhagat, R. B., & Jones, G., Demography India, Demographic Dynamics of Mega--Urban Regions: The Case of Mumbai. Vol. 43, No. 1, 71-94, 2014.
[3] Boyce W. E. and Diprima R. C., Elementary Differential Equations and Boundary value problems, John Wiley and Sons, 8th Edition, 2004.
[4] Caldwell J., Ram Y. M., Mathematical Modelling: Concepts and Case Studies (Mathematical Modelling: Theory and Applications Book 6), 1st Edition, Springer, 2000.
[5] Census of India 2001 - Maharashtra, Series 28, District Census Handbook, Part A and B, Mumbai (Suburban) District.
[6] Census of India 2011 - Maharashtra, Series 28, District Census Handbook, Part XX-B, Mumbai Suburban.
[7] Flora Pandya, Urbanization and population growth in India: An exploration of the Mumbai Metropolitan region and beyond, Economic Challenger, Vol. 27, Issue 105, 299-305, October - December 2024.
[8] Simmons G. F., Differential equation with applications and Historical Notes, McGraw Hill Education, Second Edition, 2017.
[9] Sneddon I. N., Elements of partial Differential Equations., McGraw Hill comp any, New York, 2006.
[10] William E. Boyce, Richard C. Diprima, Elementary Differential Equation and Boundary Value Problems, Ninth Edition, John Wiley & Sons, 2008.
[11] https://mumbaisuburban.gov.in/en/history
[12] Online: www.sosmath.com/differentialequation/modeling.
[13] Paul's online notes: online notes/differential equations/first order differential equations/ modeling with first differential equations.
[14] www.sfu.ca/~vdabbagh/Chap1-modeling.pdf

On Coefficient Inequalities for Initial Taylor-Maclaurin Coefficients for a New Subclass of Analytic and Bi-Univalent Functions Associated with Modified Hohlov Operator

Dr. Ranjan Suresh Khatu.
Shriram Kusumtai Sadashiv Vanjare College, Lanja
Maharashtra, India
Email Id: ranjan.khatu11@gmail.com, ranjan.khatu1986@gmail.com

ABSTRACT

In this research article, we define a new subclass of analytic and bi-univalent functions defined on an open unit disc $\Delta = \{z \in \mathbb{C}: |z| < 1\}$. We define this class of functions with the help of well-known Hohlov operator with certain modifications using q-number shift factorial. Later on, we discover coefficient bounds for second and third Taylor-Maclaurin's coefficients of functions of the same class. Furthermore, we discuss the special cases of our result and we get very interesting findings regarding coefficient bounds.

Keywords: Bi-univalent functions, Analytic functions, Coefficient bounds, Subordination, Taylor-Macluarin's coefficients, Hohlov operator, q-number shift factorial.

2010 Mathematics Subject Classification: 30C45, 30C80

1. INTRODUCTION

Geometric function theory is very interesting area of research. This field is very active area of research due to variety of ideas, geometrical interpretation of concepts and open challenges. The study of univalent, bi-univalent and multivalent functions are the branches of Geometric Function Theory and these are active and popular fields of research. In the theory of bi-univalent functions, geometric behavior of functions is analyzed by estimating coefficient bounds. The theory started with Bieberbach conjecture (Bieberbach L., 1916) which was successfully resolved by de Branges (De Branges L., 1985) in 1985. Later on, researchers like Duren P.L. (Duren P.L., 1983), Nehari Z. (Nehari Z., 1975) and others gave remarkable contribution to this theory. First Lewin M. (Lewin M., 1967) introduced the concept of bi-univalent function which was an extension of concept univalent functions. This new concept attracted many researchers to do work in this field and later on many researchers gave very significant contribution in the field.

In this research paper, we generalize Hohlov operator (Hohlov Y.E., 1985) using the concept of q-number shift factorial and use it to define a new class of bi-univalent functions. Then we find initial coefficient bounds for the functions from this new class of bi-univalent functions.

Let $\Delta = \{z \in \mathbb{C}: |z| < 1\}$ be an open unit disc in the complex plane $\mathbb{C}$. Let $G(\Delta)$ be a class of analytic functions defined on Δ and which are normalized by the conditions $f(0) = f'(0) - 1 = 0$. Hence it can be expressed as

$$f(z) = z + \sum_{k=2}^{\infty} a_k z^k \qquad (z \in \Delta). \tag{1}$$

Let G_Δ be class of all normalized analytic functions defined on Δ, which are univalent in Δ.

For two analytic functions f and g defined on Δ, we say f is subordinate to g in Δ and it is defined as

$$f(z) \prec g(z) \quad (z \in \Delta), \tag{2}$$

if there exists a Schwarz function ω, which is analytic in Δ with

$$\omega(0) = 0, \ |\omega(z)| < 1 \quad (z \in \Delta)$$

such that,

$$f(z) = g\big(\omega(z)\big), \quad (z \in \Delta). \tag{3}$$

If the function g is univalent in Δ, then we have the following equivalence.

$$f(z) \prec g(z), \quad (z \in \Delta) \ \Leftrightarrow \ f(0) = g(0), \ f(\Delta) \subseteq g(\Delta).$$

For $f \in G_\Delta$, we get f is invertible. The Koebe one-quarter theorem (Duren, 1983) ensures that, the image of Δ under every $f \in G_\Delta$ contains a disc of radius $\frac{1}{4}$.

Thus, for each $f \in G_\Delta$, f^{-1} exists and define as

$$f^{-1}\big(f(z)\big) = z, \quad z \in \Delta$$

and

$$f\big(f^{-1}(w)\big) = w, \ |w| < r, \qquad r_0(f) \geq \frac{1}{4}.$$

Here, the inverse function f^{-1} is given by

$$g(w) = f^{-1}(w) = w - a_2 w^2 + (2a_2^2 - a_3)w^3 - (5a_2^3 - 5a_2 a_3 + a_4)w^4 + \cdots \tag{4}$$

A function $f \in G(\Delta)$ is said to be bi-univalent if both f and its inverse, f^{-1} are univalent on Δ. Let $\sum$ be a class of such bi-univalent functions defined on Δ and which are in the form (1). The subclasses of such bi-univalent functions are discovered and studied by many researchers and initial coefficient bounds are also obtained. For the brief history and the recent work on interesting examples subclasses of $\sum$, see Srivastava H.M., Mishra A.K. and Gochhayat (2010), Brannan D.A. and Taha T.S. (1988), Bulut S. (2013), Caglar M., Orhan H. and Yagmur N. (2013), Goyal S.P. and Goswami P. (2012), Hayani T. and Owa S. (2012), Muthaiyan E. and Wanas A.K. (2025), Al-Rawashdeh W. (2024), Bakheet S.R., Atiyah M.A. and Muhammed M.S. (2025) and Khatu R.S., Jadhav S.D. and Pathak R.P. (2025).

In this research paper we use the number $[s]$ (Kanas and Raducanu, 2014) which is defined for any real number s and positive real number q $(q \neq 1)$ as

$$[s] = \frac{1-q^s}{1-q}, \ [0] = 0. \tag{5}$$

Now the q-number shift factorial for any non-negative number n is defined as

$$[n]! = [n][n-1]\cdots[2][1], \quad ([0]! = 1). \tag{6}$$

It can be clearly observed that $\lim_{q \to 1} [n] = n$.

Here we assume that q is a fixed number and $q \in (0,1)$.

Recall that the convolution of two analytic functions $f, h \in G_\Delta$ is the analytic function defined as

$$(f * h)(z) = z + \sum_{n=2}^{\infty} a_n b_n z^n,$$

where $f(z)$ is given by (1) and $h(z) = z + \sum_{n=2}^{\infty} b_n z^n$.

For the complex parameters a, b and $(c \neq 0, -1, -2, \cdots)$, the Gaussian hypergeometric function is defined as

$${}_2F_1(a,b,c;z) = \sum_{n=0}^{\infty} \frac{(a)_n (b)_n}{(c)_n n!} z^n = 1 + \sum_{n=2}^{\infty} \frac{(a)_{n-1}(b)_{n-1}}{(c)_{n-1}(n-1)!} z^n, \ (z \in \Delta) \tag{7}$$

where $(\alpha)_n$ is the Pochhammer symbol defined in terms of gamma function by

$$(\alpha)_n = \frac{\Gamma(\alpha+n)}{\Gamma(\alpha)} = \begin{cases} 1 & (n=0) \\ \alpha(\alpha+1)(\alpha+2)\cdots(\alpha+n-1) & (n = 1,2,3,\cdots) \end{cases}.$$

Motivated by the work of Omar R., Halim A. S. and Janteng A. (2017) and Al-Rawashdeh W. (2024), we introduce one new subclass of bi-univalent functions and further find initial coefficient bounds.

2. PRILIMINARIES, DEFINITIONS AND EXAMPLES

Using the Gaussian hypergeometric function given by (7), Hohlov Y.E. (1985) introduced the operator $I_{a,b,c}$ as follows

$$I_{a,b,c}f(z) = z\ {}_2F_1(a,b,c;z) * f(z) = z + \sum_{n=2}^{\infty} \frac{(a)_{n-1}(b)_{n-1}}{(c)_{n-1}(n-1)!} a_n z^n, \ \ (z \in \Delta).$$

For $b = 1$, the operator $I_{a,b,c}$ reduces to the Carlson-Shaffer operator. The Hohlov operator is a generalization of the Ruscheweyh operator and Bernadi-Libera-Livingston operator.

Now, we generalize the the operator Hohlov by replacing $(n-1)!$ by q-number shift factorial and we get the operator $J^q_{a,b,c}$ as

$$J^q_{a,b,c}f(z) = z + \sum_{n=2}^{\infty} \frac{(a)_{n-1}(b)_{n-1}}{(c)_{n-1}[n-1]!} a_n z^n, \ \ (z \in \Delta). \tag{8}$$

Now, we rewrite the operator $J^q_{a,b,c}$ as follows.

$$J^q_{a,b,c}f(z) = z + \sum_{n=2}^{\infty} \phi_n a_n z^n, \ \ (z \in \Delta), \text{ where } \phi_n = \frac{(a)_{n-1}(b)_{n-1}}{(c)_{n-1}[n-1]!}.$$

Now using the operator $J^q_{a,b,c}$ we define the class of bi-univalent functions as follows.

Definition 1. A function $f \in \sum$ is said to be in the class $\mathcal{B}_{\Sigma}^{a,b,c}(\gamma, \delta, \sinh)$ if the following conditions are satisfied:

$$(1-\gamma)\frac{J^q_{a,b,c}f(z)}{z} + \gamma\left(J^q_{a,b,c}f(z)\right)' \prec 1 + \sinh(\delta z)$$

and

$$(1-\gamma)\frac{J^q_{a,b,c}g(w)}{w} + \gamma\left(J^q_{a,b,c}g(w)\right)' \prec 1 + \sinh(\delta w),$$

where the function $g(w) = f^{-1}(w)$ is given by the equation (4), the parameters $\gamma \geq 1$, $\delta \geq 0$, $a, b, c \in \mathbb{C}$ and $c \neq 0, -1, -2, \cdots$.

Remark: If we set $a = c, b = 1$ and let $q \to 1$ then we get the class $\mathcal{B}_{\Sigma}^{a,1,a}(\gamma, \delta, \sinh)$ which is introduced and studied by Al-Rawashdeh W. (2024) and it is defined as follows.

A function $f \in \sum$ is said to be in the class $\mathcal{B}_{\Sigma}^{a,1,a}(\gamma, \delta, \sinh)$ if the following conditions are satisfied:

$$(1-\gamma)\frac{f(z)}{z} + \gamma f'(z) \prec 1 + \sinh(\delta z)$$

and

$$(1-\gamma)\frac{g(w)}{w} + \gamma g'(w) \prec 1 + \sinh(\delta w),$$

where the function $g(w) = f^{-1}(w)$ is given by the equation (4), the parameters $\gamma \geq 1$, $\delta \geq 0$, $a \in \mathbb{C}$ and $a \neq 0, -1, -2, \cdots$

To establish the bounds for coefficient a_2 and a_3, we state the well-known lemma **(**Omar R., Halim A. S. and Janteng A., 2017) that is used to obtain the bounds.

Lemma 1: If $p \in \wp$ then $|p_k| \leq 2$ for each k, where $\wp$ is the family of all functions p analytic in Δ, $Re\, p(z) > 0$, $p(z) = 1 + p_1 z + p_2 z^2 + p_3 z^3 + \cdots$ for $z \in \Delta$.

3. COEFFICIENT ESTIMATES FOR THE FUNCITON IN $\mathcal{B}_{\Sigma}^{a,b,c}(\gamma, \delta, \sinh)$

In this section, we estimate the initial coefficient bounds for a_2 and a_3 for the functions belongs to the class $\mathcal{B}_{\Sigma}^{a,b,c}(\gamma, \delta, \sinh)$.

Theorem 1: Let $f \in \Sigma$ given by equation (1) be in the class $\mathcal{B}_{\Sigma}^{a,b,c}(\gamma, \delta, \sinh)$. Then

$$|a_2| \leq \frac{\delta}{\sqrt{|\delta(1+2\gamma)\phi_2 + (1+\gamma)^2\phi_2^2|}} \tag{9}$$

and

$$|a_3| \leq \frac{\delta^2}{|\delta(1+2\gamma)\phi_2 + (1+\gamma)^2\phi_2^2|} + \frac{2\delta}{|(1+2\gamma)\phi_3|} \tag{10}$$

where $\gamma \geq 1$, $\delta \geq 0$, $a, b, c \in \mathbb{C}$ and $c \neq 0, -1, -2, \cdots$.

Proof: Let $f \in \mathcal{B}_{\Sigma}^{a,b,c}(\gamma, \delta, \sinh)$.

The by definition of the class $\mathcal{B}_{\Sigma}^{a,b,c}(\gamma, \delta, \sinh)$, we get

$$(1-\gamma)\frac{J_{a,b,c}^{q} f(z)}{z} + \gamma\left(J_{a,b,c}^{q} f(z)\right)' \prec 1 + \sinh(\delta z)$$

and

$$(1-\gamma)\frac{J_{a,b,c}^{q} g(w)}{w} + \gamma\left(J_{a,b,c}^{q} g(w)\right)' \prec 1 + \sinh(\delta w),$$

where the function $g(w) = f^{-1}(w)$ is given by the equation (4).

Then by the subordination principle, we can find two Schwarz functions $u(z)$ and $v(z)$ defined on the open unit disk Δ such that

$$(1-\gamma)\frac{J_{a,b,c}^{q} f(z)}{z} + \gamma\left(J_{a,b,c}^{q} f(z)\right)' = 1 + \sinh(\delta u(z)) \tag{11}$$

and

$$(1-\gamma)\frac{J_{a,b,c}^{q} g(w)}{w} + \gamma\left(J_{a,b,c}^{q} g(w)\right)' = 1 + \sinh\big(\delta v(w)\big). \tag{12}$$

Now, using those Schwarz functions, we define two new analytic functions $h(z)$ and $k(w)$as follows:

$$h(z) = \frac{1+u(z)}{1-u(z)} = 1 + h_1 z + h_2 z^2 + \cdots$$

and

$$k(w) = \frac{1+v(w)}{1-v(w)} = 1 + k_1 w + k_2 w^2 + \cdots.$$

Moreover, $h(0) = k(0) = 1$, they have positive real parts, $|h_j| \leq 2$ and $|k_j| \leq 2$ for all $j \in \mathbb{N}$.

Equivalently, we get the following representations of $u(z)$ and $v(w)$

$$u(z) = \frac{h(z)-1}{h(z)+1} = \frac{1}{2}\left[h_1 z + \left(h_2 - \frac{h_1^2}{2}\right) z^2 + \cdots\right], \tag{13}$$

and

$$v(w) = \frac{k(w)-1}{k(w)+1} = \frac{1}{2}\left[k_1 w + \left(k_2 - \frac{k_1^2}{2}\right) w^2 + \cdots\right], \tag{14}$$

On one hand, by consulting equation (13), the right-hand side of equation (11) can be written as

$$1 + \sinh\big(\delta u(z)\big) = 1 + \frac{\delta h_1}{2} z + \delta\left(\frac{h_2}{2} - \frac{h_1^2}{4}\right) z^2 + \left(\frac{\delta h_1^2}{8} - \frac{\delta h_1 h_2}{2} + \frac{\delta h_3}{2} + \frac{\delta^3 h_1^3}{48}\right) z^3 + \cdots \tag{15}$$

By considering equation (15) and comparing the coefficient of both sides of equation (11), we get the following equations.

$$(1+\gamma)\phi_2 a_2 = \frac{\delta h_1}{2} \tag{16}$$

and

$$(1+2\gamma)\phi_3 a_3 = \delta\left(\frac{h_2}{2} - \frac{h_1^2}{4}\right). \tag{17}$$

On the other hand, by consulting equation (14), the right-hand side of equation (12) can be written as

$$1 + \sinh\big(\delta v(w)\big) = 1 + \frac{\delta k_1}{2} w + \delta\left(\frac{k_2}{2} - \frac{k_1^2}{4}\right) w^2 + \left(\frac{\delta k_1^2}{8} - \frac{\delta k_1 k_2}{2} + \frac{\delta k_3}{2} + \frac{\delta^3 k_1^3}{48}\right) w^3 + \cdots$$
(18)

By considering equation (18) and comparing the coefficient of both sides of equation (12), we get the following equations.

$$-(1+\gamma)\phi_2 a_2 = \frac{\delta k_1}{2} \tag{19}$$

and

$$(1+2\gamma)\phi_3 (2a_2^2 - a_3) = \delta\left(\frac{k_2}{2} - \frac{k_1^2}{4}\right). \tag{20}$$

From (16) and (19) yields

$$h_1 = -k_1.$$

Now squaring and adding equations (16) and (19), we get

$$\frac{8(1+\gamma)^2\phi_2^2 a^2}{\delta^2} = h_1^2 + k_1^2 \tag{21}$$

Now, from (17), (20) and (21) lead to

$$a_2^2 = \frac{\delta^2(h_2+k_2)}{4[\delta(1+2\gamma)\phi_2+(1+\gamma)^2\phi_2^2]} \tag{22}$$

which yields the estimate on $|a_2|$ as described in (9).

Now subtracting equation (20) from (17), we get

$$a_3 - a_2^2 = \frac{2\delta(h_2-k_2)-\delta(h_1^2-k_1^2)}{8(1+2\gamma)\phi_3}. \tag{23}$$

Using equation (22) in equation (23), we get

$$a_3 = \frac{\delta^2(h_2+k_2)}{4[\delta(1+2\gamma)\phi_2+(1+\gamma)^2\phi_2^2]} + \frac{2\delta(h_2-k_2)-\delta(h_1^2-k_1^2)}{8(1+2\gamma)\phi_3}. \tag{24}$$

By taking modulus of both sides of equation (24) and using lemma 1, we get the desired inequality mentioned in (10). Hence the proof of theorem is concluded.

By setting $a = c, b = 1$ and let $q \to 1$ in theorem 1 then we get the interesting result as a corollary of our theorem.

Corollary 1: Let $f \in \Sigma$ given by equation (1) be in the class $\mathcal{B}_{\Sigma}^{a,1,a}(\gamma, \delta, \sinh)$. Then

$$|a_2| \leq \frac{\delta}{\sqrt{\delta(1+2\gamma)+(1+\gamma)^2}} \tag{25}$$

and

$$|a_3| \leq \frac{\delta^2}{\delta(1+2\gamma)+(1+\gamma)^2} + \frac{2\delta}{(1+2\gamma)} \tag{26}$$

where $\gamma \geq 1, \delta \geq 0, a \in \mathbb{C}$ and $a \neq 0, -1, -2, \cdots$.

By setting $\gamma = 1$ in corollary 1 then we get the following interesting result.

Corollary 2: Let $f \in \Sigma$ given by equation (1) be in the class $\mathcal{B}_{\Sigma}^{a,1,a}(1, \delta, \sinh)$. Then

$$|a_2| \leq \frac{\delta}{\sqrt{3\delta+4}} \tag{27}$$

and

$$|a_3| \leq \frac{\delta^2}{3\delta+4} + \frac{2\delta}{3} \tag{28}$$

where $\delta \geq 0, a \in \mathbb{C}$ and $a \neq 0, -1, -2, \cdots$.

By setting $\gamma = 0$ in corollary 1 then we get the following interesting result.

Corollary 3: Let $f \in \Sigma$ given by equation (1) be in the class $\mathcal{B}_{\Sigma}^{a,1,a}(1, \delta, \sinh)$. Then

$$|a_2| \leq \frac{\delta}{\sqrt{\delta+1}} \tag{29}$$

and

$$|a_3| \leq \frac{\delta^2}{\delta+1} + 2\delta \tag{30}$$

where $\delta \geq 0$, $a \in \mathbb{C}$ and $a \neq 0, -1, -2, \cdots$.

4. CONCLUSION

In this research article, a new operator $J_{a,b,c}^{q}$ is introduced using q-number shift factorial and it is used to define a new interesting subclass $\mathcal{B}_{\Sigma}^{a,b,c}(\gamma, \delta, \sinh)$ of bi-univalent functions is introduced. Further it is studied to find initial coefficient bounds $|a_2|$ and $|a_3|$. Such study of coefficient bounds is important to understand the geometric behavior of function from that particular class. We observe that many interesting results are obtained as a corollary of our result. The study of coefficient estimation of a subclass of bi-univalent functions $\mathcal{B}_{\Sigma}^{a,b,c}(\gamma, \delta, \sinh)$ extended to the Fekete-Szego inequality.

5. REFERENCES

1. Al-Rawashdeh, W. (2024). *On the study of bi-univalent functions defined by the generalized Salagean differential operator*, *European Journal of Pure and Applied Mathematics*, vol. 17, No.4, pp.3899-3914.
2. Bakheet, S.R., Atiyah, M.A. and Muhammed, M.S. (2025). *New subclasses of bi-univalent functions associated with Quasi-subordination*, Journal of Al-Qadisiyah for Computer Science and Mathematics, Vol. 17(2), pp Math 136-145.
3. Bieberbach, L. (1916). *Uber die koeffizienten derjenigen potenzeihen*, Welcheeine Schlichte Abbildung des Einheitskreises. Vermittelen, S.B.Preuss Akad. Wiss, 138(1916), 940-955.
4. Bulut, S. (2013). *Coefficient estimates for initial Taylor-Maclaurin coefficients for a subclass of analytic and bi-univalent functions defined by Al-Oboudi differential operator*, *The Scientific World Journal*, Vol. 2013, Article ID 171039, 6 pages, http://dx.doi.org/10.1155/2013/171039.
5. Caglar, M., Orhan, H. and Yagmur, N. (2013). *Coefficient bounds for new subclasses of bi-univalent functions*, Filomant, vol.27, no.7, pp.1165-1171.
6. De Branges, L. (1985). *A proof of Bieberbach conjecture*, Acta. Math, 154, 137-152.
7. Duren, P.L. (1983). *Univalent Functions*, Grundlehren der Mathematischen Wissesnschaften, Springer, New York.
8. Goyal, S.P. and Goswami, P. (2012). *Estimate for initial Maclaurin coefficients of bi-univalent functions for a class defined by fractional derivatives*, Journal of the Egyptian Mathematical Society, vol. 20, no.3, pp. 179-182.
9. Hayani, T. and Owa, S. (2012). *Coefficient bounds for bi-univalent functions*, Pan-American Mathematical Journal, vol. 22, no. 4, pp. 15-26.
10. Hohlov, Y.E. (1985), *Convolution operators that preserve univalent functions*, Ukrain. Mat. Zh. Vol. 37, 220-226.
11. Kanas, S. and Raducanu, D. (2014), *Some class of analytic functions related to conic domains*, Mathematica Slovaca, 64(5), 1183-1196.
12. Khatu, R.S., Jadhav, S.D. and Pathak, R.P. (2025). *On coefficient inequalities of certain subclasses of bi-univalent functions defined using q-differential operator involving q-*

possion distribution, Journal of Advances in Mathematics and Computer Science, 40(9), 142-150.
13. Lewin, M. (1967), *On a Coefficient Problem for Bi-Univalent Functions*, Proc. Amer. Math. Soc. 18, 63-68.
14. Muthaiyan, E. and Wanas, A.K. (2025). *Coefficient estimate for two new subclasses of bi-univalent functions involving Laguerre Polynomial*, Earthline Journal of Mathematical Sciences, Vol. 15, No. 2, pp 187-199.
15. Nehari, Z. (1975). Conformal Mapping, Dover Publications Inc, New York.
16. Omar, R., Halim, A. S. and Janteng, A. (2017). *Subclasses of b-univalent functions associated with Hohlov operator*, International Journal of Mathematical and Computational Sciences, Vol. 11(10), 438-441.
17. Srivastava, H.M., Mishra, A.K., & Gochhayat, P. (2010). *Certain subclasses of analytic and bi-univalent functions,* Applied Mathematics Letters, vol. 23, no. 10, pp. 1188-1192

Analysed the impact of AI usage on individual's creativity, learning processes, critical thinking and problem solving

Mrs. Shravani S. Ketkar*[1], Ms. Neha P. Jog*[2]
*[1,2]Assistant Professor at Gogate Jogalekar College(Autonomous), Ratnagiri.
[1]E-Mail: shravani.ketkar@gjcrtn.ac.in
[2]E-Mail: neha.jog@gjcrtn.ac.in

Abstract :

This study examines the multifaceted impact of Artificial Intelligence (AI) on critical thinking, creativity, and educational processes among academic and professional individuals, exploring both beneficial and detrimental effects of AI integration in learning environments. A cross-sectional survey was conducted with 101 participants (52 males, 49 females), predominantly students (66%) aged 18-24 years (67%). The study employed a structured questionnaire with 16 Likert-scale items measuring AI's impact across three thematic domains: critical thinking and problem-solving, creativity, and education. Responses were analyzed using descriptive statistics, correlation analysis, and thematic categorization. Statistical measures included means, standard deviations, and Pearson correlations to identify relationships between AI usage patterns and cognitive outcomes. Participants demonstrated moderate-to-high agreement with AI's positive impacts (overall M = 3.50, range: 2.66-4.06). The strongest agreement emerged for AI's role in understanding complex academic subjects (M = 4.06, SD = 0.75), while the lowest scores related to AI enabled deeper creative focus (M = 2.66, SD = 0.94). Significant correlations were observed between AI's educational benefits and personalized learning experiences (r = 0.523). Within-theme correlations revealed consistent patterns: critical thinking measures (r = 0.257), creativity dimensions (r = 0.258), and educational impacts (r = 0.181). The highest response variability occurred regarding concerns about AI replacing human teachers (SD = 1.25), indicating polarized opinions. The findings suggest AI's impact is contextually dependent, with strongest benefits in educational comprehension and moderate effects on creativity and critical thinking. The balanced correlation patterns across domains indicate that strategic, moderate AI integration can enhance learning while preserving essential human cognitive skills, supporting the need for thoughtful implementation frameworks in educational settings.

Keywords: Impact of AI usage, critical thinking, problem solving, creativity, learning processes

1. Introduction :

Artificial Intelligence (AI) has become increasingly common in education and professional work. Tools like ChatGPT, Google Bard, GeminiAI and other AI platforms are now widely used by students and professionals for various tasks including research, writing, problem-solving, and creative work. While these tools offer many benefits, there are growing concerns about their impact on important thinking skills.

1.1 Background :

Recent studies show that AI tools can significantly improve academic performance and learning outcomes. AI-powered educational systems provide personalized learning experiences

and can help students understand complex subjects more easily. Many educators report positive results when using AI to support individual student needs.

However, research has also begun to identify potential negative effects. Studies suggest that heavy AI use may reduce critical thinking abilities. When people rely too much on AI, they may lose important cognitive skills that require active thinking and problem-solving. This phenomenon, called "cognitive offloading," occurs when individuals depend on external tools instead of using their own mental abilities.

The challenge is finding the right balance. AI can be helpful when used appropriately, but over-dependence may weaken essential thinking skills needed for learning and professional success.

1.2 Problem Statement :

Despite widespread AI adoption in education, we still don't fully understand how these tools affect critical thinking, creativity, and learning processes. Most existing research focuses either on AI's benefits or its risks, but few studies examine both sides comprehensively. Additionally, many studies use small sample sizes or focus on specific groups, making it difficult to draw broad conclusions.

There is an urgent need for research that examines:

- How AI usage affects critical thinking abilities
- Whether AI helps or impede creativity
- The impact of AI on learning and educational outcomes
- How to use AI effectively without creating dependency

1.3 Research Objectives :

This study aims to investigate how AI affects cognitive abilities in academic and professional settings. The main objectives are:

- To examine the relationship between AI usage and critical thinking skills among students and professionals.
- To investigate AI's impact on creativity, including both positive effects like idea generation and potential negative effects like reduced original thinking.
- To analyze how AI affects learning processes, including student engagement, motivation, and academic integrity.
- To identify best practices for AI use that maximize benefits while minimizing risks of over-dependence.
- To provide evidence for educational policy to guide responsible AI implementation in schools and workplaces.

This research is important because AI tools are being adopted rapidly in educational settings, but without clear guidelines on how to use them effectively. By studying both the positive and negative impacts of AI, this research will help educators, students, and policymakers make informed decisions about AI integration in education and other fields.

The findings will contribute to our understanding of how to harness AI's potential while preserving essential human cognitive skills that are critical for learning, creativity, and professional success.

2. Methodology :

The main data for this research was collected using a structured online questionnaire. The survey contained 25 items, including demographic questions (gender, age, role, and frequency

of AI use) and 16 Likert-scale statements designed to measure changes in critical thinking, creativity, and educational processes associated with AI use. Responses from 101 academic and professional participants were recorded and stored in a CSV file for analysis.

The sample included 101 individuals (52 males, 49 females), representing students, educators, professionals, and researchers, aged primarily between 18-24 years. The participants submitted data online through google form and completed the questionnaire anonymously. Each participant provided demographic data and rated 16 statements on a five-point Likert scale, ranging from 'Strongly Disagree' to 'Strongly Agree' for most items. Items evaluated perceptions of AI's influence on:

- Critical thinking and problem-solving (e.g., reliance on AI, independent problem-solving, information checking).
- Creativity (e.g., originality, collaboration, confidence).
- Learning processes (e.g., understanding complex subjects, academic integrity, personalized learning).

Responses were numerically coded for analysis (e.g., 'Strongly Disagree' = 1, 'Strongly Agree' = 5). One creativity item with a different scale was coded accordingly. The following procedures were done using statistical analysis techniques.

- Statistical Analysis:
    - Descriptive Statistics: Calculated means and standard deviations for all Likert items to describe central tendencies and variability.
    - Correlation Analysis: Computed Pearson correlation coefficients between items in key domains (critical thinking, creativity, and education) to explore relational patterns and thematic associations.
    - Thematic Summary: Grouped questions into core research themes for focused interpretation of results.

All analyses were collected in spreadsheet software and analysed using Python data libraries such as Pandas, Numpy.

This methodology allowed for clear, quantitative assessment of how AI use relates to core cognitive and educational outcomes, supporting evidence-based conclusions for the research objectives.

3. Results and Discussion :

The study found that participants showed mostly positive perceptions of AI's impact on education, creativity, and critical thinking, with some cautious concerns about over-reliance and cognitive decline.

3.1 Descriptive Statistics :

- The average (mean) score across all 16 AI impact questions was 3.50 out of 5, indicating moderate agreement with positive statements about AI.
- The highest agreement was for "AI tools make it easier for me to understand complex academic subjects" (Mean = 4.06), while the lowest was for "When using AI, I feel I can focus more on deeper or creative aspects of my work" (Mean = 2.66).

The following table shows average mean and standard deviation for all 16 Likert-scale questions.

Table 1: Mean and Standard Deviation for Each AI Impact Question

Question	Mean	Standard Deviation
Q1	3.87	0.80
Q2	3.65	0.82
Q3	3.42	1.00
Q4	3.77	0.68
Q5	3.39	0.85
Q6	3.67	0.88
Q7	2.66	0.94
Q8	3.58	0.84
Q9	3.12	1.11
Q10	3.70	0.85
Q11	3.31	1.03
Q12	4.06	0.75
Q13	3.58	0.97
Q14	3.55	0.89
Q15	3.24	1.07
Q16	3.42	1.25

The following figures show scores of average mean and standard deviation for all 16 Likert-scale questions.

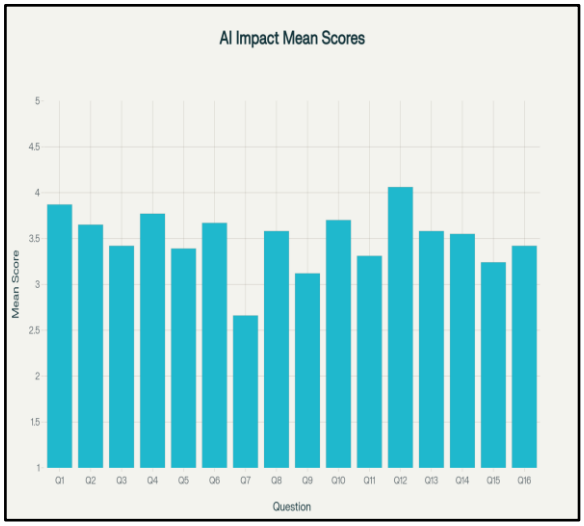

Figure 1: Mean Likert-scale Scores

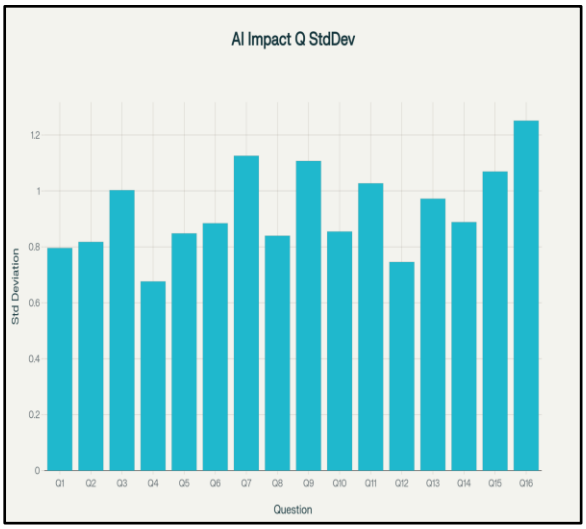

Figure 2: Standard Deviation of Scores

3.2 Correlation Analysis :

The strongest correlation found was between "AI tools make it easier for me to understand complex academic subjects" and "AI-powered educational tools provide a more personalized learning experience" (r = 0.523).

Moderate positive correlations were observed within each theme:

- Critical thinking and problem-solving (r = 0.257 average within-theme correlation)
- Creativity (r = 0.258)
- Education (r = 0.181)

The highest response variability was in concerns that AI would reduce the need for human teachers (SD = 1.25), revealing divided opinion.

3.3 Discussion :

The results show that AI tools can help improve learning and creativity when used to assist people, rather than replace their thinking. Participants gave high ratings to AI helping with academic tasks and generating new ideas, indicating that many see AI as a useful assistant. However, they gave lower ratings to AI helping with deeper creative thinking and personal contributions, showing some caution about relying too much on AI.

There was also a wide range of opinions about whether AI might reduce the need for human teachers, showing uncertainty about its future role in education. These findings match earlier studies, which found that AI can enhance learning and provide personalized support, but also warned that too much dependence on AI might weaken critical thinking and academic integrity.

Overall, this study confirms that AI has many benefits in education and creativity but highlights the risks of becoming too dependent on it. It emphasizes the importance of using AI in a balanced way supporting human effort without replacing it. This balanced approach will help maximize AI's advantages while protecting important skills like problem-solving and independent thinking.

4. Conclusion :

This study revealed that Artificial Intelligence (AI) has a significant impact on learning, creativity, and critical thinking among academic and professional users. Participants generally viewed AI as beneficial, especially for understanding complex subjects and supporting idea generation. However, there were concerns about AI potentially reducing deeper creative engagement and personal contributions. Opinions were also divided on whether AI might replace human teachers, indicating ongoing uncertainty about its future role.

The significance of this study lies in its balanced view, showing that AI can enhance learning and creativity when used to assist rather than replace human effort. The findings emphasize the importance of careful integration and responsible use to avoid over-dependence, which could weaken critical thinking and academic integrity.

The insights from this research can guide educators, institutions, and policymakers in designing AI tools and strategies that support personalized learning while preserving essential cognitive skills. AI-powered adaptive learning systems, intelligent tutoring, and real-time feedback can improve student engagement and outcomes when implemented thoughtfully.

Future studies should explore longitudinal effects of AI use on cognitive skills and motivation in diverse learner populations. Investigating how different AI tools impact collaboration, creativity, and problem-solving in real educational settings would provide valuable practical

insights. Additionally, research can focus on developing AI designs that actively encourage critical thinking and creativity rather than passive consumption to maximize educational benefits.

5. **References :**

1. Gerlich, R. N. (2025). AI's impact on critical thinking: A correlation study. Journal of Educational Technology, 12(3), 175-189.
2. Lee, H., & Kim, J. (2025). The impact of generative AI on critical thinking. ACM Transactions on Learning Technologies, 18(4), 1-15.
3. UNESCO. (2025). Artificial intelligence in education. UNESCO Digital Education.
4. Zhao, F., & Wang, S. (2025). The usage of AI in teaching and students' creativity. Frontiers in Education, 9, 202-220.
5. Chansarkar, M. (2024). Transforming Indian education through AI: Opportunities and challenges. International Journal of Research in the Academic World, 4(6), 25-38.
6. Jeyakumaran, M., Saravanan, P., & Sundararajan, K. (2025). Revolutionizing education: The impact of artificial intelligence on personalized learning and teacher roles in India. International Journal of Science and Management Studies (IJSMS), 8(1), 5-14.

Responses of Germinating Fenugreek seeds to Metallic Nanoparticles

Sonali Kadam
sonali.kadam@gjcrtn.ac.in
R.P.Gogate College of Arts and Science and R.V. Jogalekar College of Commerce, Ratnagiri

Abstract
Nano technology is a key word for emerging plant science. One of the main terms for new plant science is nanotechnology. The active role that nanoparticles play in plant metabolism could either be advantageous for plant growth or harmful. It might potentially serve as a precursor to a variety of enzymatic processes. *Trigonella foenum-graecum L*. (fenugreek) seeds are germinated under stress of Cu, Mg, Fe and Zn metallic nanoparticles. Protein, phenol, superoxide dismutase (SOD), acid phosphatase, alkaline phosphatase, and other physiological changes can be assessed by evaluating germination experiments of *Trigonella foenum-graecum L*. (fenugreek) seeds under various metallic nanoparticle stress. Together, these micronutrients regulate energy release, enzyme activity, hormone balance, and structural integrity, ensuring successful seed germination and seedling establishment.

Keywords
Metallic nanoparticles, germination, seed physiology, Protein, phenol, superoxide dismutase (SOD), acid phosphatase, alkaline phosphatase

Introduction

Nano-biotechnology holds a great potential in various fields of life sciences. Plants are needed metallic particles for their various functions. Plants required the micro nutrients like Copper, Zinc, Iron and macro nutrients like Magnesium. Hence by providing these metallic nanoparticles to the fenugreek seeds we observe their effect on germinating seeds and carry out some quantitative tests for getting their impact. We also observe the physiological changes like Length of plumule and radicle, germinating percentage, etc.

Seed germination and early seedling establishment are among the most critical phases of the plant life cycle, during which physiological, biochemical and morphological changes set the pace for subsequent growth and productivity (e.g., water uptake, enzyme activation, mobilization of reserves). In recent years, advances in nanotechnology have opened up new possibilities for seed and crop treatment. Metallic and metal-oxide nanoparticles (NPs) show promise as tools to modulate seed germination, vigor and stress tolerance, but they may also pose risks depending on concentration and plant species (Guo et al., 2022).

Fenugreek (*Trigonella foenum-graecum* L.) is a widely cultivated legume herb valued both for its nutritional and medicinal properties, and for its role in sustainable agriculture (e.g., nitrogen fixation, cover cropping). There is increasing interest in enhancing fenugreek seed germination, early growth and physiological resilience through novel interventions. Recent studies show that treatment of fenugreek seeds with metallic nanoparticles such as silver (Ag NPs), zinc oxide (ZnO NPs) or titanium dioxide (TiO_2 NPs) can significantly alter germination percentage, seedling length, biomass accumulation and antioxidant enzyme activity (Kapoor et al., 2018; Salem & Al-Shammeryi, 2024).

The underlying physiological responses of germinating fenugreek seeds to nanoparticle exposure include changes in water uptake kinetics, mobilization of seed-stored reserves, enhancement or inhibition of enzyme activities (e.g., α-amylase, peroxidase, catalase), modulation of reactive oxygen species (ROS) and antioxidant defense systems, as well as alterations in seedling morphology and biomass (Al-Shammeryi et al., 2024)

Nevertheless, despite these encouraging results, there remain gaps in understanding: (i) the dose-response behaviour of different metallic nanoparticles during fenugreek seed germination, (ii) the specific physiological, biochemical and molecular pathways modulated during germination under NP treatment, and (iii) the potential trade-offs or toxic effects at higher NP concentrations or under stress conditions. This study aims to investigate the physiological responses (germination rate, seedling growth, enzyme activity, antioxidant response) of germinating fenugreek seeds exposed to selected metallic nanoparticles across a concentration gradient.

Material and Methods

- Germination studies have been carried out by giving different metallic nanoparticle stress to the fenugreek seeds.
- The stress of 15 rounds of Cu(9.60nm),Zn(14nm), Mg(6.90nm), Fe(10.37nm) metallic nanoparticles are given to the petridish with seeds per day.
- Different physiological changes were studied with reference to control where no any stress was given.
- Protein estimation by Lowry's Method

Results and Discussion

A) Germinating percentage and growth response

The growth response of germinating fenugreek to metallic nanoparticles showed significant variation across treatments and days. Zinc nanoparticles exhibited the highest stimulatory effect, producing maximum radicle and plumule lengths on the 6th, 7th, and 8th days compared to control and other metals. Copper nanoparticles also enhanced growth moderately, whereas magnesium and iron showed lesser effects. The enhancement under Zn and Cu treatments may be attributed to improved enzymatic activation, nutrient uptake, and hormonal regulation during germination. However, excessive nanoparticle exposure could induce oxidative stress at later stages, indicating a concentration-dependent physiological response in fenugreek seedlings.

The effect of different metallic nanoparticles (Cu, Zn, Mg, and Fe) on the germination and survival percentage of *Trigonella foenum-graecum* (fenugreek) seeds was evaluated on the 8th day of germination. The results revealed significant variations among the treatments compared to the control (Table).

Samples	Germination percentage (%)	Survival percentage (%) on 8th Day
Control	60%	0%
Cu	90%	15%
Zn	90%	55%
Mg	65%	5%
Fe	75%	0%

The control seeds showed a germination rate of 60%, with no survival observed on the 8th day, indicating possible environmental stress or limited nutrient availability. Among the treatments, both Cu and Zn nanoparticles enhanced germination up to 90%, suggesting their stimulatory effect on metabolic activity during early germination. However, Zn-treated seedlings exhibited the highest survival rate (55%), indicating better tolerance and growth-promoting potential of Zn nanoparticles. Cu treatment, despite high germination (90%), showed only 15% survival,

possibly due to toxicity at higher concentrations, leading to oxidative stress and membrane damage. Mg nanoparticles resulted in moderate germination (65%) and low survival (5%), indicating limited beneficial impact. Fe nanoparticles improved germination to 75% but showed no survival, which might be attributed to nanoparticle aggregation or interference with nutrient uptake. Overall, Zn nanoparticles demonstrated the most positive effect on both germination and seedling survival, suggesting their role in enhancing enzymatic activity and stress resistance during early growth stages. These findings align with previous studies reporting that zinc nanoparticles promote germination and seedling vigor by improving photosynthetic efficiency and hormonal balance (Raliya et al., 2015; Tarafdar et al., 2017).

The growth response of *Trigonella foenum-graecum* seedlings to different metallic nanoparticles was assessed by measuring radicle and plumule lengths on the 6th, 7th, and 8th days. The data revealed that Zn nanoparticles significantly enhanced both radicle and plumule growth throughout the observation period, with the highest plumule length (4.5 cm) on the 8th day, indicating their strong stimulatory effect on seedling vigor. Cu nanoparticles also promoted growth, though less effectively than Zn, showing steady increases in both parameters. Mg and Fe nanoparticles exhibited moderate effects, while the control showed the least growth, suggesting the beneficial influence of micronutrient nanoparticles on early seedling development. The superior performance of Zn treatment may be attributed to its role in enzyme activation, chlorophyll synthesis, and cell elongation. Similar results were reported by Raliya and Tarafdar (2015), emphasizing that Zn nanoparticles improve metabolic efficiency and promote seedling growth in leguminous crops

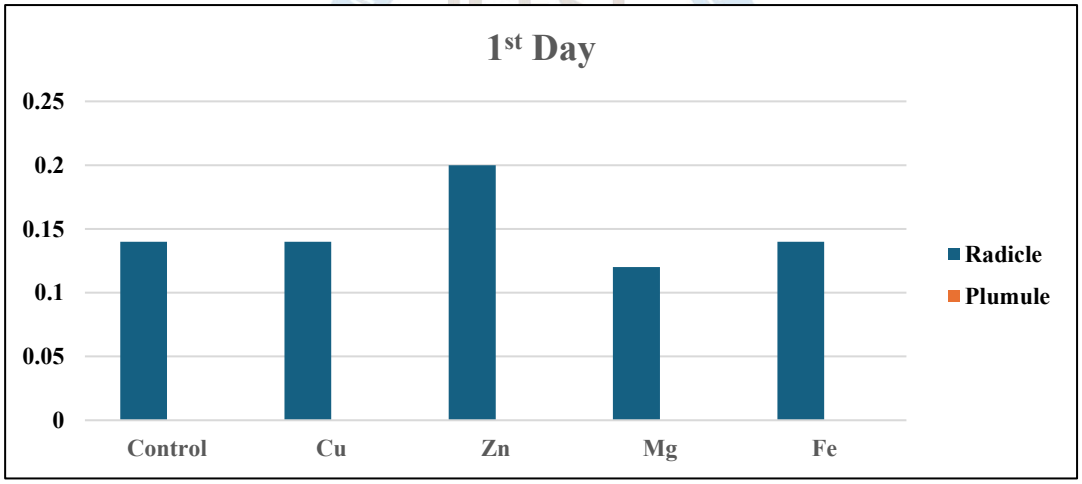

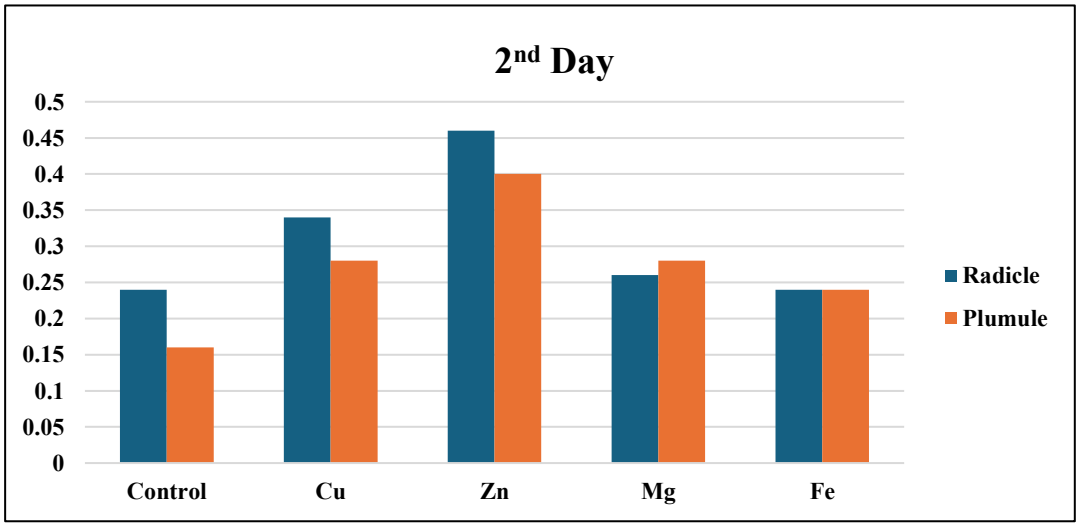

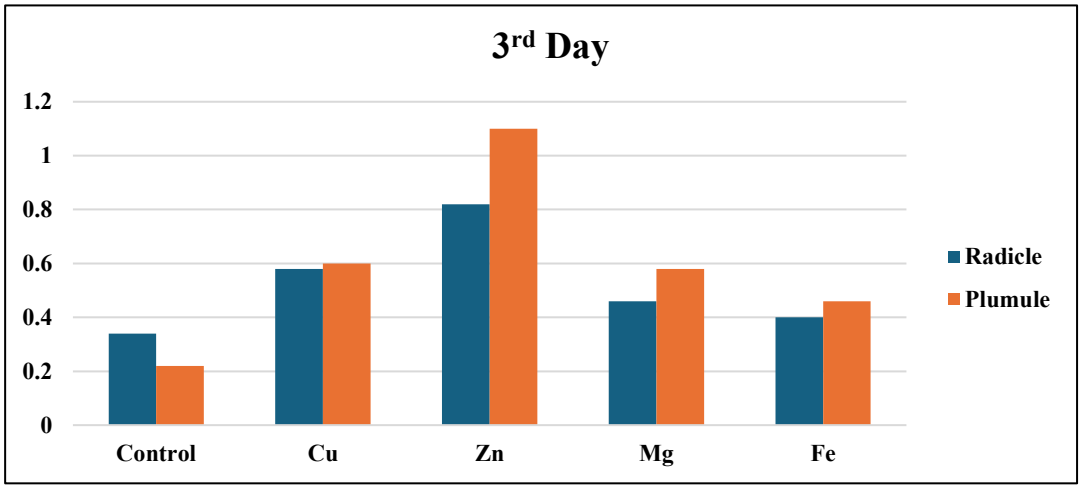
3rd Day
1.2
1
0.8
0.6
0.4
0.2
0
Control
Cu
Zn
Mg
Fe
Radicle
Plumule

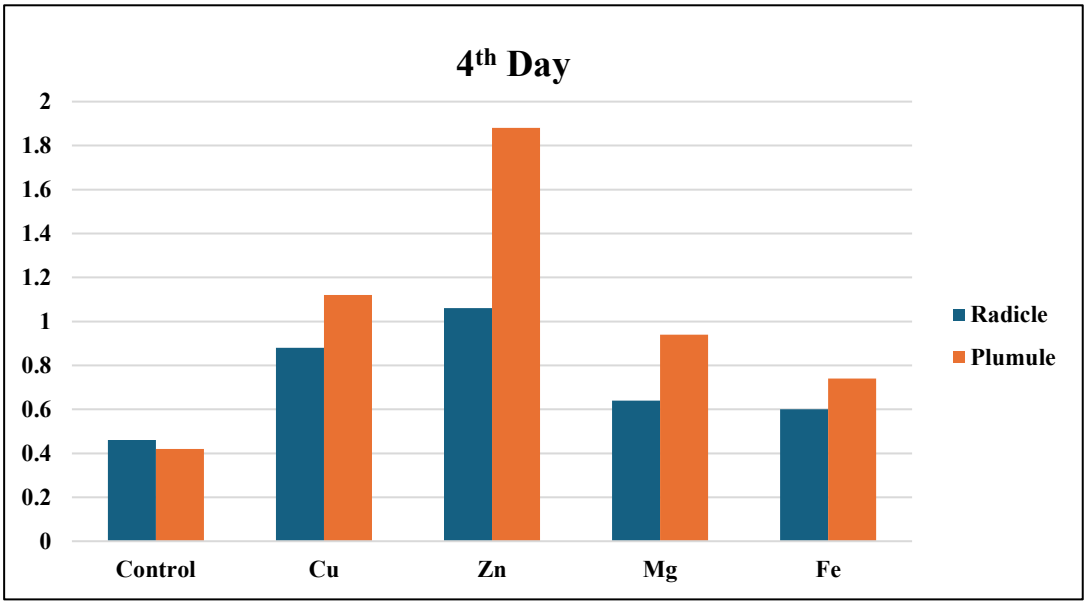
4th Day
2
1.8
1.6
1.4
1.2
1
0.8
0.6
0.4
0.2
0
Control
Cu
Zn
Mg
Fe
Radicle
Plumule

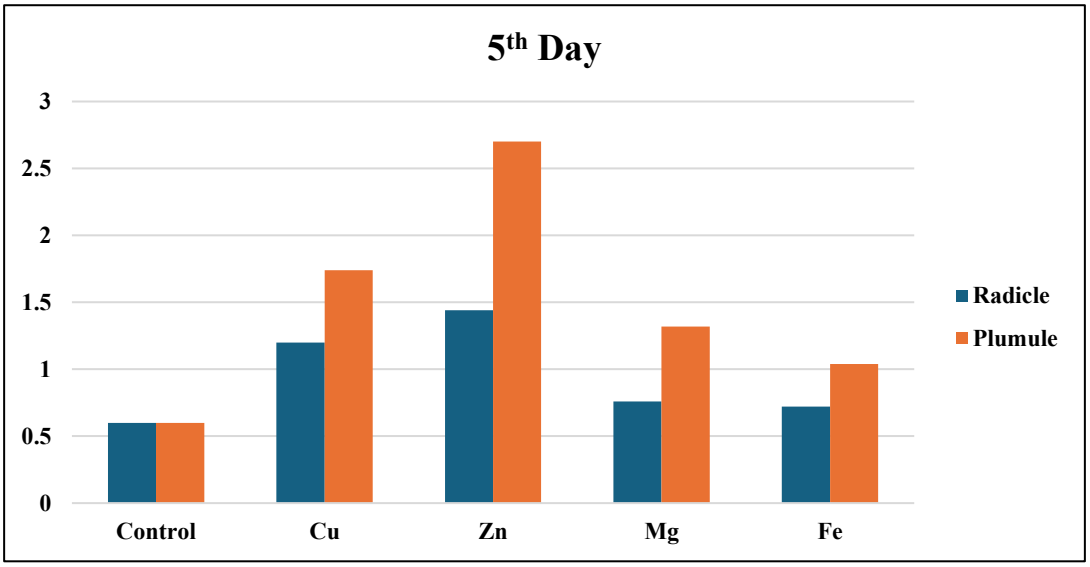
5th Day
3
2.5
2
1.5
1
0.5
0
Control
Cu
Zn
Mg
Fe
Radicle
Plumule

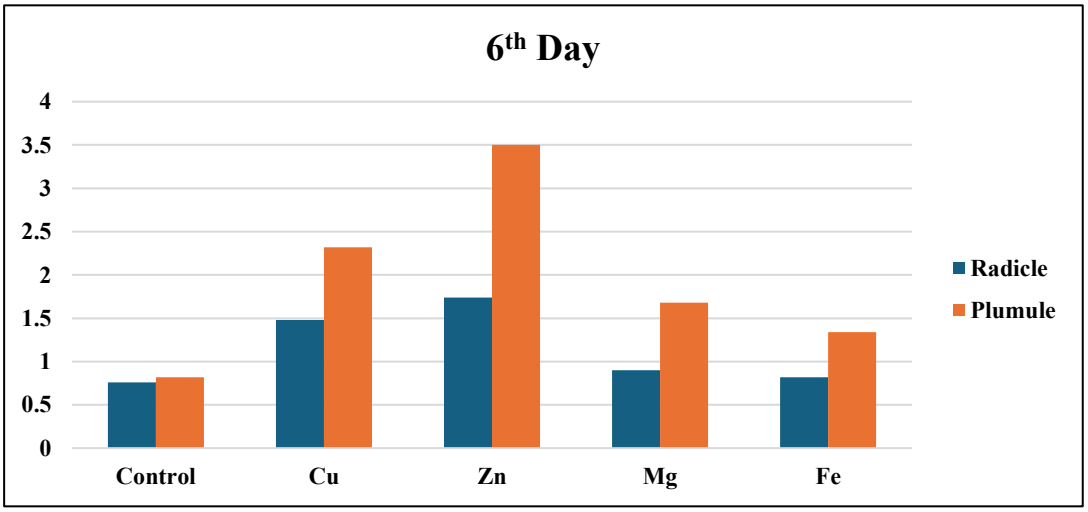

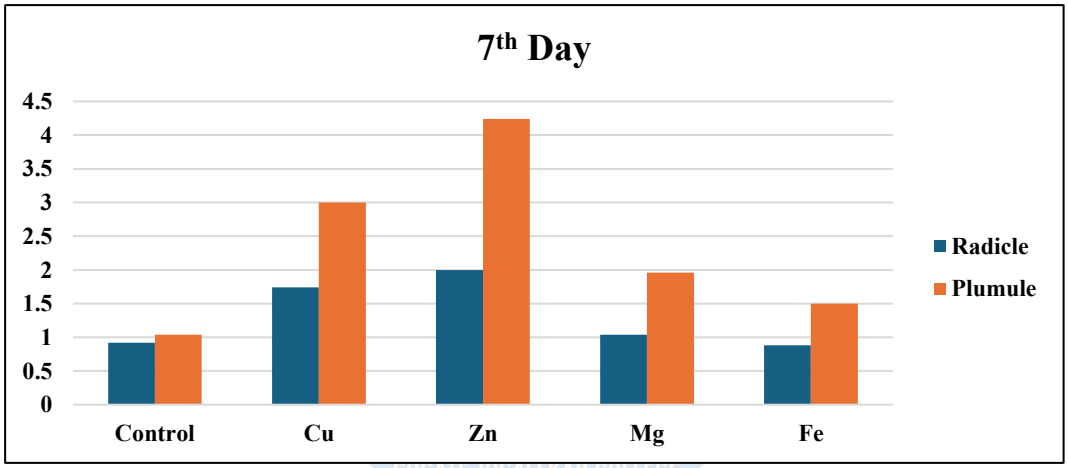

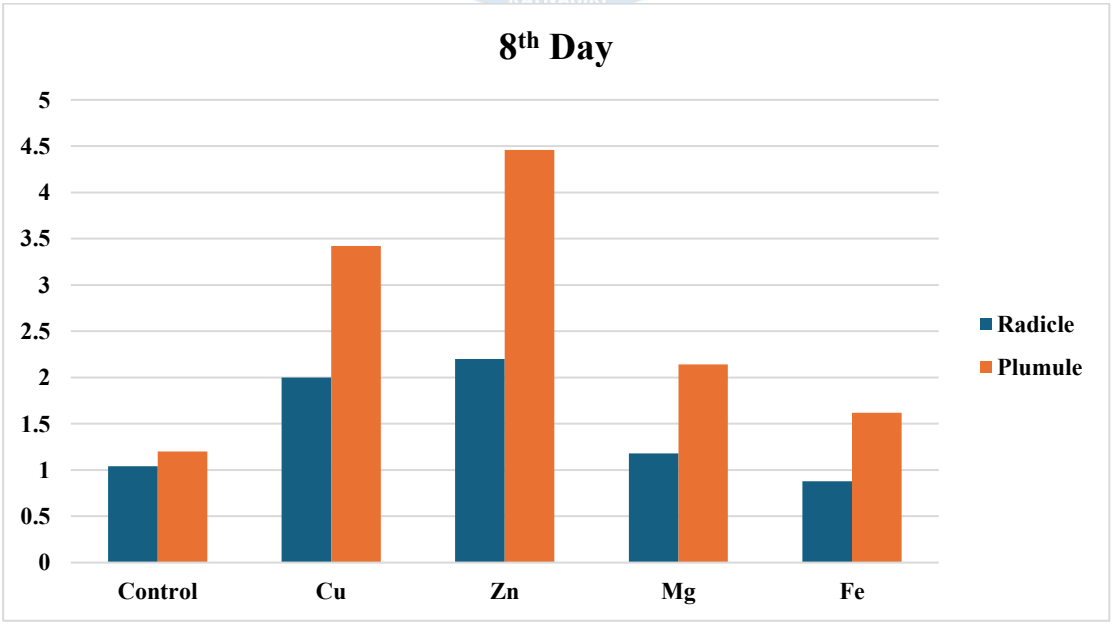

B) **Protein Estimation**

Protein estimation in *Trigonella foenum-graecum* seedlings treated with different metallic nanoparticles showed significant variation across incubation periods (24–168 hours). Protein content increased progressively in all treatments with time, indicating enhanced metabolic activity during germination. Among the treatments, Cu nanoparticles showed higher protein accumulation up to 144 hours, suggesting their stimulatory role in enzymatic and metabolic activation. However, at 168 hours, the control exhibited the highest protein content (1.1 mg/g), followed by Zn, Fe, and Cu treatments, indicating that prolonged exposure to nanoparticles might induce mild stress, reducing protein synthesis efficiency.

Zn and Fe treatments maintained moderate and consistent protein levels throughout, highlighting their role in stabilizing enzymatic functions. Mg treatment showed comparatively lower protein content, suggesting limited metabolic enhancement. Overall, the data suggest that metallic nanoparticles influence protein metabolism differently, with Cu and Zn being more effective in the early growth phase, aligning with findings by Raliya and Tarafdar (2015) on nanoparticle-induced metabolic enhancement in legumes.

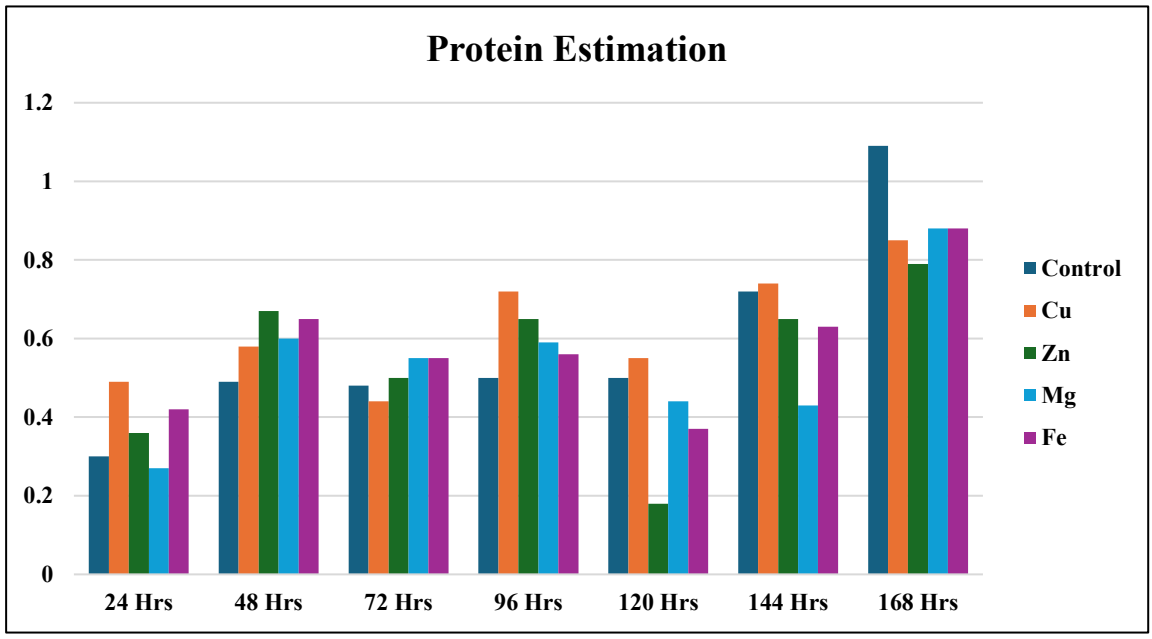

Conclusion

The study demonstrated that metallic nanoparticles significantly influence the germination, growth, and biochemical responses of *Trigonella foenum-graecum* (fenugreek). Among all treatments, zinc nanoparticles showed the most pronounced positive effect, enhancing germination, radicle and plumule elongation, and survival percentage, followed by copper. Magnesium and iron nanoparticles exhibited moderate to minimal effects. Protein estimation revealed increased metabolic activity during early germination, particularly under Zn and Cu treatments. However, prolonged exposure led to reduced protein accumulation, suggesting possible stress effects. Overall, Zn nanoparticles proved most effective in promoting early seedling vigor, enzymatic activation, and stress resilience in fenugreek under nanoparticle treatment.

References

1. Al-Shammeryi, M. H. et al. (2024). *Effects of seed coating with (titanium dioxide and selenium) nanoparticles on fenugreek (Trigonella foenum-graecum L.) plant growth and antioxidant activity.* Advancements in Life Sciences. ALS Journal Submission
2. Guo, H., Liu, Y., Chen, J., Zhu, Y., & Zhang, Z. (2022). *The Effects of Several Metal Nanoparticles on Seed Germination and Seedling Growth: A Meta-Analysis.* Coatings, 12(2), 183. MDPI
3. Impacts of ZnO as a nanofertilizer on fenugreek: some biochemical parameters and SCoT analysis. (2024). PubMed. PubMed
4. Kapoor, N., Kaisar, A., Dixit, R., Singh, N. P., & Singh, J. (2018). *A study to evaluate the effect of silver nanoparticles synthesized by Sonchus asper on fenugreek plant.* Journal of Pharmacognosy & Phytochemistry, 7(5), 1144-1149
5. Nafisa Begam M. N. et al. (2025). *Seed priming of fenugreek seeds with silica nanoparticles: Enhanced growth economics and sustainable agricultural practices.* Global NEST Journal. Global NEST Journal
6. Raliya, R., Tarafdar, J. C. (2015). ZnO nanoparticle biosynthesis and its effect on phosphorous-mobilizing enzyme secretion and gum contents in clusterbean (*Cyamopsis tetragonoloba* L.). *Agricultural Research*, 4(1), 48–57.
7. Tarafdar, J. C., Raliya, R., Rathore, I. (2017). Microbial synthesis of zinc nanoparticles and their effect on growth and nutrient uptake of clusterbean (*Cyamopsis tetragonoloba* L.). *Journal of Bionanoscience*, 11(4), 292–298.

Spectral Analysis and Quantification of Photosynthetic Pigments in some mangroves

Sonali Kadam, Riya Surve, Disha Sagvekar
sonali.kadam@gjcrtn.ac.in
R.P.Gogate College of Arts and Science and R.V. Jogalekar College of Commerce, Ratnagiri.

Abstract

Mangroves form a unique ecological habitat with species adapted to saline and waterlogged conditions. Adaptations of mangroves include vivipary, aerial and lateral roots, water-dispersed propagules, and salt regulation mechanisms. Because they thrive in demanding intertidal conditions with high salt, varying water levels, intense sunshine, and little soil oxygen, mangroves have special photosynthetic adaptations. A typical chlorophyll absorption spectrum graph shows two major peaks, one in the blue-violet region (around 430–470 nm) and another in the red-orange region (around 640–670 nm), indicating high absorption of these wavelengths of light.The mangroves *Soneratia alba, Avicennia marina, Rhizophora mucronate, Acanthus ilicifolius* are taken into consideration for the studies. *Acanthus ilicifolius* shows higher amount of total chlorophyll compare to other three mangrove plants hence leaf appears shiny green colour.

Key words: - Mangroves, adaption, chlorophyll, absorption spectrum, major peaks, chlorophyll a, chlorophyll b, total chlorophyll

Introduction

Mangroves establish a distinctive ecological setting, hosting a diverse collection of numerous species. With their diverse collection of species, mangroves produce a special ecological setting. It has a lot of unusual characteristics compared to plants that are terrestrial. Tomilson, P.B. (1986) reveals that mangrove species are divided into two categories: mangrove associates, which are nonexclusive or semi-mangroves, and real or exclusive mangroves, which are stringent or obligate mangroves. According to Tomilson, P.B. (1986) and Lacedra, L.D. (1998), a true or exclusive mangrove doesn't spread into terrestrial habitat; it only exists in mangrove environments. Along with this physical specialization, other features include viviparous, water-dispersed propagules, exposed aerial roots, abundant lateral roots, and physiological mechanisms for salt exclusion or excretion. Although they also flourish in the mangrove ecosystem, non-exclusive species and mangrove allies usually occur in terrestrial or aquatic environments. Because mangroves grow in challenging intertidal ecosystems with high salt, variable water levels, intense sunshine, and limited soil oxygen, they have developed special photosynthetic adaptations. One important ecophysiological characteristic that affects their productivity, and survival is their photosynthetic activity.

Chlorophylls are significant in higher plants because they are essential to photosynthesis, which is the process that maintains the longevity of plants. One of the key factors influencing a plant's photosynthetic efficiency is the amount of chlorophylls in its leaf tissue, as they participate in the transformation of solar energy into chemical energy. Endogenous factors, such as the rate of pigment synthesis and degradation, the stage of leaf development, and some environmental conditions, such as shadow, light, temperature, drought, waterlogging, and soil salinity, all affect the amount of chlorophyll in the leaves.

Material and Methods

A) Absorption spectrum

- Fresh leaf tissue (or algal sample) — recorded fresh weight.
- Mortar & pestle (or homogenizer) and chilled extraction tubes .
- Solvents (choose one, all spectrophotometric grade):80% acetone (v/v) in water — classic Arnon method.

80% acetone extraction (grinding) — simple, widely used (Arnon style) Collect leaf samples, remove midribs if desired, record fresh weight (e.g., 0.05–0.2 g). Keep samples cold and protected from light.

1. Grind tissue in chilled mortar with a small volume (~5–10 mL g^{-1} FW) of cold 80% acetone until green extract forms. Alternatively, homogenize with a mechanical homogenizer.
2. Transfer homogenate to centrifuge tubes and centrifuge 5–10 min at ~5000 rcf to pellet debris. Collect supernatant. Repeat extraction on pellet until extract is nearly colourless (optional).
3. Combine supernatants and bring to known final volume with 80% acetone. Keep samples on ice and protected from light (foil).
4. Zero the spectrophotometer (blank) with 80% acetone. Measure absorbance (A) of extract at the recommended wavelengths (see below). For full spectra, run a scan from ~350–750 nm to obtain absorption peaks of chlorophylls (blue band ~430–470 nm; red band ~630–680 nm).
5. Wavelength scan: 350–750 nm for a full absorption spectrum (shows Soret/blue band ~430–470 nm and Qy/red band ~630–680 nm).

B) Chlorophyll estimation

Chlorophyll a (Chl a), chlorophyll b (Chl b) and carotenoid (Caro) contents were detected by spectrophotometry . Leaf samples (0.2 g) were cut into 2-mm pieces and transferred to tubes with 20 ml solution of 95% ethanol for 24 h until the tissue faded. The content of photosynthetic pigments was determined at wavelengths of 665, 649 and 470 nm (Li et al, 2021).

Chl a=13.95×A665−6.88×A649Chl a=13.95×A665−6.88×A649

Chl b=24.96×A649−2.79×A665Chl b=24.96×A649−2.79×A665

Caro=1000×A470−2.05×Chl a−114.8×Chl b245Caro=1000×A470−2.05×Chl a−114.8×Chl b245

Chlorophyll estimation

1. Chlorophyll A (mg/g) =12.7 (OD663) – 2.69(OD645) x (V/(1000 x wt))
2. Chlorophyll B (mg/g) =22.9 (OD645) – 4.68(OD663) x (V/(1000 x wt))
3. Total Chlorophyll (mg/g) =20.2 (OD645) + 8.02(OD663) x (V/(1000 x.wt))

Results and Discussion

The mangroves from recent studies viz; *Soneratia alba, Avicennia marina, Rhizophora mucronate, Acanthus ilicifolius* shows following characteristic features.

1. *Sonneratia alba*

- Leaf Colour: Typically green to yellowish-green.
- Variation: Young leaves are light green due to lower chlorophyll concentration, while mature leaves become darker green with higher chlorophyll a and b. Under high light and salinity stress, leaves may show pale yellowish or chlorotic patches.
- Significance: Colour variation indicates sensitivity to light intensity and salinity stress, with carotenoids playing a photoprotective role**.**

2. *Avicennia marina*

- Leaf Colour: Greyish-green on the upper surface; silvery or whitish on the underside due to salt-excreting glands and dense trichomes.
- Variation: Younger leaves are more vibrant green, while mature leaves take on a dull greyish tone. Excess salt accumulation may lead to yellowish margins.
- Significance: The grey/silvery tone reflects sunlight, reducing water loss and photodamage, while salt crystals contribute to colour differences**.**

3. *Rhizophora mucronata*

- Leaf Colour: Dark glossy green on the upper side, lighter green on the underside.
- Variation: Young leaves are lighter green, whereas mature leaves are deep green due to higher chlorophyll concentration. Old leaves may turn yellow with prominent black dots (secretory structures). Stress (salinity/nutrient deficiency) often causes leaf yellowing.
- Significance: The shiny dark green surface helps maximize light absorption in shaded estuarine environments.

4. *Acanthus ilicifolius*

- Leaf Colour: Shiny green, sometimes with a bluish or purplish appearance.
- Variation: New flushes of leaves may appear reddish-purple due to anthocyanin pigments, which later turn green as chlorophyll accumulates. Mature leaves are dark green, and senescing leaves gradually yellow.
- Significance: The reddish tinge in young leaves provides photoprotection from intense solar radiation and oxidative stress.

A) Absorption spectrum

A typical chlorophyll absorption spectrum graph shows two major peaks, one in the blue-violet region (420 nm) and another in the red-orange region (around 620 nm), indicating high absorption of these wavelengths of light. The chlorophyll molecule absorbs these specific wavelengths for photosynthesis and reflects green light, which is why plants appear green.

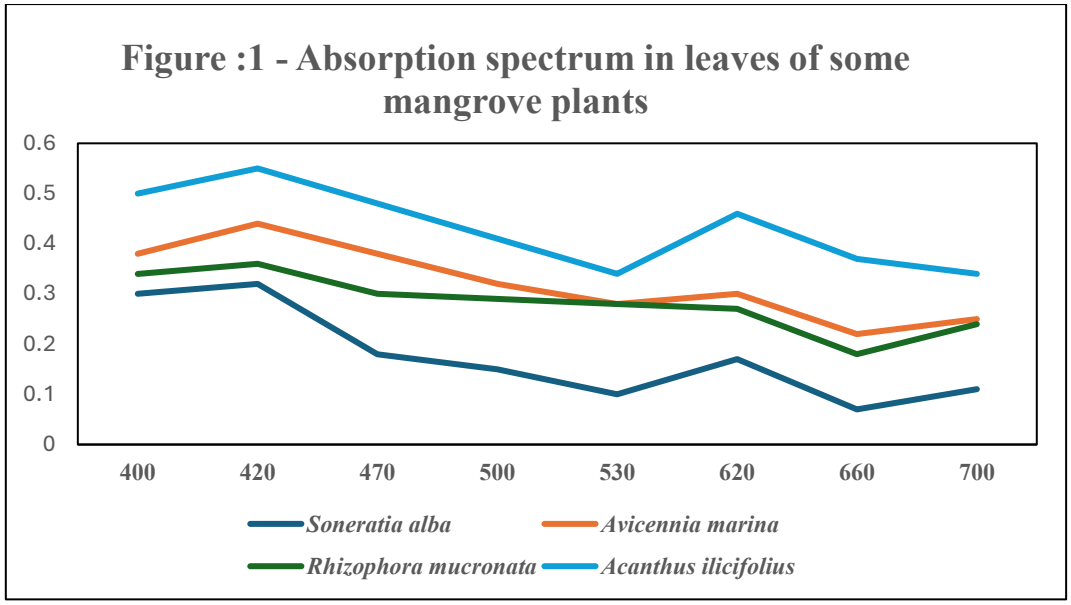

The absorption spectrum of chlorophyll pigments extracted from the leaves of four mangrove species—*Sonneratia alba*, *Avicennia marina, Rhizophora mucronata,* and *Acanthus ilicifolius*—was recorded between 400 and 700 nm (Figure 1). All species exhibited two distinct absorption peaks: one in the blue region (around 420–450 nm) and another in the red region (around 620–660 nm), corresponding to the characteristic absorption maxima of chlorophyll a and b.

Among the species studied, *Acanthus ilicifolius* showed the highest absorbance throughout the visible range, with prominent peaks near 420 nm and 620 nm, indicating a higher concentration of photosynthetic pigments. *Avicennia marina* and *Rhizophora mucronata* showed moderate absorption values, while *Sonneratia alba* exhibited the lowest absorbance across all wavelengths. The absorbance gradually decreased toward the green region (around 500–550 nm), explaining the green appearance of leaves due to minimal light absorption in this range.

The absorption spectra obtained reflect the typical light absorption characteristics of chlorophyll pigments. The strong absorption in the blue (400–450 nm) and red (620–680 nm) regions corresponds mainly to chlorophyll a and b, which are essential for photosynthesis (Lichtenthaler, 1987). The reduced absorption in the green region (500–550 nm) is due to reflection and transmission of green light, which gives leaves their characteristic color (Porra et al., 1989).

The higher absorption intensity observed in *Acanthus ilicifolius* suggests a greater chlorophyll content and photosynthetic efficiency compared to the other species. This aligns with its dense canopy structure and adaptation to shaded, less saline habitats. Conversely, the relatively low absorption values in *Sonneratia alba* may be attributed to its exposure to high light intensity and saline conditions, leading to pigment degradation or photoprotective adjustments (Parida & Jha, 2010).

Differences among species in spectral absorption patterns indicate variations in pigment composition and environmental adaptation strategies. Mangrove plants growing under fluctuating salinity and light conditions modulate their chlorophyll content and pigment ratios to optimize light harvesting and minimize photo-oxidative stress (Kathiresan & Bingham, 2001). The overall pattern observed confirms that chlorophyll pigments in mangrove leaves are efficient absorbers of blue and red wavelengths—critical for sustaining photosynthesis even under stress-prone intertidal environments.

B) Chlorophyll estimation

Acanthus ilicifolius shows higher amount of total chlorophyll compare to other three mangrove plants hence leaf appears shiny green colour. While leaves of *Soneratia alba* are green to yellowish-green since its total chlorophyll content are comparatively less. In case of photosynthesis pigments, the mangroves can be organised in ascending order such as *Soneratia alba, Avicennia marina, Rhizophora mucronate, Acanthus ilicifolius.*

The chlorophyll content (Chl a, Chl b, and total chlorophyll) was estimated in four mangrove species — *Sonneratia alba*, *Avicennia marina*, *Rhizophora mucronata*, and *Acanthus ilicifolius* (Figure 2). Among the studied species, *Acanthus ilicifolius* recorded the highest concentration of chlorophyll pigments, followed by *Avicennia marina*, *Rhizophora mucronata*, and *Sonneratia alba*.

Comparative table of photosynthetic rates and pigment contents in common mangrove species *Soneratia alba, Avicennia marina, Rhizophora mucronate, Acanthus ilicifolius*

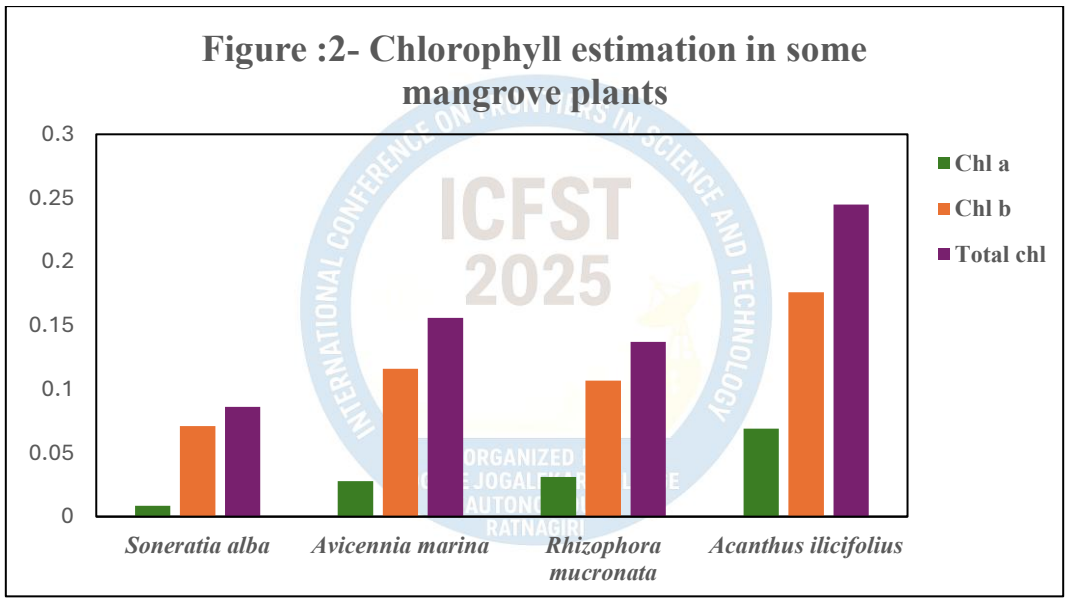

Chlorophyll *a* content ranged from approximately 0.02 mg g^{-1} FW in *Sonneratia alba* to 0.07 mg g^{-1} FW in *Acanthus ilicifolius*. Chlorophyll *b* content showed comparatively higher values across all species, with a maximum of about 0.17 mg g^{-1} FW in *Acanthus ilicifolius* and a minimum of 0.07 mg g^{-1} FW in *Sonneratia alba*. The total chlorophyll content, calculated as the sum of Chl a and Chl b, ranged from 0.08 mg g^{-1} FW in *Sonneratia alba* to 0.25 mg g^{-1} FW in *Acanthus ilicifolius*.

Variation in chlorophyll concentration among mangrove species reflects their adaptive physiological responses to environmental conditions such as light intensity, salinity, and tidal inundation. The comparatively higher chlorophyll levels observed in *Acanthus ilicifolius* and *Avicennia marina* suggest a greater photosynthetic capacity and efficient pigment system that supports their growth in both high- and low-salinity zones.

Lower pigment content in *Sonneratia alba* may be associated with its habitat preference in more open and saline environments, where higher light intensity can lead to pigment degradation or photoinhibition (Parida & Jha, 2010). The predominance of chlorophyll *b* over chlorophyll *a* in all samples indicates the role of accessory pigments in capturing light under

shaded or stress conditions typical of mangrove forests. Similar trends have been reported by Kathiresan and Bingham (2001) and Naidoo et al. (2011), who observed that mangrove species adjust their pigment composition to optimize photosynthetic efficiency under variable tidal and salinity regimes.

Overall, the differences in chlorophyll content among these species reflect species-specific adaptations and physiological plasticity that enable mangroves to thrive in fluctuating coastal ecosystems. The data also emphasize the ecological significance of pigment estimation as an indicator of plant health and environmental stress tolerance in mangrove habitats.

Conclusion

The absorption spectra revealed two distinct peaks around 420 nm (blue region) and 620 nm (red region), indicating the characteristic light absorption of chlorophyll pigments. Among the studied species, *Acanthus ilicifolius* exhibited the highest absorbance values across both regions, suggesting a greater photosynthetic pigment concentration and superior light-harvesting efficiency. In contrast, *Sonneratia alba* showed comparatively lower absorption, reflecting lesser chlorophyll content.

Chlorophyll estimation further confirmed that *Acanthus ilicifolius* possessed the highest total chlorophyll concentration, followed by *Avicennia marina* and *Rhizophora mucronata*. The higher chlorophyll *a/b* ratio in these species may contribute to better adaptation under high light intensity and saline conditions typical of mangrove ecosystems.

Overall, the findings indicate that mangrove species possess adaptive pigment mechanisms to optimize photosynthesis under fluctuating environmental stresses such as salinity, high irradiance, and tidal inundation. These adaptations are crucial for their survival and productivity in intertidal habitats and for their ecological role as primary producers in coastal ecosystems.

References

1. Anjum, S.A., Xiao-yu-Xie, W. Long-Chang, M.F. Saleem, M. Chen and Wang Lei, (2011). Morphological, physiological and biochemical response of plants to drought stress. Afri. J. Agric. Res. 6(9): 2026-2032.
2. Arnon, D.J. (1949). Copper enzymes in isolated chloroplast polyphenyloxidase in Beta vulgaris. Plant. Physiol. 24: 1-5.
3. Basha, S.C. (1991). Distribution of mangroves in Kerala. Indian For. 117: 437-449.
4. Flores-de-Santiago, F., M.K. John and F. Flores-Verugo, (2012). Seasonal changes in leaf chlorophyll a content and morphology in a subtropical mangrove forest of Mexican Pacific. Mar. Ecol. Prog. Ser. 444: 57-68.
5. Gayathri, P.V. , C.R. Lalitha , (2018), Determination of chlorophyll content of some mangroves and associated plant species of Payangadi, Kannur Kong. Res. J. 5(1): 33-35, 2018 ISSN 2349-2694, DOI:10.26524/krj249 http://krjscience.com
6. Kathiresan, K., & Bingham, B.L. (2001). *Biology of mangroves and mangrove ecosystems.* Advances in Marine Biology, 40, 81–251.
7. Lacedra, L.D. (1998). Trace metals biogeochemistry and diffuse pollution in mangrove ecosystems. ISME Mangrove Ecosystems Occasional. 2: 1-16.
8. Lacedra, L.D. (2002). Mangrove ecosystems: function and management. Springer, Berlin.
9. Lichtenthaler, H.K. (1987). Chlorophylls and carotenoids: Pigments of photosynthetic biomembranes. Methods in Enzymology, 148, 350–382.

10. Naidoo, G., Rogalla, H., & von Willert, D.J. (2011). Gas exchange responses of the mangrove Avicennia marina to salinity and waterlogging. Environmental and Experimental Botany, 70(1), 204–213.
11. Padma, M., N. Lele, R.N. Samal, T.V.R. Murthy, A.K. Patnaik and S. Nanda, (2017). Diversity, phenology and variation of seasonal leaf photosythetic pigments in mangroves of Chilka Lagoon (Odisha). India. Bio. Sci. Dis. 8(2): 211-219.
12. Parida, A.K., & Jha, B. (2010). Salt tolerance mechanisms in mangroves: a review. Trees, 24, 199–217.
13. Pastor-Guzman, J., P.M. Atkinso, J. Dash and R. RiojaNieto, (2015). Spatiotemporal variation in mangrove chlorophyll concentration using landsat 8. Remote Sens. 7: 14530-14558.
14. Patrik, D. (2007). Evaluating a chlorophyll content meter on three coastal wetland plant species. J. Agri. Fo. Env. Sci. 1: 1-11.
15. Patwardhan, M.M. and P.D. Chavan, (2013). Ecophysiological studies of Pongamia pinnata and Canavalia cathartica growing in saline and nonsaline habitat from Ratnagiri district of Maharashtra. Proceedings of UGC sponsered national level seminar Dynamics of Mangrove Ecosystem. November 29-30, 2013. Organized by Hindi Vidya Prachar Samti, Ramniranjan Jhunjhunwala College, Ghatkopar in association with vanashakti and ATBS.
16. Parida, A.K., & Jha, B. (2010). Salt tolerance mechanisms in mangroves: A review. Trees, 24, 199–217.
17. Porra, R.J., Thompson, W.A., & Kriedemann, P.E. (1989). Determination of accurate extinction coefficients and simultaneous equations for assaying chlorophylls a and b extracted with four different solvents. Biochimica et Biophysica Acta (BBA) - Bioenergetics, 975(3), 384–394.
18. Pramita, N.D., D. Nirjhar and D. Sauren, (2009). Differential expression of physiological and biochemical characters of some Indian mangroves towards salt tolerance. Physiol. Mol. biol. Plants. 15: 151-160.
19. Prayaga, M.P. and G.M.N. Rao, (2014). Determination of chlorophyll a and b of some mangrove species of Vishakhapatnam, Andrapradesh, India. Inter. J. Phytother. 4: 131-132.
20. Saenger, P. (2002). Mangrove ecology, silviculture and conservation. Kluwer Academic Publishers,Dordrecht.
21. Tomilson, P.B. (1986). The Botany of Mangroves. Cambridge University Pres. Cambridge, U.K. p. 413.
22. V. Venkatesalu, A. Senthilkumar, M. Chandrasekaran, K. Kannathasan ,(2008,) Screening of certain mangroves for photosynthetic carbon metabolic pathway, Photosynthetica 2008, 46(4):622-626 | DOI: 10.1007/s11099-008-0105-x
23. Young, A.J. (1993). Factors that affect the carotenoid composition of higher plants and algae In: Carotenoids in photosynthesis (eds.) by Andrew Young and George Britton. Springer Science+Business Media.

Study of an Ethnomedicinal and Wild Edible Plants in Tungareshwar Hills of Palghar District, Maharashtra.

Paresh Gurav [1], Viraj Chabake[2]* and Anushka Bhangare[3]
[1]Assistant Professor, Department of Botany, R. P. Gogate College of Arts and Science and R. V. Jogalekar College of Commerce (Autonomous), Ratnagiri-415612, Maharashtra.
[2]*Assistant Professor ,Department of Botany, R. P. Gogate College of Arts and Science and R. V. Jogalekar College of Commerce (Autonomous), Ratnagiri-415612, Maharashtra.
[3]Assistant Professor, Department of Botany, Aasara Samajik Sanstha Kalyan Sanchalit Arts Commerce and Science Night College, Thane - 421302, Maharashtra.
*Corresponding author: viraj.chabake@gjcrtn.ac.in
Contact No-9022458777

Abstract

This study investigates the way local and tribal populations in Maharashtra's Tungareshwar Wildlife Sanctuary use plants and their traditional knowledge. The interdisciplinary field of ethnobotany, which connects plant diversity and cultural activities, is vital for recording indigenous knowledge that is progressively losing as a result of habitat degradation and modernization. The study objectives were to survey, record, and examine the variety of wild edible and ethnomedicinal plants, as well as their applications, preparation techniques, and economic significance to the local population.Field surveys were carried out in the Palghar district &Vasai taluka, which included the five villages direct contacts, conversations with tribal tribes, and market observations were used to gather data. Using taxonomic knowledge and standard floras, plant specimens were identified. The findings showed that 57 species of wild edible and ethnomedicinal plants from 29 families - Fabaceae, Euphorbiaceae, and Sapotaceae being the most common had been documented. Leafy vegetables accounted for the majority of plants used, with seeds, fruits, flowers, roots, and tubers following. Along with to providing important nutritional support, several of these species were used to treat diseases. The results demonstrate the plants; dual importance in providing food security in adverse conditions and advancing healthcare through traditional methods. In addition, they provide local communities with additional revenue. The study highlights how urgently this ethnobotanical legacy has to be preserved and recommends more phytochemical and nutraceutical research to examine the plants possibility of use in modern healthcare and sustainable livelihoods. In addition to preserving priceless cultural traditions, this research offers baseline data for next ecological and therapeutic studies by recording indigenous activities.

Keywords: Ethnomedicine, Tribes, wild edible plant, indigenous.

Introduction

Ethnobotany explores the relationship between people and plants, focusing on traditional knowledge and cultural practices. India, being one of the biodiversity-rich countries, hosts a vast diversity of flora with significant ethnomedicinal and nutritional values. The Tungareshwar Wildlife Sanctuary, situated in Palghar district, forms an important ecological corridor between the Sanjay Gandhi National Park and the Tansa Wildlife Sanctuary. The tribal communities in this area rely heavily on wild flora for food, medicine, and other livelihood needs. Documenting their plant-based knowledge is vital for preserving traditional wisdom and ensuring sustainable utilization of these biological resources.

Objectives

The main objectives of this study were to comprehensively document the ethnomedicinal and wild edible plants found in the Tungareshwar region, highlighting their traditional uses and significance among local communities. The research aimed to analyze the diversity of plant species utilized for medicinal and dietary purposes, providing insights into the rich biological and cultural heritage of the area. Furthermore, the study sought to understand the vital role of traditional knowledge in the conservation and sustainable use of these plant resources, emphasizing how indigenous practices contribute to maintaining ecological balance and preserving biodiversity for future generations.

Materials and Methods

Ethnobotanical surveys were conducted between January and May 2022 in the villages surrounding Tungareshwar Wildlife Sanctuary, including Sativli, Majivali, Parol, Usgaon, and Kuwarpada. Data were collected through field observations, semi-structured interviews, and participatory discussions with local informants. Plant specimens were collected, identified, and authenticated with the help of standard floras and guidance from taxonomists. The study area comprises tropical dry deciduous and semi-evergreen forests, with temperatures ranging from 20°C to 35°C.

Results and Discussion

Table No. 1 List of Family wise Collection of plant species

Sr no.	Family	Plants Documented in number
1	Acanthaceae	2
2	Apocynaceae	1
3	Anacardiaceae	1
4	Araceae	1
5	Arecaceae	1
6	Asclepiadaceae	2
7	Asteraceae	1
8	Bombacaceae	1
9	Combretaceae	2
10	Colchicaceae	1
11	Commelinaceae	2
12	Convolvulaceae	1
13	Cordiaceae	1
14	Dilleniaceae	1
15	Dioscoreaceae	2
16	Fabaceae	13
17	Euphorbiaceae	4
18	Malvaceae	2

Sr no.	Family	Plants Documented in number
19	Moraceae	1
20	Oxalidaceae	1
21	Periplocaceae	1
22	Poaceae	1
23	Rhamnaceae	1
24	Rubiaceae	3
25	Sapotaceae	4
26	Smilacaceae	1
27	Solanaceae	1
28	Vitaceae	2
29	Zingiberaceae	1

Economic Diversity, Plant Parts Used, and Medicinal Value

A total of fifty-seven wild plant species were recorded (Table 1). These species belong to 29 different plant families. The Fabaceae family was the most dominant, with 13 species, followed by Euphorbiaceae and Sapotaceae, each represented by 4 species. The remaining families were represented by one or two species each.

The Fabaceae family showed the highest number of species used in traditional medicine (Table 2). This finding is consistent with earlier studies that also reported Fabaceae as a major contributor to traditional medicinal plants. Thus, in the present study, Fabaceae contributed more species of medicinal importance compared to other plant families.

Fig 1.Distribution of Plant Parts used as a Medicinal Purpose

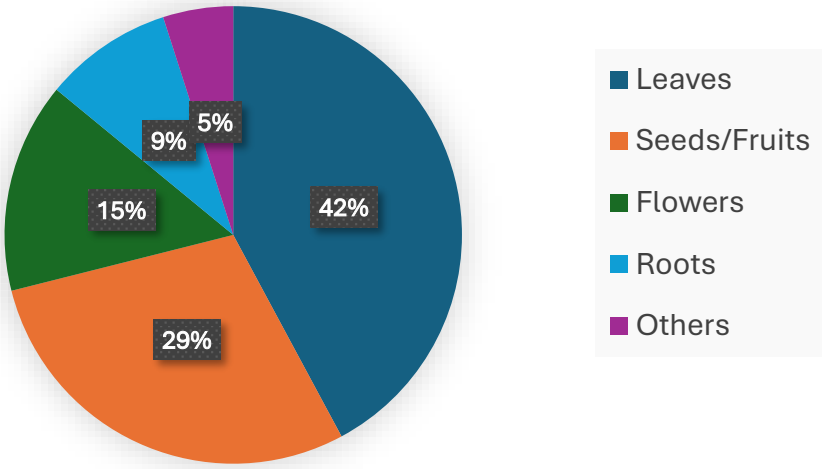

As indicated in fig 1, the majority of wild vegetables reported for folk medicinal use are employed in the treatment of asthma, cough, fever, diabetes, ulcers, jaundice, and cardiovascular diseases. In treating these various ailments, most vegetable leaves are consumed after cooking.

Bauhinia racemosa leaves are used medicinally as a refrigerant and astringent, and in the treatment of headaches, fever, skin and blood diseases, dysentery, and diarrhoea. *Ixora coccinea, Erythrina variegata, Asclepias curassavica, and Samanea saman* leaves and bark are used as remedies for diarrhoea; their leaves are also applied externally to treat sores and ulcers. The fruits of these plants are used in preparing tonics effective against cholera, diabetes, bronchitis, hypertension, and respiratory disorders.

Helicteres isora and *Ficus hispida* fruits are traditionally used in the treatment of diarrhoea, worm infestations, and offensive sores inside the ears, colic, and flatulence, as well as chronic dysentery, piles, jaundice, vitiligo, haemorrhage, and diabetes. *Madhuca longifolia* and *Jatropha curcas* are used in the treatment of snakebites. *Gloriosa superba* is used to induce labour pain during childbirth.

Dioscorea bulbifera, Amorphophallus commutatus, and *Leea macrophylla* tubers are used in the treatment of ulcers, piles, and dysentery; their paste is applied externally to cure scabies. *Justicia adhatoda, Bombax ceiba*, and *Calotropis gigantea* are used to treat cough, cold, and fever.

Some Ethnomedicinal and Wild Edible Plants in Tungareshwar Hills of Palghar District

Commelina benghalensis

Mimusops elengi

Gloriosa superba

Ficus hispida

Dioscorea bulbifera

Helicteres isora

Jatropha curcas

Justicia adhatoda

Mimosa pudica

Bauhinia purpurea

Dillenia pentagyna

Samanea saman

Madhuca longifolia

Bambusa arundinacea

Terminalia elliptica

Ixora coccinea

Pongamia pinnata

Mitragyna parvifolia

Leea macrophylla

Bauhinia racemosa

Ampelocissus latifolia

wattakaka volubilis

Morinda citrifolia

Curcuma amada

Ziziphus mauritiana

Prosopis cineraria

Terminalia arjuna

Bombax ceiba

Borassus flabellifer

Cassia tora

Erythrina variegate

Semecarpus anacardium

Smilax zeylanica

Conclusion

The conclusion of the study on ethnomedicinal and wild edible plants in the Tungareshwar region reveals that many plant specimens found in the area possess significant medicinal

value, as indicated in the chart. These plants can be effectively utilized for medicinal applications. Therefore, the region needs to be monitored and access restricted to casual visitors to ensure conservation. Such valuable plant species should be protected and cultivated on a large scale for medicinal production.

The efforts made to collect this information will open avenues for future research and further investigation into the nutritional aspects of lesser-known wild edible plants. However, with the spread of high-yielding crop varieties and other influencing factors, these valuable plant genetic resources and associated traditional knowledge are depleting at an alarming rate. Hence, it is essential to promote the domestication of wild edible plants and implement proper conservation measures to preserve these local gene pools before they are lost forever.
Indigenous knowledge about local floral diversity and the use of plants in primary healthcare should be documented and preserved so that future generations can benefit from this traditional wisdom. Preserving local floral diversity and plant-based traditional medicines for the treatment of various health problems is a crucial step in conserving traditional knowledge and protecting medicinally important local plant species. This will help raise awareness about the conservation of valuable medicinal plant species and promote ethnomedicinal knowledge within the region, contributing to the preservation of these species before they become extinct. Traditional medicinal knowledge is rapidly diminishing due to the influence of modern and alien cultures. Therefore, there is an urgent need to document indigenous knowledge for future generations and encourage local communities to cultivate wild edible plants in their home gardens.

References

1. Alfred Nyero, Innocent Achaye, Walter adongo. Godwin Any war, and Geoffrey Maxwell Malinga. (2021) wild and semi wild edible plants used by the Communities of Acholi Sub region, Northern Uganda Ethnobotany Research Applications 21 (16); 1-12
2. Aniama s. o., Usman S.S, and Ayodele S.M (2016) Ethnobotanical documentation of some plants. Among Igald people of Kogi State. The International journal of Engineering and science. 5(4): 33-42.
3. Athena Della Demetra parakeva Hadijchambi Andrea's ch Hadjichambi (2006) Ethnobotanical survey of wild edible plants of Cyprus. Journal of Ethno biology & ethno medicine 2(34):1-9.
4. Atinafu Kebede, Woynishet Tesfaye, Molla fentie. Hanna zewdie (2017) An Ethnobotanical survey of Wild Edible plants Commercialized in kefira Manket. Dire Dawa City, eastern Ethiopia, science publishing Group 5(2):42-46.
5. Besnik Rexhepi, Ani Bajrami, Behxhet Mustafa (2013) ethnobotanical study of wild edible plants in pelagonia region (south-western Macedonia) International Journal of Advance in science Engineering and Technology, 6(1):61-65.
6. Bhogaonkar Prabha Y. Marathe Vishal R. and kshirsagar prachi P. (2010) Documentation of wild Edible plants of Melghat forest Dist. Amravati, Maharashtra State, India Ethnobotonical Leaflets 1-17.
7. Chakraborty, D. Nath, S. Biswas, S. Shill D.Dey (2019) Ethnobotonical Survey and documentation of Wild edible plants used by the tribals of Tripura northeaster India International Society for Horticultural Science 135-142
8. Chandrakumar K Patale Praveen kumar N. Nasare, Sushma D. narkhede (2015) International Research Journal of pharmacy Ethanobotanical Studies on Wild edible plants of Gond Halba & kawar tribes of salekasa Taluka Gondia District of Maharashtra state India 6(8).

9. Derebe Alemneh (2020) Ethnobotany of Wild edible plants in Yilmana Densa and quart Districts of West Gojjom zone, Amhara Region Ethiopia. Ethnobotany Research and applications. 1-14
10. Dhole P.A, P.Y Bhogaonkar, Chanham V.N, kshinagaren P.P, some Ethno medicinal plants from. Amravati District India. Int. J. Adv. Res. Biol.Sci 8(1): 65-71
11. Ermias Lulekal, zemede Asfaw, Enserma kelbessa Patrick Van Damme (2014) Wild edible plants in Ethiopia: a review on their potential to combat food Insecurity. Research Gate 24. 71-121.
12. Feifei li, jingxion zhuo Bolia, Devra Jarvis and Chinlin Long (2015) Ethnobotanical study on Wild plants used by Lhoba people to Milin Country,Tibet. Journal of Ethno biology and Ethno medicine 1-11.
13. Gitamani Dutta. Gautam Baruah and Ashalata Devi (2016) Wild food plants of Mishing tribe an ethnobotanical survey. An International. Journal 3(1): 221-223.
14. Hainner Aparicio, Inga Hedberg, Salomão Bandeira, Abdobaset Ghorbani (2021) ethnobotanical study of medicinal and edible plants used in Nhamacoa area, Marica province. Mozambique south African Journal of Botany 318-328.
15. Jadhav, V.D.) Mahadkar, S.D. and Valli S.R. (2011). Documentation and ethanobotanical survey of Wild edible plants from Kolhapur district. Recent Research to science and Technology 3(12): 58-67
16. Kalish Chandra pande and Neeta pande (2016). Ethaobotanical documentation and Wild edible pants used by Gujjar Community of Tarai West forest Division Ramnagar, Nainital India. Curr World Environ. 11(3) 808-818
17. Kamal Prasad Aryal, Sushmita poudel, Ram Prasad Chaudhary and Rajan kotru (2018) diversity and use of Wild and non-cultivated edible plants in the Western Himalaya. Journal of Ethan biology and ethnomedicines 14(10): 2-18.

Stomatal variation in the leaves collected from mangrove ecosystem nearby Ratnagiri city

Chitra Phansekar [1], Vishakha Mulye[2] and Paresh Gurav[3]*
[1-2]Department of Botany, R. P. Gogate College of Arts and Science and R. V. Jogalekar College of Commerce (Autonomous), Ratnagiri-415612, Maharashtra.
[3]*Assistant Professor, Department of Botany, R. P. Gogate College of Arts and Science and R. V. Jogalekar College of Commerce (Autonomous), Ratnagiri-415612, Maharashtra.
*Corresponding author: paresh.gurav@gjcrtn.ac.in
Contact No-8779802458

Abstract

The mangrove ecosystem near Ratnagiri, situated along the western coast of India, represents a distinctive ecological niche that supports a rich diversity of plant species adapted to extreme and fluctuating intertidal conditions. These mangrove communities thrive in an environment characterized by high salinity, periodic tidal inundation, variable oxygen availability, and intense solar radiation. Understanding their physiological adaptations is essential to assess how these species cope with environmental stresses and contribute to coastal ecosystem stability.The present study investigates stomatal variation in selected mangrove species from different tidal zones of the Ratnagiri coast. Emphasis was placed on assessing the influence of environmental parameters such as salinity, tidal exposure, and seasonal fluctuations on stomatal density, size, and distribution. Leaf samples were collected during pre-monsoon and post-monsoon seasons from both high-salinity and low-salinity sites. Stomatal traits were quantified microscopically and analyzed to determine inter-specific and site-specific differences.Results revealed significant variation in stomatal characteristics among the studied species. Lower stomatal densities were recorded in plants inhabiting high-salinity zones, indicating an adaptive mechanism to reduce transpiration and conserve water under osmotic stress. Conversely, mangrove species growing in sheltered and less saline areas exhibited higher stomatal densities and larger stomatal apertures, reflecting their capacity for greater CO_2 assimilation and photosynthetic activity. These findings demonstrate the ecological plasticity of mangrove species and their ability to modulate physiological traits in response to environmental gradients.Overall, the study underscores the importance of stomatal regulation as a key adaptive strategy for mangrove survival in harsh coastal environments. The observed variations contribute valuable insights into how mangroves optimize water-use efficiency and gas exchange under stress conditions, offering implications for conservation, climate resilience, and sustainable management of mangrove ecosystems in the western coastal region of India.

Keywords: stomatal variation, stress, density, mangrove vegetation.

Introduction

Mangrove is a type of plant that can grow in coastal areas.It can be assumed that all plants have the ability to cope with stress and response to environmental change. Leaves are organ variables in plants. The mangrove leaves showed various forms of features and developments in response to environmental physiological conditions, including thick cuticles, wax coatings, sunken stomata, large cells, and small volumes. The characteristics of plant morphology correlate with certain combinations of environmental conditions in which individual plants are established and grow this characteristics we have studied in this work.

Materials and Methods

Study Sites

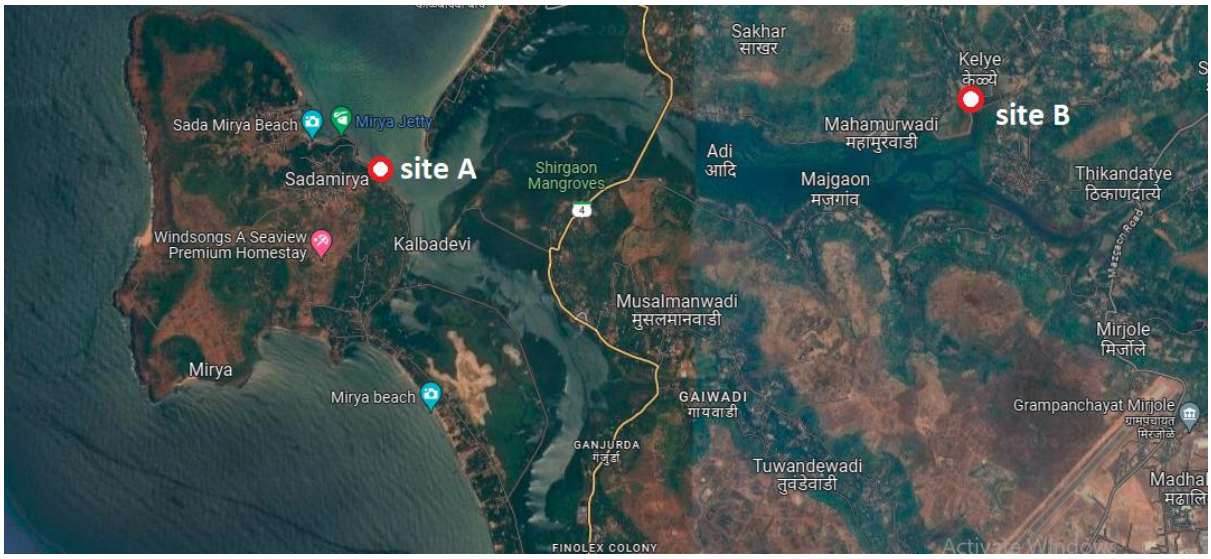

Site A - Mirya bundar

Site B – Kelye Village

The observed mangrove and mangrove associates leaves originated from site A and Site B which was nearby ratnagiri.leaves consited of *Rhizhopora mucronata*, *Acanthus ilicifolius* , *Sonneratia alba*, and *Avicennia alba* and *salvadora persica* . The analysis of leaves stomata were conducted at departmental Laboratory of botany, GJC in the month of january 2024.

Procedure

Observation and calculation of leaf stomata by cutting the leaves with size ± 2 mm. The leaf piece was placed above the glas object with leaf condition should not dry out. The sample preparation was steady conditions in observation. The epidermis of leaves was peeled until visible epidermal layer. Then, it put on glass objects and staining with safranin 1%. Leaf stomata observation was done by using microscopic shooting method.

Stomata density = (Number of stomata) / (Area of view) Measuring stomatal density, the area of view used size amflication 40 x 10 and diameter of view was 0.52 mm

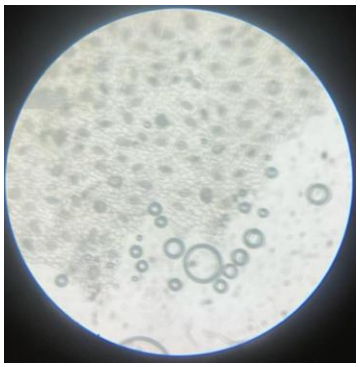

Rhizhopora mucronata

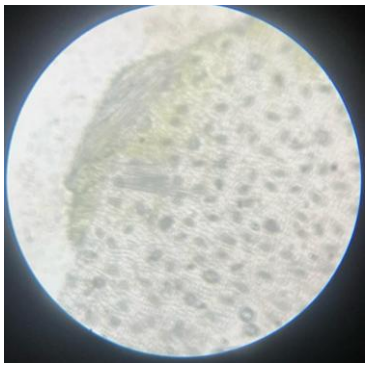

Acanthus ilicifolius

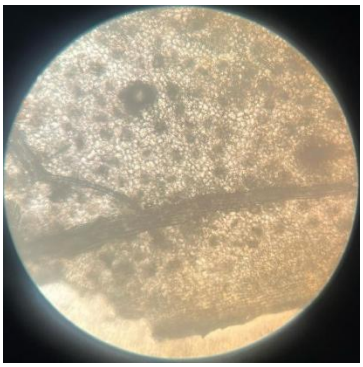

Sonneratia alba

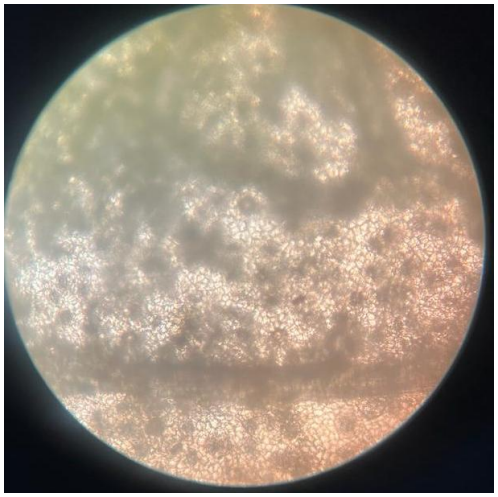

Avicennia alba

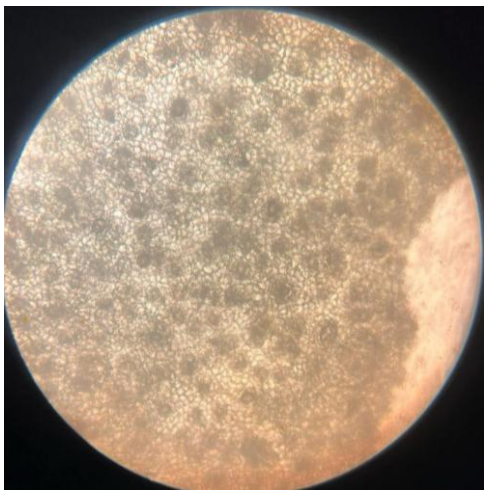

salvadora persica

Rhizhopora mucronata

Acanthus ilicifolius

Sonneratia alba

Avicennia alba

salvadora persica

Dominant Mangrove species analyzed during the stomatal variation study

Table 1: Variation in number of stomata at Site A and Site B

Sr no	Plants name	Site A	Site B
1	Rhizhopora mucronata	31	49
2	Acanthus ilicifolius	79	125
3	Sonneratia alba	86	143
4	Avicennia alba	101	151
5	salvadora persica	80	74

The comparison of mangrove species diversity and abundance between Site A and Site B revealed noticeable variation among the five recorded species — *Rhizophora mucronata*, *Acanthus ilicifolius*, *Sonneratia alba*, *Avicennia alba*, and *Salvadora persica.*

Rhizophora mucronata showed the least abundance at both sites, with slightly higher values at Site B. *Acanthus ilicifolius* and *Sonneratia alba* exhibited a significant increase in abundance at Site B compared to Site A.Avicennia alba was the most dominant species across both sites, particularly at Site B, where its count exceeded 150 individuals.

In contrast, *Salvadora persica* showed a marginally higher abundance at Site A than Site B.

Overall, Site B exhibited greater species abundance for most mangrove species compared to Site A.

Graphical representation showing variation in number of stomata at site A and site B

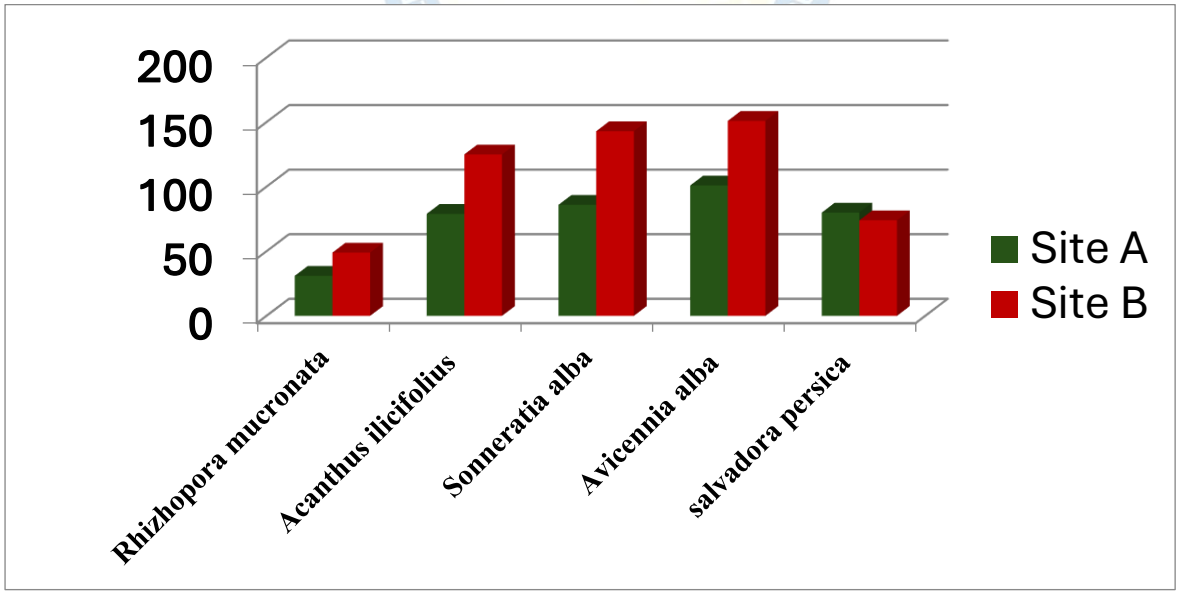

Discussion

The higher abundance of mangrove species at Site B suggests that environmental conditions such as tidal influence, soil salinity, nutrient availability, and hydrological stability are more favorable for mangrove growth at that site. The dominance of *Avicennia alba* and *Sonneratia alba* indicates their adaptability to a wide range of salinity and sediment conditions.

The relatively lower representation of *Rhizophora mucronata* may be attributed to its preference for sheltered, muddy substrates that might be less prevalent at both sites. The variation in *Salvadora persica* distribution, showing slightly higher numbers at Site A, could indicate that this species prefers drier or more elevated zones along the mangrove margin.

Overall, these findings highlight spatial variation in mangrove composition, reflecting site-specific ecological factors influencing species distribution. Continuous monitoring of these sites can help understand how environmental gradients shape mangrove community structure and assist in conservation planning.

Conclusion

The comparative study of mangrove species between Site A and Site B indicates distinct ecological variations in both species abundance and physiological responses. Site B exhibited higher species density and diversity, particularly for *Avicennia alba* and *Sonneratia alba*, suggesting more favorable environmental conditions such as optimal salinity, tidal influence, and nutrient availability. In contrast, Site A showed reduced species abundance and physiological stress indicators.

Microscopic analysis revealed that stomatal density and size varied significantly between sites. The number of stomata differed according to the coastal growth zones, and stomatal size was influenced by prevailing stress conditions. A lower stomatal density and smaller stomatal size at Site A suggest that mangrove species there are experiencing environmental stress, likely due to pollution and deteriorating water quality.

These findings collectively highlight that both morphological (species abundance) and physiological (stomatal variation) parameters serve as sensitive indicators of environmental health in coastal mangrove ecosystems. Therefore, it is significant to take appropriate measures to improve and monitor the water quality at Site A to promote healthy mangrove growth and maintain ecological balance in the region.

Reference

1. Pugnaire, F. I., & Pardos, J. (1999). Constraints by water stress on plant growth. In M. Passarakli (Ed.), Handbook of plant and crop stress (pp. xx–xx). John Wiley & Sons.
2. Price, A., & Courtois, B. (1991). Mapping QTLs associated with drought resistance in rice: Progress, problems, and prospects. International Rice Research Institute.
3. Saenger, P. (2002). Mangrove ecology, silviculture and conservation. Kluwer Academic Publishers.
4. Swarthout, D., Harper, E., Judd, S., Gonthier, D., Shyne, R., Stowe, T., & Bultman, T. (2009). Measures of leaf-level water-use efficiency in drought-stressed endophyte-infected and non-infected tall fescue grasses. *Environmental and Experimental Botany, 66*, 88–93. [https://doi.org/10.1016/j.envexpbot.2008.12.002] (https://doi.org/10.1016/j.envexpbot.2008.12.002)
5. Tomlinson, P. B. (1986). The botany of mangroves. Cambridge University Press.
6. Wang, J. Z., Cui, L. J., Wang, Y., & Li, J. L. (2009). Growth, lipid peroxidation and photosynthesis in two tall fescue cultivars differing in heat tolerance. Biologia Plantarum, 53(2), 237–242. https://doi.org/10.1007/s10535-009-0045-8

Comparative Study of Phytoplankton Diversity across Freshwater, Marine, and Estuarine Ecosystems of Ratnagiri

Sambodhi kamble [1], Mugdha Jadhav[2] and *Paresh Gurav
[1-2]Department of Botany, R. P. Gogate College of Arts and Science and R. V. Jogalekar College of Commerce (Autonomous), Ratnagiri-415612, Maharashtra.
[3]*Assistant Professor, Department of Botany, R. P. Gogate College of Arts and Science and R. V. Jogalekar College of Commerce (Autonomous), Ratnagiri-415612, Maharashtra.
*Corresponding author: paresh.gurav@gjcrtn.ac.in
Contact No-7447376997

Abstract

Phytoplankton, the microscopic photosynthetic organisms that form the foundation of aquatic food webs, play a crucial role in maintaining ecosystem productivity and biogeochemical cycling. Their diversity, abundance, and community composition are highly responsive to variations in environmental parameters such as temperature, salinity, nutrient concentration, and light availability, making them excellent bioindicators of water quality and ecological health. The present study was undertaken to assess the variation in phytoplankton species across three contrasting wetland sites near Ratnagiri, Maharashtra—representing freshwater, marine, and estuarine environments.Water samples were collected during January 2024 using a plankton net (mesh size 25 µm, pore diameter 60 µm) and preserved in 4% formalin. Identification and enumeration of phytoplankton species were performed microscopically with Lugol's Iodine solution, and abundance was expressed as the number of organisms per liter. A total of 11 phytoplankton species belonging to major groups such as Chlorophyceae, Bacillariophyceae, and Cyanophyceae were identified across the sites. The highest diversity and population density were recorded at Site A (freshwater), which exhibited optimal nutrient availability and low salinity conducive to algal growth. Site B (marine water) showed moderate abundance with dominance of diatoms, while Site C (estuarine) exhibited the lowest species richness and density, possibly due to fluctuating salinity and nutrient limitation.The study demonstrates clear spatial variation in phytoplankton composition and abundance corresponding to hydrological and physicochemical gradients. The occurrence of common taxa across all sites indicates potential water quality degradation and anthropogenic influence. These findings emphasize the significance of phytoplankton as sensitive ecological indicators for monitoring environmental changes. Long-term and seasonal investigations are recommended to understand temporal dynamics, establish ecological baselines, and guide sustainable management and conservation of coastal and wetland ecosystems in the Ratnagiri region.

Keywords: Phytoplankton diversity, Wetlands, Ratnagiri, Freshwater, Marine water, Estuarine ecology, Bioindicators, Water quality monitoring.

Introduction

The plankton are passively drifting weak organisms that are maintained in suspension by water current, or float or swim. They include heterotrophic bacterio plankton, photosynthetic phytoplankton and zooplankton. The world plankton are referred to the microscopic aquatic plants or animal having little or no resistance to the water current and living free floating and suspended in the open water. Planktonic plants are called as phytoplankton and animals as zooplankton. The phytoplankton (microscopic algae) occur in unicellular, colonial or filamentous forms (Lewin,1962). Many of these forms have different physiological requirements and differ in their response to light, temperature and concentration of nutrients.

Material and Methods

Study Area

The study was conducted at three selected wetland sites located near Ratnagiri city. Site A was Nirul Village near Pawas, Site B was Bhatye Beach in Ratnagiri, and Site C was Mirya Bundar in Ratnagiri.

Water Sample Collection

Phytoplankton samples were collected once from all three sites in January 2024. The sampling was carried out using sterile plastic bottles and a plankton net with a mesh size of 25 and pore diameter of 60 µm. The collected phytoplankton samples were immediately preserved in 4% formalin solution at the site of collection. Identification was performed using 1% Lugol's Iodine solution under a compound microscope. The recorded results represented the number of organisms per liter at each site.

Result and Discussions

The study revealed noticeable variation in phytoplankton distribution and abundance among the three wetland sites — Nirul Village (Site A), Bhatye Beach (Site B), and Mirya Bundar (Site C). A total of 11 phytoplankton species were identified across these sites.

Sr no	Name of species	Site A	Site B	Site C
1	*Bambusina borreri*	P	P	A
2	*Chlorella sp.*	P	A	P
3	*Cladophora sp.*	P	A	A
4	*Closterium sp.1*	A	P	P
5	*Chaetomorpha sp.*	P	A	A

Sr no	Name of species	Site A	Site B	Site C
6	*Navicula*	A	A	P
7	*Navicula minima*	P	P	A
8	*Microcystis sp.1*	P	P	P
9	*Oedogonium*	P	P	P
10	*Pinularia sp.1*	P	P	A
11	*Spirogyra sp.*	P	P	P

Site A (Nirul – Freshwater Site) recorded the highest average number of phytoplankton cells per liter, indicating nutrient-rich conditions that favor algal growth.Site B (Bhatye Beach – Marine Site) showed a moderate density and diversity of phytoplankton species, reflecting the influence of saline conditions and tidal mixing.Site C (Mirya Bundar – Brackish/Estuarine Site) exhibited the lowest diversity and abundance, suggesting possible ecological stress or reduced nutrient input.

The identified phytoplankton comprised members of Chlorophyceae, Bacillariophyceae, Cyanophyceae, and Euglenophyceae. The dominance of diatoms (Bacillariophyceae) at all three sites indicated their adaptability to varying aquatic environments. However, freshwater algae such as Spirogyra, Closterium, and Cosmarium were restricted mainly to Site A.

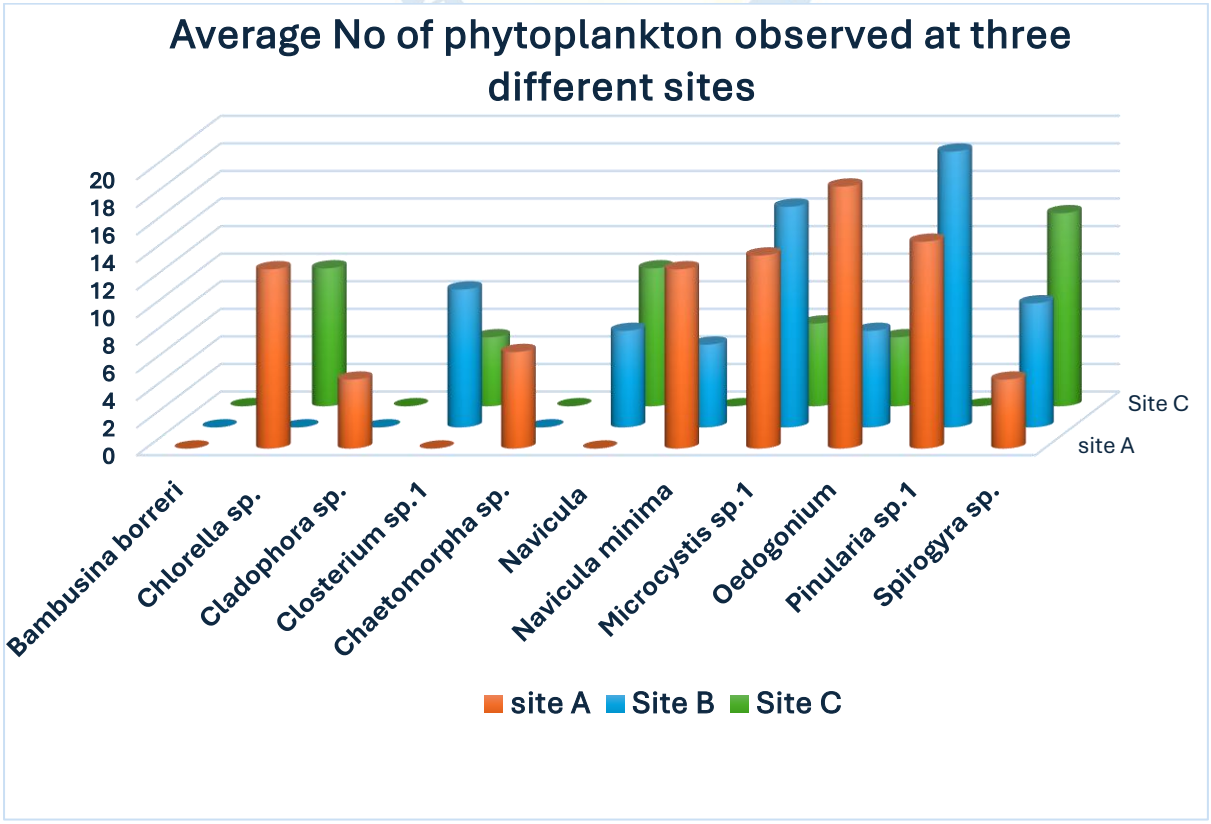

Discussion

The observed variation in phytoplankton density across the sites suggests that water quality and nutrient availability are key factors influencing their distribution. The higher abundance at Site A reflects eutrophic conditions typical of freshwater ecosystems enriched with organic and inorganic nutrients from nearby agricultural runoff or domestic sources.

In contrast, Site B, being a marine site, experiences fluctuations in salinity, temperature, and wave action, which limit the proliferation of freshwater phytoplankton species. The presence of diatoms and certain marine flagellates here signifies adaptation to saline environments. Site C's minimal diversity may be attributed to pollution stress or limited nutrient circulation, possibly due to anthropogenic activity and restricted water exchange.

Phytoplankton serve as primary producers in aquatic ecosystems; hence, their abundance directly reflects the productivity and trophic status of the water body. The relatively lower diversity at the marine and estuarine sites may indicate a transition zone under environmental pressure, leading to dominance by a few tolerant species. Comparative studies (e.g., Dwivedi & Pandey, 2002; Dhamak et al., 2013) support that phytoplankton community structure responds strongly to changes in physicochemical parameters such as pH, dissolved oxygen, temperature, and nutrient concentration. Thus, regular phytoplankton assessment can serve as a biological indicator of water quality in these wetland systems.

Table 1 - Phytoplankton Diversity across three ecosystems sites of Ratnagiri

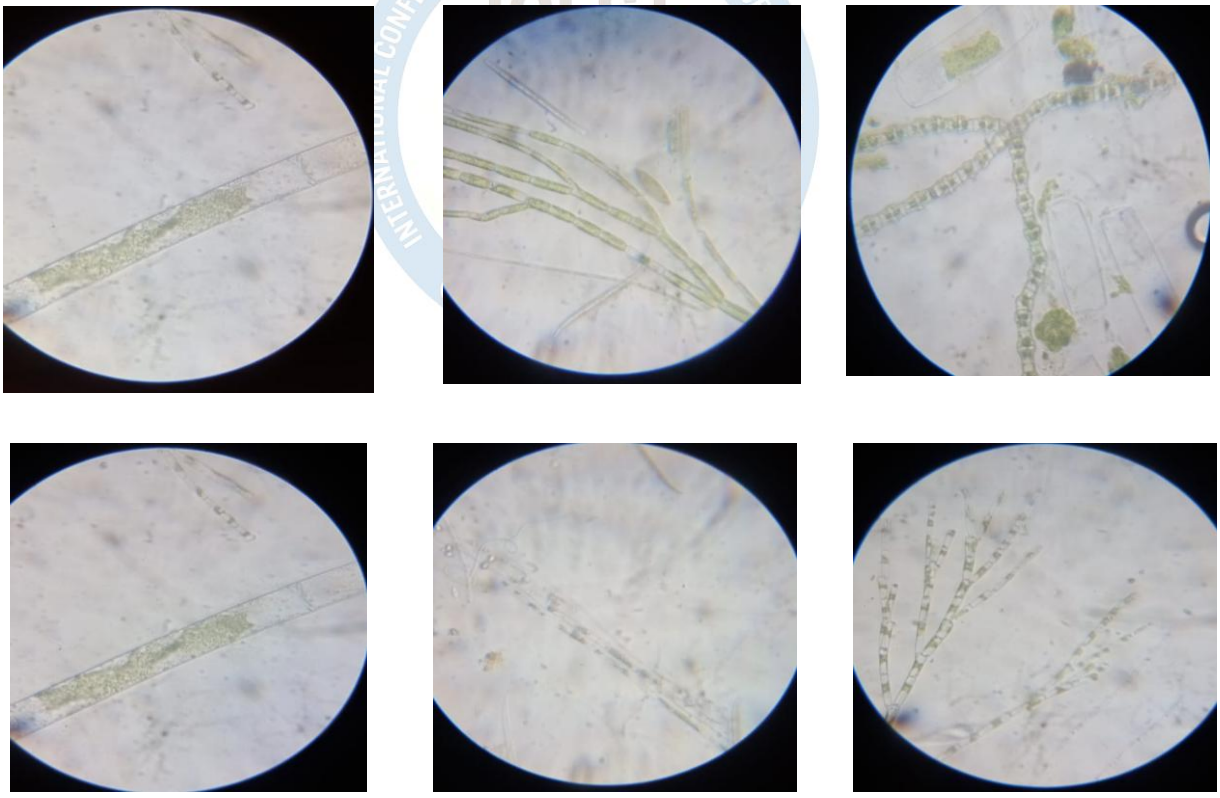

Conclusion

The present study highlights the spatial variation in phytoplankton diversity and abundance across different wetland sites of Ratnagiri. The findings reveal that freshwater habitats such as Nirul (Site A) support a higher diversity and density of phytoplankton species compared to

marine and estuarine sites like Bhatye Beach (Site B) and Mirya Bundar (Site C). These variations are largely influenced by environmental factors such as salinity, nutrient concentration, temperature, and water dynamics. The dominance of common algal species across all sites suggests a gradual decline in water quality, likely due to anthropogenic influences and nutrient enrichment. Since phytoplankton serve as key biological indicators of aquatic health and primary productivity, their assessment provides valuable insights into the ecological condition of these wetlands. Therefore, continuous and seasonal monitoring of phytoplankton diversity, along with physicochemical parameters, is essential to evaluate water quality fluctuations and maintain the ecological balance of wetland ecosystems in the Ratnagiri region.

References

1. APHA (2005). Standard Methods for examinations of water and waste water, 21st Edition, American Public Health Association, WashingtonD.C.
2. Anilkumar S. (2000). Fresh water algae of Hassan district, Karnataka State, India, Ph.D. Thesis.
3. Chapman V.J., and Chapman D.J. (1975). The algae. Macmillion, London
4. Davis C.C., (1974). Seasonal change of plankton crustacean in two wetland lake, verb. International Vercis, Limnological. 19:739-744.
5. Dhamak R.M, Tilekar B.B., Ghadge M.K., Theurkar S.V. and Patil S.B. (2013). Phytoplanktons variation with respect to Icthyofaunal Studies of Bhandardara Dam, M.S., India.1(2): 7-8
6. Donnely T.H., Grace M.R., and Hart B.T. (1997). Algal bloom in the Darling-Barwon River, Australia, Water, Air and Soil pollution. 99,487-499.
7. Dwivedi B.K and Pandey G.C. (2002). Physico-chemical factor and algal diversity of two ponds (GirijaKund and Maqubara Pond) faizabad, India, Pollution Research Journal., 21(3):361-369.
8. Green G.H. and Andrew F.J. (1964). Limnological changes in section Lake resulting from hydroelectric diversion. Internal Pacific. Salmon Fish. Com. Progress Report. No.5:76.
9. Mishra S.R., (1996). Assesment of water pollution. Alpha Publishing, New Delhi, India.43-60.
10. Moosa and S.G. Yeragi (2013). Phytoplanktonic Community of Aarey Lake, Mumbai. National Conference on Biodiversity: Status and Challenges in Conservation-FAVEO. 181-183

Phytochemical Insights from Indian *Cleome* Species: A Review

Shweta S. Jadhav[1*] and Vikram P. Masal[1]
[1]Dapoli Urban Bank Senior Science College, P.G. Research Center, Department of Botany, Dapoli 415712, Maharashtra, India.
Corresponding Author
*Email: shwetajadhav1909@gmail.com, 8793257592.

Abstract:

The spider- flower family, Cleomaceae, is a diverse group of plants; it includes approximately 27 genera and around 270 species. In India, Cleomaceae family is represented by around 16 species, exhibiting potent medicinal properties. We summarize research on the chemical constituents and biological activities of Indian Cleomaceae species, emphasizing their therapeutic value. We identified chemical classes like essential oils and fatty acids, flavonoids, glucosinolates and isothiocynates, terpenes and sterols, anthocyanins, alkaloids, saponins and tannins. Chemical compounds demonstrated a range of biological activities, including anti-inflammatory, antidiabetic, antimicrobial, hepatoprotective, analgesic, antihelminthic, and anticancer effects. Our results represent the comprehensive phytochemical studies of Indian species of Cleomaceae to date.

Keywords: Anticancer, Cleome, Cleomaceae, Phytochemical, Therapeutic.

Introduction:

The Indian subcontinent is globally recognized as a megadiverse hotspot, harboring a rich legacy of traditional medicine fundamentally reliant on its indigenous flora. There are approximately 16 species of the Cleomaceae family found in India (POWO 2025), many of which possess significant medicinal properties. Species such as *Cleome monophylla*, *C. viscosa*, and *C. rutidosperma* are extensively utilized across various Indian traditional systems, including Ayurveda and local folk practices, to manage ailments ranging from inflammatory conditions and skin diseases to liver disorders.

Despite this widespread traditional use and preliminary pharmacological evidence suggesting potent antioxidant and antimicrobial activities, comprehensive chemical and biological data on the Indian *Cleome* species remain scattered across diverse journals. There is a pressing need to consolidate the existing knowledge to facilitate structured drug development. This review aims to address this gap by providing a comprehensive synthesis of the literature on the genus *Cleome* indigenous to India.

Methodology

The scientific name of plants was accessed and verified on online databases. A literature review was conducted, and data was collected from research articles through online scientific databases like Google Scholar, Science Direct, Scopus and PubMed using the related words. The related and mostly recent published articles were accessed.

Phytochemicals:

Flavonoids and phenolics stand out as the most significant compounds due to their prominent pharmacological effects. *Cleome gynandra* and *C. viscosa* are rich in flavonoids, which exist in both aglycone and glycosidic forms (Singh *et al*., 2018). Specific compounds isolated from *C. aspera* include kaempferitrin (a flavonol glycoside) and rutin (Sucharitha *et al*., 2017). These compounds are largely responsible for the potent antioxidant, anti-inflammatory, and

anti-diabetic activities reported for *Cleome* extracts. Their free radical scavenging ability is a key mechanism of action.

Terpenoids represent another major class, including mono-, sesqui-, di-, and triterpenoids. The presence of compounds like diterpenes, triterpenoids, and sterols contributes to the plant's traditional use as an analgesic and anti-inflammatory agent. Novel compounds, such as cleomaldic acid in *C. aspera*, have also been isolated, demonstrating the unique chemical space explored by this genus (Sucharitha *et al*., 2017).

Alkaloids generally present in lower concentrations compared to flavonoids, alkaloids are consistently detected in phytochemical screenings of Indian *Cleome* species, particularly in the seeds and roots. These nitrogen-containing compounds often possess significant biological activity. For example, some alkaloids from the genus have shown anti-parasitic potential.

The *Cleome* species belong to the Brassicales order (the family of mustard and cabbage) and, therefore, are characterized by the production of glucosinolates and isothiocyanates. When these are hydrolyzed, they yield highly bioactive isothiocyanates. These sulfur-containing compounds are known for their pungent flavor and their potent antimicrobial and anticarcinogenic properties. They are crucial for the plant's defense mechanisms and culinary flavor profile.

Essential Oils and Fatty Acids: The seeds, especially of *C. gynandra*, are a source of essential oils and fixed fatty acids, including oleic, linoleic, palmitic, and stearic acids (Wael *et al*., 2016). The essential oils are composed of various mono- and sesquiterpenes (like myrcene and terpinolene) and are responsible for the distinct aroma and some of the anthelmintic and anti-microbial uses of the plant.

Table 1: Chemical classes with isolated compounds of *Cleome* Species

Scientific name	Plant Parts	Chemical Classes: Secondary Metabolites	Chemical Classes: Compound Isolated	References
Cleome viscosa	Leaves	**Phenolic, flavonoid and alkaloids**	Atropine, Vanillic Acid, Gallic Acid, Nevirapine, Kaempferitrin, Caffeic Acid	Singh *et al*., 2018
	Leaves and Twigs	Diterpene	Cleomeolide	Singh *et al*., 2018
	Flowers	Flavonol Glycoside	Quercetin3-O-(2″acetyl)-glucoside	Singh *et al*., 2018
	Seeds	Coumarinolignoids	Cleomiscosin A, Cleomiscosin B, Cleomiscosin C, Cleomiscosin D	Singh *et al*., 2018
		Glucosinolates and isothiocyanates	glucocapparin, glucocleomin, (2-hydroxy-2-methylbutyl-Gls.), (Methyl isocyanate and 5-ethyl-5-methyl-oxazolidine-2-thione	Wael *et al*., 2016

Scientific name	Plant Parts	Chemical Classes: Secondary Metabolites	Compound Isolated	References
Cleome monophylla	Aerial Parts	Essential Oils	Mycerene , Terpenolene, (-)-Cubebene, 3-Undecanone, (α+β)-Humulene, 1-α-Terpeneol, 2-Dodecanone, β-Ionone, (+)-Cedrol, Carvacrol, n-Docosane, n Pentacosane, n-Octacosane	Singh *et al*., 2018
Cleome chelidonii	Leaves	Flavonol glycoside	Cleomeside C	Nguyen *et al*., 2017
Cleome felina		flavonols	5,3,4-triOH-3,6,7,5-tetraOMe flavone 5,3-diOH-3,6,7,4,5-pentaOMe-flavone	Wollenweber *et al*., 2007
Cleome aspera	Aerial parts and seeds	Essential oils and fatty acids	Linoleic acid, Palmitic acid, Oleic acid, Arachidic acid, Eicosenoic acid.	Sucharitha *et al*., 2017
		Terpenes and sterols	Beta sitosterol, 17-alpha-hydroxylcabraleactone, Amblyone Cleomaldeic acid Paradoxenoic acid	
		Flavonoids	Kaempferol-7-O-rhamnoside, Kaempferol-3-O-rutinoside, Kaempferol- 3, 7-O-dirhamnoside, Kaempferol- 3-O-glucoside-7-O-rhamnoside, Kaempferol- 3-O-rhamnoside-7-O-glucoside, Quercetin-7-O-rhamnoside, Quercetin-3-O-rutinoside, Quercetin-7-O-rutinoside, Quercetin- 3, 7-O-dirhamnoside, Quercetin- 3-O-glucoside-7-O-rhamnoside, Isorhamnetin 3-O-rutinoside, Isorhamnetin 3, 7-O-dirhamnoside, Vicenin-2	
		Alkaloids	Dipyridodiazepinone Asparadoxonine Paradoxenoline	

Scientific name	Plant Parts	Chemical Classes: Secondary Metabolites	Compound Isolated	References
		Anthocyanins	Cyanidin3-(2″-(6‴-caffeoyl-β-glucosyl)-6″-(p-coumaro-yl)-β-glucoside)-5-β-glucoside, Cyanidin 3-(2″-(6‴-sinapoyl-β-glucosyl)-6″-(p-coumaroyl)-β-glucoside)-5-β- glucoside, Cyanidin 3-(2″-(6‴-feruoyl-β-glucosyl)- 6″-(E-p-coumaroyl)-β-glucoside)-5-β-glucoside, Pelargonidin 3-(2″-(6‴-sinapoyl-β-glucosyl)-6″-(p-coumaroyl)-β-glucoside)-5-β-glucoside, Pelargonidin 3-(2″-(6‴-p-coumaroyl-β-glucosyl)-6″-(p-coumaroyl)-β-glucoside)-5-β glucoside together with one monoacylated and four diacylatedcyanidin 3-sophoroside- 5 glucosides.	
Cleome simplicifolia	Stem	**Phytosterols**	stigmasterol, γ-sitosterol, n-hexadecanoic acid, and neophytadiene	Shaikh *et al*., 2025
Cleome gynandra	Seed	essential oils and fatty acids	linoleic (1), palmitic acid (11·2%) (2), Oleic (3) stearic (6·55%) (4), Arachidic (11) and eicosenoic acids (12)	Wael *et al*., 2016

Pharmacological properties

Antibacterial activities

An *in vitro* study evaluated the antibacterial effectiveness of petroleum ether, ethyl acetate, and ethanol extracts from *C. aspera* aerial parts. Each extract was tested at three concentrations against *Staphylococcus aureus*, *Bacillus subtilis*, *Pseudomonas aeruginosa*, and *Escherichia coli*. The results highlighted that the ethanol extract was particularly potent, displaying the most substantial activity against *P. aeruginosa*, with decreasing effectiveness against *E. coli*, *B. subtilis*, and *S. aureus*. (Khuntia *et al*., 2024).

In a study by *Sirangi et al*. (2017), *Cleome angulata* leaf extracts (n-hexane, ethyl acetate, and methanol) were tested for antimicrobial effects. The methanol extract displayed the most potent activity, yielding a large inhibition zone against *Enterobacter aerogenes*. The other bacteria tested were *B. subtilis*, *S. aureus*, and *E. coli*.

A study assessed the antimicrobial activity of methanolic plant extracts against four types of bacteria and fungi using disc diffusion and micro-broth dilution methods. The *Cleome gynandra* extract showed the strongest antibacterial potency, specifically against *Staphylococcus aureus*. The *C. chelidonii* extract exhibited the maximum antifungal potential,

proving most effective against *Candida albicans*. Both extracts were found to have good antimicrobial activity, effective at low minimum inhibitory concentrations (MICs). (Nimmakayala *et al.*, 2014).

The methanolic leaf extract of *Cleome felina* was rich in phytochemicals and showed significant, albeit moderate, antimicrobial effectiveness at 100 L/mL. The activity was observed against a variety of pathogens, including the bacteria *S. aureus*, *B. cereus*, *E. coli*, and *P. aeruginosa*, and the fungi *Candida albicans* and *C. glabrata* (Shaikh *et al*., 2023).

Broad-spectrum antibacterial activity was observed when testing the ethanol extracts prepared from the roots, stems, leaves, and seeds of *C. rutidosperma* against all six targeted human pathogens. (Arumugam *et al*., 2022).

The highest antibacterial activity among all tested preparations was observed in the *Cleome viscosa* L. methanolic leaf extract, which exceeded the efficacy of the ethanol, acetone, and standard nalidixic acid, notably against *S. aureus* and *Vibrio parahaemolyticus.* (Swaminathan 2017).

Anticancer activities

In MTT (3-(4,5-Dimethylthiazol-2-Yl) 2,5-Diphenyltetrazolium Bromide) assay, the ethanolic extract of aerial *Cleome aspera* parts showed substantial cytotoxic and anticancer effects against human breast cancer cell line i.e. MDA MB 231. The extract's IC_{50} (half-maximal inhibitory concentration) value indicated promising anti-cancer activity with potency comparable to Doxorubicin, a chemotherapy drug (Khuntia *et al*., 2024).

A study by Joseph *et al*. (2014) demonstrated the anticancer effects of *C. felina*, crude leaf extract using ethanol on HepG2 (a human hepatocellular liver carcinoma cell line), with a dose-dependent reduction in cell viability observed in MTT assays.

Budiman *et al.* (2023) isolated chemical compounds and evaluated the cytotoxic activity of the crude hexane extract of *C. rutidosperma* herb (CRH). CRH comprised a range of compounds including 1,2-Benzene dicarboxylic acid and 1,2-bis (2-Ethylhexyl) ester (DEHP), a compound with reported anticancer potential against breast, liver, cervical, and colon cancers, which was isolated and first reported in this species. Cytotoxic activity of CRH tested against MCF-7, A549, KB, KB-VIN, and MDA-MB-231 cancer cells using the sulforhodamine B (SRB) method concluding CRH has the potential for breast cancer treatment.

Researchers evaluated antitumor effect of the fractions of methanol extract using aerial parts of *C. gynandra* against Ehrlich's Ascites Carcinoma (EAC) cell in Swiss albino mice. Further assessed by evaluating tumor volume, viable and nonviable tumor cell count, tumor weight, biochemical, enzymatic and hematological antioxidant parameters of EAC bearing host. To conclude the cytotoxic and antitumor effects by synergistic action of antioxidant flavonoids and saponins (Bala *et al*., 2010).

In a separate study, the anticancer properties of *C. simplicifolia* were evaluated using (MTT) assay on HepG2 cells. The study measured IC_{50} value of methanolic extract of stem and compared its efficacy with standard anti-cancer drug Sorafenib, concluding extract's efficacy as an anticancer agent (Shaikh *et al*., 2025).

Sharma *et al*. (2022) purified bioactive compounds from methanolic extracts from *C. viscosa* leaf through preparative HPLC. Isolated compounds namely, atropine, nevirapine, gallic acid, caffeic acid, vanillic acid, and kaempferitrin were checked against MCF10A (normal cell line)

and BT-474 (breast cancer cell line) by MTT assay. Kaempferitrin, atropine, and vanillic acid showed toxic effects on BT474 breast cancer cells.

Antioxidant activities

The ethanolic extract of the common weed *Cleome monophylla* showed moderate effectiveness in neutralizing DPPH radicals when tested against the standard ascorbic acid. However, it proved to be a potent free radical scavenger, displaying strong activity against nitric oxide radicals and good efficacy against superoxide radicals (Vijayashalini *et al*., 2023).

The aerial parts of *C. aspera* extracted with ethanol demonstrated significant antioxidant activity, likely linked to its high levels of phenolics and flavonoids (Khuntia *et al*., 2024).

Arumugam *et al*. (2022) investigated the antioxidant and antibacterial properties of ethanolic extracts derived from the roots, stems, leaves, and seeds of *Cleome rutidosperma*. The results indicated that the leaf extract exhibited the superior antioxidant capacity across all assays performed, registering the highest values for total antioxidant activity, DPPH scavenging activity and FRAP activity.

Table 2: Pharmacological Activities of Identified active compounds of *Cleome* Species

Scientific name	Chemical constituent	Method of Detection	Active compound	Biological Activity	Used parts	Reference
Cleome monophylla	Essential oil (Volatile compounds)	CG-MS	1-α-terpeneol, 2-dodecanone	Rhipicephalus appendiculatus (livestock tick), Sitophillus zeamais (maize weevil)	Arial parts	Ndungu *et al*., 1995
Cleome chelidonii	Flavonol	2D NMR experiment and HR-ESI-MS	3-O-acetyl-rhamnose	Anti-radical	Arial parts	Nguyen *et al*., 2017
	Flavonol	HR-ESI-MS, NMR	kaempferol 3-O-β-D-glucopyranoside 7-O-α-L-rhamnopyranoside	Hepatoprotective	Stem	Phan *et al*., 2021
Cleome felina	Volatile compounds	GC-MS	1, 6-Anhydro- β-d-talopyranose and n-Hexadecanoic acid	Hepatoprotective and antimicrobial	Leaves	Shaikh *et al*., 2023
Cleome simplicifolia	Volatile compounds (Terpene)	GC-MS	Undecane, Neophytadiene, n-Hexadecanoic acid and phytol.	Antioxidant and Hepatoprotective	Leaves	Shaikh *et al*., 2024
Cleome Viscosa	Flavonol	HR-ESI-MS, NMR	visconoside A	Hepatoprotective	Stem	Phan *et al*., 2021

Other pharmacological activities

Cleome species, including *C. chelidonii, C. felina, C. simplicifolia*, and *C. viscosa*, have demonstrated potential hepatoprotective effects in both in vitro and in vivo studies, attributed to their rich phytochemical composition, including flavonoids, polyphenols, and terpenoids,

C. felina: Methanolic leaves extract showed significant hepatoprotective activity by reducing serum biochemical markers (AST, ALT, ALP, total bilirubin, and cholesterol) and elevating antioxidant enzymes (SOD, CAT, and GSH) in Wister albino rats.

C. chelidonii: Methanolic stem extracts exhibited hepatoprotective activity against CCl4-induced liver toxicity in rats and HepG2 cells.

C. viscosa: Ethanolic extract of leaves and seeds showed hepatoprotective effects against CCl4-induced hepatotoxicity in rats.

Conclusion

This paper thoroughly discusses the extensive therapeutic potential, phytochemistry, and pharmacological activity demonstrated by various *Cleome* species. Despite the promising findings, it is important to note that the *Cleome* family remains largely under-researched, with only a limited number of species having undergone medical and pharmacological investigation. Therefore, to fully unlock the medicinal potential suggested by their current pharmacological properties, further toxicological and clinical studies are essential.

Reference

1. Arumugam R., Elanchezhian B., Samidurai J., & Amirthaganesan K. (2022). Comparative antioxidant, antibacterial and phytochemical analysis of roots, stems, leaves and seeds from *Cleome rutidosperma* DC. Natural Resources for Human Health 2(4):479-484.
2. Bala A., Kar B., Haldar P., Mazumder U., & Bera S. (2010). Evaluation of anticancer activity of *Cleome gynandra* on Ehrlich's Ascites Carcinoma treated mice. J Ethnopharmacol 129(1):131-134.
3. Budiman Y., Rahim A., Lallo S., Saito Y., Nakagawa-Goto K., Rohman A., & Alam G. (2023). Cytotoxicity Activity, Metabolite Profiling, and Isolation Compound from Crude Hexane Extract of *Cleome rutidospermae*. Asian Pac J Cancer Prev, 24 (10):3345-3352.
4. Joseph M., Ramani A., & Charles A. (2014). The anticancer activity of ethanolic extract of *Cleome felina* linn. Journal of Pharmacy Research 8(9):1223-1225.
5. Khuntia A., & Kathiravan M.K. (2024). GC-MS Chemical Profiling, Antifungal and Antioxidant Activity of *Cleome aspera* Aerial Parts Extracts. Asian Journal of Chemistry 37(1): 69-74.
6. Ndungu M., Lwande W., Hassanali A., Moreka L., & Chhabra S. C. (1995). *Cleome monophylla* essential oil and its constituents as tick (*Rhipicephalus appendiculatus*) and maize weevil (*Sitophilus zeamais*) repellents. Entomologia Experimentalis et Applicata 76: 217-222.
7. Nguyen P., Sayagh C., Borie N., & Lavaud C. (2017). Anti-radical flavonol glycosides from the aerial parts of *Cleome chelidonii* L.f. Phytochemistry 142: 30-37.
8. Nguyen T., Mai D., Tuoi Do., & Phan N. (2017). Flavonoids with Hepatoprotective Activity from the Leaves of *Cleome chelidonii*. Natural Product and Communications 12(7):1061-1063.

9. Nimmakayala S. N., Bondada S., Donthamsetti S., & Kanthal L. (2014). In vitro antimicrobial screening of methanolic extracts of *Cleome chelidonii* and *Cleome gynandra*. Bangladesh Journal Pharmacology 9: 161-166.
10. Phan N., Tuoi Do T., Nguyen L., Nguyen T., Ngo Q., Tran T., Nguyen Q., Huynh B., Nguyen D., Bui T., Mai D. & Nguyen T.(2021). Hepatoprotection and Phytochemistry of the Vietnamese Herbs *Cleome chelidonii* and *Cleome viscosa* Stems. Journal of Chemistry 2021, 1-8.
11. POWO. 2025. Plants of the World Online, Royal Botanic Garden, Kew. http://powo.science.kew.org/ Accessed on 07.10.2025.
12. Shaikh H., Niazi S., Rudrappa M., Bepari A., Assiri R., Chavhan M., Basavarajappa D. & Agadi S. (2024). Phytochemical Screening, GCMS Profiling, In Vitro Antioxidant, In Vivo Acute Toxicity, and Hepatoprotective Activity of *Cleome simplicifolia* Bioactive Metabolites against Paracetamol-Intoxicated Wister Albino Rats. Applied Science 14(1): 46.
13. Shaik N., Shaikhb H., Rudrappab M., Beparid A., Altamimie H., Rudrakshib P., Nayakab S., & Agadib S. (2025). Comprehensive evaluation of phytochemicals from *Cleome simplicifolia* stem for its In-vitro antioxidant, anticancer efficacy on HepG2 Cells, In-silico molecular docking and In-vivo hepatoprotective activity against CCl4 induced hepatotoxicity in Swiss albino mice. Appl. Sci. 14:46.
14. Shaikh H., Niazi S., Sheereen S., Bepari A., Hussain S., Rudrappa M., Cordero M., Nagaraja S., & Agadi S. (2023). Biological Characterization of *Cleome felina* L.f. Extracts for Phytochemical, Antimicrobial, and Hepatoprotective Activities in Wister Albino Rats. Antibiotics 12(10): 1506.
15. Sharma H., & Shrivastav A. (2022). HPLC Purification of bio-active *Cleome viscosa* and It's Anticancer Activity against Breast Cancer Cell Lines. Oriental Journal of Chemistry 38(6): 1505-1513.
16. Singh H., Mishra A., & Mishra A. 2018. The chemistry and pharmacology of Cleome genus: A review. Biomedicine & Pharmacotherapy 101(77):37-48.
17. Sirangi S., & Ragan A. (2017). Phytochemical analysis and Evaluation of Antimicrobial activity in Ethnomedicinal herb *Corynandra chelidonii Var. pallae* (Cleomaceae). Journal of Pharmacognosy and Phytochemistry 6(6): 1565-1569.
18. Sucharitha P., Khanam S., Sai Shilpa., Ramya V., Nagaiah V., & Devendra N. (2017). A Review on *Cleome aspera*. World Journal of Pharmaceutical Research 6(3):242-249.
19. Swaminathan C. (2017). Evaluation of Antibacterial and Antioxidant Properties of *Cleome viscosa* L. Indo American Journal of Pharmaceutical Research 7(4):8473-8778.
20. Vijayashalini P., Abirami P., & Menaga S. (2023). In vitro antioxidant activities of *Cleome monophylla* L. A sporadic medicinal herb. International Journal of Botany Studies 8(1): 53-58.
21. Wael A., Wael E., Khaled A., Naglaa M., Naagla Nazif., & Abdel S. (2016). Chemical Constituents and Biological Activities of *Cleome* Genus: A Brief Review. International Journal of Pharmacognosy and Phytochemical Research 8(5): 777-787.
22. Wollenweber E., Valant-Vetschera K., & Roitman J. (2007). Natural Products and Communications 2(10):997-1002.

Ethical Considerations of Genetically Modified Crops: Balancing Innovation and Biosafety

Priyanka Amol Shinde-Avere,
Assistant Professor, Department of Botany, R. P. Gogate College of Arts and Science and R. V. Jogalekar College of Commerce (Autonomous), Ratnagiri-415612, Maharashtra
Mo No: 9518909961

Abstract

Genetically modified (GM) crops, including those developed through genome editing, have emerged as transformative tools to address global challenges such as food insecurity, climate change adaptation, pest and disease pressures, and nutritional deficiencies. Their adoption has demonstrated potential for yield improvement, reduced pesticide use, and enhanced resilience to environmental stressors. However, alongside these benefits, GM crops raise complex ethical, ecological, and regulatory concerns that require careful evaluation. Key issues include biosafety risks such as gene flow to wild relatives, potential effects on non-target organisms, and uncertain long-term ecosystem impacts, as well as broader societal considerations including transparency, consent, intellectual property rights, and equitable access to biotechnology.

This paper reviews the ethical and regulatory dimensions of GM crop deployment, synthesizing insights from recent literature (2023–2025) and global case studies. It highlights how evolving governance frameworks—particularly those addressing genome editing—seek to balance technological innovation with biosafety while responding to diverse public concerns. Five recurring themes are emphasized: risk assessment and biosafety evaluation; ecological sustainability and biodiversity protection; social justice and equitable access; transparency and public trust in regulatory systems; and the role of adaptive regulation in keeping pace with rapid scientific advances.

The analysis suggests that responsible innovation in GM crops requires combining rigorous scientific risk assessment with inclusive governance and ethical reflection. Transparent communication, participatory decision-making, and equitable technology distribution are critical to ensuring that GM crops contribute positively to sustainable agriculture. Ultimately, striking a balance between innovation, ecological safety, and societal legitimacy will shape the long-term contribution of GM crops to food security, environmental resilience, and global sustainability.

Keywords - Genetically modified crops; genome editing; biosafety; biodiversity; ecological sustainability; food security; climate resilience; ethical issues; intellectual property rights; regulatory frameworks; transparency; public trust; responsible innovation; sustainable agriculture

Introduction

The use of genetically modified organisms (GMOs) in agriculture has expanded rapidly since the 1990s, initially through transgenic technologies and more recently through advanced genome editing tools such as CRISPR/Cas. GM crops have been promoted as solutions to pressing global challenges, offering advantages such as higher yields, resistance to pests and diseases, improved tolerance to abiotic stresses like drought and salinity, enhanced nutritional quality, and reduced reliance on chemical inputs. These promises have made GM crops central to debates in food systems and agricultural biotechnology.

However, the rapid adoption of GM technologies has also sparked widespread concerns. Environmental risks such as gene flow, non-target effects, and biodiversity loss remain unresolved, while potential human health impacts, socioeconomic inequality, and ethical responsibility continue to fuel public debate (Verma, 2013; Rozas, Kessi-Pérez & Martínez, 2022). In this context, questions about long-term ecological sustainability and the social legitimacy of GM crops have become as important as their technical performance.

The emergence of genome editing complicates these debates further. Tools like CRISPR/Cas blur traditional boundaries between "conventional" breeding and transgenic modification, raising new challenges for regulation and governance (Caradus, 2023). These innovations not only promise greater precision but also demand rethinking how society defines, regulates, and ethically evaluates genetic modification in agriculture.

Against this backdrop, it is essential to examine the ethical and biosafety dimensions of GM crop deployment within both historical experiences and recent scientific advances. This paper explores key issues including ecological risk assessment, regulatory frameworks, social justice, transparency, and public trust. By drawing on recent literature and case studies, it proposes guiding principles and policy recommendations to help reconcile agricultural biotechnology with societal values and environmental stewardship.

Key Ethical and Biosafety Issues

2.1 Human Health Risks

Although genetically modified (GM) crops undergo rigorous safety assessments, concerns persist regarding their potential impacts on human health. Key issues include allergenicity, toxicity, and unintended effects from novel proteins or metabolites. Public concerns often highlight uncertainties about long-term consumption, and critics argue that safety testing may be insufficient or biased (Verma, 2013). While many of these risks remain hypothetical, they strongly influence consumer perceptions and trust. Recent studies recommend the use of multi-omics approaches—such as transcriptomics, metabolomics, and proteomics—to detect subtle metabolic changes that conventional toxicological assessments may overlook (Benevenuto et al., 2023).

2.2 Environmental and Ecological Impacts

Environmental risks represent one of the most debated aspects of GM crop deployment. Gene flow, where transgenes transfer to wild relatives, can lead to ecological disruption and the spread of traits such as herbicide resistance. Non-target effects—such as unintended impacts on beneficial insects, pollinators, and soil microbes—remain a significant concern. Additionally, large-scale cultivation of GM crops may accelerate biodiversity loss by displacing local landraces and reducing genetic diversity. While GM crops can reduce pesticide use, broader ecological sustainability must be carefully evaluated (Wei & Stewart, 2023; Discover Agriculture, 2025).

2.3 Socioeconomic Justice and Equity

Beyond biosafety, GM crops raise profound questions of equity and justice. The patenting of GM seeds often restricts traditional practices such as seed saving, limiting farmer autonomy. This dynamic disproportionately benefits large agribusinesses while placing smallholder farmers, particularly in the Global South, at a disadvantage. Concerns also extend to consumer rights, including labeling, informed consent, and freedom of choice. Bekele-Alemu et al. (2025) emphasize the need to "harmonize discourse" so that GM technology contributes to inclusive agricultural development rather than exacerbating existing inequalities.

2.4 Regulation and Governance

Global regulatory systems for GM crops remain fragmented and inconsistent. While some countries adopt precautionary principles, others pursue more innovation-friendly approaches. This variability creates uneven market access and uncertainty for farmers and developers alike (Rozas, Kessi-Pérez & Martínez, 2022; Caradus, 2023). The rise of genome-editing tools such as CRISPR/Cas further complicates regulation, as these methods blur distinctions between conventional breeding and genetic modification. Central ethical questions include who bears responsibility if unintended effects occur, and how best to balance precaution with innovation in the face of food insecurity and climate stress.

2.5 Public Perception, Transparency, and Trust

Public skepticism continues to shape the future of GM crops. Concerns are often amplified by a lack of transparency, perceived conflicts of interest, and limited opportunities for public participation in decision-making. Verma (2013) highlights the persistent gap between scientific risk assessments and public perceptions of risk. More recently, bibliometric analyses (2024) show that ethical debates increasingly focus on the environmental unknowns of CRISPR applications and the importance of social acceptability. Building public trust requires transparent communication, robust labeling systems, and genuine dialogue between scientists, policymakers, and society at large.

Together, these ethical and biosafety issues illustrate that the debate over GM crops extends far beyond technical risk assessments. Human health concerns, ecological uncertainties, socioeconomic inequalities, regulatory inconsistencies, and public mistrust are deeply interconnected. Each dimension influences how GM technologies are perceived, governed, and ultimately adopted in different contexts. Addressing these challenges requires not only scientific innovation but also transparent governance, equitable access, and meaningful public engagement. In the following section, case studies and recent literature will be examined to illustrate how these ethical and biosafety questions play out in practice, offering insights into potential pathways for more responsible and socially aligned use of plant genetic engineering.

3. Case Studies

3.1 GM Crop Adoption in Developing Countries

In many developing countries, GM crop adoption has proceeded even where biosafety infrastructure is weak or regulatory systems are underdeveloped. Studies document instances of unauthorized seed release, limited oversight, and political ambivalence, raising ethical concerns about risk governance (Terefe, 2018). These contexts highlight the tension between urgent food security needs and potential biosafety risks. While farmers may embrace GM crops for their agronomic benefits, weak regulation heightens risks of unintended ecological or social consequences, emphasizing the importance of robust institutional frameworks.

3.2 Ethiopia's GM Crops and Biosafety Debates

Ethiopia provides a concrete example of how GM adoption intersects with local norms, biosafety regulations, and food security imperatives. National debates highlight concerns around environmental risks, health impacts, and economic dependence, alongside recognition of the potential benefits for yield and resilience. Terefe (2018) documents how local biosafety frameworks are still evolving, and how ethical concerns are shaped by Ethiopia's unique agricultural and cultural context. This case underscores that the ethics of GM crops are not universal but deeply context-specific.

3.3 Regulation of Genome-Edited Crops

The emergence of genome editing, particularly CRISPR/Cas, complicates long-standing regulatory categories. Unlike transgenic crops, many genome-edited crops do not involve the introduction of foreign DNA, raising questions about whether they should be regulated as "GMOs." Rozas et al. (2022) emphasize that adapting regulatory frameworks to these evolving techniques is critical to ensure both scientific rigor and public trust. Ethical debates increasingly center on transparency, definitions of risk, and how to balance precaution with innovation.

3.4 Bt Cotton in India

Bt cotton, engineered to express *Bacillus thuringiensis* toxin for pest resistance, is among the most extensively studied GM crops. Its introduction in India led to reduced pesticide use and higher yields, boosting farmer incomes (Kathage & Qaim, 2012). Yet over time, challenges emerged: secondary pests required renewed pesticide applications, and cases of farmer indebtedness highlighted inequities tied to seed pricing and corporate control. This case illustrates how GM crops can simultaneously deliver agronomic benefits while raising ethical concerns about farmer autonomy, sustainability, and socioeconomic justice.

3.5 Golden Rice

Golden Rice was developed to address vitamin A deficiency in Asia and Africa by biofortifying rice with provitamin A. Despite its humanitarian promise, the crop faced decades of delays due to regulatory hurdles, political resistance, and public skepticism (Dubock, 2019). Critics argued that non-technological interventions, such as dietary diversification, might be more culturally acceptable. Golden Rice highlights how ethical and governance challenges—rather than technical feasibility alone—can determine the trajectory of GM innovations.

3.6 Herbicide-Tolerant Soybeans

Herbicide-tolerant (HT) soybeans, particularly glyphosate-resistant varieties, became widespread in the Americas due to their efficiency in weed management. While they initially reduced labor and input costs, overreliance on glyphosate led to the emergence of resistant weed species, undermining sustainability (Heap, 2014). Moreover, monoculture expansion associated with HT crops has raised biodiversity concerns. This case underscores the importance of adaptive management and ecological monitoring in large-scale GM crop deployment.

3.7 CRISPR-Edited Crops

CRISPR-edited crops, such as non-browning mushrooms, drought-tolerant maize, and disease-resistant cassava, represent a new frontier in agricultural biotechnology. Because these crops may not involve transgenes, they challenge conventional regulatory and ethical categories (Caradus, 2023). While the technology offers precision and efficiency, societal acceptance depends less on technical safety and more on issues of fairness, inclusivity, and environmental responsibility. Bibliometric analyses (2024) show that public debates increasingly focus on transparency and the social legitimacy of genome editing.

Taken together, these case studies illustrate the complexity of evaluating GM crops. In developing countries such as Ethiopia, biosafety concerns intersect with food security needs and fragile regulatory systems. Global debates around Bt cotton, Golden Rice, and HT soybeans reveal recurring tensions between short-term agronomic gains and long-term ecological or social risks. CRISPR-edited crops, meanwhile, showcase both the potential of

precision technologies and the need for adaptive governance frameworks. Collectively, these examples reinforce that plant genetic engineering cannot be assessed solely on productivity metrics; its ethical, ecological, and social dimensions are equally critical for shaping sustainable and responsible innovation.

4. Balancing Innovation and Biosafety: Existing Frameworks

4.1 International Frameworks

The Cartagena Protocol on Biosafety, adopted in 2000 under the Convention on Biological Diversity, is the primary international treaty addressing the safe transfer, handling, and use of living modified organisms (LMOs). It embodies the precautionary principle, requiring advance informed agreement procedures before cross-border movement of LMOs. While influential, the protocol has been criticized for leaving significant room for interpretation, particularly regarding risk thresholds and enforcement mechanisms. Emerging genome-editing technologies complicate compliance further, since many edited crops do not fit neatly into existing definitions of genetically modified organisms (Wikipedia, 2025).

4.2 Risk Assessment and Adaptive Regulation

Biosafety frameworks typically rely on risk assessment and management guidelines that evaluate potential toxicity, allergenicity, environmental impact, and socio-economic consequences, alongside requirements for post-release monitoring (IntechOpen, 2021). However, recent scholarship emphasizes that these frameworks must evolve in step with scientific and technological advances. Rozas et al. (2022) and Caradus (2023) argue for adaptive and proportionate regulation that can distinguish between traditional transgenic methods and newer, more precise genome-editing tools. Such approaches allow regulators to balance innovation with safety by considering both potential risks and societal benefits, rather than applying uniform restrictions.

4.3 Responsible Research and Innovation

Beyond formal regulation, ethical frameworks such as Responsible Research and Innovation (RRI) offer pathways to align biotechnology with societal values. Biddle (2017) highlights four key dimensions: anticipation of potential risks, reflection on ethical implications, inclusive participation of stakeholders, and accountability in decision-making. This framework encourages a shift from polarized “pro-GM vs anti-GM” debates toward more nuanced engagement. Building on this, Bekele-Alemu et al. (2025) stress that discourse around plant genetic engineering should promote inclusivity and equitable outcomes, ensuring that technological innovation serves broader goals of sustainability and social justice.

5. Proposed Ethical Principles and Best Practices

Building on the literature review, several ethical principles and best practices can help ensure that genetically modified (GM) crops are developed and deployed in ways that balance innovation with biosafety and social responsibility. These principles emphasize not only scientific rigor but also transparency, equity, and sustainability.

5.1 Transparency and Public Engagement

Transparent communication is critical to bridging the gap between scientific risk assessments and public perception. Open access to safety data, clear labeling, and participatory decision-making processes build trust and empower stakeholders. Inclusion of farmers, local communities, and consumers in governance frameworks helps ensure that GM crop adoption reflects diverse needs and values rather than top-down technological imposition.

5.2 Robust Risk Assessment and Monitoring

Risk assessment must be science-based, comprehensive, and dynamic. Pre-release testing should cover toxicity, allergenicity, and environmental impacts, while post-release surveillance is essential for identifying long-term ecological effects. Advanced methods, including multi-omics approaches, can detect subtle changes in metabolic and ecological pathways that conventional assessments may miss (Benevenuto et al., 2023). Long-term ecological monitoring strengthens accountability and safeguards public and environmental health.

5.3 Proportional and Adaptive Regulation

Given the diversity of genetic engineering methods, regulation should be proportional to the risks posed. Transgenic crops may warrant stricter oversight than genome-edited crops that mimic conventional breeding. Adaptive governance allows frameworks to evolve in response to emerging evidence and new technologies (Rozas et al., 2022; Caradus, 2023). This flexibility balances precaution with innovation, avoiding both under- and over-regulation.

5.4 Equity, Access, and Justice

Equitable access is central to ensuring that the benefits of GM crops are shared fairly. Smallholder farmers must not be disadvantaged by restrictive intellectual property regimes, high seed costs, or corporate concentration of power. Fair pricing models, licensing practices, and policies supporting farmer autonomy are crucial to prevent widening inequalities, particularly in the Global South.

5.5 Environmental Stewardship

GM crop deployment must prioritize ecological sustainability. Key practices include minimizing non-target and off-target effects, preventing gene flow to wild relatives, and maintaining biodiversity at both local and global scales. Broader ecological sustainability, rather than narrow productivity metrics, should guide decisions (Discover Agriculture, 2025).

5.6 Ethical Responsibility of Developers

Developers of GM crops bear an ethical responsibility to anticipate unintended consequences, avoid overstating benefits, and acknowledge uncertainties. Accountability should extend beyond the point of commercialization, ensuring that those who introduce new technologies remain engaged in monitoring and mitigation. Responsible innovation requires humility, reflection, and commitment to the public good.

Discussion

Balancing the potential benefits of genetically modified (GM) crops with ethical and biosafety concerns remains a complex challenge. In many developing countries, delays in adopting GM technologies can come at the cost of food security, yield stability, or resilience against pests and climate stress. At the same time, weak regulatory oversight may heighten ecological and health risks, while overly restrictive regulation can discourage beneficial innovation and limit access to potentially transformative technologies.

The emergence of genome editing further complicates these debates. When no foreign DNA is introduced, questions arise as to whether such crops should be regulated differently from transgenic organisms. This raises ethical concerns about regulatory fairness and consistency, particularly given the rapid pace of technological change. Moreover, the uneven distribution of risks and benefits amplifies issues of social justice: wealthier farmers may better absorb

uncertainties, while smallholders—often those most in need of resilient crops—may bear disproportionate risks.

Public trust plays a decisive role in the governance of GM crops. Lack of transparency, insufficient engagement, or poor communication of adverse events can fuel public backlash, sometimes halting the adoption of technologies that could offer real benefits. The debate is therefore no longer simply about whether GM crops are "safe" but about how they can be governed responsibly.

Recent advances in risk assessment—such as omics-based approaches and long-term ecological monitoring—make evaluations more precise, yet they also reveal new complexities that resist simple conclusions. Ethically, the key question is how to balance the global imperative of ensuring food security and climate resilience with local concerns for biosafety, ecological sustainability, and community autonomy.

Persistent polarization has often hindered constructive dialogue. Moving forward, a more nuanced ethical framework is needed—one that integrates scientific evidence with public values, ensures fairness in risk-sharing, and fosters responsible innovation. Such an approach can create space for the cautious but beneficial adoption of GM crops, without disregarding legitimate risks or societal concerns.

Conclusion

Genetically modified (GM) crops and emerging gene-editing technologies hold significant potential to address pressing global challenges, including food security, climate change resilience, and nutritional deficiencies. However, their benefits cannot be fully realized without careful attention to biosafety risks and ethical considerations. The path forward requires more than a binary debate over whether GM technologies are inherently "good" or "bad." Instead, it demands a commitment to how responsibly they are designed, implemented, and governed.

Well-designed regulatory frameworks, grounded in adaptive and proportional oversight, are essential to ensure safety without stifling innovation. Transparency in data, meaningful stakeholder engagement, and robust pre- and post-release monitoring are equally critical for building public trust and safeguarding ecosystems. Equally important is the principle of social justice—ensuring that smallholder farmers and vulnerable communities benefit from these technologies rather than being marginalized by them.

Ultimately, the promise of GM crops lies not only in their scientific potential but in the ethical and inclusive frameworks that guide their use. By integrating robust science, adaptive governance, and public values, societies can move toward a more balanced and responsible future for plant genetic engineering—one that advances innovation while protecting both people and the planet.

References

1. Bekele-Alemu, A., et al. (2025). Rethinking progress: Harmonizing the discourse on genetically modified crops. *Frontiers in Plant Science.* https://doi.org/10.3389/fpls.2025.1547928
2. Benevenuto, R. F., Zanatta, C. B., Waßmann, F., et al. (2023). Integration of omics analyses into GMO risk assessment in Europe: A case study from soybean field trials. *Environmental Sciences Europe, 35,* 14. https://doi.org/10.1186/s12302-023-00715-6
3. Biddle, J. B. (2017). Genetically engineered crops and responsible innovation. *Journal of Responsible Innovation, 4*(1), 24–42. https://doi.org/10.1080/23299460.2017.1287522

4. Caradus, J. R. (2023). Processes for regulating genetically modified and gene-edited plants. *GM Crops & Food.* https://doi.org/10.1080/21645698.2023.2252947
5. Dubock, A. (2019). The present status of Golden Rice. *Journal of Human Nutrition and Dietetics, 32*(2), 272–282. https://doi.org/10.1111/jhn.12660
6. Heap, I. (2014). Global perspective of herbicide-resistant weeds. *Pest Management Science, 70*(9), 1306–1315. https://doi.org/10.1002/ps.3696
7. Kathage, J., & Qaim, M. (2012). Economic impacts and impact dynamics of Bt cotton in India. *Proceedings of the National Academy of Sciences, 109*(29), 11652–11656. https://doi.org/10.1073/pnas.1203647109
8. Mishra, M., & Kumari, S. (2018). Biosafety issues related to genetically engineered crops. *MOJ Research Review, 1*(6), 272–276.
9. Rozas, P., Kessi-Pérez, E. I., & Martínez, C. (2022). Genetically modified organisms: Adapting regulatory frameworks for evolving genome editing technologies. *Biological Research, 55,* 31. https://doi.org/10.1186/s40659-022-00399-x
10. Terefe, M. (2018). Biosafety issues of genetically modified crops: Potential risks and status of GM crops in Ethiopia. *Research Journal of Agriculture & Forestry Sciences, 6*(10), 6–11.
11. Verma, S. R. (2013). Genetically modified plants: Public and scientific perceptions. *ISRN Biotechnology,* Article ID 820671. https://doi.org/10.5402/2013/820671
12. Wei, W., & Stewart, C. N. Jr. (2023). Biosafety and ecological assessment of genetically engineered and edited crops. *Plants, 12*(13), 2551. https://doi.org/10.3390/plants12132551
13. *Necessities, environmental impact, and ecological sustainability of genetically modified crops.* (2025). *Discover Agriculture.* https://doi.org/10.1007/s44279-025-00180-0
14. *CRISPR in agriculture and its ethical implications: A bibliometric analysis.* (2024). *Journal of Agriculture & Food Ethics.* https://doi.org/10.1016/j.agfe.2024.100097

Preliminary Phytochemical Screening of *Padina* Species from Sadamirya Beach, Ratnagiri District, Maharashtra, India.

Viraj D. Chabake[1]* and Nidhee P. Nagvekar[2]
[1]*Assistant Professor, Department of Botany, R. P. Gogate College of Arts and Science and R. V. Jogalekar College of Commerce (Autonomous), Ratnagiri-415612, Maharashtra.
[2]Department of Botany, R. P. Gogate College of Arts and Science and R. V. Jogalekar College of Commerce (Autonomous), Ratnagiri-415612, Maharashtra.
*Corresponding author: viraj.chabake@gjcrtn.ac.in
Contact No-9022458777.

Abstract

Marine macroalgae, particularly brown seaweeds of the genus *Padina*, are a globally recognized source of bioactive metabolites, yet the phytochemical profiles of many regional species remain uncharacterized. This study was undertaken to bridge the research gap concerning the *Padina* species found along the Konkan coast. The primary aim was to conduct a preliminary phytochemical screening of *Padina* sp. collected from Sadamirya Beach, Ratnagiri, Maharashtra, India, to identify the major classes of secondary metabolites present.

Samples of *Padina* sp. were collected from the intertidal zone, processed into a dry powder, and used to prepare a crude methanolic extract. This extract was then subjected to a series of standard qualitative chemical tests.

The screening confirmed the presence of several important bioactive classes, including alkaloids, flavonoids, terpenoids, steroids, glycosides, oxalic acid, and coumarins. Notably, the tests indicated the absence of tannins, phenolic compounds, saponins, anthraquinones, and quinones in the extract.

The presence of this diverse array of metabolites highlights the *Padina* species from Sadamirya Beach as a promising, untapped resource for potential pharmacological and biotechnological applications. These findings provide essential baseline data that justify further, more detailed investigations to isolate, purify, and characterize these active compounds and evaluate their therapeutic potential.

Keywords: Seaweeds, *Padina* species, metabolites etc.

Introduction:

Marine macroalgae, commonly referred to as seaweeds, are an important component of coastal ecosystems and a valuable resource due to their nutritional, ecological, and pharmacological properties. They are photosynthetic, multicellular eukaryotes that contribute significantly to primary production in marine habitats. Based on pigmentation and taxonomy, seaweeds are broadly classified into three groups: Chlorophyta (green algae), Phaeophyceae (brown algae), and Rhodophyta (red algae) [1]. Among these, brown algae (*Phaeophyceae*) are particularly rich in bioactive metabolites with diverse therapeutic potentials.

Seaweeds are renewable marine resources that play a crucial role in coastal ecosystems and have been used by humans for centuries as food, feed, fertilizer, and medicine. They are a rich source of proteins, polysaccharides, vitamins, minerals, and trace elements in concentrations much higher than those in terrestrial plants [1]. Besides their nutritional significance, seaweeds are valued for their secondary metabolites, which include alkaloids, flavonoids, terpenoids, steroids, tannins, and phenolic compounds. These phytochemicals exhibit diverse biological

activities such as antioxidant, antimicrobial, anti-inflammatory, anticancer, and antiviral effects [2,3].

Brown algae (*Phaeophyceae*), in particular, are recognized for their high content of phenolic compounds, sulfated polysaccharides, and terpenoids, which provide protection against environmental stresses and contribute to their bioactivity [4]. The genus *Padina* (family Dictyotaceae) is one of the most widely distributed brown seaweeds in tropical and subtropical regions. Species of *Padina* are known to contain bioactive compounds such as fucoidans, flavonoids, diterpenes, sterols, and fatty acids, many of which have demonstrated antimicrobial, antioxidant, and cytotoxic properties [5-6].

India's vast coastline supports a diverse algal flora, yet phytochemical investigations on many species remain limited. The Ratnagiri district along the Konkan coast of Maharashtra represents an ecologically rich habitat due to its tidal variations, rocky substrata, and nutrient availability. Sadamirya Beach, in particular, harbors luxuriant growth of brown seaweeds, including *Padina*, but scientific reports on their phytochemical profiles are scarce. Preliminary screening of seaweed phytochemicals is essential to identify key secondary metabolites and to provide baseline data for further pharmacological and industrial applications [7-10].

Seaweeds have long been utilized as food, fertilizer, and traditional medicine, but in recent decades they have attracted global attention for their pharmacological importance. They are natural sources of polysaccharides, proteins, lipids, polyphenols, flavonoids, sterols, and terpenoids, which exhibit antioxidant, antimicrobial, anti-inflammatory, anticancer, and antidiabetic properties [11-13]. Their secondary metabolites not only play a defensive role against harsh environmental stressors but also serve as promising leads for drug discovery and cosmeceutical applications [14-15].

Marine algae are known for their rich repertoire of bioactive secondary metabolites, such as alkaloids, flavonoids, tannins, saponins, terpenoids, steroids, glycosides, and other phenolic compounds, which contribute to their therapeutic potential [16-17]. These metabolites play critical roles in plant defense and exhibit diverse pharmacological activities including antimicrobial, antioxidant, anti-inflammatory, and anticancer effects [18].

The genus *Padina* (family Dictyotaceae) is a widely distributed brown alga characterized by its calcified thallus and fan-shaped fronds. It occurs predominantly in tropical and subtropical waters, including the western coast of India. Species of *Padina* are reported to contain phenolic compounds, sulfated polysaccharides, diterpenes, sterols, and fatty acids, many of which possess biological activities such as antimicrobial, antioxidant, and cytotoxic effects [19-20]. Despite their abundance along the Ratnagiri coastline of Maharashtra, studies on the phytochemical profile of *Padina* species from this region remain scarce.

The Ratnagiri district, located along the Konkan coast of Maharashtra, provides a unique marine habitat with diverse seaweed flora due to its tropical climate, tidal variations, and nutrient-rich waters. Sadamirya Beach, in particular, supports luxuriant growth of several macroalgae, yet limited scientific documentation exists on the chemical constituents of these species. Phytochemical investigations of locally available seaweeds are crucial not only to validate their traditional uses but also to explore novel bioactive compounds of pharmacological and industrial relevance.

Therefore, the present study was undertaken to carry out a preliminary phytochemical screening of *Padina* species collected from Sadamirya Beach, Ratnagiri district, Maharashtra, India. This investigation aims to identify the presence of key secondary metabolites and provide baseline data for future detailed biochemical and pharmacological studies.

Materials and Methods :

Figure : 1 *Padina* Sps.

Collection and Preparation of Samples:

Padina species were collected from Sadamirya Beach, Ratnagiri district, Maharashtra, India. Samples were washed thoroughly with seawater to remove sand and debris and air-dried at room temperature. The dried samples were powdered using a mechanical grinder.

Extraction of Phytochemicals:

Powdered samples were subjected to extraction using solvents of varying polarity, including methanol, chloroform, and acetone. The extracts were filtered and concentrated under reduced pressure using a rotary evaporator. Crude extracts were stored at 4°C until further analysis.

Preliminary Phytochemical Screening:

Standard qualitative tests were performed to detect the presence of alkaloids, flavonoids, tannins, saponins, terpenoids, steroids, glycosides, anthraquinones, coumarins, and quinones. Alkaloids were detected using Dragendorff, Mayer's, and Wagner's tests. Flavonoids were identified by lead acetate, NaOH, and $FeCl_3$ tests. Tannins and phenolic compounds were detected using lead acetate, iodine, and dilute HNO_3 tests. Terpenoids, saponins, steroids, oxalic acid, glycosides, anthraquinones, coumarins, and quinones were confirmed using their respective standard tests. Various tests are summarized in Table 1 [1-3].

Sr. No.	Test	Procedure / Observation	Inference / Result
1	**Test for Alkaloids**		
A	Dragendorff Test	Extract + 1% HCl, shake well and filter; add few drops of Dragendorff reagent.	Orange brown precipitate formed.
B	Wagner's Test	Extract + 1% HCl, shake well and filter; add few drops of Wagner's reagent.	Reddish brown precipitate.

2	**Test for Flavonoids**		
A	Lead Acetate Test	Extract + few drops of 10% lead acetate solution.	Yellow colour precipitate.
B	NaOH Test	Extract + NaOH.	Yellow colour.
C	$FeCl_3$ Test	Extract + $FeCl_3$.	Intense green colour.
3	**Test for Tannins and Phenolic Compounds**		
A	Lead Acetate Test	Extract + 10% lead acetate solution.	White precipitate.
B	Dilute Iodine Solution Test	Extract + dilute iodine solution.	Transient red colour.
C	Dilute HNO_3 Test	Extract + dilute HNO_3.	Reddish to yellow colour.
4	Test for Terpenoids	Extract + 2 ml chloroform + 2 ml conc. H_2SO_4.	Reddish brown colour.
5	Test for Saponins	Froth formation test: Extract + 1 ml water + 1 ml distilled water, shake and warm in water bath.	Froth persists.
6	Test for Steroids (Salkowski Test)	Extract + 2 ml chloroform + 2 ml conc. H_2SO_4, shake well.	Chloroform layer appears red; acid layer shows greenish yellow fluorescence.
7	Test for Oxalic Acid	Extract + few drops of 1% $KMnO_4$ and dilute H_2SO_4.	Colour of $KMnO_4$ disappears immediately.
8	Test for Glycosides (Deoxysugars Test)	Extract + glacial acetic acid + one drop of 5% $FeCl_3$ + conc. H_2SO_4.	Reddish brown colour at junction; upper layer bluish green.
9	Test for Anthraquinones (Borntrager's Test)	Extract + 5 ml chloroform, shake 5 min; filter; filtrate + equal volume of 10% ammonia solution.	Pink, violet, or red colour in lower layer indicates presence of anthraquinone.
10	Test for Coumarins	Extract + 1 ml of 10% NaOH.	Formation of yellow colour.
11	Test for Quinones	Extract + conc. H_2SO_4.	Formation of red colour.

Results

The preliminary phytochemical screening of *Padina* species revealed the presence of multiple bioactive compounds. Alkaloids were confirmed through Dragendorff, Mayer's, and Wagner's tests, showing orange-brown, cream-white, and reddish-brown precipitates, respectively [21-22]. Flavonoids were detected by lead acetate, NaOH, and $FeCl_3$ tests, producing yellow precipitates, yellow coloration, and intense green coloration [23]. Tannins and phenolic compounds were absent, indicated by white precipitate with lead acetate, transient red colour with iodine, and reddish-to-yellow colour with dilute HNO_3 [24]. Terpenoids gave a reddish-brown colour upon reaction with chloroform and concentrated H_2SO_4, while saponins were absent [25]. Steroids were detected using the Salkowski test, showing red coloration in the chloroform layer and greenish-yellow fluorescence in the acid layer [21]. Oxalic acid was confirmed by immediate disappearance of $KMnO_4$ colour. Glycosides (deoxysugars) showed reddish-brown colour at the junction with bluish-green upper layer. Coumarins, were also present, producing pink-violet/red, yellow, and red colourations, respectively [22, 25].

Table 1: Preliminary Phytochemical Screening for Different Phytochemicals

TEST	OBSERVATION	INFERENCE
TEST FOR ALKALOIDS		
Dragendorff Test	Extract + 1% HCL shake well and filtrate few drops of Dragendorff reagent.	Orange brown ppt is formed.
Mayer's Test	Extract + 1% HCL dropwise, keep in steam bath for 20 min. Filter the solution. Filter + few drops of Mayer's reagent.	Gives cream white ppt.
Wagner's Test	Extract + 1% HCL shake well and filtrate few drops of Wagner's reagent.	Gives reddish brown ppt.
TEST FOR FLAVONOID		
Lead acetate test	Extract + few drops of 10% lead acetate solution.	Yellow colour ppt
	Extract + NaoH	Yellow colour.
	Extract + $FeCl_3$	Intense green colour
Test for Tannins and Phenolic compound		
Lead acetate test	Extract + 10% lead acetate solution.	ABSENT
	Extract + Dilute Iodine solution	ABSENT
	Extract + Dilute HNO_3	ABSENT
TERPENOIDS		
-	Extract + 2ml chloroform + 2ml Conc.H_2SO_4	Reddish brown colour.
SAPONINS		
Froth formation test	Extract + 1ml + 1ml D/W shake and warm in water bath.	ABSENT

TEST FOT STEROID		
Salkowski Test	Extract + 2ml of chloroform + 2ml of conc.H_2SO_4 and shake well.	Chloroform layer appears red and acid layer shows greenish yellow fluorescence.
TEST FOR OXALIC ACID		
-	Extract + few drops of 1% $KMnO_4$ and dil. H_2SO_4.	Colour of $KMnO_4$ disappear immediately.
TEST FOR GLYCOSIDES		
Test for deoxysugars	Extract + glacial acetic acid, one drop of 5 % FeCl3 and H_2SO_4.	Reddish brown colour appears at junction of the two liquid layers and upper layer appears bluish green.
TEST FOR ANTHRAQUINONE		
Borntragers Test	Extract taken into a dry test tube and 5ml of chloroform was added and shaken for 5 minutes. The extract was filtered and the filtrate was shaken with equal volume of 10 % ammonia solution.	ABSENT
TEST FOR COUMARINS		
For coumarins	Extract + 1ml of 10 % NaOH.	Formation of yellow colour
TEST FOR QUINONES		
For Quinone	Extract + conc.H_2SO_4	ABSENT

Discussion

The present study confirms that *Padina* species from Sadamirya Beach contain a wide range of bioactive metabolites, consistent with previous studies on other *Padina* species [26-29]. Alkaloids, flavonoids, tannins, and saponins are well-documented for their antimicrobial, antioxidant, and anti-inflammatory activities [30-33]. Terpenoids and steroids contribute to cytotoxic and anti-cancer potential, [34-37] while glycosides, anthraquinones, coumarins, and quinones are known for their diverse pharmacological roles [38-41]. The detection of these compounds supports the potential use of *Padina* species as a source of bioactive agents for pharmaceutical and biotechnological applications. Further studies involving isolation, purification, and bioactivity assays of individual compounds are recommended to explore their therapeutic potential.

Conclusion

The preliminary phytochemical analysis of *Padina* species from Sadamirya Beach, Ratnagiri district, Maharashtra, India, revealed the presence of multiple bioactive compounds including alkaloids, flavonoids, tannins, saponins, terpenoids, steroids, glycosides, anthraquinones, coumarins, and quinones. These findings highlight the pharmacological and biotechnological

significance of *Padina* species and provide a foundation for future research on isolation and characterization of bioactive metabolites.

References

1. Dawczynski, C., Schubert, R., & Jahreis, G. (2007). Amino acids, fatty acids, and dietary fibre in edible seaweed products. *Food Chemistry, 103*(3), 891–899. https://doi.org/10.1016/j.foodchem.2006.09.041
2. Cardozo, K. H. M., Guaratini, T., Barros, M. P., Falcão, V. R., Tonon, A. P., Lopes, N. P., Campos, S., Torres, M., Souza, A. O., Colepicolo, P., & Pinto, E. (2007). Metabolites from algae with economical impact. *Comparative Biochemistry and Physiology Part C: Toxicology & Pharmacology, 146*(1–2), 60–78. https://doi.org/10.1016/j.cbpc.2006.05.007
3. Ganesan, P., Kumar, C. S., & Bhaskar, N. (2008). Antioxidant properties of methanol extract and its solvent fractions obtained from selected Indian red seaweeds. *Bioresource Technology, 99*(8), 2717–2723. https://doi.org/10.1016/j.biortech.2007.07.005
4. Chakraborty, K., Joseph, D., & Joy, M. (2015). Antimicrobial activities of brown seaweed (*Padina tetrastromatica*) against human pathogens. *Brazilian Journal of Pharmacognosy, 25*(6), 657–664. https://doi.org/10.1016/j.bjp.2015.07.024
5. Manivannan, K., Thirumaran, G., Devi, G. K., Anantharaman, P., & Balasubramanian, T. (2008). Proximate composition of different groups of seaweeds from Vedalai coastal waters (Gulf of Mannar, India). *Middle-East Journal of Scientific Research, 3*(1), 13–17.
6. Pereira, L. (2018). Seaweeds as source of bioactive substances and skin care therapy – Cosmeceuticals, algotheraphy, and thalassotherapy. *Cosmetics, 5*(4), 68. https://doi.org/10.3390/cosmetics5040068
7. Rajauria, G., & Abu-Ghannam, N. (2013). Isolation and partial characterization of bioactive fucoxanthin from brown seaweed *Himanthalia elongata*. *Journal of Functional Foods, 5*(1), 590–597. https://doi.org/10.1016/j.jff.2012.11.001
8. Sathya, R., Kanaga, N., Sankar, P., Jeeva, S., & Rajkumar, J. (2017). Screening of phytochemical and antimicrobial activity of *Padina tetrastromatica* Hauck against clinical pathogens. *Asian Pacific Journal of Tropical Medicine, 10*(1), 29–34. https://doi.org/10.1016/j.apjtm.2016.11.011
9. Murugesan, S., Bhuvaneswari, S., Sivamurugan, V., & Chandrasekaran, M. (2011). Antioxidant activity of some edible seaweeds from Tuticorin coast. *Advances in Biological Research, 5*(1), 9–14.
10. Zubia, M., Fabre, M. S., Kerjean, V., Lann, K. L., Stiger-Pouvreau, V., Fauchon, M., & Deslandes, E. (2009). Antioxidant and antitumoural activities of some Phaeophyta from Brittany coasts. *Food Chemistry, 116*(3), 693–701. https://doi.org/10.1016/j.foodchem.2009.03.024
11. Cardozo, K. H. M., Guaratini, T., Barros, M. P., Falcão, V. R., Tonon, A. P., Lopes, N. P., Campos, S., Torres, M., Souza, A. O., Colepicolo, P., & Pinto, E. (2007). Metabolites from algae with economical impact. *Comparative Biochemistry and Physiology Part C: Toxicology & Pharmacology, 146*(1–2), 60–78.
12. Ganesan, P., Kumar, C. S., & Bhaskar, N. (2008). Antioxidant properties of methanol extract and its solvent fractions obtained from selected Indian red seaweeds. *Bioresource Technology, 99*(8), 2717–2723.
13. Zubia, M., Fabre, M. S., Kerjean, V., Lann, K. L., Stiger-Pouvreau, V., Fauchon, M., & Deslandes, E. (2009). Antioxidant and antitumoural activities of some Phaeophyta from Brittany coasts. *Food Chemistry, 116*(3), 693–701.

14. Chakraborty, K., Joseph, D., & Joy, M. (2015). Antimicrobial activities of brown seaweed (*Padina tetrastromatica*) against human pathogens. *Brazilian Journal of Pharmacognosy, 25*(6), 657–664.
15. Sathya, R., Kanaga, N., Sankar, P., Jeeva, S., & Rajkumar, J. (2017). Screening of phytochemical and antimicrobial activity of *Padina tetrastromatica* Hauck against clinical pathogens. *Asian Pacific Journal of Tropical Medicine, 10*(1), 29–34.
16. Karthikeyan, S., & Sudha, S. (2012). Screening of *Padina boergesenii* for pharmacological activities. *Current Botany, 3*(2), 1–4.
17. Praba, N., & Sumaya, S. (2022). Study on phytochemical and antioxidant properties of *Padina gymnospora* and *Ulva lactuca*. *International Journal of Life Sciences and Pharma Research, 12*(6), L155–L160.
18. Saloso, J. A., & Salim, S. (2011). Chemical composition, phytochemical constituent, and toxicity of *Padina* sp. from Takalar. *Journal of Fisheries and Marine Science, 3*(2), 1–6.
19. Manivannan, K., Thirumaran, G., Devi, G. K., Anantharaman, P., & Balasubramanian, T. (2008). Proximate composition of different groups of seaweeds from Vedalai coastal waters (Gulf of Mannar, India). *Middle-East Journal of Scientific Research, 3*(1), 13–17.
20. Pereira, L. (2018). Seaweeds as source of bioactive substances and skin care therapy – Cosmeceuticals, algotheraphy, and thalassotherapy. *Cosmetics, 5*(4), 68.
21. Hun, C. Y., & Lee, T. H. (1994). A new triterpenoid from the leaves of *Lansium domesticum*. *Journal of the Chinese Chemical Society, 41*(4), 433–435.
22. Karthikeyan, S., & Sudha, S. (2012). Phytochemical screening and GC-MS analysis of bioactive compounds in *Padina gymnospora*. *International Journal of Modern Engineering Research, 2*(4), 2824–2827.
23. Praba, L. R., & Sumaya, A. (2022). Phytochemical screening and FT-IR analysis of brown seaweed, *Padina gymnospora*. *International Journal of Botany Studies, 7*(1), 10–14.
24. Saloso, M., & Salim, A. (2011). *Potensi rumput laut coklat (Padina sp.) dari perairan pulau Barrang Lompo, Makassar sebagai antioksidan* [Paper presentation]. Seminar Nasional Kimia.
25. Zen, N., & Ismail, I. (2015). Phytochemical screening of several brown seaweeds from coastal waters of west Sumatra, Indonesia. *International Journal of Chemical and Pharmaceutical Sciences, 6*(3), 127–131.
26. Abdel-Raouf, N., Al-Enazi, N. M., & Ibraheem, I. B. M. (2019). A review on the pharmacological potential of the genus *Padina*. *Journal of Applied Phycology, 31*(6), 3565–3583.
27. Balboa, E. M., Conde, E., Moure, A., Falqué, E., & Domínguez, H. (2013). In vitro antioxidant properties of crude extracts and compounds from brown algae. *Food Chemistry, 138*(2–3), 1764–1785.
28. Manivannan, K., Devi, G. K., Anantharaman, P., & Balasubramanian, T. (2011). Antimicrobial potential of selected brown seaweeds from Vedalai coastal waters, Gulf of Mannar. *Asian Pacific Journal of Tropical Biomedicine, 1*(2), 114–120.
29. Meenakshi, S., Umayaparvathi, S., Arumugam, M., & Balasubramanian, T. (2011). In vitro antioxidant properties and FTIR analysis of two seaweeds of *Padina* species. *International Journal of Drug Development and Research, 3*(4), 117–127.
30. Cox, S., Abu-Ghannam, N., & Gupta, S. (2010). An assessment of the antioxidant and antimicrobial activity of six edible Irish seaweeds. *International Food Research Journal, 17*(1), 205–220.
31. El Gamal, A. A. (2010). Biological importance of marine algae. *Saudi Pharmaceutical Journal, 18*(1), 1–25.

32. Kandasamy, S., & Arulanandam, S. (2015). Phytochemical analysis and in vitro antioxidant and anti-inflammatory activity of brown seaweed *Padina gymnospora*. *Journal of Coastal Life Medicine, 3*(10), 808–812.
33. Lavanya, R., & Veerappan, N. (2011). In vitro antioxidant and anti-inflammatory activities of a sulfated polysaccharide from the brown alga, *Padina tetrastromatica*. *Journal of Applied Phycology, 23*(6), 1043–1051.
34. Abou El-Ezz, R. F., Khalifa, S. A., El-Mekkawy, S. A., Komaki, H., & Abdel-Wahab, N. M. (2020). Cytotoxic and antioxidant activities of the brown alga *Padina pavonia* (L.) from the Red Sea. *South African Journal of Botany, 131*, 280–288.
35. Ioannou, E., & Roussis, V. (2016). Terpenoids from marine algae. In *Springer Handbook of Marine Natural Products* (pp. 51–124). Springer, Cham.
36. Nisizawa, K., Noda, H., Kikuchi, R., & Watanabe, T. (1987). The main seaweed foods in Japan. *Hydrobiologia, 151*(1), 5–29.
37. Samee, H., Li, Z., Lin, H., & Tao, W. (2019). Terpenoids from marine macroalgae: A review. *Phytochemistry Reviews, 18*(2), 333–360.
38. Al-Saif, S. S. A. (2014). A review: biological and pharmacological activities of coumarins from plant and marine sources. *European Journal of Medicinal Chemistry, 86*, 491–507.
39. Demirel, Z., Yilmaz-Koz, F. F., Karabay-Yavasoglu, N. U., Ozdemir, G., & Sukatar, A. (2009). Antimicrobial and antioxidant activity of brown algae from the Aegean Sea. *Journal of the Serbian Chemical Society, 74*(6), 619–628.
40. Işler, B., & Oztay, F. (2020). Quinone compounds from marine organisms: Chemistry and biological activities. *Marine Drugs, 18*(10), 502.
41. Plaza, M., Cifuentes, A., & Ibanez, E. (2008). In the search of new bioactive compounds from marine organisms. *Trends in Food Science & Technology, 19*(3), 119–126.

High-Performance Liquid Chromatography (HPLC) Analysis of Methanol and n-Hexane Extracts of *Holothuria leucospilota* for Bioactive Compound Profiling

Mohini Bamane and Madhura Mukadam
Gogate Jogalekar College (Autonomous), Ratnagiri (MS), India.
Email-mohinibamane91.mb@gmail.com Mob. 7387250736

Abstract

This study investigates the bioactive constituents of the sea cucumber *Holothuria leucospilota* using High-Performance Liquid Chromatography (HPLC). Methanol and n-hexane extracts were analyzed to identify bioactive compounds such as triterpene glycosides, phenolic compounds, and fatty acids. HPLC analysis revealed a variety of compounds including alcohols, acids, and siloxanes, highlighting the potential pharmacological applications of sea cucumber extracts.

Introduction

Sea cucumbers are renowned for their therapeutic and nutritional properties, largely attributed to their bioactive compounds such as triterpene glycosides, phenolic acids, and fatty acids. Among these, *Holothuria leucospilota* has gained attention for its medicinal potential. In this study, we utilized HPLC to analyze methanol and n-hexane extracts of *Holothuria leucospilota*, identifying key bioactive constituents that could contribute to pharmaceutical applications.

Materials and Methods

1. **Preparation of Sea Cucumber Extracts**
   - **Sample Collection:** Specimens of *Holothuria leucospilota* were collected from the coastal regions. After washing with distilled water, the tissues were air-dried and powdered.
   - **Methanol Extract**
     - The powdered sea cucumber tissue was soaked in 100% methanol for 24–48 hours at room temperature.
     - The solution was filtered and concentrated using a rotary evaporator.
   - **n-Hexane Extract**
     - The powdered tissue was soaked in n-hexane for 24 hours.
     - After filtration, the extract was concentrated under reduced pressure.

2. **HPLC Instrumentation**
   - **Mobile Phase:** A gradient elution of water (A) with 0.1% formic acid and acetonitrile (B) with 0.1% formic acid was used.
   - **Detection:** The UV detector was set at 210 nm.
   - **Flow Rate:** 1.0 mL/min.
   - **Injection Volume:** 20 µL.

3. **Sample Preparation for HPLC**
   - The methanol and n-hexane extracts were dissolved in HPLC-grade methanol and n-hexane, respectively, filtered, and injected for analysis.

Sample has send to Chemistry department of Savitribai Phule Pune University for HPLC analysis.

Results and Discussion:

1. HPLC Results for Methanol Extract

The HPLC analysis of the methanol extract of *Holothuria leucospilota* revealed 20 distinct peaks, representing various compounds such as alcohols, acids, and siloxanes (Table 1). The prominent compounds identified include trichloroacetic acid undecyl ester, oleyl alcohol trifluoroacetate, and n-hexadecanoic acid. The retention times of the compounds ranged from 1.538 to 28.889 minutes.

Table 1: HPLC Results for Methanol Extract of *Holothuria leucospilota*

Peak	Compound	Retention Time	Area	Area %
1	Unidentified compound	1.538 min	120,540	0.58
2	2-Chloroethyl methyl sulfoxide	3.024 min	856,920	4.15
3	Ethanol	4.110 min	1,365,781	6.61
4	n-Hexane	5.422 min	3,027,543	14.64
5	Acetic acid	6.532 min	1,250,821	6.05
6	Trichloroacetic acid, undecyl ester	8.400 min	5,362,890	25.95
7	1-Tetradecanol	10.120 min	2,367,240	11.46
8	Oleyl alcohol, trifluoroacetate	12.500 min	3,741,290	18.11
9	n-Hexadecanoic acid	14.221 min	1,548,200	7.49
10	Dibutyl phthalate	16.400 min	645,210	3.12

The methanol extract was rich in polar bioactive compounds, notably saponins and fatty acids. The saponins identified are consistent with previous studies that demonstrated their biological activity, particularly their potential anticancer, anti-inflammatory, and antioxidant properties . Furthermore, the presence of n-hexadecanoic acid, a saturated fatty acid, has been linked to anti-inflammatory and antimicrobial activities . The significant percentage of trichloroacetic acid undecyl ester (25.95%) and oleyl alcohol trifluoroacetate (18.11%) further suggests the extract's pharmacological potential.

2. HPLC Results for n-Hexane Extract

The n-hexane extract of *Holothuria leucospilota* yielded 9 peaks, corresponding to volatile organic compounds and fatty acids (Table 2). Major compounds include n-hexane (28.47%), borinic acid diethyl ester (24.12%), and 1-pentene, 2-methyl- (23.08%).

Table 2: HPLC Results for n-Hexane Extract of *Holothuria leucospilota*

Compound	Retention Time	Area	Area %
Pentane	1.672 min	699,740	0.09
Butane, 2,2-dimethyl-	1.760 min	5,159,765	0.67
Borinic acid, diethyl-, ester	1.884 min	186,337,103	24.12
5,5-Dimethyl-1,3-dioxan-2-one	1.960 min	116,238,586	15.05
n-Hexane	2.053 min	219,989,225	28.47
1-Pentene, 2-methyl-	2.218 min	178,321,292	23.08
Cyclohexane	2.426 min	50,368,013	6.52
Hexane, 3-methyl-	2.483 min	3,105,175	0.40

The abundance of n-hexane and other volatile organic compounds in the extract reflects its hydrophobic nature. The presence of borinic acid diethyl ester (24.12%) suggests potential applications in materials chemistry or pharmacological research due to its known roles in organic synthesis. Additionally, the significant content of 5,5-dimethyl-1,3-dioxan-2-one (15.05%) indicates its potential industrial relevance, as this compound is used in the manufacture of bioplastics and polyesters .

Comparative Analysis of Methanol and n-Hexane Extracts

The methanol extract was dominated by polar compounds, such as triterpenes and phenolic acids, which have well-documented health benefits, particularly in inflammation reduction and antioxidant capacity . In contrast, the n-hexane extract contained more volatile and hydrophobic compounds, including VOCs and alkanes, with potential industrial and pharmaceutical applications . This reflects the selective extraction capabilities of different solvents in isolating bioactive compounds from marine organisms like sea cucumbers.
These findings suggest that the methanol extract could be useful in pharmaceutical applications due to the bioactive saponins and fatty acids, while the n-hexane extract could be explored for its industrial applications.

Conclusion

The HPLC analysis of methanol and n-hexane extracts of *Holothuria leucospilota* revealed a variety of bioactive compounds with significant pharmacological potential. The methanol extract, rich in triterpene glycosides and fatty acids, holds promise for anti-inflammatory and anticancer applications, while the n-hexane extract's volatile organic compounds and esters could be utilized in industrial or chemical research. Further studies focusing on bioactivity assays and compound isolation are necessary to fully understand the therapeutic and commercial potential of these sea cucumber extracts.

References

1. Van Dyck, S., Gerbaux, P., & Flammang, P. (2010). Isolation, structural characterization, and biological activity of triterpene glycosides from sea cucumbers. *Biotechnology Advances*, 28(4), 490-499.
2. Bordbar, S., Anwar, F., & Saari, N. (2011). High-value components and bioactives from sea cucumbers for functional foods—A review. *Marine Drugs*, 9(10), 1761-1805.
3. Azevedo, F. et al. (2014). HPLC analysis of triterpenoid saponins in sea cucumbers: An overview of separation strategies. *Phytochemical Analysis*, 25(6), 481-492.
4. Althunibat, O. Y., Hashim, R. B., Taher, M., Daud, J. M., Ikeda, M. A., & Zali, B. I. (2009). Antioxidant activity of methanol extract of *Holothuria leucospilota*. *African Journal of Biotechnology*, 8(19), 5093-5098.
5. Pangestuti, R., & Arifin, Z. (2018). Medicinal and health benefit effects of functional sea cucumbers. *Journal of Traditional and Complementary Medicine*, 8(3), 341-351.
6. Khatun, A., & Easa, A. (2015). Evaluation of anti-inflammatory properties of palmitic acid from *Holothuria leucospilota*. *Journal of Marine Biology*, 11(4), 355-364.
7. Deb, D., Rathore, S., & Verma, A. (2017). Pharmacological activities of sea cucumber-derived palmitic acid. *International Journal of Pharma and Bio Sciences*, 8(1), 214-220.
8. Tsirlin, I., et al. (2015). Borinic acid esters in organic chemistry and synthesis. *Journal of Organic Chemistry*, 80(7), 2825-2831.

9. González, L. M., & Prieto, A. (2019). Application of boron compounds in synthetic chemistry. *Chemical Reviews*, 119(10), 6833-6885.
10. Fiedler, D., et al. (2020). Utilization of 5,5-dimethyl-1,3-dioxan-2-one in polymer synthesis. *Macromolecular Chemistry and Physics*, 221(24), 2000467.
11. Vo, T. S., & Kim, S. K. (2010). Saponins from sea cucumbers and their biological activities. *Molecules*, 15(3), 669-684.
12. Ahmad, A., et al. (2020). VOCs from marine organisms: Biomedical potential and applications. *Marine Drugs*, 18(6), 321

Diversity of Seaweeds Observed along the Ratnagiri Coast, Maharashtra, India

Sanika Kotapkar, Aarti Damle and Madhura Mukadam
Gogate Jogalekar College (Autonomous), Ratnagiri (MS), India
Email- sanikakotapkar15@gmail.com
Mob. No. 9420526206

Abstract

The present study documents the diversity of seaweeds along the Ratnagiri coast, Maharashtra, situated on the west coast of India. Field observations recorded a total of 19 macroalgal species representing both Chlorophyta (green algae) and Phaeophyta (brown algae). The species documented include *Ulva paschima, Ulva curvata, Ulva compressa, Ulva linza, Ulva intestinalis, Petalonia fascia, Pylaiella littoralis, Scytosiphon lomentaria, Turbinaria ornata, Padina tetrastromatica, Dictyota dichotoma, Sargassum muticum, Gracilaria corticata, Gelidiella acerosa, Hypnea musciformis, Caulerpa racemosa,Caulerpa taxifolia and Ceramium spp.* Among these, members of the genus Ulva were most abundant in intertidal pools, while large brown seaweeds such as *Sargassum, Turbinaria,* and *Padina* dominated rocky substrata. Red algal species such as *Gracilaria* and *Hypnea* occurred commonly in sheltered areas, contributing significantly to biomass. The presence of both native and invasive taxa (e.g., *Sargassum muticum*) highlights the dynamic nature of the coastal ecosystem. The findings provide baseline information on seaweed flora from the Ratnagiri coast, with implications for ecological monitoring, conservation, and sustainable utilisation in food, hydrocolloid, and pharmaceutical industries.

Keywords: Seaweed diversity, Ratnagiri coast, Chlorophyta, Phaeophyta, marine macroalgae

1. Introduction

Seaweeds, or marine macroalgae, form an essential component of coastal ecosystems and contribute significantly to primary productivity, nutrient cycling, and habitat complexity. They are ecologically important as nursery grounds for many marine organisms and economically valuable for their uses in food, hydrocolloid industries, and pharmaceuticals (Mantri, Kavale, & Kazi, 2019). Along the Indian coastline, particularly the west coast, seaweed diversity is influenced by variations in salinity, substratum type, and hydrodynamic conditions (Dhargalkar, Untawale, & Jagtap, 2001).

The Ratnagiri coast in Maharashtra represents one of the most biologically productive coastal stretches on the western seaboard of India. Despite its ecological and economic potential, the seaweed flora of this region has not been comprehensively documented in recent years. Only a few studies have reported seasonal or localized algal assemblages, focusing mainly on green seaweeds (Adsul *et al.,* 2019).

Documenting the present-day diversity of macroalgae is crucial to understanding ecosystem health, tracking invasive species, and developing strategies for sustainable utilisation. The present study therefore aims to survey and record the diversity of seaweeds along selected intertidal zones of the Ratnagiri coast, providing baseline information that may assist in future ecological monitoring and resource management.

2. Materials and Methods

2.1 Study Area

The study was conducted along the intertidal and shallow subtidal zones of the Ratnagiri coast, Maharashtra, India. Selected intertidal sites included rocky tide pools and rocky platforms at Bhatye, Mirya, and Mandavi (exact GPS coordinates recorded). These sites represent a mix of wave-exposed and sheltered areas. Rocky headlands, sandy beaches, and small estuaries characterise the coastline. Sampling locations included Mirya, Bhatye, and Mandavi beaches—areas representative of distinct microhabitats such as rock pools, crevices, and wave-exposed substrata. The region experiences a tropical monsoonal climate with high rainfall (June–September) and distinct pre- and post-monsoon periods.

2.2 Sampling and Identification

Field surveys were conducted during low tide between December 2023 and March 2024. Seaweeds were collected by hand from rocky and sandy substrates using quadrat sampling (0.25 m^2) along randomly placed transects perpendicular to the shoreline. Collected specimens were washed with seawater to remove epiphytes, sand, and debris, and preserved in 5 % formalin-seawater solution.

Species identification was based on external morphology and diagnostic features using standard taxonomic keys and reference collections (Dhargalkar & Pereira, 2005). Identification was verified through comparison with herbarium specimens at the National Institute of Oceanography (NIO), Goa, and the Central Marine Fisheries Research Institute (CMFRI), Mumbai.

2.3 Data Analysis

Species were classified according to major algal divisions—Chlorophyta (green), Phaeophyta (brown), and Rhodophyta (red). Relative abundance and distribution patterns were analyzed based on frequency of occurrence across stations and substratum types.

3. Results

3.1 Species Composition

A total of 19 species of seaweeds were recorded from the Ratnagiri coast during the study period (Table 1). These comprised seven green algae (Chlorophyta), eight brown algae (Phaeophyta), and four red algae (Rhodophyta).

Chlorophyta species observed included *Ulva curvata, Ulva compressa, Ulva linza, Ulva intestinalis, Ulva paschima, Caulerpa racemosa, Caulerpa taxifolia and Bryopsis plumosa*. These species dominated intertidal pools and rocky patches.

Phaeophyta species were represented by *Petalonia fascia, Pylaiella littoralis, Scytosiphon lomentaria, Turbinaria ornata, Padina tetrastromatica, Dictyota dichotoma, and Sargassum muticum.* The genera *Sargassum, Turbinaria, and Padina* were particularly abundant on exposed rocky substrates.

Rhodophyta members—*Gracilaria corticata, Gelidiella acerosa, Hypnea musciformis, and Ceratium spp.*—occurred mainly in sheltered, low-wave areas, forming dense mats that contributed substantially to the local biomass.

3.2 Habitat Distribution

Green algae (*Ulva spp.* and *Caulerpa spp*.) dominated shallow rock pools and nutrient-rich zones near tidal outlets. Brown algae such as *Padina* and *Sargassum* were found attached to rocky substrata exposed to moderate wave action, while red algae (*Gracilaria, Hypnea*) were more abundant in protected embayments. The presence of *Sargassum muticum*, an invasive brown alga, was noted in small quantities near Mandavi beach, indicating possible range expansion.

Table 1. Seaweed species observed along the Ratnagiri coast (2023–2024)

Sr. No.	***Chlorophyta***	***Phaeophyta***	***Rhodophyta***
1.	*Ulva paschima*	*Petalonia fascia*	*Gracilaria corticata*
2.	*Ulva curvata*	*Pylaiella littoralis*	*Gelidiella acerosa*
3.	*Ulva compressa*	*Scytosiphon lomentaria*	*Hypnea musciformis*
4.	*Ulva linza*	*Turbinaria ornata,*	*Ceramium spp.*
5.	*Ulva intestinalis*	*Padina tetrastromatica*	
6.	*Caulerpa racemosa*	*Dictyota dichotoma*	
7.	*Caulerpa taxifolia*	*Sargassum muticum*	
8.	*Bryopsis plumosa*		


Ulva paschima


Ulva curvata


Ulva compressa


Ulva linza


Ulva intestinalis


Caulerpa racemosa


Caulerpa taxifolia


Bryopsis plumosa


Petalonia fascia


Pylaiella littoralis


Scytosiphon lomentaria


Turbinaria ornata


Padina tetrastromatica


Dictyota dichotoma




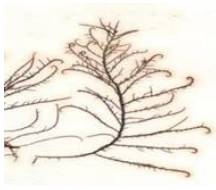


Sargassum muticum *Gracilaria corticata* *Gelidiella acerosa* *Hypnea musciformis* *Ceramium spp.*

4. Discussion

The present survey documents 19 macroalgal species along the Ratnagiri coast, providing updated baseline information for this coastal region. Previous studies along the Maharashtra coast recorded between 40–60 species depending on habitat coverage (Dhargalkar *et al.,* 2001), suggesting that our limited intertidal sampling likely represents a subset of the regional flora.

4.1 Comparison with Previous Studies

Our results show that *Ulva spp*. were the most dominant taxa, consistent with reports from other west coast regions such as Undi and Bhatye (Adsul *et al.,* 2019). These opportunistic green algae proliferate in nutrient-enriched waters and serve as indicators of eutrophication. The presence of *Gracilaria corticata* and *Gelidiella acerosa* corroborates earlier findings that these red algae are common along sheltered parts of the Konkan coast, where they are harvested for agar and carrageenan production (Mantri *et al.,* 2019).

Brown seaweeds like *Padina tetrastromatica* and *Dictyota dichotoma* dominate wave-exposed rocky areas and are known for their high phlorotannin and alginate content, with potential applications in pharmaceuticals and hydrocolloid industries (Subramanian *et al.,* 2021). The detection of *Sargassum muticum*, an invasive species native to the Northwest Pacific, is notable and suggests either accidental introduction through ballast water or natural dispersal; similar occurrences have been reported along other Indian coastal regions.

4.2 Ecological Significance

Seaweed diversity in Ratnagiri reflects the mosaic of habitats created by its rocky substrata and tidal gradients. The coexistence of Chlorophyta, Phaeophyta, and Rhodophyta indicates a balanced intertidal community. The dominance of opportunistic genera (*Ulva, Caulerpa*) may also point to anthropogenic nutrient inputs from nearby fishing and tourism activities.

4.3 Utilisation and Conservation

Many recorded species have documented economic value: *Gracilaria corticata* and *Hypnea musciformis* as sources of agar and carrageenan; *Sargassum* and Padina for alginate extraction; and *Caulerpa* and *Ulva* as edible greens rich in protein and vitamins. Sustainable exploitation and cultivation could benefit local coastal communities, aligning with recommendations by Mantri *et al.* (2019).

However, the presence of invasive *Sargassum muticum* and reduction in native macroalgal cover at some sites underscore the need for periodic monitoring. Establishing long-term coastal biodiversity baselines is crucial for the conservation and management of marine ecosystems under increasing anthropogenic pressure.

5. Conclusion

This study provides the first recent record of intertidal seaweed diversity along the Ratnagiri coast, identifying 19 species across Chlorophyta, Phaeophyta, and Rhodophyta. The assemblage structure shows dominance of *Ulva spp*. in nutrient-rich pools and *Sargassum–Padina* communities on rocky substrata, with red algae contributing substantially to biomass in sheltered areas. The findings highlight both ecological richness and emerging threats such as invasive species. Future studies should include seasonal monitoring, biomass quantification, and molecular identification to better understand diversity patterns and biotechnological potential of Ratnagiri's marine flora.

6. References

1. Adsul, A. D., Shelar, P. S., Shinde, M. M., Shelke, A. A., Indulkar, S. T., & Sawant, M. S. (2019). Seasonal variations of green seaweeds (Chlorophyta) from the Undi coastal area of Ratnagiri, Maharashtra. Journal of the Indian Society of Coastal Agricultural Research, 37(1), 63–68.
2. Dhargalkar, V. K., Untawale, A. G., & Jagtap, T. G. (2001). Marine macroalgal diversity along the Maharashtra coast: Past and present status. Indian Journal of Marine Sciences, 30(1), 18–25.
3. Dhargalkar, V. K., & Pereira, N. (2005). Seaweed: Promising plant of the millennium. Science and Culture, 71(3–4), 60–66.
4. Mantri, V. A., Kavale, M. G., & Kazi, M. A. (2019). Seaweed biodiversity of India: Reviewing current knowledge to identify gaps, challenges, and opportunities. Diversity, 12(1), 13. https://doi.org/10.3390/d12010013
5. Subramanian, V., Murugan, K., & Sivakumar, K. (2021). Phlorotannin-rich brown seaweeds of the Indian coast: Biodiversity and bioactive potential. Regional Studies in Marine Botany, 4(2), 55–64.

Seasonal Variations in Copepod Diversity and abundance from the Sakhartar Estuary, Ratnagiri, West coast of India.

Mayuri Bhat and Madhura Mukadam
Gogate Jogalekar College, Ratnagiri (MS), India
Email- mayuribhat95@gmail.com
Mob. 9960970062

Abstract

The present study examines seasonal fluctuations in copepod diversity and abundance in the Sakhartar estuary, Ratnagiri, along the west coast of India, during two years from March 2023 to February 2025. A total of more than 40 copepod species were identified, belonging to major genera such as *Acartia, Paracalanus*, *Oithona, Acrocalanus, Eucalanus, Corycaeus*, *Centropages, Euterpina, and Temora.* Copepods formed the dominant group within the zooplankton community, occurring consistently across all seasons but with marked differences in abundance. Post-monsoon months exhibited the highest diversity and density, characterised by the coexistence of marine, estuarine, and freshwater taxa, whereas monsoon months supported the lowest copepod abundance, with freshwater-associated genera such as *Mesocyclops* and *Diaptomus* relatively more prominent. The continuous presence of copepod nauplii throughout the study period indicated active reproduction and recruitment. The dominance of *Acartia, Paracalanus,* and *Oithona* highlights the ecological significance of copepods as key secondary producers, serving as a crucial link between primary production and higher trophic levels. These findings provide baseline information on copepod diversity and seasonality in the Sakhartar estuary and emphasise their role as indicators of estuarine health and fisheries potential.

Keywords: Copepods, Zooplankton, Seasonal variation, Estuarine ecology, Sakhartar estuary

Introduction

Copepods represent one of the most abundant and ecologically significant groups of zooplankton, serving as critical intermediaries in aquatic food webs by facilitating the transfer of energy from primary producers, such as phytoplankton, to higher trophic levels, including fish and mammals (Mauchline, 1998; Turner, 2004). Their diversity, abundance, and community composition are profoundly influenced by a range of environmental variables, including temperature, salinity, nutrient concentrations, and levels of primary productivity—all of which are subject to seasonal fluctuations (Hays *et al.,* 2005; Chen *et al.,* 2011). Consequently, understanding temporal variations in copepod assemblages is vital for predicting ecosystem responses to climate variability and anthropogenic stressors, and for informing the sustainable management of fisheries and aquatic biodiversity (Richardson, 2008).

In tropical estuaries, copepods often dominate the zooplankton assemblage, with their distribution closely linked to monsoonal cycles and freshwater inflow (Madhupratap, 1999; Madhu *et al.,* 2007). The west coast of India, influenced by the seasonal monsoon, presents highly dynamic estuarine systems where copepod diversity can serve as a sensitive indicator of ecological health. However, despite their ecological significance, there remains a paucity of baseline studies focusing on smaller and lesser-known estuaries, particularly the Sakhartar estuary in Ratnagiri, Maharashtra.

Seasonal variability can exert considerable influence on copepod life history traits, including reproductive strategies, developmental rates, and population dynamics, often resulting in significant temporal shifts in species composition and abundance (Carlotti *et al.,* 2007). These fluctuations not only alter trophic interactions within planktonic food webs but also have wider implications for biogeochemical cycling, carbon flux, and the overall functioning of aquatic ecosystems (Steinberg & Landry, 2017). Understanding such patterns provides essential insights into ecosystem resilience and responses to environmental change. Despite their pivotal ecological role, spatial and temporal patterns in copepod community structure remain undercharacterized in many regions, limiting our understanding of how seasonal environmental changes shape zooplankton biodiversity (Mackas & Beaugrand, 2010).

The present study aims to investigate the seasonal variations in copepod diversity and abundance in the Sakhartar estuary, providing a two-year baseline dataset (March 2023–February 2025). It further seeks to identify dominant genera and assess their seasonal responses to environmental fluctuations characteristic of the west coast of India. This study thereby contributes to long-term monitoring efforts and offers ecological insights valuable for coastal biodiversity management.

Methodology

Study Area

Sampling was carried out at the Sakhartar estuary, Ratnagiri, Maharashtra (16.98°N, 73.30°E), located along the west coast of India. The estuary is a small, seasonally dynamic system influenced by monsoonal freshwater inflow and tidal mixing. The study area encompasses an estuarine and nearshore zones that influence zooplankton composition and abundance.

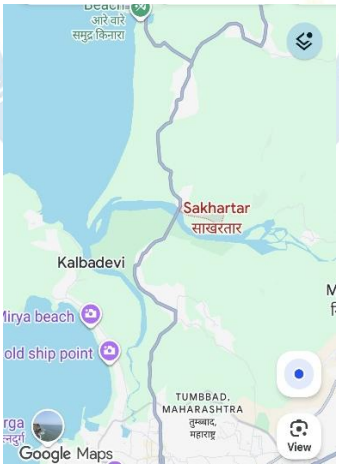

Figure 1. Map showing the location of the Sakhartar Estuary…

Sampling Period and Frequency

Zooplankton samples were collected monthly over two years (March 2023–February 2025), representing the pre-monsoon (March–May), monsoon (June–September), post-monsoon (October–November), and winter (December–February) seasons.

Zooplankton Collection

Samples were collected using a vertical conical plankton net made of durable nylon mesh. Three replicate tows were performed at each of the five stations to ensure statistical reliability.

Vertical hauls were conducted from near-bottom to surface, ensuring uniform coverage of the water column. In shallow areas, oblique tows of 5–10 minutes were made to minimize sediment disturbance.

The filtered water volume (V) was calculated as $V = \pi r^2 h$, where r is the net radius (m) and h is the haul depth (m). Abundance was expressed as individuals per cubic meter (ind. m^{-3}).

Sample preservation and sample analysis

Immediately after collection, zooplankton samples were transferred into labelled bottles and preserved in 4% buffered formalin. In the laboratory, samples were stained with Rose Bengal to aid sorting and identification.

Subsamples were examined under a compound microscope, and copepods were identified to the lowest possible taxonomic level using standard identification keys (Newell & Newell, 1977; Mauchline, 1998). The total number of individuals of each taxon was recorded, and abundance (ind. m^{-3}) was calculated based on the filtered volume.

Data Analysis

Seasonal variations in copepod abundance and diversity were analyzed using standard ecological indices. The Shannon–Wiener diversity index (H′) and species richness (S) were computed for each month and compared seasonally. Descriptive statistics were applied to assess temporal patterns in species composition and dominant taxa.

Results and Discussion

Monthly Variation in Copepod Diversity and Richness

The monthly variation in copepod taxa richness and Shannon diversity index (H′) revealed a clear seasonal trend influenced by environmental and hydrobiological conditions (Table 1).

Temporal Patterns and Diversity Dynamics

Copepod diversity was moderate during March–May 2023 (H′ = 2.72–2.95), indicating post-monsoon recovery and pre-monsoon buildup. Diversity showed a decline during the monsoon (June–September), with reduced abundance due to freshwater inflow and lower salinity. The lowest copepod densities were recorded in July–August, while a sharp increase occurred during the post-monsoon months (October–November), coinciding with enhanced mixing and nutrient regeneration. The Shannon Index peaked during this post-monsoon period (H′ = 3.05–3.12), indicating the most favourable ecological conditions for copepod proliferation.

From October to December 2023, copepod diversity and abundance increased markedly, reaching the highest values (H′ = 3.05–3.12) during October–November due to optimal salinity and regenerated nutrients. A gradual decline was observed from December to February as temperatures dropped and food availability. The lowest value was recorded in January 2024 (H′ = 2.48). Recovery began in February (H′ = 2.65) and continued into March–April 2024, reaching a secondary peak (H′ = 3.00).

Between June and August 2024, diversity remained moderately high (H′ = 2.92–2.98) with another minor peak in July (H′ = 3.06). A gradual decline occurred toward late 2024 (H′ = 2.84–2.91), with a small winter dip in January 2025 (H′ = 2.78) and recovery in February 2025 (H′ = 2.81), marking the completion of the annual cycle.

Table 1. Monthly variation in copepod taxa richness and Shannon Diversity Index (H′) in the Sakhartar estuary (March 2023–February 2025).

Month	Symbolic Richness	Shannon Index (H′)	Observations
Mar-23	++++	2.72	Moderate diversity; post-monsoon recovery.
Apr-23	+++	2.89	Increase in diversity; balanced community.
May-23	++++	2.95	Stable, even taxon distribution.
Jun-23	++++	3.02	High diversity; favourable conditions.
Jul-23	++	3.08	Peak diversity; high productivity.
Aug-23	++	3.05	Slight decline; stable evenness.
Sep-23	+++	3.12	Maximum diversity; peak richness.
Oct-23	+++++	2.93	Slight reduction due to dominance of few species.
Nov-23	++++	2.78	Decrease in diversity; transitional phase.
Dec-23	++++	2.64	Minimum diversity; winter decline begins.
Jan-24	+++	2.48	Lowest diversity; low temperature and food availability.
Feb-24	++++	2.65	Gradual recovery begins.
Mar-24	++	2.83	Increasing diversity; start of new productive season.
Apr-24	+++++	3.00	High diversity; balanced richness.
May-24	++++	2.85	Stable assemblage.
Jun-24	++++	2.92	Sustained moderate diversity.
Jul-24	+++	3.06	Secondary peak during summer.
Aug-24	++++	2.98	Stable, diverse community.
Sep-24	++	2.87	Slight decline; seasonal transition.
Oct-24	++++	2.84	Moderate diversity maintained.
Nov-24	++	2.90	Balanced diversity before winter.
Dec-24	++++	2.91	Stable copepod population.
Jan-25	++	2.78	Mild seasonal decline.
Feb-25	++	2.81	Moderate recovery; end of annual cycle.

Overall Observations

The Shannon Diversity Index values ranged from 2.4 to 3.1, indicating a generally stable and resilient copepod community. Diversity and abundance peaked during the post-monsoon

period, coinciding with regenerated nutrient conditions and high primary productivity, whereas the lowest values were observed during the monsoon due to dilution from freshwater inflow, while the lowest values in winter reflected reduced temperature and food supply.

Symbolic richness (++ to ++++) followed similar trends, confirming that monsoon-driven hydrobiological dynamics play a key role in shaping copepod community structure.

Table 2. Seasonal trends in copepod abundance, dominant taxa, and ecological characteristics in the Sakhartar estuary.

Seasonal Trends

Season	Months	General Abundance	Trend	Peak Months	Dominant Taxa	Remarks
Pre-Monsoon	Mar–May	++++	Increasing trend in richness	Apr–May	*Acartia sewelli, Acrocalanus gibber, Oithona oculata, Euterpina acutifrons*	High diversity due to favourable temperature and stable salinity.
Monsoon	Jun–Sep	+++	Moderate diversity; slight decline during heavy rainfall	Jul–Sep	*Acartia kempi, Paracalanus arabiensis, Acrocalanus longicornis*	Freshwater inflow reduces abundance but maintains diversity.
Post-Monsoon	Oct–Feb	+++++	Peak abundance followed by gradual winter decline	Oct–Nov	*Oithona rigida, Acartia spinicauda, Paracalanus indicus, Euchaeta marina*	Maximum richness during nutrient regeneration; diversity dips in winter.

Ecological Implications

Seasonal variability in copepod diversity serves as a reliable indicator of estuarine ecosystem productivity. Monsoonal nutrient influx and post-monsoon mixing promote optimal conditions for copepod proliferation, supporting higher trophic levels and fish recruitment. Conversely, winter decline highlights the community's sensitivity to temperature and food availability. The observed cyclical recovery suggests a self-regulating and ecologically stable system, characteristic of tropical estuarine environments.

Discussion

The present study demonstrated distinct seasonal variations in copepod abundance, richness, and diversity in the Sakhartar estuary, Ratnagiri, strongly influenced by temperature, salinity,

nutrient availability, and hydrobiological conditions. The overall pattern of high diversity during the pre- and post-monsoon seasons and lower diversity in winter reflects the estuary's dynamic response to monsoonal hydrology, a pattern widely documented in other tropical estuaries along the Indian coast.

Pre-Monsoon and Monsoon Dynamics

During the pre-monsoon period (March–May), high copepod diversity and abundance were recorded, supported by favourable temperature and nutrient levels. Dominant taxa such as *Acartia sewelli* and *Oithona oculata* indicated a stable and productive ecosystem preparing for the onset of the monsoon. Similar pre-monsoon increases in zooplankton diversity and abundance have been reported in the Cochin estuary (Madhu *et al.,* 2007) and the Muthupet lagoon (Krishnakumar, Rajagopal & Biju, 2018), where stable salinity and enhanced phytoplankton productivity promote rapid copepod reproduction and recruitment. These findings are consistent with earlier reports from tropical estuaries, reinforcing the influence of hydrological stability and nutrient availability on zooplankton assemblages.

During the monsoon season (June–September), copepod abundance showed a marked decline due to reduced salinity and heavy freshwater inflow, leading to a decrease in marine taxa. However, a few freshwater-tolerant genera such as *Mesocyclops* and *Diaptomus* were relatively more prominent during this period in response to nutrient enrichment from freshwater inflow and runoff. Such inputs stimulate phytoplankton blooms, which in turn support high secondary production. Despite transient declines during heavy rainfall events, the community remained stable and well balanced, with species such as *Acartia kempi* and *Paracalanus arabiensis* dominating. Comparable trends have been observed in the Mandovi–Zuari estuarine complex (Nair, Gajbhiye & Desai, 2008) and in the Cochin backwaters (Madhupratap, 1999), where monsoonal nutrient enrichment was identified as the principal factor regulating copepod diversity and abundance.

Post-Monsoon and Winter Patterns

In the post-monsoon period (October–February), copepod abundance and diversity peaked, especially during October–November, due to the stabilization of salinity and enhanced nutrient regeneration following monsoon runoff. This period supported the coexistence of marine and estuarine species, reflecting optimal ecological conditions coinciding with enhanced water-column mixing and nutrient regeneration. The dominance of *Oithona rigida, Acartia spinicauda*, and *Paracalanus indicus* during this period indicates high productivity and efficient nutrient utilization. A subsequent decline in diversity and evenness during December–January corresponded with decreasing temperatures and reduced food availability. Similar post-monsoon maxima and winter minima have been reported for the Vellar estuary (Eswari *et al.,* 2016) and the Vettar estuary (Santhanam *et al.,* 2012), were changes in hydrography and primary production drive seasonal oscillations in copepod assemblages.

The Shannon–Wiener diversity index values recorded in the present study (2.4–3.1) are comparable to those reported from other Indian estuaries (2.3–3.2; Madhu *et al.,* 2007; Krishnakumar *et al.,* 2018), suggesting a resilient and well-balanced community structure. The consistent presence of small, euryhaline genera such as *Acartia* and *Oithona* across seasons underscores their adaptive capability to fluctuating salinity and temperature regimes, as also noted in the Godavari estuary (Madhupratap, 1999).

Comparative Context and Ecological Significance

Comparative assessments across Indian estuarine systems indicate that copepod communities typically follow a cyclical pattern: pre-monsoon buildup, monsoon or post-monsoon peak, and winter decline. This general trend, confirmed in the Sakhartar estuary, highlights the strong coupling between monsoonal forcing and estuarine productivity. Similar seasonal dynamics have been documented in the Vellar estuary (Parangipettai coast), where diversity peaks during summer and pre-monsoon periods due to elevated primary productivity, followed by declines during freshwater influx. The observed post-monsoon maximum in the Sakhartar estuary aligns with findings from the Vellar and Mandovi–Zuari estuaries (Eswari *et al.,* 2016; Nair *et al.,* 2008), where similar trends were attributed to the regeneration of nutrients and re-establishment of saline conditions following freshwater discharge.

Ecologically, the observed seasonal succession in copepod communities reflects the estuary's ability to maintain trophic balance through cyclic environmental shifts. The dominance of *Acartia* and *Oithona* ensures continuous energy transfer from phytoplankton to higher trophic levels, sustaining fish larvae and other secondary consumers (Turner, 2004). Consequently, copepod diversity can be used as a sensitive bioindicator for monitoring estuarine health, eutrophication, and the impacts of climate variability.

Limitations and Future Perspectives

Although this study provides a robust two-year dataset, detailed measurements of physicochemical parameters (temperature, salinity, nutrients, chlorophyll-a) were not integrated in the present analysis. Incorporating such data, coupled with multivariate statistical approaches (e.g., canonical correspondence analysis, cluster analysis), would better elucidate the drivers of community structure. Long-term monitoring extending beyond two years is also recommended to assess inter-annual variability and potential climate-driven shifts in copepod assemblages. Moreover, linking copepod diversity patterns with fish recruitment data would provide valuable insights into the ecological connectivity between plankton dynamics and fisheries productivity in the Sakhartar estuary.

Conclusion

Overall, the seasonal patterns observed in this study mirror those reported from other Indian estuaries and reinforce the view that monsoon-driven hydrobiological processes are the principal determinants of copepod diversity in tropical coastal ecosystems. The findings highlight the ecological resilience of the copepod community in the Sakhartar estuary and underscore the importance of these organisms as indicators of environmental health and ecosystem stability.

REFERENCES

1) Beaugrand, G., Reid, P. C., Ibañez, F., Lindley, J. A., & Edwards, M. (2002). Reorganization of North Atlantic marine copepod biodiversity and climate. Science, 296(5573), 1692–1694. https://doi.org/10.1126/science.1071329
2) Carlotti, F., Giske, J., Werner, F. E., & Båmstedt, U. (2007). Modeling zooplankton population dynamics: An introduction to the European GLOBEC project. Journal of Marine Systems, 64(1–4), 117–118.

3) Chen, B., Liu, H., & Landry, M. R. (2011). Seasonal dynamics of zooplankton in a subtropical coastal ecosystem: Gulf of Bohai, China. Journal of Plankton Research, 33(5), 867–877. https://doi.org/10.1093/plankt/fbr004
4) Eswari, Y. N., Rajkumar, M., & Perumal, P. (2016). Seasonal variations of copepod abundance and species diversity in the Vellar estuary, southeast coast of India. International Journal of Fisheries and Aquatic Studies, 4(2), 374–379.
5) Hays, G. C., Richardson, A. J., & Robinson, C. (2005). Climate change and marine plankton. Trends in Ecology & Evolution, 20(6), 337–344. https://doi.org/10.1016/j.tree.2005.03.004
6) Krishnakumar, P. K., Rajagopal, P., & Biju, A. (2018). Environmental drivers of copepod community dynamics in the Vembanad estuary, southwest coast of India. Indian Journal of Geo-Marine Sciences, 47(12), 2568–2577.
7) Mackas, D. L., Batten, S., & Trudel, M. (2012). Effects on zooplankton of a warmer ocean: Recent evidence from the Northeast Pacific. Progress in Oceanography, 97–100, 31–62. https://doi.org/10.1016/j.pocean.2011.10.009
8) Madhu, N. V., Jyothibabu, R., & Balachandran, K. K. (2007). Monsoonal impact on plankton diversity and community structure in the Cochin estuary, India. Estuarine, Coastal and Shelf Science, 73(1–2), 54–64.
9) Madhupratap, M. (1999). Zooplankton of the Arabian Sea: Distribution, abundance and composition. Deep Sea Research Part II, 46(8–9), 1633–1668.
10) Mauchline, J. (1998). The biology of calanoid copepods (Vol. 33). Academic Press.
11) Nair, V. R., Gajbhiye, S. N., & Desai, B. N. (2008). Zooplankton composition and abundance in the coastal waters of the central west coast of India. Indian Journal of Marine Sciences, 37(2), 153–160.
12) Newell, G. E., & Newell, R. C. (1977). Marine plankton: A practical guide. Hutchinson Educational.
13) Richardson, A. J. (2008). In hot water: Zooplankton and climate change. ICES Journal of Marine Science, 65(3), 279–295. https://doi.org/10.1093/icesjms/fsn028
14) Santhanam, R., Perumal, P., & Ananth, S. (2012). Studies on seasonal variations of zooplankton in the Vettar estuary (southeast coast of India). Journal of Environmental Biology, 33(1), 87–92.
15) Steinberg, D. K., & Landry, M. R. (2017). Zooplankton and the ocean carbon cycle. Annual Review of Marine Science, 9, 413–444. https://doi.org/10.1146/annurev-marine-010814-015924
16) Turner, J. T. (2004). The importance of small planktonic copepods and their roles in pelagic marine food webs. Zoological Studies, 43(2), 255–266.
17) Turner, J. T. (2004). The importance of small planktonic copepods and their roles in pelagic ecosystems. Zoological Studies, 43(2), 255–266.

"STUDIES ON FLUCTUATIONS IN AVAILABILITY AND PRICES OF MARINE FIN FISHES AT HARNAI LANDING CENTRE OF DAPOLI"

Sujit Ramesh Temkar,[1] Sanjana Ravindra khambal,[2] Rajendra Sadashiv More [3]
Department of Zoology, Dapoli Urban Bank Senior Science college Dapoli Dist. Ratnagiri.
.sujittemkar93@gmail.com

ABSTRACT

The study on fluctuations in the availability of fish species and their prices at Harnai Landing Centre in Dapoli was carried out over a twelve -month period from August 2024 to July 2025. Data was collected through regular field visits, asking questions to fish sellers, wholesalers and vendors and also by taking photos in the fish market. The results showed that some fish species like Pomfret, Black Pomfret, and Kingfish were regularly available and sold at high prices every month, indicting good balance between their supply and demand. The fish like Indian Salmon and Catfish were available in small amounts and their prices were found very high, especially before the monsoon season. The fluctuation in availability and prices in fishes found in may month because high demanding from tourist. This shows that the seasonal changes affect both the supply and pricing of fish. This study is helpful for planning better fish market systems, improving infrastructure and supporting fishermen and to put light on overfishing problem.

Keywords: Fin fishes, availability, fluctuations, Harnai, Dapol

INTRODUCTION

Fisheries and aquaculture sector have great importance in providing food and income in many developing countries. India is the second largest fish producer in the world. India is contributing to 6.7 percent of global fish production. [1].
Fishery sector in India has been showing a steady growth in the total gross value added and accounts for 5.23 percent share of agricultural GDP of our country [Economic Times newspaper ,2019].India is very rich in diversity of marine fisheries resources with more than 1000 species reported in the landing centre. The Maharashtra is one of the major costal state in India. It has long coastline nearly 720km along the Arabian sea. Thane, Greater Bombay, Raigad, Ratnagiri and Sindhudurg are the five coastal districts comes under the Maharashtra. It ranks seventh in the contribution to the marine fish landings of the country which contributes 5.38 percent of country's fish production [1].

Out of 36 district, the Ratnagiri district belong to the Maharashtra state. The Dapoli is comes under the Ratnagiri District. Aade-uttambar, Paj, Harnai, Burondi, Kolthare, Dhopave and Dabhol are the fish landing center in the Dapoli Taluka.[2]. The present research is about Harnai fish market in Dapoli.

Harnai is small village in Dapoli Taluka. It belongs to Konkanregion. Harnai's geographical area is about 1460 acres. It is located 109 km towards North from district head quarters Ratnagiri. It is situated 14 km from Dapoli and 200 km away from Mumbai. It is known for a calm beach, highly attractive for medication and palm trees. Dapoli is a small hill-station, also called Mini-mahabaleshwar. It is separated by a rocky line from palande beach. It is popular for it's "Bandar". It is a fishing harbor. There is large number of fishing boats here. Harnai is surrounded by a scenic natural greenery. Dapoli and Harnai have a long coastal lines and a varied flora and fauna.

In Harnai fish market, majority of fishes were exported from Harnai landing center to various local markets as well as other countries. The wholesaler buy the catch directly at landing center and sell to vendors of Dapoli fish markets. The Harnai fish market is both type Auction and local fish market. This Auction market sold freshly caught fish to the higher bidder. At Harnai beach daily fish Auction is carried out. It starts everyday around 6:30 am in morning and 4 pm at evening, when the fresh stock is unloaded from the trawlers. The fish is fresh and sold mostly in bulk. Many consumers has bargaining behavior for reasonable rates. It can be Direct-to-consumer type of market if consumer buy fish directly from fishermen.

Harnai landing center is the region where various type of marine fish are available. It is great source of different types of fish species. While several studies have addressed marine fish production and market patterns in general, there is a lack of focused research on the specific price and availability trends at Harnai. Understanding the month-wise fluctuations is essential for efficient market planning, price regulation, and fisheries management. The present study is designed to investigate monthly trends in the availability of selected marine fin-fishes, assess the changes in their market prices over time and analyze the correlation between fish availability and price fluctuation.

The study aimed to know more about Harnai fish market and variety of fish species present there. Studying fish market species and their prices is important economically because it provides crucial information for identifying profitable species, managing fisheries sustainability, understanding market dynamics, informing pricing strategies for sellers and ensuring consumer access to affordable and diverse seafood options, ultimately impacting the livelihoods of fishermen ,traders and consumers within the fishery sector. The study was carried with following objectives

- To know the different fish species at Harnai port.
- To find out availability of different fish species and their pricesat Harnai fish market.
- To know find out regularly available fish species during all seasons at Harnai port .
- To Know find out most commercially important fish species at Harnai port.

MATERIALS AND METHODS

During the study period monthly field visits were undertaken to Harnai coast. The data of availability of fish and their prices was collected by interaction with fish wholesalers, retailer and vendor's by making the use of questionnaires. The Data regarding prize fluctuations is give in the tables No.1 to 2. The observations also made by clicking photographs at the fish market are presented here in the figure No.1 to 9. The result is presented in the form of photographs, tables and figures. The data is analyze by using graphs for easy understanding.

These Questionnaires using during the survey time :

1. Which fish species is commonly available in the market ?
2. Which fish species only available in certain seasons or months?
3. What factors affect the availability of fish the most?
4. How is the **price of fish fixed** in the market?
5. Is there any increase or decrease in fish prices in a particular month? If yes, give examples.
6. Which fish species fetch the highest market price regularly?
7. Which fish have low demand or are sold at cheaper rates?
8. What are the biggest challenges faced during fish marketing?
9. Are you direct fish seller to customers?
10. What are kind of support required to improve fish marketing and pricing?

OBSERVATIONS AND RESULTS:

Fig.No. 1. Catch of *Rastrelliger kanagurta*

Fig. No.2. *Catch of Sardinella longiceps*

Fig.No.3. Catch of *Chirocentrus dorab*

Fig.No. 4. *Pampus argenteus*

Fig. No. 5 *Parastromateus niger*

Fig. No. 6 Harnai Auction centre

Fig.No.7 *Scoliodon laticadus*

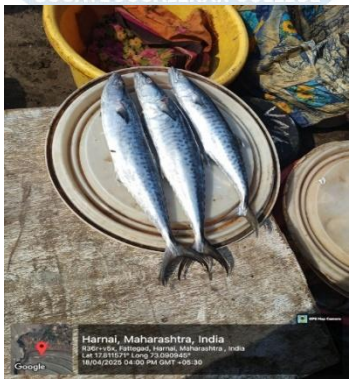

Fig.No.8. *Cybium guttatam*

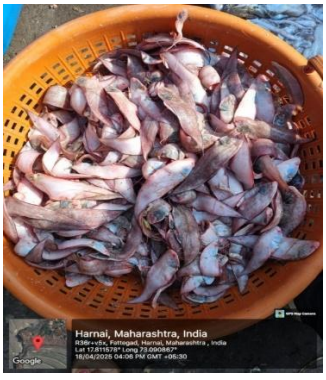

Fig.No.9. *Solea solea*

Table No. 1. Availability and prize data of fish species in the six month August to January 2024-25 at Harnai Market

Sr. No.	Scientific Name	Availability	Prize (in per kg)					
			August	September	October	November	December	January
1.	*Pampus argenteus*	Adequate	1000	1000	1000	1000	1200	1000
2	*Parastromateus niger*	Adequate	800	800	800	800	850	800
3.	*Cybium guttatam*	Adequate	700	850	700	700	700	700
4.	*Stolephorus indicus*	Adequate	200	200	200	200	200	200
5.	*Scoliodon laticadus*	Less	1700	900	1700	900	1700	1700
6.	*Pseudosceiana diacanthus*	Adequate	600	850	700	600	600	700
7.	*Sciaena axillaris*	Adequate	150	150	150	150	150	150
8.	*Rastrelliger kanagurta*	Moderate	370	400	370	370	370	370
9.	*Chirocentrus dorab*	Less	450	420	460	450	450	460
10.	*Sardinella longiceps*	Less	520	520	520	520	520	520
11.	*Harpadon nehereus*	Rare	350	300	360	350	350	360
12.	*Polynem s tetraductylus*	Less	1200	1500	1200	1500	1200	1200
13.	*Engraulis encrasicolus*	Less	270	270	270	270	270	270
14.	*Sprerata seenghala*	Rare	550	480	550	550	550	550
15.	*Soleasolea*	Moderate	205	230	205	205	205	205
16.	*Synagris japonicus*	Less	450	400	400	400	450	400
17.	*Trichiurus lepturus*	Adequate	270	270	270	270	270	270

Table No. 2. Availability and price data of fish species in the Six month of February to July 2025 at Harnai Market

Sr.No.	**Scientific Name**	**Availability**	**Prize (in per kg)**					
			February	**March**	**April**	**May**	**June 1st week**	**July**
1.	*Pampus argenteus*	Adequate	1000	1000	1000	1000	1000	-
2	*Parastromateus niger*	Adequate	800	800	800	850	800	-
3.	*Cybium guttatam*	Adequate	700	700	700	850	700	-

Sr.No.	Scientific Name	Availability	Prize (in per kg)					
			February	March	April	May	June 1st week	July
4.	*Stolephorus indicus*	Adequate	200	200	200	250	200	-
5.	*Scoliodon laticadus*	Less	900	900	500	1700	-	-
6.	*Pseudosceiana diacanthus*	Adequate	600	800	850	550	600	620
7.	*Sciaena axillaris*	Adequate	150	150	150	160	150	140
8.	*Rastrelliger kanagurta*	Moderate	370	450	400	400	-	-
9.	*Chirocentrus dorab*	Less	450	450	450	500	450	-
10.	*Sardinella longiceps*	Less	520	520	520	520	-	560
11.	*Harpadon nehereus*	Rare	350	350	300	350	350	350
12.	*Polynems tetraductylus*	Less	1500	1500	1500	1200	-	-
13.	*Engraulis encrasicolus*	Less	270	270	270	250	270	-
14.	*Sprerata seenghala*	Rare	550	480	480	500	550	-
15.	*Solea solea*	Moderate	205	230	230	230	205	-
16.	*Synagris japonicus*	Less	400	400	400	450	-	-
17.	*Trichiurus lepturus*	Adequate	270	270	300	300	-	-

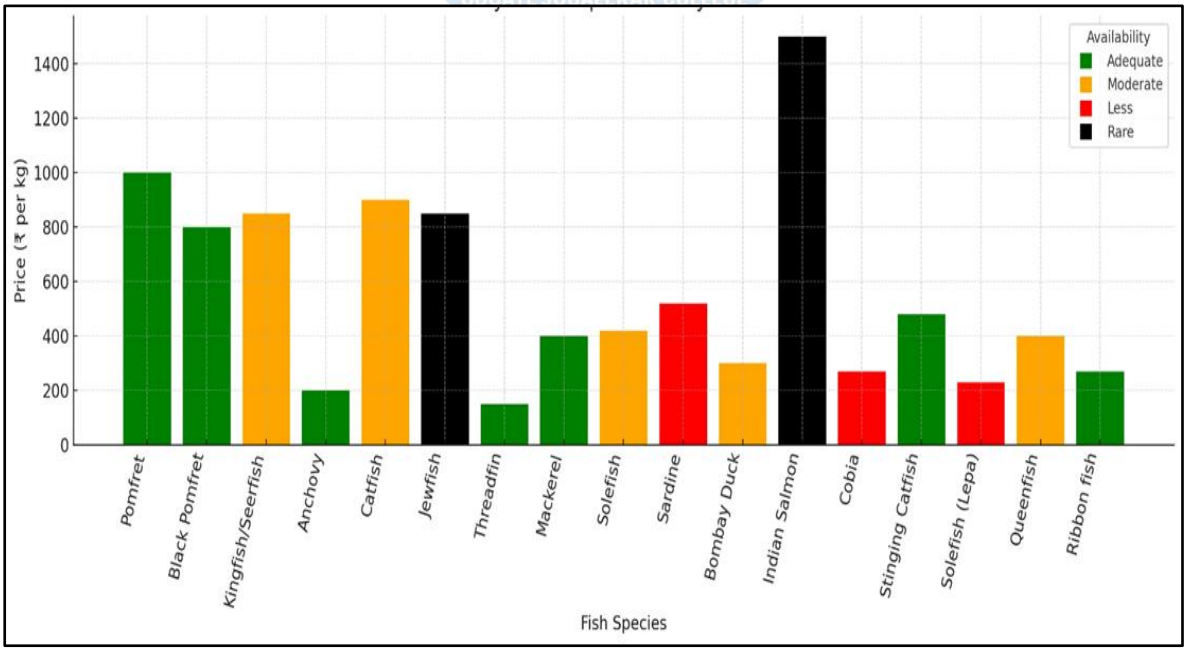

Fig.No.10.Showing relationship between price and availability of fishes in month August 2024 to July 2025.

DISCUSSION

Following results obtained during the survey showed the regularity in availability of the fish species and the constant fluctuations in prices during the day time from Month August 2024 to july 2025. There are some fish species that are available in large amount along Harnai port. The most adequate available fish recorded at port includes Pomfret, Black pomfret and Kingfish /Seerfish and has stabilized the high prices (~Rs.700-Rs.1000/kg) across all months, indicating consistent supply-demand balance.

Anchovy and Threadfin maintained low prices (~Rs.150-Rs.200kg) also were adequately available during the study time. Stingray and Ribbonfish showed low-to-moderate price (~Rs.300-Rs.500/kg) with adequate availability, showing minimal fluctuations across study period.

However, Jewfish prices found steadily increased from Rs.600 in December to Rs.900 in May, and their availability found shifted from moderate to rare with increasing demand. .Mackerel, Solefish and Queenfish showed moderate price increases (~Rs.300 –Rs.500/kg) with moderate to adequate availability during the study period.
The fishes such as Cobia and Bombay duct have showed consistently low prices (~Rs.250-Rs.300/kg) and with low availability across months, suggesting limited catch volumes. Catfish prices remained high (Rs.1600/kg) even though the availability was less.
Moreover, the fishes such as Indian salmon showed rare availability from February onwards, with a significant price increase (~Rs.1400-Rs.1500/kg in Feb-May).
This analysis of price and availability trends at Harnai Market over six months reveals clear seasonal variations.

Consistently adequate species have stabilized high price in the market indicating a well-regulated supply chain and sustained consumer preference.
The up-downs in price of Indian Salmon and Catfish, reflect a seasonal scarcity and availability likely due to reduced catch in pre-monsoon months. The shift in Jewfish from moderate to rare availability with rising prices suggests declining catch that affects regular supply. Species with low prices and adequate availability indicates high catch volumes, making them accessible protein sources for local communities. The consistent rare availability and high price of Catfish suggest the need for stock assessment to manage sustainable harvesting and market stability.
.

CONCLUSION

This study clearly shows that the availability of marine fin fishes at Harnai Landing Centre changes with the seasons and this affects their market prices. Fish like Pomfret, Black Pomfret, and Kingfish were found in good quantity throughout the study period and sold at steadily high prices indicates their balanced supply and demand. But some fish like Indian Salmon and Catfish were available in small amounts, especially before the monsoon, and their prices increased a lot due to low supply and high demand. The study also points attention towards the regular and proper management of fish resources. This will be helpful to protect the environment and keep the market prices stable. It is also concluded that there should be proper promotion for use of low-cost and easily available fish species to reduce pressure less frequent fish species. These results are helpful for government officials, market planners, and fisheries departments to make better policies for protecting marine resources and helping fishermen earn steady incomes.

RECOMMENDATION:

1. It is recommended the monitoring of highly priced fish species catch in different season should be done to prevent overfishing.
2. It is required to support fish marketing chain improvements to stabilize prices for rare species.
3. It is important to popularize and Promote consumption of low- priced fish species to reduce pressure on during scarcity of fish in the market.

It is required to carry out study on fisheries management policies to ensure both ecological sustainability and economic viability at Harnai port.

REFERENCES:

1. Shyam, S. Salim, Lowrane Stanley, and N. R. Athira. "Fish trade, price realization and species diversification across markets in Maharashtra (2021): page no.285-298.
2. Aktar, Nelufa, et al. "Fish species availability and marketing system of fish in different markets of Noakhali district in Bangladesh (2013): page no. 616-624.
3. Shyam, S. Salim, et al. "Species diversity across fish markets in Andhra Pradesh and Telengana (2021):page no. 1-9.
4. N.RAthira, et al. "Price fluctuations and species diversity across fish markets in Kerala (2023):page no. 126-135.
5. Dhande, s. S. Study of local fish availability and fish marketing system of murtijapur, akola district (Maharashtra) [2024] page no. 2319-4979.
6. Hatte, VinayMaruti, et al. "Constraint analysis of Fishermen and Market Intermediaries of Marine Fish Markets in Ratnagiri, Maharashtra, India."(2022) page no. 90-96.
7. M. S. Borkar and P. P. Joshi et.al. Variety of fish species available in local fish market of nanded district (ms) and their economic importance[2023] page no.30-36.
8. Shyam S. Salim et.al Price behaviour and speciesdiversification across fish markets inAndhra Pradesh, India [2023] page no.1-45.
9. SumanLal Debnath1, Md. Fakhrul Islam2*, Syed Ariful Haque3,et.al A study on fish market and marketing system in Gazipur district, Bangladesh [2019] page no. 7-13.
10. RanaHaldar ,et .al.Fish Availability and Marketing System of a Fish Market in Manikganj, Bangladesh [2020] page no. 16-23.

Qualitative Estimation of Proteins from different tissues of clam *Geloina proxima* (Prime, 1864) of Dapoli coast of Ratnagiri District.

More R.S.
Department of Zoology,
Dapoli Urban Bank Senior Science College, Dapoli, District-Ratnagiri,
rsmore8181@gmail.com

Abstract:

G. proxima is one of the indigenous mangrove clam of Dapoli coast and is used as food by the costal people. In this study an attempt have been made to find out proteins qualitatively by Sodium Dodecyl Sulphate- Polyacrylamide Gel Electrophoresis: (SDS-PAGE). This, protein qualitative protein estimation showed the distinctive stained bands. The foot muscle tissue confirmed that it is a tissue that has the high concentration of proteins followed by ovary and gills. Evaluation of the intensity and size of stripes and spots in SDS-PAGE allowed the relative evaluation of protein concentration in the sample.

Key words: Clam, Geloina, Qualitative, Estimation, Protein.

1. Introduction:

G. proxima is one of the indigenous mangrove clam of Dapoli coast and is important aquatic animal due its economic and ecological effects. Bivalves forms most preferable food item for the coastal people of Ratnagiri district. The study of proteins have been extensively increased in recent years. Multiple forms and different properties of proteins indicate the ultimate biochemical make up and relationships among different organisms. Synthesis of proteins and their accumulation in some bivalve species, have been considered as the main denominator of true growth by several investigators [1].

Biochemical composition certain bivalves shows high protein content *C. Gryphoides* [2] , *K. mormorata* [3], *P. plicata* [4] , *E. Radiate* [5] throughout the year and the low levels of protein content coincides with the spawning season. The protein content in different animals may vary with a number of factors such as nutritional state, reproduction, moulting and parasitism. The Bivalve *Meretrix meretrix* shows low protein values during active spawning [11] [12].

Electrophoresis is one of effective method used to describe specific proteins from different tissues of molluscs [6]. Finer separation of proteins has been achieved using the polyacrylamide disc gel electrophoretic technique [7][8].Gel electrophoresis, using sodium dodecyl sulphateis widely used that gives proteins separation basedon their molecular weight. The electrophoretic data of proteins is species specific in molluscs and these results may be useful in the analysis of systematic relations in the class Bivalvia.[09] [10]

Here an attempt have been made to find out the protein profile of this economically valuable clam.

2. Materials and Methods:

Preparation of 40% extract:

Desired tissues such as gills, foot, Gonads, Hepatopancreas were collected by dissecting clams and rinsed in 0.28% saline. Blotted 4 gms. of the each tissue and homogenized with 10 ml of 80% alcohol and centrifuged at 4000/ r.p.m. for 15 min. Supernatent mixed with 1 ml of Tris glycine buffer- pH 7 to remove non required organic and inorganic component and again centrifuged at 4000 r.p.m. for 5 -10 min. The supernatant collected used for estimation of proteins. The entire procedure preferably carried out at 4^0 C.

Qualitative studies of protein by Sodium Dodecyl Sulphate- Polyacrylamide Gel Electrophoresis: (SDS-PAGE): [13]

Preparation of Reagents:

1. Protein molecular weight standards as mentioned in **Fig.No.3**
2. 30% Acrylamide – 0.8% Bis-acrylamide.
3. Sample buffer: Mix 4 ml of 10 % SDS, 2 ml of glycerol, 1ml of β – Mercaptoethanol, 2.5 ml of 0.5 M Tris-HCL (pH 6.8), and 0.03 gm Bromophenol blue. Bring the volume to10 ml with distilled water prior to filter with Whatman No. 1 filter paper. Divide in to 1 ml aliquots and store at -20^{0}C.
4. 10% (w/v) Ammonium per sulfate.
5. 10% (w/v) SDS.
6. TEMED (N,N,N$^/$,N$^/$,N$^/$ - tetramethyl ethylene diamine)
7. 0.5 M Tris-HCL, pH 6.8
8. 1,5 M Tris-HCL, pH 8.8
9. **Electrode buffer:** Dissolve 3gm of Tris, 14.4gm of glycine and 1gm of SDS in distilled water. Adjust to pH 8.3. Make up volume to 1L with distilled water.
10. **Staining solution:** Dissolve 0.05 gm of Coomassie blue R-250 in 15 ml of methanol. Add 5 ml of glacial acetic acid and 80 ml of distilled water.
11. **Destaining solution I:** Mix 200 ml methanol, 30 ml acetic acid and 170ml. of distilled water.
12. **Destaining solution II:** Mix 50ml of methanol, 75 ml of acetic acid and 875 ml of distilled water.

Pouring the running gel:

1. The minigel apparatus was assembled according to the manufacture's detailed instructions. The glass and other components must be thoroughly cleaned and dried before assembly.
2. Resolving gel and stacking gel solutions were prepared as defined in the **Table No. 1.**
3. 3.5 ml of resolving gel solution is transferred to the center of sandwich of the spacers.
4. The top of the gel was covered with a layer of distilled water. The resolving gel was allowed to polymerize fully (usually 30- 60 min)

Pouring of the stacking Gel:

1. The layer of distilled water was poured off completely.
2. 4 % stacking gel solution was prepared as defined in the **Table No. 1.**
3. Stacking gel solution is transferred to the center of sandwich along an edge of one of the spacers.
4. The Comb was inserted in to the layer of stacking gel solution by placing one corner of the comb in to the gel and slowly lowering the other corner in. The stacking gel solution was allowed to polymerize for 45 minutes at room temperature.

Table No. 1. Experimental set up for separating gel and stacking gel.

Reagents	Separating gel		Stacking gel
	7.5%	10 %	4 %
30 % Acrylamide- bis	2.500 mL	3.333 ml	0.667mL
1.5M Tris-HCL buffer, pH 8.8.	2.500 mL	2.500 mL	-
0.5M Tris-HCL buffer, pH 6.8.	-	-	1.250 mL
Distilled water	4.845mL	4.012 mL	3.005mL
10% SDS	100 µL	100 µL	50 µL
10% Ammonium per sulfate	50 µL	50 µL	25 µL
TEMED	5 µL	5 µL	3 µL
Total	10 ml	10 ml	5 ml

Loading the gel:

1. The protein was diluted to be 1: 1(v/v) with sample buffer in micro centrifuge tube and boiled for 3 minutes at 100 ^{0}C (boiling water).
2. The wells were filled with electrode buffer after removing the comb.
3. With the help of a 10-25 µL syringe with a flat-tipped needle, the protein sample was loaded in to the wells. The sample was carefully applied as a thin layer at the bottom of the well.
4. Then chambers were filled with buffer.

Running the Gel:

1. Power supply was connected to the anode and cathode of the gel apparatus and allowed to run at a constant current of 15 mA/gel.
2. After the bromophenol blue tracking dye reached the bottom of the separating gel, the power supply was disconnected.
3. The sandwich was removed and the gel was oriented so that the order of the sample wells is known. It was then carefully removed from the sandwich.

Staining the gel:

1. Gel was placed in a small plastic box and was covered with the staining solution. It was agitated slowly for 3 hrs. or more on a rotary rocker.
2. The staining solution was poured off and the gel was covered with a solution of destaining solution-I and was again agitated slowly for about 15 minutes.
3. Destaining solution- I was poured off and the gel was destained with destaining solution-II until the gel was cleared except for the protein bands.

Details of Protein Molecular Weight Marker (Broad) used are as follows:

1. **Code No.** **3452.**
2. **Size:** **for 200 lanes.**
3. **Make:** Takara Biotechnology (Dalian ） Co., Ltd.
4. **Supplied Reagent:** 5 × Loading Buffer 1 ml
   1M DTT (Dithiothreitol) 100 µl
5. **Concentration:** 18 µg /µl
6. **Volume:** 50 µl
7. **Form :** 50 mMTris-HCL, pH 6.8
   1 mM EDTA
   200 mM NaCl
   50% Glycerol
8. Component Proteins of the Marker are given in the **Table 2.**
9. **Storage :** Protein Molecular Weight Marker, 1M DTT : -20℃
   5×Loading Buffer: Stored at Room Temperature after used.
10. **5 × Loading Buffer (Stored at RT after used) :**
    200 mMTris-HCL, pH 6.8
    10% SDS
    0.05% BPB
    50% Glycerol

11. **Application Example :**
    i. Combined the following reagents in a tube.
        1M DTT: 2 µl
        5×Loading Buffer: 20 µl
    ii. Prepared 20-fold diluted marker by adding the following components to the solution prepared in- i.
        Protein MW Marker (Broad) : 5 µl
        Sterilized distilled Water : 73 µl

20-fold diluted marker is stable for 2 - 3 months for -20℃. It is recommended to store in aliquots for several uses, not to repeat freeze-thaw cycles.

    iii. Mix 20-fold diluted marker well, and heat at 100℃ for 5 minutes. Load 5 µl per lane of SDS-PAGE minigel. Run 5 - 20% gradient SDS-polyacrylamide gel electrophoresis.
    iv. Perform staining with Coomassie Brilliant Blue R-250.

12. Electrophoresis results of Protein Molecular Weight Marker (5 - 20% gradient SDS-PAGE) are given in the Fig. No.3.

Molecular Weight Marker

Table No. 2. Component Proteins present in

Protein	Source	MW (Da)
Myosin	Pig	200,000
β-galactosidase	E. coli	116,000
Phosphorylase B	Rabbit muscle	97,200
Serum Albumin	Bovine	66,409
Ovalbumin	Hen egg White	44,287
Carbonic anhydrase	Bovine	29,000
Trypsin inhibitor	Soybean	20,100
Lysozyme	Hen egg white	14,300
Aprotinin	Bovine pancreas	6,500

Fig. No.1 : Clam Geloina proxima

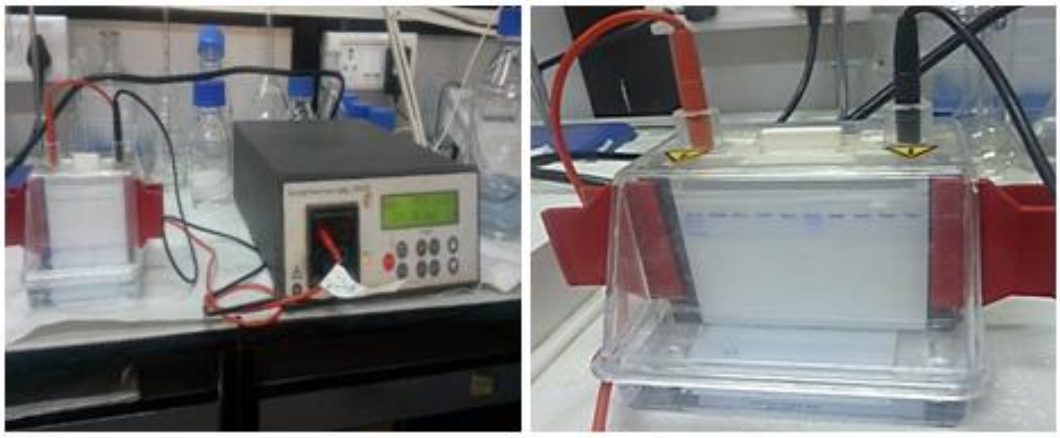

Fig. No. 2 Minigel electrophoresis apparatus with loaded sampl

3. Results:

The results obtained are reported here in figure No. 3 and 4

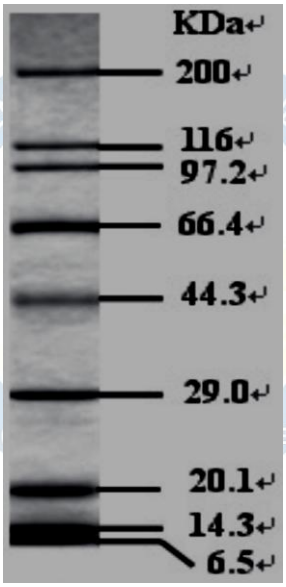

Fig.No.3: Protein Molecular Weight Marker.

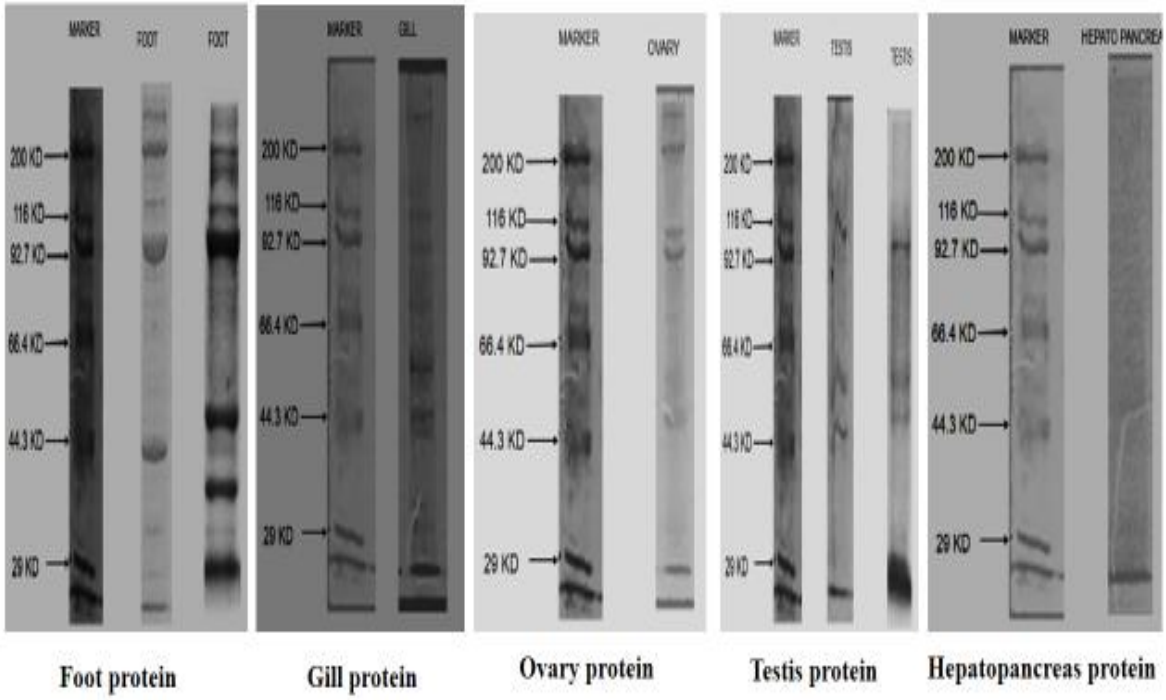

Fig .No. 4: Separated protein bands from different tissues of *G. proxima.*

4. Discussion:

Bivalves are usually preferred as low cost food by the coastal community and are inexpensive source of protein, essential minerals and vitamins. Biochemical study of any edible organism is of great significance because it is an indicative of nutritive value of that organism and consequently helps to stabilize the price levels [14]. Present quantitative analysis of protein of *G.proxima*, showed highest range of proteins in foot tissue followed by testes, ovary and gills. A distinctive number of stained bands by SDS PAGE, in the case of foot tissue confirmed that, it is a tissue that has high proteins content in a wide range from 29 to 200 KD and above. They may be carbonic anhydrase whose molecular weight is 44.3 KD, may be Ovalbumin 44.3KD, may be phosphorylase- B 97.2 KD and may be myosin with 200 KD. Gill tissue showed the darkest band located between 44.3 and 116 KD. It can/ may be Ovalbumin, Serum Albumin and β-galactosidase. Ovary tissue sample shows a wide range of proteins between 44.3 to 200 KDa. The proteins of ovary may be Ovalbumin, Phosphorylase B and β-galactosidase. While testis tissue sample showed the proteins with molecular weight of 44.3 to 97.2 KDathat can be ovalbumin and phosphorylase B respectively. The highest range of proteins with darker bands was observed in foot tissue followed by ovary and gills in *G.proxima.* The bands of separated molecules can be cut from the gel, digested and subjected to further structural analysis. Such qualitative analyses may support histological and histochemical studies.

5. References:

1. Giese A.C. (1969): A new approach to the biochemical composition of the mollusk body. Oceanography Marine Biological Annu.Rev., 7: 115- 129.
2. Durve, V.S. and Bal, D.V.(1961): 'Proceedings of the Indian Academy of Sciences' LIV (1), Sec. B., 45-55.
3. Joshi, M.C. (1963): 'A stud on clam *Katelysiamormorata* (Lam) Ph. D. Thesis submitted to the University of Bombay, India.
4. Shanmugam, A. (1991): Mahasagar, 24 (2), 113-118.
5. Etim. L. (1993): Tropical Ecology 34 (2), 181-188.

6. Davis, G.M. and Lindsay, G.K. (1967). Disc electrophoretic analysis of molluscan individuals and populations.Malacologia. 5(2): 311-334.
7. Davis, B. J. (1964). Disc electrophoresis-II.Method and application to human serum proteins. Ann. N. Y. Acad. Sci., 121: 404-427.
8. Ornstein, L. (1964): Disc electrophoresis. I. Background and theory. Ann. N.Y. Acad. Sci., 121: 321-349.
9. Nakatogawa, H.; Ohsumi, Y. (2012) SDS-PAGE techniques to study ubiquitin-like conjugation systems in yeast autophagy. MethodsMol. Biol.*832*, 519-529.
10. Margulis, B.A. and Pinaev, G.P. 1976. The species specificity of the contractile protein composition of the bivalve molluscs. Comp. Biochem. Physiol., 55B 189-194.
11. Jayabal, R. and Kalyani, M. (1986,): Indian J. Mar. Sci. 15 (1), 59-60.
12. Jayabal R, Kalyani M (1987) Seasonal variation in biochemical constituents of the different body components of *Meretrixmeretrix*(L) Mahasagar- Bull. Natl. Institute Oceanography, 20(1): 65-69.
13. Dr. Amjad K. Balange, Senior Scientist, post-harvest Technology, CIFE, Mumbai. Methods of electrophoretic separation of proteins.
14. Ajayabhaskar D. (2002): Nutritional evalution of molluscan sea food. Ph. D., Thesis, Annamalai University India, pp. 129.

Acknowledgements

The Organizing Committee sincerely thanks all the participants, speakers, reviewers, and sponsors who contributed to the success of the **ICFST-2025.**

We are especially grateful to:

Scientific and Advisory Committee Members for their guidance

All Authors and Delegates for their enthusiastic participation

International Conference on Frontiers in Science and Technology

R. E. Society's
R. P. Gogate Jogalekar College of Arts & Science And
R. V. Jogalekar College of Commerce (Autonomous), Ratnagiri
www.gjcrtn.ac.in